Radio Antenna Engineering

EDMUND A. LAPORT

Chief Engineer, RCA International Division
Radio Corporation of America
Fellow, Institute of Radio Engineers

McGraw-Hill Book Company, Inc.
New York Toronto London
1952

RADIO ANTENNA ENGINEERING

Copyright, 1952, by the McGraw-Hill Book Company, Inc. Printed in the United States of America. All rights reserved. This book, or parts thereof, may not be reproduced in any form without permission of the publishers.

Library of Congress Catalog Card Number: 51–12624

IV

THE MAPLE PRESS COMPANY, YORK, PA.

PDF file generated: Sat May 21 14:54:48 PDT 2005

Electronic edition Copyright © 2005 by David C Platt

Permission is granted for noncommercial copying and distribution

For complete information and copyright terms, please visit:

http://snulbug.mtview.ca.us/books/RadioAntennaEngineering/

Preface

Antenna engineering has developed into a highly specialized field of radio engineering which in turn is subdivided into many special branches. This treatise will deal with antennas made of wires, masts, and towers for frequencies up to about 30 megacycles. Antennas for higher frequencies are nowadays factory-designed and factory-built, and the operating and plant engineers are relieved of the design problems.

There is a very extensive experience with antennas within our range of interest, but unfortunately there is only a relatively small amount of published material on techniques. In contrast, there is a vast literature on antenna and radiation theory. It is the purpose of this book to attempt to compile a sufficient amount of useful engineering information to enable nonspecialists to handle many of the ordinary antenna problems that arise in point-to-point, ground-to-air, and military communications, and in broadcasting. Some of the more advanced antenna designs suggested by very-high-frequency and ultrahigh-frequency techniques are included because the day is approaching when these principles will have to be applied at the lower frequencies as the spectrum conditions become more difficult.

Transmission lines are inseparably related to antennas, so a chapter on this subject is included, together with a chapter on impedance-matching networks.

An author of a book on techniques is confronted with many difficult situations because he must try to convey a sense of judgment in significant values and wise compromise in the presence of the many empirical conditions that surround each individual problem. The successful solution of an engineering problem involves many arbitrary decisions and is largely a matter of personal ingenuity and resourcefulness in applying sound electrical and mechanical principles. For that reason some of our statements made in the discussion of the various topics should not be interpreted too rigorously. Our intention has been to provide a certain amount of guiding counsel for those who need it even though it was necessary to oversimplify to some extent.

There are three basic aspects of antenna engineering. The first per-

tains to radiation characteristics and includes all matters of the distribution of radiant energy in space around an antenna system, as well as the current distributions that produce the radiation pattern. The second pertains to antenna circuitry and involves such matters as self- and mutual impedances, currents, potentials, insulation, and feeder systems that will yield the desired current distributions. Third there is the structural engineering which has to do with all the mechanical details of supports, rigging, materials, strengths, weights, hardware, assembly, adjustability, stability, and maintenance. While each aspect must be separately developed, the final design must be an integration of the three, with a minimum of compromise and within reasonable economic limits.

The purpose of a transmitting antenna is to project radiant energy over a given wave path in the most effective and economical manner. The purpose of a receiving antenna is to absorb a maximum power from a passing wave field, with the maximum exclusion of noise and interfering signals. The transit of a wave field between the two depends upon the physics of wave propagation. The antenna engineer must be familiar with wave propagation to be able to design antenna systems of maximum effectiveness. Wave propagation is a vast and complicated statistical subject, and for that reason the space that can be devoted to the subject in this book is limited to the barest essentials. Sources of detailed information are indicated for reference and study. It may be expected that future developments in our knowledge of propagation will have their influence on future antenna design.

The design formulas for the various types of antennas are presented without proof and may be regarded as recipes. Their theory and derivation may be found in the literature, together with more complete information of a related nature. Also, many data curves and tables are taken from recognized sources, although these are sometimes rearranged for greater utility. Some of the information is from unpublished sources and includes much original material. The appendixes contain reference data of general use to the antenna engineer.

The nomenclature used for bands of frequencies is based primarily on their propagation characteristics. These terms are also approximately in accord with the nomenclature adopted by the International Telecommunications Union at its Atlantic City conference in 1947. The use of these broad terms has a brevity and convenience that is very desirable in writing and talking about frequencies, provided that one thinks about them as having indistinct boundaries.

One must recognize rather large overlaps in the bands of frequencies propagated as listed, and the bands shown are indicative only. They blend gradually from one into the other, the amount and the extreme ranges varying with the state of the ionosphere and ground characteristics.

The three frequency groupings also roughly define three different classes of design technique for antennas, and we have taken them up in this order. To a certain extent, high-frequency design techniques may be applied to antennas used for optical propagation, but antennas for the frequencies propagated optically become still another class of techniques based on rigid prefabricated structures.

Term	Abbreviation	Approximate band	Most useful propagation
Low frequency (long wave)	LF or lf	Up to 500 kilocycles	Ground waves
Medium frequency (medium wave)	MF or mf	200–5,000 kilocycles	Both ground and sky waves
High frequency (short wave)	HF or hf	3–40 megacycles	Sky waves propagated by way of the ionosphere

Wherever possible we have used the meter-kilogram-second system of units in the formulas. However, in a practical work of this nature it is necessary to adhere to prevalent engineering usage of heterogeneous systems of units. For example, in the United States it is standard engineering practice in broadcasting to base the performance of an antenna on millivolts per meter at 1 mile and to use conductivities in the centimeter-gram-second electromagnetic system of units. The general use of the English system of measurements leads also to the frequent use of such units in formulas. To avoid confusion, the particular units used are explicitly given where necessary, even though this requires a certain amount of repetition. This is done so that one can select and use an isolated formula conveniently.

Nomenclature with respect to wave polarization follows the standardized usage where the orientation of the electric vector of the wave field with respect to the earth defines the polarization. Vertical polarization is understood when the electric vector of the wave is normal to the earth's surface, and horizontal polarization when the electric vector is parallel to the earth. Intermediate polarizations also exist.

Comprehensive bibliographies are given at the end of each chapter, and a more general bibliography is given in Appendix I. The papers listed are those which have a definite reference value to the antenna engineer when he is searching for fundamental information, experimental data, and history of the art, as reported in original researches. Collectively they comprise many thousands of pages of information that cannot possibly be condensed into any single volume. As one advances further and further in the antenna-engineering art, the need for reference to these original sources becomes more pressing and the value of an extensive bibliography becomes evident.

Superscript numbers are used in the text to indicate relevant sources of information. Numbers under 1000 relate to those references listed at the end of the particular chapter in which they are cited. References in the 1000 series are to be found in Appendix I.

The book *Antennas* by J. D. Kraus[1002] is a useful one for those desirous of becoming familiar with the theoretical principles of antennas. It is a synthesis of the latest theories of radiation from antennas and the methods for computing radiation patterns and impedances, and reduces the need to refer to the large number of original research papers distributed through the literature of many years.

I acknowledge with thanks the encouragement of Keith Henney, Editor-in-Chief of *Radio Engineering Handbook*, who suggested that this book be written, at the time he received the manuscript for the chapter on Antennas which appears in the Fourth Edition of the Handbook.

I am deeply indebted to many coworkers and associates, present and past, for information and instruction on antenna technology and wave propagation over many years. There is a special debt of gratitude to acknowledge to Dr. George H. Brown, Phillip S. Carter, Clarence W. Hansell, and Henry E. Hallborg of the RCA Laboratories Division for the use of information from their published and unpublished researches. I express my gratitude to Robert F. Holtz for carefully reviewing the early manuscript and making many valuable suggestions. The final manuscript was again painstakingly reviewed by J. D. Fahnestock, whose professional editorial effort has greatly improved the style and arrangement.

The following men kindly contributed some of the photographs showing construction details: R. F. Guy of the National Broadcasting Company; J. L. Finch of RCA Communications, Inc.; H. B. Seabrook and J. B. Knox of the RCA Victor Company, Ltd.; A. O. Austin, Barberton, Ohio; Lt. D. V. Carroll of the Royal Canadian Navy; J. A. Ouimet and J. E. Hayes of the Canadian Broadcasting Corporation; Harold Bishop of the British Broadcasting Corporation; E. J. Wilkinson of the Australian Postmaster-General's Department; W. M. Witty, Dallas, Texas. E. W. Davis of the Mutual Broadcasting System contributed the map reproduced in Appendix VIII.

I acknowledge with sincere thanks the kindness of the following organizations which have granted the right of reproduction of certain figures under their copyrights: Institute of Radio Engineers; Institution of Electrical Engineers; Amalgamated Wireless (Australasia) Ltd.; His Majesty's Stationery Office, London; McGraw-Hill Publishing Company, Inc.; Marconi's Wireless Telegraph Company, Ltd.; Institution of Radio Engineers (Australia).

EDMUND A. LAPORT

GLEN RIDGE, N. J.
January, 1952

Contents

Introduction

Radio communication is accomplished by the transmission and reception of electromagnetic waves that are propagated between two geographical locations by the phenomenon of electromagnetic radiation. A radio-frequency generator, called a radio transmitter, delivers its output power to a transmitting antenna. The transmitting antenna transforms the radio-frequency energy in the antenna circuit to the wave field that is radiated into surrounding space. The waves originating as a disturbance at the transmitting antenna are propagated as detached electromagnetic fields which travel through air with the velocity of light c, where c is 3×10^8 meters per second.* In other mediums, the velocity of propagation of plane electromagnetic waves[1001] is

$$v = c\left[\frac{\mu_r\epsilon_r}{2}\left(\sqrt{1+\frac{\sigma^2}{\epsilon_v{}^2\epsilon_r{}^2\omega^2}}+1\right)\right]^{-\frac{1}{2}} \quad \text{meters per second}^{1001}$$

This equation is in the rationalized meter-kilogram-second (mks) system of units. Here, μ_r is the magnetic permeability relative to free space, and ϵ_r is the dielectric constant, or inductivity, of the medium relative to free space. ϵ_v is the permittivity of free space, which has the value of 8.85×10^{-12} farad per meter. σ is the conductivity of the medium in mhos per meter. ω is $2\pi \times f$, the frequency in cycles per second.

When electromagnetic waves are propagated into the earth (soil), water, metals or any other materials, the velocity may become very low with respect to air owing to the sometimes large values for σ, μ, and ϵ in the material.

A transmitting antenna emits one wave for each period of the exciting potential, or a total number per second equal to the transmitted frequency f. The wavelength λ of the emitted waves is therefore

$$\lambda = \frac{v}{f}$$

The wavelength is in the same units as used for the velocity.

* This is the value used for ordinary engineering purposes. The latest measurements give the velocity as 299,792 kilometers per second.

The size of an antenna is related to the wavelength of emission in some manner; it may have a length of a half wavelength, a quarter wavelength, one-twelfth wavelength, or in some cases one or more wavelengths. The range of wavelengths primarily concerning us in this book is from about 10 meters to perhaps 20,000 meters. One can realize immediately that an antenna one wavelength high at 10 meters is a simple matter, whereas one 20,000 meters high, as a fixed structure, is impractical. For this reason, the use of the longer wavelengths imposes mechanical restrictions on the designer, which in turn introduce difficult electrical conditions.

One wavelength being generated per period of the exciting frequency, we can speak of one wavelength as being 360 electrical degrees and use the electrical degree as a unit of physical length which always bears a fixed relationship to the wavelength. In this book antenna dimensions will usually be given in electrical degrees, which is a convenience in engineering because of its direct relation to trigonometric angles used in computations. When we speak of an electrically short antenna, it means one that has a length very small with respect to the wavelength emitted. In accordance with the principle of similitude, the performance of an antenna in free space, infinitely removed from earth, is the same for all antennas of the same electrical size, without regard to their mechanical sizes. Use is made of this principle in making large-scale or small-scale antenna models as a means for obtaining physical data on projected systems.

The transmitting antenna comprises the "load" circuit for the radio transmitter, and the power delivered to the antenna is dissipated in heating the conductors, the insulators, and the ground and surrounding parasitic objects and in radiation. The transmitting-antenna resistance therefore is composed of several components which account for these various power losses. The energy "lost" from the antenna circuit because of the radiation of waves into space is of course the *useful* loss, and that component of antenna resistance which is associated with the radiation of energy is called the "radiation resistance." The efficiency of the antenna system is the ratio of its radiation resistance to its total resistance. In antenna engineering one of the objectives is to make this ratio as large as possible. At the shorter wavelengths efficiencies very near to 1.0 can be achieved conveniently, while for the longer wavelengths the best that can be achieved is much less than this, and sometimes as low as 0.05.

Antennas are in general open-circuit systems of electrical conductors projecting into the space in which the radio waves are propagated. These conductors are connected to the transmitting and receiving apparatus, which are closed-circuit devices. The charges moving in the transmitting

antenna cause disturbances in the surrounding space which generate the waves propagated outward into space, with attenuation and variations which increase with the distance from the transmitting antenna. The passing wave field induces the movement of charges in the conductors of the receiving antenna, which causes currents and potentials to be built up in various parts of the system and combined at the point where the radio receiver is connected to the antenna system. The receiver input power is amplified, detected, and delivered to an electromechanical transducer of a type which will be actuated by the signal received and will disclose the intelligence which it contains.

In a book of this nature we shall take for granted the dynamic relationships established in the electromagnetic theory between electric charge, electric flux, electric field strength, electric current, magnetic flux, and magnetic field strength and shall apply these relations in the manner of the engineer. The reader who wishes to have a full understanding of the theoretical foundations of electromagnetic theory and electromagnetic radiation may consult many excellent modern treatises, such as Stratton,[1001] Skilling,[1004] and Kraus.[1002] For the present practical purposes it will suffice to utilize the proven results of the theory, extracting useful formulas out of context as the need arises. One that must be extracted and examined, because it will be used frequently, concerns the field around a very short doublet in free space composed of a straight conductor of length l in which a sinusoidal alternating current of frequency f is flowing. The current is assumed to be uniform throughout the length of this doublet. The instantaneous value of the current i as a function of time t can be expressed as

$$i = I_0 \sin \omega t$$

Consider further that the middle of this doublet is the center of a system of polar coordinates with the axis of the conductor along the θ axis of the coordinate system. The angle θ is measured from this axis and may be called a "colatitude angle." The longitude angle ϕ is measured from some arbitrary reference direction in the equatorial plane. The distance from the origin of coordinates will be designated by r. When the electric field is measured at a point in space several wavelengths from the doublet and this point has the coordinates θ, ϕ, and r,

$$E_\theta = \frac{377Il \sin \theta}{2r\lambda} \cos\left(\frac{2\pi r}{\lambda} - \omega t\right) \qquad \text{volts per meter}$$

This equation expresses the absolute magnitude and relative phase of the field at all values of θ and r; but, owing to axial symmetry, the field is independent of ϕ. If we consider only the factor giving the magnitude of the field, it is seen to be directly proportional to the current and to the

length of the doublet; that it is proportional to the sine of θ and is therefore zero in the direction of the doublet axis and maximum in the equatorial plane where $\theta = 90$ degrees; and that it is inversely proportional to the distance and to the wavelength when r, l, and λ are measured in meters. If instead we change both the length of the doublet and the wavelength to electrical degrees, we shall obtain the same result. As a valuable example, let us assume that the current is unity, l is 1 electrical degree, λ is 360 degrees, and r is 1,610 meters (1 mile). When these values are substituted in this equation, we compute a value of 325×10^{-6} volt per meter, for $\theta = 90$ degrees. Therefore a doublet with a moment of 1 degree-ampere corresponding to the above conditions will produce a free-space field strength of 325 microvolts per meter at 1 mile from the doublet. This is an important fact to remember in practice—that each degree-ampere will contribute this amount to the total free-space field normal to the doublet axis.

This field equation is for the radiation field only. Near the doublet, there are two additional terms for the total field (which are omitted from our equation) that are described as the static field and the induction field, which vary inversely as r^3 and r^2, respectively, and which therefore quickly fall to negligible values as the distance increases. The induction field has decreased to 1 per cent of the value of the radiation field at a distance of 16 wavelengths.

The values of E plotted in all directions, but at constant distance from the center of the system, describe the space characteristic, or radiation pattern. The pattern for a free-space doublet is the fundamental unit used to derive the radiation pattern for antennas having various spatial distributions of currents. Each element of length of a wire in an antenna system contributes as a doublet to the over-all field for the antenna system made up of the contributions from all the current-carrying elements. The pattern for an antenna is understood to be determined at a distance so large with respect to the largest dimension of the antenna that the rays from each doublet portion are essentially parallel and the effect of the different values of r from each doublet portion to the distant point are essentially equal. This is the so-called "Fraunhofer region," where the shape of the pattern is independent of r. The radiation pattern then is the integration of all the elements of radiation contributed by all the currents of the system, taking into account their relative magnitudes, initial phase differences, and the phase differences introduced by their propagation over different path lengths.

The basic relation for the radiation field from an elementary doublet is

$$E \propto I \sin \theta$$

This gives its fundamental pattern shape and relative magnitude. The

pattern for any antenna system is the integration of the contributions of all its elementary doublets.

These basic facts can be brought down to a very useful summary if we consider a doublet that has an electrical length of 1 degree, with a uniform current of 1 ampere flowing throughout its length. The field strength produced by a moment of 1 degree-ampere in free space has already been shown to be 325 microvolts per meter at 1 mile from the doublet in the direction normal to the doublet axis. So long as all the currents in a system of coaxial doublets are cophased, each degree-ampere contributes 325 microvolts per meter in this direction. When reversed currents are present, the antenna field will be the algebraic sum of the fields produced by the positive and negative degree-amperes.

When a doublet is located over a perfectly conducting infinite flat plane and oriented either horizontally or vertically, the maximum field strength produced by the combined direct and reflected wave fields is twice that from the doublet in free space. Therefore, over perfectly conducting flat earth, each degree-ampere contributes 650 *microvolts per meter* at 1 mile to the total field in the maximum direction. When the doublet is horizontal, the maximum field will be at some angle to ground determined by its electrical height; and if the height be large electrically, there will be several such maximums. Again, the field maximums occur normal to the doublet.

A straight half-wavelength dipole in free space having sinusoidal current that is in time phase throughout its length but distributed sinusoidally in magnitude as a function of the distance in electrical degrees from either end of the dipole has an integrated radiation field which is completely expressed by the relation

$$E_\theta = \underbrace{\frac{60 I_0 \sin \omega t}{r}}_{A} \underbrace{\frac{\cos (90 \cos \theta)}{\sin \theta}}_{B} \underbrace{e^{j360r/\lambda}}_{C} \quad \text{volts per meter}$$

where I_0 is the instantaneous peak value of the current at the center of the dipole.

This equation has the factors indicated as A, B, and C which have the following physical meanings:

A. This is the amplitude factor which shows that the field strength is proportional to the current varying sinusoidally in time, with a peak instantaneous value of I_0 at the center of the dipole, and that the field strength is inversely proportional to the distance r from the dipole. The constant 60 sets the absolute value in volts per meter at unit distance, and is $377/2\pi$, very nearly, where 377 (ohms) is the intrinsic impedance of free space to a plane wave.

B. This factor results from integrating the distant fields from the distribution of doublets with their relative currents along the dipole (sinusoidal current distribution) and is the radiation pattern for an idealized half-wave dipole as a function of θ. This factor is often used alone in engineering studies where only the shape of the radiation pattern is of interest.

C. This factor states that the phase of the electric field is leading that of the field at the source at any instant by 360 degrees per wavelength, measured along the propagation path. This is because of the finite propagation for a wavefront to arrive at the distance r, during which time the phase of the source has fallen behind this wavefront by $360r/\lambda$ electrical degrees.

In using half-wavelength (or half-wave) dipoles as elements in more extensive antenna systems, the radiation patterns may be computed on a relative rms basis using the relation

$$F_\theta = \frac{I \cos (90 \cos \theta)}{\sin \theta}$$

where I is the rms current at the center of the dipole and the electric force F_θ is now in arbitrary relative units. If instead of using the colatitude angle θ we wish to measure θ_1 as a latitude angle from the equatorial plane of the system, as we do frequently, we take θ_1 as the complement of θ and by substitution, to obtain

$$F_\theta = \frac{I \cos (90 \sin \theta_1)}{\cos \theta_1}$$

A half-wave dipole has a moment of 114.5 degree-amperes per ampere at its center. This produces a field strength of 37.3 millivolts per meter at 1 mile from the antenna for each ampere of antenna current. Over perfectly conducting ground, the image radiation (waves reflected from the ground) contribute an equal amount to the resultant field, producing a field strength of 74.6 millivolts per meter at 1 mile per ampere at those angles where the direct and reflected waves add in phase.

From now on, with this information, we can use the half-wave dipole as the fundamental element in an antenna array composed of half-wave dipoles, integrate the contributions of each such dipole to the total field of the array, and thereby compute the radiation pattern for the array.

At this point one can summarize the basic physical facts of doublets and dipoles in easily remembered form as follows:

The free-space radiation pattern for a very short doublet is the solid of revolution generated by a circle tangent to the doublet.

The free-space radiation pattern for a half-wave dipole is the solid of

revolution generated by an oval tangent to the dipole with its major axis normal to the dipole. The minor axis of the tangent oval is 90 per cent of the major axis.

These facts will be used extensively throughout the book in dealing with radiation patterns. However, because practical antennas must usually be built close to the earth, the symbols for the reference angles will be changed to α for the elevation angle from the horizon and β for the azimuth angle from the *normal* to a dipole, or clockwise from true north, or some other reference in systems using vertical radiators.

The magnetic force H of a plane electromagnetic wave can be derived from the electric force, or electric field strength E, through the relation

$$H = \frac{E}{377} \qquad \text{ampere-turns per meter}$$

in air. In this relation E is in volts per meter, and 377 is a constant known as the "intrinsic impedance" η of free space in ohms. It is obtained from the relation

$$\eta = \frac{E}{H} = \sqrt{\frac{\mu_v}{\epsilon_v}} = \sqrt{\frac{4\pi \times 10^{-7}}{8.85 \times 10^{-12}}} = 377 \text{ ohms}$$

where μ_v is the permeability of free space, which is $4\pi \times 10^{-7}$ henry per meter.

Whereas the intrinsic impedance of free space for a plane electromagnetic wave is the ratio of E and H, the vector product of E and H gives the Poynting vector P, or the power flow in watts per square meter in the direction of propagation or in the plane of the equiphase surface of the wave. Both E and H are vector quantities in that they both have direction and magnitude at any point in space. They are perpendicular to each other and to the direction of propagation. Through these simple equations, which are consequences of using the meter-kilogram-second (mks) system of units, plane-wave relations become analogous to Ohm's and Joule's laws for circuits. Therefore we can go on to other obvious relations such as

$$P = \frac{E^2}{377} = 377H^2$$

Most field-strength meters are calibrated in terms of volts per meter, millivolts per meter, or microvolts per meter. From a measurement of field strength one can determine directly the power flow in watts per square meter. If the effective pickup area (or the effective aperture) of a receiving antenna is known, the total power delivered at the receiver input from the passing wave field becomes known. It is assumed in

this statement that the wave field is arriving from the direction of maximum response of the receiving antenna.

The classical original method of computing the radiation resistance of an antenna was to compute its radiation pattern at great distance in terms of field strength and square the field strengths at all points on an enclosing hemisphere (in the case of an antenna located near the ground). The radiation pattern then is in terms of power flowing outward through the hemisphere, and the integration of power flow over the surface of the enclosing hemisphere gives the total radiated power from the antenna. The radiation resistance then is the ratio of the radiated power and the square of the antenna current. Since the antenna current is usually a function of position in the antenna, the value of radiation resistance will depend upon what point in the system it is referred to—usually the point where the antenna is fed by the transmitter or at a point of maximum current.

Radio transmission sometimes is to specific targets, as in point-to-point communication, and sometimes to a multiplicity of targets of general geographic distribution, as in broadcasting. The radiation of electromagnetic waves to specific fixed targets permits the use of antennas that are directive and concentrate the radiant energy like a searchlight beam in the desired direction. Directive antennas make use of the principles of wave interference to combine the fields from a multiplicity of radiators synchronously excited so that they add their effects in the desired direction and cancel partly or wholly in other directions. The suppression of radiation in unwanted directions causes reinforcement of the energy in the wanted direction, and this increase in the intensity of the wave field is equivalent to increasing the effective radiated power in this direction. The increase in field due to directivity as compared with a nondirective antenna gives rise to the antenna characteristic known as "gain."

In reality there is no known type of antenna that is not directive in some way, although the "isotropic" antenna having equal radiated field strength in all directions (spherical radiation, like the radiation of light from an isolated point source of illumination) is taken as a theoretical standard of reference. Every kind of practical radio antenna is directional to some extent because of the doublet field distribution for a straight conductor and also because of interference between radiations from each infinitesimal element of its geometric configuration and interference between the waves radiated directly into space with those reflected from the earth and other objects against which the waves inevitably impinge. Therefore even antennas that are regarded as omnidirectional are so only in a certain sense—usually in the sense that the antenna is nondirective geographically in the earth plane.

The receiving antenna has the function of extracting the maximum power from a passing wave field and at the same time intercepting a minimum of other radiations inevitably present owing to unwanted signals from other stations that cause interference and to natural or man-made electrical noise. The most important factor at the radio receiver is the signal-to-noise ratio, in this case considering interfering signals from unwanted stations as a component of the total noise present. Radio communication is impractical when signal-to-noise ratios fall below certain values, the values depending upon the kind of communication, whether telegraph, telephone, facsimile, television, etc. (see Appendix VII). The minimum value of signal-to-noise ratio below which the transmission is impaired to the point of interrupting communication may be due to weak incoming signals or to high noise pickup. When the ambient noise pickup is very small, the limiting noise may be that due to thermal agitation in the antenna conductors and in the receiver input circuits.

The propagation of radio waves over a given path between transmitting antenna and receiving antenna is beyond human control; in this respect, radio communication differs from other forms of electrical communication where the propagation medium is specifically designed and built for the purpose. In each chapter of the book dealing with the three different classes of antenna design, a résumé is given of the characteristics of propagation, leading up to the antenna-design techniques best adapted to the special propagation conditions existing in the relevant portions of the radio spectrum.

In free space devoid of all substance, including air or gases, an electromagnetic wave is propagated without any dissipation of its energy. The inverse relationship between field strength and distance is due to the expansion of the wave in three dimensions and the distribution of radiant energy over a larger and larger volume of space, so that the power flow follows the inverse-squares law with respect to distance.

In a macroscopic sense, therefore, radio waves are spherical waves. However, in view of the relatively small portion of this spherical wave utilizable at a typical distant radio receiving position, the equiphase wavefront in this small region may be considered in a microscopic sense as a plane wave. The laws of reflection and refraction for plane waves are easily formulated and applied practically. A plane wave impinging upon the plane interface between empty space and some other medium of different permeability and permittivity splits the wave into two components, one reflected from the interface and the other refracted into the second medium, where it is propagated at different velocity and in a different direction. The exact nature of this phenomenon depends upon

the orientation of the electric vector of the wave with respect to the interface—whether parallel to it, normal to it, or oblique, with both parallel and normal components. It also depends upon the intrinsic impedance of the second medium, whether it is a perfect conductor, a perfect dielectric, or a complex (imperfect) dielectric having both inductivity and conductivity. The surface of the earth, which we often call simply "ground," is always a complex dielectric.

This fact complicates the quantitative details of wave reflection from the ground to such an extent that in ordinary engineering usage little attempt is made to deal with the effect quantitatively. For one reason, the empirical constants of the ground over the areas and the depths that are involved in any particular problem can be ascertained only approximately by the best available techniques. The most exact values, of course, are for water, where the measurement of a small sample can be made in the laboratory. Soil is not so homogeneous, and furthermore its constants can vary greatly with moisture gradients and with weather and also with frequency owing to the different depths of penetration of earth currents.

It is general practice to postulate antenna performance on an idealized basis, considering the antenna itself to be lossless and the ground to be perfectly conducting. With this as a standard, the compromises due to surrounding empirical effects which cause losses and modify the radiation pattern can be taken into account separately to the extent that the problem warrants. The empirical factors are omitted entirely in many ordinary engineering problems, with satisfactory practical results.

The empirical characteristics of the ground have an important effect on the technique of designing ground systems to collect ground currents in the most efficient way. One technique consists virtually in "metal plating" the ground so that the ground currents associated with the antenna flow almost wholly in buried wires, with very small current densities in the ground itself. The other basic technique is to use ground collector electrodes or capacitance areas in such a way that the current densities in the ground are as uniformly diffused as possible throughout the volume of ground in which there are appreciable currents associated with the antenna circuit.

In homogeneous imperfect dielectrics the attenuation of a plane electromagnetic wave[1001] is

$$\alpha = \omega \left[\frac{\mu_v \mu_r \epsilon_v \epsilon_r}{2} \left(\sqrt{1 + \frac{\sigma^2}{\epsilon_v^2 \epsilon_r^2 \omega^2}} - 1 \right) \right]^{\frac{1}{2}} \quad \text{nepers per meter}^{1001}$$

All units are in the meter-kilogram-second (mks) system.

When $\sigma^2/\epsilon_v^2\epsilon_r^2\omega^2 \gg 1$, conduction currents predominate over displacement currents and the equation for attenuation reduces to

$$\alpha = 1.987 \times 10^{-3} \sqrt{\mu_r f \sigma} \qquad \text{nepers per meter}^{1001}$$

Appendix II gives the so-called "skin depth" of ground currents (depth at which the wave attenuation is 1 neper or 8.686 . . . decibels) for this case. [For conversion from meter-kilogram-second (mks) to electromagnetic centimeter-gram-second (cgs) units, $\sigma_{mks} = 10^{11}\sigma_{cgs}$.]

When $\sigma^2/\epsilon_v^2\epsilon_r^2\omega^2 \ll 1$, displacement currents predominate over conduction currents and the equation for attenuation reduces to

$$\alpha = 188.3\sigma \sqrt{\frac{\mu_r}{\epsilon_r}} \qquad \text{nepers per meter}^{1001}$$

For geologic materials μ_r is 1, usually.

SYMBOLS FREQUENTLY USED IN TEXT

Symbols	*Meaning*
A	Area included in current-distribution plot, degree-amperes; also a symbol for special quantities
C	Capacitance in farads
c	Free-space wave velocity (3×10^8 meters per second)
D	Distance
d	Diameter; distance
E	Electric field strength, volts per meter
F	Field strength; a functional notation
f	Frequency; a functional notation
f_0	Fundamental frequency
G	Length of a conductor, electrical degrees
G_h	Length of a horizontal conductor, electrical degrees
G_v	Length of a vertical conductor, electrical degrees
G_0	Length of a vertical conductor, radians
h	Height above ground
I	Current, amperes
j	Operator $\equiv \sqrt{-1}$ = a 90-degree rotation counterclockwise
L	Inductance in henrys
l	Length (physical)
Q	Dissipation factor X/R; a standing-wave ratio I_{max}/I_{min}
R	Resistance, ohms
r	Radial distance
V	Potential, volts
v	Velocity of propagation, meters per second
W	Power, watts

Symbol	*Meaning*
X	Reactance, ohms
Z	Impedance, ohms
Z_0	Characteristic impedance, ohms
Z_m	Mutual impedance, ohms
α	Angle above the horizontal; also the attenuation factor in the propagation constant
β	Azimuth angle from some reference direction
ϵ	Inductivity or dielectric constant
θ	A colatitude angle in polar coordinates; also occasionally used as general designation for an angle
λ	Free-space wavelength in meters
λ_0	Fundamental wavelength in meters
ρ	Radius
σ	Conductivity
ϕ	Phase difference; a longitude angle in polar coordinates
ψ	Phase difference; a latitude angle
ω	Angular frequency $2\pi f$

CHAPTER 1

Low-frequency Antennas

1.1. Introduction

Practical radio communication began with the use of the low frequencies and for several years the trend was toward lower and lower frequencies. It was believed at that time, early in the twentieth century, that the range of a station was a matter of a certain number of wavelengths, so that the longer the wavelength the greater the range. This continued until the middle 1920's, when the possibilities of high-frequency communication became evident. For a time, high-frequency transmission captured the imagination of the radio-communication world, with the consequence that for many years low frequencies were believed to be discarded. For this reason low-frequency techniques almost became a lost art, even though the applications for low frequencies have been constantly growing throughout the world. If it were not for the relatively congested condition of the low-frequency spectrum, there would be more extensive uses for this band from 15 to 500 kilocycles.

An important factor in the ever-increasing importance of the lower radio frequencies is that of their comparative propagation stability. The variations that occur are small with respect to those usually encountered on high-frequency circuits. There are circumstances where this characteristic outweighs all the disadvantages of the lower frequencies, such as when reliability is the dominant objective. Reliability in this case includes not only propagation stability but also relative immunity to jamming. Another characteristic value is the deep penetration of ground currents (which are really waves propagated in the ground or in water), which makes it possible to communicate at considerable depths under the sea or under ground.

It is well known that the strength of atmospheric static increases as the frequency becomes lower. This kind of interference is a controlling factor in the effectiveness of low-frequency communication. While the strength of the transmitted wave remains relatively steady, the rise and fall of the noise levels during a typical day may cover a range of 20 decibels. Thunderstorms in the general area of the receiving station may increase this range to 80 or 100 decibels on occasion. The variations

for frequencies down to 100 kilocycles for the different noise zones for different hours of the day can be deduced from the curves reproduced as Appendix VII. These curves explain why the range of a low-frequency station is determined by ambient noise rather than by actual fading of the radio wave. These curves also indicate the very large differences in noise conditions between the various noise zones from grade 1 to grade 5. It is a fortunate fact that the world's auroral zones are regions of lowest atmospheric noise for low-frequency propagation, because these are also the regions of greatest instability for high-frequency propagation. This permits low frequencies to be easily substituted for high frequencies, and communication can take place with very moderate powers and with relatively inefficient antennas. This is one reason why the lower frequencies have exceptional importance in the high latitudes.

For many years the backbone of the North American airways navigation system was the four-course radio-range system using frequencies between 200 and 400 kilocycles. This basic system is being replaced by newer systems using the very high frequencies, but the older low-frequency system will remain for many years. In Europe this band has long been reserved for broadcasting. Marine communication makes extensive use of the low radio frequencies.

In presenting a chapter on low-frequency-antenna design it must not be thought by the general reader that this is a historical subject only. Low-frequency-antenna engineering is an active modern subject, and one where the sources of information are few and the problems difficult. The author has been impressed by this lack of specific information on low-frequency antennas even after so many years of engineering effort devoted to them, as well as enormous sums of money. The reason evidently is that the compromises that have to be made in design are so extreme that the designer has no particular pride in the result and says as little as possible about it in his technical reports to the profession. Almost all papers in technical journals about low-frequency antennas are strictly descriptive and lack the detailed discussions of how the designs were conceived and developed that one misses so much when searching for engineering guidance. This chapter will provide some useful information and explain something about the nature of the compromises that one must make in practice. Large low-frequency antenna systems involve large capital outlays, and one may pay dearly for ignorance of the practical importance of the several controlling design factors and the compromises the designer finally accepts.

1.2. Low-frequency-wave Propagation

Low-frequency radio waves are propagated by means of radiating structures which are, in terms of wavelength, electrically very close to

earth. Thus all propagation which can be utilized is in this region close to the interface between earth and air, where the ground plays a very important role in the propagation physics.

The field in the space above the earth is accompanied by a wave of ground currents in the earth or water (hereafter referred to as "ground"). The lower the frequency, the more negligible the displacement component of the ground currents with respect to the conduction component. Both conductivity and inductivity of the ground determine the depth of penetration of ground currents. The density of such ground currents decreases exponentially with depth below the surface when the soil is homogeneous. (See Appendix II.)

Losses in the ground cause attenuation of the wave field in space immediately above the surface of the earth, since energy from this field is dissipated continuously in the ground as the wave passes over it. This loss causes the electric vector to be tilted forward in the direction of propagation, producing a component of electric intensity parallel to the direction of propagation and another normal to it and to the surface.

The wave mechanics at the interface between air and ground are very complicated even under the simplest physical circumstances. The solution of Maxwell's equations in this region has long been in dispute, and serious work on the subject continues.

Nothing can be done about the electrical characteristics of the ground or the topography along the path between transmitting and receiving antennas. By choice, it is possible to locate the antennas in areas of the best available soil conductivity, thus to increase the terminal efficiency to some extent, and to increase this efficiency still further by proper design of the grounding system.

Optimum ground-wave propagation is obtained over salt water because of its conductivity (many times that of the best soils to be found on the land) and its uniform topography. Undulations in the topography of land cause losses in propagation greater than the loss produced by conductivity alone because the impingement of a wave against a tilted surface creates wave reflections that produce scattering of the energy in directions other than the original direction of propagation. The energy loss due to scattering is dependent upon the electrical height and the slope of the surface undulations. The greater the electrical heights of hills and mountains, the greater the loss due to scattering and the greater the wave attenuation. Behind mountains greater than approximately one-half wavelength high, there may appear genuine shadows, but unless other obstructions occur, this shadow will gradually be filled in as distance is increased, owing to diffraction.

In choosing a site for a station operating on a low frequency, therefore, these general facts must be taken into consideration by using the best

available land in terms of flatness, soil depth, and soil conductivity and by choosing the flattest available profile in the direction of dominant interest. Whenever possible, sites are located near the sea for overseas transmission or reception.

1.2.1. Ground-wave Propagation of Low Frequencies. Ground-wave transmissions in general require vertical polarization of the wave field; that is, the electric vector lies in the vertical plane through the direction of propagation.

Low-frequency antennas therefore are designed for vertical polarization, the useful radiations being derived from currents in the vertical portions of the antennas. Radiations from horizontal portions of antennas at low frequency are lost by cancellation of their image radiations. Currents in the conductors of a flat-top should be balanced with respect to the center where the down lead is taken off. For this reason, T antennas are preferable to inverted-L types* except for the case where multiple tuning is used.

The fact that, at low and very low frequencies, practical vertical heights are usually a very small portion of a wavelength is the cause for two important basic facts in low-frequency-antenna design: (1) the vertical-radiation pattern is always that due to a very short vertical radiator and follows the equation

$$f(\alpha) \propto \cos \alpha$$

where α is the angle above the horizon, and (2) the radiation resistance is always very low, often very much lower than any other resistances in the system. For that reason, the radiation efficiency, defined as the ratio of power radiated to total power input to the antenna system, is generally low.

The attenuation of a ground wave passing over a given path increases with frequency, as one may observe from the data of Table 1.1. This table lists the attenuation for a ground wave propagated over a smooth, spherical earth for sea water, soil of good conductivity, and soil of poor conductivity. Most soils encountered in practice will come between these "good" soil and "poor" soil limits. The specifications for these soils are given in the table.

Relatively low attenuation constitutes one of the advantages to the use of a low frequency from the propagation standpoint. But there are two opposing factors which penalize the low frequencies from a communication standpoint. One is the reduction in radiation efficiency which attends the use of lower and lower frequencies, due to the limited

* Many old textbooks tell us that an inverted-L antenna is directive in its horizontal pattern. The amount of such directivity is too small to consider.

electrical size of practicable antennas. This factor is equivalent to loss of as much as 10 to 12 decibels at the source for the lowest radio frequencies or for other frequencies where the radiation efficiency may be of the order of 6 per cent. The other factor is that relatively high noise

TABLE 1.1. GROUND-WAVE PROPAGATION—SMOOTH SPHERICAL EARTH

Distance, miles	Wave-path attenuation, decibels			
	50 kilocycles	100 kilocycles	200 kilocycles	400 kilocycles
Sea water ($\sigma = 4 \times 10^{-11}$ electromagnetic unit; $\epsilon = 80$)				
1	0	0	0	0
10	20	20	20	20
20	26	26	26	26
50	34	34	34	34
100	40	40	41	42
200	47	49	50	51
500	56	59	64	70
1000	62	66	86	98
Good soil ($\sigma = 2 \times 10^{-13}$ electromagnetic unit; $\epsilon = 30$)				
1	0	0	0	0
10	20	20	20	21
20	26	26	26	28
50	34	34	35	37
100	40	41	42	45
200	47	48	52	55
500	55	58	66	77
1000	63	68	89	111
Poor soil ($\sigma = 10^{-14}$ electromagnetic unit; $\epsilon = 4$)				
1	0	0	0	0
10	21	21	22	26
20	28	28	29	37
50	37	39	42	56
100	44	48	54	70
200	51	58	69	86
500	62	72	99	121
1000	70	85	135	160

levels generally prevail at these frequencies. While these noise levels vary considerably with time and geography, they seriously limit the range of transmission by requiring relatively high field strengths for practical working signal-to-noise ratios. The only way of overcoming

this range limitation is by employing high-power transmitters. Furthermore, it is not feasible to obtain appreciable power gains by using directive antennas as is so easily done at much higher frequencies. Some advantage of directivity can be realized at the receiving location by employing loop or, preferably, wave antennas.

1.2.2. Sky-wave Propagation at the Low Frequencies. If low-frequency-wave propagation was entirely by means of the ground wave, there would be negligible variations in received signal strengths. Actually there is some propagation by atmospheric paths above the earth with reflection or refraction of these sky waves back to earth. During the daylight hours, the lower radio frequencies seem to experience reflection from the D layer, an ionized stratum of atmosphere below the E layer. Like the latter, the D layer disappears during the hours of darkness, but this does not eliminate all signal-strength variations that are attributed to sky-wave propagation. Any such sky waves interfere with the dominant ground wave and produce the variations observed on long circuits, even at the lowest radio frequencies in use. However, the magnitude of these variations is relatively small with respect to those experienced at the higher frequencies.

1.3. Low-frequency Antennas

Low-frequency antennas are characterized generally as being electrically short. This means that they operate at frequencies that are low with respect to the fundamental frequency of the antenna system. This is because realizable structures are small in proportion to the radiated wavelength. One of the design objectives is to have an antenna of a given mechanical size appear electrically as long as possible within the economic limitations of good investment.

The means one may adopt to achieve this end depend very much upon the specifications for the communication system, of which the antenna is one element. If communication over long distances in the presence of high electrical noise is the objective, very high power may be necessary. The need for high power brings with it the need for special design techniques for the naturally large antenna currents and antenna potentials that result. The bandwidth required, depending on the type of emission used, may also be a determining factor in the design of an antenna. In another case, the range of transmission may be simply that which is possible within a specified capital cost.

Of course, the operating frequency itself is a dominant factor. The band embracing the so-called "low" and "very low" frequencies is from 300 kilocycles down to the lowest that have been used, something of the

order of 12 kilocycles. For the purposes of the present book, we shall regard low frequencies as those below about 500 kilocycles, for the reason that the same basic techniques are usually employed for antennas within this range. Cognizance is taken of certain opportunities to apply the special techniques which have been developed for the medium-frequency broadcast band for frequencies below 500 kilocycles, where steel masts and towers are used as radiators instead of systems of wires. However, aerial wire systems constitute the majority of antennas for the low frequencies.

The design of antennas for frequencies below about 30 kilocycles is a very specialized field of engineering, and problems within this range arise very infrequently in general practice. Except for casual mention of certain details as they arise in connection with our general subject, we are omitting reference to this very low range.

Radiation engineering, in the sense of controlling the radiation pattern of the system in special ways for special purposes, is virtually absent from low-frequency-antenna engineering. To a limited degree, radiation control is applied to low-frequency navigational aids such as the four-course radio-range systems (see Sec. 1.13.3). In general, however, low-frequency-antenna engineering is principally a problem in circuits and how to obtain maximum efficiency from an electrically short antenna.

1.3.1. Vertical-antenna Current Distribution. The principles of the electrically short antenna are better understood from Fig. 1.1, in which the natural sinusoidal current distribution along a straight uniform-section quarter-wavelength vertical antenna is used for reference. A straight uniform vertical antenna with a height of 20 degrees would have the relative current distribution shown for the sine curve above the 20-degree level *A*. In the same way, one with a height of 30 degrees would have the relative distribution above the level *B*. An antenna with a vertical height of 10 degrees, but with top loading sufficient to give it a total electrical length of 30 degrees, would have the current distribution shown between *A* and *B*, and the top loading would be equivalent to an additional 20 degrees of vertical

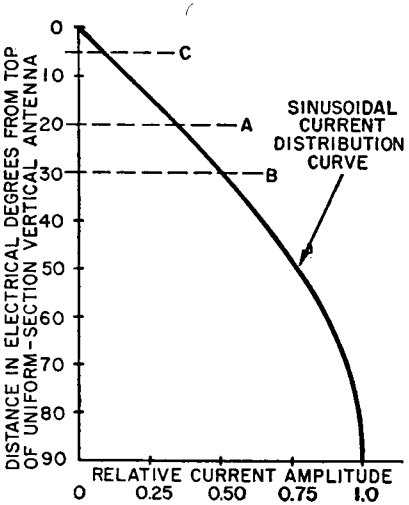

FIG. 1.1. Relative current distributions on electrically short vertical radiators.

antenna so far as the shaping of the current distribution on the vertical portion is concerned.

A vertical 5-degree antenna, with a relative current distribution like that shown above the level C, is a comparatively ineffective radiator because of its very small exposure to space and consequent small resistance due to radiation.

In low-frequency-antenna design there is no optimum design. One can "squeeze" here and there to get a little more performance. The designer must decide where to stop. This decision may be the most important of all, since the performance-cost relations run into the law of diminishing returns. No one can specify in a general way how far one should go in this direction. The tendency is to go too far into diminishing returns as a part of the squeezing process.

It is helpful at this point to think of the results in decibels, since any improvement having appreciable cost should yield not less than 1 decibel of increase in radiation. If one can afford to be exhaustive in his preliminary engineering, which means that engineering cost is not a factor, detailed cost estimates can be obtained for a succession of design variations in the approach to an optimum investment.

1.4. Fundamental Frequency of a Straight, Uniform Vertical Radiator

The fundamental frequency f_0 of a vertical radiator is the lowest frequency for which the reactance is zero at the feed point between the lower end of the radiator and ground. At this frequency, the electrical length of the antenna is 90 degrees, or one-quarter wavelength.

In practice, an antenna that is a quarter wavelength *electrically* is somewhat shorter than a quarter wave long *physically*. The difference is due to *end effect*, which results from the finite ratio of antenna length to antenna diameter. Table 1.2 shows the effect of height (length)-to-diameter ratio h/d on physical length G for a cylindrical vertical radiator for the condition of zero reactance with no artificial end loading.

TABLE 1.2

h/d	G
10	81.5
20	81.5
40	82.5
100	84.2
200	85.0
400	85.7
1,000	86.4
2,000	87.1
4,000	87.4

From this table, the fundamental frequency of a vertical radiator can be determined from its geometry. For example, a cylindrical conductor with $h/d = 200$ has a physical height of 85 degrees. Its fundamental wavelength is $\lambda_0 = 360h/85.0$, and its fundamental frequency is

$$f_0 = 3 \times 10^8/\lambda_0$$

For an *idealized* uniform vertical antenna *without end effect*, the fundamental wavelength in meters is

$$\lambda_0 = 4h_{\text{meters}} = 1.22h_{\text{feet}}$$

These relations are useful in deriving a simple equivalent vertical antenna that has the same fundamental frequency as an antenna of any arbitrary configuration. The current distribution along the vertical portion can thus be determined and from that the radiation resistance, and eventually the field strength per ampere at a unit distance can be calculated.

1.5. Radiation Efficiency

Low-frequency antennas characteristically have low radiation resistance and relatively high capacitive reactance. The most practical form of power feed employs series resonance in the antenna circuit, using an inductance to neutralize the antenna reactance. The design of this tuning inductance is an important part of the design of an antenna system. Because of the high currents that flow through the inductance, its resistance becomes a prominent, if not dominant, component of the resistance of the system. Therefore, the tuning inductance becomes a limiting factor in ultimate efficiency of the transmitting plant.

In the absence of more precise information, one may assume that a well-designed low-frequency antenna and ground system will have a radiation efficiency of roughly 75 per cent of the equivalent electrical length in degrees of the antenna system at the working frequency. In other words, an antenna system having a vertical height of 11 degrees, with top loading that makes it equivalent to 25 electrical degrees, should have a radiation efficiency of the order of 18 per cent, excluding tuning-coil losses. While this estimate is necessarily a rough one, it will serve as a reasonable starting point for computations.

The best guide for initial assumptions is information on systems that have already been built and measured. Such direct information can then be applied to a new problem by similitude. Some reference information of this nature is included later.

The antenna-design problem will always assume one of three basic forms: the limitations on the ultimate design to be those of a reasonable investment; or a maximum height (where physical height is limited by

conditions other than cost); or a fixed amount of money available. The design considerations are weighed differently for each of these three forms. Height is the most costly dimension for an antenna system, and so the determination of height is one of the most important considerations in any given problem. It is also the most important choice with respect to maximum realizable radiation efficiency, since radiation resistance is in general proportional to the square of the height.

Since the radiation pattern is not under control in low-frequency-antenna design, the radiation efficiency is purely a circuit problem. The object is to obtain the highest ratio of radiation resistance to total antenna-circuit resistance.

The total antenna resistance is the sum of five separate components:

Radiation resistance R_r

Ground-terminal resistance R_g

Resistance of tuning inductance R_c

Resistance equivalent of insulation loss R_i

Resistance equivalent of conductor loss R_w

The radiation efficiency of an antenna is therefore

$$\eta = \frac{R_r}{R_r + R_g + R_c + R_i + R_w}$$

Ground resistance often is larger than the radiation resistance even when large investments are made in the ground system. The tuning-coil resistance may be relatively large, even after careful engineering design, because of the large reactance usually necessary and because of practical limitations in minimizing the dissipation factor Q. The characteristically high operating potentials on the antenna, owing to its small resistance and high reactance, cause insulator-loss equivalent resistance to become appreciable and sometimes of great importance in relation to the radiation resistance. The conductor resistance can also become appreciable in systems where mechanical considerations dictate the use of high-strength alloy materials having effective resistivities two to three times greater than copper. Also, the great lengths of wire required for low-frequency antennas add to conductor-loss equivalent resistance.

The absolute values of ground, insulation, and conductor resistance are unattainable by direct measurement and must in any event be estimated from final system-resistance measurements. In the design stage, unfortunately, no significant estimates can be made because of the great range of values encountered within the scope of low-frequency design. From a knowledge of the current distribution in the antenna, the conductor resistance referred to the feed point can be computed by making a summation of I^2R losses over the complete system.

1.6. Radiation Resistance

The radiation resistance is essentially due to the distribution of current on the vertical portions of the antenna. Typically the current in all vertical parts is in phase but varies in amplitude with distance along the vertical, with the maximum value at the base, near ground. If the vertical part has a uniform cross section throughout its length, the current distribution will be some portion of a sine wave. If the antenna consists solely of a vertical part, with no top loading, the current at the top will be zero and the distribution will be sinusoidal as measured from the top. Since a sine wave is practically linear from zero to 30 degrees, a uniform vertical radiator of height 30 degrees or less will have a linear current distribution. Thus current distribution plotted against electrical height forms a right triangle as shown in Fig. 1.1.

When there is capacitive top loading attached to such a vertical antenna, its electrical length is effectively increased. The current I_t at the top of the vertical is no longer zero but has a value that is proportional to the capacitance of the top loading. In almost every practical case it is less than the base current I_b. With top loading, the plot of relative current against position along the vertical now becomes a right-angled trapezoid, which as a practical limit may ultimately approach a rectangle. This is realizable only with an electrically short vertical section having a very large amount of top loading.

The radiation resistance of an antenna less than an electrical quarter wavelength long is increased by top loading and by increasing height. A straight vertical radiator of height 30 degrees or less has a radiation resistance R_r following the equation

$$R_r = 10G_0^2$$

where G_0 is the electrical height *in radians*. (One radian is 57.3 degrees.)

Referring again to the geometric form of current distribution with height (Fig. 1.1), this relation holds for the triangular distribution. If the base current I_b is always taken as 1.0 for comparative purposes, we can say that radiation resistance varies as the square of the area of the degree-ampere plot. We can transform this relation into a very useful form that shows the radiation resistance as a function of the degree-ampere area A of the plot of current distribution. This is

$$R_r = 0.01215A^2$$

The utility of this relation is that it holds for any shape of inphase current distribution. It permits direct computation of the radiation resistance from a known current distribution for an electrically short

antenna. A top-loaded antenna having a trapezoidal current distribution has a degree-ampere area

$$A = \frac{G_v}{2}\left(\frac{I_t}{I_b} + 1\right)$$

where G_v is in degrees of vertical height and I_t and I_b the currents at the top and at the base of the vertical, respectively.

These relations can be used for any arbitrary system where the current distribution in degree-amperes is known, the value of A can be computed, and the base current is taken as unity.

A chart of the values of radiation resistance as a function of physical height G_v in electrical degrees and the ratio I_t/I_b is shown in Fig. 1.2 over the domain where the vertical current distributions are linear.

1.6.1. Relation between Degree-amperes and Field Strength. When the actual value of degree-amperes on the vertical part of the antenna with a given power input to the system and the base current is all known, the unattenuated field strength at a unit distance can be computed directly. There is a linear relationship between actual degree-amperes A_0 and field strength as expressed by

$$F = kA_0$$

When F is the field strength in millivolts per meter at 1 mile, $k = 0.650$, and when F is given in volts per meter at 1 kilometer, $k = 0.00104$.

First Example. An example of the application of these relations is the solution of the following problem: A radiophare (or omnidirectional beacon) antenna for operation with low power on 200 kilocycles is desired. We can expect a total antenna resistance of the order of 3.5 ohms (judging from experience), and we want a radiation efficiency of about 15 per cent. The radiation resistance of the antenna system therefore should be 0.53 ohm. By examination of Fig. 1.2 it is found that this resistance can be obtained by any of the realizable structures listed in Table 1.3.

TABLE 1.3

Electrical (vertical) height, degrees	Actual height, feet	I_t/I_b
13	180	0
12	164	0.1
11	150	0.2
10	137	0.3
9.4	128	0.4
8.7	118	0.5
8.2	111	0.6
7.7	104	0.7

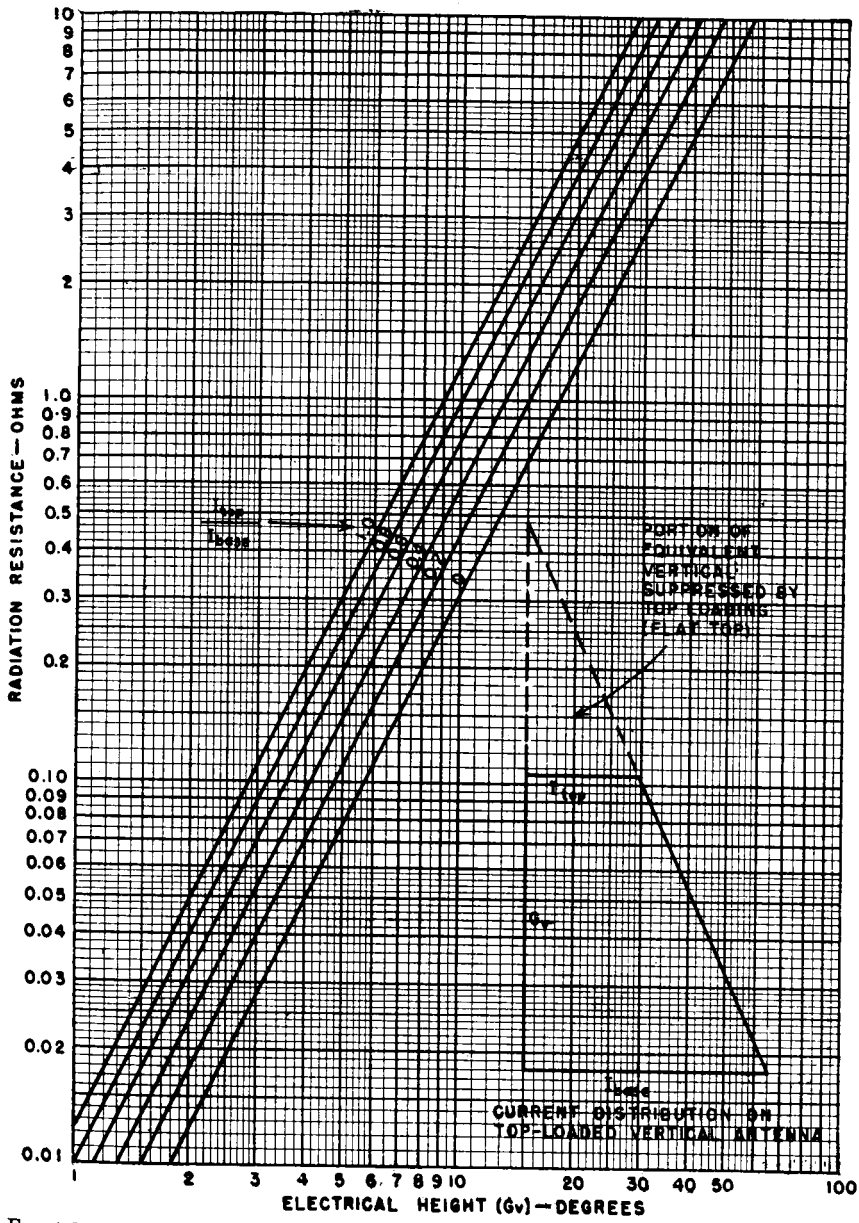

FIG. 1.2. Radiation resistance for electrically short antennas versus height of vertical portion (degrees) and ratio of currents at top and base of vertical portion.

We therefore have to choose between one vertical radiator of 180 feet or two or more towers higher than 100 feet to support some form of top-loaded wire antenna. If the radiophare is near an airport, there may be objections to the 180-foot radiator as an obstruction. The 104-foot height takes a large amount of top loading to attain a ratio of 0.7 between currents at the top and base of the antenna. This creates additional mechanical loads, and more than two supports may be required.

Let us assume that we choose the 104-foot height in order to avoid the cost and complications of remotely controlling the transmitter. It is now desired to know what the fundamental frequency of the antenna must be.

Graphically, this is quickly solved by a diagram of height plotted against relative antenna current distribution. If we let 1.0 be the base current and 0.7 the current at 104 feet, a straight line drawn through these points and extended upward until it intersects with $I_t/I_b = 0$ will give the height of the equivalent vertical radiator with the same fundamental frequency. This height is found to be about 347 feet (25 degrees at 200 kilocycles). To get the required current taper on the 104-foot antenna the flat-top must simulate the capacitance of the upper 243 feet (17.3 degrees) of this equivalent vertical radiator.

A vertical radiator with a length of 25 degrees at 200 kilocycles would, by direct proportion, be 90 degrees at a frequency

$$f = {}^{90}\!/_{25} \times 200 = 719 \text{ kilocycles}$$

The antenna under study must therefore be built to have a fundamental frequency of about 719 kilocycles for a vertical height of 104 feet.

If the power input to the system is to be 250 watts, the antenna current will be 8.47 amperes if the system resistance is 3.5 ohms. The vertical section of the antenna will then have a degree-ampere area of

$$A_0 = \frac{7.7(0.70 + 1) \times 8.47}{2} = 55.5 \text{ degree-amperes}$$

The unattenuated field strength at 1 mile is

$$F = 0.650 \times 55.5 = 36.8 \text{ millivolts per meter}$$

Second Example. As another example, let us compute the radiation resistance, radiation efficiency, and field strength of an antenna that has been constructed and has the following measured values at an operating frequency of 50 kilocycles:

Fundamental frequency 176 kilocycles

Physical height of vertical portion 450 feet

Electrical height of vertical portion 8 degrees at 50 kilocycles
Electrical length of entire antenna 25.5 degrees at 50 kilocycles
Measured resistance at 50 kilocycles 2.8 ohms

The current distribution on the vertical portion is computed from the fundamental frequency of 176 kilocycles. A straight vertical antenna for this frequency would be approximately

$$h = \frac{3 \times 10^8}{1.22f} = 1{,}398 \text{ feet}$$

and this equivalent system also has an electrical length of 25.5 degrees at 50 kilocycles. Its current distribution would therefore correspond to 25.5 degrees of a sine wave as measured from the top end. The lower 8 degrees of this equivalent portion would correspond exactly to the vertical portion of the actual antenna under study. The top loading of the antenna is equivalent to the upper 945 feet (17.5 degrees) of the equivalent straight vertical antenna.

The ratio of top current to base current is

$$\frac{I_t}{I_b} = \frac{\sin 17.5}{\sin 25.5} = \frac{0.300}{0.430} = 0.70$$

Now, referring to Fig. 1.2, we read (for a vertical height of 8 degrees and an I_t/I_b ratio of 0.7) a radiation resistance of 0.56 ohm. The radiation efficiency is therefore

$$\eta = \frac{0.56}{2.8} = 0.20$$

With 100 kilowatts input, the antenna current would be 190 amperes. The degree-ampere area A_0 is 1,290, which produces an unattenuated field strength of 1.34 volts per meter at 1 kilometer.

1.7. Characteristic Impedance of a Vertical Antenna

The usual concept of the characteristic impedance of a transmission line is quite rigorously defined in terms of uniformly distributed fundamental constants of L, C, R, and G. At high frequencies, this becomes

$$Z_0 = \sqrt{\frac{L}{C}} \equiv \frac{1}{vC}$$

where v is the propagation velocity.

A vertical antenna is not a transmission line in the purest sense because its constants vary with distance from ground and the time of propagation of the fields from real and image charges is not small with respect to one period of the emitted wave. From a practical standpoint, however, these deviations from theoretical ideals are of small consequence. The

concept of the characteristic impedance of an electrically long wire, vertical or otherwise, is of great practical convenience because it permits us to refer circuit conditions in an antenna to those so well known for transmission lines. To use the characteristic impedance quantitatively, however, we must be content with approximate values. The error, in most cases, is fortunately within that of the many other empirical factors with which one must deal in engineering.

The characteristic impedance of a vertical antenna of any cross section can be calculated with suitable accuracy by considering a sample 1-meter unit of length at a height h above ground and the corresponding portion of its image. The characteristic impedance can then be obtained from electrostatics, using the theory of logarithmic potentials. A short discussion of this useful theory is given in Chap. 6. For a vertical antenna (a down lead or any vertical radiating portion of an antenna, whose diameter is small with respect to its length) a compromise value of Z_0 for the entire vertical part can be calculated at the mid-height. The capacitance per meter C for the cross section used is computed from logarithmic-potential theory and the characteristic impedance calculated directly from the equation

$$Z_0 = \frac{1}{3 \times 10^8 C} \quad \text{ohms}$$

A vertical antenna with capacitive end loading in the form of a flat-top of any configuration can then be treated as a capacitively terminated transmission line of length G_v degrees and characteristic impedance Z_0 (where G_v is the physical length of the vertical portion of the antenna in electrical degrees). The flat-top in turn can be treated as a transmission line or as several lines in parallel, and its approximate reactance can be calculated at the point of connection with the vertical, using Eq. (8), Chap. 4. These general facts can be used to calculate the fundamental frequency and the reactance of low-frequency antennas.

The characteristic impedance of a horizontal wire or system of parallel wires can also be computed from logarithmic-potential theory within satisfactory limits of accuracy in certain simple cases. For example, the characteristic impedance of the horizontal portion of an inverted-L or a T antenna can be found by using the principles of electrostatics and the same equations one would use for transmission lines. The method is limited to single wires or to systems of parallel wires well removed from the fields of other parts of the antenna system. In the following section the application of such methods will be demonstrated.

For suitable characteristic impedance formulas, consult Cases I, II, and III, Chap. 4, as examples.

1.8. Antenna Reactance

The impedance of a low-frequency antenna at the operating frequency must be known to determine the power input and the antenna potential. The resistance portion of the impedance has been discussed separately. Prior to actual construction and measurement (or lacking measurements on other similar systems), the total resistance can only be estimated. From this the order of the antenna current for a given power input can be deduced. The antenna potential can then be found approximately if the reactance is known. The size of the tuning inductance must also be determined by the antenna reactance.

Low-frequency antennas encounter very high potentials normally. The power input to an antenna is limited by potential due to corona, pluming, and flashover from the conductors as well as the insulators. The cost of insulation may be a large portion of total antenna cost, and great care is required in the design of medium- and high-power-antenna systems to reduce antenna potential and to design properly the insulation and the conductors. Reducing antenna reactance also reduces tuning-coil losses by decreasing the amount of reactance required for tuning.

Antenna potential is reduced by minimizing antenna reactance at the working frequency. This in turn is accomplished by minimizing the characteristic impedance of the antenna system and by top loading it with as much capacitance as can be afforded. Once the antenna potential gradients are under the limiting values which produce corona and pluming, the designer must carefully avoid excess costs which arise from a large and heavy aerial requiring several heavy-duty supporting structures. Once the potential gradients are reduced below a certain critical value for the maximum anticipated power input, insulation is cheaper than steel and copper.

Applying the transmission-line analogy, the reactance of an open-circuited line of characteristic impedance Z_0 and electrical length G is

$$X = -jZ_0 \cot G$$

With capacitive top loading of a vertical radiator of electrical height G_v and characteristic impedance Z_0 with a flat-top of reactance X_1 at a frequency f_1, the reactance at the feed point would be

$$X_a = Z_0 \frac{X_1 \cos G_v + jZ_0 \sin G_v}{Z_0 \cos G_v + jX_1 \sin G_v}$$

Both X_1 and G_v are functions of frequency, so that a computation of X_a can be made over a frequency band. At the fundamental frequency of the antenna, $X_a = 0$, under which condition the numerator in this equation must be equal to zero.

1.8.1. Practical Flat-top Design. In low-frequency applications, G_v is always less than 90 degrees so that X_a is always capacitive. The value of G_v is determined by the size of the antenna and has a dominant influence on its cost. The value of Z_0 and X_1 must therefore be minimized once the limits of G_v are determined economically and structurally.

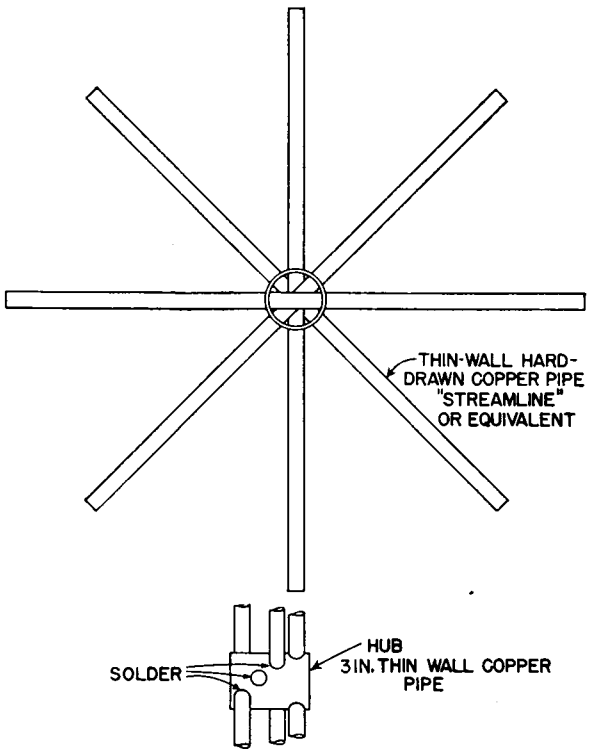

FIG. 1.3. Strong lightweight inexpensive cage spreader (four to eight spokes).

Recognizing that $Z_0 = 1/vC$, we must seek means for increasing C per unit length. This is done by increasing the cross section of the antenna. Increasing the diameter of the conductors increases the weight faster than it reduces Z_0 (assuming solid conductors), and so one resorts to several conductors in parallel. To get the maximum benefit from the conductors, they should be arranged to carry equal currents. This requires that they be arranged in a conical or a cylindrical cage. In a flat configuration, the currents concentrate in the outer wires and depreciate the contributions of the inner wires to the desired result unless they have very large electrical spacing. A useful design for a cage spreader is shown in Fig. 1.3.

A cage of four wires in a square cross section is a desirable one from both mechanical and electrical standpoints for ordinary antennas. Its construction is relatively simple, the mechanical stresses are easily equalized among the wires, it has moderate wind resistance, and it gives the maximum increase in capacitance per unit length for practical spacings for the amount of copper required.

For a square cage of four wires located a height h above ground, with wires of radius ρ spaced a distance a, the capacitance in farads per meter is

$$C_4 = \frac{1}{34.5v \log_{10} \dfrac{16h^4}{\rho a^3 \sqrt{2}}}$$

A single wire of the same radius at the same height has a capacitance of

$$C_1 = \frac{1}{138v \log_{10} \dfrac{2h}{\rho}}$$

The ratio of the capacitance of the cage to that of the single wire is therefore

$$\frac{C_4}{C_1} = \frac{4 \log_{10} \dfrac{2h}{\rho}}{\log_{10} \dfrac{16h^4}{\rho a^3 \sqrt{2}}}$$

Figure 1.4*A* is a curve of this ratio for a particular case for a given height and wire size as a function of a. Figure 1.4*B* shows curves of the capacitance ratios for a particular height and wire size for cylindrical cages of various numbers of uniformly spaced wires and cage diameters.

For *two* wires in parallel, spaced a distance a,

$$\frac{C_2}{C_1} = \frac{2 \log_{10} \dfrac{2h}{\rho}}{\log_{10} \dfrac{4h^2}{\rho a}}$$

For a *six-wire* cage, the capacitance ratio is

$$\frac{C_6}{C_1} = \frac{6 \log_{10} \dfrac{2h}{\rho}}{\log_{10} \dfrac{10.67h^6}{\rho a^5}}$$

If one wishes to use four wires spaced a uniform distance a in a flat plane, the ratio of capacitance to that of a single wire can be obtained with the

following equations, which include the solution for k, the ratio of charges on the two inner wires to those on the two outer wires:

$$\frac{C_{1v}}{C_1} = \frac{2(1+k)\log_{10}\dfrac{2h}{\rho}}{\log_{10}\dfrac{4h^2}{3a\rho} + k\log_{10}\dfrac{2h^2}{a^2}} \qquad k = \frac{\log_{10}\dfrac{2a}{3\rho}}{\log_{10}\dfrac{2a}{\rho}}$$

To test the practical application of these principles, we can analyze an antenna of known characteristics to see how closely the computed values compare with the measured values.

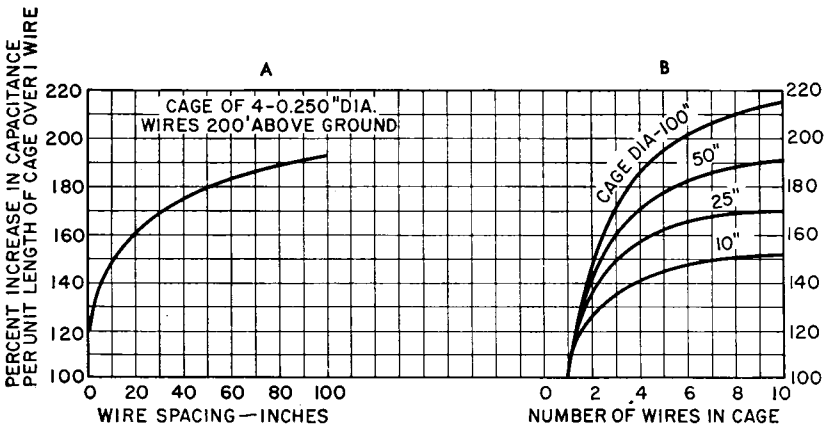

FIG. 1.4. Capacitance ratio per unit length of cylindrical cages versus single wire when $h = 200$ feet and $\rho = 0.125$ inch.

Identical Antennas at Different Locations. Consider the antenna shown in Fig. 1.5. Let us try to verify the reactance values at 100 kilocycles as measured at the three different locations. At the outset we recognize some important empirical factors not amenable to quantitative prediction, for instance, the end effect as the cages of the flat-top converge to a point, the capacitance of the insulators at the point of convergence, and the stray capacitance to the grounded supporting towers and to the supporting cables. At 100 kilocycles the vertical height is 9 degrees, and each arm of the flat-top will be 9 degrees plus an estimated additional 0.5 degree (5 per cent) to account for all spurious end effects. Thus we consider each arm of the T (G_h) as 9.5 degrees. The entire system is a four-wire square cage of 0.129-inch-radius wires spaced 48 inches from each other. The average height of the flat-top is about 270 feet, or 3,240 inches. The capacitance per meter of the flat-top is then calculated.

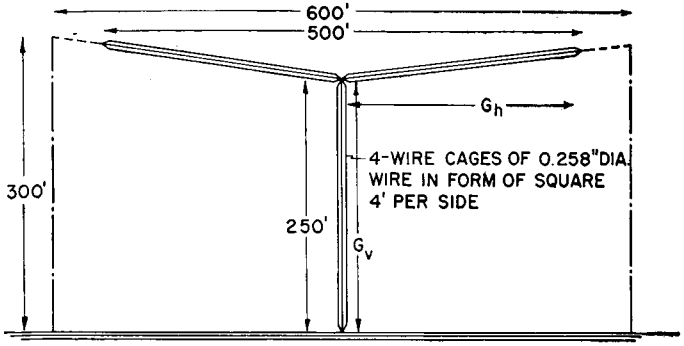

GROUND SYSTEM: 120-500' BURIED RADIALS AND 1-4'x4' COPPER PLATE BURIED ON EDGE UNDER CENTER OF RADIAL SYSTEM.
MEASUREMENTS OF 3 IDENTICAL ANTENNAS AT DIFFERENT LOCATIONS

	STATION #1		STATION #2		STATION #3	
f-kc	X	R	X	R	X	R
50	-j1315Ω	—				
60	1130	—				
70	975	—				
80	848	—				
90	745	—				
100	655	2.5Ω	-j625	2.25Ω	-j640Ω	1.3Ω
150	375	3.1	425	3.0	400	3.0
200	222	5.0	267	4.1	250	5.3
250	130	7.4	148	5.8	158	8.0
300	65	10.5	67	8.3	83	11.3
350	25	14.0	11	11.6	16	15.3
400	+j15	18.3	+j45	16.0	+j40	20.1
450	70	23.8	108	21.4	95	25.5
500	120	32.5	165	27.6	152	31.3
f	0	390kc	0	360kc	0	363kc

FIG. 1.5. Cage T antenna characteristics.

$$C \doteq \frac{1}{34.5 \times 3 \times 10^8 \times \log_{10} \dfrac{16(3{,}240)^2}{0.129 \times 48^3 \times 1.414}} \text{ farads per meter}$$

$Z_0 = \dfrac{1}{vC} = 343$ ohms = characteristic impedance of flat-top cage

$G_h = 9.5°$ (electrical length of one arm). cot $9.5° = 5.976$

X_h = reactance of one horizontal arm of T at junction

$= -j(343 \times 5.976) = -j2{,}050$ ohms

With the two arms in parallel, the total terminal reactance of the flat-top is approximately

$$\frac{X_h}{2} = -j1{,}025 \text{ ohms}$$

The characteristic impedance of the vertical cage, which we shall take

at the mid-point (h = 1,500 inches) is of the order of

$$Z_0 \doteq 34.5 \log_{10} \frac{16 \times 1{,}500^4}{0.129 \times 1.414 \times 11 \times 10^5} = 297 \text{ ohms}$$

The input reactance at 100 kilocycles is computed to be, using Eq. (8), Chap. 4,

$$X_a = 297 \frac{(-j1{,}025) \cos 9 + j297 \sin 9}{297 \cos 9 + j(-j1{,}025) \sin 9} = -j635 \text{ ohms}$$

This compares with 625 ohms, 640 ohms, and 655 ohms measured values at the three stations. Apparently the end effect was correctly estimated. The reader may wish to compute the reactance of a single-wire antenna of the same dimensions.

1.8.2. Reducing Potential Gradients. Potential gradients may be reduced by increasing conductor diameter or by using several conductors in parallel so that the charge per unit length on each conductor is reduced. Sharp edges and points on metallic hardware are smoothed to reduce localized gradients. The over-all capacitance loading is made as large as economically feasible so that, for a given power input, the potential is made as small as possible by decreasing the antenna reactance X_a. In high-power low-frequency systems the amount of top loading and the final design of the aerial system are determined by the potential considerations rather than merely radiation resistance. Fortunately, the design factors that minimize the potential on the antenna are also those which increase the bandwidth capabilities and increase radiation efficiency.

1.8.3. Aerial Insulators. The aerial insulators should have high electrical and mechanical strength. They are of two basic types for strain duty—special cylindrical porcelain tubular insulators with cemented end fittings, and the oil-filled safety-core type.

Porcelain tubular strain insulators have been made for radio applications in sizes up to 6 feet long and 6 inches outside diameter, with an ultimate mechanical strength of 35,000 pounds and a steady working load of about 12,000 pounds. Where greater working loads are encountered, two, three, and four such tubular insulators have been used in parallel, with yokes that equalize the load on the individual insulators. Safety-core-type insulators, as made by A. O. Austin, have rated mechanical loads as high as 1,000,000 pounds.

Tubular porcelain insulators have small impact resistance, and an insulator capable of supporting a steady tension load of 6 tons may break when accidentally struck with a wrench or other tool. They must be handled with great care to avoid accidental breakage.

The strength of tubular insulators is often limited by the strength of

the cemented end fittings, which may be of malleable iron, bronze, or aluminum. Thermal stress on the porcelain may at times be the cause of failure in service due to unequal expansion of the porcelain and the metal. Sometimes the casting will split or the porcelain be crushed. The kind of cement used for attaching the end fitting to the insulator can also be a cause of failure due to weathering and expansion of the cement.

There is appreciable leakage loss on plain tubes, and when they are used in multiple, this loss is increased. Losses are often further increased by cross discharge between the insulators when moisture and drip-water

FIG. 1.6. Oil-filled safety-core strain insulator, rated at 150 kilovolts. (*Photograph courtesy of Royal Canadian Navy.*)

distribution is irregular. For this reason it is best to use a minimum number of units, preferably only one, provided that the unit can sustain the requisite mechanical duty. Leakage loss can be reduced by using grading rings or rain shields, but these reduce the pluming potential, which is then limited by the shields. In the presence of drip water, a uniformly distributed roughness in the form of a wire mesh or expanded metal is more effective than a smooth metallic shield in preventing pluming.

The oil-filled safety-core insulator of modern design is available with very high electrical and mechanical ratings and high reliability. Figure 1.6 is a photograph of one form of strain insulator of this type, rated at 150 kilovolts working potential when wet and a working load of 60,000 pounds. Other safety-core insulators appear in Figs. 1.38, 1.41, and 1.43.

1.8.4. Scale-model Measurements. The search for the simplest and most economical antenna configuration that will give a desired value of radiation resistance with top loading is complicated by many factors.

Computations are practical only for rather simple systems, such as for inverted-L, T, and X configurations. For large, complicated capacitance areas made up of many wires of different lengths and orientations it is easier to make and measure small-scale models than to attempt to compute the values.

Antenna scale models make use of the fact that there is a fixed relationship in systems of identical electrical dimensions. An accurate scale model one-fiftieth the size of the original will have the same electrical dimensions when operated at fifty times the frequency. Scales as small as one one-thousandth have been successfully used for low-frequency design engineering.

The technique is to lay out a large metallic surface, very large with respect to the area of the proposed model, to serve as a ground plane. Towers, guys, antenna rigging, and placement of insulators are modeled carefully, including the relative cross section of the wires, sags, etc. Usually the only measurements necessary from a model are the fundamental frequency and the reactances in the region of the scaled operating frequency. The fundamental frequency can be measured by using shielded coupled buzzer excitation with a calibrated receiver as a frequency meter. The reactances can be measured with a Q meter, taking necessary precautions with body effect of the operator in some cases. With small expense and very little expenditure of time, a good model will yield the desired information and permit studies of such things as insulated versus grounded towers, placement of guy insulators, and alternative wire configurations. All the data needed to compute the performance of a full-scale system can be obtained except those factors associated with the ground system. The characteristics of ground systems and flow of ground currents in imperfect dielectrics do not follow the same principle of similitude as do fundamental frequency, reactance, and radiation resistance.

The value of scale-model measurements in low-frequency-antenna design cannot be overemphasized, both for economy of engineering time and for precise forecasting of performance. By this technique it is possible to obtain a great deal of empirical information that cannot be reliably calculated. System costs can be minimized by experimentally developing the most conservative structure for a given performance.

1.9. Transmission Bandwidth of a Low-frequency Antenna

Antenna selectivity is usually the limiting selectivity factor in a low-frequency transmission system. Transmitter, receiver, and other selective circuits associated with the system should be examined, however, in all applications where special attention to bandwidth is required. Selec-

tivity limits transmission speed and contributes to telegraph distortion because, by filtering the side frequencies inherent in the modulated signal and shifting their relative phases, the signal loses definition. In the case of telegraphic on-off keying (an example of 100 per cent amplitude modulation with a square wave) a long series of symmetrical side frequencies, all in correct phase and amplitude relationships, is necessary for distortionless transmission. As the dot length is decreased and the dot frequency increased, the spectrum of the symmetrical side frequencies must be greater. If the spectrum width exceeds the bandwidth of the system, the higher side frequencies are lost or so modified in phase and amplitude that the carrier envelope is seriously distorted. Beyond a certain point, it may be impossible to regenerate the signal envelope at the receiver.

In the case of teleprinter operation, there are strict limits on telegraph distortion for correct printing. In speech transmission, inadequate bandwidth capability will seriously restrict the frequency range that can be transmitted. In pulse transmission, antenna selectivity may produce serious pulse distortion, making it difficult or impossible to match two separate pulses at the receiver because of lack of definition at the leading edges where two separate pulses are compared. Therefore, in all but the most elementary applications, special attention to the bandwidth capabilities of the antenna (both transmitting and receiving) must be examined critically during design.

A corollary condition of high selectivity is accuracy of tuning. Any mistuning causes asymmetry of side-frequency transmission with resultant distortion. Unless the bandwidth of the system is considerably greater than required, there is little or no tolerance in the tuning.

An electrically short antenna has a reactance very large with respect to its total resistance, which permits us to use the ratio X/R as the Q of the antenna. Such an antenna, when tuned for operation by means of series inductance, forms a series-resonant circuit. The bandwidth of the antenna can therefore be defined in the usual way as

$$BW = \frac{f}{Q}$$

where f is the frequency of resonance and BW is the total bandwidth, in cycles, between the upper and lower points of 3-decibel attenuation (45-degree phase angle.)

It is seen that the bandwidth is inversely proportional to antenna (or total circuit) Q. To decrease Q, the same design considerations are required as for the reduction of antenna potential. Therefore the same measures may be required in the design of a low-power system for large

bandwidths as for a high-power system for narrow bandwidths, with the exception of the insulation.

To transmit the fundamental and third-harmonic sidefrequencies of a square pulse of dot frequency F, the bandwidth required is $7.4F$. Therefore, the maximum permissible Q of the antenna is

$$Q_{max} = \frac{f}{7.4F}$$

If it is desired to operate a standard five-unit start-stop teleprinter (60-word speed of 23 dot cycles per second with equal mark and space intervals) at 40 kilocycles, the Q of the antenna must not exceed 235. Furthermore, at this value, the tuning must be exact at all times, or excessive telegraph distortion would result and impair the accuracy of operation. To be more precise, the entire selectivity in the transmitter and receiver systems together should not exceed an equivalent total Q of this value. The transmitting antenna should therefore have a Q less than this value in considering system performance and allowing for tuning tolerance to accommodate inevitable variations in antenna capacitance with weather.

One method of increasing bandwidth is to use an antenna of very large cross section. A cage or a tower is more effective in this respect than a single thin wire. A number of towers or vertical conductors with large separation and operated in parallel, either by individual feed or by multiple tuning, is a further step in this direction and one which is quite practical. In addition to the advantages of improving ground-current distribution and transforming the feed-point impedance to more convenient values, multiple tuning is a desirable method for increasing the bandwidth of the system. The disposition and the number of vertical leads in the system can simulate flat or circular current sheets having intrinsically much larger bandwidth characteristics than conventional single-tuned antennas.

1.10. Multiple Tuning

The most extreme conditions of low radiation resistance and high reactance are encountered at the lowest frequencies, and some extreme measures are necessary to obtain acceptable radiation efficiencies. The antenna represents a very great investment in structures and rigging, usually many times the cost of the associated transmitting equipment.

The most successful method of improving the radiation efficiency is that of multiple tuning. The antenna consists of a large elevated capacitance area with two or more down leads that are tuned individually as indicated in Fig. 1.7. The total antenna current is thus divided equally

among the down leads, each of which has its own ground system. The down-lead currents are in phase, and because of their electrically small separation there is no observable effect on the radiation pattern, which is always nearly circular. Power is fed into the system through *one* of the down leads.

When arranged for multiple tuning, an antenna behaves as a number of smaller antennas in parallel, voltage being fed through the flat-top system. Thus, a system with triple tuning is essentially three antennas in parallel, one of which is fed directly by coupling to the transmitter and the other two at high potential (voltage feed) through their common

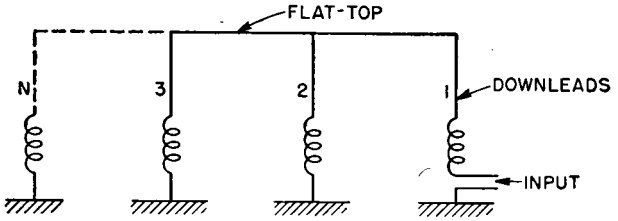

FIG. 1.7. Principle of multiple tuning.

flat-top. From a radiation standpoint, the same effect would be realized if the different portions of the antenna were not physically connected through their common flat-top but instead were separately fed from a common transmitter and feeder system in the manner of a directive antenna. Practically it is simpler to take advantage of the fact that almost all antennas for the lowest radio frequencies must of necessity employ flat-tops for capacitive loading and merely to add the extra down leads for multiple tuning. In this way, there is only one feed point, and the problems of power division, phasing, and impedance matching are automatically minimized.

A simplified explanation of the manner in which multiple tuning increases the radiation resistance as seen from the power feed point is the following: Assume a certain antenna system which, on the basis of ordinary single tuning, has a radiation resistance of 0.04 ohm but has a total resistance of 0.90 ohm as measured at the feed point. For a power input of 100 kilowatts, the antenna current with single tuning would therefore be 333 amperes. If now this same system is multiple-tuned, using three down leads with idential ground systems for each down lead, the current of 333 amperes is divided approximately equally among them, giving 111 amperes per down lead. At the one fed by the transmitter, 100 kilowatts input now produces a current in that down lead of 111 amperes. From this it is reckoned that the total antenna resistance at that point is about nine times its original value, or some 8.1 ohms. If

the radiation efficiency were not changed, the radiation resistance at this point would be transformed to 0.36 ohm. However, the radiation efficiency is improved over that of single tuning by virtue of the decreased total ground resistance resulting from reductions in the density of ground currents of each collecting point. Thus the ratio of radiation resistance to total resistance is effectively increased by multiple tuning.

If N represents the number of multiple-tuning down leads carrying equal currents, the new radiation resistance R_{rr} is related to that for single tuning R_r by the equation

$$R_{rr} = R_r N^2$$

The total antenna resistance with multiple tuning R_{tt} is, in general, less than $R_t N^2$, and from this $R_{rr}/R_{tt} > R_r/R_t$.

In addition to improving the radiation efficiency, multiple tuning also provides a more convenient input impedance at the feed point and increases bandwidth.

The full explanation of multiple tuning is much more complex than indicated here, where only the basic principle is explained. Some of the modifying factors are as follows: The effective capacitance of the flat-top is divided among the down leads so that each requires a larger tuning inductance than in the case of single tuning. The resistances of these tuning inductances are in series with the radiation resistance of each down lead, as are the conductor and insulation resistance components of loss, and these are also transferred to the feed point through the factor N^2. For the same coil Q, the larger inductance required for multiple tuning introduces a proportionately larger resistance per coil. However, the total loss in the inductances with multiple tuning is also less than in the case of single tuning, assuming equal Q's for all the inductances.

Multiple tuning is best adapted to operation on a single frequency. Where it is necessary to tune the antenna to several operating frequencies from time to time, single tuning is the most convenient.

1.10.1. Umbrella Antenna. Figure 1.8 illustrates an antenna of the umbrella type made up of three diamond antennas supported by seven towers and mechanically arranged so that each section can be raised and lowered separately. In turn, each diamond can be divided at the center for sleet melting if required, and therefore the down lead from each diamond has two conductors as shown at 1-2, 3-4, and 5-6, each pair connected in parallel near ground. The cross triatic of each diamond has a low-tension insulator (represented by a dot) at the middle to divide the antenna for sleet-melting purposes.

Let us assume that power is to be introduced at the down lead 3-4. The coupling apparatus will be located under this point. Only the

multiple-tuning inductors are located under the other two points. This requires that the flat-tops of the three sections be electrically connected at some point, such as at the center. This could be done by base insulating the central tower for the whole antenna potential and placing the cable winches on the tower above these insulators. Keeping in mind the sleet-melting circuit (if used), three-phase Y connections could be made with the neutral connected to this central tower and the three phases connected to points 1, 3, and 5.

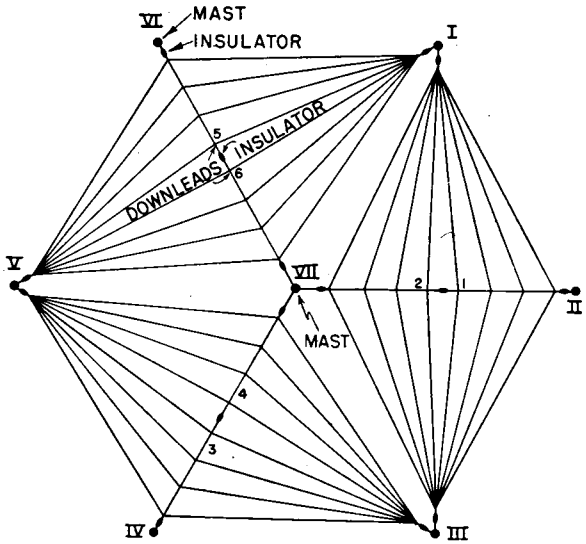

FIG. 1.8. An arrangement of three diamond sections to form a flat-top for a very low frequency antenna.

There is another arrangement that should not be overlooked. The towers I, III, and V could be adequately base-insulated and employed as the down-lead conductors and the tuning points located near their bases. This would eliminate the insulators from the end points of the diamonds, which would be thus connected directly to the three insulated towers. The aerials would be insulated from the other four towers. The desired mechanical flexibility of three separate flat-top sections could be realized very well, but the sleet-melting circuits would be somewhat different. Balanced three-phase power could be applied directly at the base of the three insulated towers. This would be an excellent arrangement for the sleet-melting circuits since, with the wire configuration shown, there would be an optimum equalization of the sleet-melting currents in the wires of the flat-tops.

The procedure of multiple tuning a circularly symmetrical antenna

system, after computing the approximate values, is to adjust all tuning inductances to identical values until there is a condition of zero reactance between ground and the inductance in the power lead. The system will then be adjusted for equality of currents in all down leads.

1.10.2. Multiple Tuning for Impedance Transformation. One of the characteristics of multiple tuning has been shown to be the transformation of impedance at the feed point when power is fed into only one of several down leads. Advantage of this principle can be taken in some

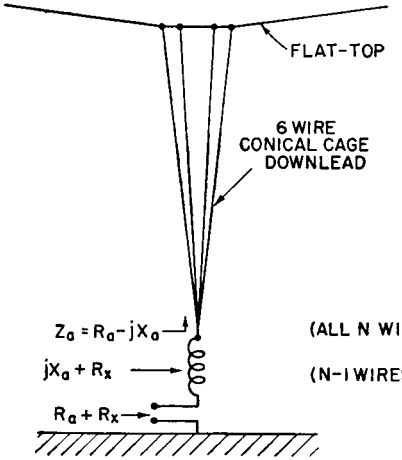

FIG. 1.9. Flat-top antenna with conical cage down lead.

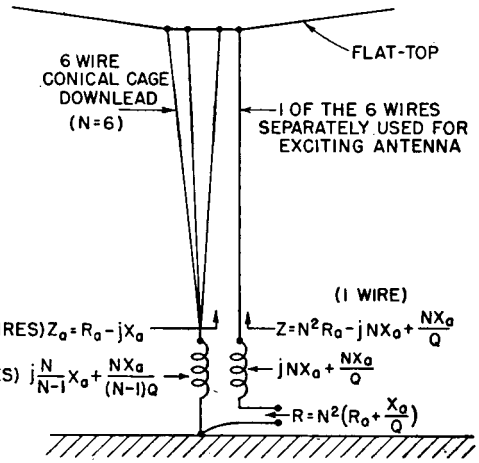

FIG. 1.10. Multiple tuning applied to the system of Fig. 1.9 for impedance matching.

cases to obtain a more favorable input impedance, principally an increase in the input resistance, for coupling and matching purposes. The technique can be applied in the following manner:

In Fig. 1.9 we have shown the schematic representation of a multiple-wire down lead for a single-tuned low-frequency antenna. There are 6 down leads in this cage, and the antenna current is divided equally among them. Let us say that this system has a measured resistance of 3 ohms and a reactance of $-j320$ ohms at the operating frequency. It will take an inductance with a reactance of 320 ohms to tune this system to series resonance by conventional means. This impedance is a very unfavorable value to use as a termination for a long feeder. The impedance transformation that must be used with practical feeders must be very large. The network that provides the desired ratio will store a large amount of energy, thus adding to the over-all selectivity of the system.

By the multiple-tuning technique, we can produce a practical transformation ratio in the antenna itself and therefore simplify the coupling

problem. The antenna can be fed through any one of the six wires. This will multiply the input resistance by $6^2 = 36$. At this stage it must be remembered that the quantity multiplied will be the total antenna resistance, which includes the resistance of the load coil as well as that of the antenna itself. The resistance of the antenna, excluding the load coil, has been given as 3 ohms. The load coil Q must now be estimated. Let it be arbitrarily assumed, for the frequency and anticipated design, to be 500.* The load-coil resistance will be 320/500, or 0.64, ohm. The total resistance will then be 3.64 ohms. Now, if power is fed into one of the six wires, the input resistance will be $3.64 \times 36 = 131$ ohms. This is now a value of resistance that can be a direct termination for certain types of unbalanced open-wire transmission line after tuning out the input reactance with a series inductance.

The total tuning reactance required is 320 ohms. This can be lumped all in one coil; or each of the six wires could be kept separated and a series reactance of $6 \times 320 = 1{,}920$ ohms used in each wire. If the coil Q were the same as for one lumped inductance, the same result would be obtained. In the example, where we feed into one of the six wires, we can use a load coil with a reactance of 1,920 ohms. Since the other five wires are connected together, a single load coil of reactance $1{,}920/5 = 384$ ohms can be used. The circuit is now as shown in Fig. 1.10. The overall performance of the system is identical with single series tuning except that the input impedance has been transformed from $3.64 - j320$ ohms to $131 - j1{,}920$ ohms. The reactance is tuned out with the second coil of 1,920 ohms, so that the actual feed-point impedance is 131 ohms resistive. This may be used as a direct termination for a transmission line having a characteristic impedance of approximately 130 ohms. A coupling network is thus eliminated in an efficient and inexpensive way.

The transformation ratio can be varied by using different numbers of down-lead wires in parallel and by changing the ratio of currents in the wires. The foregoing example assumed a circular disposition of the wires in which the antenna current was uniformly divided among them. Other system cross sections can be used which will provide unequal division of currents to modify the transformation ratio, more or less at will. The system efficiency, the total antenna current, the potentials and bandwidth of the entire radiating system are the same as if simple single tuning had been used.

1.10.3. Increasing Bandwidth of Vertical Radiators Used for Broadcasting. The multiple-down-lead technique offers excellent possibilities for low-frequency broadcast antennas where bandwidth is a special

* Antenna tuning inductors have been built with a Q of as high as 10,000 at 15 kilocycles.

problem. The requirement of a very large diameter vertical radiator as a means of increasing the bandwidth can be met by using a central steel mast with an outrigger at the top to support a cage of vertical wires having a substantial diameter without excessive weight or cost. Let us take, for example, a wide-band vertical radiator for broadcast purposes for a carrier frequency of 218 kilocycles. A steel mast 200 meters high (52.3 degrees at 218 kilocycles) must have a cylindrical height-to-diameter ratio of 20 in order to have a response within 2.5 decibels for the upper and lower 10-kilocycle side frequencies. This information can be computed from the impedance data of Figs. 2.15 and 2.16, taking into account that the electrical height of the antenna will vary from 49.9 degrees at 208 kilocycles to 54.7 at 228 kilocycles. To obtain a ratio of height to diameter of 20, the requisite diameter of 10 meters can be obtained by using an outrigger at the top of the mast to support at least eight vertical wires in the form of a cage enclosing the mast. A larger number of wires would more nearly approximate a complete cylinder.

The self-impedance of a radiator of these dimensions at 218 kilocycles is of the order of 11 ohms resistance and 80 ohms reactance. Ground resistance and other loss resistances must be added to this. The antenna current will be equally divided, by symmetry, among the eight vertical wires, and a residual portion of the total current will flow in the steel central supporting mast. The exact proportion of the total antenna current flowing in the mast itself can be computed by means of logarithmic-potential theory, but we shall assume for the present that it is the same as that in one of the vertical wires. The system therefore is equivalent to a nine-wire antenna with equal current division. We may choose to use a double tuning system, by including anywhere from one to eight wires in the fed portion, the remainder being tuned directly to ground. There is therefore a range of input impedances available for feed purposes, as shown in Table 1.4.

TABLE 1.4

Wires in fed portion	Input R, ohms	Input X, ohms
1	890	720
2	275	360
3	99	240
4	55	180
5	35	144
6	25	120
7	18	103
8	14	90
9 (self-impedance)	11	80

In the resistances given in the table the ground and other loss components have been omitted for simplicity. It is seen immediately that a wide range of input resistances is available according to the number of wires (with the supporting mast counted as a wire) included in the fed portion of the system, and with the remaining wires multiple-tuned in such a way as to maintain equal currents in all wires. It is interesting

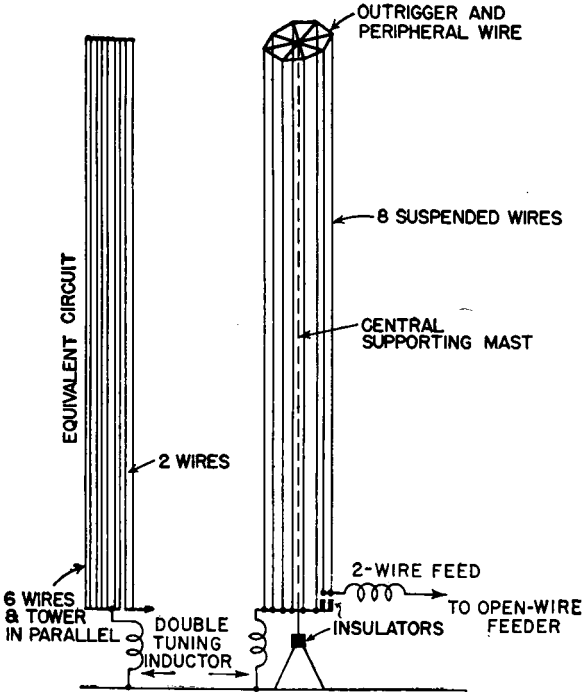

FIG. 1.11. Multiple-tuned low-frequency broadcast antenna.

that, with two wires in the fed portion, the resistance is of a value that would permit direct matching of convenient types of open-wire feeders. With four fed wires, the value is suitable for direct matching with coaxial feeders. The antenna-tuning gear consists of two inductors only, and the full bandwidth capabilities of the radiator are utilized by avoiding the use of more complicated networks having additional energy storage.

Figure 1.11 illustrates this arrangement when two-wire feed is used to match an open-wire feeder.

1.11. Antenna Potential

The power input to a low-frequency antenna is limited by potential. Any electrically short antenna having low resistance and high reactance

will require a relatively high exciting potential for any given power input. The formation of corona and standing arcs, or plumes, causes high loss, and a plume can be very destructive. The maximum safe potentials can be found from the data in Sec. 4.9 (see ref. 59, Chap. 4).

Low-frequency antennas are commonly fed in series between the down lead and ground. At this point the antenna resistance R_a includes those components of resistance due to radiation, insulation losses, corona losses, conductor heating, and ground loss. If the antenna tuning inductance is included as part of the antenna instead of part of the transmitter, its resistance is also included in the system resistance. Then, for a power input to the system of W_a (watts), the antenna current at the feed point will be

$$I_a = \sqrt{\frac{W_a}{R_a}}$$

The feed-point potential at the bottom of the down lead will be

$$V_a = I_a(R_a - jX_a)$$

where X_a is the antenna reactance at the working frequency.

In general, X_a is very large with respect to R_a so that the antenna potential becomes simply

$$V_a \doteq I_a X_a$$

For typical top-loaded antennas having an electrical length of less than 20 degrees at the working frequency, the antenna potential is identical within 3 to 5 per cent over the entire antenna. For any practical design purposes, one may arbitrarily assume that the maximum potential existing on any ordinary low-frequency-antenna design due to potential build-up from its standing-wave potential-distribution pattern will not exceed

$$V_a \doteq \frac{I_a X_a}{\cos G}$$

For practical purposes it is quite sufficient simply to add a few per cent to the value of the product $I_a X_a$. The potential need be known only approximately in ordinary cases in order to estimate the insulation requirements of the system and the potential gradients at critical points. The gradients must be below those which produce corona and pluming (standing arcs) at the altitude of the site. The conductors of the antenna must be of sufficient diameter and their physical arrangement planned so as to keep all potential gradients below critical values. For high-power systems, this becomes a major engineering problem, necessitating

the use of large and heavy conductors with their attendant mechanical and economic problems.

The critical corona-producing gradients vary with the atmospheric pressure, the turbulence of the air, and the frequency. Another important factor is the energy of the system, which may be more than sufficient to sustain large and destructive plumes as well as self-propagating arcs that produce actual flashovers to ground. Therefore high-potential engineering on high-power antenna systems has two distinct phases—that of not overstressing the air dielectric around the conductors and metallic parts, and that of the selection of solid insulation for isolating the antenna conductors from ground and supporting structures.

It is evident from the direct proportionality between antenna potential and antenna reactance, all other factors remaining constant, that all the techniques mentioned in Sec. 1.8 for reducing reactance will minimize the antenna potential for any given power input. Such techniques therefore raise the maximum power-handling capability of the system. They also tend to increase the bandwidth of the system as explained in Sec. 1.9.

The potential gradients to be expected in various parts of a multiwire antenna are at times impossible to compute accurately. Satisfactory approximations for engineering purposes can usually be made by simple methods. The computation starts with the value of potential existing at the surface of the conductor. This is determined from a measurement of the antenna impedance and the antenna current for the power input to the antenna and from the estimated build-up of potential above the feed point, which depends upon the configuration and the potential distribution.

Several wires in parallel or in close proximity at the same potential reduce the potential gradients as compared with a single isolated wire at the same potential. A single wire that is separated from ground, supporting towers, and other wires of the system by a distance of a few hundred wire diameters can be assumed to have a strictly radial electrical field at the wire surface. The equipotential surfaces close to it will be concentric with the axis. To solve for the potential gradient near such a wire, we may assume its image charge to be uniformly distributed over an imaginary cylindrical surface at a considerable distance like the outer conductor of a concentric transmission line. We can apply the principles of a concentric transmission line and consider that the isolated wire is the central conductor of a concentric transmission line having a characteristic impedance of large value, say 300 ohms or more. This requires that the outer concentric conductor have a very large diameter. In this analogy, the potential gradients in the vicinity of the antenna wire will approximate, with acceptable accuracy, those which would exist for the

same size wire at the same potential used as the central conductor of this equivalent concentric line.

The maximum safe operating potential for an antenna conductor can be computed from the information given in Sec. 4.9.

When there are other wires at the same potential in the vicinity of a wire, as when there are several wires in parallel, the maximum safe operating potential for the same wire size is increased somewhat. When the wire is in the vicinity of grounded structures or wires of opposite potential, the maximum safe operating potential is reduced. High localized potential gradients, which are incipient sources of weakness, can sometimes be reduced by applying corona shields or insulated controls. Corona shields reduce local potentials by distributing the electric charge over a larger area and thus reduce the electric-flux density below critical values that produce ionization. The insulated control is used for the same purpose, but it functions in a different manner. It reduces localized gradients by placing dielectric material in the high-intensity electrical field and smooths the discontinuity between metallic surfaces with a dielectric constant of infinity and air which has a dielectric constant of about 1.0. The layer of dielectric material acts as a corona shield.

Many localized weak points in a low-frequency antenna system can be corrected by the use of insulated controls. For example, the corona limit for a wire system is raised if the wires are coated with certain insulating varnishes with a high dielectric constant. The varnish also reduces the rate of corrosion of the conductors. A projection that causes corona can often be neutralized by attaching a mass of insulating material in the high-strength field, but in such a way that small dead-air spaces are completely absent; otherwise there may be ionization in the dead-air regions. Plastic as well as solid dielectrics are useful in many borderline brushing problems. Plastics are usually more convenient than corona shields made of metal. An insulated control is usually more effective with drip water than a metallic shield where the drip water may be the source of brushing or pluming from the metal surfaces.

When it is desired to increase transmitter power at an existing low-frequency station, it may be found that some modifications are needed to make the antenna safely withstand the increased potential. In most cases these problems will be localized. Special measures applied to the weak points, as just mentioned, will often remove the limitations at relatively small expense. The indication of an optimum antenna design is when the potentials are limited by corona or pluming on the linear conductors throughout the system and there are no local weak spots. It is necessary then only to ensure that the limiting potentials are well above the operating values.

1.12. Low-frequency Ground Systems

The principles of grounding low-frequency antennas differ from those used at higher frequencies for two main reasons: it is usually impractical to employ electrically long buried-wire systems (1) because of the relatively greater wavelengths and (2) because the low frequencies penetrate the soil to a relatively greater depth. This is in contrast with the situation at medium broadcast frequencies where radial ground systems of the order of one-half wavelength long are practical and economical. In such systems, most of the electrical flux that causes return ground conduction currents to enter the base of the antenna as antenna current is collected over the top of the ground system so that the current density in the soil beneath is very small. In the case of low frequencies, with electrically short ground wires, a considerable portion of the field is completed to ground beyond the limits of the ground system, and currents flow back to the antenna at considerable depth under the ground system. It then is important to collect ground currents in such a way as to minimize current densities in the soil to reduce ground loss.

There are essentially three methods for the design of low-frequency ground systems: radial buried ground systems (Fig. 1.12); star grounds (Fig. 1.13); counterpoises (Fig. 1.14).

1.12.1. Radial-buried-wire Ground System. The radial-buried-wire system is similar to that used at broadcast frequencies (see Sec. 2.5) where from 15 to 150 radial wires, centered at the antenna base, are buried in the soil. Because of the relatively great conductivity of the wires with respect to the soil, there is a tendency for the current in the soil to be diffracted into the lower resistance paths formed by the wires. The earth currents are at their maximum density at the surface of the ground where the wires are buried so that a substantial portion of the ground current is conducted by the radial wires if they are sufficiently long and sufficiently numerous. But since it is seldom convenient to use electrically long radial wires, a considerable loss may occur in the ground beyond the limits of the buried wires. A considerable loss can also occur because of the deep currents flowing beneath the buried wires, especially at points of concentrated collection such as the base of the antenna.

There are several ways in which a ground system can be designed to minimize current densities at low frequencies.

1. Ground rods can be attached at the ends of the radials to intercept as much current as possible vertically at the periphery of the system. Ideally, the ground rods should reach down to the depth corresponding to the skin thickness for the soil conductivity and the operating fre-

quency. This is not usually practical, but it is desirable to use the longest available ground rods.

2. The ground wires may be brought out of and above the surface of the soil at some distance from the antenna base. This requires the deep currents to rise to the surface uniformly at a distance sufficient to prevent

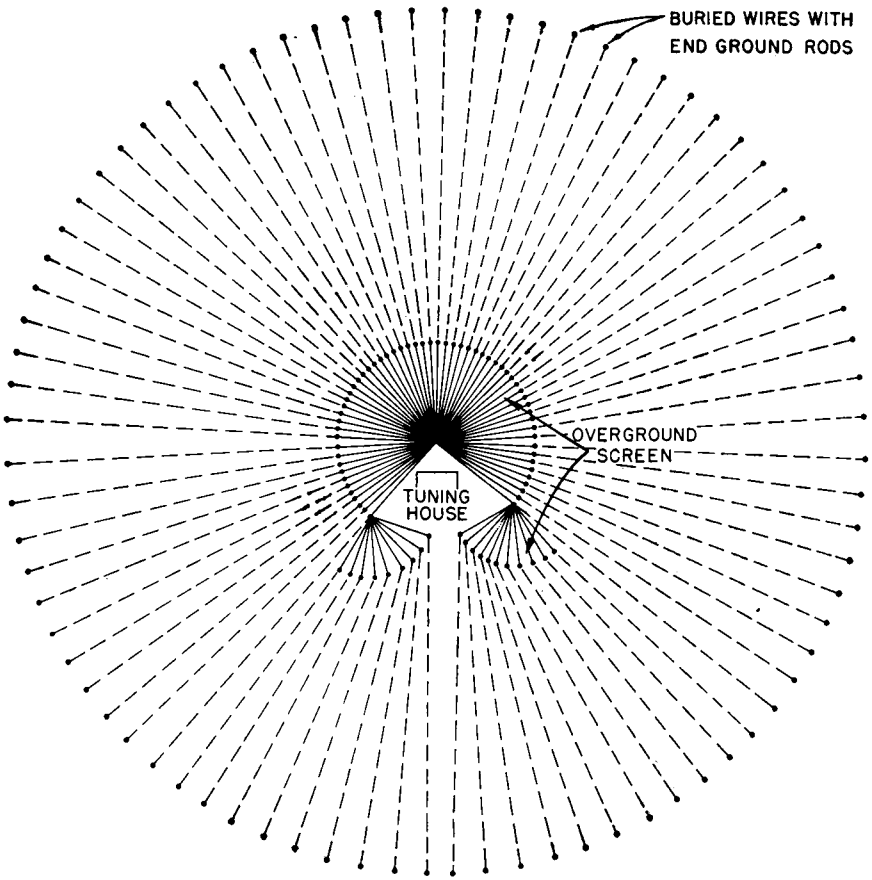

FIG. 1.12. Low-frequency buried-radial ground system with elevated central portion forming ground screen.

excessive concentration at the circle of collecting points. It is also beneficial to employ ground rods at the point where the radials emerge from the ground. The ground rods should be driven at an angle of 45 degrees toward the center of the system. The inner ground rods, driven in at this angle, reduce still further the concentration of ground currents coming up from below.

3. The radials that emerge and come to the base of the antenna above

ground also form an electrostatic ground screen to shield the ground from the intense electric field near the base of the antenna. At this point the antenna potential is high, and the ground screen prevents large dielectric loss in the soil. The exposed portions of the radials are insulated from ground at all points after they emerge from the ground. The exposed portion of the radials should be of the order of 1 electrical degree at least.

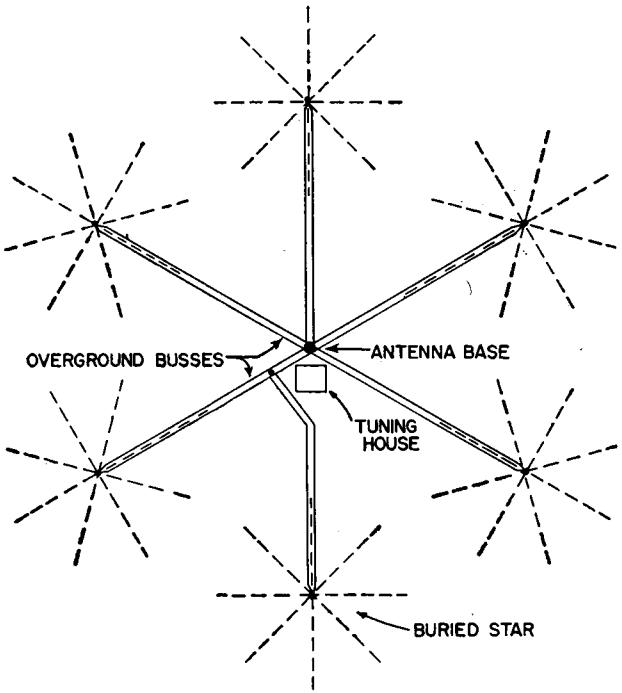

FIG. 1.13. A single circle of star grounds.

4. The length of the buried radials should be made as great as land and budget will permit. The number of radials used should also be as large as budget will permit, up to a maximum of 150 or 180.

5. There should be no closed conductive loops in the ground system in which eddy currents can circulate to increase copper loss.

6. The size of the wire used will depend upon the amount of current collected by each wire for the power and antenna used, taking the precaution to avoid excessive copper loss. This is a factor of great importance where large antenna currents are involved.

1.12.2. Multiple-star Ground System. The star ground system utilizes the principle that if a number of short buried-wire radial systems, simulating large ground plates, are placed at uniform distance around

the antenna base and their centers connected together at the base of the antenna with *overground* bus wires, the current densities in the soil can be made relatively small. A system of such star radials can reduce the current densities at the collecting areas to almost any degree desired depending on the number used. When two or more concentric circles of stars are used, inductors are placed in series with the busses for the inner stars to equalize the currents—otherwise the inner ones would collect the most current. The inductors may be simply a few turns in the bus wire wrapped around the supporting poles for the over-ground return circuit. The size and number of radial wires in each star and the number of stars used per circle have to be determined by tests. The greater the amount of current to be collected, the greater should be the number of stars and the number of circles of stars. This will in turn depend upon the antenna resistance and the power input. A star of eight 50-foot radials may be mentioned as a suggestion for 100-kilocycle use. At higher frequencies the radials can be decreased eventually to 25 feet in length. It is better to use more stars of short radial length than to use fewer stars with long radials. The need for ground rods at the ends of each radial must be determined by experimental tests.

1.12.3. Counterpoise. The counterpoise is an insulated net of radial wires assembled above ground to form a large capacitance with the ground. From the earliest days of radio the merits of the counterpoise as a low-loss ground system have been recognized because of the way in which the current densities in the ground are more or less uniformly distributed over the area of the counterpoise. Any tendency toward nonuniformity of current distribution in the ground will increase the portion of ground current toward the edge of the counterpoise. It is inconvenient structurally to use very extensive counterpoise systems, and this is the principal reason that has limited their application. The size of the counterpoise depends upon the frequency. It should have sufficient capacitance to have a relatively low reactance at the working frequency so as to minimize counterpoise potentials with respect to ground. The potential existing on a counterpoise may be a physical hazard which may also be objectionable.

All three of these ground systems require exposed over-ground wires near the antenna base. The buried radial ground system with the wires brought above ground near the antenna is possibly the best choice at stations where there is ample land for an extensive buried-wire system. In this system, the over-ground wires are not dangerous since they are at ground potential. The buried radial system accomplishes current-density reduction and decreases ground losses out to the distance of the buried radials. The over-ground portion forms an excellent ground screen as

well. In restricted areas, the star system seems to offer the best possibility of obtaining low ground resistance without the inconvenience and exposed potentials of the counterpoise. However, if the disadvantages of the counterpoise can be tolerated, it may be superior to the star system for low ground resistance. Figures 1.15 and 1.16 show useful details of counterpoise construction.*

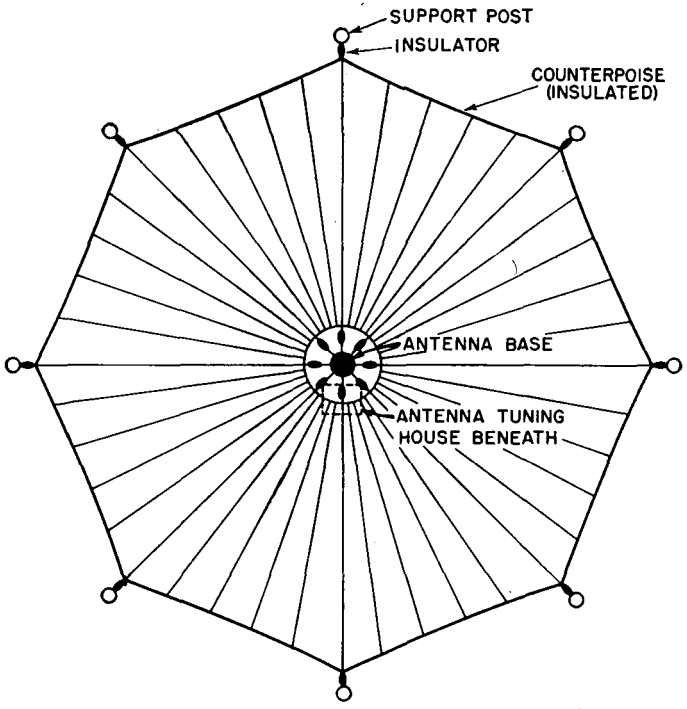

FIG. 1.14. Counterpoise (capacitance) ground.

These comparisons are not to be regarded as absolute, for they have not been proved quantitatively over a sufficient range of conditions to be considered as fact. They are the author's opinion from the information at his disposal. The soil conductivity and the frequency for any particular case may modify the controlling factors sufficiently to affect the final choice. For frequencies from 15 kilocycles to 500 kilocycles and soil conductivities from 10^{-14} to $5{,}000 \times 10^{-14}$ electromagnetic unit (sea water) the conditions vary a great deal.

* Figures 1.15 and 1.16 are photographs of an electrostatic ground screen and not a counterpoise. However, the mechanical construction of a counterpoise can be exactly as illustrated in these figures except that the inner ring of Fig. 1.15 should be fully insulated from ground. There should not be any connection to actual ground in the antenna circuit when a counterpoise is used.

The depth of penetration of ground currents at the low frequencies (see Appendix II) makes it important to consider the nature of the subsoil to the depth known as the "skin thickness." The search for a station site should include an examination of the subsoil characteristics

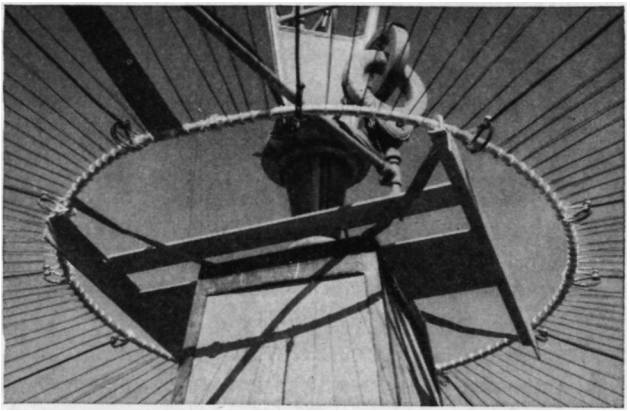

FIG. 1.15. Ground screen construction—center detail. (*Photograph courtesy of W. M. Witty, consulting engineer.*)

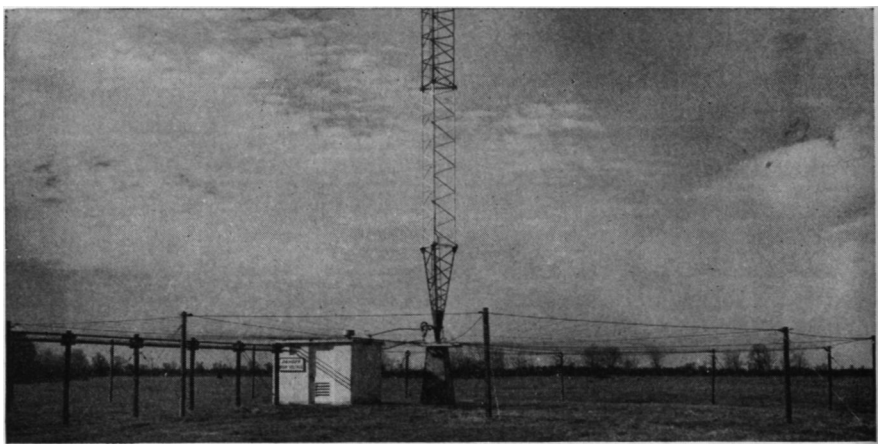

FIG. 1.16. Ground screen for a vertical radiator. (*Photograph from Radio Station KTBS, courtesy of W. M. Witty.*)

with the purpose of obtaining soil of best available conductivity to a sufficient depth. A thin covering of good-conductivity topsoil overlying a base of poor conductivity is usually a poor location for a low-frequency station.

1.13. Low-frequency Directive Antennas

1.13.1. Loop Antennas. Directive antennas for use on the low frequencies are limited to those which function with electrically close spac-

ing. For receiving, the loop antenna giving a figure-of-eight pattern, and the loop, in conjunction with a vertical sense antenna, giving the cardioid pattern, has long been used for direction finders particularly. The cardioid pattern from a loop and a vertical antenna is obtained by phasing the current in the latter at 90 degrees with respect to that in one side of the loop and by carefully balancing their relative current amplitudes to obtain the full null of the cardioid. This principle is amply described in all radio textbooks, particularly those dealing with direction finding. Ships and aircraft continue to be the principal users of direction finders as navigational aids. In recent years, the automatic direction finder has been developed to indicate continuously the bearing of the station used as the beacon. However, the use of loops for fixed point-to-point services has been marginal and of small importance.

1.13.2. Wave Antenna. The wave, or Beverage, antenna has for many years been the principal low-frequency directive antenna for the fixed services, especially for frequencies below 100 kilocycles. It was apparently the first antenna to be developed using the traveling-wave principle. Since 1920, this principle has been applied to many other forms of antennas for frequencies over the entire present-day range of radio frequencies.

The wave antenna, as used for low-frequency reception, consists of a horizontal wire one wavelength or more long and oriented in the direction of a desired arriving signal. It is usually suspended 15 to 30 feet above ground on ordinary telephone poles.

The simplest form consists of a single wire terminated in its characteristic impedance to ground at the end nearest to the sending station. The other end terminates in the receiver. This type of antenna is responsive to vertically polarized waves by virtue of the fact that the electric vectors of a wavefront, when passing over the imperfectly conducting earth, are tilted forward in the direction of propagation. This produces a component of electric force that is parallel to the wire and induces a current in it. This current flows in the direction of wave travel, which is toward the receiver end of the wave antenna. All portions of the antenna collect additional energy from the impinging wavefront in space, and the energy extracted from the passing wave field is cumulative so long as the phase of the wave in the antenna does not become greatly different from that of the exciting field.

The length of the wave antenna can be increased to advantage up to the point where destructive interference begins to take place between the wave field and the wire field. Where this cumulative effect reaches its optimum value depends upon the conductivity of the soil surrounding the antenna, the frequency of the incoming wave, and the orientation of the antenna with respect to the direction of wave travel in cases where

the antenna is not oriented in that direction. This latter condition is responsible for the wave antenna's pronounced directivity pattern, together with the condition of far-end termination, which dissipates all energy traveling in the opposite direction in the antenna. These effects are characteristic of all traveling-wave antennas.

The best location for a wave antenna is where the soil conductivity is lowest to a considerable depth (preferably as deep as the skin thickness). Unlike most other site requirements where the highest possible soil conductivity is desired, in the low-frequency wave antenna low conductivity is desired to obtain maximum wave tilt and the maximum exposure of the wire to the tilted wave field.

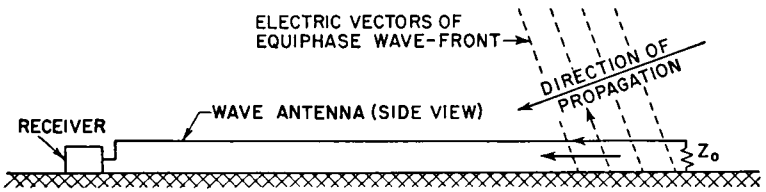

FIG. 1.17. Simplest form of wave antenna.

The characteristic impedance of the wave antenna is that of an unbalanced transmission line. It can be computed from the cross-sectional geometry of the antenna. One or more wires may be used to obtain characteristic impedances between 300 and 500 ohms.

Single-wire wave antennas will suffice for many applications. It is often desired to reverse the direction of maximum response in order to receive stations from two reciprocal directions at different times, or perhaps simultaneously. There are situations where it is more convenient to locate the receiving equipment near the blind end.

These requirements are easily met by using a wave antenna consisting of two parallel wires as shown in Fig. 1.18*A*. The wave field impinges upon these two wires simultaneously, and equal currents are caused to flow in both wires in the direction of wave travel. These currents continue to flow until they reach the far end of the antenna, where a reflection transformer is used to transform the collected current from unbalanced to balanced form. The energy thus transformed is then propagated backward along the antenna to the receiver. In this case, the receiver is connected between the two wires instead of from the wires to ground. The input impedance of the receiver is made equal to the impedance of the two wires functioning as a transmission line. To suppress pickup from the opposite direction, the neutral point of the balanced input circuit is connected to ground through a resistance equal to the characteristic impedance of the two wires to ground.

The reflection transformer shown in Fig. 1.18*A* is an inductive transformer having a ratio of Z_{01} unbalanced to Z_{02} balanced, and connected as shown. Z_{01} designates the characteristic impedance of the two wires unbalanced to ground, and Z_{02} is the balanced characteristic impedance between wires. In this diagram, reception is intended from one direction only, using one receiver.

In Fig. 1.18*B*, two receivers are used for simultaneous reception from two reciprocal directions. The input to one receiver is matched to Z_{02} balanced and the other to Z_{01} unbalanced and connected as shown. In

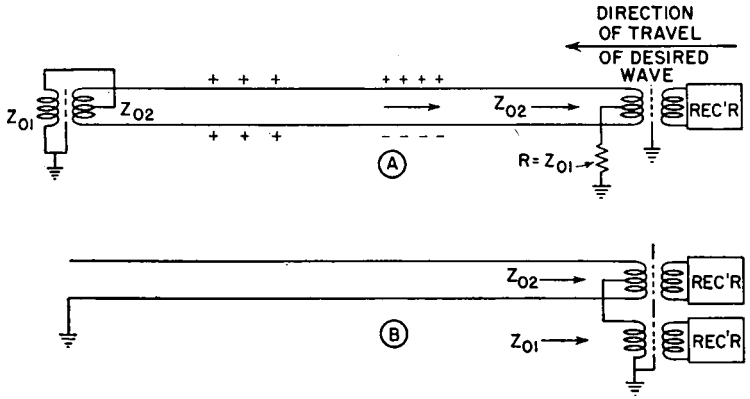

FIG. 1.18. Two-wire wave antenna with reflection transformer for separate reception from reciprocal directions and an alternative form of bidirective wave antenna without reflection transformer.

this diagram, reflection from the far end is accomplished by grounding one wire and leaving the other open-circuited. This balances the current received from the right but has no effect on the unbalanced current received from the left. In order to obtain sufficiently correct balances in the transformers, an electrostatic shield is indicated.

The characteristic impedance Z_{01} is in general a function of frequency, varying from the value computed from standard formulas which assume a perfectly conducting earth. It is desirable to measure the characteristic impedance of a system at the working frequencies after erection. This involves special techniques in view of the uncertainties of the ground terminals.

Directivity of Wave Antennas. The approximate polar pattern in the horizontal plane for a wave antenna having a length of one wavelength (360 degrees) is shown in Fig. 1.19. A pattern of this type is somewhat dependent upon the underlying soil at a given frequency because of its effect upon the propagation velocity within the antenna system.

Additional directivity can be obtained by combining two or more wave antennas in an array. The array can be lateral or longitudinal or a combination of both. Ordinary transmission lines are used to guide the received energy from the antennas to the receivers, and differences in the phases and amplitudes of the different signals, due to inequalities in the transmission-line lengths, are corrected by means of appropriate phasing networks and attenuators at the combining points. The combining technique may employ either active or passive means in such a way as to avoid interaction between the several antennas.

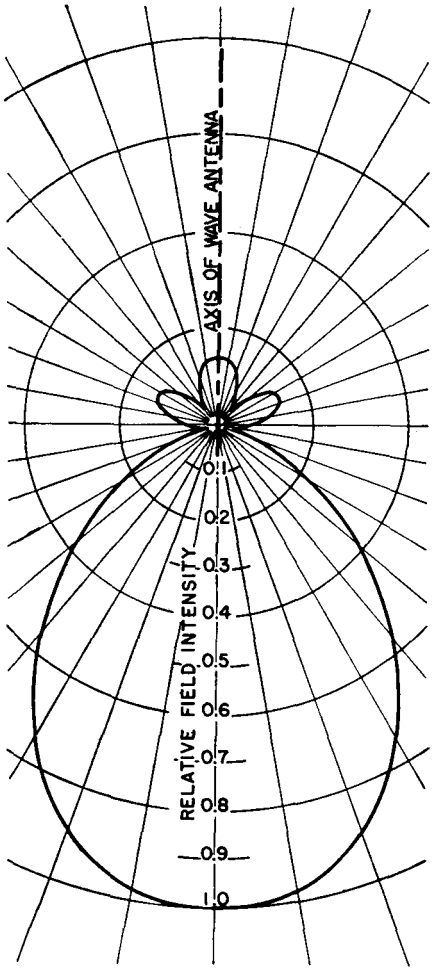

FIG. 1.19. Ideal horizontal response pattern for a one-wavelength wave antenna.

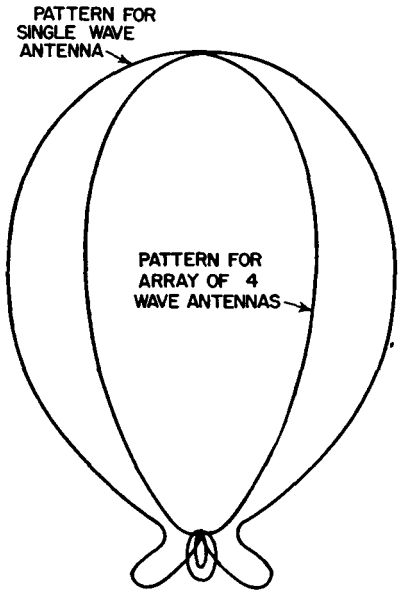

FIG. 1.20. Measured response patterns for one element and for an array of four wave antennas used at the receiving station of the American Telephone & Telegraph Co. at Houlton, Maine.

Figure 1.21 shows the circuitry employed for the low-frequency trans-atlantic-telephone wave-antenna system at Houlton, Maine. Four wave antennas, each 320 degrees long, are arranged in two pairs and are all parallel. Antennas A and B form the first pair, spaced laterally 25

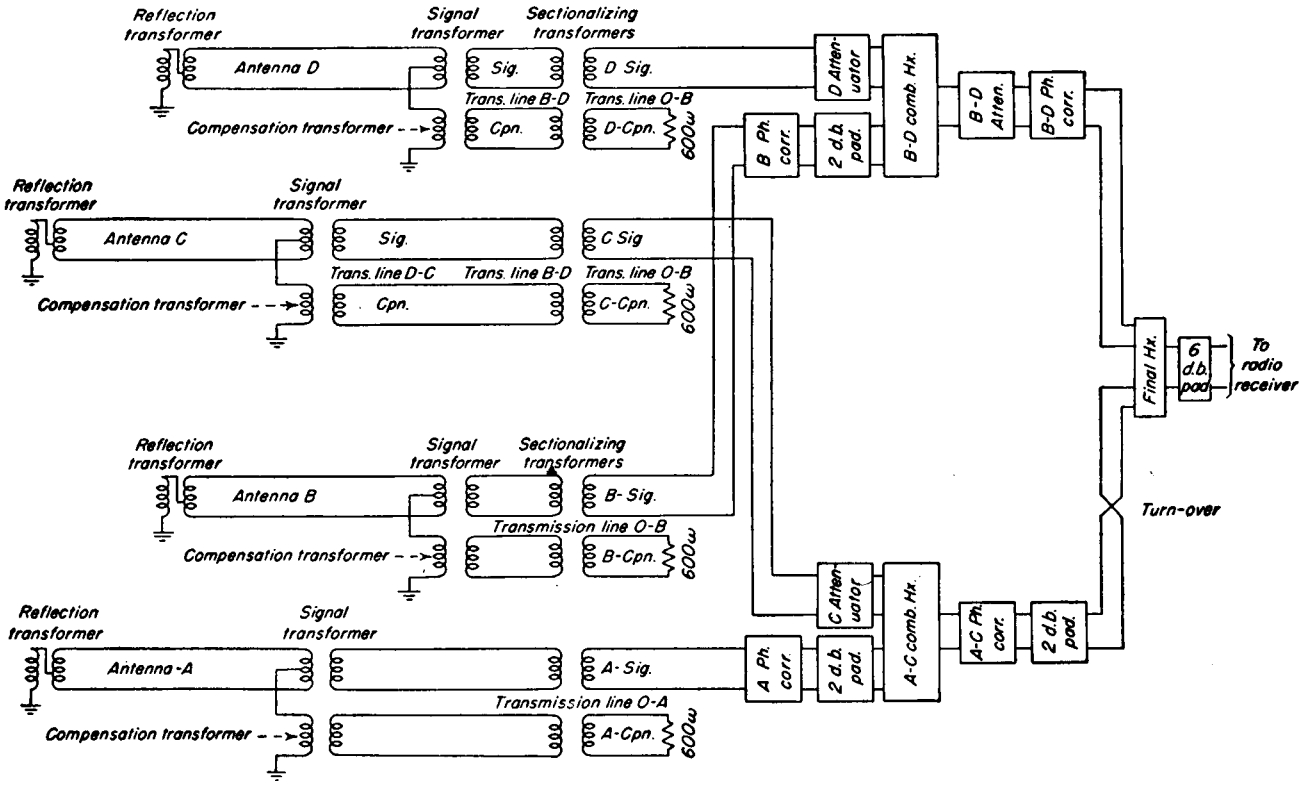

FIG. 1.21. Circuitry for the wave-antenna array at Houlton, Maine.

degrees and longitudinally 78 degrees. A second identical pair, composed of antennas C and D, are spaced laterally 220 degrees. The array therefore utilizes both lateral and longitudinal effects to obtain improved directivity, and the over-all pattern for the array is shown in Fig. 1.20.

The wave antenna has the property of substantial aperiodicity and therefore is especially desirable in wide-band systems.

1.13.3. Adcock Antenna. Another principle for low-frequency directive transmission and reception is used in the Adcock antenna. This

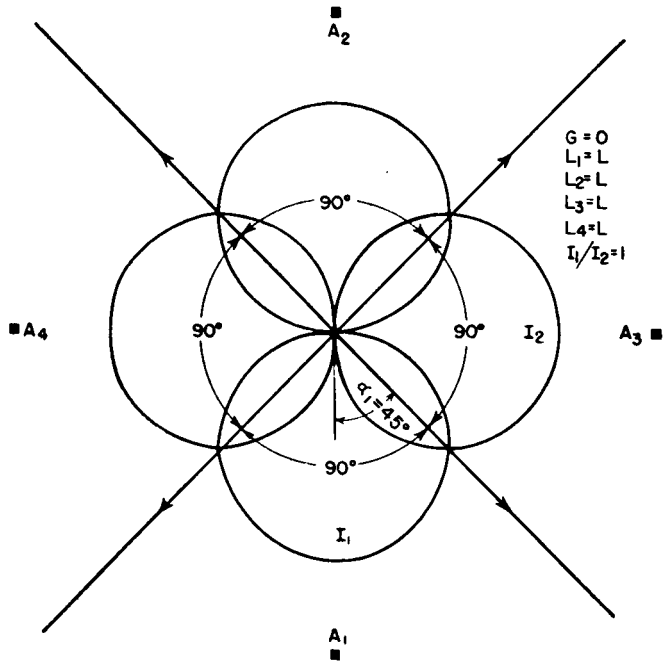

FIG. 1.22. Adcock array for four 90-degree courses.

antenna basically consists of two spaced vertical radiators with their currents in (or very near) phase opposition. Such a pair of radiators has substantially the characteristics of a loop antenna, but with the additional property that the feeders between the two radiators are made nonradiating. (They are often in the form of buried coaxial feeders.)

The system of two crossed Adcock antennas has been widely used for many years in the low-frequency four-course radio ranges for airways navigation in the North American continent and in other parts of the world. In its simplest form, four vertical radiators are located at the corners of a 600-foot square. Diagonal pairs constitute two Adcock arrays. If each pair is energized with equal-amplitude antiphased

currents, and energized alternately in some interlocked keying sequence such as the commonly used A-N method, the crossed patterns produce symmetrical courses at 90-degree azimuths (see Fig. 1.22). If now the currents in one pair are decreased with respect to the other pair, as shown in Fig. 1.23, the two reciprocal pairs of courses are squeezed. If the phase of the currents of one Adcock pair is made different from 180 degrees by a small amount, an asymmetrical figure-of-eight pattern is generated. When combined with the pattern of the opposite pair of

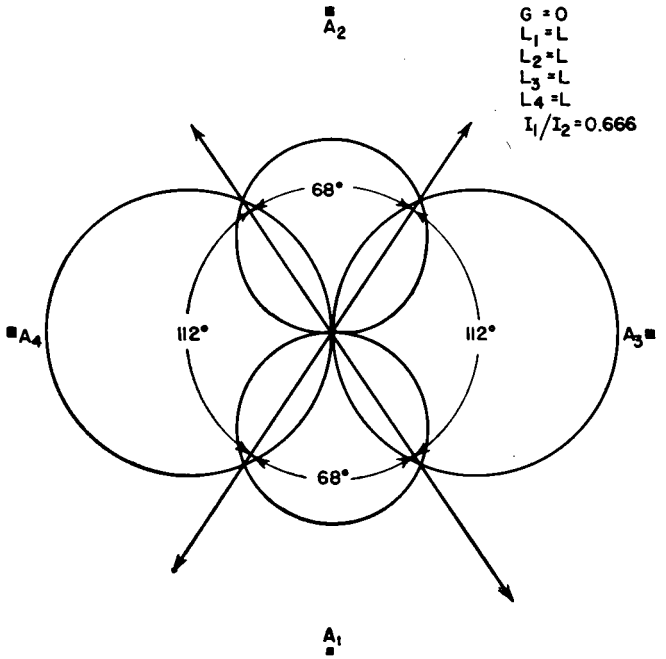

FIG. 1.23. Adcock array with squeezed courses.

radiators, the equisignal bearings can be bent in varying amounts to set up four-course guidance at specified azimuths.

The merit of this system of navigation is that an ordinary receiver is used in the aircraft. When equal signals are obtained from both the A and the N sides of the radio-range system, a steady signal is heard by the pilot and he is on one of the four courses. The apparent width of a course is of the order of 3 degrees. Outside of this zone, the difference in signal level is apparent, and the A or the N signal can be distinguished to indicate which side of the course the aircraft is on. This is indicated in Fig. 1.24, which shows the transition of the signal from a pure N to a pure A and passing one equisignal (on-course) bearing.

Feeding A-N *Arrays.* The two Adcock pairs in this system are fed through a cross-coil goniometer having two primaries and two secondaries. The A signals are fed across one primary and the N signals across the other. One secondary excites the first pair of diagonal radiators and

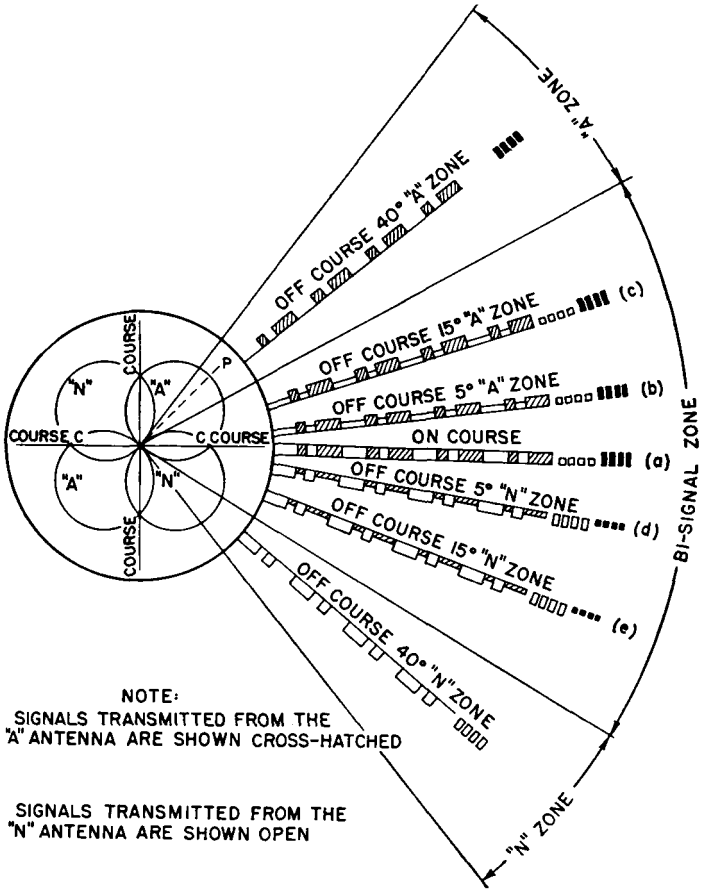

FIG. 1.24. Principle of course and quadrant identification in the Civil Aeronautics Authority four-course Adcock radio range.

the other the second pair. The goniometer is designed to be rotatable, so that when in other than the zero position the currents of the two pairs are actually distributed among the four radiators. The field pattern rotates with the goniometer rotation. The goniometer position is therefore a factor in the resulting pattern, when in other than the zero position, and plays a part in the bending of the courses to prescribed azimuths.

The installation, adjustment, and calibration of a four-course radio

range of this type (by flight checks) may require that only two of the courses be aligned to specified azimuths, in which case the others may fall at random. In other cases three or all four of the courses may have to be oriented at specified azimuths. Out of the great variety of possible combinations, Figs. 1.25 to 1.28 are included to show the effects of the goniometer position and the effects of feeder line lengths in adjusting the

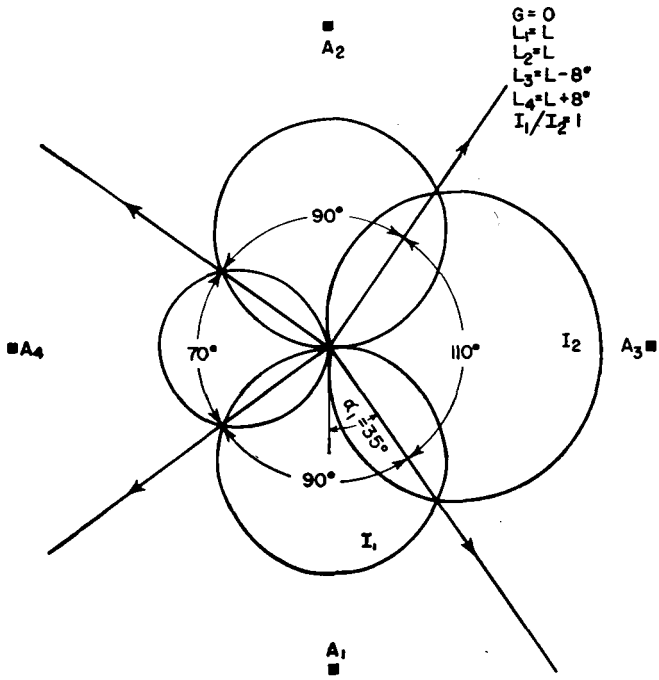

FIG. 1.25. Adcock array pattern with one antiphased pair and one pair out of antiphased relationship.

phase differences in one or both pairs of radiators. In these diagrams the locations of the four radiators are shown. Each legend gives the goniometer position in degrees from reference position, G, the differential in the electrical lengths L_1 and L_2 of feeders to the radiators A_1 and A_2, and the differential in the electrical lengths L_3 and L_4 to radiators A_3 and A_4.

Each feeder to each tower includes a straight run of coaxial feeder and an adjustable artificial-line network which builds out the electrical length of each feeder until it is equivalent to 90 degrees, approximately, from the goniometer. Therefore there is a total of about 180 degrees in the feeding system between a pair of radiators in the reference optimum initial condition. To produce phase differences between the currents of

a pair, this total feeder length is held constant, and the goniometer is, in effect, moved off the center of the feeder, by removing, say, 4 degrees of length from the artificial-line network on one side and adding the same amount on the other side. The same is done independently in the feeding of both Adcock pairs (see also refs. 40 and 28, Chap. 2).

Figure 1.22 shows the perfectly symmetrical pattern with reciprocal 90-degree courses when the goniometer is in its zero position and the

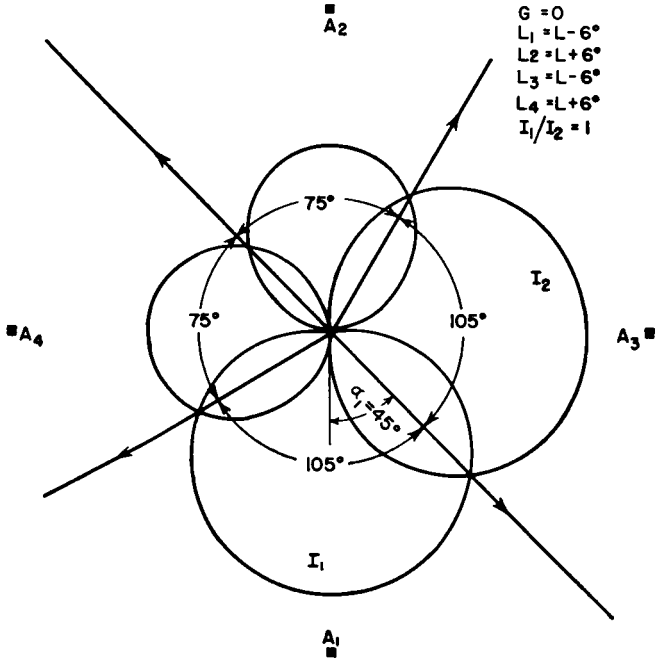

FIG. 1.26. Adcock array pattern with both pairs out of antiphased relationship.

currents of each pair are identical and exactly antiphased. Figure 1.23 is the same except that now an attenuator has been introduced in the feeder to the first pair to decrease the currents in that pair with respect to the currents in the second pair. This retains the same pattern shape for the first pair, but its amplitude is reduced. At the same time it squeezes the courses as shown but retains their reciprocal relationship.

In Fig. 1.25, the goniometer remains at zero. The currents of the first pair are in exact antiphased relationship, but the currents of the second pair are now 16 degrees out of antiphased relation. As a result, one pair of courses is squeezed, and the opposite pair is expanded. The two reciprocal intermediate angles remain at 90 degrees. The symmetrical figure-of-eight pattern of the first pair is combined with the asym-

metrical figure-of-eight pattern of the second pair. In Fig. 1.26 both pairs have the asymmetrical figure-of-eight pattern due to a phase difference of 12 degrees from antiphase condition. It can be seen that the angle between adjacent courses is the same on opposite sides of the whole pattern. The goniometer remains in the zero position.

Figure 1.27 is the same as Fig. 1.22 except that a 30-degree rotation of the goniometer has rotated the pattern 15 degrees. Figure 1.28 shows

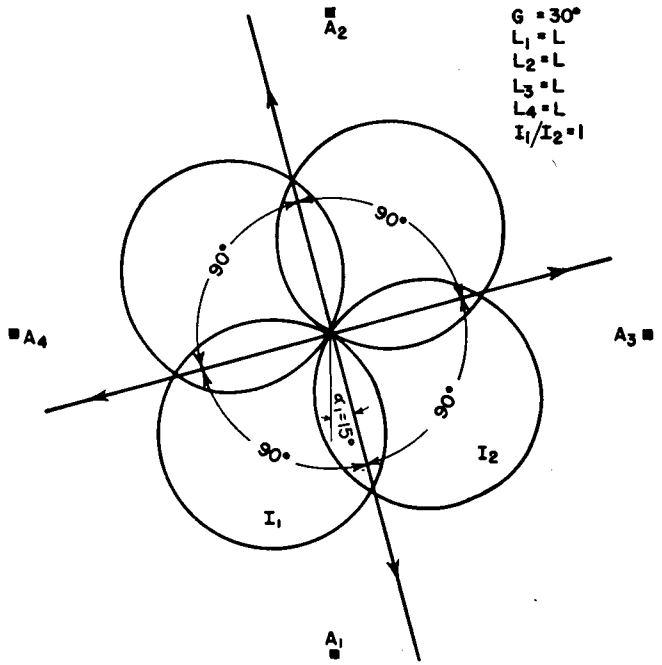

FIG. 1.27. Rotation of four 90-degree courses by means of goniometer rotation.

equal 20-degree phase deviations from antiphase for both pairs, but the goniometer is now set at 75 degrees. The patterns from the two pairs are seen to be unequal, and the angles between courses are all different.

In all the above cases except Fig. 1.23 the currents in the two pairs have been the same. In this case the ratio was changed by connecting an attenuator in the feeder to one pair. The adjustment of this current ratio between pairs, the setting of the goniometer, and the phasing of the two pairs provide the means for obtaining the very great range of course settings used in practice.

The use of approximately one-half wavelength of feeder between the radiators of a pair, consisting of coaxial line and artificial building-out networks having the same characteristic impedance, gives the maximum

intrinsic stability of the system in the presence of radiator impedance variations due to weather and other influences. When it is recalled that the radiators are electrically short and have low resistance and high reactance at the frequencies between 200 and 400 kilocycles, it can be expected that variations that might ordinarily be negligible can readily become important in such a phase- and amplitude-sensitive system. The special properties of the half-wavelength line are employed to main-

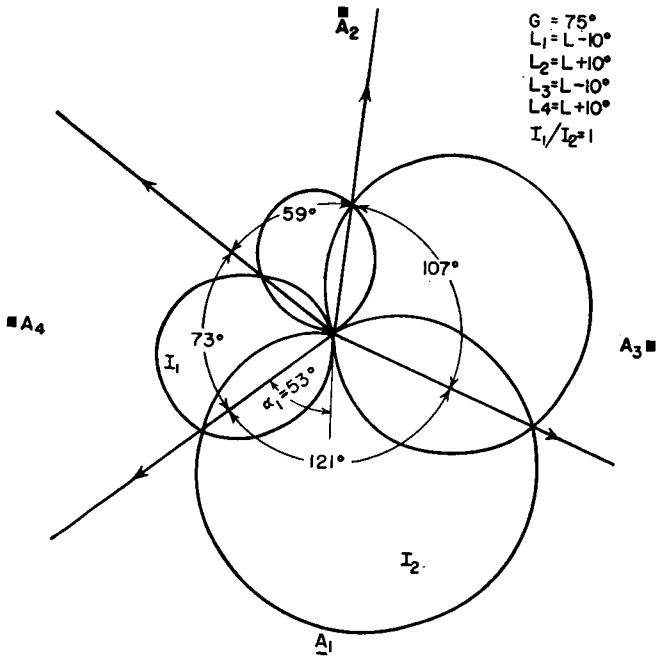

FIG. 1.28. Adcock array pattern illustrating arbitrary relations between courses by combination of current phasings and goniometer position.

tain a high degree of stability with the impedance variations inevitably encountered in service.

In the design and installation of the radiators and the ground systems every effort is made to minimize impedance variations due to changes in soil characteristics, the movement of the radiators in the wind, the presence of moisture films and water on the insulators at the base and the feed bushings, and many other effects which are of lesser importance but which cumulatively can be disturbing. Other variations are imposed by the cooling and heating of the tuning inductances due to power dissipation and to solar radiation and weather conditions throughout the seasons.

The radio range is also used for the transmission of voice signals for instructions and information to pilots. In the nonsimultaneous type

using only the four radiators previously discussed, all four radiators are excited in phase when the voice signals are transmitted. This involves switching from the four course navigational form of system excitation to parallel excitation for omnidirectional transmission, and the navigational facilities are absent during the voice transmission.

A later form of radiating system, known as the "simultaneous" radio range, places a fifth radiator at the center of the array, and voice signals can be transmitted from this central radiator without interrupting the navigational signals. In the receiver, the 1,020-cycle tone modulation used for navigation is selected by a filter to provide the navigational signals, while the voice circuit filters out this tone so that it will not interfere with the reception of voice signals. One receiver equipped with this reciprocal filter system provides the two types of signals in two output circuits simultaneously.

The cross-Adcock antenna system has also been used for fixed direction-finding stations for low- and high-frequency applications.

1.14. Reference Data on Certain Forms of Low-frequency Antennas

In Figs. 1.29 to 1.34 and their related tables some useful reference information is given on several forms of low-frequency antennas. Some of these data were obtained from full-scale antennas as constructed, and others were obtained from scale models.

f(kc)	X (ohms)	CALCULATED Rrad (ohms)
45	-j 785	0.49
50	690	0.60
60	555	0.85
70	450	1.20
80	375	1.55
90	320	2.00
100	268	2.40
120	188	3.6
140	125	5.2
160	75	7.2
180	30	9.9
195	0	12.8

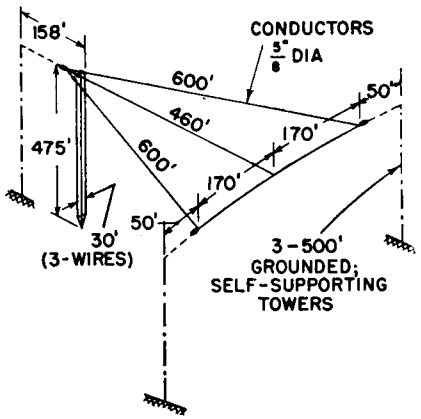

FIG. 1.29. Single-tuned inverted-L antenna with horizontal portion expanded.

By means of these data the approach to a new antenna problem is greatly simplified. The configurations presented will often be directly usable or will provide information that will be applicable to similar configurations. While one may conceive of a wide variety of antennas, economy restricts the number that are practically reasonable.

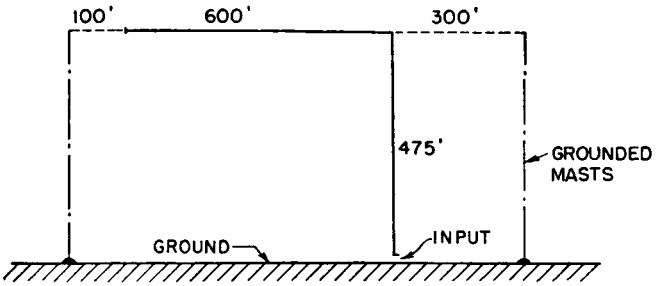

MODEL	ANTENNA CROSS-SECTION (UNIFORM) P = 0.40 INCH (ALL WIRES)		f_o(kc)	−jX (ohms) 44 kc	100 kc
A	•	1 WIRE	224	1350	520
B	S	2 WIRES SPACING 200 INS.	223	1040	433
C	• •	2 WIRES SPACING 250 INS.	222	1030	427
D	• •	2 WIRES SPACING 300 INS.	221	1022	412
E	• •	2 WIRES SPACING 400 INS.	221	985	412
F	• •	2 WIRES SPACING 600 INS.	222	975	416
G	S • • •	3 WIRES SPACING 100 INS.	220	910	394
H	S • • • •	4 WIRES SPACING 67 INS.	219	845	365

FIG. 1.30. Inverted-L antennas.

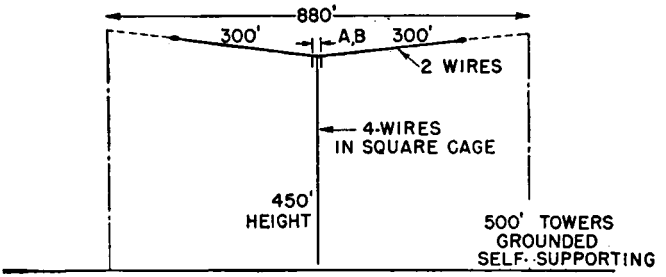

f kc	X (ohms) A	B
50	-j855	-j785
60	705	635
70	590	535
80	508	450
90	440	394
100	380	340
150	175	153
200	40	30
217	0	0

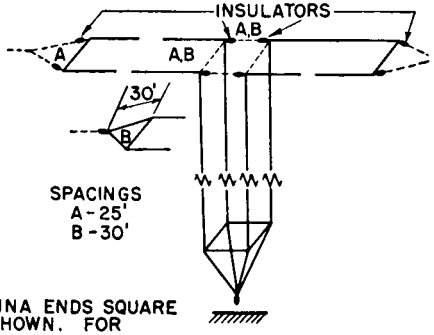

NOTE:
FOR SPACING A, ANTENNA ENDS SQUARE AND INSULATED AS SHOWN. FOR SPACING B, END DETAIL WAS CHANGED TO V SHAPE USING ONE INSULATOR ONLY IN TRIATIC.

FIG. 1.31. Two-wire T antenna.

The application of vertical radiators to the lower frequencies is increasing steadily as greater heights become practical. Where once a height of 1,000 feet was considered excessive, such a height is not considered unusual now. A height of 1,500 feet is already regarded as practical.

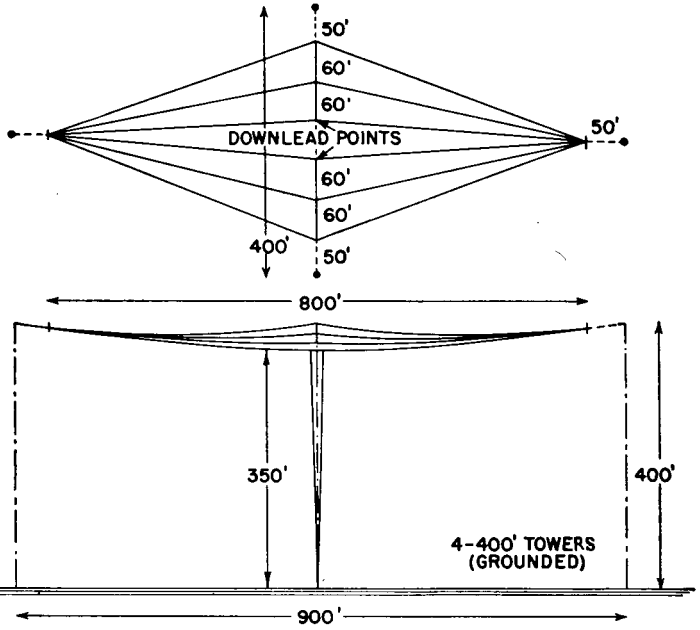

f(kc)	X(ohms)
40	-j680
60	395
80	265
100	185
120	130
140	85
160	50
195	0

FIG. 1.32. Diamond antenna.

1.15. Structural Design

Low-frequency antennas usually involve a great deal of mechanical engineering. In some cases the mechanical problems are more extensive than the electrical. For this reason the radio engineer often requires the aid of civil and mechanical engineers when design responsibilities exceed his normal competence. The design of supporting structures for radio antennas is now a special field of engineering practiced by those engaged in the business of supplying masts and towers. When these structures must support extended aerial wire systems many of the

mechanical problems are taken over by the tower engineers. Nevertheless the radio engineer should be familiar with certain elements of structural design in order to orient his preliminary antenna design toward forms that will be practical and economical. These elements are the same as those required for high-frequency antennas and transmission lines; therefore Secs. 3.26 and 4.13 should be consulted.

LOW-FREQUENCY ANTENNA SYSTEM

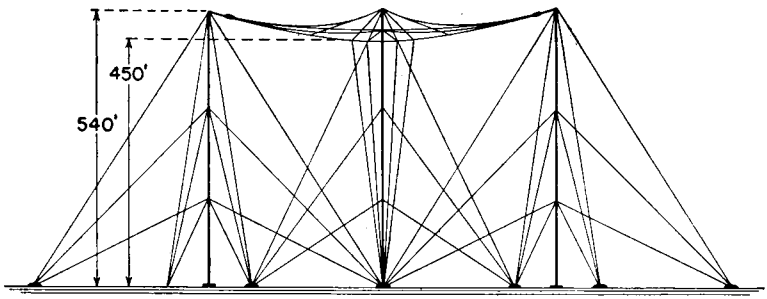

MEASURED CHARACTERISTICS

f (kc)	ELEC. LENGTH G-DEGREES	R(ohms)	X(ohms)
40	20.4	2.7	-j 520
50	25.5	2.8	408
60	30.6	3.0	327
70	35.8	3.3	263
80	41	3.7	223
90	46	4.2	185
100	51	4.8	155
110	56	5.5	130
120	61	6.3	102
140	71.5	8.4	60
160	81.6	11.1	25
176	90	—	0

FIG. 1.33. Triangular flat-top antenna (elevation).

Various good examples of assembly details for low-frequency antennas are presented photographically in Figs. 1.35 to 1.43. These details will serve as a guide to good engineering practices for a wide range of applications.

The mechanical loadings on members of a low-frequency antenna are often rather large, and it becomes necessary to use high-strength conductors, even though electrical conductivity has to be sacrificed. It is customary to use stranded conductors of phosphor bronze, Calsun bronze, and copper-clad steel when exceptional strength is needed. Some high-strength alloys require great care in construction to avoid annealing during soldering, which reduces the strength. The same effect is obtained

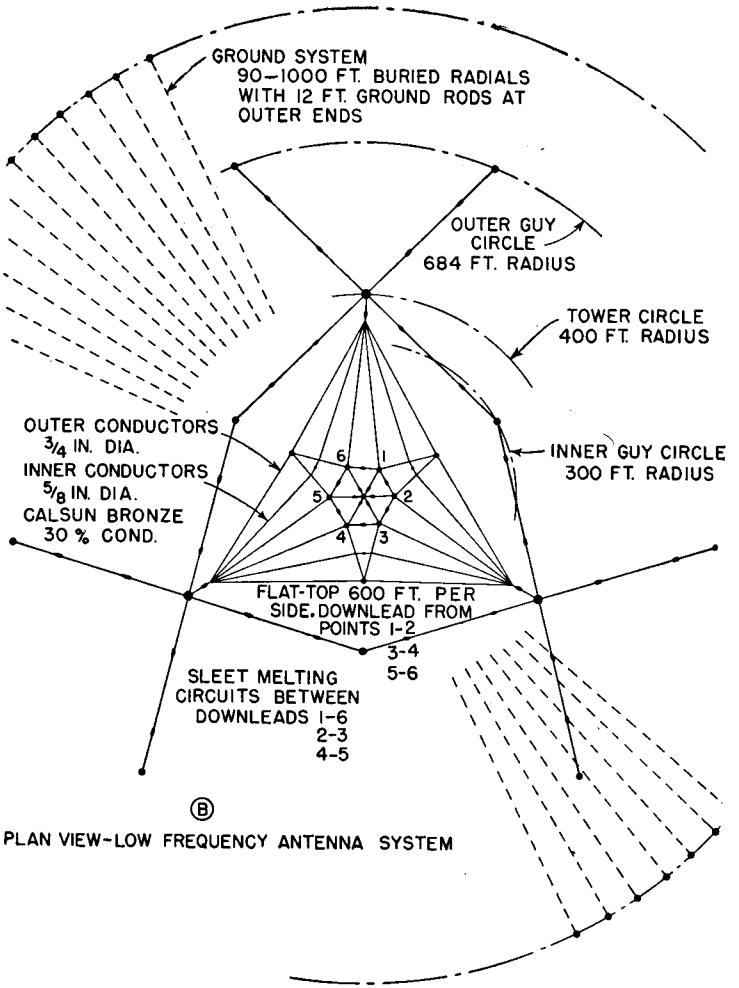

FIG. 1.34. Plan view of antenna shown in Fig. 1.33.

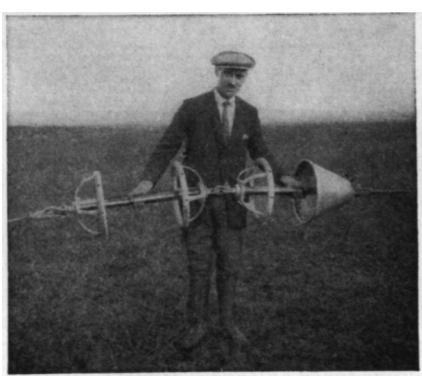

FIG. 1.35. Assembly of two antenna strain insulators in series, both fitted with potential-grading rings and one with a rain shield.

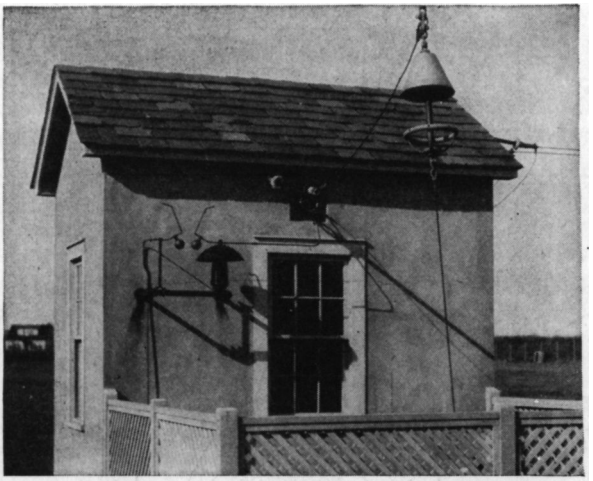

FIG. 1.36. Antenna down-lead and coupling-house-entrance detail as used at medium-power low-frequency stations.

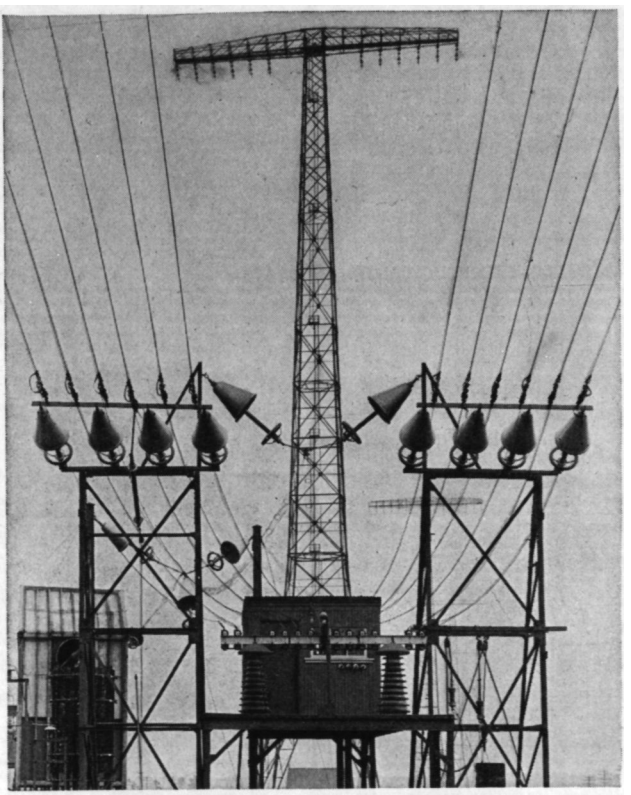

FIG. 1.37. Antenna down-lead details for the Rocky Point, New York, high-power very-low-frequency multiple-tuned antenna. (*Photograph courtesy of RCA Communications, Inc., and Drix Duryea.*)

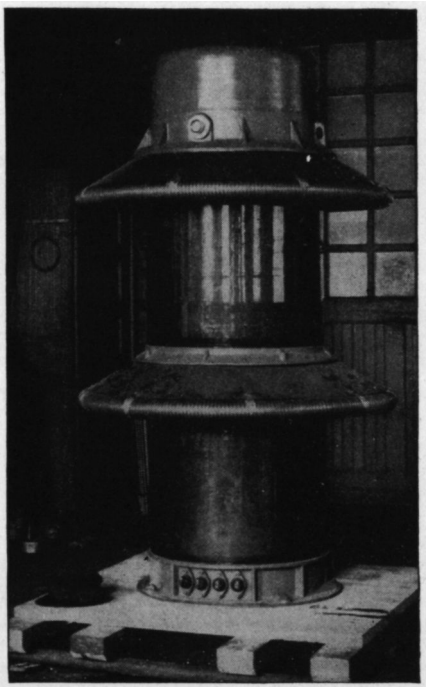

FIG. 1.38. High-voltage oil-filled safety-core tower-base insulator with tower-lighting transformer inside the insulator. (*Photograph courtesy of A. O. Austin.*)

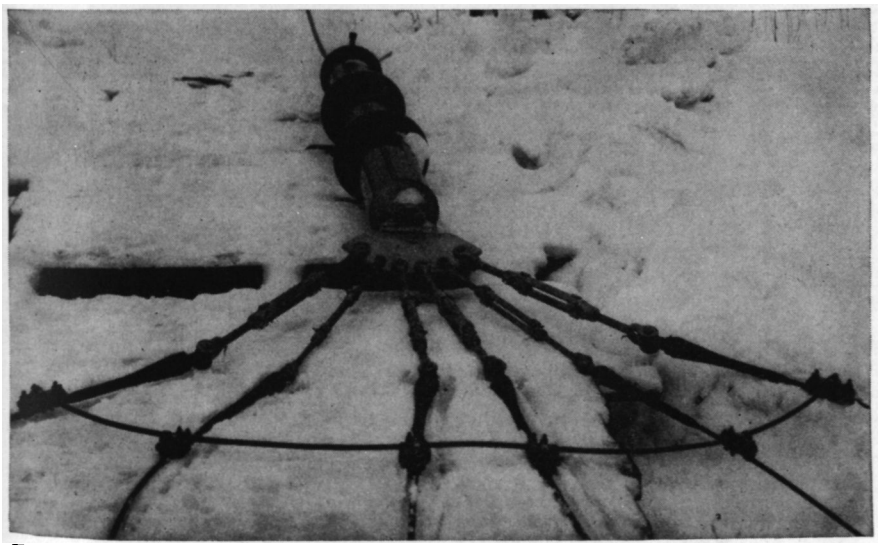

FIG. 1.39. Detail showing the assembly of wires to the strain insulator at the corners of antenna flat-top system of antenna in Figs. 1.33 and 1.34. (*Photograph courtesy of Royal Canadian Navy.*)

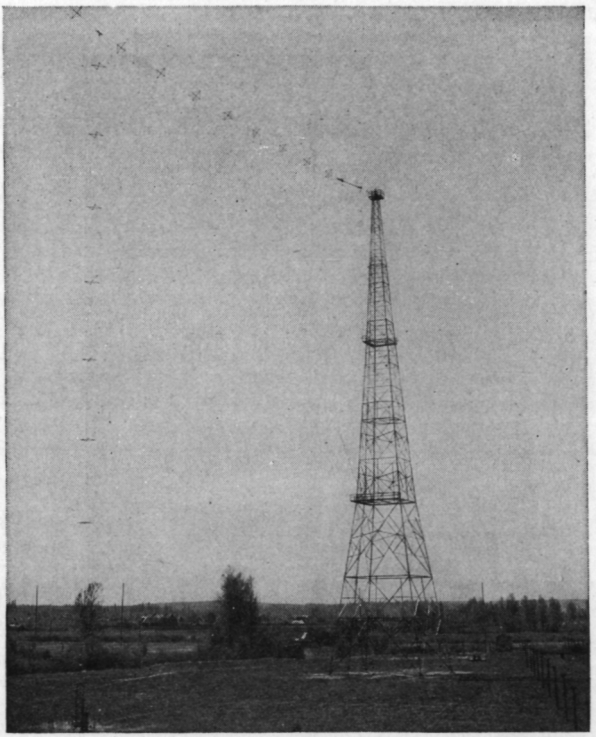

FIG. 1.40. Four-wire cage T antenna built according to the dimensions of Fig. 1.5. (*Photograph courtesy of Royal Canadian Navy.*)

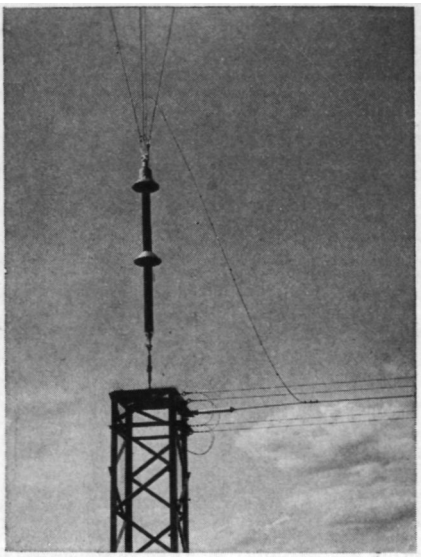

FIG. 1.41. Down-lead insulator and the end of the six-wire unbalanced unmatched feeder for the antenna of Fig. 1.5.

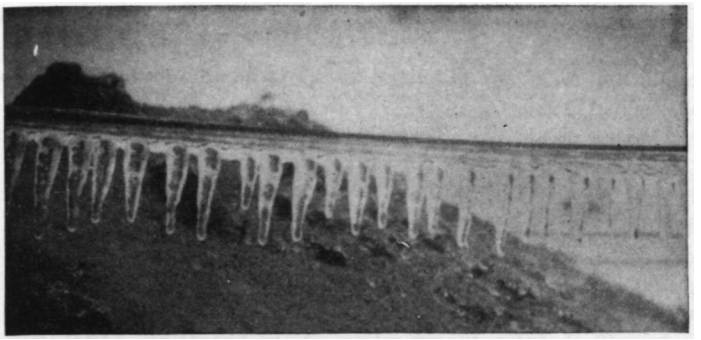

FIG. 1.42. Example of heavy icing on an antenna wire. (*Photograph courtesy of J. S. Hall and C. I. Soucy.*)

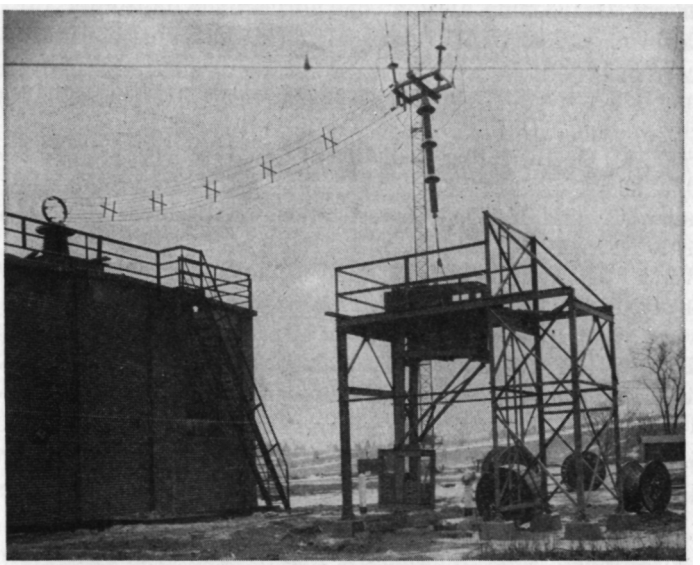

FIG. 1.43. Antenna down-lead detail for antenna built according to Figs. 1.33 and 1.34, showing down-lead counterweight and precautions at tuning-house entrance for large currents and high potentials. (*Photograph courtesy of Royal Canadian Navy.*)

if the conductors are overheated by sleet-melting currents when current is allowed to flow long after the ice has been removed from the wires. This also points out the reason why it is essential to design sleet-melting circuits so that ice is removed uniformly from all the conductors of the system in about the same time—otherwise some of the conductors may be overheated before ice is removed from others.

BIBLIOGRAPHY

1. Alexanderson, E. F. W., Trans-atlantic Radio Communication, *Proc. IRE*, **8**:263, August, 1920.
2. Alexanderson, E. F. W., Transoceanic Radio Communication, *Gen. Elec. Rev.*, October, 1920.
3. Ashbridge, N., H. Bishop, and B. N. MacLarty, Droitwich Broadcasting Station, *J. IEE*, **77**:447, Discussion 474, October, 1935.
4. Bailey, A., S. W. Dean, and W. T. Wintringham, Receiving System for Long-wave Transatlantic Radiotelephony, *Bell System Tech. J.*, **8**:309, April, 1929.
5. Eckersley, T. L., An Investigation of Transmitting Aerial Resistances, *J. IEE (London)*, **60**:581, 1922.
6. Kear, F. G., Phase Synchronization in Directive Antenna Arrays with Particular Application to the Radio Range Beacon, *J. Research, Natl. Bur. Standards*, **11**:123, July, 1933.
7. Lindenblad, N., and W. W. Brown, Main Considerations in Antenna Design, *Proc. IRE*, **14**:291, June, 1926.
8. Mann, H. F., and F. Hollinghurst, Replacement of Main Aerial System at Rugby Station, *P.O. Elec. Eng. J.*, April, 1940, p. 22.
9. Morgan, M. G., Increasing Radiation at Low Frequencies, *Electronics*, July, 1940, p. 33.
10. Rosseler, G., and K. Vogt, Investigations on Umbrella Aerials, abstract, *Wireless Engr.*, **20**:141, March, 1943.
11. Grover, F. W., Methods, Formulas and Tables for the Calculation of Antenna Capacity, *Natl. Bur. Standards Sci. Papers*, **568**: 569, 1928.
12. Howe, G. W. O., Calculation of Aerial Capacitance, *Wireless Engr.*, **20**:157, April, 1943.
13. Smith, C. E., and E. M. Johnson, Performance of Short Antennas, *Proc. IRE*, **35**:1026, October, 1947.
14. Bolt, F. D., Ice Formation on Aerials, *BBC Quart.*, **4**:1, winter, 1950–1951.

CHAPTER 2

Medium-frequency Broadcast Antennas

2.1. Review of the Development of Broadcast Antennas

Prior to 1924, almost all engineering experience with antennas was derived from electrically short antennas of the type that had been used for low and very low frequencies since the dawn of radio. It seems remarkable that it required such a long time to develop the principles of the vertical radiator. The recognition and proof of the theoretical aspects of vertical radiators, together with the realization of their practical forms, required several years.

The natural sequence of events was to apply to the broadcast frequencies the same techniques of theory and construction that were common to the low-frequency systems. These antennas usually consisted of two or more towers or masts supporting an aerial system of wires comprising the antenna. Also in conformance with typical low-frequency practice, these antennas were always operated at a frequency equal to or considerably less than their fundamental frequency.

Little was known among practical engineers about radiation patterns. As designed, the radiation resistance of the original broadcast antennas was low, running from about 5 to 35 ohms, the larger of these values being rare. Ground-system design was still in the black-magic stage. With the exception of a few theoretical studies, made mostly by physicists, there was very little thought directed toward antenna development. What little text and reference material existed on the subject was pertinent to the low-frequency applications, the understanding being that as the frequency increased one simply used smaller dimensions.

The publication by Ballantine,[1008,1009] of two historic papers led to the development of the modern broadcast antenna. In one of these papers it was shown that for vertical antennas higher than one-quarter wavelength the radiation resistance continued to rise and went to very high values when the height approximated one-half wavelength. This then pointed to a method of increasing radiation efficiency by using antennas

having a radiation resistance very large with respect to the ground resistance, the principal loss factor of the antenna system. A way was at hand to make the radiation efficiency about as high as one wished, by employing vertical height sufficient to arrive at some desired large value of radiation resistance.

The second of Ballantine's papers disclosed a hitherto unknown fact: there was an optimum height of vertical radiator for obtaining maximum ground-wave field strength. This resulted from the space wave pattern produced by waves directly radiated above the ground interfering with those reflected from the ground. The result produced a vertical directivity which concentrated the radiant energy normal to the antenna, that is, along the surface of the earth. In a system such as broadcasting, dependent on ground-wave propagation, the existence of an optimum height of antenna from a radiation-effectiveness viewpoint was of great importance.

Still a third important consequence of Ballantine's principle was to appear later. As the power of broadcast stations gradually increased, the situation soon appeared where the ground wave was interfered with by waves reflected from the ionosphere. Interference between these two waves produced serious selective fading at a rapid rate. In the annular regions surrounding a station where both waves were of about equal intensity, destructive interference was maximum, and any coverage in these regions was rendered virtually useless at night. This fading wall became a major obstacle to further increases in power, at least at night. The only hope in sight was to use Ballantine's optimum-height antenna to reduce the amount of energy radiated skyward at high angles and at the same time to increase the radiation along the ground. This should push the fading wall farther from the station. When practical means were found to construct antennas using this principle, this effect was indeed verified.

The theory of the vertical radiator was developed around the condition that the current distribution along the antenna was sinusoidal from its upper end. It was believed, though not proved at that time, that the current distribution was naturally sinusoidal, or very nearly so. At that time, however, the practical realization of optimum-height vertical radiators was not at hand. The first applications of the new principle were made to the T-type wire aerial operating at a frequency above its fundamental frequency and supported in the usual way by two high towers. This gave a worth-while improvement in radiation efficiency but failed to provide sufficient reduction in fading. At this stage, the knowledge of wave propagation probably had not quite developed to the state where the fading-reduction properties of the optimum-height antenna were apparent. From 1925 to about 1930 the T antenna,

operating at about 1½ times its fundamental frequency, was the dominant type of broadcast antenna, and many of the systems constructed during this period continued in use many years thereafter.

2.1.1. The Tower Radiator. The next significant step in the progression of improvement was the advent, in 1930, of the guyed cantilever steel tower of a height in conformance with Ballantine's optimum-height formula, which was five-eighths wavelength. At the same time, the use of an extensive system of long radial ground wires centered about the base of the radiator was introduced. This was also an important step forward.

Unfortunately, the original form of cantilever radiator was not of uniform cross section. It tapered from a point resting on the base insulator to a maximum thickness just below mid-height and then tapered again to a point at the top. The guys were attached at the waist, or maximum cross section point. This structure was a success mechanically but did not yield full expected performance, because its double taper modified the current distribution in a way that reduced its vertical directivity. Nevertheless, this type of radiator performed sufficiently near to expectations to provide a satisfactory proof of the antifading properties of such systems. The deficiency of the double-taper tower was finally verified by field-strength measurements in aircraft and by scale-model measurements of current distribution.[23]

Tower design then evolved to the form now prevalent, using either very slender self-supporting towers, or guyed towers of uniform cross section.

The advent of the tower radiator was novel in yet another respect—it used the steel structure as the antenna directly. The use of a steel mast as a radiator had been tried as far back as 1906 at Brant Rock but was never adopted as a design for an antenna. The economic advantages of the tower radiator are quite apparent. A tower radiator is less costly than two towers of similar height supporting a wire antenna. Furthermore, supporting towers, being in the strong field of the antenna, often had large currents induced in them, which made them secondary radiators and produced directive effects in the horizontal pattern which were often undesirable. The tower radiator became essentially an ideal radiator with electrical and mechanical requirements satisfied by a single structure. The tower radiator could also be adapted to use in directive arrays.

Further study of the optimum-height antenna disclosed eventually that the conditions of maximum ground-wave field gain and best antifading characteristics were not obtained with the same height. The height that gave the highest field strength (225 degrees) had a rather large secondary lobe of high-angle radiation. This lobe could be reduced

to a point where its effect was negligible at some small sacrifice in horizontal field-strength gain. The optimum choice for antifading over land was experimentally established at about 190 degrees, or slightly over one-half wavelength in height. Over salt water the 225-degree radiator has certain advantages, as will be explained later.

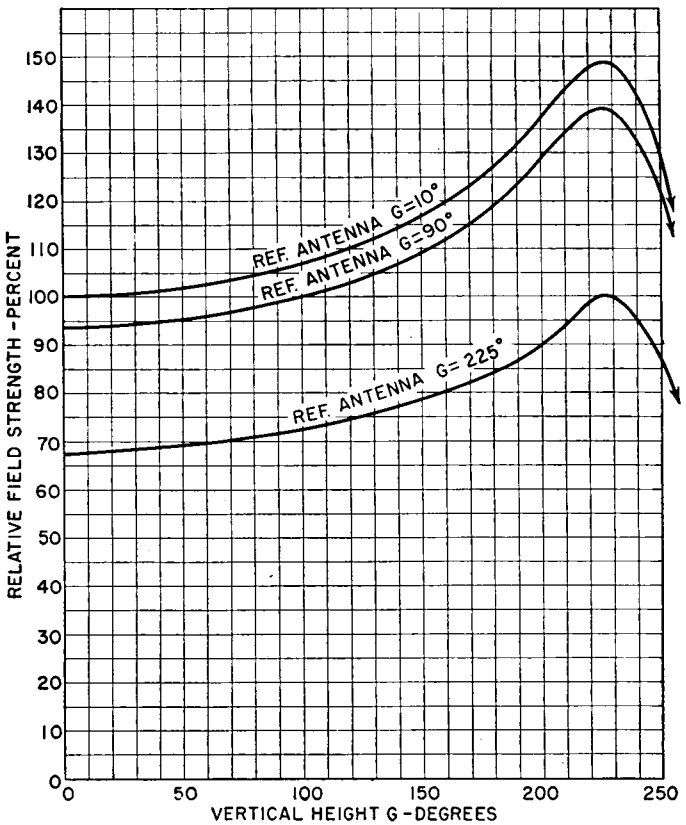

FIG. 2.1. Relative field strength versus height of a uniform straight vertical radiator with sinusoidal current distribution.

Subsequent special modifications were introduced to obtain optimum-height operation characteristics with shorter structures, as often necessitated by airways near the transmitter site. One form was the top-loaded vertical radiator which employed a horizontal circular steel capacitance area at the top to substitute for a certain amount of missing vertical height.[23] The amount of top loading was limited structurally to values equivalent to 15 to 30 degrees of electrical height. When the top-loading structure was insulated from the tower and its reactance reduced by

means of a series inductance, its electrical effect could be somewhat enhanced. Another approach was to sectionalize the tower with insulators at a point somewhat above three-tenths wavelength from ground and insert a series inductance to reduce the reactance of the upper section. The whole tower could then be physically shorter than optimum height and still perform as an optimum-height antenna.

By about 1934, the modern broadcast radiator had evolved to its present state. The tower radiator was the essential element for the directive broadcast antenna, which is presently of utmost importance in the development of ever-increasing broadcast services within the limited frequency spectrum.

2.1.2. Development of Ground Systems. It has been known theoretically since the works of Pierce and Ballantine that, for the condition of perfectly conducting flat ground, a very short vertical radiator will produce, within about 6 per cent, the same field strength as a radiator one-quarter wavelength high for the same power input. This is illustrated in Fig. 2.1. For greater heights, the field-strength gain increases very slowly to well beyond three-eighths wavelength. Only as the radiator approaches the optimum heights previously discussed does any real gain occur.[6]

One important conclusion one draws immediately from Fig. 2.1 is that there is very little difference in the performance of a radiator in the range up to about 120 degrees from the standpoint of field strength. If we compare a 60-degree radiator with one of 120 degrees, the gain of the latter is trivial with respect to the increase in cost for a structure of twice the height. However, the bandwidth requirements of an antenna may dictate the use of higher radiators without regard to the comparative radiation efficiency.

The question naturally arises: Why not use very short radiators? Several factors make this impractical in most cases. The shorter the radiator, the lower its radiation resistance. Practical ground systems can be constructed to have very low resistance, but as radiation resistance becomes very small, the ground resistance becomes an increasingly important factor in the circuital efficiency of the antenna system. For this reason it is difficult to realize the desired over-all circuital efficiency, with the result that short antennas are usually very inefficient.

Furthermore, very short antennas have very high reactance, so that high reactances are needed for tuning. The inductor loss therefore becomes large with electrically short radiators. The low-resistance and high-reactance systems have relatively small bandwidth, also. For these reasons a radiator for medium-frequency broadcasting is seldom made less than 60 degrees high.

Since stations of low and medium power do not usually require antifading antennas, it was obvious that it would be desirable to investigate synthetic perfectly conducting grounds for obtaining optimum efficiency from electrically short radiators. Experimental research and theoretical studies of earth currents near radiators of various heights yielded a simple and practical ground system that fully satisfied the requirements. This work[6] established immediately a uniform ground-system design for broadcast stations in the medium frequencies. A system of 120 radial wires, spaced 3 degrees and having a length of about one-half wavelength, approaches the condition of a perfectly conducting ground within about 2 per cent for radiator heights of 45 degrees or more. Ground rods at radial ends and various other departures from simple straight buried wires are of negligible benefit in such a system at the medium frequencies.

Diligent research and experiments have been conducted for other possible broadcast principles that might equal or surpass those disclosed by Ballantine.[3] Various natural and unnatural current distributions have been studied and tried, as well as circles of radiators,[25] controlling the velocity of propagation and using great heights. Some such devices produce equivalent performance at much greater cost and design complication—others are definitely inferior. Only one form, the uniphased antenna developed by Franklin for high-frequency use, holds promise of surpassing the straight vertical antenna of uniform cross section and of height 190 to 225 degrees. The Franklin antenna is realizable at medium frequencies by extremely high structures, insulated at the current nodes and tuned to produce uniphased currents on each side of such current nodes.

The medium-wave broadcast radiator is thus in that happy state where, so it seems in the light of present knowledge, a standardized optimum design exists. Also, the optimum ground-system design exists. These optimum designs are practical, as proved by extensive application at hundreds of stations whose performance has been carefully measured. The design formula is very simple. The performance is predictable with very high accuracy, and this performance is very close to the theoretical maximum. Furthermore, the cost of such systems is within economically practical values.

While one may wonder, in reviewing this story of progress, why it took so long to solve such a simple problem, it can be said that it is seldom in technology that such an important problem is so completely solved in such a short time.

2.1.3. Directive Broadcast Arrays. In the middle of the 1930's, spectrum congestion in the medium-frequency broadcasting band began

to be solved by the use of directive antennas. These were composed of two or more vertical radiators, usually towers, disposed geometrically and excited electrically to produce radiation patterns that control the field strength radiated toward another station. By this method, the interference can be maintained within prescribed limits in the area of other stations on the same or adjacent frequency assignments.

The success of the directive-antenna technique in North America has led to a much more intensive utilization of the available frequency band than would have been possible otherwise. At the present time several hundred broadcast stations employ directive systems for mutual protection, administered under precise technical standards by international treaty.

This remarkable branch of antenna engineering has developed rapidly under the ever-increasing complexity of the allocation situation as the number of stations in service increased. The number of radiators needed to produce the more complex radiation patterns has been increasing year by year until, at the present time, systems of nine radiators are being used or proposed, with even more extensive systems likely to be used in the future.

Appendix VIII is included to show the development of the 620-kilocycle channel as of 1949, using directive antennas.

2.2. Prediction of Medium-frequency Coverage

The antenna and the power of the transmitter determine the unattenuated field strength at unit distance, which we take to be 1 mile (1.61 kilometers). Table 2.1 shows the theoretical maximum field strength in millivolts per meter at 1 mile with uniform-section vertical radiators for different practical heights (in electrical degrees) and different powers. These are the values one would measure on the 1-mile circle around the antenna if the earth were a perfect conductor and the antenna system 100 per cent efficient. By proper design of ground system and proper choice of site, measurements corrected for attenuation within the first mile should approach these values closely.

The prediction of coverage proceeds directly from the use of ground-wave propagation curves, such as those included in the Federal Communications Commission Standards of Good Engineering Practice Concerning Standard Broadcast Stations.[20] Plotted for reference values of 100 millivolts per meter unattenuated at 1 mile, they show field strength versus distance for soil conductivities ranging from the best existing in nature (over sea water) to values corresponding to the worst ordinarily

encountered, and for different frequencies between 550 and 1,600 kilocycles. Figure 2.2 shows the curves for the range 970 to 1,030 kilocycles. If the soil conductivities are known throughout the region to be served

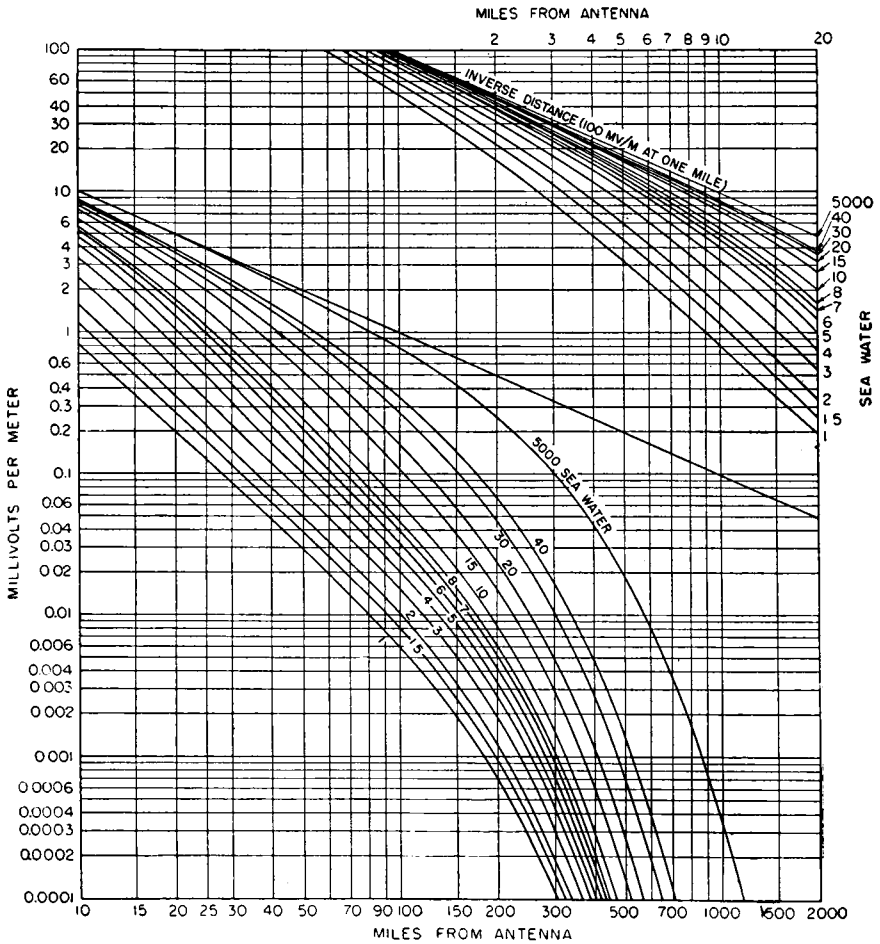

FIG. 2.2. Ground-wave field-strength versus distance curves for 970 to 1,030 kilocycles based on 100 millivolts per meter unattenuated at 1 mile along the ground. (*Federal Communications Commission.*)

by direct ground waves, the field strengths over a whole region can be predicted.

When the electrical characteristics of the ground are not known, one with long experience in such propagation problems can often estimate it from an examination of the soils and geology of a region. Otherwise,

soil-conductivity measurements must be made. Conductivity* is not always the same over a large area. When it is not, a composite attenuation curve must be developed along each radial from the antenna base to all points of prime interest. The ground-wave propagation curves shown in Fig. 2.2 are adjusted for the actual field strength at 1 mile for the frequency, antenna, and power used, by proportion to the 100 millivolts per meter used for these curves. For example, if the expected field intensity at 1 mile is to be 1,100 millivolts per meter, then all field strengths will be eleven times those shown on the curves.

2.2.1. Field-strength Contour Mapping. To construct a field-strength contour map of a station, a number of field-strength versus distance curves are measured and plotted for several radials from the antenna out to a distance where the signal approaches the ambient-noise level. The location of various field strengths can then be transcribed on a map and the various signal strength contours drawn in.[22] The choice of contours depends on the region, the population distribution, and the situation with regard to interference, if any, on the channel.

The usual purpose of such a map is to show service areas of different classes served by direct ground wave. These represent the daylight coverage, but not necessarily the nighttime coverage, because interference between ground waves and sky waves causes selective fading that may reduce the satisfactory service range appreciably under some conditions.

A typical example of the manner in which a composite-conductivity radial is computed is the following: A station on 1,000 kilocycles, operating with a power of 10,000 watts with a vertical radiator 60 degrees high and an optimum ground system, is situated on a plain having a conductivity of 7×10^{-14} electromagnetic unit. In one direction, this conductivity extends for a distance of 6 miles, then becomes fresh water for a distance of 11 miles with a conductivity of 10×10^{-14}. From here on, there is sandy and rocky soil with an average conductivity of 2×10^{-14}.

* In speaking of soil conductivity it must be remembered that it is not a "constant" but is actually a function of frequency, in addition to being variable in depth as well as in area. Soil texture and composition are likely to vary greatly with depth, as will also the moisture content, which affects both conductivity and inductivity. Since the depth of penetration of earth currents tends to be greater with lowering of frequency, the characteristics of the lower subsoil become increasingly important for the lower frequencies. At higher frequencies, penetration depth may be determined by the inductivity, especially where the water table is relatively near the surface. The effective conductivity of any given soil is therefore an empirical value in any given area and cannot be measured statically by using small samples in the laboratory. When we speak of conductivity here, we refer to the actual effective value at a given frequency, taking account of the fact that the effective conductivity of a particular soil will, in general, be different for other frequencies.

TABLE 2.1. UNATTENUATED FIELD STRENGTHS AT 1 MILE FROM UNIFORM-CROSS-SECTION VERTICAL RADIATORS HAVING ESSENTIALLY SINUSOIDAL CURRENT DISTRIBUTION, AS FUNCTIONS OF ELECTRICAL HEIGHT G DEGREES AND RADIATED POWER

(To convert to the basis of 1 kilometer, multiply all values by 1.61. Field strengths in millivolts per meter)

G, degrees	Power radiated, watts									
	10	25	100	250	1,000	5,000	10,000	50,000	100,000	1,000,000
10	18.6	29.4	58.9	93	186	417	589	1,320	1,860	5,890
20	18.6	29.4	58.9	93	186	417	589	1,320	1,865	5,895
30	18.7	29.6	59.2	93.5	187	419	592	1,327	1,870	5,920
40	18.8	29.7	59.5	94.1	188	421	595	1,333	1,880	5,950
50	18.9	29.9	59.8	94.6	189	423	598	1,341	1,890	5,980
60	19.0	30.1	60.2	95.1	190	426	602	1,350	1,900	6,020
70	19.1	30.2	60.5	95.6	191	428	605	1,357	1,910	6,050
80	19.3	30.5	61.1	96.6	193	432	611	1,369	1,930	6,110
90	19.5	30.8	61.7	97.6	195	437	617	1,384	1,950	6,170
100	19.7	31.2	62.4	98.6	197	442	624	1,400	1,970	6,240
110	20.0	31.6	63.3	100.	200	448	633	1,420	2,000	6,330
120	20.3	32.1	64.3	101.6	203	455	643	1,442	2,030	6,430
130	20.7	32.8	65.5	103.7	207	464	655	1,470	2,070	6,550
140	21.1	33.4	66.8	105.6	211	473	668	1,500	2,110	6,680
150	21.6	34.2	68.4	108.1	216	484	684	1,532	2,160	6,840
160	22.1	35.0	70.0	110.7	221	495	700	1,568	2,210	7,000
170	22.8	36.1	72.2	114	228	511	722	1,620	2,280	7,220
180	23.6	37.4	74.7	118	236	529	747	1,675	2,360	7,470
190	24.5	38.8	77.6	123	245	549	776	1,740	2,450	7,760
200	25.5	40.3	80.8	128	255	571	808	1,810	2,550	8,080
210	26.5	41.9	84.0	133	265	594	840	1,880	2,650	8,400
220	27.3	43.2	86.5	136	273	612	865	1,940	2,730	8,650
230	27.6	43.7	87.5	138	276	618	875	1,958	2,760	8,750
240	26.8	42.4	84.9	134	268	600	849	1,900	2,680	8,490
250	24.4	38.6	77.3	122	244	547	773	1,733	2,440	7,730
260	20.5	32.4	65.0	103	205	459	650	1,453	2,050	6,500
300	6.0	9.5	19.0	30	60	135	190	427	600	1,900

The field at one mile, from Table 2.1, is 602 millivolts per meter. From Fig. 2.2 for 1,000 kilocycles and a conductivity of 7×10^{-14}, we find that the field strength has fallen to 11 per cent of the unattenuated value of 1 mile, or to 66 millivolts per meter at 6 miles. In passing over the fresh water a distance of 11 miles, a distance between 6 and 17 miles

from the antenna, the signal is decreased to 23 per cent of 66 millivolts per meter, or to a value of 15 millivolts per meter.* From here on, the conductivity of 2×10^{-14} attenuates the signal as listed:

Distance from antenna, miles	Ratio of field strength at distance to that at water's edge 17 miles from antenna	Expected field strength, millivolts per meter
17	1.00	15
25	0.42	6.2
50	0.16	2.4
75	0.04	0.6
100	0.02	0.3
150	0.0064	0.096

If the ambient-noise level during daylight hours at a town on this radial at a distance of 150 miles averages 30 microvolts per meter, the signal-to-noise ratio average would be approximately 10 decibels.

In the same way, each radial can be computed, and the service range of the station in terms of signal-to-noise ratios or in terms of actual field strengths can be determined. The same procedure is followed if a directive antenna is used, except that in the latter case the field strength along the ground at 1 mile will vary with the azimuth angle depending upon the directive pattern of the array.

2.2.2. Soil-conductivity Measurements. When the soil conductivities are not known, they must be measured in some manner. The best known method is to use a test transmitter to radiate signals and to measure the field strengths with a suitable field-strength meter. If a test transmitter is used, it is best to operate at the frequency for which the data are desired. Sometimes measurements can be made on another radio station operating at some other frequency and the data converted to conductivity in the manner prescribed in detail in the FCC Standards of Good Engineering Practice Concerning Standard Broadcast Stations.[20] This same procedure is standard with all nations that are parties to the North American Regional Broadcasting Agreement (NARBA).

For ordinary use where precision of the result is not important, and

* This method is adequate for practical purposes when the differences in conductivities for different portions of the ground path are small. The method is subject to errors of importance when, for example, a land path with a conductivity of 2×10^{-14} changes to sea water. In such cases, more accurate results may be obtained by computing the same path in both directions by the method outlined, interchanging the locations of transmitter and receiver, and averaging the two curves point by point along the radial.

for longer distances from the transmitting site, the conductivity may be obtained by the ratio method. Measurements of field strength are made on a known frequency at large-distance intervals (such as every 5 miles or more) and a sufficient number of measurements made in each locale to establish a reliable average field strength at these distances. During the measurements the transmitting-antenna current is maintained at a constant value. Then, by taking the ratio of the measured fields at, say, 5 and 10 miles on the same radial ,one can refer to the ground-wave propagation curves for that frequency and find the conductivity curve that gives the same field-strength ratio for these same distances. The conductivity curve giving the same ratio may then be taken as the value of conductivity for this interval. The same is done for other intervals of distance. The intervals may be chosen according to convenience of access and measurement and would normally include regions of special interest in coverage studies.

By this method, a few careful measurements can quickly establish a working value of conductivity to use in any subsequent studies. If the test frequency is other than that to be used for operation, the value of conductivity found is transferred to the propagation curves for the desired frequency and the field strengths calculated therefrom. If soil characteristics are obviously constant over a very large area, one ratio measurement may suffice. Where the soil or topography varies in character, the ratios and conductivities for several intervals of distance are required.

As an example of how this is applied, let us assume that measurements of field strength were made on a frequency of 1,000 kilocycles, and the result was a value of 17 millivolts per meter at 6.5 miles. At 13 miles the average value on the same radial was 4.85 millivolts per meter. The ratio is 3.5. Looking now at the propagation curves for 1,000 kilocycles (Fig. 2.2), at these same distances, it is found that a conductivity of 4×10^{-14} electromagnetic unit gives this same ratio. This is taken as the conductivity for the terrain between 6.5 and 13 miles.

There is a practical precaution to observe in this process. Since the field-strength ratios must be precisely determined (because a small difference in the ratio may make a substantial error in the conductivity figure), care should be taken wherever possible to use distance intervals that will permit the two sets of measurements to be made on the same attenuator position of the field-strength meter. There is almost always a small error between attenuator positions, which is ordinarily negligible but which in this type of measurement cannot be tolerated. This error becomes inconsequential when large-distance intervals and higher frequencies are used to give rather large field-strength ratios.

A more exact method of determining conductivity is that in which a

TABLE 2.2. GROUND-WAVE FIELD STRENGTH VERSUS DISTANCE

[Field strength in per cent of the field strength (unattenuated) at 1 mile from the antenna]

Distance, miles	Distance, kilometers	Conductivities × 10^{-14} electromagnetic unit						
		Sea water 5,000	40	20	10	5	2	1
A. 610 kilocycles per second								
1	1.61	100	99	98	96	93	85	72
2	3.22	50	49	48	47	43	38	29
5	8.05	20	20	19	18	16.1	11.7	7.3
10	16.1	10	9.7	9.0	8.2	6.9	4.1	2.1
20	32.2	5	4.6	4.2	3.6	2.6	1.1	0.49
50	80.5	1.9	1.67	1.35	0.90	0.45	0.134	0.068
100	161	0.83	0.68	0.45	0.230	0.090	0.030	0.015
200	322	0.29	0.20	0.105	0.041	0.0145	0.0044	0.0022
500	805	0.028						
B. 790 kilocycles per second								
1	1.61	100	99	98	96	91	77	60
2	3.22	50	49	4.8	47	43	32.5	22.5
5	8.05	20	19.5	19.2	17.2	14.2	8.7	5.0
10	16.1	10	9.5	8.6	7.5	5.6	2.55	1.30
20	32.2	5.0	4.38	3.8	2.9	1.73	0.61	0.30
50	80.5	1.85	1.42	1.03	0.58	0.240	0.078	0.043
100	161	0.82	0.51	0.29	0.120	0.046	0.017	0.0092
200	322	0.270	0.125	0.052	0.0173	0.0065	0.0022	0.00115
500	805	0.023						
C. 1,000 kilocycles per second								
1	1.61	100	99	97	93	87	68	49
2	3.22	50	49	4.7	44	39	26.4	17.2
5	8.05	20	18.3	17.4	15.3	12.0	6.0	3.35
10	16.1	10	8.8	8.0	6.3	4.15	1.58	0.83
20	32.2	5	3.95	3.26	2.1	1.04	0.35	0.200
50	80.5	1.8	1.15	0.72	0.324	0.127	0.048	0.028
100	161	0.79	0.35	0.160	0.062	0.026	0.010	0.0057
200	322	0.25	0.067	0.0234	0.0082	0.0032	0.00115	0.00067
500	805	0.0185						

TABLE 2.2. GROUND-WAVE FIELD STRENGTH VERSUS DISTANCE. (*Continued*)

Distance, miles	Distance, kilometers	Conductivities × 10^{-14} electromagnetic unit						
		Sea water 5,000	40	20	10	5	2	1
		D. 1,210 kilocycles per second						
1	1.61	100	98	96	91	81	59	41
2	3.22	50	49	46	42	35	21.3	13.3
5	8.05	20	18.3	17.0	14.0	9.6	4.3	2.43
10	16.1	10	8.6	7.2	5.25	2.85	1.102	0.590
20	32.2	5	3.7	2.7	1.53	0.650	0.230	0.144
50	80.5	1.8	0.95	0.48	0.190	0.080	0.032	0.021
100	161	0.78	0.244	0.092	0.037	0.0154	0.0066	0.0042
200	322	0.24	0.037	0.012	0.0044	0.00182	0.00070	0.00043
500	805	0.016						
		E. 1,380 kilocycles per second						
1	1.61	100	97	95	89	77	53	36.4
2	3.22	50	48	45	40	32	18.5	11.2
5	8.05	20	18	16	12.5	8.2	3.45	1.95
10	16.1	10	8.2	6.6	4.35	2.18	0.71	0.48
20	32.2	4.9	3.40	2.30	1.15	0.47	0.185	0.118
50	80.5	1.8	0.77	0.35	0.133	0.061	0.0265	0.017
100	161	0.78	0.176	0.065	0.027	0.0125	0.0050	0.0032
200	322	0.23	0.024	0.008	0.00305	0.00125	0.00038	0.00032
500	805	0.0135						
		F. 1,600 kilocycles per second						
1	1.61	100	96	93	85	71	45	31
2	3.22	50	48	43	37.5	28	14.5	9.4
5	8.05	20	17.2	15.0	10.8	6.2	2.5	1.6
10	16.1	10	6.6	5.8	3.4	1.54	0.58	0.39
20	32.2	4.8	2.95	1.76	0.79	0.32	0.137	0.096
50	80.5	1.76	0.57	0.23	0.092	0.044	0.0195	0.0127
100	161	0.75	0.113	0.041	0.018	0.0084	0.0037	0.0026
200	322	0.215	0.0145	0.0043	0.0018	0.00077	0.00046	0.00023
500	805	0.011						

large number of field-strength measurements are made along a radial line and the complete attenuation curve is plotted from these data out to any given distance. From such a curve, the slope as a function of distance indicates the conductivity, by direct comparison with the ground-wave propagation curves. When the measured curve is plotted on exactly the same paper as used for the reference propagation curves, and to the same scales, the conductivities can be found by matching the slopes of the measured and reference curves, at the various distances.

Table 2.2 provides the basic information for the plotting of accurate ground-wave propagation curves for the frequency range 600 to 1,600 kilocycles.[20] By interpolation between the values given, the values for all intermediate frequencies, conductivities, and distances can be obtained. For practical use, these data can be plotted on log-log coordinate graph paper, one sheet for each frequency. Other sheets should be made for intermediate frequencies, since there is enough change with frequency to require a different curve about every 50 kilocycles in this band.

2.2.3. Intermittent Coverage from Sky Waves. In circumstances where cochannel interference at night is negligible, it is frequently desired to know what service can be rendered intermittently at night by sky waves. The variability of the ionosphere makes this a statistical problem.

Considerable data on this type of propagation have been reduced to convenient curves. The FCC Standards of Good Engineering Practice Concerning Standard Broadcast Stations includes curves of sky-wave field strengths exceeding various percentages of the time from 5 to 95 per cent, for varying distances. Several representative values taken from these curves are given in Table 2.3. These data are used for allocation purposes in the 550- to 1,600-kilocycle band. If one wished to know approximately what field strength could be delivered to a locality at some particular distance such that the only signal received there would be sky wave at night 95 per cent of the time (corresponding to nearly 100 per cent reliable night signals), the values read from the curve are adjusted to correspond to the actual field strength delivered at 1 mile in the right direction and at the proper vertical angle to arrive at the locality by reflection from the ionosphere. The vertical angle of radiation of the waves for a given distance may be determined by the curves of Fig. 2.3.

From the ambient-noise levels, the signal-to-noise ratios for a certain portion of time can be calculated as a statistical average.

To show how this information is used, consider the following case: A station contemplates using 50,000 watts in a region where grade 4 noise (see Appendix VI-A to VI-D) prevails for more than 6 months a year. It is desired to deliver a semiservice at night in certain cities varying

in distance from 200 to 400 miles. What type antenna should be used, and what kind of service can be expected in these cities? (No interference from other stations is encountered on the frequency to be used.)

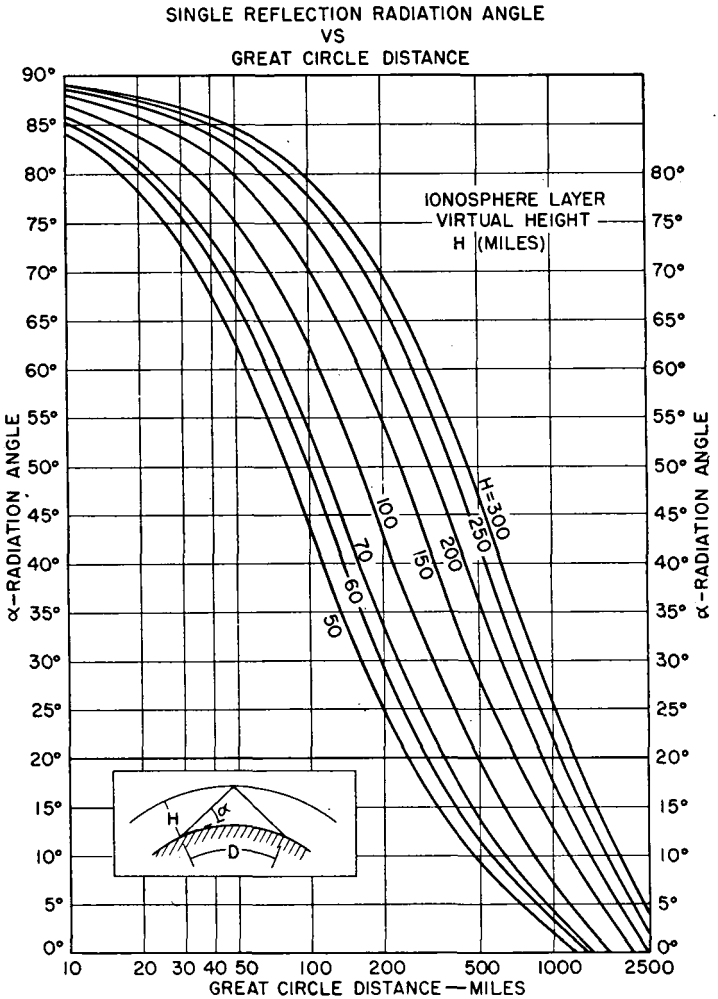

FIG. 2.3. Vertical radiation angles for sky-wave propagation.

From Fig. 2.3, the vertical angles of radiation for these distances vary from 30 to 15 degrees for a 60-mile-layer height. The antenna used must therefore have strong radiation at these angles. Guided by information from Fig. 2.6, we select an antenna approximately one-half wavelength high to obtain good ground-wave efficiency and yet have adequately large field strengths at vertical angles as high as 30 degrees. Referring to

TABLE 2.3. AVERAGE SKY-WAVE FIELD STRENGTH (HOURS OF DARKNESS)
(In per cent of field strength 1 mile from antenna at relevant vertical radiation angle)

Distance, miles	Distance, kilometers	Vertical radiation angle, degrees	Value of field strength exceeded		
			10 per cent of time	50 per cent of time	90 per cent of time
0	0	70–90	0.30	0.088	0.030
100	162	53	0.27	0.088	0.030
200	324	33.5	0.230	0.084	0.035
400	648	17.3	0.156	0.064	0.0200
600	972	10.6	0.097	0.042	0.0128
800	1,296	6.7	0.057	0.0250	0.0075
1,000	1,620	4.0	0.032	0.0135	0.0043
1,200	1,944	2.0	0.019	0.0075	0.00255
1,400	2,268	0.2	0.0123	0.0048	0.00163
1,600	2,592	....	0.0090	0.0034	0.00115
1,800	2,916	....	0.0067	0.0025	0.00085
2,000	3,240	....	0.0052	0.0020	0.00064
2,200	3,564	....	0.0041	0.0016	0.00046
2,400	3,888	....	0.0033	0.0013	0.00033

Table 2.1, for 50,000 watts radiated by an antenna 180 degrees high, the field strength along the ground at 1 mile, unattenuated, should be 1,675 millivolts per meter. At the vertical angles, the field strengths would be as follows:

Vertical angle, degrees	Distance, miles	Field at 1 mile, millivolts per meter	Field at this distance 50 per cent of nighttime, millivolts per meter
15	460	1,460	0.730
20	350	1,320	0.925
25	280	1,160	0.925
30	230	970	0.800
35	190	790	0.660

A minimum acceptable service requires a signal-to-noise ratio of 15 decibels 90 per cent of the time. During the dark hours the above field strengths are essentially those which will provide such a ratio according to Appendix VI-I. During the months when grade 3 noise exists, there is a somewhat better signal-to-noise ratio, provided that man-made

noise does not dominate natural atmospheric noise on which this information is based.

2.3. Radiation Characteristics of a Vertical Radiator

The type of radiator that is generally used for medium-frequency broadcasting is the straight uniform vertical with its lower end near ground. This type is also used for certain limited applications at the higher frequencies, and to some extent at lower frequencies. Such antennas may be steel towers used as radiators or supported vertical wire antennas. Extensive experience has been gained with vertical radiators at many hundreds of broadcast stations, each employing one or more for omnidirectional or directive radiation.

The radiation pattern for a vertical radiator is uniform in the horizontal plane (nondirective) but is directive in the vertical plane. The vertical directivity pattern depends on the distribution of currents in the radiator. If the radiator is of uniform cross section throughout its length, the current distribution is virtually sinusoidal; that is, the amplitude of the current is a sinusoidal function of the electrical distance from its upper end. This approximation does not lead to very serious deviations from physical fact for ordinary engineering purposes, and the simplifications in computations are desirable.

Pure sinusoidal distribution is the consequence of a pure standing wave on the radiator, which means that there are no losses whatever in the system. In fact, energy loss due to radiation and circuital loss requires that the actual current distribution be composed of a standing wave and a smaller component of traveling wave, the latter supplying the actual losses. In measurements that have been made of current distributions, the effect of the feed current due to the traveling-wave component is conspicuous only in the region of a current node, where instead of the current becoming zero, as it would from a pure sinusoidal distribution, it passes through a minimum value. At this minimum, the current has changed phase by 90 degrees and is then in phase with the antenna potential. The impedance therefore appears as a pure resistance at this point.

It is very helpful to the antenna engineer to have a clear physical concept of the manner in which waves are propagated in a linear conductor such as a vertical radiator and how the potentials, currents, and antenna impedance vary with its electrical length. For engineering purposes, the concept is sufficiently exact if the antenna is treated as an open-ended transmission line of uniform characteristic impedance.

In Figs. 2.4*A* and 2.4*B* there is represented graphically the solution of the current and potential distributions and the vector relations between

potential and current at all points along a vertical radiator 190 degrees high.

Figure 2.4*A* represents an attenuated traveling wave propagated in the antenna when excited by a generator connected between its base and

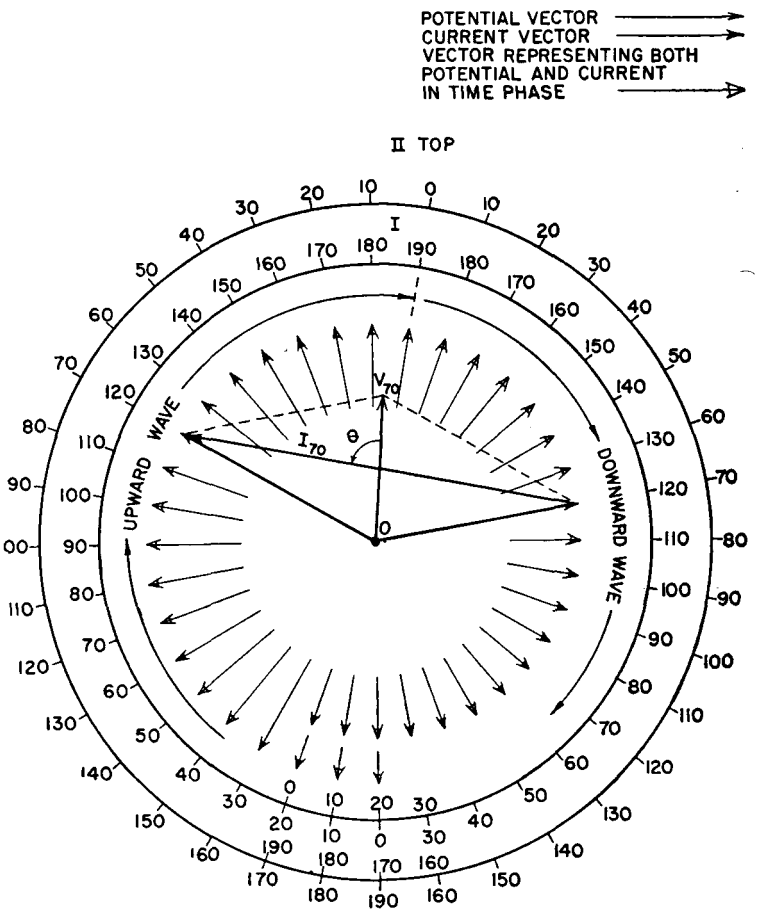

FIG. 2.4*A*. Development of current and potential distributions on a uniform vertical radiator 190 degrees high, representing the attenuation of a transmitted and reflected wave of charges, when the radiator is fed between its base and ground.

ground. For the time it takes to propagate this wave from the generator to the top of the antenna and back, the antenna appears to the generator as a resistance equal to its characteristic impedance. Therefore the potential and current vectors of the upward wave and the downward wave

of charges are in phase. The envelope of these vectors of the traveling wave that goes up and down the antenna is a logarithmic spiral.

Owing to the complete reflection of this traveling wave from the open end of the antenna, the vector sum of the currents from the upward and

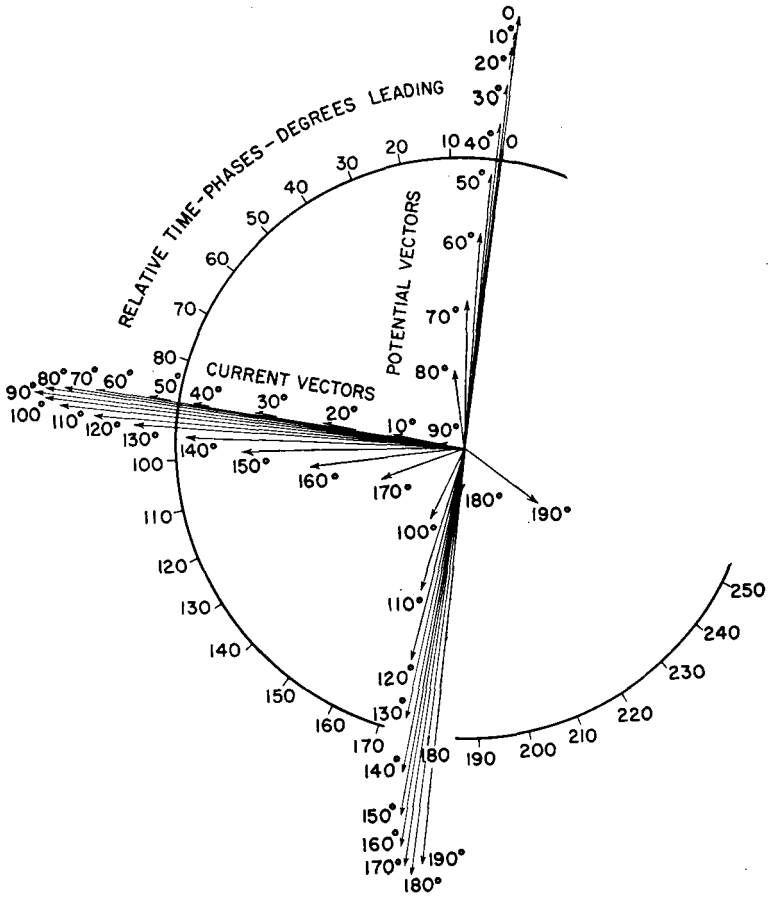

FIG. 2.4*B*. Development of current and potential distributions on a uniform vertical radiator 190 degrees high, representing the attenuation of a transmitted and reflected wave of charges, when the radiator is fed between its base and ground.

the downward waves must cancel to zero at the open end. This is accomplished by a reversal of the current vector in the downward wave. The potential vectors at the top add to double the potential of the traveling wave at that point.

The potential (and current) at any point in the antenna are the vector sums of the potentials (and currents) at that point due to the upward wave

and the downward wave with their propagation time-phase differences from that point to the top end and back again. This effect is illustrated for the point 70 degrees from the upper end in Fig. 2.4*A*, where the resultant potential at that point is shown to be obtained by *adding* the potential vectors for the two traveling waves and the resultant current by *subtracting* the current vectors. It is seen that at this point the resultant current vector leads the resultant potential vector by an angle θ less than 90 degrees. The antenna impedance at this point looking toward the open end is therefore $R - jX$.

Figure 2.4*B* is a polar plot of the resultants of performing similar vector additions of the potential vectors and vector subtractions of the current vectors at 10-degree intervals along the entire 190-degree antenna. These relations are more accurately tabulated in Table 2.4. Since in this diagram we are using the electrical distance from the top of the antenna, the 190-degree point is at the base near ground where the system

TABLE 2.4
(Computed values based on a traveling-wave attenuation of 2 decibels per wavelength)

Distance from open end, degrees	Potential		Current	
	Magnitude	Phase, degrees	Magnitude	Phase, degrees
0	1.000	0	0	
10	0.99	0	0.174	88
20	0.945	0	0.342	88
30	0.865	0.5	0.500	88
40	0.765	1.0	0.642	88.2
50	0.640	1.6	0.765	88.3
60	0.505	3.0	0.860	88.6
70	0.348	6.0	0.937	89
80	0.180	15	0.982	89.5
90	0.056	90	1.000	90
100	0.186	162	0.988	90.6
110	0.348	171	0.938	91.5
120	0.505	173	0.870	92.4
130	0.646	175	0.770	93.6
140	0.775	176.5	0.647	95.2
150	0.870	177.3	0.507	98.3
160	0.930	178	0.279	104.5
170	0.990	179	0.201	119
180	1.000	180	0.105	180
190	0.978	181.2	0.212	240

is usually fed. Therefore the vector ratio V_{190}/I_{190} represents the input impedance of the antenna between ground and its lower end. This of course omits consideration of any additional stray capacitance in parallel with this impedance which would be introduced by the physical construction of an actual antenna.

When the resultant potential and current vectors of Fig. 2.4*B* are plotted as in Fig. 2.5, we see the potential and current distributions in the manner most frequently displayed and described. In this diagram, only the magnitudes are shown, whereas in Fig. 2.4*B* both magnitude and phase are shown. The comparison with sinusoidal theory is indicated also.

From Fig. 2.4*B* it can be seen how the impedance looking toward the upper end from any point varies with the location of the point. It is evident that:

1. At all points less than 90 degrees from the upper end the impedance is $R - jX$ and that R increases and X decreases as the distance from the end increases.
2. At the 90-degree point, the impedance is pure resistance, and the resultant potential vector has turned 90 degrees from the open end.
3. Between 90 degrees and 180 degrees the potential vector leads the current vector so that the impedance looking upward from any of these points is $R + jX$, with resistance and reactance both increasing with increased distance from the top.
4. At the 180-degree point the current is in phase with the potential, and their ratio is such as to give an impedance that is a high value of resistance. Therefore the reactance had to change from a high value at some point less than 180 degrees to fall rapidly to zero at the 180-degree point.
5. Beyond the 180-degree point we see the beginning of another cycle of events where the potential is falling, the current is rising, and the current is leading the potential. It is evident, therefore, that between 180 degrees and 270 degrees the antenna impedance would be $R - jX$ again, but with both R and X decreasing with increase of length.
6. All these cycles of changing sign of reactance and changing values of resistance and reactance are typical of an open-circuited transmission line with attenuation. Qualitatively the analogy is satisfactory. Quantitatively the analogy fails to provide sufficient accuracy so that empirical data like that of Figs. 2.15 and 2.16 have to be used for engineering-design purposes.

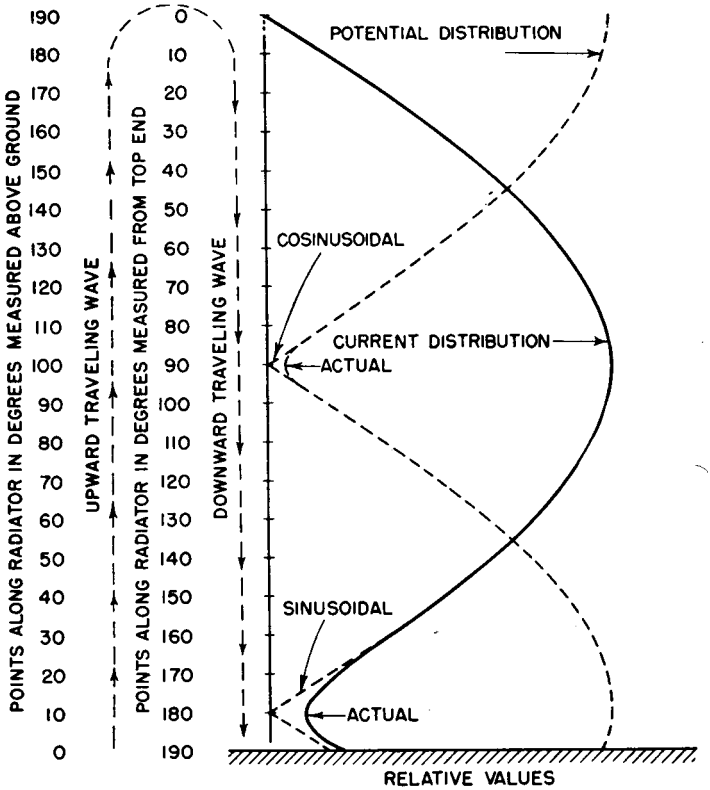

FIG. 2.5. Comparison of current distributions for sine and actual relative values on a 190-degree uniform vertical radiator.

2.3.1. Radiation Patterns for Sinusoidal Current Distribution. The radiation pattern for a vertical radiator with sinusoidal current distribution may be found from the following equation, in which G may be any value, large or small, and α is the angle above the horizon:

$$f(\alpha) = \frac{\cos (G \sin \alpha) - \cos G}{\cos \alpha (1 - \cos G)}$$

When $G = 90$ degrees (height is one-quarter wavelength), this equation reduces to

$$f(\alpha) = \frac{\cos (90 \sin \alpha)}{\cos \alpha}$$

When $G = 60$ degrees, the following equation may be used for the vertical radiation pattern:

$$f(\alpha) = \cos \alpha$$

These equations only give the *shape* of the pattern in relative values of field strength.

Figure 2.6 shows the vertical patterns, in rectangular coordinates, for vertical radiators from 45 to 225 degrees high, based on sinusoidal current distribution. Table 2.5 gives the relative values of the vertical pattern, in more convenient form for computational purposes, for eight

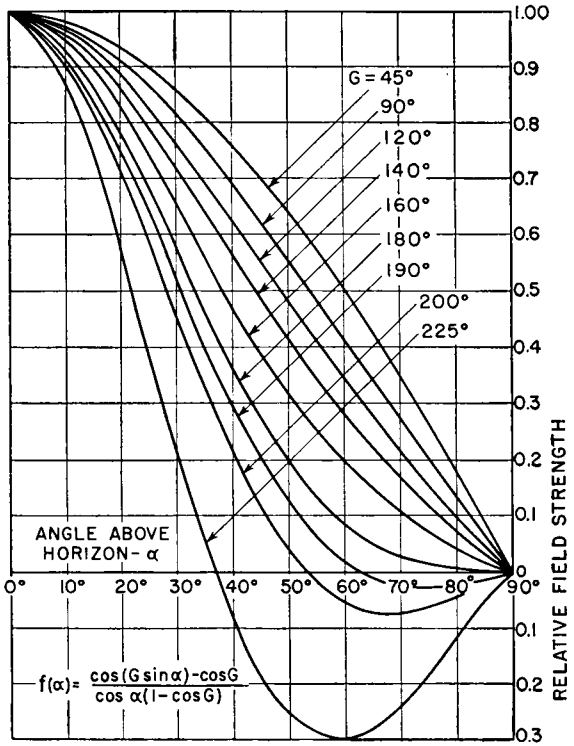

FIG. 2.6. Relative vertical radiation patterns for vertical radiators with sinusoidal current distributions for various electrical heights (G).

different heights corresponding to those of most frequent application for broadcasting. In this table are included the approximate values of the patterns in the region of a pattern null, which is the result of the fact that in practice the current never is zero at a node. The occurrence of a minimum instead of zero current at a node in the radiator produces an analogous effect on the radiation pattern, in that the pattern will have a minimum instead of a complete null. The phase of the electric field goes through the same kind of transition in passing a minimum as did the phase of the current in passing a node. There is a minimum in the vertical radiation pattern for every current minimum along the radiator.

Broadcasting applications almost never make use of radiators having more than one node, not counting the one that exists at the top of the antenna. The node at the top of the antenna has its radiation counterpart as a null in the pattern directly above the vertical radiator, or where $\alpha = 90$ degrees.

TABLE 2.5. VERTICAL RADIATION PATTERNS FOR VERTICAL RADIATORS OF DIFFERENT ELECTRICAL HEIGHTS WITH SINUSOIDAL CURRENT DISTRIBUTIONS

α	60°	90°	120°	150°	165°	180°	195°	210°
0	1.000	1.000	1.000	1.000	1.000	1.000	1.000	1.000
5°	.....	.....	.....	.....	.....	.....	0.981	0.977
10°	0.980	0.976	0.970	0.961	0.954	0.943	0.928	0.909
15°	0.958	0.950	0.937	0.913	0.896	0.873	0.844	0.804
20°	0.929	0.916	0.888	0.851	0.820	0.785	0.734	0.675
25°	0.890	0.869	0.833	0.777	0.736	0.683	0.616	0.524
30°	0.845	0.816	0.768	0.695	0.645	0.578	0.490	0.375
							(0.510)‡	(0.400)‡
35°	0.792	0.756	0.702	0.610	0.548	0.470	0.368	0.234
40°	0.735	0.695	0.629	0.527	0.458	0.370	0.256	0.111
						(0.390)‡	(0.270)‡	(0.150)‡
45°	0.673	0.628	0.554	0.446	0.370	0.278	0.159	0.008
50°	0.607	0.559	0.483	0.371	0.293	0.203	0.081	−0.066
						(0.225)‡	(0.125)‡	(0.160)‡
55°	0.536	0.488	0.413	0.301	0.227	0.136	0.022	−0.115
60°	0.464	0.414	0.344	0.238	0.170	0.087	−0.017	−0.143
						(0.110)‡	(0.080)‡	(−0.200)‡
65°	0.388	0.345	0.281	0.187	0.125	0.052	−0.040	−0.149
70°	0.312	0.271	0.218	0.140	0.088	0.025	−0.048	−0.138
						(0.050)‡	(0.075)‡	
75°	0.237	0.204	0.162	0.098	0.058	0.010	−0.047	−0.113
80°	0.158	0.138	0.106	0.063	0.036	0.003	−0.036	−0.082
85°	0.079	0.070	0.053	0.031	0.017	0.001	−0.020	−0.043
90°	0	0	0	0	0	0	0	0
*	190	195	203	216	225	236	250	265
†	306	314	326	348	362	380	402	426

* Unattenuated field strength at 1 mile with 1,000 watts radiated, in millivolts per meter.

† Unattenuated field strength at 1 kilometer with 1,000 watts radiated, in millivolts per meter.

‡ Figures in parentheses represent very nearly the actual values encountered in practice, taking into account the deviation from sinusoidal current distribution due to radiation losses in the antenna, shown only where the differences are of importance.

Having now the shape of the vertical patterns for simple vertical radiators, it remains to set the actual values of field strength that will result from a given power radiated from a given vertical radiator. Table 2.1

gives the values of unattenuated field strength at the surface of the ground at a distance of 1 mile from the radiator, for various values of G and power radiated.

A radiator of nonuniform cross section has a current distribution that departs from sinusoidal distribution from trivial to considerable amounts, depending on the geometry of the radiator. The distribution then becomes empirical and has to be solved as an individual case. The resulting vertical pattern is also empirical. Solutions for such cases have been published.[3,23]

It can be seen from the figures in Table 2.1 that the vertical directivity has an important influence on the horizontal field strength at 1 mile. The effect can be seen more clearly in Fig. 2.1, which shows the field strength at unit distance as a function of electrical height G for constant radiated power, using three different radiator heights as 100 per cent.

2.3.2. Choice of Vertical Radiation Pattern. An intelligent choice of a vertical radiation pattern for a particular application is made only after a computation of the ground-wave and sky-wave field strengths over the desired propagation paths. These two wave fields are separately computed, and special attention is directed to the distances at which their ratio is less than 2 to 1, because objectionable selective fading will occur at night at these distances. The location of this fading ring, or fading "wall" as it is often called, sometimes can be adjusted by the choice of vertical radiation pattern to fall where the least number of listeners is located. The variability of the sky-wave field strength from day to day will cause this fading ring to move about accordingly. Over ground where the direct wave is very rapidly attenuated, the fading ring may be quite narrow.

Consider a simple case of a broadcast station on 1,000 kilocycles in the center of a region having a uniform conductivity of 4×10^{-14} electromagnetic unit. The station will operate with a power of 10,000 watts. It is desired to see what the coverage will be with an antenna of 60 degrees height compared with one of 190 degrees. It is assumed that there are no regulatory reasons why either cannot be used. It is a grade 3 noise area. The data of Fig. 2.7 are computed and plotted from the vertical patterns for these two antennas and the ground-wave and sky-wave propagation information and noise data provided, using the given power and frequency.

The direct ground-wave intensity for the 60-degree radiator reaches the 15-decibel signal-to-noise threshold of 560 microvolts per meter at a distance of 49 miles, and for the 190-degree radiator at 55 miles. The 60-degree-radiator sky wave, for 10 per cent of the time at night, equals the ground-wave field strength at distance 49 miles (where it is also

noise-limited) and the fading ring for 2 to 1 direct and indirect signal ratio extends from 39 miles to 62 miles 10 per cent of the time. For 50 per cent of the time, the center of the fading ring would be at about 73 miles and the near edge of the ring under these conditions at about 57 miles.

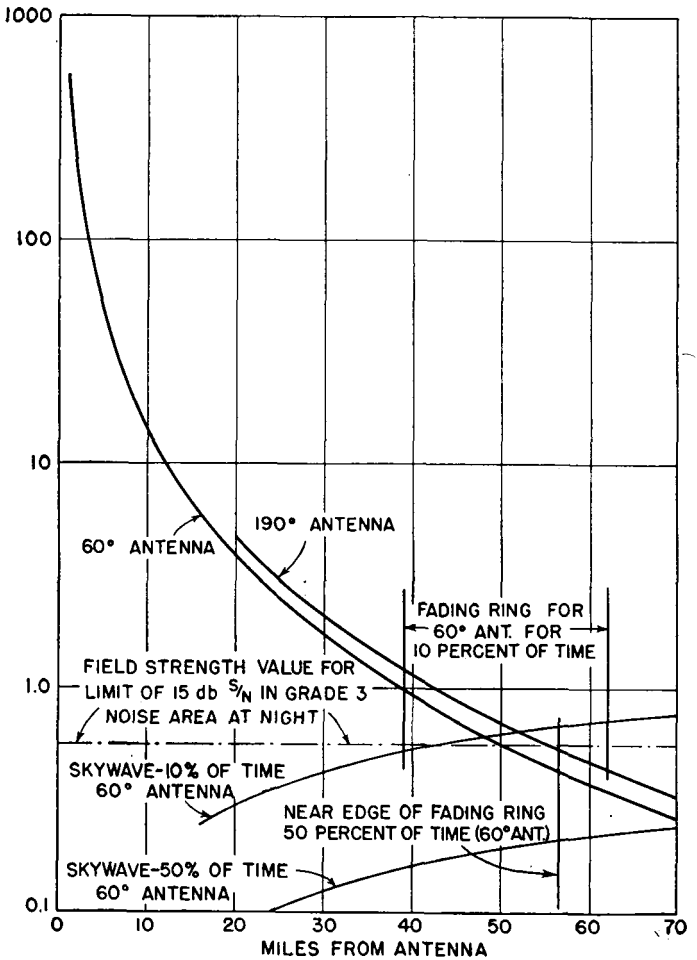

FIG. 2.7. Ground-wave and sky-wave curves for 10 kilowatts radiated from a 60-degree and a 190-degree radiator where $\sigma = 4 \times 10^{-14}$ electromagnetic unit, $f = 1{,}000$ kilocycles, in grade 3 noise area.

In this zone it appears that the signal is noise-limited before it is fading-limited, with this power.

For the 190-degree radiator, the sky-wave fields are not shown because it is known immediately from the chart thus far computed that the signal

will be severely noise-limited before arriving at the distance where fading is objectionable.

This example was chosen to demonstrate the influence of natural atmospheric noise on the solution of a problem of this type. One can readily see that, *under these circumstances*, it would be wasteful to invest in a 190-degree radiator when a 60-degree radiator will provide essentially the same fading-free and noise-free coverage. However, this example should not be used for any conclusion for other cases without completely calculating the problem in the manner outlined. The use of lower powers and higher frequencies in regions of lower conductivities and equal or higher noise levels would always show poor justification for expenditures for high radiators. For higher powers on lower frequencies, in regions of lower noise levels and higher conductivities, there would almost always be a case to justify investments in higher radiators. Intermediate combinations of frequency, power, conductivity, and noise conditions will always require specific detailed study of the actual data before a decision can be made.

Some marginal intermittent service is given by daytime sky-wave propagation due to E-layer reflections. The computations for such propagation can be made by reference to the data published by the Central Radio Propagation Laboratory of the National Bureau of Standards, following the methods used for computing high-frequency propagation. The effects of E sporadic layers may also be computed from these data.

2.3.3. Shunt-fed Radiators. A grounded vertical radiator may be shunt-fed as shown in Fig. 2.8. With shunt feed,[34,36] the radiator is grounded at its base, and the system is excited at the point where the shunt-feed wire is connected. By using a sloping wire, as shown in *B* of Fig. 2.8, a number of wire lengths and tapping points are available. The feed wire acts as a transformer which is adjustable over a certain range. In typical use, the feed wire is adjusted to bring a predetermined value of resistance at the input, which may be the value necessary to terminate a given transmission-line characteristic impedance. There is always an inductively reactive component of impedance present also, which is neutralized by a series capacitance. Any radiator can be shunt-fed in this way, provided that an adjustment can be found that will give a desired input impedance, or more usually it is necessary only to provide a given resistance component.

A shunt-fed vertical radiator does not use base insulators and therefore does not require any isolation circuits for tower-lighting circuits or for any top-mounted very-high-frequency antennas that may be present. By virtue of its direct grounding, it is somewhat less vulnerable to lightning

damage than a series-fed radiator. However, with a direct lightning hit on the tower, destructive potentials are sometimes transferred to the input to the feed wire, so that safety from lightning damage is not as complete as might be supposed.

A given vertical radiator, arranged for series feed, will have a series impedance at its base, which we shall designate as Z_{ab}, at a specified frequency. When this same radiator is grounded and fed with a shunt-feed connection, it is adjusted to give an input impedance Z_{as}. The shunt feeder thus acts as a transformer which converts Z_{ab} to Z_{as}. An equivalent circuit of such a transformer can be derived as a network, in the form of a T or L. While the transformation ratio is known, the phase shift between the current at the feed point and the current in the radiator is indeterminate.

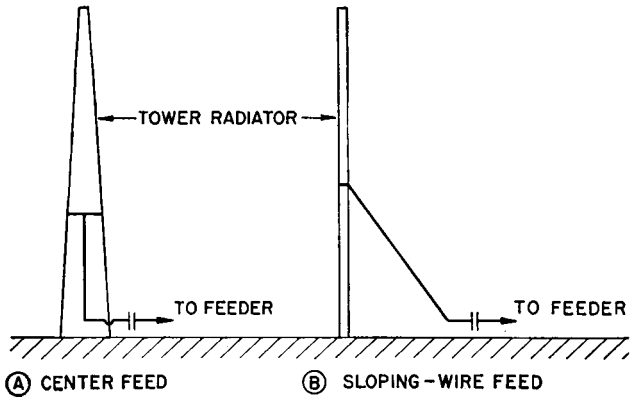

FIG. 2.8. Shunt-fed vertical radiators.

The optimum application for shunt feed is with a vertical quarter-wave radiator working into a low-impedance feeder. When the radiators are considerably more or less than 90 degrees high, the feed-wire adjustment requires that the loop formed between the feed wire, the radiator, and ground become relatively large, and this loop becomes a considerable radiator itself, modifying the intrinsic radiation properties and the current distribution of the radiator below the tapping point.

The quarter-wave shunt-fed radiator is the unbalanced analogy to the delta feed so commonly used for horizontal dipoles at high frequencies. In the latter system, the shunt feed is balanced. In both cases, the transforming action of the shunt feed is relatively small, and the reactive component introduced by the feed wire is not excessive, giving input impedances of relatively high power factor. Furthermore, the feed loop is not sufficiently large to cause excessive radiation, though there is some.

The amount of parasitic radiation that can be tolerated from the feed loop is something the designer must decide.

In broadcast applications, radiation from the feed loop causes the vertical radiation pattern for a single radiator to be distorted and eliminates the cone of silence directly above the radiator. High-angle radiation is therefore increased in all vertical planes, especially at the very high angles where, with series feed, the field strength would be zero.

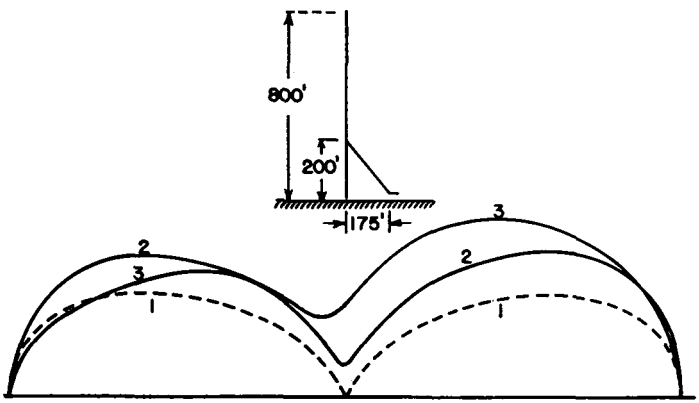

1. IDEAL VERTICAL PATTERN FROM SINUSOIDAL THEORY
2. MEASURED PATTERN NORMAL TO FEED-WIRE PLANE
3. MEASURED PATTERN IN PLANE OF FEED-WIRE

FIG. 2.9. Comparison of measured vertical patterns from series-fed and sloping-wire shunt-fed radiator of same height.

Figure 2.9 shows the measured vertical-plane patterns for a shunt-fed vertical half-wave radiator in the plane of the feed wire and in the plane normal to the feed wire. For comparison, the normal series-feed pattern is also shown by the dotted line. Figure 2.10 shows the measured current distribution along the vertical radiator which gave these radiation patterns. The distortion of the current distribution is rather extreme owing in part to the shunt feed and in part to the structural taper for this particular tower, which was self-supporting and tapered from 40 feet per side at the base to 1.5 feet per side at the top, 800 feet above ground. These data were obtained by model measurements by Brown and Epstein of the RCA Laboratories (not published), simulating an actual tower under study. They found that the area of the feed loop for this antenna could be greatly reduced by running the feed wire up the center of the tower, as shown in Fig. 2.8*A*, instead of using the usual external sloping wire. This made a considerable improvement in the measured vertical

radiation patterns, proving that radiation from the sloping feed-wire loop was an important modifying factor in the entire radiating system. The current distribution for these two types is illustrated in Figs. 2.11 and 2.12. Running the feed wire up the center of the tower seems very desirable when shunt-fed radiators are used in a directive array requiring moderate or high degrees of radiation suppression at some angles.

Shunt-fed antifading antennas introduce three factors that require special attention in design. One is the modification of the current dis-

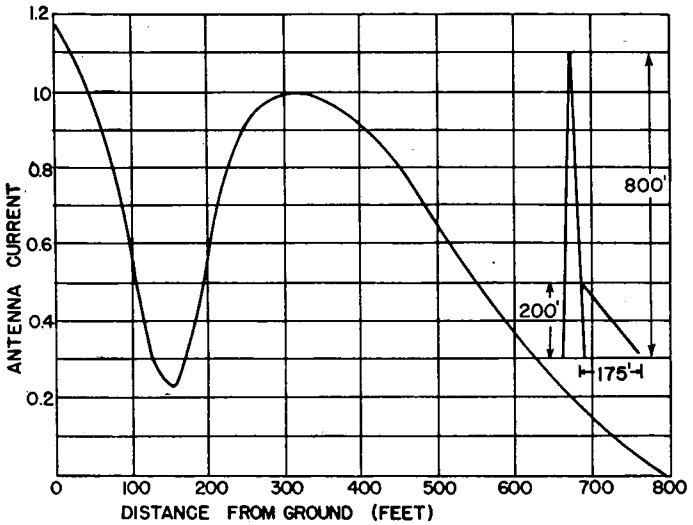

FIG. 2.10. Measured current distribution on vertical radiator shunt-fed and producing the patterns shown in Fig. 2.9 (curves 2 and 3).

tribution in the radiator below the feed point, which causes the current at the base of the radiator proper to be many times that present with series feed. This requires attention to reducing ground-system resistance as much as possible to maintain high radiation efficiency. This can be done by using a larger number of longer ground wires. The other point is the appearance of relatively high potentials at the feed point due to its high reactance when adjusted for the usual 50- to 70-ohm resistance to terminate a coaxial feeder. The high potential encountered at the feed point is the consequence of the feed current flowing into the high reactance of the input impedance. Precautions must be included to accommodate this condition, which in itself does not present a very difficult problem. The same factors that give a high input reactance will also contribute to selectivity. Attention must therefore be directed to this aspect of the application whenever bandwidth has to be considered.

The shunt-fed radiator is a system which appears to be more simple

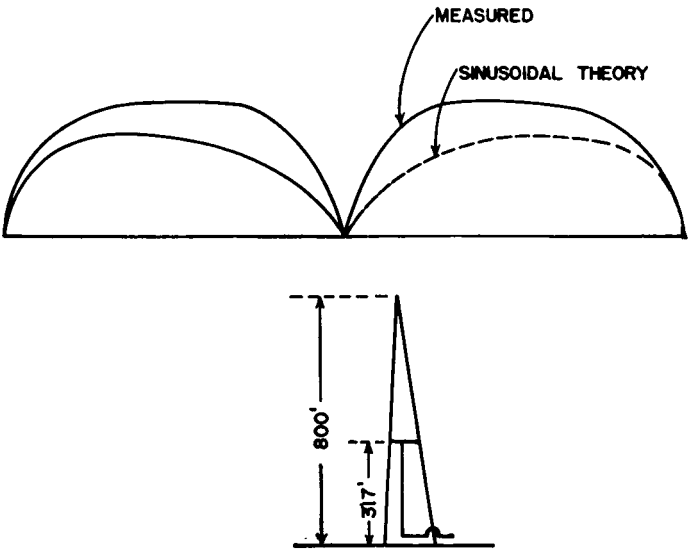

FIG. 2.11. Measured vertical patterns for axial shunt-fed vertical radiator.

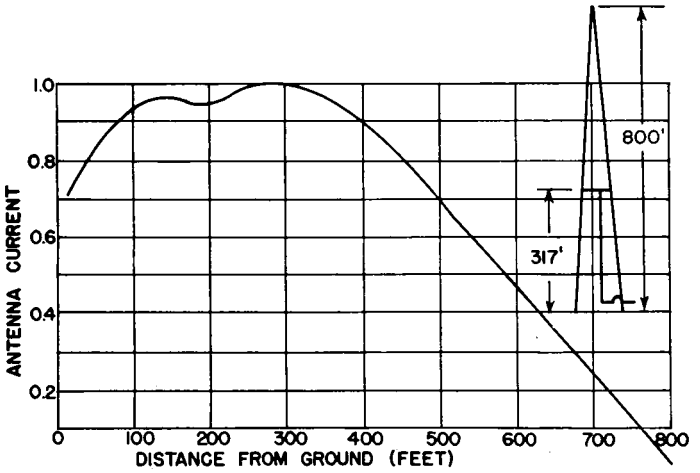

FIG. 2.12. Measured radiator current distribution for system producing the pattern of Fig. 2.11.

than it actually is. It must therefore be applied with caution in exacting circumstances. For instance, the use of the sloping-wire feed on an antifading radiator nullifies some of the important properties for which such a radiator is used. As an element in a directive array, it is cumbersome to design because all available reference data on which the performance of a directive array is predicted are for series feed. Shunt feed introduces the

impedance-transformer action, which is difficult to predict, especially when mutual impedances are taken into account. The sloping-wire feed, in addition to modifying the vertical pattern of each radiator, will introduce mutual impedances between feed wires which will, in general, be indeterminate during the design stage of the work. The coupling circuits must therefore be designed after measurements have been made on the final radiator system. There is also the complication that the phase and amplitude relations of the currents at the feed points will not be those prevailing in the radiators, and it is necessary to monitor radiator currents on the radiators above the tapping point. The design of a directive array of shunt-fed elements will usually require an enormous expenditure of engineering effort that may offset any structural economy. However, these remarks should not discourage the application of the shunt-fed radiator in cases where its simplicity and economic advantages can be realized and where the detrimental factors discussed are of minor importance.

2.3.4. The Folded Unipole. An alternative method of shunt feeding a vertical radiator one-quarter wavelength tall is that shown in Fig. 2.13, which may be called a folded unipole, from very-high-frequency terminology. By this method, which is one-half of a folded dipole, the total antenna current is divided between two conductors which are paralleled at their current nodes (at the top), and power is fed into one leg only. As with a folded dipole, the resistance at the feed point in one leg increases in proportion to the inverse square of the current ratio for the fed wire. This is evident from the following:

Let R_0 represent the base resistance of the radiating system operating as a simple series-fed antenna, and let I_0 represent the total base antenna current when the system has a power input of W watts. When excited as a folded unipole, the total antenna current for the same power input will be I_0 as before, except that, with one conductor grounded and the other fed by the transmitter, the latter carries only a portion M of the total current. Then, if R_1 designates the input resistance when excited as a folded unipole,

$$R_1 = \frac{R_0}{M^2}$$

The value of M will differ with the relative radii of the two conductors and will be 0.5 when the two conductors are identical, so that the total antenna current is equally divided between the two. However, when one conductor is a grounded quarter-wave tower and the other is a wire, the great disparity in radii will cause the value of M to be very much less than 0.5. If the tower and the "drop" wire were both continuous uni-

form-section cylindrical conductors, the value of M could be obtained from the relation

$$M = \frac{1}{1 + \dfrac{\log_{10} \dfrac{a}{\rho_1}}{\log_{10} \dfrac{a}{\rho_2}}}$$

where ρ_1 is the radius of the larger conductor, ρ_2 the radius of the smaller conductor, and a the axial separation between the two. However, if a

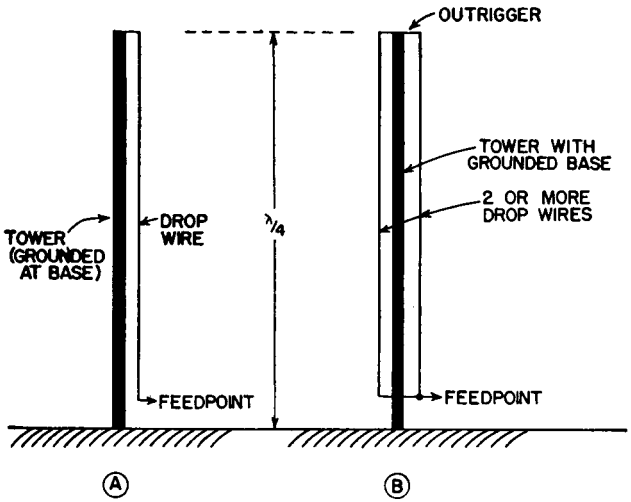

FIG. 2.13. Folded unipole principle for shunt-feeding vertical radiators.

steel tower that is not cylindrical is the larger conductor, an approximate value of M can be found by supposing the tower to be equivalent to a cylinder with the same sectional periphery.

A large tower and a small drop wire, as shown in Fig. 2.13*A*, will often yield rather small values of M. If one wishes to raise the value of M, two or more drop wires may be used, all insulated from the tower throughout their length except at the top and connected together at the bottom, where they are fed, as shown in Fig. 2.13*B*. Thus the transformation ratio of the drop wire can be varied more or less at will to bring a predesired value of resistance at the feed point. This may be a value of resistance that will directly match a given feeder characteristic impedance.

This method is best adapted to quarter-wave uniform-section radiators which are self-resonant by virtue of their height. Tapered towers can be made to be substantially of uniform section by using other drop wires suspended from a spreader at the top having the same width as the tower

base and connecting these wires to the tower proper. Then the additional drop wires for forming the unipole are affixed where they will not interfere with the former. Figure 2.14 shows a plan view of a tapered square radiator using drop wires for feeding and to equalize the tower cross section.

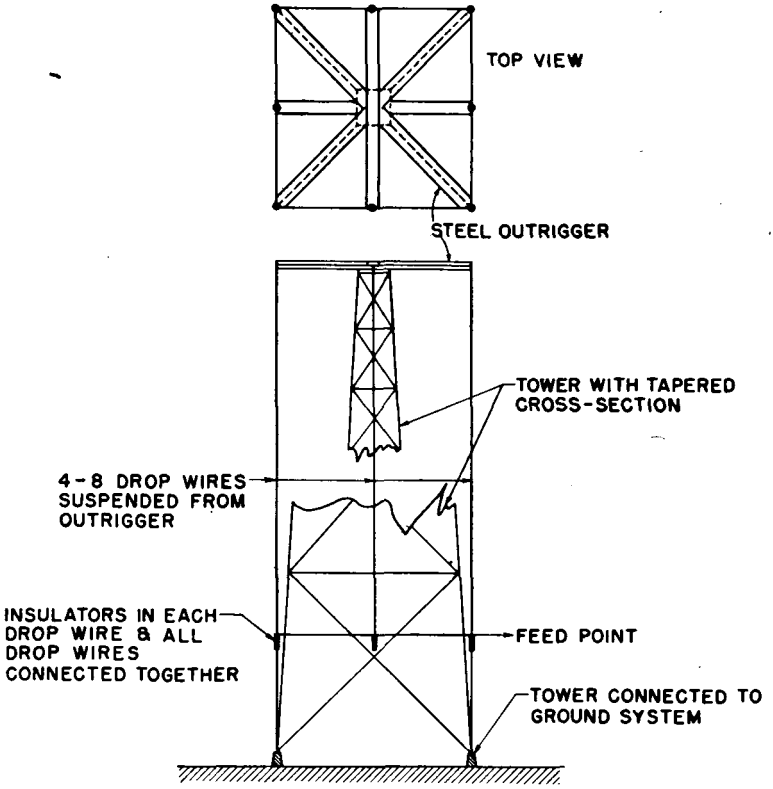

FIG. 2.14. Method of transforming a tapered tower to one of nearly uniform electrical section and using the folded unipole feed.

A folded unipole of this type allows all of the conveniences afforded by the use of directly grounded towers without compromising the natural current distribution or introducing pattern distortion from a sloping wire. The input impedance can be made almost purely resistive with a value that will directly match open-wire feeders of common types, designed for the proper characteristic impedance.

2.4. Impedance of Uniform-cross-section Vertical Radiators

The series impedance of a vertical radiator is a function of several variables, of which the dominant ones are the height, the longitudinal

and cross-sectional geometry, and the characteristics of the ground system. The series impedance under idealized conditions may be referred to as the "intrinsic impedance." This is the value obtained from theoretically pure conditions, using the methods of the electromagnetic

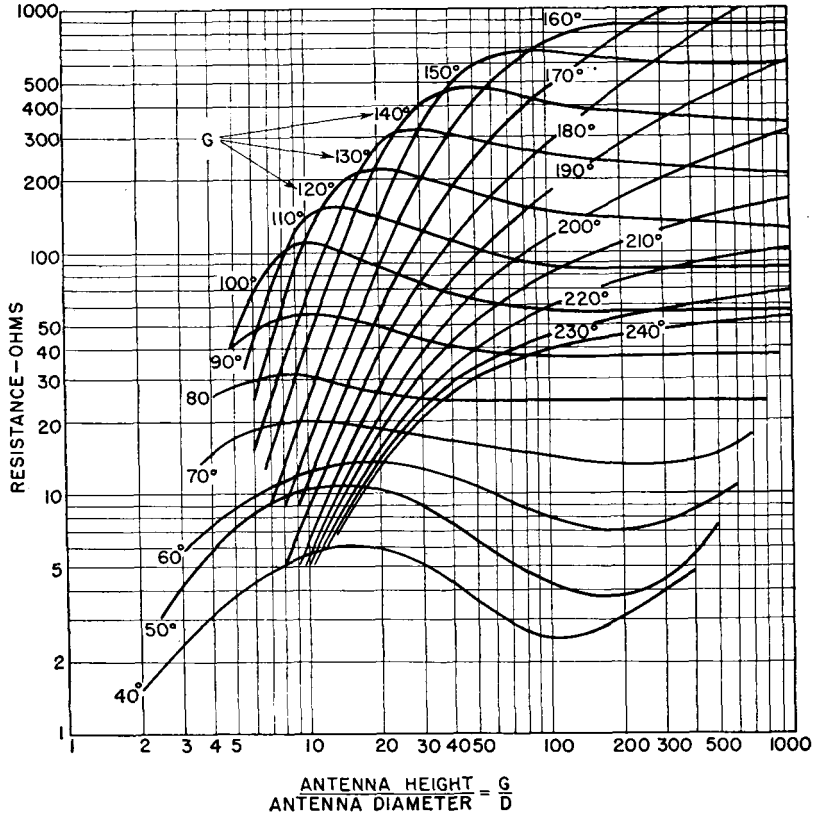

FIG. 2.15. Measured base (series) resistance for cylindrical vertical radiators over perfectly conducting ground. (*After Brown and Woodward.*)

theory, assuming perfectly conducting ground, zero base capacitance, and no internal losses. A continuous cylindrical vertical radiator of perfect conductivity, with its lower end very near to a perfectly conducting flat earth plane, has a resistance and a reactance that may be computed from published formulas.[1002] For practical use it is more convenient to refer to Fig. 2.15 for resistance and to Fig. 2.16 for reactance for cylindrical antennas of height G and height-to-diameter ratio G/D. These figures were derived from systematic measurements of scale models under carefully controlled laboratory conditions[1018] and are therefore of basic

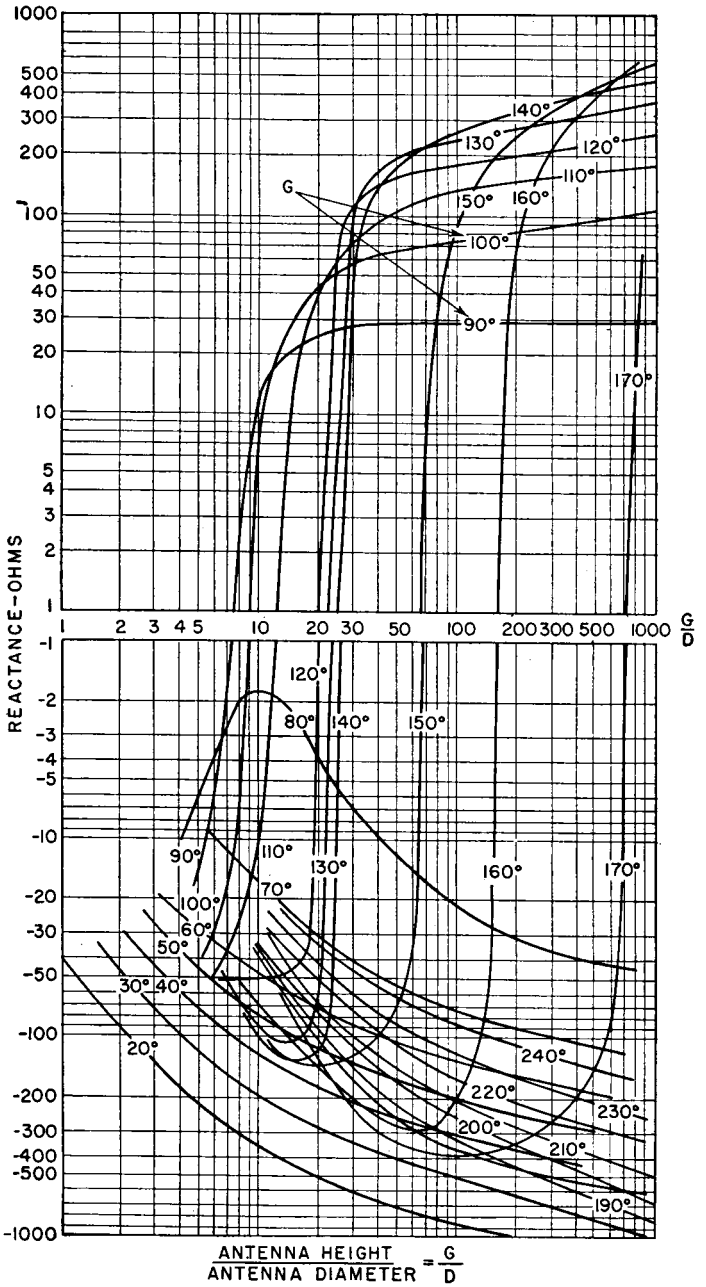

FIG. 2.16. Measured base (series) reactance for cylindrical vertical radiators over perfectly conducting ground. (*After Brown and Woodward.*)

importance for practical design. The values can be read with adequate accuracy for most purposes (see ref. 18, Chap. 5).

The intrinsic impedance of an antenna is modified by a number of empirical influences so that the impedance as seen from the accessible terminals of the system will differ from the idealized values. These empirical influences may be due to such factors as the capacitance introduced by a base insulator, the effects of attached guys, the ground system, proximity to nearby objects that reradiate, and attachments for power feed to tower lights, feeders for frequency-modulation or television antennas that may be mounted on the radiator, spark gaps, and other devices. The impedance is also modified by practical cross-sectional configurations for a fabricated mast or tower and by nonuniform cross section.

It is apparent from the foregoing that one must be content with approximate estimated values of radiator impedance values during preliminary design, leaving for the final stage the measurements to be made after erection. Typical coupling networks for energizing the system have sufficient adjustability so that they will accommodate any ordinary discrepancies between the preliminary estimated values and the final working values. When two or more radiators are to be employed in a directive array, the estimated impedances must be derived with care if the feeding networks are to be precalculated with acceptable accuracy.

An example of the use of the intrinsic impedance data to estimate the input impedance to a vertical radiator under actual working conditions is the following:

A vertical radiator of height $G = 125$ degrees at a frequency of 600 kilocycles will have a square cross section 10 feet per side. The base insulator to be used has a capacitance of 60 micromicrofarads. A tower-lighting transformer and spark gap will add another estimated 75 micromicrofarads in parallel with the base insulator. No other attachments are needed. What will input impedance be at 600 kilocycles?

The periphery of the antenna should be equivalent to a cylinder having a diameter of about 12 feet. At 600 kilocycles this diameter expressed in electrical degrees is 2.63. The ratio $G/D = 47.6$. For this form factor and height 125 degrees, Fig. 2.15 shows a resistance of about 240 ohms, and Fig. 2.16 shows a reactance of about $j185$ ohms. These are the components of the intrinsic impedance of the antenna without any spurious influences. If now the effect of the capacitance of 135 micromicrofarads added across the base of the radiator is computed, it is found that the input impedance to the system will then be

$$Z_{in} = 289 + j165$$

When tower-lighting power is fed through an isolating inductor, an inductive reactance may then appear across the base insulator, which neutralizes a portion of the base-insulator capacitive reactance. In addition, the resistance of such an inductor parallels the antenna resistance, owing to its finite dissipation factor Q. If this inductor is self-resonant at the working frequency, its presence modifies only the resistance. If its resonant frequency is lower than the working frequency, it will act as a shunt capacitance. In some instances the reactance of the isolation inductor can be made equal to that of the base insulator and of sufficiently high Q so that the input impedance to the system is very nearly equal to the intrinsic antenna impedance.

The transformed impedances of vertical radiators are of special interest in directive arrays where the design of the entire system must proceed on computed values of impedances and networks. This is because it is physically impractical to measure the desired impedances until the array is functioning correctly. It must be remembered that the theoretical values of mutual impedance are also intrinsic values. The input impedance to each radiator in an array is computed first with intrinsic values of self- and mutual impedances. These different impedances are then transformed to true accessible impedances through the masking impedances of the various attachments, base insulator, etc. It is in such cases that one may desire to design light-feed isolation inductors to neutralize the reactance of the base insulator so that intrinsic and observed impedances will be in accord.

2.5. Ground Systems for Broadcast Antennas

Antenna performance is standardized with reference to the ground being a perfectly conducting flat plane. Such an assumption serves a very useful purpose in revealing the ultimate possibilities of a certain radiator in terms of its dimensions and longitudinal and sectional geometry at a given frequency. All practical deviations from this norm are due to a number of empirical circumstances, of which one is the earth itself.

A line of electric force (displacement current) extends from the top of the antenna through surrounding space to the earth. Upon entering a perfectly conducting earth it becomes a conduction current which returns to the base of the antenna and becomes a portion of the antenna current. The electric lines of force of the antenna field are thus seen to be the continuation current of a closed circuit through surrounding space. With a perfectly conducting earth, the electric line of force is always normal to the surface. When the earth is imperfectly conducting, the line of force tilts forward in the direction of propagation. This means

that the Poynting vector at the surface of the earth is tilted downward and has a component that points into the earth where it is dissipated. The component parallel to the earth represents the power propagated onward in the half space above the ground.

A vertical radiator above natural earth without any sort of ground system, energized by an electromotive force between the antenna and the earth, would require all earth currents to return to the antenna through a very imperfect conductor. The earth is actually an imperfect dielectric in that it has both finite conductivity and inductivity. The range of values encountered in engineering practice in various soils and various amounts of water may be said to be the following:

For land:

Conductivities—from 1×10^{-14} to 100×10^{-14} electromagnetic unit for land of various kinds

Inductivities—(ordinary dielectric constant) from 2 to 25, depending upon the amount of water in the soil

For fresh water:

Conductivities of the order of 10×10^{-14} electromagnetic unit. Inductivity about 81.

For typical ocean water:

Conductivity of about $5{,}000 \times 10^{-14}$ electromagnetic unit. Inductivity about 81

The above values are expressed in electromagnetic units because most available propagation data are prepared in these units for engineering use. The procedure of using the factor 10^{-14} permits the relative conductivity to be immediately apparent from reading the value of the coefficient, the value 1×10^{-14} being low enough to include almost the poorest kind of soil that would be encountered. Values of conductivity lower than this are equivalent values for attenuation conditions due not only to the soil characteristics but to losses due to wave scattering. Therefore it may be found that in topographically rugged country it appears that the average conductivity is below 1×10^{-14}, whereas the earth itself, if flat, would in almost all cases be above this value. The additional attenuation of a wave due principally to scattering by reflections from the irregular terrain is then equivalent to that over a flat earth with much lower conductivity.

When a plane electromagnetic wave with its electric field normal to the direction of propagation impinges upon the surface of an imperfect dielectric, the power propagated into the dielectric sets up conduction

currents and displacement currents, both in quadrature to each other. The ratio of the two is dependent upon the frequency, the conductivity, and the inductivity. At the lowest radio frequencies, conduction currents are very large with respect to the displacement currents, permitting the latter to be neglected. With increasing frequency, displacement currents become more important relatively, and eventually a frequency is reached where displacement currents predominate over conduction currents.

Conduction-current density is maximum at the surface of the ground and decreases exponentially with depth. The depth at which the magnitude of the current density has fallen to $1/e$ of its surface value (about 37 per cent) is called the "skin depth," which we shall designate by the letter S. The conduction-current skin depth in meters can be computed from the relation

$$S_m = \frac{1}{\sqrt{4\pi^2 f\sigma \times 10^4}}$$

where σ is in electromagnetic units and f in cycles per second. Appendix II shows the skin depths for the range of frequencies and soil conductivities of general interest. The skin depth equals one-half wavelength at the velocity of propagation in the soil and about 90 per cent of all the loss in the soil occurs within this depth.

The earth currents return to the base of a vertical antenna along radial lines. At the base of the antenna, all the ground currents add together to enter the antenna as the antenna current. The total ground loss is the integrated losses at all points due to all the returning ground currents. In ordinary soils this loss is considerable, and measures have to be taken to minimize ground loss by the use of systems of buried radial wires that conduct the returning ground currents to the base of the antenna through high-conductivity circuits.

The distance from the antenna at which returning ground currents are of such a low value as to be negligible is of the order of 0.5 wavelength. Beyond about 0.4 wavelength, the gain in efficiency with increased length is seldom a good economic investment, when a sufficiently large number of radials is used. Systematic measurements[6] have shown that the effective length of a buried wire decreases as the number of radial wires is decreased. Ground resistance decreases as both the length and the number of buried radial wires are increased. However, when the number of radials exceeds 120 and their length exceeds 0.4 wavelength, one reaches the region of diminishing returns. With such a ground system, the circuital and radiational characteristics of a vertical radiator of the type used for broadcasting approach very nearly those computed from theory for a

perfectly conducting earth. Figure 2.17 shows how the field strength varies as a function of antenna height and the number of 0.412-wavelength radial ground wires. Figure 2.18 shows the same thing, but with 0.137-wavelength radials. Figure 2.19 shows the field strength and the antenna resistance of a 77-degree radiator as a function of the number of 0.412-wavelength radials used. These data were obtained from experimental studies at 3,000 kilocycles.[6]

The ground system performs solely as a circuital element with the shorter vertical radiators, serving to reduce ground losses. With a system of 120 radial wires buried near the surface of the soil to a length of 0.4 to 0.5 wavelength, almost all of the ground current is collected from the electric field above the ground system and current densities below the ground system are very small. Currents in the soil between the radials are quickly diffracted into the wires.

With high radiators of the antifading type, however, the ground system performs another function—that of providing a reflecting surface of high reflectivity for those electromagnetic fields which produce cancellation of high-angle radiation. Surface-reflection losses cause incomplete wave interference because the reflected field strength is decreased in amplitude by these losses.

From the principles of the reflection of a *plane* electromagnetic wave from the boundary between air and an imperfect dielectric of conductivity σ and inductivity ϵ at a frequency f in cycles, the reflection coefficient K_v for vertically polarized waves is the following vector (Fresnel) equation:

$$K_v = |K_v|e^{j\psi_v} = \frac{\left(\epsilon - j\frac{2\sigma}{f}\right)\sin\alpha - \sqrt{\epsilon - \cos^2\alpha - j\frac{2\sigma}{f}}}{\left(\epsilon - j\frac{2\sigma}{f}\right)\sin\alpha + \sqrt{\epsilon - \cos^2\alpha - j\frac{2\sigma}{f}}}$$

in which α is the angle above the horizon and is the complement of the angle of incidence. This is the Fresnel equation for vitreous reflection, and the value of σ in this equation is in *centimeter-gram-second electrostatic units*. To convert from customary electromagnetic units to electrostatic units, use the relation

$$\sigma_{esu} = 9 \times 10^{20} \times \sigma_{emu}$$

It is evident from this equation that the complex reflection coefficient is a function of the conductivity and the inductivity of the ground, the frequency, and the angle of elevation above the ground. This means that there is always a decrease in the magnitude of the reflected wave with respect to the incident wave, and there is a change of phase ψ_v as

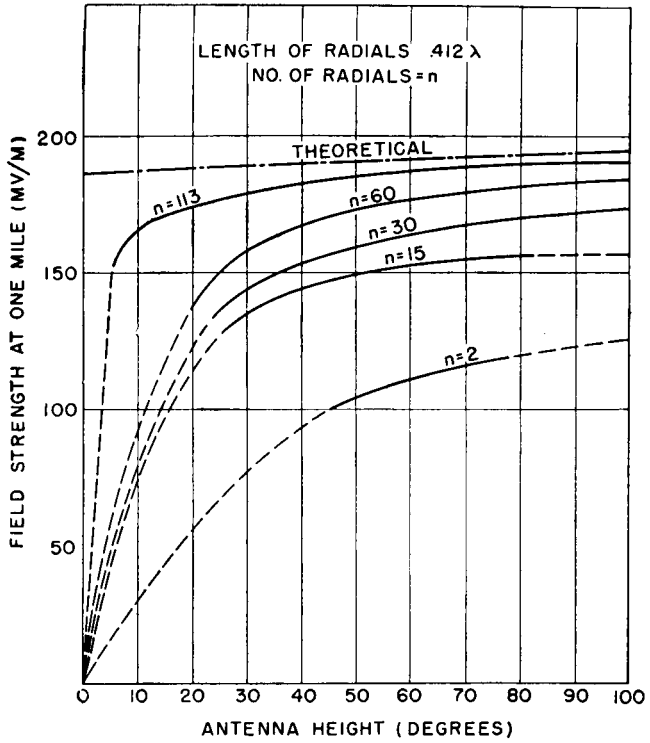

FIG. 2.17. Field strength as a function of antenna height and the number of 0.412-wavelength radial ground wires, 1,000 watts antenna input. (*After Brown, Lewis, and Epstein.*)

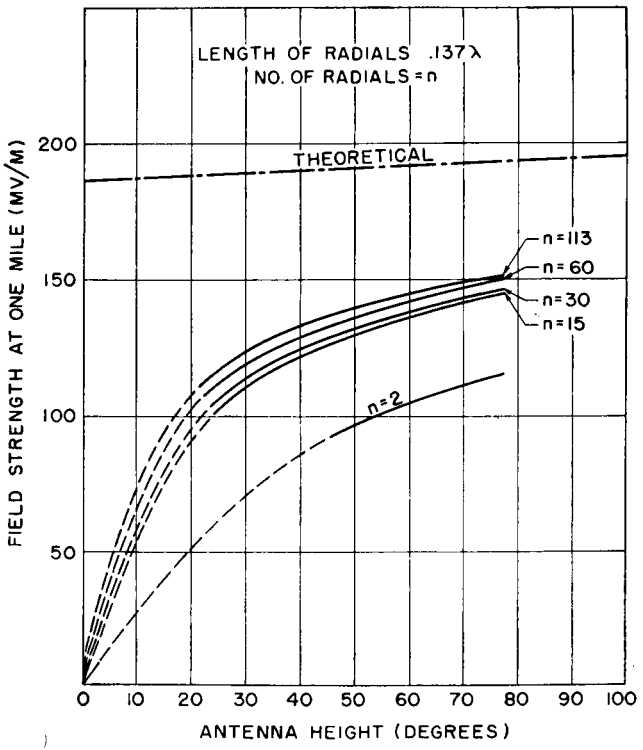

FIG. 2.18. Field strength as a function of antenna height and the number of 0.137-wavelength radial ground wires, 1,000 watts antenna input. (*After Brown, Lewis, and Epstein.*)

well. When the computation is made for the values of $\bar{K}_v$ as α varies from 0 to 90 degrees, it will be found that at some angle α_b the amplitude $|K|$ is a minimum, and at this elevation the value of ψ is -90 degrees. The elevation angle α_b is known as the "pseudo-Brewster angle." If the ground were a perfect isotropic dielectric ($\sigma = 0$), it would be found that $|K| = 0$ at the Brewster angle.

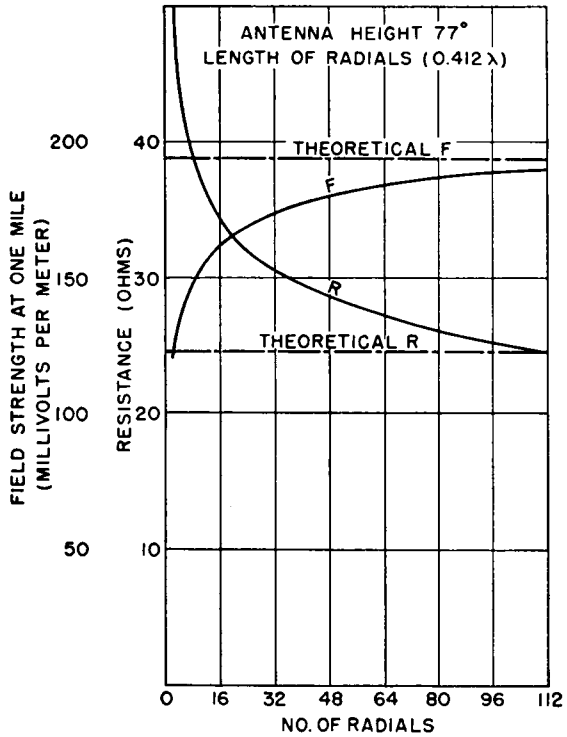

FIG. 2.19. Field strength for a 77-degree vertical radiator as a function of the number of 0.412-wavelength radial ground wires, 1,000 watts antenna input. (*After Brown, Lewis, and Epstein.*)

The significance of these facts is that a vertical radiation pattern at a very great distance differs from that which is computed without taking into account the imperfect conductivity and the inductivity of the ground. Up to this point all discussion of vertical radiation patterns has followed the assumption that the ground was of perfect conductivity. The construction of an optimum practical ground system for a vertical radiator tends to approach this ideal condition from a circuital standpoint and for wave reflections that occur within the radius of the ground system. For waves reflected from the surface beyond the limits of the

ground system, the actual ground constants may impose a substantial change in the vertical radiation pattern at the low angles, by modifying both its amplitude and its shape.

Table 2.6 will provide a general idea of the importance of these facts for two values of conductivity when the frequency is 1 megacycle.

TABLE 2.6. REFLECTION COEFFICIENTS $\bar{K}_v$ AT 1 MEGACYCLE IN TERMS OF THE MODULUS $|K|$ AND THE PHASE ANGLE ψ

Elevation angle α, degrees	Ocean water $\sigma = 5{,}000 \times 10^{-14}$ electromagnetic unit $\epsilon = 81$		Good moist soil $\sigma = 11 \times 10^{-14}$ electromagnetic unit $\epsilon = 20$	
	$\|K\|$	ψ, degrees	$\|K\|$	ψ, degrees
0	1.00	−180	1.00	−180
5	0.95	−3	0.40	−72
10	0.97	−2	0.55	−32
15	0.98	−1.5	0.66	−20
20	0.985	−1	0.73	−16
25	0.98	−0.5	0.78	−12
30	0.99	0	0.81	−10
40	0.99	0	0.85	−8
50	0.99	0	0.87	−6
60	0.99	0	0.88	−6
70	0.99	0	0.90	−6
80	1.00	0	0.90	−6
90	1.00	0	0.90	−6
Pseudo-Brewster angle α_b	Between 0 and 1 degrees		4 degrees	
	0.41	−90	0.39	−90

2.5.1. Ground-system Design. The radial disposition of wires in a buried or a surface ground system is dictated by the natural paths for returning ground currents. Meshes of crossed wires, which were once widely used, should not be used with vertical radiators, because the return paths are not direct and eddy-current losses in the closed loop circuits of the mesh can be appreciable.

If the radial wires are of optimum length, sufficient to have virtually zero current as one approaches the ends of the wires, there is no need to add ground rods. The test for the desirability of ground rods is to drive one ground rod, connect one of the radial wires to it, and measure the current distribution along the wire up to the end. If it is evident that

any appreciable current exists at the end of the wire in using the ground rod, their desirability may be indicated. The same applies to the use of a circular bonding wire around the periphery of the system. It is only when the lengths of the radials are insufficient that there is justification for using peripheral bonding and ground rods.

The size of the ground wires has only a secondary effect on the performance of the system. Usually the wire size is that which will with-

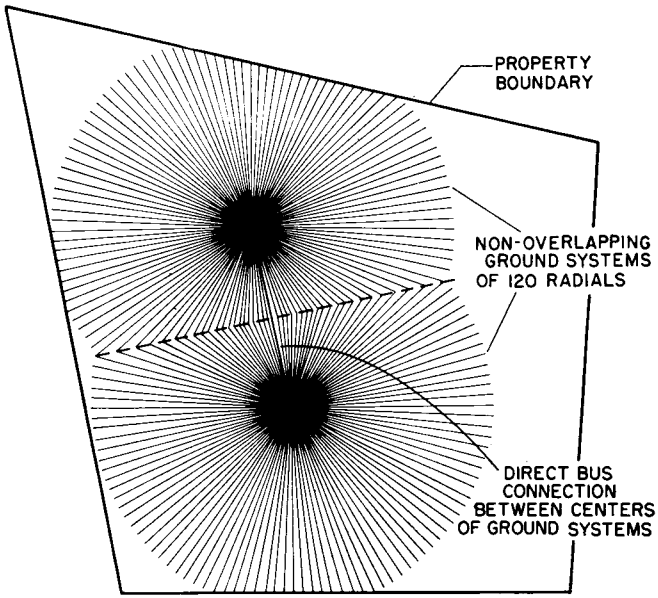

FIG. 2.20. Example of radial ground system for a two-element directive array, on limited plot.

stand the mechanical duty of the plowing-in process. If one desires to increase the amount of copper in the ground system, it is best to employ the copper in the form of more and longer wires rather than heavier wires, unless the antenna current has a very large value, causing high current densities in the individual wires.

When the available plot of ground for the ground system is insufficient for a complete circular layout, certain compromises must be used. If the boundaries of the property limit some of the radials to less than optimum length, the use of ground rods at the ends of the short radials, driven in to a depth equal to the skin depth, will generally be beneficial in minimizing ground loss. If the property is so small as to limit radial lengths in all directions to those well below optimum, ground rods and peripheral bonding may be used to advantage.

In a directive array using several vertical radiators, each with a radial ground system of its own, the ground systems usually overlap. There is no useful purpose in overlapping the ground systems, and the ground radials may be terminated at the intersections, as shown in Fig. 2.20. In nonoverlapping regions, the radials of each system should be continued out to their optimum length. Bonding of radials at intersections is frequently used and is probably desirable.

The depth of the wires is immaterial, whether the soil be moist or dry. They may be placed on the surface except that they are then subject to injury and prevent the use of the land for other purposes. When the

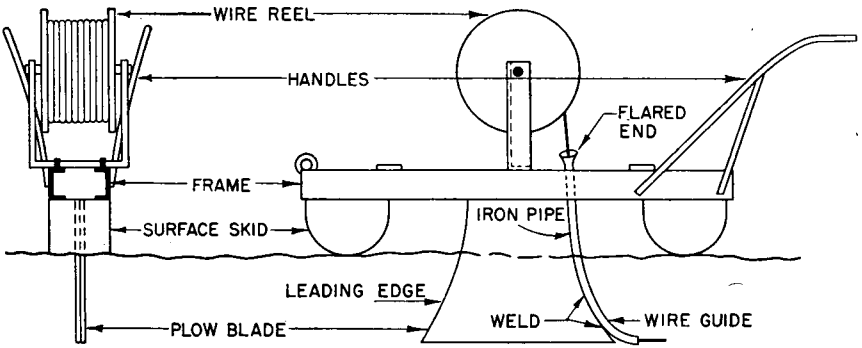

FIG. 2.21. Design for elementary plow for burying ground wires.

plot is to be cultivated, the wires must be far enough below plowing depth so as not to be injured by plowing. However, it is desirable to bring the ground wires to the surface a short distance from the radiator base so as to form a good ground screen above the soil near the antenna base where the electric field strengths are high. The exposed portion of the ground system can be protected by a fence if necessary.

The burial of ground wires is a simple procedure in soils where a wire plow can be used. Such a plow is easily made from a piece of sheet steel from $\frac{3}{8}$ to $\frac{1}{2}$ inch thick, cut as shown in Fig. 2.21. The leading edge is sharpened so as to cut its way through the soil. The trailing edge has a small iron pipe welded to it to act as a guide for the ground wire. This pipe is turned backward on a radius that will not cause too much friction on the wire as it passes through the pipe. When a hand or tractor plow of this type is used, it cuts a thin groove in the soil at the desired depth into which the wire is fed as the plow moves along. The reel of wire is often mounted on the plow. The photograph (Fig. 2.67) shows another type of ground-wire plow drawn by a tractor.

The ground system is laid out from the center, using a transit to set the angles between radials. Stakes are then set at the proper distance

to mark the end of a radial. The ground wires are plowed in by running the wires as directly as possible from center to one of the stakes or from the stake toward the center. The soil grooves will fill in a short time with the erosion of the sides of the groove.

The inner ends of the radials should center at the base of the radiator, and not to one side. They should be securely soldered to a ring or plate to which is connected the metallic parts of the lower end of the base insulator (see Fig. 2.65). From this common ground-wire junction, the ground connection to the antenna coupling network should be taken, and all other grounding wires to conduits and other metallic objects in the field of the antenna. Care should be taken not to introduce coupled loop circuits that often result from grounding several objects with the same ground wire. Separate insulated ground wires, connected back to the central junction for the ground radials, will avoid many of the instability troubles that occur in directive systems. Grounding connections should be securely bonded by welding or soldering so as not to be vulnerable to corrosion. The stability of the ground system and the various ground connections should be tested by measuring the antenna resistance with a sensitive balance indicator such as an impedance bridge. When one can touch, pull, or shake any grounded objects in the vicinity of the radiator base without observing a change of resistance, the system is likely to be stable.

The ground bus from the radial system to the coupling network should be of very low reactance. A wide strip of sheet copper is desirable. Alternatively, several insulated wires in parallel and mounted so as to simulate a sheet of conductors are very satisfactory.

Some of the ground radials are often impeded by the presence of the house for the antenna coupling equipment. Unless the ground radials can run under the house, the best practice is to bring the ground radials to the surface as they approach the house and to continue them in insulation around the house to the junction point. Insulating the wires will avoid erratic variations in impedance when the wires are cabled to pass around the house. Bunching several bare ground wires before they reach the common junction is to be avoided always.

2.6. Bandwidth of a Radiator

In modern design, cognizance is taken of the bandwidth of emission characteristic of the type of emission to be radiated from the antenna. Both resistance and reactance of an antenna vary with frequency, and it is desirable that the system have the least practicable variation in

impedance between the center frequency and the maximum and minimum side frequencies. In general, the bandwidth capabilities of a radiator are increased (for a given amount of impedance variation) as the cross section of the radiator is increased. Thin wire antennas have much greater selectivity than steel tower radiators of substantial cross section. When the desired cross section is greater than is structurally or economically desirable for a given bandwidth to be transmitted, an outrigger at the top of the tower can be used to support vertical wires or cables some distance away from the supporting center tower, as in Fig. 2.14.

Experience has shown that not enough attention was given to bandwidth in many existing systems. Bandwidth should be one of the primary considerations in planning any type of radiating system.[48] Whenever the bandwidth exceeds 1 per cent of the carrier frequency, special design considerations are certainly involved. In choosing the final design to accommodate a specified bandwidth, there are no absolute criteria, other than the designer's good judgment, to determine when a satisfactory set of parameters has been found.

In any applications involving extreme bandwidths, care must be taken to avoid selectivity in the feeder coupling network. The smaller the amount of stored energy in all the reactive elements of a coupling network, the smaller its intrinsic selectivity.

Minimum selectivity is afforded by using a feeder having a characteristic impedance equal to the actual working resistance of the antenna system at the center frequency of the transmission band and then using a simple series reactance to cancel the antenna reactance at this center frequency. Occasionally it may be found impractical to provide transmission lines of the correct characteristic impedance for direct resistance match to an antenna. With coaxial feeders it is practical to obtain characteristic impedances of 15 to 75 ohms, using paralleled lines if necessary. With open-wire lines of the single-end (unbalanced) type, characteristic impedances from 150 to 350 ohms are easily obtained, and by special measures, including paralleled lines, the gap between 75 and 150 ohms can be closed, using open-wire lines. A total resistance range of 15 to 350 ohms can therefore be accommodated for direct resistance match between feeder and antenna if required.

When coupling networks are used between feeder and antenna and between transmitter and feeder, but where precautions are desirable to avoid unnecessary selectivity, conservative networks of minimum total stored energy should be chosen and the changes in impedance levels at coupling points minimized as much as practicable. Standing waves on a transmission line also represent stored energy and add to the selectivity

of the system. Feeders of tapered characteristic impedance may be used instead of networks to effect moderate impedance changes. These matters are treated in Chap. 4.

The bandwidth of a series-resonant circuit is usually defined as the frequency band between the limits where the input impedance has equal resistance and reactance components. At these two limits, above and below the resonant frequency, the phase angle of the impedance is 45 degrees, and the circuit response with a zero-impedance generator is 3 decibels below that at resonance. An antenna circuit may be viewed as a series-resonant circuit in the same way, even though the resistance as well as the reactance changes with frequency.

In broadcasting, it is customary to allow only about 1 decibel attenuation for the side frequencies produced by the highest modulating frequency. The phase angle of the antenna impedance for these side frequencies to maintain 1 decibel response in the antenna must not exceed 27.5 degrees. For any other response limit in decibels, the maximum phase angle of the impedance ϕ is found from

$$\cos \phi = \frac{1}{\log_{10}^{-1} \frac{\text{db}}{20}}$$

2.6.1. Calculation of Bandwidth. The resistance and reactance curves of Figs. 2.15 and 2.16 can be used to compute bandwidth. It will be noted that the ratio G/D has a major influence on the reactance as the value of G changes with frequency.

To illustrate the prediction of antenna response, we shall consider a practical problem of computing the response of a 60-degree vertical radiator at 550 kilocycles to side frequencies of +10 and −10 kilocycles. This radiator is 300 feet high and has a uniform triangular cross section with 5.2 feet per side. The periphery of this radiator is 15.6 feet, which we assume to be equivalent to a cylindrical section with the same periphery and thus having a diameter of 5 feet. Then the ratio of height to diameter $G/D = 60$. By plotting out the readable data for resistance and reactance from Figs. 2.15 and 2.16 so as to interpolate for small increments of G in the vicinity of $G = 60$ degrees and $G/D = 60$, we obtain the following information:

Variation of reactance—6.8 ohms per degree change in G
Variation of G with frequency—1.2 degrees per 10 kilocycles
At 550 kilocycles—$Z_a = 9.8 - j118$
At 540 kilocycles—$Z_a = 9.2 - j126$
At 560 kilocycles—$Z_a = 10.4 - j110$

If all reactance is tuned out at 550 kilocycles with an inductor of reactance $j118$, then at the two opposite side frequencies we find:

Frequency, kilocycles	R	X	ϕ, degrees	Decibels
540	9.2	$-j8$	41.7	−2.52
550	9.8	0	0	0
560	10.4	$+j8$	40.5	−2.36

It is evident from this that the high-frequency-modulation response of a transmitter working into this particular antenna would be limited by the intrinsic bandwidth of the antenna. A further limitation may be imposed by the antenna coupling networks.

One should avoid drawing general conclusions from this single example, except possibly that the response characteristics of a radiator have to be studied whenever the reactance of an antenna is high and its resistance low and whenever the transmission bandwidth is more than 1 per cent.

The response can be easily computed from measurements that have been made on a radiator already constructed. If it is found that the bandwidth of the antenna is inadequate for the quality of emission desired, the effective diameter of the radiator can usually be increased by means of vertical wires hung from an outrigger at the top or by booms attached to the tower a short distance from the top. The requisite number of wires and their distance from the tower to obtain the desired bandwidth can then be determined experimentally.

A suspended wire antenna has smaller intrinsic bandwidth because of its small diameter. To increase the bandwidth of a wire antenna, the system can be constructed as a large cage or several wires can be connected in parallel or as a fan in a common plane with considerable separation of the wires.

In the case of a directive array, the bandwidth of the complete radiator feeder system can be computed if one has the patience to undertake the labor involved. In some cases the effort is not justified. One should watch for the situation where mutual impedances may reduce the input resistance of one radiator to a very low value, with the reactance remaining high. The bandwidth of the one radiator can then be computed, using the expected values of resistance and reactance when the system is operating properly. If intolerable selectivity is found, other alternatives of design may have to be adopted, including, in some cases, a different kind of array configuration.

The response of a finished directive array can be determined by measuring the impedances at the common input to the system at the frequency

limits of the desired transmission band and computing the response therefrom. The procedure is the same as that for a single elementary circuit.

2.7. Input Impedance to Each Radiator in a Directive Array

Before one can design the feeder system for a directive array, it is necessary to predetermine the input impedance to each radiator *when it is functioning properly in the final working system.* Any impedance computation for this purpose therefore presupposes that the system is energized so as to provide the proper current amplitude and phase in each radiator and that the system is producing the desired pattern. From here on, the circuit-design problem is to energize each radiator as a separate load with its correct current and phase when energized from a common generator—the transmitter.

The self-impedance of each radiator at the working frequency must first be known with an accuracy of a few per cent, and especially the nature of its reactive component must be certain. In preliminary computations the self-impedance may be estimated from measurements that were previously made on a similar radiator, or from measurements made on the same design of radiator, or from interpolated values from a number of sources of data that one may have from former experience. Without such previous-experience data, general data such as those from Figs. 2.15 and 2.16 may be used, with the addition of the effects of base insulators, guys and guy insulators, tower-light circuits, and other attachments that must be present in the final working system. Eventually it will be necessary to make measurements on the radiators, after they have been erected, to confirm the preliminary computations and the feeder-circuit design.

The voltage at the base (feed point) of each radiator will be

$$V_1 = I_1Z_{11} + I_2Z_{21} + I_3Z_{31} + I_4Z_{41} + \cdots + I_nZ_{n1}$$

In this equation, *all the currents and impedances are complex numbers,* referred to some one spot in the system such as radiator 1 as a basis of reference of phases and amplitudes. This equation shows that the voltage at the base of radiator 1 is the sum of its own current times its own self-impedance, the induced voltage from radiator 2 is a result of its current times the mutual impedance between radiators 2 and 1, and the same for all the other radiators. In general, these are all complex numbers. Thus the value of V_1 will have an amplitude and also a phase relation to I_1. The ratio V_1/I_1 is the input impedance to radiator 1 and is generally complex, meaning that it has both resistance and reactance. Occasionally a radiator will have an input impedance which has a nega-

tive-resistance component. This means that this radiator is giving back power to the generator and thus acts as a second generator instead of as a load. This condition requires special precautions in the feeder-network design, because its power will be flowing in a reversed direction.

It is preferable to rewrite the foregoing equation in the rectangular form that employs the inphase and quadrature current components and the resistances and reactances of the impedances. Then the equation becomes

$$Z_1 = \frac{V_1}{I_1} = (R_{11} + jX_{11}) + \frac{I_2}{I_1}(\cos \phi_2 + j \sin \phi_2)(R_{21} + jX_{21}) + \cdots + \frac{I_n}{I_1}(\cos \phi_n + j \sin \phi_n)(R_{n1} + jX_{n1})$$

in which ϕ_n is the phase difference between the current in radiator n and that in radiator 1 which is used as the reference for all currents in the system. This equation can be solved graphically by means of vectors or by arithmetic after inserting the correct numbers and signs for all values.

When one is merely interested in impedances, I_1 is assumed to be unity. Then all the other currents are merely expressed as ratios with respect to I_1, and the value found for V_1 is then exactly equal to the impedance of radiator 1 in resistance and reactance. The values for the mutual impedances must be carefully handled because they may lie in any of the four quadrants, and the resistive component of a mutual impedance in the second and third quadrants is therefore *negative*. Also, the phase of the different radiator currents may lie in any of the four quadrants.

This operation is repeated for each radiator in the system, unless symmetry of a problem makes it unnecessary for certain radiators. For example, the impedance of the second radiator will be

$$Z_2 = \frac{V_2}{I_2} = \frac{I_1}{I_2} Z_{12} + Z_{22} + \frac{I_3}{I_2} Z_{32} + \cdots + \frac{I_n}{I_2} Z_{n2}$$

and so on, through all n radiators. For mutual-impedance data consult Appendix III and refs. 4, 9, 44, 1002, 1011, and 1023.

2.7.1. Circuits for Cancellation of Mutual Impedances in a Two-element Array. It is possible to feed such an array in a manner that will cancel mutual impedance. The principles are exemplified in Figs. 2.22 and 2.23. By simultaneously exciting both radiators with equal cophased currents and equal antiphased currents and with any arbitrary phase or amplitude relationships between these two pairs of currents, mutual

impedance is balanced out, as shown in the vector diagram. Then any desired excitation of the radiators in phase and amplitude, to obtain any pattern that is possible with the chosen spacing between radiators, requires only power division and phasing between the two pairs of feeders, while the terminal conditions of the array remain constant at the inputs

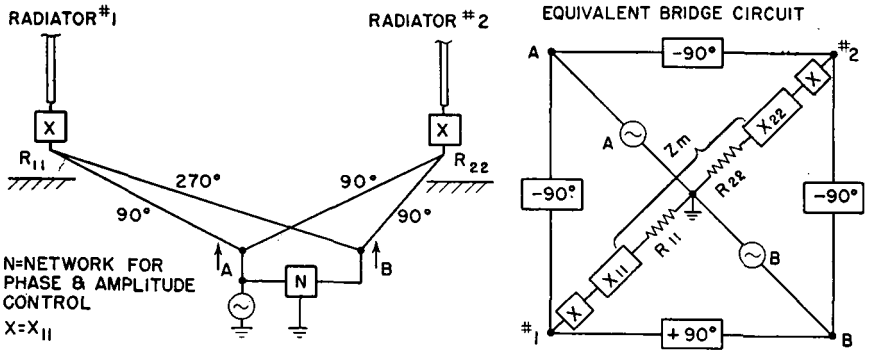

FIG. 2.22. Circuits for mutual-impedance cancellation in a system of two radiators.

A and B (Fig. 2.22). This method is useful where a variable pattern is required. In the vector diagram (Fig. 2.23) $A1$ and $A2$ (equal and in phase) are the currents in radiators 1 and 2 due to excitation by the A branch; $B1$ and $B2$ are the radiator currents due to antiphased excitation by branch B. The angle ϕ_1 is the phase difference, and the amplitudes of $B1$ and $B2$ are the difference due to power ratio controlled by the network N. The relative amplitudes I_1 and I_2 and phase ϕ_0 of the resultant radiator currents are seen to be controllable by varying ϕ_1, A, and B. This can all be done with one network.

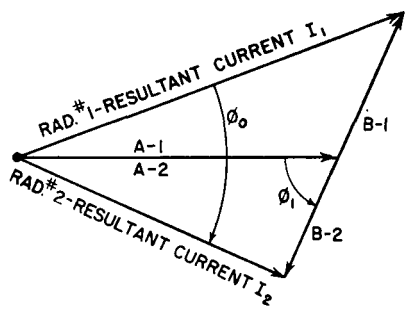

FIG. 2.23. Vector representation of mutual-impedance cancellation.

In this circuit the self-reactance of each radiator is canceled by the series reactance X, and the feeders are made with a characteristic impedance equal to the self-resistance of the radiators R_{11} and R_{22}.

The equivalent bridge circuit of Fig. 2.22 will aid in understanding what follows and shows why the generators A and B are mutually uncoupled and why the loads R_{11} and R_{22} are also mutually uncoupled. When the B side of the bridge is removed, the situation always seen by generator A is apparent, and vice versa. With B removed, A sees a

load impedance of $Z_1 = Z_{11} + Z_m$ because the currents in the two loads are cophased. Having made $Z_0 = R_{11}$, the feeders are unmatched. Consider that the A side of the bridge is absent and see that the load currents are now antiphased but that the lines are also mismatched because now $Z_1 = Z_{11} - Z_m$. When both sides of the circuit are synchronously excited, each generator sees an impedance of Z_1 through each of its lines. The series reactance X was added so that each line will see R_{11} only, and the lines are matched.

Now the relative phase and amplitude of currents from A and B can be changed at will without any reaction between them, and each sees a constant load. It is interesting to note that when A and B are equal and cophased, the current in radiator 2 is doubled and that in 1 goes to zero. Then all the power is in one radiator, and the array is nondirective. When equal and antiphased, all the power is in radiator 1.

The power in the array is contributed by generators A and B. The amount of power from A is $2 \times I_A^2 R_{11}$, and that from B is $2 \times I_B^2 R_{11}$. The sum of these powers, less any losses in the feeders and network, is the total power input to the antenna array.

Arbitrary line lengths other than 90 degrees can be used if building-out (or shortening) sections are inserted in each line to obtain the effect of 90-degree lines. Lines of characteristic impedance other than $Z_0 = R_{11}$ can be used if impedance-matching networks are inserted in each feeder which have equal phase characteristics in the generalized case or are designed for zero phase shift of input and output currents when lines of 90 degrees length are used.

This same circuit has application in the paralleling of synchronous transmitters without reaction, by making R_{22} the useful load and R_{11} a dummy load. Then when the transmitters are not perfectly cophased, nothing happens except that some power is lost in the dummy load. The phasing can be adjusted by observing the current through the dummy load, which will read zero when A and B are precisely equal in phase and amplitude. Under this condition, all the power from both generators is delivered to the useful load.

2.7.2. Feeder Circuits For Directive Arrays. When the working input impedance to each radiator in an array is known, the next step in design is to compute the networks of the feeder system. The design starts with a consideration of the arrangement of transmission lines, of which there may be several choices from a cost standpoint. For example, one may choose to run a separate transmission line from each radiator to the transmitter and join these feeders together in a network near the transmitter. Or it may be decided to run one line from the transmitter to one of the radiators and go on from there to the others in succession, with

coupling and power-dividing networks at each radiator along the line to the last. Or there may be combinations of these two basic methods. Then there is the choice of matching each line at each point in its characteristic impedance or allowing certain standing waves to exist, with the consequent transformation of impedance by the unmatched lines. Here again the choice is one of economy in engineering time and materials if the mismatches are not large.

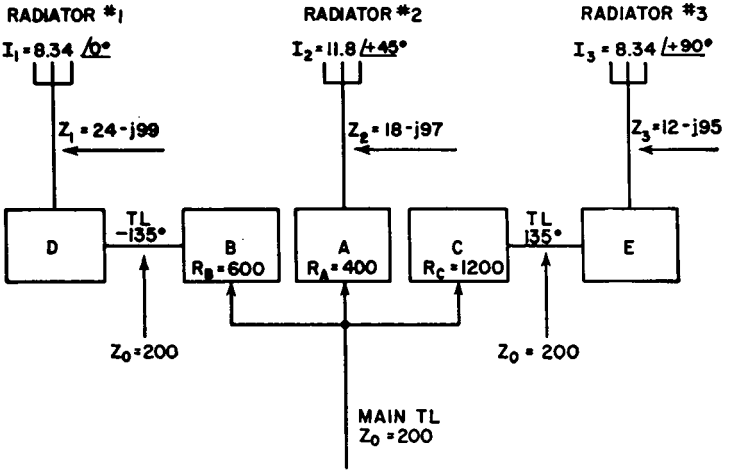

FIG. 2.24. Basic circuits for the array feeder system.

The easiest system to design is one using separate lines from each radiator to the transmitter, each line being correctly matched in its characteristic impedance. If perchance the power input to each radiator is the same and the lines have the same characteristic impedance, they can all be connected directly in parallel near the transmitter. The phasing of the different radiator currents is accomplished in each radiator by the combination of the electrical length of each line and the phase difference effected by its impedance-matching network at the radiator.

In general, however, the radiator input powers will be different, in which case it is necessary to feed each line with the potential that will transmit the proper amount of power down each line. This requires the use of power-dividing networks, and the inputs to these networks are paralleled to obtain the correct impedance for the transmitter. These power-dividing networks will introduce phase shifts in each branch so that now the correct radiator current phasing is accomplished by adding the phase shifts of the power-dividing network, the line, and the radiator coupling network. Since the phase difference on a matched line is

always negative (lag), it may be necessary to employ either positive or negative phase differences through the power-dividing network or the radiator coupling network or both to obtain the full range of phase differences required in practice.

In the case of successive feeding, the full transmitter power is fed into a common line to the first radiator. Here one network extracts the proper power for that radiator through a coupling network with a predetermined phase shift, positive or negative. The remainder of the power is fed through the line to the next radiator, where again a portion is taken out for the second radiator and the rest sent on, etc. The last radiator has simply a coupling network, from which it receives the remaining power that it requires. The phase shifts, as well as the proper impedance matches, are built into each network along the system. Allowance is made for losses and attenuation in the lines also.

It is helpful to start the design of the feeder system by making a block diagram showing every network and every section of line, with points of paralleling included. If matched lines are to be used everywhere, as is usually preferred by engineers, the phase lag for each section of line is immediately known from its length and is so marked in the diagram. Specified phase shifts are then assigned to the different networks of the system, making arbitrary divisions between two or three networks that may occur in one branch so long as the total phase shift is correct. When all the phases have been assigned, the diagram can be marked with input and output impedances for each block. Power dividing is usually done by paralleling networks, using different resistance values to effect the power division when energized with a common potential. The input resistance to the paralleled networks is made that which will terminate the transmission line.

When the block diagram is completed with the terminal impedances and phase shift of each block shown, the synthesis of each network then proceeds in a routine manner. The electrical design is followed by the design of the reactive components and then by the mechanical assembly of each network.

In low-power systems it is often feasible to house the networks of small components in weatherproof boxes located near each radiator. When this becomes impractical because of size, a cabin is made to house the equipment.

Since all vertical radiators for medium-frequency broadcasting have ground as one side of the circuit, it is desirable to employ unbalanced transmission lines in the feeder system. It is a needless complication to employ balanced lines in such cases and thus have to make balanced-to-unbalanced conversions in the circuits.

2.7.3. Computation of a Feeder System for a Three-radiator Array. The preceding principles will now be applied to an example. An in-line array of three identical 60-degree vertical radiators spaced 135 degrees is to be fed for a power input of 5,000 watts in the following manner:

Radiator	Current ratio	Phase difference, degrees
1	1.00	0
2	1.41	+45
3	1.00	+90

At the working frequency the self-impedances

$$Z_{11} = Z_{22} = Z_{33} = 16 - j90 \text{ ohms}$$

From symmetry, it is evident that

$$Z_{12} = Z_{21} = Z_{23} = Z_{32}$$

and

$$Z_{13} = Z_{31}$$

From Appendix III, Fig. *D*, the following values are read

$$Z_{12} = 2 - j7 \text{ ohms}$$
$$Z_{13} = -4 + j1 \text{ ohms}$$

The input impedance to each radiator is then computed.

$$Z_1 = \frac{V_1}{I_1} = Z_{11} + \frac{I_2}{I_1}Z_{21} + \frac{I_3}{I_1}Z_{31} = Z_{11} + 1.41\underline{/+45}(Z_{21}) + 1.0\underline{/+90}(Z_{31})$$
$$= 16 - j90 + (1 + j1)(2 - j7) + j1(-4 + j1)$$
$$= 24 - j99 \text{ ohms}$$
$$Z_2 = \frac{V_2}{I_2} = \frac{I_1}{I_2}Z_{12} + Z_{22} + \frac{I_3}{I_2}Z_{32}$$
$$= (0.5 - j0.5)(2 - j7) + 16 - j90 + (0.5 + j0.5)(2 - j7)$$
$$= 18 - j97 \text{ ohms}$$
$$Z_3 = \frac{V_3}{I_3} = \frac{I_1}{I_3}Z_{13} + \frac{I_2}{I_3}Z_{23} + Z_{33}$$
$$= -j(-4 + j) + (-j + 1)(2 - j7) + 16 - j90$$
$$= 12 - j95 \text{ ohms}$$

The power input to the system is

$$W = I_1^2R_1 + I_2^2R_2 + I_3^2R_3$$

but using the current ratios,

$$W = I_1^2[R_1 + (1.41)^2R_2 + R_3]$$

By arithmetic, after substituting the resistances,

$$W = I_1^2(24 + 36 + 12) = I_1^2 72$$

$$I_1 = \sqrt{\frac{W}{72}} = \sqrt{\frac{5{,}000}{72}} = 8.34 \text{ amperes}$$

Then

$$\begin{aligned} W_1 &= 8.34^2 \times 24 = 1{,}670 \text{ watts} \\ W_2 &= 11.8^2 \times 18 = 2{,}500 \text{ watts} \\ W_3 &= 8.34^2 \times 12 = 835 \text{ watts} \\ \text{Total} &= 5{,}005 \text{ watts} \end{aligned}$$

Now that all the input-impedance information has been determined, decisions can be made regarding the feeder system. It is noted that

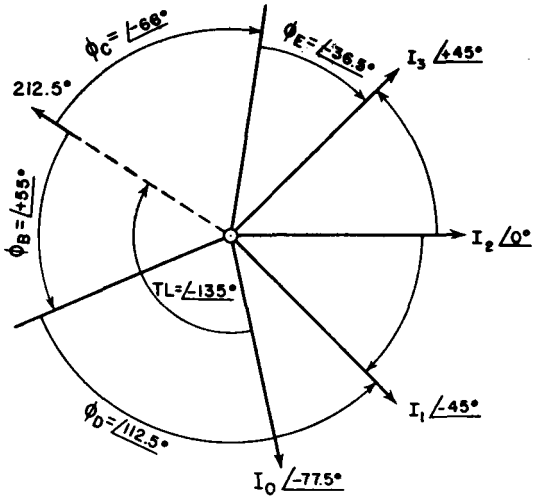

FIG. 2.25. Phasing diagram chosen for the array.

half of the total power is in radiator 2. It will probably be well to bring the main transmission line up to this radiator and use the simplest possible network—a simple two-element L circuit. Then power to the two outer feeders can be fed each way from the middle, with lines running between the radiators. The block diagram of Fig. 2.24 illustrates the problem. Network *A* will couple radiator 2 to the main feeder. Network *B* will divide power and take enough from the main feeder to excite radiator 1, and network *C* will do the same for radiator 3. Network *D* will terminate the line on the left and couple into radiator 1, and network *E* will do the same for the right-hand line. Networks *A*, *B*, and *C* in parallel will match the main feeder.

Choosing a convenient open-wire line of characteristic impedance such as 200 ohms, the potential on the main line will be

$$V = \sqrt{WZ_0} = \sqrt{5{,}000 \times 200} = 1{,}000 \text{ volts}$$

For 2,500 watts into network A, its input resistance must be

$$R_A = \frac{V^2}{2{,}500} = 400 \text{ ohms}$$

For 1,670 watts into network B, its input resistance must be

$$R_B = \frac{V^2}{1{,}670} = 600 \text{ ohms}$$

For 835 watts into network C, its input resistance must be

$$R_C = \frac{V^2}{835} = 1{,}200 \text{ ohms}$$

Networks A, B, and C in parallel give a resistance value of

$$\frac{1}{R} = \frac{1}{R_A} + \frac{1}{R_B} + \frac{1}{R_C}$$

$$\frac{1}{R} = 0.0025 + 0.00167 + 0.00083 = 0.00500$$

from which $R = 200$ ohms.

At this point the impedance-matching requirements are known for each network, as follows:

Network	Input impedance	Output impedance
A	$400 + j0$	$18 - j97$
B	$600 + j0$	$200 + j0$
C	$1{,}200 + j0$	$200 + j0$
D	$200 + j0$	$24 - j99$
E	$200 + j0$	$12 - j95$

The required phase shift in each network must now be determined. This phase shift pertains to the *currents* of the system. The phase length of the terminated lines between radiators is the same as their electrical length of 135 degrees—the spacings between radiators.

Using an L network at A makes us dependent upon the phase shift that happens to come out of the imposed conditions, because with an L network there is no independent control of phase shift. Hence before going further this network will be solved. The result is shown in Fig. 2.26, and the phase shift is +77.5 degrees.

The total phase lag between the currents of radiators 2 and 1 must be 45 degrees. From the main line to radiator 2 there is a phase advance of 77.5 degrees. From the main line to radiator 1 there must therefore be a total phase advance of $77.5 - 45 = 32.5$ degrees. There is already a phase lag of 135 degrees in the line, so that there must be a phase advance of $135 + 32.5 = 167.5$ degrees introduced by networks B and D. The choice of networks is arbitrary, but advantage can be taken of simpler circuits if one of these networks is an L, using only two elements. If B is so made, we tie down its phase shift. Upon solution of the circuit of Fig. 2.27 we find the phase shift to be $+55$ degrees. This leaves

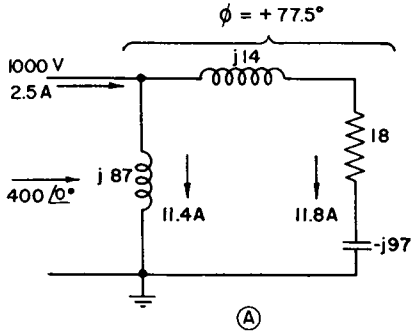

FIG. 2.26. Network A.

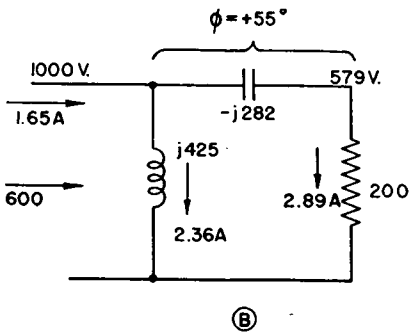

FIG. 2.27. Network B.

$+112.5$ degrees to be obtained in network D, which is obtained by the circuit of Fig. 2.29.

Network C can be made in the form of an L also because the phase remainder can be taken up in E. The total phase shift between the main feeder and radiator 3 must be -237.5 degrees, of which there is -135 degrees in the line. Between networks C and E there must be a total phase shift of $-237.5 + (-135) = 102.5$ degrees.

2.7.4. Phase Diagrams. These phase relations are confusing until set out in a separate diagram like Fig. 2.25, which shows all of the phases of the system. It is to be noted that the desired phase can be attained usually in two ways—by advancing phase or retarding it. The choice is important from the standpoint of network economy and minimum storage of energy in all the circuits of the system, a factor in its selectivity characteristic. The nearest rule that one can suggest for the choice is to go in the direction, positive or negative, that gives the smallest total phase shift in the networks of a branch circuit.

In the phase diagram for this problem (Fig. 2.25), I_2 is taken as reference phase. I_1 will lag by 45 degrees, and I_3 will lead by 45 degrees. The phase shift across A was found to be 77.5 degrees, the current I_2

leading the main line current I_0 by this amount. This brings I_0 at -77.5 degrees in the diagram. Next the phase lag in the secondary lines is shown with reference to I_0, so that the 135-degree line and A together total -212.5 degrees. An auxiliary vector is drawn for this.

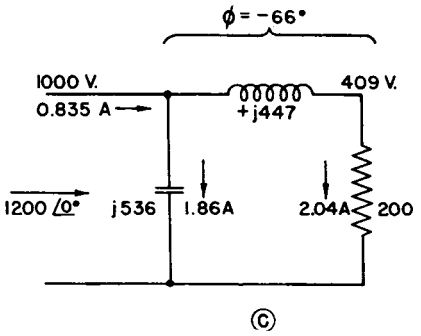

FIG. 2.28. Network C.

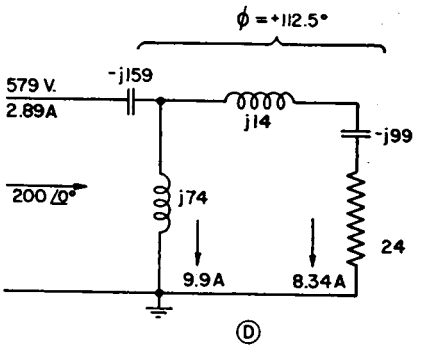

FIG. 2.29. Network D.

It is seen that the smallest angle between this auxiliary vector and I_1 is counterclockwise, the direction of advance of phase. The angle is 167.5 degrees. Network B has been computed to have an advance of 55 degrees, leaving a phase advance of 112.5 degrees to be obtained in network D.

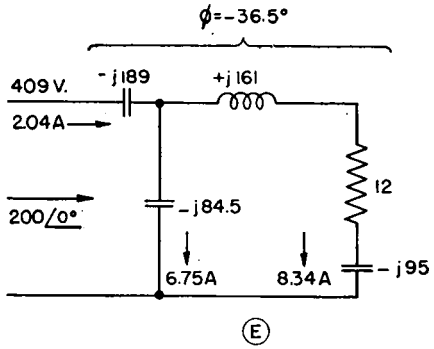

FIG. 2.30. Network E.

For the last branch of the circuit, it is noted that the angle between the auxiliary vector at 212.5 degrees and I_3 is -102.5 degrees (clockwise). If C is an L network, its phase lag is 66 degrees, and the values are as shown in Fig. 2.28. This leaves a lag of 36.5 degrees for network E.

After completing the synthesis of network E we have the circuits and values shown in Fig. 2.30.

Now we note that networks A, B, and C all have a parallel reactance directly across the main line. Thus, their combined parallel value can be obtained by using one reactance instead of three. There are values of $j87$, $-j536$, and $j425$ in parallel, which is equivalent to $j83.5$ ohms. Combining all the circuits for the system, we have the diagram of Fig. 2.31. See Chap. 5 for a simple method of network synthesis for problems of this type.

2.8. Broadcast Antennas on Buildings

When a broadcast antenna is to be placed on top of a building, as occasionally happens with low-power stations, there are special problems of feeding and grounding. The radiator is usually electrically short, that is, much less than one-quarter wavelength high. Its input impedance is therefore low in resistance and may have a substantial reactance, and tuning is accomplished with a series inductance. It is assumed that in any event a single insulated steel tower or mast would be used for the radiator.

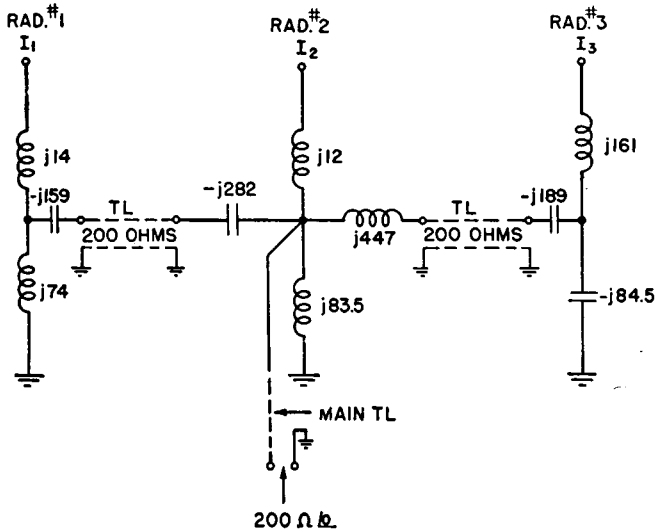

FIG. 2.31. Combined networks and feeder circuits.

The ground terminal must be constructed on the roof. If the roof is of sufficient area, a symmetrical counterpoise of 20 or more radial wires (insulated from all supports with light-duty insulators) may be a satisfactory ground. Since these conditions are seldom present, the system shown in Fig. 2.32 may be used. This is an adaptation of the principle of the Brown very-high-frequency ground-screen antenna. From two to four horizontal radial wires are centered under the radiator, each having an electrical length of one-quarter wavelength when loaded with inductance as shown. Each wire, when tuned naturally or with inductance, brings a virtual zero-potential point at the center which is taken as the ground point for the system. The full wire length can sometimes be used by allowing the excess length beyond the roof limits to hang down along the side of the building, properly secured and insulated.

The ground radials can be tuned by connecting two opposite wires in series and making symmetrical tuning adjustments in each inductance. The wires are disconnected from the mid-point during the tuning. A power oscillator of the correct working frequency is then coupled inductively to the two wires. Tuning is done by maximum current in the two

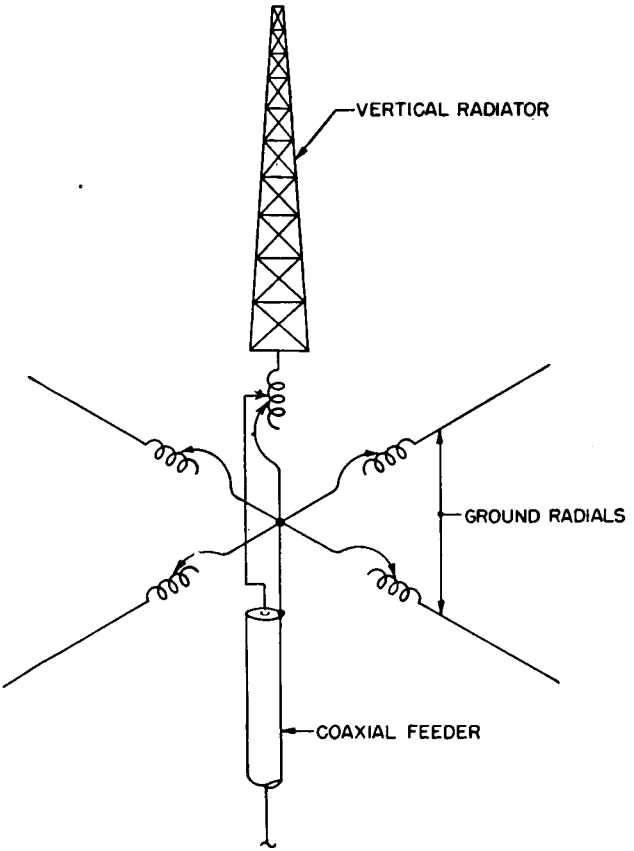

FIG. 2.32. Elementary grounding system for roof antenna.

wires, using a center-connected ammeter or a wavemeter near one of the coils away from the oscillator to avoid direct pickup from the oscillator. This tunes two wires to resonance as a half-wave system. This is repeated for the other two wires. Then they are connected permanently to a common mid-point. No loading inductors are necessary in using full-length wires, in which case the wire length should be about 0.24 wavelength to the end insulator.

The antenna is then tuned, using an impedance bridge if one is avail-

able, by connecting the correct amount of tuning inductance between the base of the radiator and the ground point.

The best feeder to use structurally in such a situation is a flexible coaxial cable of 50 to 60 ohms characteristic impedance. The sheath of the cable is terminated by connecting it to the ground point. The inner conductor, extended beyond the sheath by a flexible extension and clip, is attached to some point on the antenna tuning inductance, where it will present the impedance needed for a satisfactory matching of impedance of the cable. For a perfect match, the feeder clip and the clip attached to the ground point both require adjustment, but the match will usually be very nearly correct if only the feeder clip is moved after the antenna is originally tuned to resonance. The feeder clip will be near the lower end of the antenna tuning coil and will have to be adjusted carefully by fractions of turns.

The antenna tuning inductor may be housed, or if properly designed for the purpose, it may be in the open.

2.9. Antenna Potential

The root-mean-square potential V_a at the base of an antenna of measurable impedance $Z_a = R_a + jX_a$, for a power input of W watts, is simply

$$V_a = I_a Z_a \qquad I_a = \sqrt{\frac{W}{R_a}}$$

where I_a is the antenna current measured at the accessible terminals to the antenna system.

If the antenna has an electrical height G less than 75 degrees, the approximate potential V_m on the upper end is

$$V_m = \frac{V_a}{\cos G}$$

(This may also be used as a rough guide to the estimation of upper-end potential for antennas of heights from 110 to 225 degrees. It should not be used at all in the region of a potential minimum in the distribution occurring within 15 degrees each side of the point 90 degrees from the upper end of the antenna.)

For potentials at intermediate points, with the same limitations set forth above, adequate practical accuracy is obtained by considering that the potential varies cosinusoidally with distance from the upper end.

The antenna potential implied here is the potential at a point on the antenna itself with respect to ground. This is a physically unmeasurable quantity but has some significance in relation to guy insulation. It has

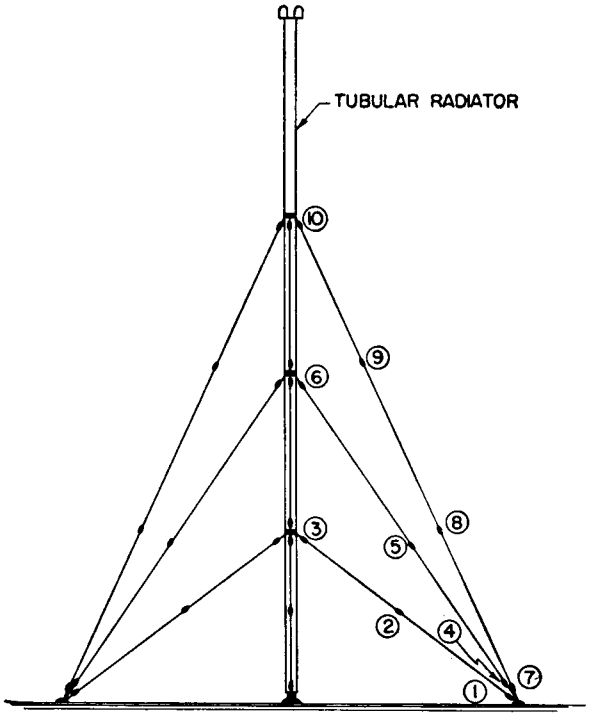

FIG. 2.33. Geometry of antenna and guys on which potentials of Table 2.7 were measured. (*After Brown.*)

TABLE 2.7. MEASURED VOLTAGES ACROSS THE INSULATORS NUMBERED ACCORDING TO FIG. 2.33 WITH 1,000 WATTS ANTENNA INPUT

Insulator	Heights, degrees		
	51.5	71.0	192
1	50.8	29.2	26.0
2	91.5	44.1	44.3
3	134.0	82.0	65.0
4	63.6	35.4	37.0
5	97.0	47.8	44.3
6	130.2	104.0	53.4
7	50.8	26.0	26.5
8	54.2	32.2	33.5
9	82.0	47.0	34.8
10	160	131.0	46.7

further significance in certain extreme applications of very large power, or a very small antenna conductor, or both, where the electric intensity at the surface of the conductor is required in the computation of potential gradients and the probability of corona formation.

Figure 2.33 shows the dimensions and layout of a tubular steel radiator, with the locations of guy cables and insulators.[9] The potential across each insulator was measured with a voltmeter, at known power input, operating at frequencies that gave this antenna electrical lengths of 51.5, 71.0, and 192 degrees. The voltages for 1,000 watts antenna input are shown in Table 2.7.

2.10. Aircraft Obstruction Lighting for Tower Radiators

Grounded supporting towers do not require any special isolation means, and the conduits for the lights are run directly up the tower from ground. When the tower is the radiator and is series-fed, as is common practice, the lighting circuits must pass by the insulated base and the antenna coupling circuits in such a manner as to appear as very high reactance at the operating radio frequencies.

There are three more or less standard methods for conducting lighting power for the tower past the antenna base.

1. The use of a toroidal tower-lighting transformer. The primary is toroidally wound on a circular iron core, and the secondary is an ordinary winding. The latter is cross-linked with the primary like two links of a chain. The primary is attached to the ground side of the tower base, and the secondary is attached to the lower part of the tower proper, above the insulator. The primary and secondary are thus separated by a large air space. At radio frequency this transformer acts as a simple capacitance in parallel with the base insulator.

2. Forming the power wires into an inductance having a sufficiently high impedance to have negligible effect on the feed-point impedance of the antenna. This lighting choke is formed with the two wires of the lighting circuit wound in parallel and is designed to have a sufficiently high Q not to cause excessive power loss.

3. Using a motor generator, the motor located on the ground side, and driving the generator, at tower potential and located on the tower proper, through a coupling shaft of dielectric material.

Aircraft obstruction-lighting requirements are dictated by regulations that vary somewhat in different countries. These specify the power of lamps to be used, the heights of lamps, the number to be used at each specified level, and the use of flashing beacons at the top and at intermediate levels in special cases. The specifications are sometimes based on the proximity of the tower to airports or airways and on the tower

height. In some countries, towers below certain heights or towers located outside of practical flying areas are not required to be lighted.

A high tower with several levels of double lamps and a large flasher

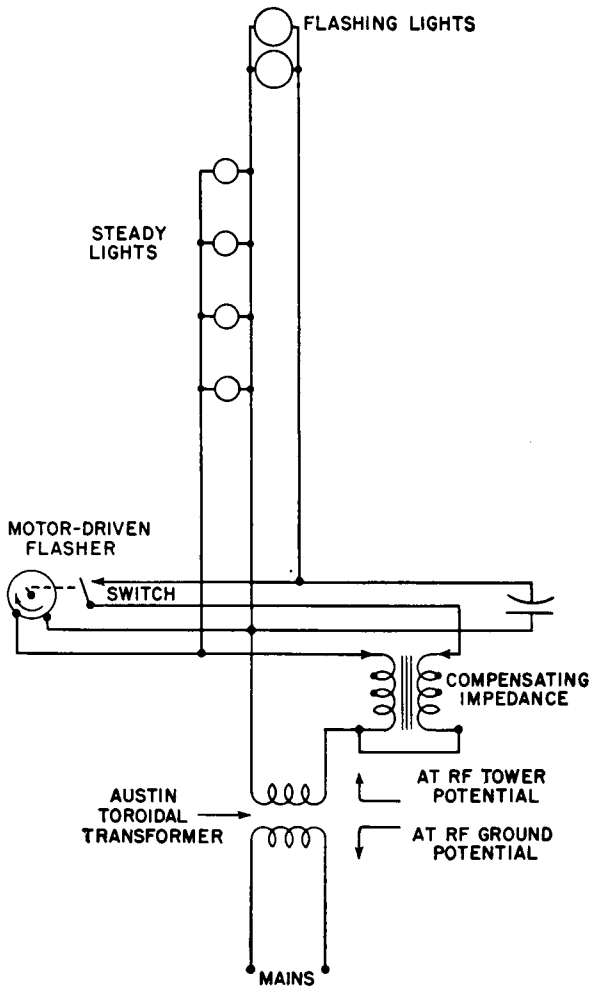

FIG. 2.34. Radio-tower-lighting system.

beacon at the top and at an intermediate level requires, in some cases, 2 kilowatts or more of lighting power.

The changing of lamps on towers is usually inconvenient, and the frequency of changing is minimized by operating the lamps at 5 to 10 per cent below rated voltage. This reduces the light intensity slightly but increases the life of incandescent lamps tremendously. Beacon lamps

are usually required in duplicate, with automatic change-over in case of failure of one.

A circuit diagram of a tower-lighting system using a tower-lighting transformer is shown in Fig. 2.34.

2.10.1. Frequency-modulation or Television Antennas on Amplitude-modulation Broadcast Antennas. The mounting of an antenna for frequency modulation or television on a medium-frequency tower antenna

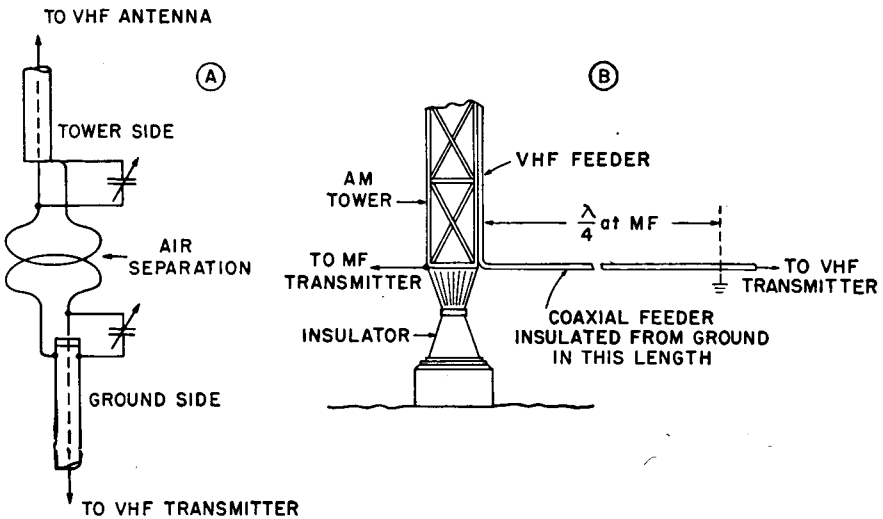

FIG. 2.35. Two methods of by-passing tower-base insulator to feed a very-high-frequency antenna on tower. (*After Holtz.*)

in such a way as to increase its height or produce the effect of top loading will affect its feed-point impedance. Corresponding changes in coupling and feeding adjustments are then required.

Separately feeding the very-high-frequency antenna and the medium-frequency antenna can be carried out as shown in Fig. 2.35.[26] In this figure, *A* shows inductive coupling between the two very-high-frequency feeders, one on the tower and one from the transmitter. Except for the capacitance between the small inductances providing the coupling, there is no effect on the medium-frequency coupling system. In *B*, the very-high-frequency feeder is continuous from transmitter to the antenna on the tower. It is attached to the tower directly but is insulated from ground a distance of one-quarter wavelength of the operating medium frequency, at which point the outer sheath of the very-high-frequency feeder is grounded. This quarter-wave section, grounded at one end, provides a virtually infinite impedance at the operating medium frequency as seen from the tower-base end feed point. Should the feeder

be less than one-quarter wavelength long, any length deficiency can be corrected for by using a small tuning capacitance between the sheath of the very-high-frequency feeder and ground at the base of the tower.

2.11. A Single Vertical Radiator for Two Different Frequencies

One radiator can be used to transmit two different frequencies simultaneously provided that the frequencies are not too close together and that the radiation characteristics at the two frequencies are satisfactory.

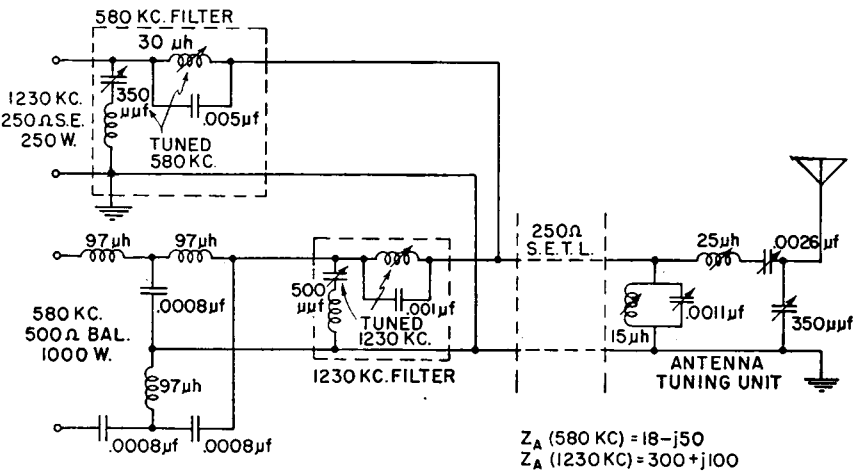

FIG. 2.36. Example of feeding vertical radiator from two broadcast transmitters.

Feeders from each transmitter are brought to a common junction through networks that are designed to provide the proper impedance match at one frequency and simultaneously to act as a stopper circuit for the other frequency. This prevents energy from one transmitter finding its way into the output circuits of the other transmitter, where it would cause cross talk between the two programs.

A stopper circuit is one that appears to be an infinite impedance at one of the frequencies, while having some specified impedance at the other.

Using complementary stopper circuits in each feeder near their common junction provides the requisite unidirectional power flow from each transmitter into the common circuit and thence to the antenna. At the antenna, the coupling network must match the antenna impedance to the feeder at the two frequencies, taking into account the fact that the antenna impedance will be different at each of the frequencies. Furthermore, all this must be done without impairing the bandwidth requirements for each transmitter.

The solution of such a problem depends entirely upon the conditions prevailing and perhaps upon the ingenuity of the designing engineer. The problem gets more serious as the two frequencies get closer together. In general it can be said that the frequencies should differ by 100 kilocycles or more in the medium-frequency broadcast band, but at least one case is known where the frequency difference was less than this.

It may be instructive to describe the circuits for one such problem, in which a broadcast transmitter having a 500-ohm balanced output and working on 580 kilocycles was to be used in parallel with another transmitter of 250 ohms unbalanced output on 1,230 kilocycles. A 250-ohm unbalanced open-wire line was used from the antenna to the radio station, and so it was necessary to employ a balance-to-unbalance network, 500/250 ohms, between the 580-kilocycle transmitter and its feeder branch. Figure 2.36 shows the circuits and values computed for the system. When installed, only minor trimming adjustments were needed to obtain the desired parallel performance with a single radiator.

2.12. General Equations for the Patterns of Multielement Arrays of Vertical Radiators

Not all of the problems of broadcast directive arrays can be solved with patterns of 90 or 180 degrees symmetry. In practice, asymmetrical arrays are frequently required. The computation of patterns is thus greatly complicated because direct solutions are very seldom possible. Various mechanical and electronic calculating machines have been devised to reduce the labor required to find a pattern of the desired characteristics by trial. Cumulative experience with such problems increases the facility of approach and reduces the time required to attain a solution. There are no simple rules to guide one in such cases, and usually one may not even know how many radiators are needed to obtain an acceptable asymmetrical pattern. Since there is almost no probability of any two directive broadcast situations being the same, each problem becomes a new one.

The equations for a generalized multielement array of identical vertical radiators can be expressed in several different forms, the most useful and the simplest being the vector form.

Let one radiator be the zero space-time reference, and let all other spacings, directions, phasings, and current ratios be reckoned from it. Let zero azimuth be true north, and measure azimuths β clockwise. Reference radiator is represented by subscript 0 and other parameters associated with other radiators by subscripts 1, 2, 3, etc., to $m = n - 1$ for an n-radiator array.

Then, the horizontal pattern is written

$$f(\beta) = 1 + k_1 e^{iX_1} + k_2 e^{iX_2} + \cdots + k_m e^{iX_m}$$

in which $f(\beta)$ is the relative horizontal pattern of field strength,

$$k_m = \frac{I_m}{I_0}$$

(may be greater or less than unity), e^{iX_m} is a unit rotating vector at an angle X with respect to reference unit vector, X_m is the phase angle of the mth radiator field due to space and time differences with respect to reference radiator field, and $X_m = S_m \cos(\beta - \beta_m) + \phi_m$, where S_m is the electrical spacing of radiator m from radiator 0 and is always reckoned positive, β_m is the azimuth of the line through radiator m and radiator 0 and ranges clockwise through 360 degrees, and ϕ_m is the time-phase difference between the currents I_m and I_0.

Since the geographical data which the pattern must fit are always in terms of azimuths with respect to true north, it is best to compute the pattern in the same coordinates.

The vertical pattern $f_\beta(\alpha)$ through any azimuth angle β is derived from

$$f_\beta(\alpha) = f_1(\alpha)(1 + k_1 e^{iY_1} + k_2 e^{iY_2} + \cdots + k_m e^{iY_m})$$

in which $f_\beta(\alpha)$ is the relative field strength at an angle above the horizon, $f_1(\alpha)$ is the relative vertical pattern for a single radiator, and $Y_m = S_m \cos[(\beta - \beta_m)\cos\alpha + \phi_m]$. All other symbols are the same as for the preceding equations.

Once calculated, the absolute field strengths are found by making a root-mean-square measurement of the pattern, placing this root-mean-square value at the field strength corresponding to the power used and the known realizable radiation efficiency of the array, and replotting the pattern to a convenient scale of field strengths.

These general vector equations are useful for checking the patterns for an array derived by any other method.

When the radiators of a system are symmetrically disposed in a straight line, with uniform or systematic symmetrical current distributions, the trigonometric form for the radiation patterns is more convenient for computation. The final pattern can be synthesized by employing the patterns for pairs of radiators having equal fields and, if the radiators are identical, having equal currents. Certain types of problems are best solved by multiplying pair patterns and others by adding pair patterns which are cocentered. The use of these different methods will be illustrated elsewhere. Actually, radiation patterns can be expressed in a variety of ways, and the choice is finally determined by the convenience

of manipulation and computation. The vector form just discussed is perfectly general and can be used without restriction of array geometry or the phases and amplitudes of the radiator currents. The vector method is convenient for graphical computations. In performing the computations arithmetically, the vector form is best converted to its real and imaginary components, adding all the real (cosine) terms, then all the imaginary (j sine) terms, and finally solving for the scalar value of the right triangle which they mutually form.

In synthesis techniques where the minimums of the pattern are being placed to achieve certain suppressions of field strength and where linear arrays with systematic current distributions can be used, the multiplication form of the pair patterns offers special advantages. However, when Fourier current gradings are employed to shape patterns in some specified manner, the trigonometric series of pair patterns is used.

2.12.1. Directive Antennas to Produce a Null at a Specified Angle in the Vertical Plane. The problem of designing an antenna to produce a null at some specific vertical angle is frequently encountered in broadcast directive-antenna design. If the suppression at the desired vertical angle can be on the array axis, the solution of this problem is relatively simple.

For example, a two-element array is to be used to suppress radiation to a prescribed value which is very small (but not necessarily zero) at an angle of 45 degrees in the vertical plane in one direction only. The approach is exactly as though a null at 45 degrees were desired in the horizontal plane also, which is obtained by

$$f(\alpha) = \cos\left(\frac{S}{2}\cos\alpha + \frac{\phi}{2}\right) = 0 \text{ at } 45 \text{ degrees}$$

$$\frac{S}{2}\cos 45 + \frac{\phi}{2} = 90$$

There is a range of values of S and ϕ that will satisfy the problem. The final choice will depend upon the suitability of a particular resulting horizontal pattern.

In any in-line array of identical radiators the pattern in the vertical plane through the radiators is obtained by multiplying the horizontal pattern $f(\beta)$ by the vertical pattern for one of the radiators $f_0(\alpha)$. If the array were composed of isotropic radiators, $f_0(\alpha)$ would be unity at all angles and so this vertical pattern would be identical to the horizontal pattern. This being so, there will be a null (or minimum) in the vertical pattern at the same angles from the ground as occur in the horizontal pattern, measuring from the line through the radiators. Then, if the vertical pattern $f_0(\alpha)$ for the vertical radiator includes one or more nulls

of its own, the main vertical pattern under discussion will contain nulls at these vertical angles as well as those derived from the horizontal pattern.

To illustrate this, assume that we require a directive-antenna pattern which, among other requirements, must have a null in the vertical plane through the array, in one direction, at 45 degrees. After some explora-

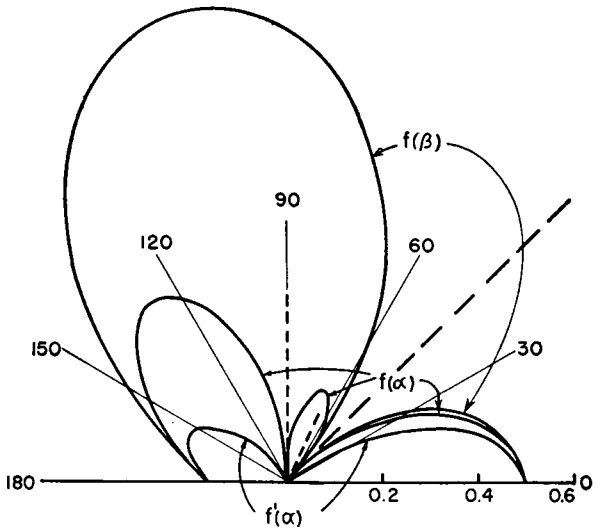

FIG. 2.37. Horizontal and two vertical patterns in the vertical plane through two radiators spaced 200 degrees and having equal currents with a phase difference of 45 degrees.

tory computations, we have found that an acceptable horizontal pattern is obtained by using two radiators spaced 200 degrees with a phase difference between their currents of 39 degrees. The horizontal pattern for this array is obtained from the following equation:

$$f(\beta) = \cos (100 \cos \beta + 19.5)$$

The relative pattern values from this equation are tabulated in the first column of Table 2.8. There is one null on each side of this pattern at 45 degrees from the line of the radiators.

Column 2 of this table is the vertical pattern for a short vertical radiator, short enough so that we can say that its pattern $f_0(\alpha) = \cos \alpha$. In using vertical radiators of this type, the main vertical pattern for the array will be the product of column 1 and column 2, which is $f(\alpha)$, tabulated in column 3, with the null at 45 degrees as required.

If instead it were desired to employ 190-degree vertical radiators in this array having the vertical pattern $f_0'(\alpha)$ listed in column 4, then the

main vertical pattern for the array would become that of column 5, which was obtained by multiplying values in column 1 by those in column 4. In this case, there is the null at 45 degrees due to interference between the spaced radiators, and another null at about 65 degrees contributed by the vertical radiator pattern.

TABLE 2.8

α and β	1 $f'(\beta)$	2 $f_0(\alpha)$	3 $f(\alpha)$	4 $f_0'(\alpha)$	5 $f'(\alpha)$
0	−0.500	1.000	−0.500	1.000	−0.500
10	−0.470	0.985	−0.462	0.94	−0.441
20	−0.407	0.940	−0.382	0.76	−0.310
30	−0.292	0.866	−0.253	0.52	−0.152
40	−0.139	0.766	−0.107	0.25	−0.035
45	0	0.707	0	0.21	0
50	+0.105	0.642	+0.067	0.14	0.0147
60	0.342	0.500	0.171	+0.03	0.010
70	0.588	0.342	0.201	−0.02	−0.0118
80	0.799	0.174	0.139	−0.02	−0.016
90	0.940	0	0	0	0
100	1.000	−0.174	−0.174	−0.02	−0.02
110	0.970	−0.342	−0.332	−0.02	−0.019
120	0.866	−0.500	−0.433	+0.03	+0.026
130	0.719	−0.642	−0.461	0.14	0.100
140	0.545	−0.766	−0.407	0.25	0.136
150	0.391	−0.866	−0.338	0.52	0.203
160	0.276	−0.940	−0.260	0.76	0.210
170	0.208	−0.985	−0.204	0.94	0.196
180	0.174	−1.000	−0.704	1.000	0.174

$f_0(\alpha) = \cos \alpha$ (for short vertical radiators).
$f_0'(\alpha) = [\cos (90 \cos \alpha) \cos (190 \sin \alpha)]/\sin \alpha$ (for 190-degree vertical radiator).

The patterns for columns 1, 3, and 5 are plotted in Fig. 2.37 for comparison. Note that $f'(\alpha)$ has only a tiny lobe of radiation above 45 degrees so that there is practically no radiation between 45 and 90 degrees on the right-hand side of the diagram. Using the short radiators, there is a rather large high-angle lobe in this space. The admissibility of this lobe would depend upon the problem at hand.

Using this same illustration, the locus of all the nulls in the three-dimensional pattern for this array can be found immediately by drawing Fig. 2.38. This is a plane orthographic projection of the hemisphere enclosing the array. The chord line 1-2 is the locus of nulls due to the

spacing and phasing of the two radiators and passes through the 45-degree points each side of the array axis where $\alpha = 0$ (horizontal plane) and also $\alpha = 45$ degrees in the main vertical plane through $\beta = 0$. At other orientations the nulls follow the chord. The null in the vertical plane through $\beta = 30$ degrees is seen to be at about 37 degrees above the hori-

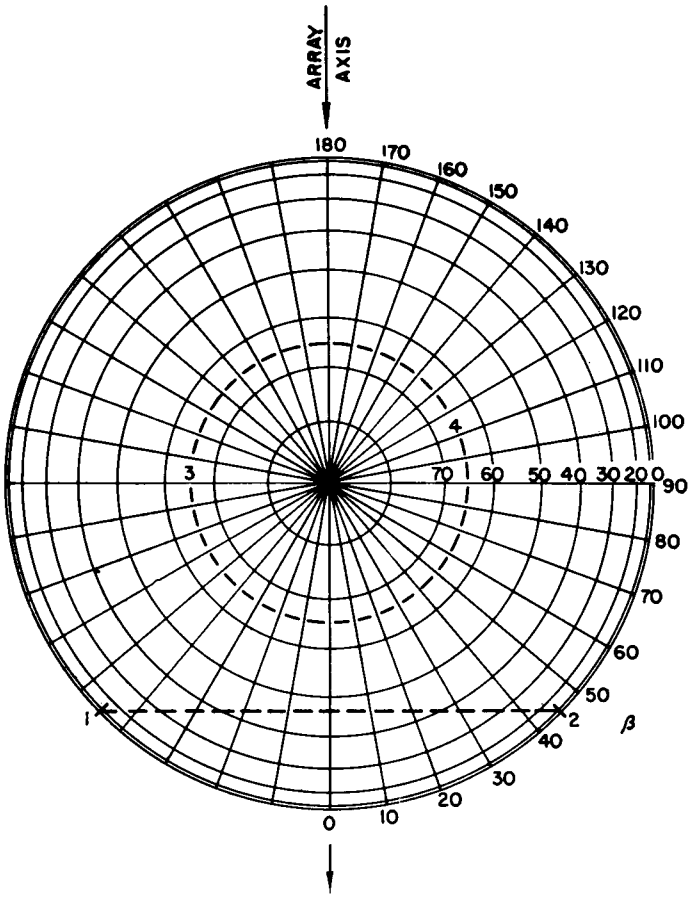

FIG. 2.38. Example of location of null lines (dotted) at higher angles.

zon, and in the direction $\beta = 40$ degrees the null occurs at about 24 degrees above the horizon.

Now consider the dotted circle 3-4 at 65 degrees above the horizon in all directions. This is the null circle for the 190-degree vertical radiator. The only null in the vertical plane for a radiator less than 180 degrees high is at 90 degrees (zenith).

This example points the way to a rapid solution for the null angles in

the three-dimensional pattern for any *linear* array of identical vertical radiators. An orthographic projection of the hemisphere is drawn, placing a pole at the zenith and laying out the angles β from the axis of the array from zero to 180 degrees each way. The latitude (α) lines are laid out orthographically by drawing circles through points that divide the radius in proportion to cos α, as in Fig. 2.38. With the hemispherical coordinates prepared in this way, place points on the periphery at the angles that correspond to null angles in the horizontal pattern for the array, symmetrically, and draw chords across the chart to connect corresponding nulls on each side of the axis. Then draw circles from the center at any vertical angle for a null in the vertical pattern for the radiator to be used, if there is one. From these the location of the nulls in all other vertical planes can be read directly from the diagram thus prepared.

From a diagram of this type one can form a mental picture of the vertical pattern at any azimuth when the horizontal pattern for the array and the vertical pattern for a single radiator are known. It will be recalled that in the direction broadside to the array the vertical pattern for the array will be identical to a single radiator.

When the array consists only of two vertical radiators, the null zones in the three-dimensional pattern occur wherever

$$\cos \alpha \cos \beta = \frac{180 - \phi}{S}$$

2.13. Directive Antenna with Maximum Gain for Two Radiators

It often occurs that directivity is desired to increase field strength in one direction only. Intuitively one thinks of using a cardioid pattern for this purpose. With a two-radiator cardioid pattern, the maximum field strength is about 1.43 times that for the same power into one radiator. The feed system for such an array is relatively complicated because of the need for dephasing the currents in the two radiators, and this in turn causes unequal powers in them. Therefore, unless the suppression of radiation in the backward direction is also a requirement along with the desire to increase signal in the forward direction, this type of system does not provide the best solution.

Reference to the polar patterns for two radiators with equal currents that include the effect of mutual impedance (see Appendix IV-A) shows good possibilities for high gain when the currents are equal and cophased. The patterns are bidirectional, but the horizontal directivity gain can reach values of the order of 1.75 in terms of relative field strength for the same power into one radiator. This is obtained with radiator spacings

between one-half and five-eighths wavelength. The maximum value occurs at a spacing of five-eighths wavelength.

The feeder system for a two-element cophased array with equal currents can be very simple, because the electrical symmetry of impedances and power division permits the system to be energized by a symmetrical feeder system. Figure 2.39 shows the simplest arrangement of a symmetrical feeder system for such an array. The equality of antenna impedances makes it necessary only to apply equal cophased potentials at each radiator base. This can be done by providing identical distances from the transmitter to each radiator.

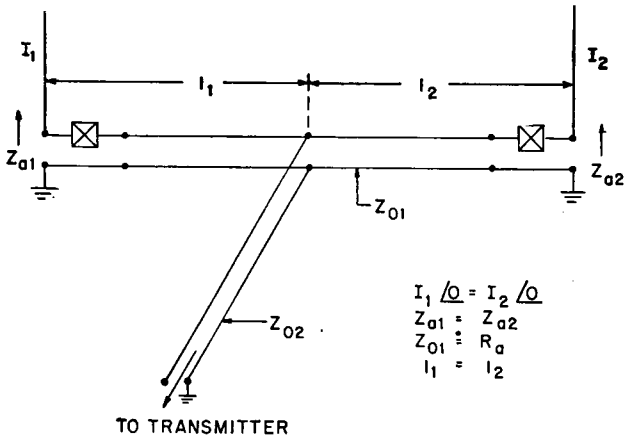

FIG. 2.39. Feeder system for a two-element array with equal cophased currents using only transmission lines for impedance matching.

As illustrated in Fig. 2.39, a main feeder attaches to the center of a secondary feeder running between the two radiators. These feeders may or may not be matched in their terminal impedances. The admissibility of mismatches will depend only on the magnitude of standing waves and the consequent feeder losses. In cases where standing waves on feeders must be avoided the characteristic impedance of the secondary feeder can be made equal to the input resistance of the radiator and identical series reactances used (shown as X) to neutralize any input reactance at the radiators. Otherwise the main feeder, terminated by whatever impedance exists at the middle of the secondary feeder, would in general be mismatched. One can employ a simple L network at this junction to match the main feeder, or one may use a value of characteristic impedance to give an exact or an approximate self-match, together with series neutralization of the existing reactance at the junction. Alternately, the mismatch may be allowed and the input impedance matched to the transmitter with a simple network.

2.14. Directive Antennas Using Unequal-height Radiators

A directive-antenna system using two or more radiators of identical physical dimensions, and therefore having intrinsically equal, or near-equal, self-impedances, is computed on the basis that the field strength contributed from each radiator is proportional to the radiator current. Therefore we can talk about radiation patterns directly in terms of radiator currents. When a directive array includes radiators of unequal heights and other dissimilar physical dimensions, it is impossible to use a direct proportionality between radiator currents and their contributing fields. The effective field strength of each radiator must be taken into account in computing a pattern. The use of unequal radiators greatly increases the engineering complications of a design.

In an array of dissimilar radiators, the current ratios for equal horizontal field strength must be computed first. When the desired pattern has been determined, the field contributions from each radiator may be ascertained. The current ratios for the different radiators in the system are then derived. The different self-impedances are then entered into the network equations with their associated currents and mutual impedances to determine the input impedance and the power input to each radiator. After this the synthesis of the phasing, impedance-matching, and power-dividing networks can be carried out, taking into account the arrangement of the feeders.

The computation of the vertical radiation patterns for the array in various directions is also complicated by the fact that the vertical pattern for each radiator of different physical dimensions will be different.

Mutual impedances between vertical radiators of unequal heights, over the range of values ordinarily encountered in broadcast arrays, have been published.[44,1011,1023]

Precautions must be taken to avoid excessive ground-terminal losses in any array when the input resistance to any radiator is driven down to a very low value by virtue of mutual impedances—especially if a substantial amount of power is to be put into such a radiator. In a system of unequal-height radiators this effect has to be more carefully watched because of a lower self-resistance of a short radiator and the probable need for a higher current in it to produce the desired effective field strength.

In general, very short radiators in a system of higher radiators are justified only where a radiator is required to make only a small contribution to the pattern and where input power and base current will be relatively small. Where unequal radiators are used, there are usually no more than two different radiator sizes. The purpose of such a practice is to avoid the expense of a full-size radiator when only a small portion

of the total power is to be contributed by it. Occasionally, the reason is that some existing towers are employed together with one or more new radiators. Dissimilarity is also introduced when a television or other very-high-frequency antenna is mounted on top of one radiator in an otherwise uniform system of identical radiators.

2.15. Directive Antennas for Wide Angles of Suppression

This section is devoted to a demonstration of certain principles that can be employed to obtain radiation patterns having wide angles of suppression. Four methods are presented by means of the solution of type problems, each of which suggests a basic principle. The suitability of any one of these principles in any specific engineering problem depends upon the nature of that problem.

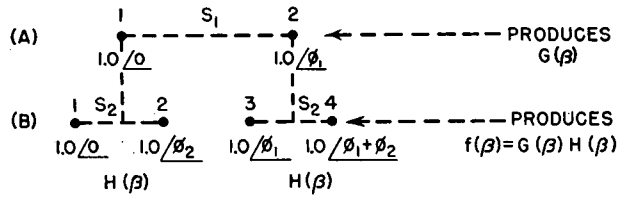

FIG. 2.40. Array synthesis by successive pairings to control location of zeros.

Under the existing allocation standards of the FCC and the North American Regional Broadcasting Agreement, the problem of suppressing radiation over wide azimuth angles frequently arises. On class 1 channels the entire border of a country may have to be protected from interference, or the entire night sky-wave secondary-service area of a station must be protected. The design of antennas capable of such performance presents a special problem.

The fundamental unit of an array of this type is a pair of identical radiators with equal currents. The final array is a synthesis of several such pairs. The economical objective is to make one radiator do multiple duty by being a part of more than one basic pair.

2.15.1. Wide-angle Suppression, Using Lobe-splitting Technique. Let $G(\beta)$ be the radiation pattern for a pair of radiators (each radiator having a circular pattern) with spacing S_1 in electrical degrees and equal currents of such phase (ϕ_1) as to place a null at an angle of β_1 each side of the axis. This arrangement is illustrated in Fig. 2.40*A*. Then

$$G(\beta) = \cos\left(\frac{S_1}{2}\cos\beta - \frac{\phi_1}{2}\right)$$

Now consider the case where each radiator is replaced by the center of a pair of radiators having the pattern $H(\beta)$ with axis coincident with

that of $G(\beta)$, as shown in Fig. 2.40*B*. Then $H(\beta)$ is specified by spacing S_2 and phase difference ϕ_2 so that

$$H(\beta) = \cos\left(\frac{S_2}{2}\cos\beta - \frac{\phi_2}{2}\right)$$

This pattern is such as to produce a null at an angle $\pm\beta_2$ from the array axis. Then, the pattern for an array of two pairs along a common axis with equal currents is

$$f(\beta) = G(\beta)H(\beta)$$

and it will have nulls at $\pm\beta_1$ and $\pm\beta_2$ from the array axis.

This method of using two pairs is sure to provide at least two nulls on each side of the axis, which can be placed as desired. In the case where $S_1 = S_2$, radiators **2** and 3 become coincident, and the effect of two pairs is achieved with three radiators. The current in the middle radiator must be the vector sum of those for radiators 2 and 3 considered separately.

This process can be continued in further similar steps as desired. The following is given to illustrate a case where this operation has been performed three times.

Example. Wanted a radiating system providing suppression of radiation over an angle of at least 90 degrees on one side of the pattern, the field strength within this angle to be less than 3 per cent of the maximum field from the array (± 45 degrees from the axis). Using the principles outlined, let us arbitrarily begin with a basic pair that has nulls at ± 43 degrees from the axis of the array, using 180 degrees spacing between radiators. Such a pattern is obtained when $\phi_1 = 48$ degrees.

$$f_1(\beta) = \cos(90\cos\beta + 24)$$

The pattern for this pair is shown by curve *A* in Fig. 2.41. Let us now use this pair as a directive source for a second pair, using the same spacing, but adjusting the phase to bring nulls at ± 30 degrees. The fundamental pair of circular sources gives

$$f_2(\beta) = \cos(90\cos\beta + 12)$$

This pattern is plotted as curve *B* in Fig. 2.41.

If at this stage we synthesize the composite pattern

$$f_1(\beta)f_2(\beta) = \cos(90\cos\beta + 24°)\cos(90\cos\beta + 12°)$$

we obtain nulls at ± 30 degrees and ± 43 degrees. This is plotted as curve *C* in Fig. 2.41. It is seen that insufficient suppression occurs between 0 and ± 30 degrees.

Another pair of radiators spaced 180 degrees and having $\phi = 8$ degrees may be added. This pair will produce a null at $\beta = \pm 19$ degrees. Again

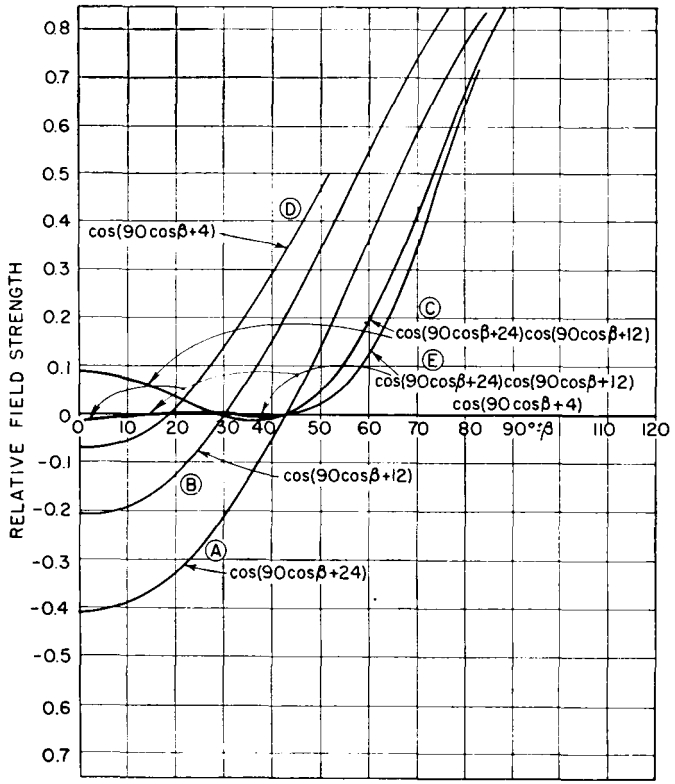

FIG. 2.41. Plots of successive development of broad null region by placing the zeros in successive pairings.

using circular-radiation sources, the radiation pattern (Fig. 2.41, curve *D*) is

$$f_3(\beta) = \cos (90 \cos \beta + 4)$$

If now this pair is made up of a pair of systems having the pattern $f_3(\beta)f_2(\beta)$, we obtain

$$f(\beta) = f_1(\beta)f_2(\beta)f_3(\beta)$$
$$= \cos (90 \cos \beta + 24) \cos (90 \cos \beta + 12) \cos (90 \cos \beta + 4)$$

This is plotted as curve *E* in Fig. 2.41. The radiation is less than 3 per cent of maximum over a range of ± 52 degrees. Throughout most of this angle (± 40 degrees) the field strengths are actually less than 1 per cent of maximum. This is desirable, because some operating margin is almost always desirable for arrays of this sort.

Array Synthesis. It remains to determine the actual array which will produce this pattern. This is accomplished by the three steps illustrated in Fig. 2.42*A*, *B*, and *C*.

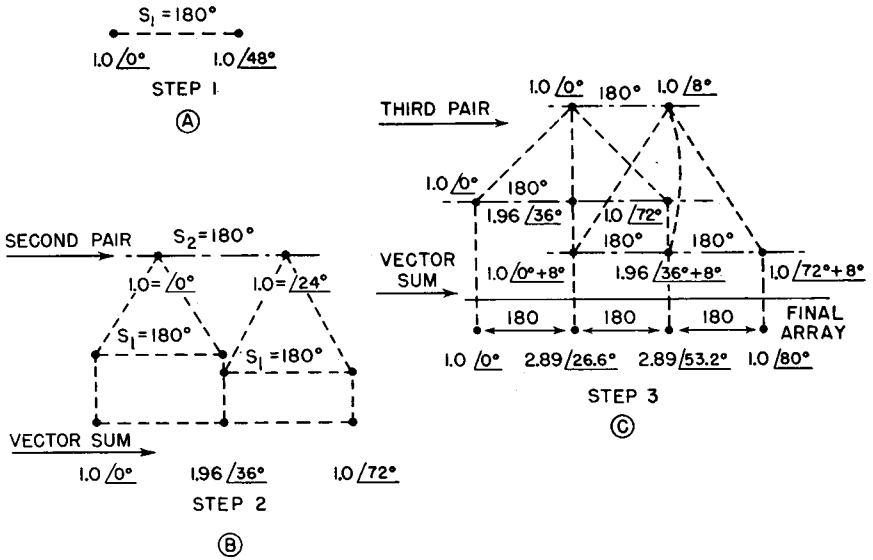

FIG. 2.42. Synthesis of array current distributions for system of Fig. 2.41.

To check the correctness of the foregoing synthesis, the vector method can be applied in the following manner; for the azimuth = ± 43 degrees, the location of one of the nulls

$$
\begin{aligned}
f(\beta) = 0 &= 1 + 2.89e^{j(180\cos 43 + 26.6)} + 2.89e^{j(360\cos 43 + 53.2)} + e^{j(540\cos 43 + 80)} \\
&= 1 + 2.89e^{j158} + 2.89e^{j316.2} + e^{j474.5} \\
&= [1 - 2.89(0.9272) + 2.89(0.74) - 0.4146] + j[2.89(0.3746) \\
&\qquad - 2.89(0.69) + 0.91] \\
&\doteq 0.045 - j0.003
\end{aligned}
$$

The real and imaginary parts equate to very nearly zero by omitting the use of some of the fractions of degrees in obtaining the sines and cosines. This is a satisfactory check on the synthesis process. This vector check provides some idea of the stability required to maintain the pattern. By changing the coefficients corresponding to current amplitudes by small increments the effect on the field in the null regions is quickly found.

2.15.2. Wide-angle Suppression Using Three Radiators. Examination of a chart of pair patterns (Appendix IV-A) shows that for $S = 5\lambda/8$ and $\phi = 180$ degrees both + and − lobes of the pattern have a very wide angle over which the field strength is constant. This leads us to use this

pattern in a system requiring a wide null angle. We note further that apparently a spacing slightly less than 0.625λ would be more constant in value over a range of angles (by comparing parallelism with the reference circle). We can test the possibilities by calculating from a spacing of 216 degrees (0.60λ). Such a pair will have the pattern

$$f_1(\beta) = \cos\left(\frac{216}{2}\cos\beta + \frac{180}{2}\right) \equiv -\sin(108\cos\beta)$$

from which we compute Table 2.9.

TABLE 2.9

α or β	$f_1(\beta)$	$f_2(\beta)$	$f(\beta) = 0.505[f_1(\beta) + f_2(\beta)]$	$f(\alpha) = f(\beta)\cos\alpha$
0	−0.951	0.975	0.024	0.024
10	−0.956	0.975	0.012	0.012
20	−0.978	0.975	0.009	0.009
30	−0.998	0.975	−0.0015	−0.013
40	−0.993	0.975	−0.011	−0.0084
50	−0.937	0.975	+0.187	+0.012
60	−0.809	0.975	0.083	0.042
70	−0.602	0.975	0.188	0.064
80	−0.326	0.975	0.327	0.057
90	0	0.975	0.492	0
100	+0.326	0.975	0.660	
110	0.602	0.975	0.795	
120	0.809	0.975	0.900	
130	0.934	0.975	0.963	
140	0.993	0.975	0.994	
150	0.998	0.975	1.000	
160	0.978	0.975	0.986	
170	0.956	0.975	0.975	
180	0.951	0.975	0.970	

In order to cancel the negative lobe of $f_1(\beta)$ over its angle of constancy we added $f_2(\beta) = 0.975$, corresponding to a circular source of radiation of relative strength 0.975, located at the center of the pair. The sum of the patterns from the pair and from the central radiator has been calculated and, after normalizing to a maximum relative value of 1.00, tabulated in Table 2.9. The horizontal pattern is plotted in Fig. 2.43.

Examination of these values shows that over an angle of ±50 degrees the field strength is less than 2.5 per cent of maximum. Without further calculation it appears that a blind angle of about 102 degrees is possible

with this array without exceeding 2.5 per cent of maximum field. Furthermore in the vertical plane $f(\alpha)$, using 60-degree radiators, the field does not exceed 6.4 per cent of maximum at any angle, and it is below 3 per cent at vertical angles up to 50 degrees. If higher radiators are used, the vertical pattern can be reduced much below these values at the higher angles.

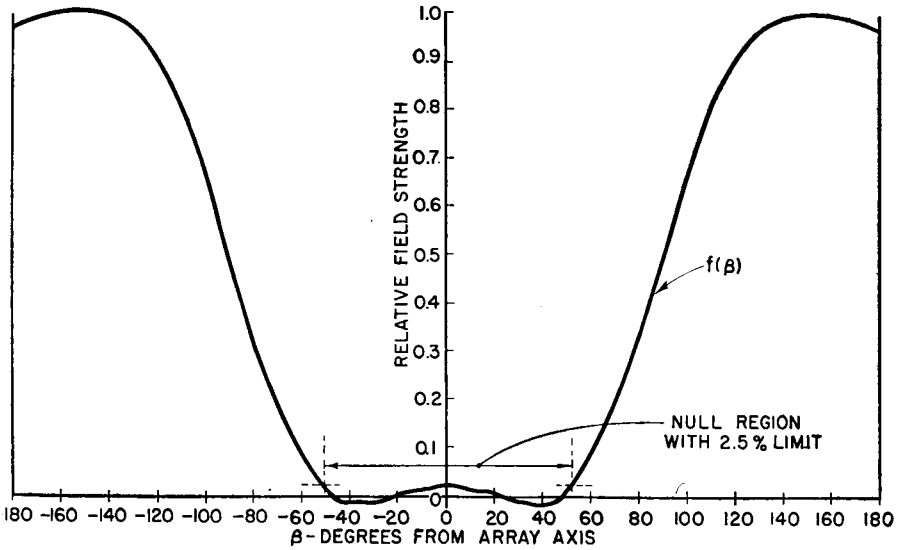

FIG. 2.43. Pattern for three-element array with cancellation of fields over a wide angle on one side.

The broad beam on the opposite side is constant over the same wide angle.

The normalized pattern specification is

$$f(\beta) = [0.975 - \sin (108 \cos \beta)]0.505$$

For the fields to add in this manner, the central-radiator current must be in quadrature with the currents in the outer radiators.

A rectangular plot of the pattern is shown in Fig. 2.43. The current relations will be

$$1.0/\underline{0}, \qquad 0.975/\underline{90}, \qquad 1.0/\underline{180}$$

The pattern can be inverted by reversing the polarity of the current in the central radiator.

2.15.3. Wide-angle Suppression Using Binomial Current Distributions. *Example.* A North American Regional Broadcasting Agreement class 2 station of 50 kilowatts is to be located on a class 1-B channel. The

directive antenna must provide for the protection of the 500 microvolts per meter night sky-wave areas (50 per cent of the time) of two class 1-B stations by suppression of radiation so that, at the protected sky-wave boundaries, the new station's signals will be less than 25 microvolts per meter all but 10 per cent of the time. Referring to appropriate maps and propagation curves, it is determined that the field strengths at 1 mile cannot exceed the values in Table 2.10.

TABLE 2.10

	Azimuth (true), degrees	Maximum permissible field at 1 mile along the ground, millivolts per meter
Station *A*	10	600
	12	310
	15	162
	20	130
	30	121
	40	140
	45	160
	50	275
	55	550
Station *B*	305	460
	310	190
	320	160
	330	165
	335	190
	340	410

These data are represented graphically in the upper part of Fig. 2.44. Mid-angle of the open gap between zones of protection = 356 degrees. The axis for the array will be placed on this bearing. The angles of maximum suppression will be placed at ± 40 degrees with respect to the array axis.

The directive pattern must be such as to fall well within these boundary values in operating at 50 kilowatts. The amount of signal suppression is rather extreme since 50 kilowatts into a nondirective one-fourth-wave radiator produces a field strength at 1 mile of about 1,200 millivolts per meter (175 millivolts per meter at 1 mile with 1 kilowatt).

We look at a chart of patterns for antenna pairs (Appendix IV-A) for a suggestion to start. It is noted that the angle between the two directions of greatest required signal suppression is about 80 degrees. We must then search for a possible pattern which will bring two symmetrical nulls 80 degrees apart, or 40 degrees from the axis of the array, also taking into account the client's desire for a maximum of radiation southwest-

ward if possible. From the chart of patterns for radiator pairs we find one for $S = 0.375\lambda$, $\phi = -90$ degrees which looks promising. The null angles may not be correct, and we see, in proportion to the unit circle,

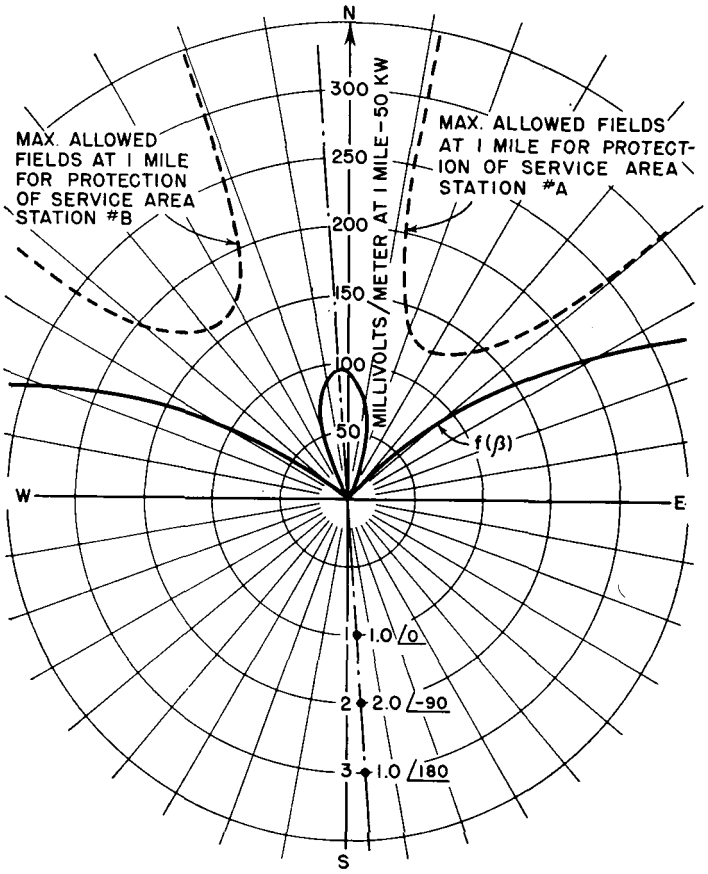

FIG. 2.44. Minor lobe reduction and null broadening using a squared pattern from a binomial array.

that the field strength of the minor lobe is about one-half that of non-directive operation, which is too large. Also, the nulls are not wide enough for our needs. But we must examine the requirements for a null angle 40 degrees each side of the axis and find the spacing required to give this. This is done as follows:

As before, the equation for all these patterns is

$$f(\beta) = \cos\left(\frac{S}{2}\cos\beta + \frac{\phi}{2}\right)$$

We know $\beta = 40$ degrees and $\phi = 90$ degrees and $\cos 40 = 0.77$. Hence

$$\cos\left(0.77\,\frac{S}{2} + 45\right) = 0$$

For the cosine of an angle to be zero, the angle must be 90, 270, 450 degrees, etc. In this case we use 90 degrees. Then

$$\frac{0.77S}{2} + 45 = 90$$

from which

$$S = 116 \text{ degrees}$$

Knowing S, we can then calculate the whole pattern as shown in Table 2.11. This pattern shows the minor lobe to be too large for use. However, if we square the values in the table, the amplitude of the minor lobe

TABLE 2.11

β, degrees	$f(\beta)$	β, degrees	$f(\beta)$
0	0.225	100	0.819
10	0.208	110	0.906
20	0.156	120	0.961
30	0.087	130	0.990
40	0.000 (minimum)	140	1.000 (maximum)
50	0.139	150	0.996
60	0.276	160	0.988
70	0.423	170	0.978
80	0.573	180	0.974
90	0.707		

changes from 0.225 to 0.051 of maximum value for the pattern and the nulls are broadened. Let us then tabulate the squares of these values and get Table 2.12.

We must now determine the *actual* field strengths in the critical regions at 50 kilowatts to see whether or not we are within limits everywhere. To do this, we must change this pattern from a relative set of values to an absolute set of field strengths. This requires finding the root-mean-square value of the pattern. For simple arrays of this type this is obtained in two ways: (1) With a polar planimeter, measure the area of a polar plot of the above pattern, and construct a circle having exactly the same area.*

* The method of obtaining the root-mean-square value of a pattern by integrating the horizontal pattern only, as was done here, is not sufficiently accurate for any but the very simple systems. The correct determination of root-mean-square pattern values requires integration of the pattern over the complete hemisphere enclosing the antenna system. For methods, consult refs. 44 and 45.

The radius of this circle is the relative field for the same power nondirectional; and we know what this should be in millivolts per meter from the antenna efficiency and the power. From this we can assign values to all parts of the directive pattern. (2) All the squared pattern values of Table 2.12 can be squared again, added, and divided by the number of values added (19 in Table 2.12). Then the square root of this value is taken, and this is the radius of the root-mean-square circle, in proportion to the arbitrary dimensions of the pattern as calculated. This again is known to be so many millivolts per meter, which in our case is 1,200 millivolts per meter.*

In the above case, the radius of the root-mean-square circle is 0.645 = 1,200 millivolts per meter. The magnitude of the minor lobe at $\beta = 0$ is $(0.051/0.645) \times 1{,}200 = 95$ millivolts per meter. This is well under what is allowed. The pattern is then calculated in field

TABLE 2.12

β	$f^2(\beta)$	β	$f^2(\beta)$
0	0.051	100	0.668
10	0.043	110	0.82
20	0.024	120	0.92
30	0	130	0.98
40	0	140	1.00
50	0.019	150	0.99
60	0.076	160	0.98
70	0.178	170	0.96
80	0.328	180	0.94
90	0.500	Root-mean-square value	0.645

strengths by multiplying the above tabulated values by 1,860 (obtained by putting 1,200/0.645 = 1,860). The pattern is now plotted on another sheet in a convenient scale of millivolts per meter versus angle and oriented in azimuth so that the nulls fall at the correct geographical angles, as shown in Fig. 2.44. In this case the axis of the array and its pattern is 356 degrees (4 degrees west of true north). Upon further examination of protections over all the angles required, it is found to be satisfactory, with ample margins.

To square such a pattern, as required in the above problem, the radiating system is derived as shown in Fig. 2.45. The pattern would be squared if each radiator of the pair had a pattern the shape of that given in Table 2.11, instead of a circular pattern, as they actually have. To

* This disagrees with the value in Table 2.1 because in this case we are considering a typical value for 50 kilowatts input to the antenna instead of 50 kilowatts radiated power.

obtain this same effect, we must use a pair of pairs, each pair spaced and phased relatively in the same way, and on the same axis. When we do this, we find that radiator *b* of the first pair coincides with radiator *c* of the second pair. Again we get a pair of pairs by using only three radiators, since one does double duty, as shown by the current being twice as much as the current in the end radiators. The current magnitudes and phase angles are shown in the various steps and in the final array.

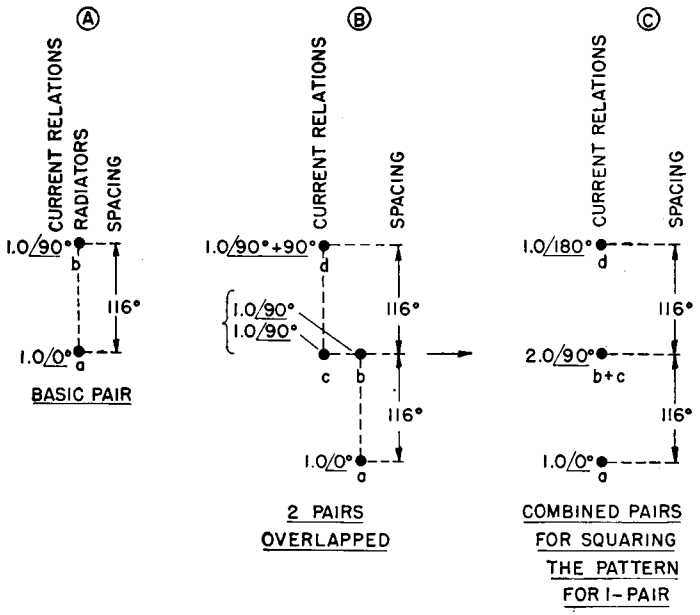

FIG. 2.45. Synthesis of the binomial array having the pattern of Fig. 2.44.

The horizontal pattern for this array then, taking into account its geographical orientation at 356 degrees and its root-mean-square field value of 1,200 millivolts per meter for 50 kilowatts, is

$$f(\beta) = 1{,}860 \cos^2 [58 \cos (\beta + 4) + 45] \quad \text{millivolts per meter at 1 mile}$$

2.15.4. Wide-angle Suppression Using Crossed Pairs. Where it is desired to produce two reciprocal wide-angle null zones, there are other means which provide wider nulls than demonstrated in Sec. 2.15.3. We can use two symmetrical pairs of radiators at right angles. Pair *A* consists of two cophased radiators spaced 270 degrees (0.75λ) and another pair of cophased radiators with its axis normal to the first, and spaced 180 degrees (0.5λ). This is suggested by a study of Appendix IV-A,

where we note that the two reciprocal minor lobes for the pair where $S = 0.75$ and $\phi = 0$ degrees have apparently the same general shape as the pattern for the pair having $S = 0.5$ and $\phi = 0$ degrees. The pattern amplitudes of the second pair are 0.707 of those in the first, and the two patterns are mutually cophased.

Since both pairs have a common center point, their resulting patterns can be added algebraically angle by angle.* These patterns are symmetrical about 0 and 90 degree axes and are tabulated in Table 2.13.

TABLE 2.13

β	$f_A(\beta)$	$f_B(\beta)$	$F(\beta) = f_A(\beta) + f_B(\beta)$
0	−0.707	+0.707	0
10	−0.682	0.678	−0.004
20	−0.602	0.608	+0.006
30	−0.454	0.500	0.046
40	−0.242	0.374	0.132
50	+0.052	0.254	0.306
60	0.380	0.148	0.528
70	0.695	0.071	0.766
80	0.921	0.021	0.942
90	1.000	0	1.000

The pattern $F(\beta)$ is plotted in Fig. 2.46, which shows that, for a field strength less than 2 per cent of maximum, the null width is ± 25 degrees on each side of the pattern, or 50 degrees total.

This example suggests a further experimentation with the same idea to see whether or not even broader nulls can be obtained. If the spacing of the first pair is increased to 0.875λ (315 degrees) and the spacing of the second pair reduced to 160 degrees, a further broadening of the null region is realized. Computing the pattern for the condition where the maximum field strength of the second pair just cancels the maximum of the negative lobe of the first pair, the normalized pattern is

$$f(\beta) = 0.86[\cos (157.5 \cos \beta) + 0.924 \cos (80 \sin \beta)]$$

This pattern is superimposed on that for the preceding example (Fig. 2.46) for comparison, and we find that the field strength can be held at

* Special attention is directed to the fact that the pattern-field ratios are not necessarily the same as the current ratios between pairs in problems involving the *addition* of patterns. The current ratios result directly when patterns are synthesized by multiplication.

or below 2 per cent of maximum over an angle of ±36 degrees, or 72 degrees total, on each side of the pattern.

2.16. Producing Symmetrical Multiple-null Patterns

A great variety of symmetrical patterns having multiple nulls (or minimums) with a linear array of three radiators can be derived by the following simple method, illustrated by a random example.

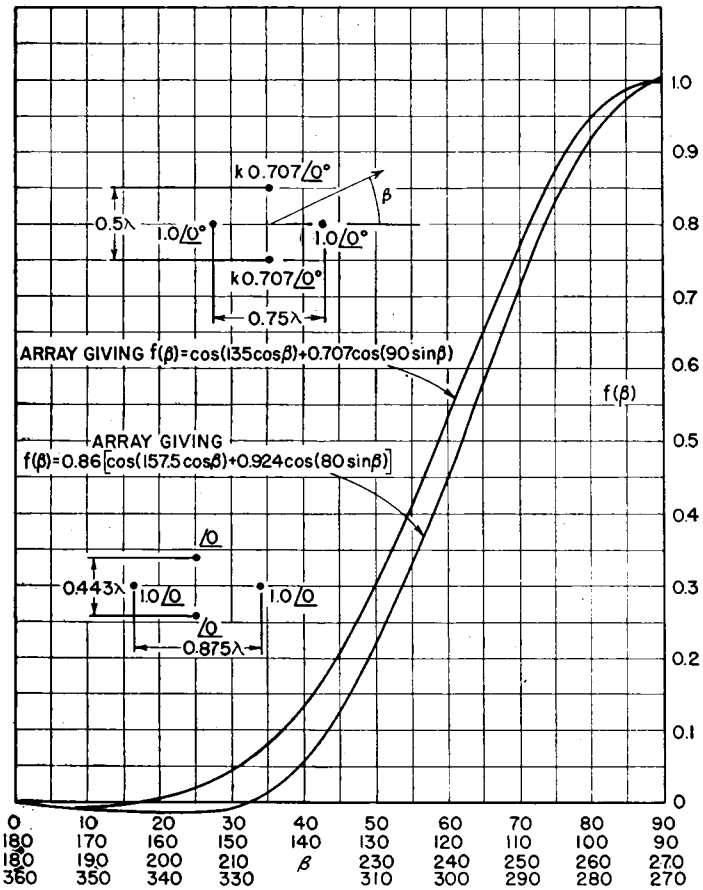

FIG. 2.46. Broad nulls obtained by crossed pairs of radiators.

We take the pair of radiators $S = 360$ degrees, $\phi = 90$ degrees, calculate its pattern in the usual way, and tabulate the values in Table 2.14. In the two right-hand columns we have added the field produced by a single nondirective radiator located at the center of the pair. We have

chosen a relative field strength of +0.76 to obtain $f_2(\beta)$ and −0.76 to obtain $f_3(\beta)$.

TABLE 2.14

β	$f_1(\beta) = \cos(180 \cos \beta + 45)$	$f_2(\beta) = f_1(\beta) + 0.76$	$f_3(\beta) = f_1(\beta) - 0.76$
0	−0.707	+0.053	−1.467
10	−0.743	0.017	−1.503
20	−0.829	−0.069	−1.589
30	−0.934	−0.174	−1.694
40	−0.999	−0.239	−1.759
50	0.946	−0.186	−1.706
60	−0.707	+0.053	−1.467
70	−0.292	0.468	−1.052
80	+0.242	1.002	−0.518
90	0.707	1.467	−0.053
100	0.970	1.730	+0.210
110	0.956	1.716	0.196
120	0.707	1.467	−0.053
130	0.326	1.086	−0.434
140	−0.056	0.704	−0.816
150	−0.358	0.402	−1.118
160	−0.559	0.201	−1.319
170	−0.669	0.091	−1.429
180	−0.707	0.053	−1.467

These three patterns are plotted in rectangular coordinates in Fig. 2.47 for clarity. It can be seen in this way that the addition of the fields from a nondirective source at the center of the pair simply "biases" the zero line of the pattern upward for a negative polarity of the center radiator field and downward for a positive. The intensity of the central source adjusts the angles at which the nulls occur. We need only have plotted $f_1(\beta)$ and moved the axis to positions shown by the dotted lines.

A practical application of this principle would involve an exploration for the best pattern for the pair and then the intensity and polarity of the center radiator field to bring the nulls at the desired angles and to provide an acceptable pattern between the nulls.

In exploring for such a solution, one can study the polar patterns for various pairs, marking the polarity of the lobes of these patterns (if not initially so marked) and then drawing circles to represent the central radiator pattern with an assigned polarity of + or −. From these directive and nondirective patterns, one can visualize qualitatively the locations of nulls (the intersections of the circle with the lobes of opposite

polarity) and the algebraic sum of the two, between nulls. After so determining in a rough way a satisfactory starting point, quantitative computations are made. The problem of bringing two or more nulls at correct angles with a satisfactory pattern otherwise cannot be solved directly but must be approached by successive trials. Rectangular

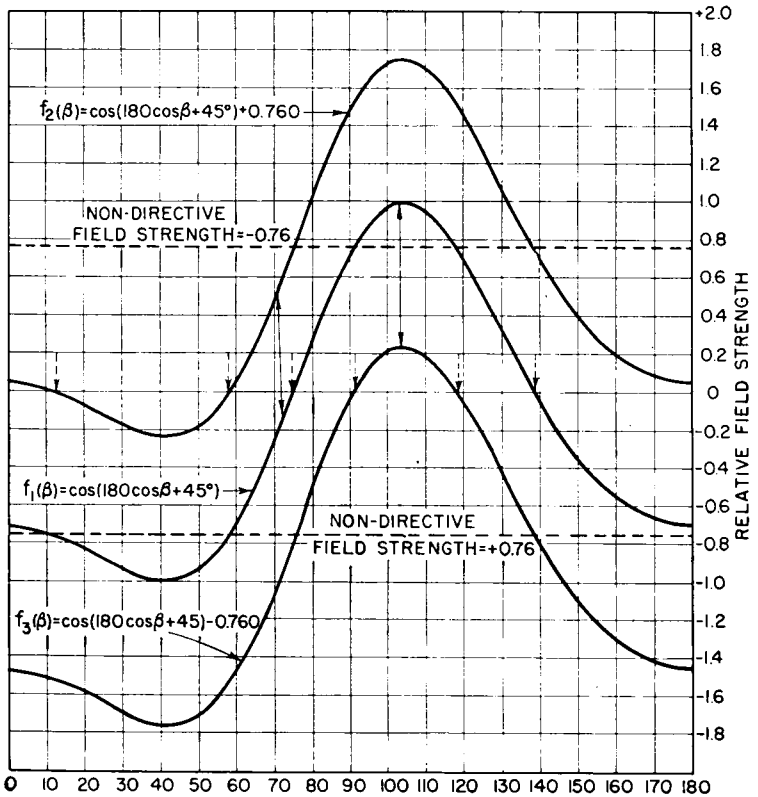

FIG. 2.47. Adjustment of pattern zero positions by using a biasing field from a central radiator with a pair.

coordinates are the most convenient for this purpose if graphical computation is used.

Anyone having frequently to make such calculations would have a large number of the pair patterns predrawn in rectangular coordinates and would use a transparent straightedge over the patterns until a desired choice is found.

The radiation pattern for this kind of array is obtained by the algebraic additions of the pair pattern with that of the constant value contributed by the central radiator. However, when it comes to determining the

phase of the current in the central radiator with respect to currents in the pair, the central-radiator current must always have a phase that is midway between the phases of the currents in the outer radiators. We may call this "mid-phasing." If in this example we refer all space and phase relations to the center of the array, the phases of the currents in the three radiators will have to be 45, 0, and -45 degrees; or taking one end radiator as reference, the phases must be 0, -45, and -90 degrees in succession.

The current ratio for the central radiator with respect to the pair, and therefore the division of power between them, must be separately computed, taking into account the mutual impedances and therefore the gain of the pair as compared with the single central radiator.

2.17. Parallelogram Arrays

Four identical vertical radiators arranged in the form of two crossed pairs with identical centers constitute a parallelogram array. Such arrays provide a very large variety of useful radiation patterns both symmetric and asymmetric. The resultant pattern from two crossed, cocentered pairs is the sum of the two pair patterns, provided that the phase reference for the currents in both pairs is taken to be zero at the center of the array. The relative size of each pair pattern can be changed by altering the power distribution between pairs. The individual patterns are in terms of field strengths, with the polarity of the electric field in each lobe indicated.

Given two overlapping patterns, one can be rotated with respect to the other by changing the angle between the axes of the two pairs.

The independent variables in a paralellogram array are the following:

1. Spacing between radiators in each pair, S_1 and S_2
2. Phase differences between the currents in each pair, $\pm\phi_1/2$ and $\pm\phi_2/2$
3. Relative current amplitude differences between pairs, I_1/I_3
4. Angle between the axes of the two pairs, β_x (this angle can lie anywhere in four quadrants)
5. Orientation of the entire array, β_0

2.17.1. Graphical Solution of Array Problems. Once the patterns are calculated for each pair with their correct relative field-strength values for a particular ratio of pair amplitudes, they can be separately plotted in rectangular coordinates on semitransparent graph sheets. They can then be superimposed and examined. If each pattern can be drawn with the axis of each array as zero azimuth reference, the coincidence of these axes would show the possibilities of one limit of the array when the parallelogram is squashed into a single line. By sliding one pattern with

respect to the other along the azimuth scale, one is effectively rotating the angle β_x between the pair axes. For this purpose, one of the pair patterns should be repeated from 360 to 720 degrees so that there is no break in the one pattern as it is slid along over the other. It is also helpful, in locating null angles, to draw the pattern for the second pair with inverted polarity with respect to the first, because then there will

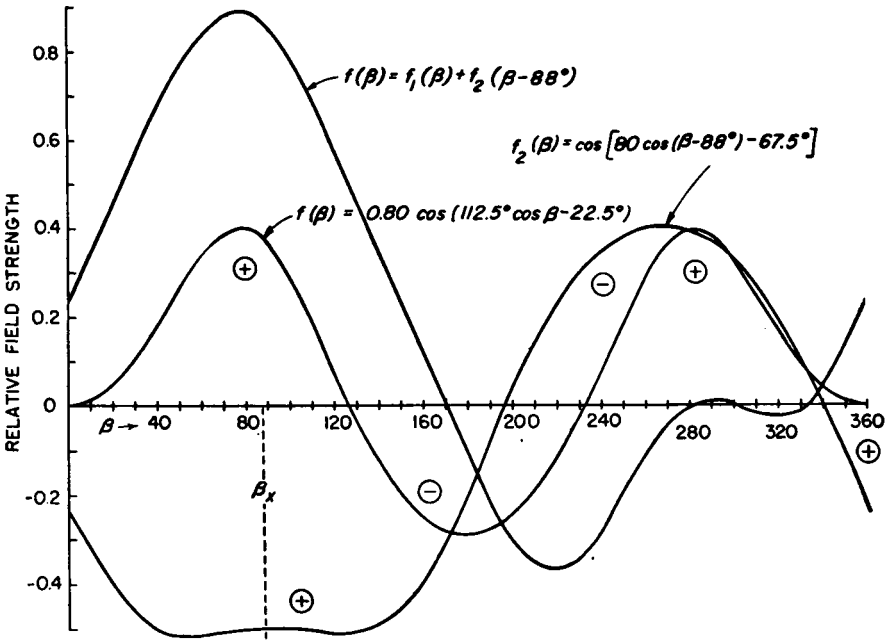

FIG. 2.48. Example of pattern from two crossed pairs forming a parallelogram array.

be a null indicated directly by the intersection of any point on one pattern with that of the second—points of equal fields but opposite polarity.

This graphical method is one way of searching for a possible solution of a given allocation problem. Its advantage is that all possible effects of varying the angle between any two trial pairs can be examined very quickly. One can also form some qualitative idea of the effects of changing the current ratio between the pairs, thus often indicating possible solutions in this direction. This method reduces the number of tries that may be necessary to find the required array specifications for a desired arrangement of nulls and maximums in the final pattern. The person who must frequently solve such problems finds it advantageous to plot all such patterns in a uniform manner and accumulate them over a period of time. Then when a new problem arises, the stock of ready-made patterns leaves only the procedure of superimposing them before a

bright light. The inversion of polarity of the lobes can be accomplished by turning a sheet over.

When the graphical method reveals a solution, an accurate recomputation can be made from the indicated array parameters.

Figure 2.48 demonstrates an overlay of two pair patterns from which the resultant pattern can be plotted directly with a pair of dividers, using the distance between the curves for each azimuth. It is seen that zeros occur at 171, 282, 298, and 334 degrees and that very low fields exist between 275 and 336 degrees, not exceeding 2.9 per cent of the maximum lobe through this interval of 61 degrees. The polar resultant pattern is given in Fig. 2.49.

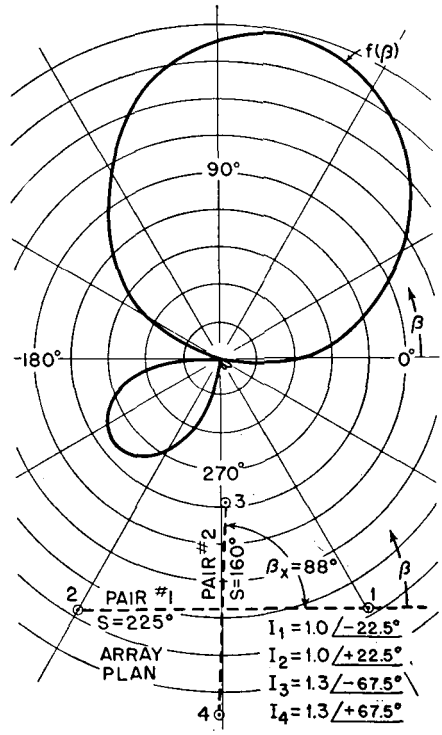

FIG. 2.49. Polar resultant pattern redrawn from Fig. 2.48.

This example was chosen to illustrate a further point of importance in making this kind of synthesis: by choosing pair patterns that cancel over a wide range of angles the resulting pattern can be made to suppress radiation over a wide angle.

In general, parallelogram arrays have azimuthal patterns derivable from the following equation:

$$f(\beta) = Af_1(\beta) + Bf_2(\beta - \beta_x)$$

In this equation A and B are scalar coefficients for the maximum field strength for the pattern of each pair, the other symbols being the same as those previously introduced.

It must now be apparent that a parallelogram array degenerates into a three-element array as the minor axis approaches zero (a single central radiator). On the other hand, as β_x approaches zero, the parallelogram again degenerates into a four-element linear array, with one pair inside the other if $S_1 \neq S_2$.

The parallelogram array is composed of only two cocentered pairs. Obviously more than two cocentered pairs could be employed to form still more extensive possibilities for radiation patterns, using the same method of pattern synthesis as developed for the two-pair system. A fifth

radiator located at the geometric center of the array and at 0 reference phase will provide additional pattern possibilities.

2.18. Direct Synthesis of an Array for Any Specified Azimuthal Pattern

It is of interest to discuss a direct method for deriving the array specifications that will provide an arbitrarily prescribed azimuthal radiation pattern. The method will always provide an exact solution, though this solution is not always economically practical. It is frequently of value to apply this general method at first because a more practical array may be suggested from the final results. We shall indicate only the broad outlines of the mathematical procedure and refer the reader to more detailed sources for some of the elements of the method.

Wolf described a method of synthesizing an array for any arbitrary symmetrical pattern using the principles of complex Fourier analysis.[1087] In his method, the pattern from a pair of radiators supplies a term in an infinite series derived from the Fourier analysis of the desired pattern in terms of spherical harmonics, each of the form

$$f_i(\beta) = \cos\left(\frac{S_i}{2}\sin\beta - \frac{\phi_i}{2}\right)$$

The present method utilizes the method of Wolf in the course of its development.

Any radiation pattern $F(\beta)$ in the equatorial plane of a multiplicity of parallel identical linear radiators is periodic in 2π and can therefore be treated with the general methods of Fourier analysis. Any arbitrary pattern may be classed as even and symmetric if $F(\beta) = F(-\beta)$, as odd and symmetric if $F(\beta) = -F(-\beta)$, or as uneven (asymmetric) if in nonconformance with both of the foregoing. An even function can be obtained from a linear broadside array with symmetrical Fourier current distributions. An odd function can be obtained from a linear end-fire array with a symmetric but inverted Fourier current distribution. An uneven function can be obtained by the combination of the even and the odd functions.

Let $F(\beta)$ in Fig. 2.50 represent a prescribed azimuthal radiation pattern for a particular application in the domain from $-\pi$ to π. This is shown to be an uneven function with respect to the reference azimuth $\beta = 0$. If we designate the function between 0 and π as X and that between 0 and $-\pi$ as Y, it can be demonstrated that the even and odd components of this uneven function are

$$F_e(\beta) = \frac{X + Y}{2}$$

and

$$F_o(\beta) = \frac{X - Y}{2}$$

and also that $F_e(\beta) + F_o(\beta) = F(\beta)$. The even and the odd components of $F(\beta)$ are shown dotted in Fig. 2.50. It is therefore obvious that since we have means for generating any desired even radiation function and also any desired odd radiation function, we can apply this method and

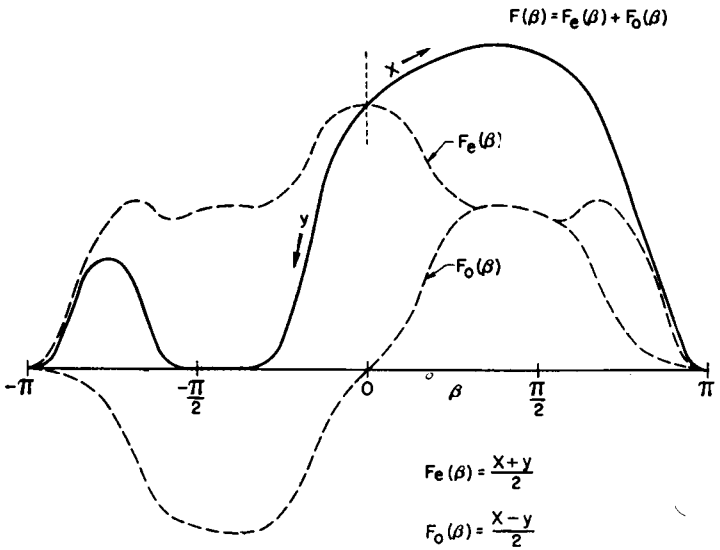

FIG. 2.50. Resolution of an asymmetric function $F(\beta)$ into its component even $F_e(\beta)$ and odd $F_o(\beta)$ functions.

obtain means for exactly generating any arbitrary asymmetric radiation pattern.

The application of Wolf's method is straightforward mathematically, though it remains for the engineer using it to decide on the minimum number of terms in the Fourier series that will give a satisfactory approximation to the desired result. By adding terms, which means adding pairs of radiators, one can approach the desired result as closely as economic considerations will permit.

The Fourier array, while it always provides a theoretical solution, frequently does not provide a practical or economical solution for an asymmetric pattern problem. One must then resort to the use of random, or nonsystematic, arrays. There are no known systematic methods for synthesizing such arrays except trial and error, reference charts of

patterns for nonsystematic arrays of three[44] or more radiators, or using an analog computer such as the RCA Antennalyzer.[7]

2.19. Distortion of Radiation Patterns Close to an Array

All radiation patterns are computed for distances that are very large with respect to the largest dimension of the array. It is assumed that the rays from each radiator at the point of field measurement are virtually parallel. The pattern is not fully "formed" at distances less than some

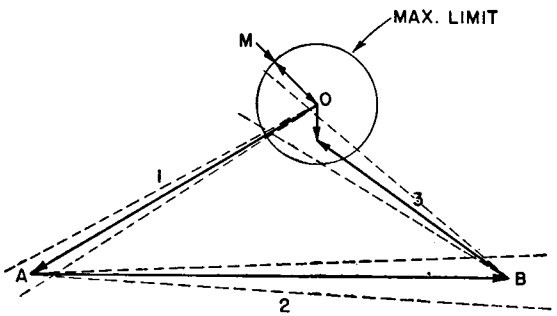

FIG. 2.51. Examination of pattern stability by vector diagram of fields in null region.

ten times the largest dimension of the array or greater. The region in which the pattern shape is a function of distance is called the "Fresnel region." Beyond this it is called the "Fraunhofer region." One can be greatly deceived in the adjustment and proof of performance of an array if patterns are measured in the Fresnel region. Distance is measured from the geometric center of the array plan.

2.20. Stability of Directive Broadcast Arrays

In almost every modern application of a broadcast directive array the conditions that have to be maintained are rather critical. Once adjusted and performance-proved, it is essential that the system maintain its adjustment and its pattern with a very high degree of stability. Work on the several hundred broadcast directive arrays in North America, using from two to six radiators (and with more extensive arrays in prospect), has revealed some fundamental principles that should be observed to obtain stability.

The commonest causes of instability include the following:

1. Variable resistance connections between sections of steel towers. All sections should be bonded at all corners by welding.
2. Loose or faulty connections in the ground system.
3. Loose or faulty connections in the feeder and network system.
4. Corrosion of connections.

5. Destructive corrosion of the ground wires in some acid soils.

6. The presence of flexible conduits in the field of ground wires and circuits of the feeder system, which causes a parasitic variation in impedance sufficient to produce considerable instability in some cases. The safest practice is not to use any flexible conduit for any purpose near the antenna circuits.

7. Static discharges over the antenna guy insulators, sometimes sustained by a power arc, which may be intermittently blown out by the wind and rekindled by static-charge accumulations. The cure for this condition is not always the same, but static leaks in the form of needle gaps across the insulators with a large-value heavy-duty resistor in series have given some measure of relief.

An experienced directive-antenna engineer does not start any work on system adjustment until the self-impedance of each radiator has been measured and until the radiator resistance remains constant within 1 or 2 per cent when the radiator is vibrated, the ground connections are pulled and vibrated, and all the various conduits and wiring in the coupling house are touched, shaken, and grounded. If there is no wind to shake the tower, it can be set into vibration by pounding a guy or by pulling on a guy with a rope. When the radiator resistance remains constant under these various tests, the adjusting procedure starts.

When the network adjustments have been made and confirmed by field-strength measurements, permanent connectors of rigid form are installed and the pattern measurements are again confirmed. All connections are then brazed or soldered and all variable elements locked in place. The phase monitors and remote ammeters, having been previously calibrated, are also bonded and sealed to prevent false indications of trouble. Finally, the equipment is locked up so as to be inaccessible to everyone except an authorized person. Tamperproofing is an important factor in array stability.

Until one has had the personal experience of adjusting a critical directive array, there is small significance to the innumerable points of technique that come into notice during measurement.

The intrinsic electrical stability of a directive array depends upon the design parameters of the system. In general, the greater the degree of radiation suppression, the more sensitive is this null to small variations in the phases and amplitudes of the various radiator currents. The latter are in turn responsive to changes in system or individual radiator impedances. As the specifications for pattern stability become more stringent, greater attention must be given to every detail of design and construction to ensure constancy of impedances under all weather conditions over long periods of time. The stability demands of certain modern medium-

FIG. 2.52. Aerial view of a high-power broadcasting station (Radio Station WJZ when it was located at Bound Brook, New Jersey), showing the station building, the 750-foot radiator, and the freshly furrowed ground where the ground wires were plowed into the soil. (*Photograph courtesy of National Broadcasting Company.*)

frequency directive arrays with extreme suppression over wide angles are indeed extreme and require great ingenuity in design and skill in adjustment.

The intrinsic stability of a proposed pattern can sometimes be examined very simply and quickly in a way which will inform the designer of the

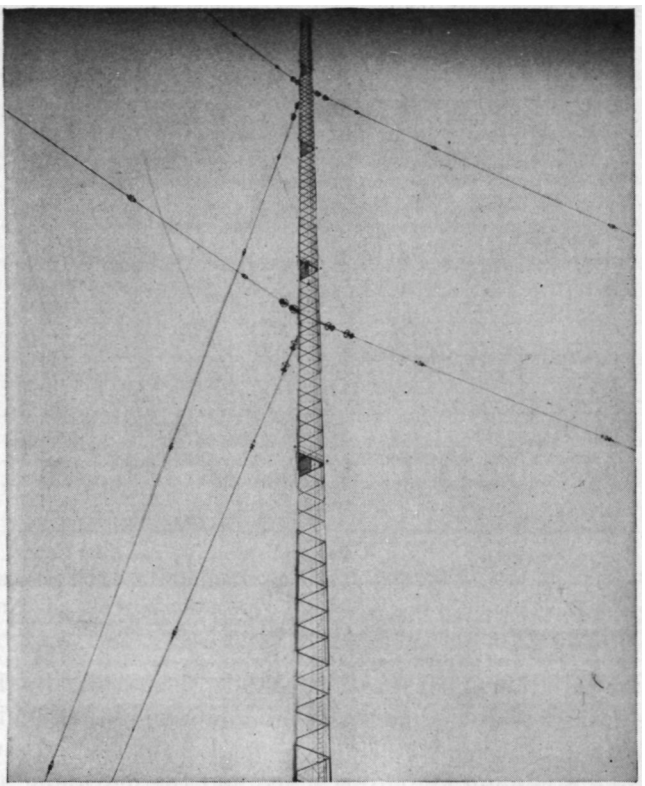

FIG. 2.53. Aerial portion of a 750-foot guyed broadcast vertical radiator used by Radio Station WJZ. (*Photograph courtesy of National Broadcasting Company.*)

critical parameters and the tolerances he must maintain. This is done graphically by plotting the vectors for a null or minimum point according to the equation on page 148. If, for instance, a three-element array requires a very deep minimum at some angle, this is the angle where the field-strength vectors due to the three radiators add to a zero or some relatively small value with respect to any of the three vectors. By drawing these vectors carefully to scale, with their correct relative amplitudes and phases for the null direction, one may then proceed to the graphic study of the effect on the scalar-value resultant field of varying the amplitudes and phases of the individual vectors. If the resultant field must be kept under a certain limit, one can determine whether or not the

pattern stability can be maintained within the necessary tolerances in practice.

An example of this sort is given in Fig. 2.51. This shows a desired resultant field-strength vector R, which is the sum of vectors 1, 2, and 3 from the three radiators. A circle of radius M represents the maximum allowable field strength under operational tolerances. Vector 1 must be

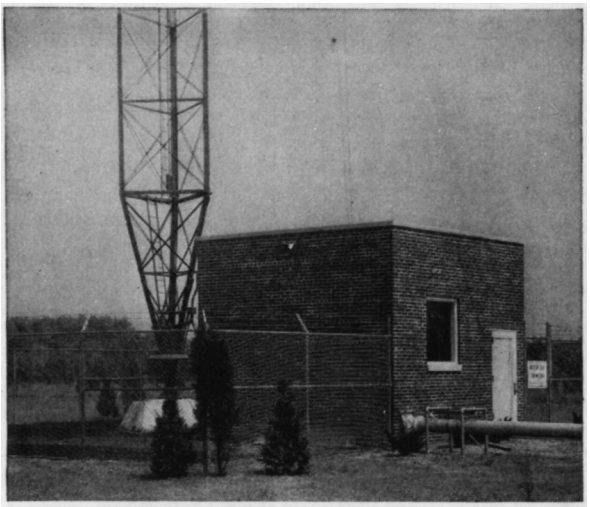

FIG. 2.54. Base of a guyed broadcast vertical radiator, coupling house, protective fence, and the 10-inch concentric transmission line suitable for 500-kilowatt service. Radio Station WJZ at Bound Brook, New Jersey (location now at Lodi, New Jersey). (*Photograph courtesy of National Broadcasting Company.*)

allowed some variation of phase and amplitude, as indicated by the dotted angular deviations and maximum and minimum amplitude limits. The end of vector 1 can therefore lie in a small rectangle A between the maximum and minimum amplitude limits and the maximum and minimum angular limits. Vector 2 starts somewhere within this area, at the end of 1, and must, of itself, have certain possible limits of amplitude and phase, bringing its end somewhere in a larger rectangular area B. The same takes place in turn with 3, and the possible area of total variation due to 3 with the cumulative deviations of the other two must always fall within the circle M.

Mutual impedances make it impossible for any one vector to vary independently from normal, so that a deviation in one implies a deviation in the others. If more than three vectors are involved, the problem is that much more complicated. An exploratory examination of this sort is qualitative only (unless one undertakes all the labor required to recompute the entire impedance network of the system with each change of value), but with experience a great deal of information regarding stability

tolerances and the degree of refinement that may be required to maintain operational limits can be gained by such a qualitative study.

Array instability is due to changes in the impedances of the system at the frequency for which it was designed, the impedance changes being caused by spurious influences. The same kind of effect occurs when the impedances change, not because of spurious effects, but with a change of

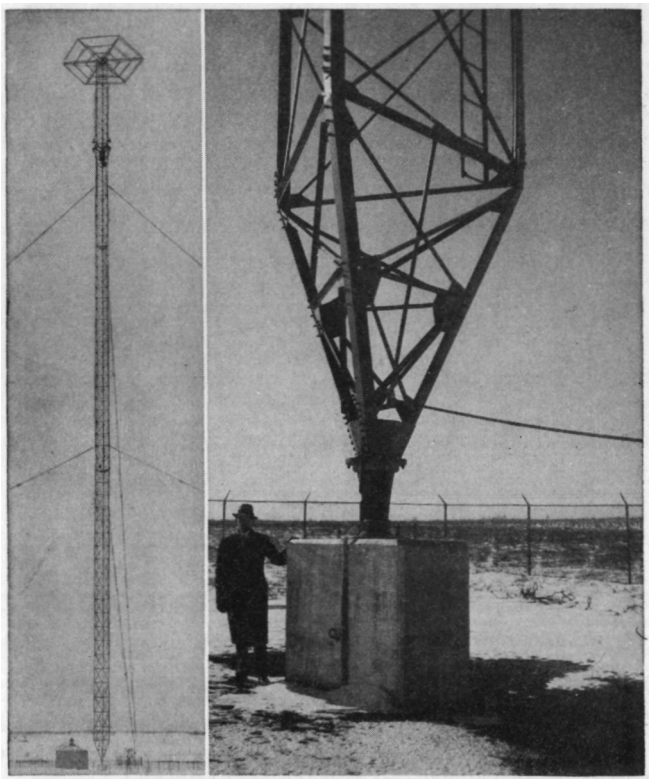

FIG. 2.55. A top-loaded sectionalized guyed vertical radiator and its base detail. Radio Station WMAQ, Chicago, Illinois. (*Photograph courtesy of National Broadcasting Company.*)

frequency, as during modulation. The impedances are different for each side frequency, the difference increasing with increased side-frequency separation. The impedance changes cause deviations in the amplitude and phase of the various radiator currents with consequent deviations in the pattern shape. In systems with high degrees of suppression, the carrier frequency may be sufficiently suppressed, but the side frequencies may leak out of a null during modulation and cause some interference. This is another reason why the bandwidth of the system as a whole has to be engineered to avoid or to minimize this effect.

2.21. Structural Details

The photographs (Figs. 2.51 to 2.70) are included to show certain structural details that have been used successfully at a number of broad-

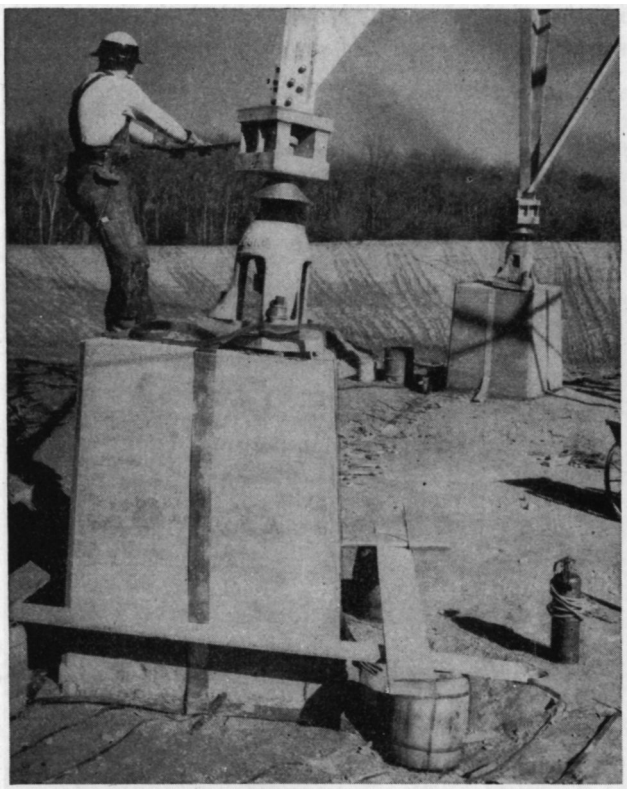

FIG. 2.56. Base of a self-supporting broadcast radiator during construction. Notice tractor and plow tracks in background where ground wires have been plowed into the soil. (*Photograph courtesy of National Broadcasting Company.*)

cast stations. The range of variation in design of structural details is naturally very great, and a few examples can suggest only a few methods that can be used. The figures also show some of the types of radiators in current use—both guyed and self-supporting—together with base and guy-anchor details.

Since the advent of steel vertical radiators for broadcast applications the radio engineer has been spared the duties of antenna mechanical and structural design. This is now delegated to the tower engineers, who have performed very creditably. Manufacturers of towers are generally familiar with radio requirements and often understand the electrical requirements as well as the structural.

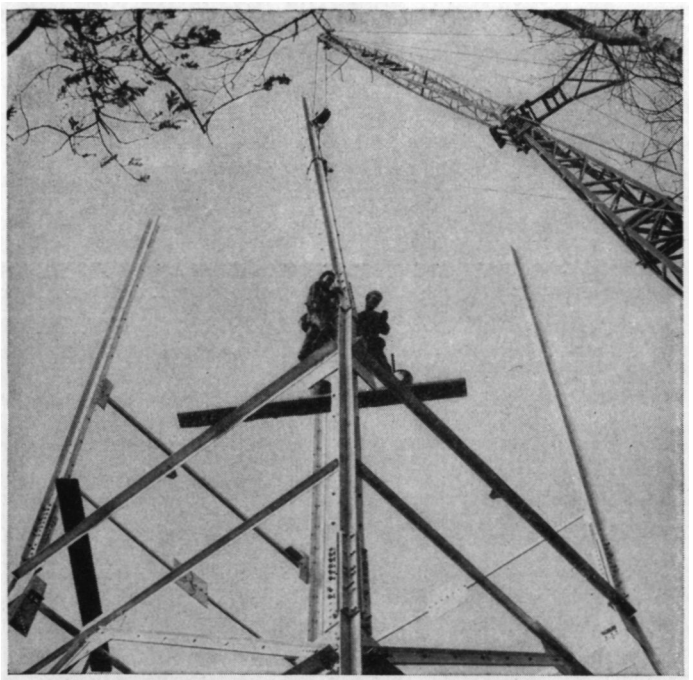

FIG. 2.57. A self-supporting broadcast radiator during construction.

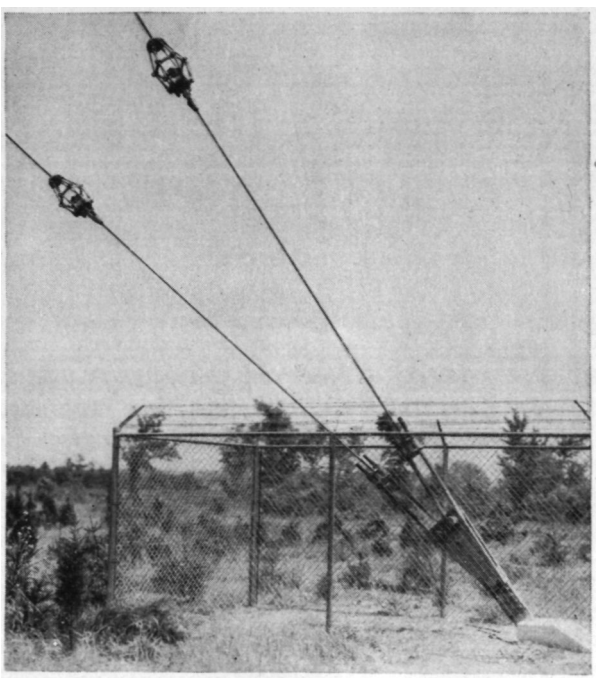

FIG. 2.58. Anchor for guy cables for two levels, used with a guyed broadcast vertic radiator. (*Photograph courtesy of National Broadcasting Company.*)

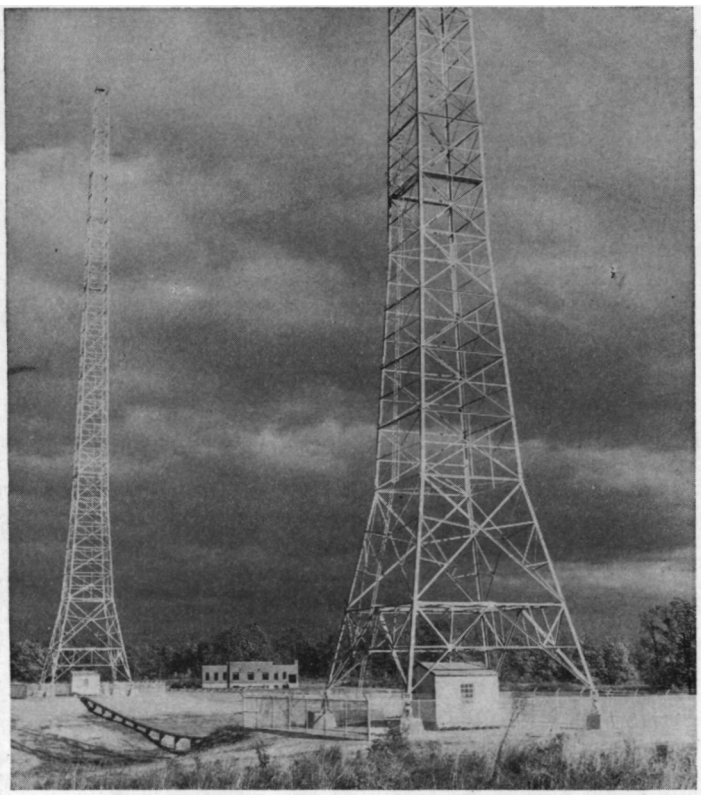

FIG. 2.59. Two self-supporting towers used in a two-element directive array at Radio Station WNBC, Port Washington, New York. (*Photograph courtesy of National Broadcasting Company.*)

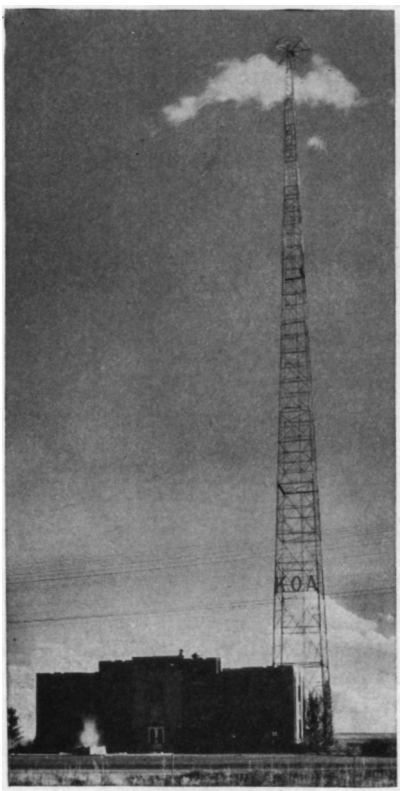

FIG. 2.60. A broadcast vertical radiator of the self-supporting type with capacity loading at the top. (*Photograph courtesy of National Broadcasting Company.*)

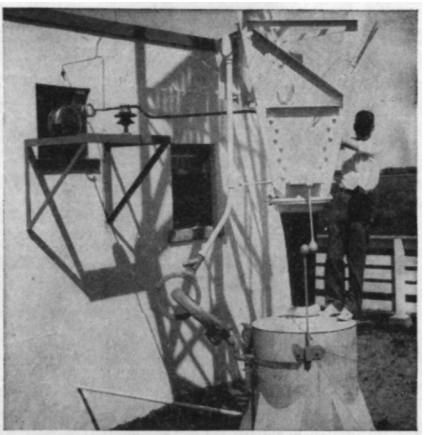

FIG. 2.61. Base details for a 550-foot broadcast vertical radiator with tower-lighting transformer and coupling-house entrance connection. Radio Station CBK, Watrous, Saskatchewan, Canada.

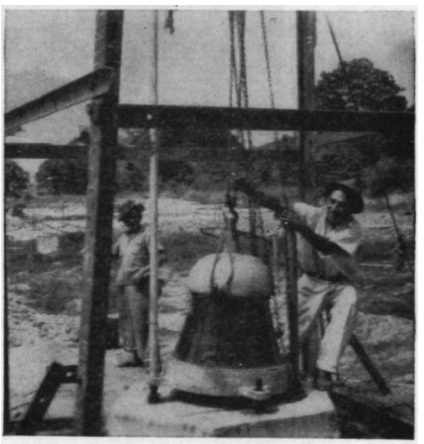

FIG. 2.62. The first step in the construction of a guyed vertical radiator for broadcasting—setting the base insulator. This photograph was taken in Peru. (*Photograph courtesy of R. E. Lee.*)

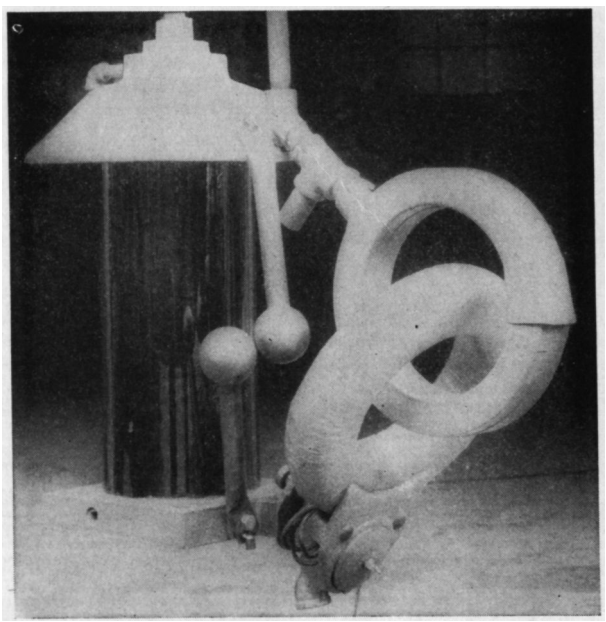

FIG. 2.63. A safety-core oil-filled tower-base insulator with a tower-lighting transformer and safety gap assembled. (*Photograph courtesy of A. O. Austin.*)

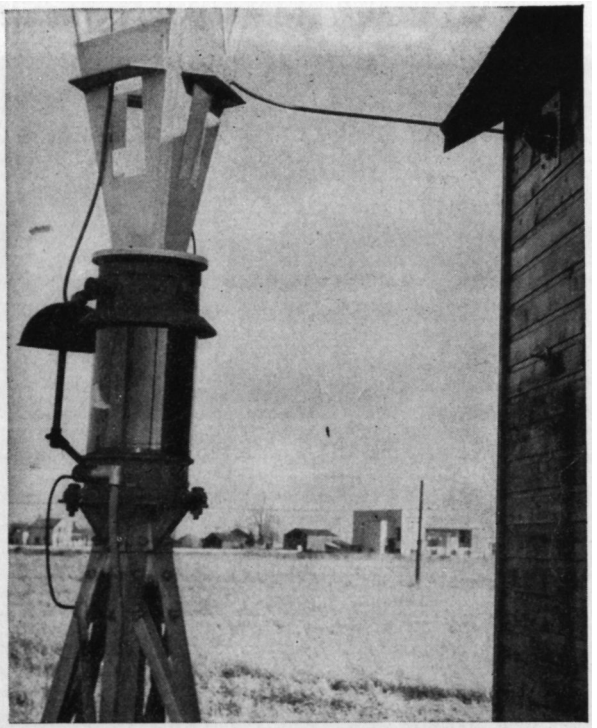

FIG. 2.64. Base insulator of the Austin oil-filled safety-core type with the tower-lighting transformer located inside the base insulator, at Station CKLW. (*Photograph courtesy of RCA Victor Company, Ltd., Montreal.*)

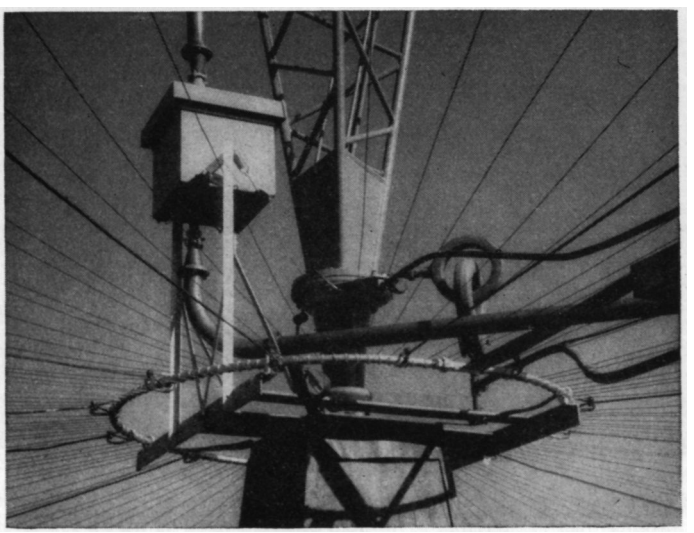

FIG. 2.65. Detail of guyed tower base with radial ground screen, toroidal tower-lighting transformer, and very-high-frequency feeder isolation network (in box). This is one radiator of a six-element array at Station KTBS. (*Photograph courtesy of W. M. Witty, Dallas, Texas.*)

FIG. 2.66. View of Station KTBS six-element directive array. Note pylon antenna for frequency modulation on top of third radiator from the left. (*Photograph courtesy of W. M. Witty, Dallas, Texas.*)

FIG. 2.67. A tractor-drawn wire plow for burying ground wires. The plow blade is of sheet steel that cuts a thin furrow. The wire is fed into the furrow as the plow advances. Horse-drawn hand plows of similar principle are often used.

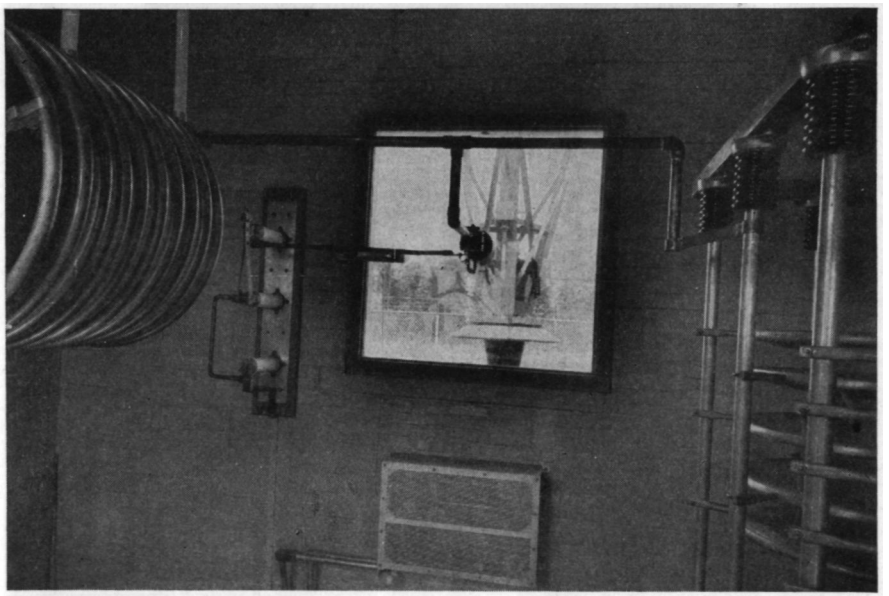

FIG. 2.68. View inside antenna coupling house, showing part of the antenna coupling-network elements, the antenna grounding switch, monitoring rectifier, plate-glass window insulator for antenna lead, and the base of the guyed vertical radiator. Radio Station WTAM, Brecksville, Ohio. (*Photograph courtesy of National Broadcasting Company.*)

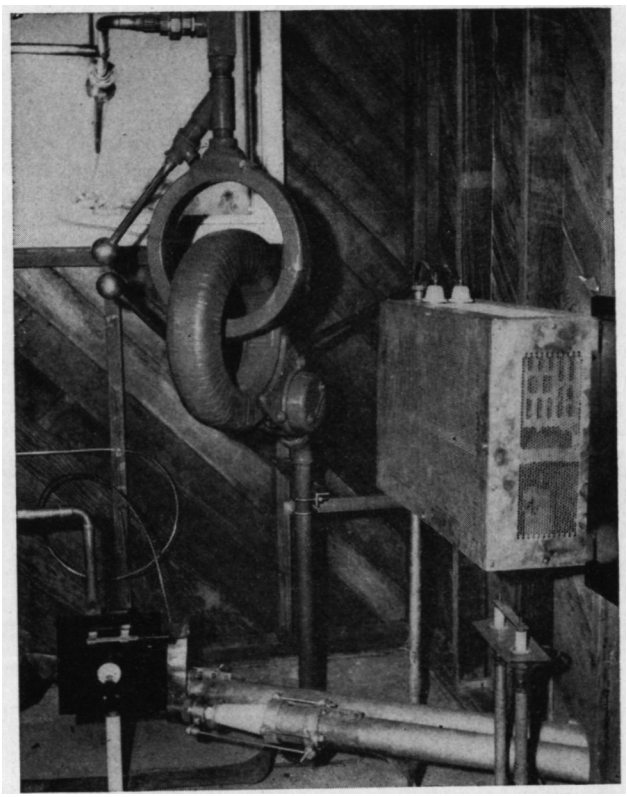

FIG. 2.69. Antenna coupling-house interior for a broadcast station (WNBC) with a plate-glass window insulator, Austin tower-lighting transformer, a monitoring rectifier, and the end of a 3½-inch concentric feeder. (Photographed during station construction. *Courtesy of National Broadcasting Company.*)

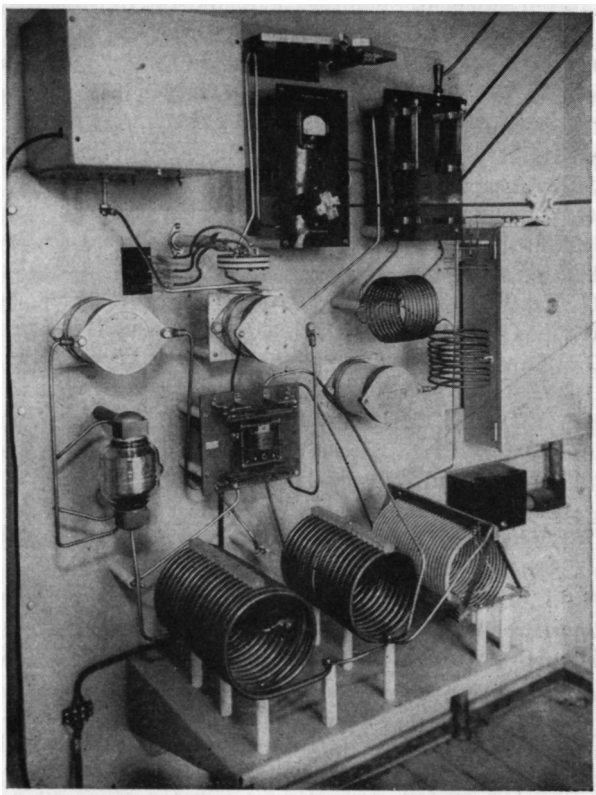

FIG. 2.70. View of antenna coupling network for one element of four-element array (night pattern) and two-element array (day pattern) for Station CKLW (50 kilowatts). The coupling, phasing, and monitoring components, with switching from day to night patterns, are assembled openly and located in a cabin. (*Photograph courtesy of RCA Victor Company, Ltd., Montreal.*)

BIBLIOGRAPHY

1. Andrew, V. J., and A. M. McGregor, Low Cost Wooden Mast; Station WJBC, *Electronics*, **9**:46, May, 1936.
2. Boudoux, P., Current Distribution and Radiation Properties of the Shunt-excited Antenna, *Proc. IRE*, **28**:271, June, 1940.
3. Brown, G. H., Critical Study of the Characteristics of Broadcast Antennas as Affected by Antenna Current Distribution, *Proc. IRE*, **24**:48, January, 1936.
4. Brown, G. H., Directional Antennas, *Proc. IRE*, **25**:78, January, 1937.
5. Brown, G. H., and J. G. Leitch, Fading Characteristics of the Top-loaded WCAU Antenna, *Proc. IRE*, **25**:583, May, 1937.
6. Brown, G. H., R. F. Lewis, and J. Epstein, Ground System as a Factor in Antenna Efficiency, *Proc. IRE*, **25**:753, June, 1937.
7. Brown, G. H., and W. C. Morrison, The RCA Antennalyzer—An Instrument Useful in the Design of Antenna Systems. *Proc. IRE*, **34**:992, December, 1946.
8. Brown, G. H., WTAR Directional Array, *Electronics*, **11**:38, January, 1938.
9. Brown, G. H., Consideration of the Radio Frequency Voltages Encountered by the Insulating Materials of Broadcast Towers, *Proc. IRE*, **27**:566, September, 1939.
10. Brown, G. H., and J. M. Baldwin, Adjusting Unequal Tower Broadcast Arrays, *Electronics*, **16**:118, December, 1943.
11. Chamberlain, A. B., and W. B. Lodge, Broadcast Antenna, *Proc. IRE*, **24**:11, January, 1936.
12. Cox, C. R., Phasing Networks for Broadcast Arrays; Graphical Methods Applied, *Electronics*, **17**:120, June, 1944.
13. Dewitt, J. H., Jr., and A. D. Ring, Significant Radiation from Directional Antennas of Broadcast Stations for Determining Sky-wave Interference at Short Distances, *Proc. IRE.*, **32**:668, November, 1944.
14. Duttera, W. S., Directional Antenna Chart, *Electronics*, February, 1940, p. 33.
15. Duttera, W. S., Design Chart for Phase Shifting and Amplitude Control Networks, *Electronics*, **15**:53, October, 1942.
16. Duttera, W. S., Adjustment of Directional Antennas, *Electronics*, **16**:91, April, 1943.
17. Eckersley, P. P., T. L. Eckersley, and H. L. Kirke, Design of Transmitting Aerials for Broadcasting Stations, *J. IEE*, **67**:507, April, 1929.
18. Eppen, F., and A. Gothe, Uber die schwundvermindernde Antenne des Rundfunksenders Breslau, *Elek. Nachr.-Tech.*, **10**(4), 1933.
19. Everest, F. A., and W. S. Pritchard, Horizontal Polar Pattern Calculator for Directional Broadcast Antennas, *Proc. IRE*, **29**:355, June, 1941.
20. FCC Standards of Good Engineering Practice Concerning Standard Broadcast Stations, Federal Communications Commission, Washington, D.C.
21. Feld, J., Radio Antenna Suspended from 1,000 Foot Towers, *J. Franklin Inst.*, **239**:363, May, 1945.
22. Fitch, W. A., and W. S. Duttera, Measurement of Broadcast Coverage and Antenna Performance, *RCA Rev.*, **5**:396, July, 1938.

23. Gihring, H. E., and G. H. Brown, General Consideration of Tower Antennas for Broadcast Use, *Proc. IRE*, **23**:311, April, 1935.
24. Glas, E. T., Efficiency-rating of Transmitting Aerials for Broadcasting Distribution, *Exptl. Wireless*, **7**:665, December, 1930.
25. Harbich, H., and W. Hahnemann, Wirksame Bekampfung des Nahschwundes im Rundfunk durch Dendeantennengebilde bestimmter Form, *Elek. Nachr.-Tech.*, **9**(10), October, 1932.
26. Holtz, R. F., Isolation Methods for FM Antennas Mounted on AM Towers, *Broadcast News*, **44**:42, October, 1946.
27. Hutton, W. G., and R. W. Pierce, Mechanical Calculator for Directional Antenna Patterns, *Proc. IRE*, **30**:233, May, 1942.
28. Kear, F. G., Maintaining the Directivity of Antenna Arrays, *Proc. IRE*, **22**:847, July, 1934; **22**:1313, November, 1934.
29. Kirby, Samuel S., Radio Field Intensity and Distance Characteristics of a High Vertical Broadcast Antenna, *Proc. IRE*, **24**:859, June, 1936.
30. Kleinwachter, H., Determination of the Radiation Diagrams of Radiator Groups; Directive or Anti-fading Aerial Systems and Acoustic Radiators; an Electro-mechanical Method; abstract, *Wireless Engr.*, **19**:576, December, 1942.
31. Labus, J. W., Broadcast Antenna for Low Angle Radiation, *Proc. IRE*, **23**: 935, August, 1935.
32. Laport, E. A., Directional Antenna Design, *Electronics*, **9**:22, April, 1936.
33. Leeman, A., Modified Protective Gap for Transmitting Antennas, *Electronics*, **16**:128, May, 1943.
34. McKinnon, K. A., Experimental Comparison of Shunt- and Series-excitation of a High Uniform Cross-section Vertical Radiator, *Can. J. Research*, November, 1939, p. 227.
35. McPherson, W. L., Electrical Properties of Aerials for Medium and Long Wave Broadcasting, *Elec. Commun.*, **16**:306, April, 1938; **17**:44, October, 1938.
36. Morrison, J. F., and P. H. Smith, Shunt-excited Antenna, *Proc. IRE*, **25**:673, June, 1937.
37. Morrison, J. F., Simple Method for Observing Current Amplitude and Phase Relations in Antenna Arrays, *Proc. IRE*, **25**:1310, October, 1937.
38. Morrison, J. F., Simplifying Adjustments of Antenna Arrays, *Electronics*, January, 1940, p. 70.
39. Prestholdt, Ogden, WABC's New Two-way Antenna, *Electronic Inds.*, **4**:88, February, 1945.
40. Roder, H., Elimination of Phase Shifts between the Currents in Two Antennas, *Proc. IRE*, **22**:374, March, 1934.
41. Rountree, J. G., Calculator for Two-element Directive Arrays, *Proc. IRE*, **32**:760, December, 1944.
42. Sinclair, D. B., Impedance Measurements on Broadcast Antennas, *Communications* (*N.Y.*), **19**:5, July, 1939.
43. Smith, Carl E., Critical Study of Two Broadcast Antennas, *Proc. IRE*, **24**: 1329, October, 1936.

44. Smith, C. E., *Directional Antennas*, Cleveland Institute of Radio Electronics, Cleveland, Ohio, 1945.
45. Spangenberg, K., Charts for the Determination of the rms Value of Horizontal Radiation Pattern of Two-element Broadcast Arrays, *Proc. IRE*, **30**:237, May, 1942.
46. Taylor, J. P., Cathode-ray Antenna Phasemeter, *Electronics*, **12**:62, April, 1939.
47. Williams, H. P., Machine for Calculating Polar Diagrams, *Electronics*, **16**:196, September, 1943.
48. Doherty, W. H., Operation of AM Broadcast Transmitters into Sharply-tuned Antenna Systems, *Proc. IRE*, **37**:729, July, 1949.

CHAPTER 3

High-frequency Antennas

3.1. Review of High-frequency Antenna Development

In the earliest days of radio communication, the frequencies below about 200 kilocycles were employed for high-power transmission. For marine communication, frequencies as high as about 1,000 kilocycles were used. At the time broadcasting was becoming established on the medium frequencies, about the middle of the 1920's, high-frequency transmission for long-distance services made its appearance.

The fundamentals of directive antennas were developed prior to the high-frequency era. They provided a basis for the arrays that were required for the new services. The general theory of radiation from elements and arrays was well established among physicists and was also available for engineering use when the need arose, even though now, many years later, some of the fine points of radiation from antennas are still open for study and experiment.

The use of high frequencies began at about the time of a sunspot maximum and was ushered in by some phenomenal results with low power. This provided a strong incentive to make extensive use of the high frequencies. However, by the time a large-scale conversion had been made, the low part of the sunspot cycle had been reached and there was some disappointment in the results achieved during this period in the late 1920's and early 1930's. The reason was lack of knowledge of the ionosphere. The relation of radio transmission to sunspot activity was established about 1926, but even in this field of study it was not until 1948 that the discordance between total sunspot numbers and ionosphere conditions was explained.

The importance of ionospheric study was recognized at a very early date in high-frequency history, and many experimenters in the field of pure science and in communication engineering devoted their efforts to this intricate problem. Measurements were made of layer heights and critical frequencies, and the effects of skip distances were observed. Multipath transmission began to be understood. There is a great deal

of literature on this subject which emphasizes the magnitude of the puzzle that had to be solved. This field of research is necessarily endless and must be continued into the future without interruption. Great impetus was given this work during World War II, when the strategic value of ionospheric information for operational purposes led to the establishment of ionospheric sounding stations in many parts of the world. The accumulation and correlation of these data provided the kind of information that permitted the most effective use of frequencies on a day-to-day engineering basis. It is now possible to predict some months in advance the conditions of the ionosphere throughout the world with considerable exactness. After the war, this service was made available to everyone under the Central Radio Propagation Laboratory of the National Bureau of Standards. Almost all the major countries of the world cooperate in providing data for this service.

The vagaries of the ionosphere posed some serious problems for the antenna engineer, which could not be alleviated by his backlog of theoretical antenna information. It took several years to decide, from long experience, whether to use vertical or horizontal polarization. The earliest high-frequency beam antennas used vertical polarization, but subsequent evolution has caused the almost universal use of horizontal polarization. There may be a reversion to vertical polarization in the future for certain applications.

Long studies were made of the best vertical beam angles and whether to use broad or sharp vertical beams. In point-to-point services it was at first believed that very sharp horizontal beams could be used advantageously with consequent gain, but rather wide deviations were observed in the azimuths of arrival of signals, which limit the beam sharpness that can be used at the receiving point.

Finally, quantitative study of the multipath problem was possible for the first time with the availability of modern ionospheric information, and this led to the important discovery of a method for reducing multipath distortion by using complementary antennas at both ends of a circuit, the right frequency at the right time to obtain selective angular penetration, and the need to change the antenna characteristics as ionosphere conditions change by seasons and by years. Engineering practice has not yet made extensive use of these latest principles.

It is virtually impossible to measure the complete performance of a beam antenna system. In the past, it was customary to obtain statistical performance by measuring the fields at some distant point. This required the interpretation of performance of a transmitting antenna, for instance, to be made through a veil of uncertainty introduced by the propagation medium and by the receiving antenna. The difficulty can be compre-

hended if we consider what is involved in the attempt to measure a few decibels difference in gain through a medium varying at random, even over short intervals of time, from 20 to 80 decibels. With better propagation data now available, the desired radiation patterns can be selected and the required array designed. If there are any direct measurements wanted, a scale model is made and measured using the ultrahigh-frequency techniques and instruments.

The development of antennas proceeded along two main lines—those using standing waves and those using traveling waves. The various dipole and harmonic-wire arrays are of the standing-wave type, while the Beverage, fishbone, and rhombic antennas exemplify the traveling-wave type. Evolution of antenna design has included both these types for vertical and horizontal polarizations.

Among antennas of the standing-wave type there were developed broadside and end-fire arrays. The former is the type where the beam is normal to the plane of the radiators, and the latter is the type where the beam is in the plane of the radiators. Evolution seems to have eliminated end-fire arrays from high-frequency practice. The nearest approach to the end-fire condition is the use of long-wire radiators with both standing and traveling waves. Such systems have their main radiation lobe at a small angle to the wire when their length is several wavelengths.

Many of the early beam antenna designers went to great extremes to achieve very high directivities and gains. The passage of time brought the economic factors into prominence, and there followed an era of simplification in design, with gradual compromise of technical perfection in the interests of lower capital costs. This was fully justified in one respect, because designs had actually been pushed far into the region of diminishing returns.

The growth of high-frequency broadcasting induced certain new studies of the transmission problem because there were basic differences from fixed point-to-point working. One of the principal differences was a complete lack of control over the design and location of the myriad individual receiving stations. Listening hours were fixed not by technical conditions but by personal habit. The coverage of a substantial geographical region also differed from delivery of the best signal at some fixed point. Most receivers were naturally located in places of high noise level. The only engineering possible from a system standpoint had to be done at the transmitting end. Broadcasting antenna design made considerable use of radiotelegraph experience but went on from there to satisfy its own requirements as well as it could.

In broadcasting there is still a need to increase power; and when very

high power comes into use, there will be some new antenna-design problems. Furthermore, the economics of broadcasting are completely different from those in the fixed services, and the amount of capital one is justified in investing in antennas is not wholly determined by technical considerations.

The 1947 Atlantic City Conference of the International Telecommunications Union brought about two points that may have a profound influence on future antenna design. The first was the limitation in the number of frequencies assigned to fixed services (actually a considerable reduction from previous assignments), which means that more and more traffic must be handled with fewer channels. This will require the utmost utilization of the propagation medium by multiplexing in various ways, which in turn requires a better solution of the multipath problem that limits working speeds.

The second point is the adoption of a plan for world-wide sharing of frequencies on an engineered basis as a means of more intensive utilization of the available frequencies. This brings a need to clean up some of the antenna patterns by elimination of large parasitic side lobes and backward radiations that now cause interference without having any beneficial value. The presently known way to achieve this cleanup of radiation patterns is to adopt some of the principles that have been applied to ultrahigh-frequency antennas, such as neutral-screen reflectors to suppress backward radiation and graded current distributions to reduce side lobes. This will require more extensive and costly systems of the dipole type if these particular principles are followed. Any further influence on antenna design will include the newer facts of high-frequency propagation as they appear, which in turn may result eventually in low-power one-hop relaying on routes that have land masses at the desired relaying points. It is already known that in such a way very high telegraphic speeds can be maintained over long distances with great economy of power, but at the expense of using more frequencies. Relaying via the tropical latitudes will benefit from greater ionosphere stability due to large auroral-zone clearance and much higher usable frequencies, with lower attenuation. Refined antenna engineering will play an important role in the eventual achievement of better utilization of the high-frequency spectrum.

A review of high-frequency antenna engineering in the light of present-day developments in very-high- and ultrahigh-frequency antenna engineering makes it evident that the former is in a very elementary state. The difference in the wavelengths naturally excludes certain very-high-frequency techniques from being applied to the high frequencies. Nevertheless there are many techniques that can be applied

in the future as the pressure of circumstances justifies greater investments in new antennas for the fixed services.

Another conclusion from such a review pertains to the significance of antenna gain. Gain was for many years a primary objective in antenna designing, on the supposition that this augmented the effective transmitted power and gave the maximum received signal energy, both with consequently improved signal-to-noise ratios. This concept is valid only with an absolutely stable propagation medium. It is now recognized that the matching of the transmitting and receiving antenna patterns to the conditions of the very unstable propagation medium is the dominant engineering objective, and antenna gain is actually an incidental consideration.

3.2. High-frequency Propagation

The antenna engineer must have a comprehensive understanding of wave propagation to adapt his antennas to the most favorable conditions of radiation. High-frequency propagation is a very complex field of study, and new facts of basic importance are appearing from time to time. It is a statistical subject. The extent of this treatment must of necessity be limited to the barest essentials for the guidance of the antenna designer.

The ionosphere is composed of layers of free electrons of heights and thicknesses that vary over wide limits. During the hours of darkness when the upper atmosphere is not in sunlight, there is a relatively permanent layer known as the "F layer." During daylight hours, starting as soon as sunlight bombards the upper atmosphere, this layer usually breaks into two strata, known as "F_1" and "F_2," the latter being the higher in altitude. At sunrise there is formed a lower layer of ionization called the "E layer," which is quite stable and constant. At sunset it disappears. There are transient regions of ionization called "E sporadic" (E_s) which may exist during the day and night hours more or less at random.

The virtual heights of the ionosphere layers vary with latitude, with the hours of the day and the seasons, and with sunspot activity. Over the earth on any particular day the variations of height are of the order of 2 to 1. Monthly average heights at any one location usually follow a fairly constant pattern. In older texts typical heights were assigned to these layers, but such rough information can be misleading. For specific information the reader should consult refs. 1 and 2 at the end of this section.

In terms of the earth's radius (6,378.4 kilometers) the various ionosphere layers form a thin shell around the earth. The height of the F layer

averages around 5 per cent of the earth's radius but in some instances reaches nearly 10 per cent. The E-layer height is generally of the order of 1.8 per cent.

When the electromagnetic wave enters one of these ionized regions, it will do one of three things, depending on the frequency of the wave. If the frequency is above a certain critical value, the wave will pass through the ionized region and out into space. If the frequency is equal to or less than the critical frequency, the wave will be bent or reflected back toward earth. If the frequency is much less than the critical frequency, much of the energy will be absorbed in the ionized layer. Thus the critical frequency is the maximum usable frequency (MUF) that will be reflected by the ionized layer back to the earth at a given point.

Since the maximum usable frequency is rather critical, stable operation in practice requires the use of a frequency near to maximum usable frequency but somewhat below it. Experience has established the optimum working frequency (OWF) at about 85 per cent of maximum usable frequency.

3.2.1. Propagation by Reflection. High-frequency propagation takes place between the surface of the earth and the one or more shells of ionized atmosphere that exhibit sufficient conductivity to reflect the waves back to earth. One reflection from the ionosphere is called one "hop," and the number of hops made by a wave before arriving at the desired receiving point is the number of successive reflections from the ionosphere. We shall use the word "ionosphere" in its most general sense, sometimes involving three or more distinct layers at different heights, each with its own relative reflectivity as determined by its state of ionization.

Transmission over long distances takes place by successive reflections from the ionosphere to earth and back into upper space. There is some attenuation to a wave traversing the lower atmosphere during the daytime, when solar bombardment induces a condition of ionization of the molecules of the air. This solar ionization causes reduction in field strength. During prolonged darkness, after equilibrium of the atmosphere has been reestablished, the neutral atmosphere acts very much as free space from an absorption standpoint.

There is always some loss of wave energy at reflection from any boundary between mediums which are imperfect conductors, or dielectrics. The amount of loss is a function of the angle of incidence of the wave, the frequency of the wave, and the directions of the electric and magnetic vectors with respect to the plane of the boundary. The ionosphere is therefore an imperfect reflector, and there is a loss of energy at reflection which depends upon the state of ionization where the reflection occurs.

The earth's surface is also an imperfect reflector for downcoming waves.

When the point of earth reflection is on a large body of water, such as the ocean, the reflection loss is small. When reflection occurs at a point where the terrain is very rugged, such as a region of mountains, the loss by poor reflectivity and wave scattering can be very large.

In high-frequency communication engineering, consideration is given to the condition of the ionosphere and the characteristics of the earth at all points along the wave path. The total attenuation over a path is the sum of attenuations due to solar absorption in the atmosphere, all of the losses due to ionosphere reflections, and all of the losses due to earth reflections, together with the inverse-distance attenuation due to normal expansion of the wavefront with distance. It is evident that a space circuit having the fewest losses at reflections and the lowest solar absorption will yield the highest field strength at the receiving point.

In multihop circuits it will be recognized that successive ionosphere reflection points are a considerable distance apart. Therefore it is unlikely that the ionosphere will have the same characteristics at any two such points. If one point happens to be in a daylight region and another in a night region, the conditions for reflection of the same frequency can be vastly different. The optimum working frequency for one reflection point may completely penetrate at another. The maximum frequency that can be used for the circuit is therefore the one that will be low enough to reflect from the point having the lowest maximum usable frequency at that instant along the entire circuit.

Thus a multihop optimum working frequency may be a frequency that gives high losses at some reflection points; but if reflection can occur, the signal will be transmitted to the destination, however much reduced in intensity. Under such a condition, relatively high power may be needed for acceptable communication.

The maximum usable frequency for any given path involving ionospheric reflections varies continuously. However certain days are considered typical within certain seasons, and operating frequencies are based on them. It is naturally impractical to have a continuous change of operating frequency on a circuit that follows exactly the variations of the maximum usable frequency, and so some compromise frequency is used for certain hours during which the maximum-usable-frequency changes are within certain limits. Then at the times when the maximum usable frequency changes greatly, some new compromise frequency is chosen for a certain other number of hours.

3.2.2. Ionosphere Data. Figure 3.1 is an example of how measured ionosphere data are presented. The curves on the left show the critical frequencies for the various layers compared with predictions made 5 months in advance. At the upper right are shown the measured

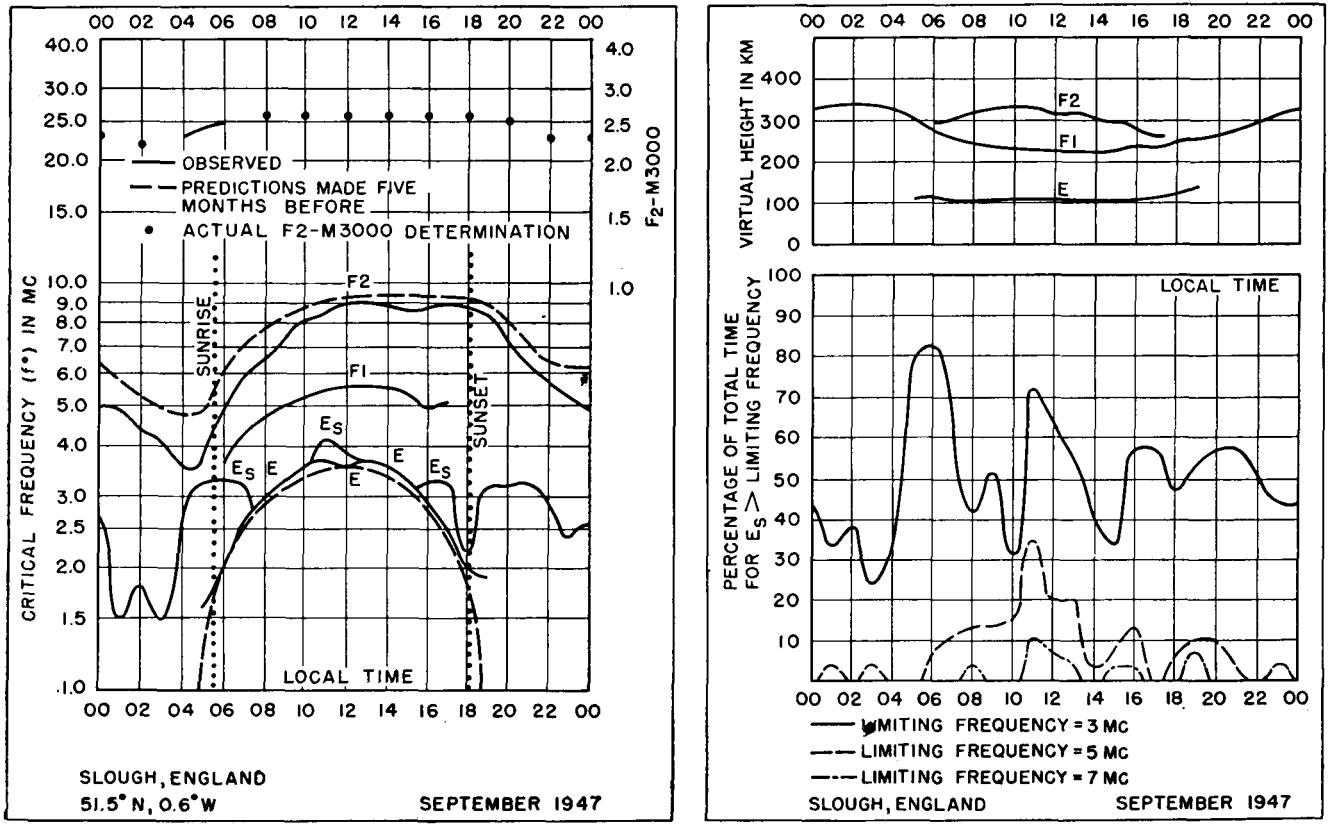

FIG. 3.1. Example of measured monthly average ionosphere characteristics. (*After Central Radio Propagation Laboratory.*)

virtual heights. At the lower right is a chart showing the percentages of total time that the critical frequency for E sporadic regions exceeded 3, 5, and 7 megacycles during this particular month of observations. These figures are median values compiled for a month of observations. They should be regarded not as typical but merely as isolated examples because of the variability of conditions. This particular example was chosen because it shows clearly defined E, F_1, and F_2 layers during the daylight, a condition that does not always exist. The figure was reproduced from the CRPL-F publication mentioned in ref. 2 on page 217.

Figures 3.2 and 3.3 are sample charts showing critical frequencies for vertical incidence (F_2 zero) and for a 4,000-kilometer hop (F_2 4,000) for the F layer in the western geomagnetic zone (which includes all of South America and almost all of North America) as they were predicted for January, 1941. Figures 3.4 and 3.5 are samples of the same sort for E and E sporadic layers for the same zone and the same month. These are reproduced from the CRPL-D26 publication of October, 1946, and are the type of data now available for computing the frequencies for high-frequency transmission, using the methods described in ref. 4, page 217.

The maximum usable frequency over a given path also varies with sunspot activity. There is no simple relationship for this effect, because in addition to the dominant 11-year sunspot cycle, there are others—including a prominent one of approximately 83 years. When these two major cycles coincide at their maximums (1947) or at their minimums (1900), there exist the greatest extremes in sunspot numbers, with corresponding effect on the maximum usable frequency for any path. During the 11-year cycle ending with its maximum in 1943 the maximum-usable-frequency range over the 11 years was 2 to 1, with greatest maximum usable frequency coinciding with maximum sunspot activity.

3.2.3. Choosing a Working Frequency. The choice of working frequency is a compromise between efficient propagation, the necessary total portion of time that service must be maintained, and the technical complexities of operation involved. It requires skillful operation and coordination at transmitter and receiver to make frequent frequency changes without excessive lost time, but if this can be done and frequencies can be allocated for the purpose the very best propagation would be realizable.

Figure 3.6 is a sample diurnal frequency characteristic, more or less typical of tropical-belt conditions at a time near a sunspot maximum. It exemplifies clearly some basic ionosphere properties. Just before sunrise, the long period of darkness has permitted a gradual reduction in ion density by recombination of the molecules of the atmosphere in the ionospheric regions of the F layer. Therefore the maximum usable frequency

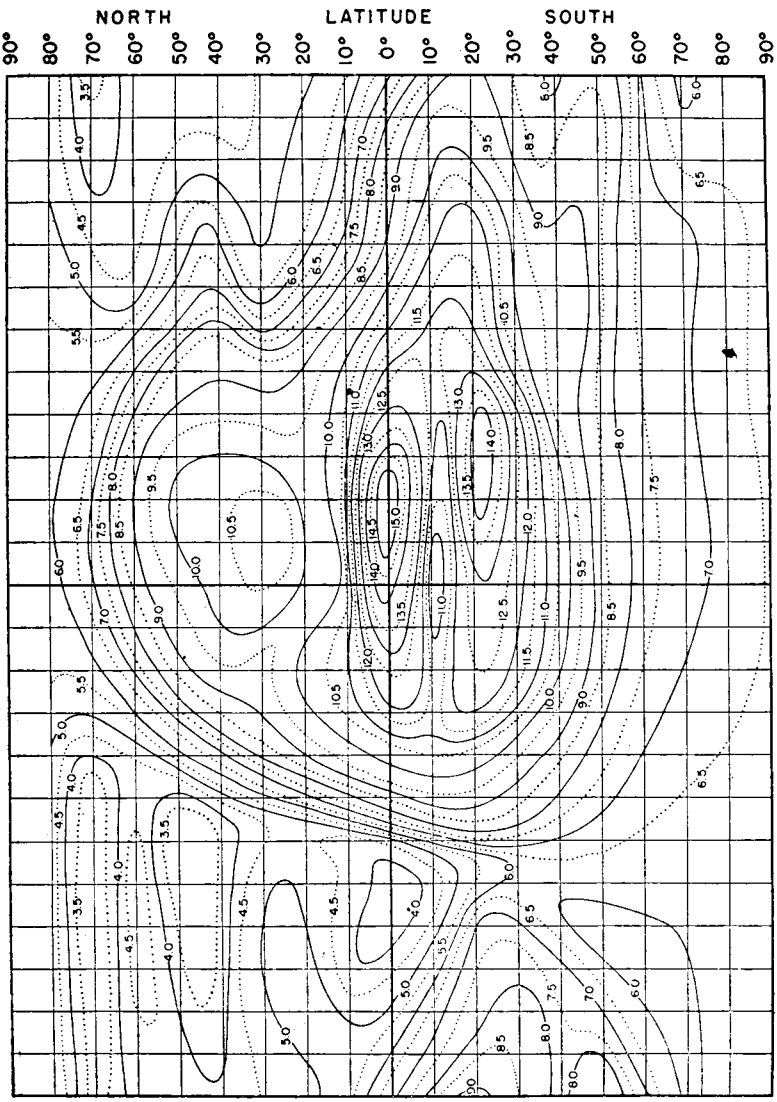

FIG. 3.2. F_2 zero—maximum usable frequency in megacycles W zone, predicted for January, 1947. (*After Central Radio Propagation Laboratory.*)

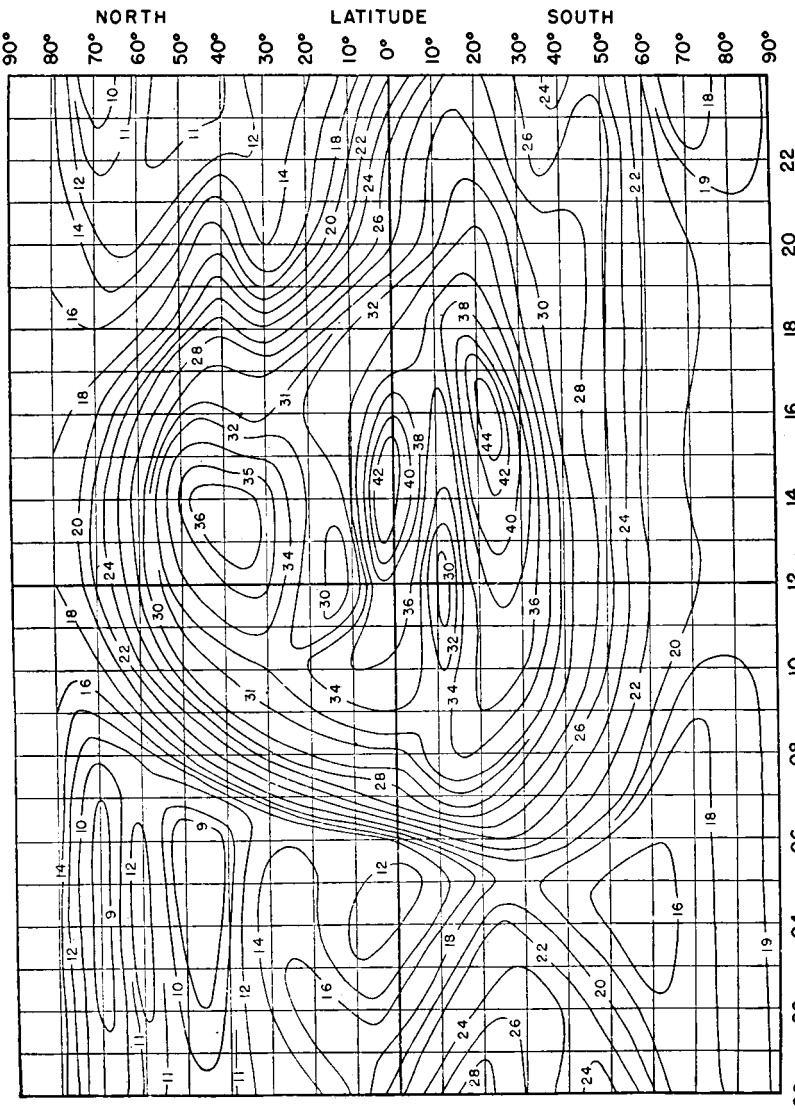

FIG. 3.3. F_2 4,000—maximum usable frequency in megacycles W zone, predicted for January, 1947. (*After Central Radio Propagation Laboratory.*)

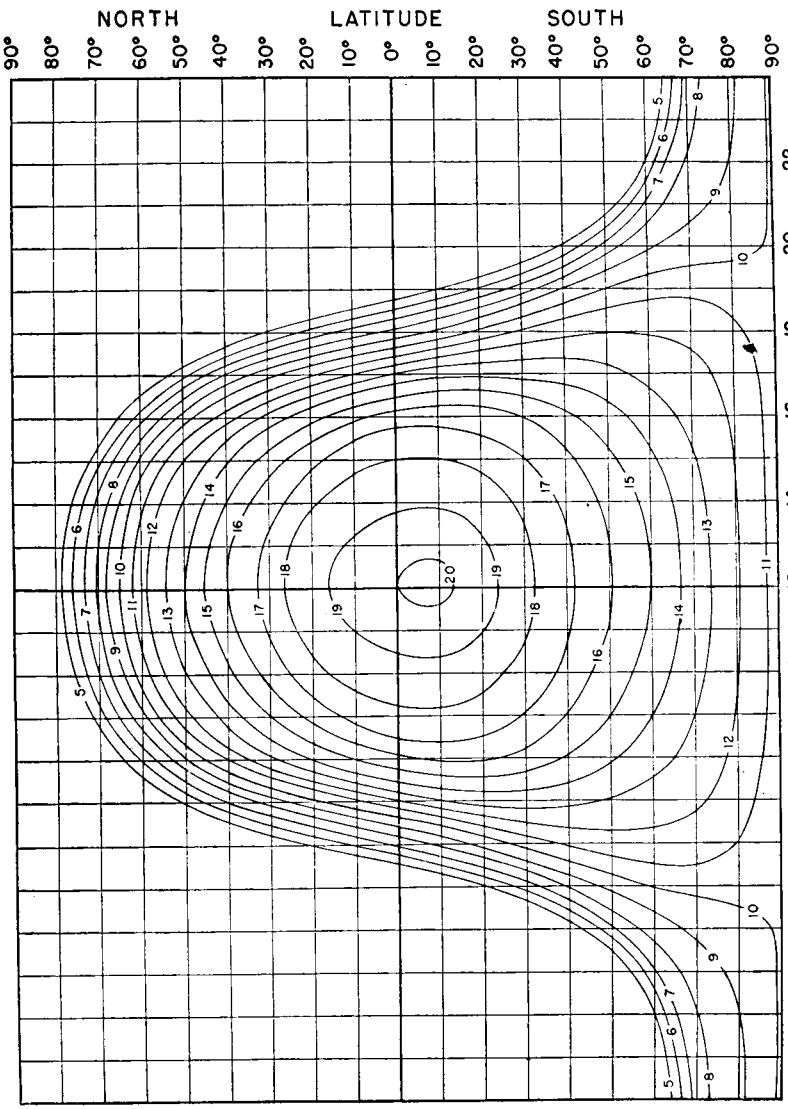

FIG. 3.4. E layer 2,000—maximum usable frequency in megacycles, predicted for January, 1947. (*After Central Radio Propagation Laboratory.*)

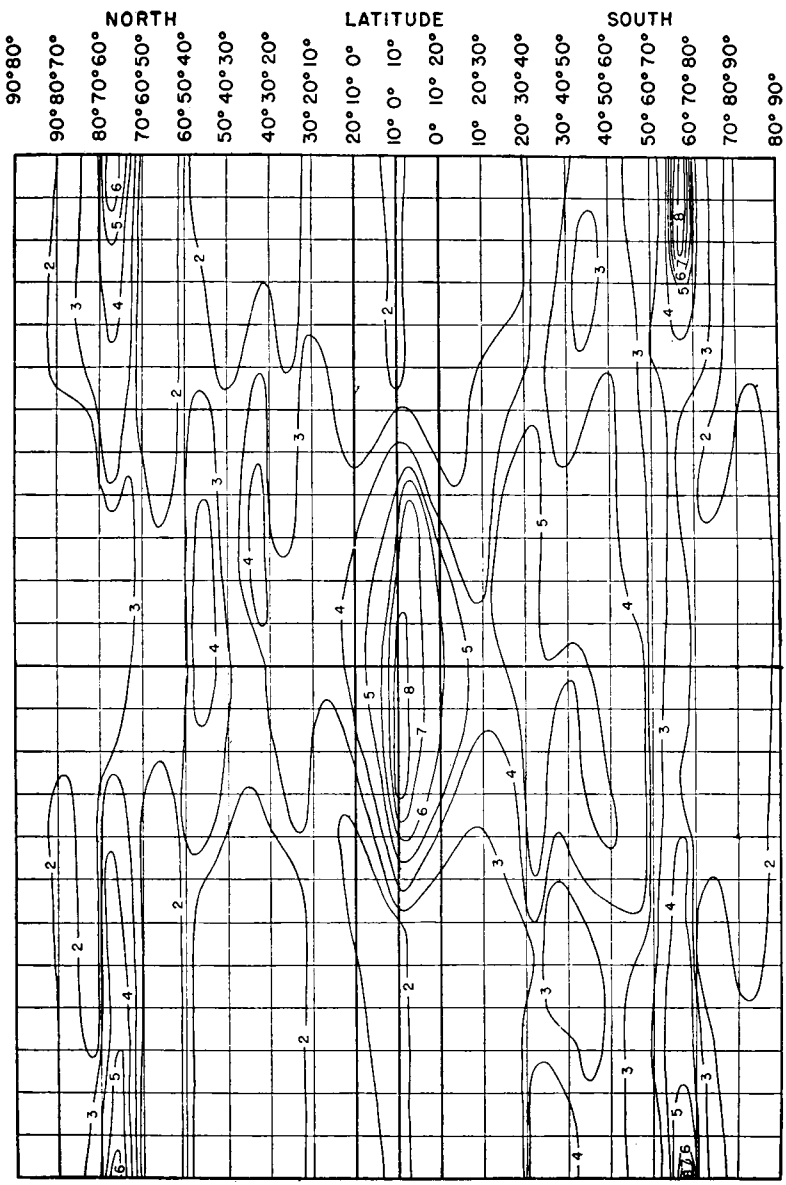

FIG. 3.5. Median E sporadic, in megacycles, predicted for January, 1947. (*After Central Radio Propagation Laboratory.*)

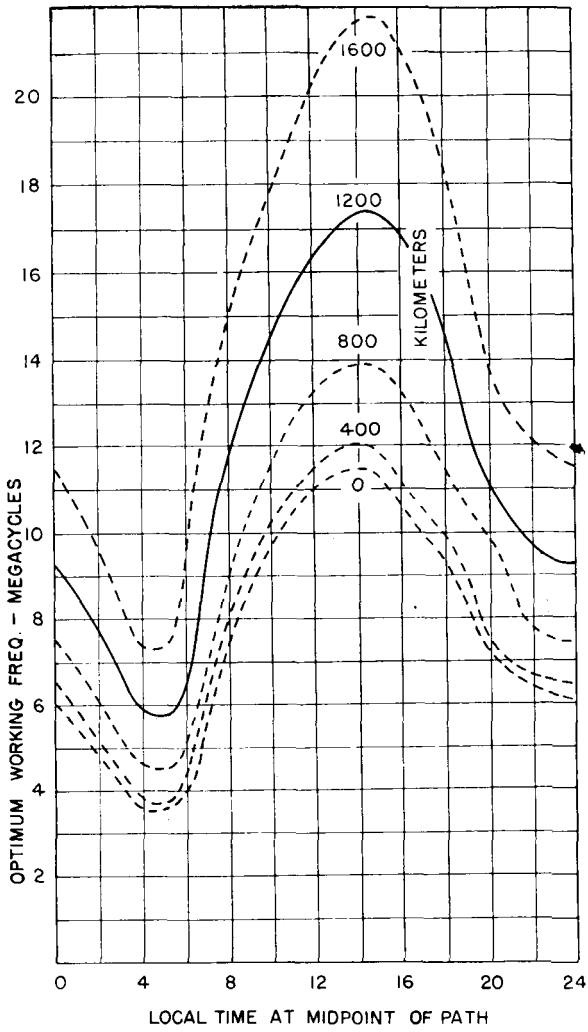

FIG. 3.6. Optimum working frequency for September, 1945, latitude 10 degrees north, west zone.

falls gradually to a minimum. When the upper atmosphere is again subjected to sunlight bombardment, before sunrise is evident on the ground, ionization commences and maximum usable frequency shows a sharp rise. The rate of rise is very rapid, and this phenomenon on the maximum-usable-frequency and optimum-working-frequency curves is called the "sunrise wall." Ionization intensity (and accordingly the maximum usable frequency) rises to a maximum shortly after local noon at the place

of wave reflection, following which it diminishes steadily into the presunrise period.

Every geophysical propagation path will have its own diurnal characteristics, and this changes month by month and year by year throughout the sunspot cycle. There will be some daily variations that are now predictable about 6 days in advance from direct sunspot observations, as these spots move into a certain part of the solar disk. These transient disturbances cause deviations from the typical diurnal frequency characteristic for any given path.

The propagation studies that must precede a choice of working frequencies can be made following the data and instructions issued by the Central Radio Propagation Laboratory (see refs. 1, 3, and 4, page 217). Since this is essential material for all modern high-frequency transmission, the reader should refer to the complete details and instructions in the application of the Central Radio Propagation Laboratory ionospheric data.

Another series of Central Radio Propagation Laboratory data (ref. 2, page 217) includes details of the various ionosphere heights. From these data the necessary information is available for determining the best angles of radiation in the vertical plane, depending upon the particular layer that is controlling as to frequency at any particular interval of time. These data are of special interest to the antenna engineer because the design of the antenna radiation patterns for best utilization of the medium proceeds from them. More extensive application of the frequency-height data permits the computation of multipath delays and angles of arrival of various wave groups from the different layers which are of importance in receiving antenna design.

The orientation of a wave path in the earth's magnetic field is another source of signal variability. Certain types of sunspots cause magnetic storms on the earth, and the effect on the ionosphere is greatest toward the magnetic poles, where the earth's magnetic field strength is greatest. It was found by Hallborg (ref. 9, page 217) that greatest disturbance to high-frequency transmission occurs when reflections take place from the ionosphere within or near the earth's auroral zones. Later researchers have established the boundaries of these zones more precisely, as shown in Fig. 3.7. It is therefore a rule of high-frequency propagation engineering to avoid all transmission through, or reflection within, these zones whenever possible. Where a transmission path must pass close to or into the auroral zone, much higher power is necessary to maintain any given circuit reliability.

The angular clearance of a wave path with respect to the boundaries of the auroral zone is called the "auroral-zone clearance" (AZC).

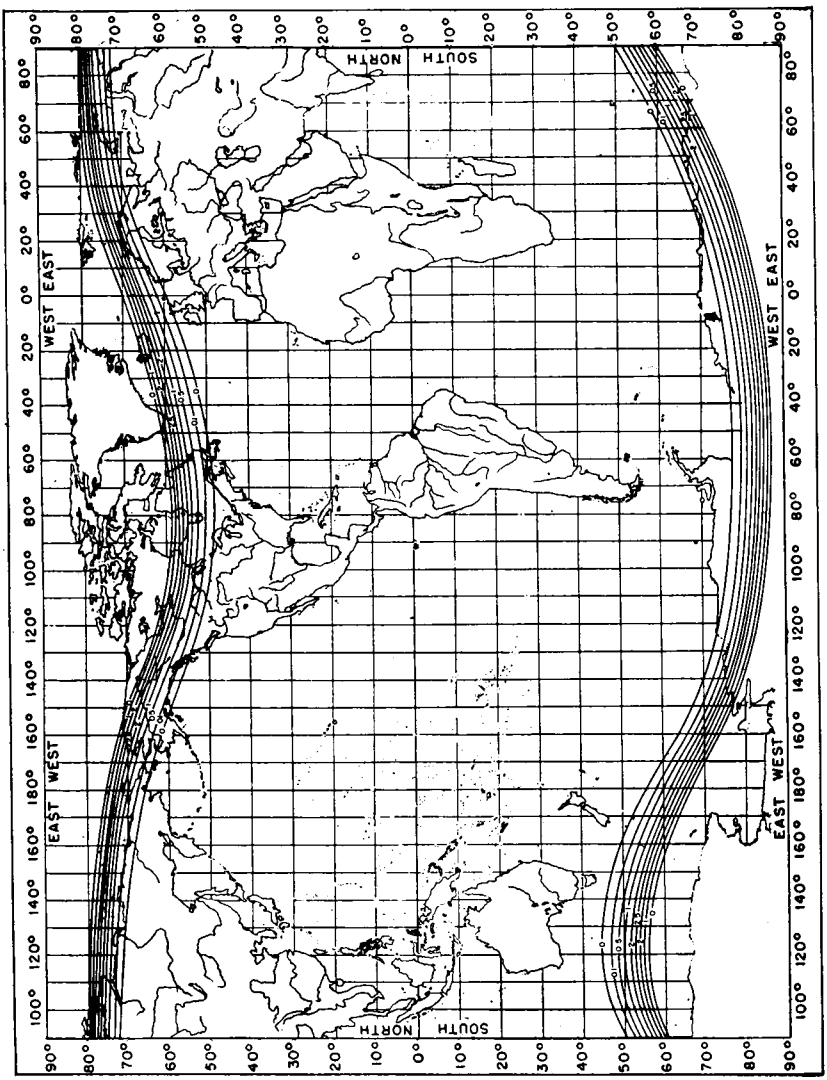

FIG. 3.7. Aurora-zone-absorption map. (*After Central Radio Propagation Laboratory.*)

The principles of multipath circuits are largely geometric, but the extent of layer penetrations at different angles of incidence and at different frequencies must be obtained from the characteristics of the ionosphere. Figure 3.8 is a simplified representation, on a flat-earth basis, of a circuit that can be worked with one hop, but there may be other higher-order hops present if there is a broad vertical lobe of radiant energy from the transmitting antenna. The angle of arrival for the one hop will be the lowest and will vary as the actual effective height of the controlling layer varies through the usual range. The E layer, when it exists, during the daylight hours, is at a relatively constant height and is

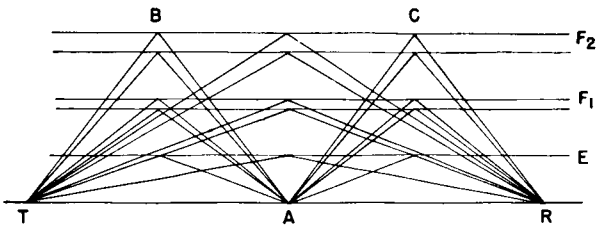

FIG. 3.8. Flat-earth representation of a radio circuit from T to R by several possible wave paths.

shown as a single line. The F_1 and F_2 layers are subject to considerable variation in height from time to time, and arbitrary upper and lower limits are shown by the two lines for each.

At a frequency that would penetrate E and F_1 with also some degree of reflection, there can arrive at the receiver three one-hop signals, one from each layer. The waves from the higher layers, having traversed the greater distance, will arrive at the receiver with increasing delays. Then consider two hops from each layer as shown, giving rise to three more wave groups with other time delays, the longest being that via F_2. Other higher-order hops might also exist.

One may eliminate E-layer reflections completely by choosing a frequency high enough to penetrate the E layer. If the frequency is close to the maximum usable frequency and F_2 is controlling, then F_1 reflections might be absent or very small. In such a case, there may be one-hop and two-hop F_2 waves, with their time differences of arrival. But if it happened that the large angle of incidence at F_2(B) and F_2(C), B and C being the reflection points on the F_2 layer, caused the waves at these points to penetrate without reflection also, only the one-hop F_2 signals would arrive. Under such conditions, only one wave would arrive completely free of multipath interference. At the other extreme, the operating frequency could be chosen so low that it would not penetrate the E layer at all, thus eliminating all F_1 and F_2 reflections. However, there

may remain multipath E-layer signals unless the antenna radiation patterns at transmitting and receiving locations provide very low response at the higher angles at which multipath E-layer signals would be propagated.

The same situation exists when the example is changed into the spherical terrestrial geometry. The known methods of attack on the multipath problem involve these three factors: (1) the use of a frequency that will cause reflection from one layer only, as nearly as possible; (2) the use of a frequency near to the critical one for reflection at the point of lowest angle of incidence so that complete penetration occurs at other points in the same layer where the angle of incidence is higher; (3) the use of antenna directivities at both ends of the circuit that will focus the energy at the angle of one dominant wave group and discriminate against other multipath signals by relatively low response to all other angles.

High-frequency signals do not always follow a great-circle path. Some long circuits that have their terminals in northern and southern hemispheres, or in daylight and darkness, show large deviations from great circle in the angle of arrival of waves. The physics of this phenomenon are insufficiently understood at present, but it is evident that a wave will tend to follow a path of lowest propagational impedance when passing from one region to another of different propagational characteristics. The phenomenon is believed to be due in part to tilting of the ionized layers.

Angular deviations in azimuth and in the vertical plane can cause excessive signal variations at the receiver input if the antenna responses at both ends of the circuit change rapidly with the angle. The ideal antenna pattern is one that has uniform response over an angular sector in both horizontal and vertical planes and zero response at all other angles. Characteristics of this sort are not practically realized with present-day high-frequency antenna-design techniques and with present-day economics.

3.2.4. Signaling Speed. The maximum signaling speed, say in telegraphy, is determined by the maximum delay resulting from multi-path signals of appreciable relative intensity. If the signaling speed is such that a prominent delayed wave in the multipath group surpasses 20 per cent of the shortest pulse in the signal, there results mutilation because of elongation of the pulse. It is then necessary to reduce signaling speed to maintain accuracy.

On one-hop circuits it might be relatively easy to apply any one or all three of the forementioned principles for reducing multipath and thus maintaining a very high signaling speed; but on a multihop circuit, with different ionosphere characteristics at each point of reflection and the

need to use a frequency that is limiting at one of these, the best frequencies would be severely compromised from the standpoint of selective layer and angular penetration. Also, there may be multipath signals with considerable delays coming in at overlapping angles so that there could

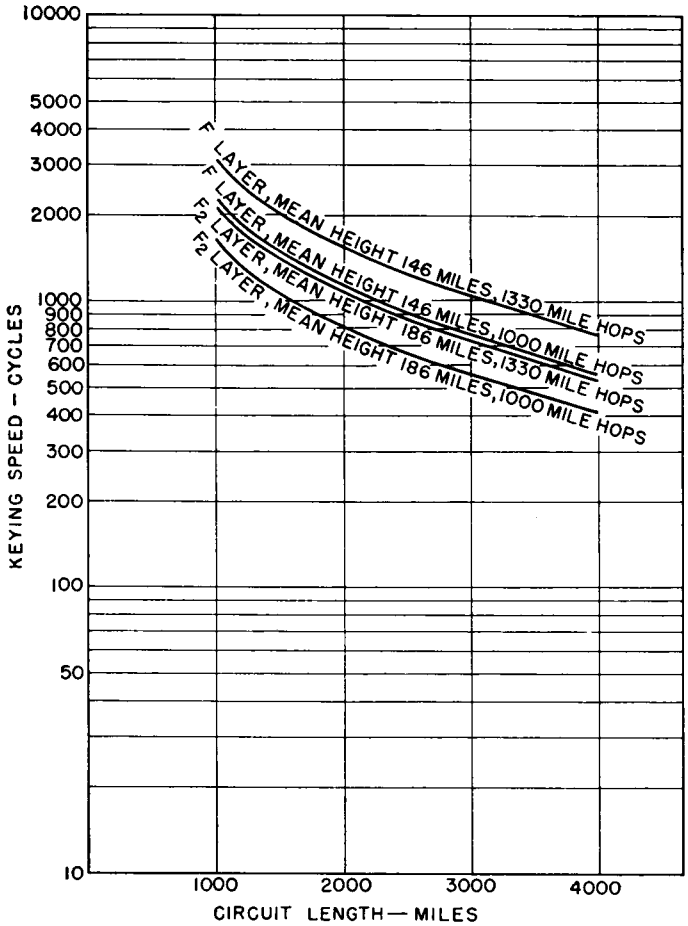

FIG. 3.9. Computed keying speeds for 25 per cent dot elongation, when speed limitation is 10 per cent instantaneous height variation only and hop lengths are 1,000 and 1,330 miles, using complementary antennas. (*Hallborg data.*)

not be angular discrimination by the antennas. As a consequence, such circuits have limited signaling speeds, and the amount of traffic that can be passed over them in a given time is reduced.

Figure 3.9 shows calculated keying speeds versus distance for one particular path, using one particular pair of transmitting and receiving antennas.

The advent of teleprinters in radiotelegraph service brought with it the need for vastly improved standards for telegraph signal distortion because a relatively pure signal must be delivered to a printer to ensure correct response to a code character. A circuit may be performing very well for a certain period on four-channel time-division multiplexed teleprinters; then a sunspot may enter the critical zone of the sun, and the circuit will be disturbed so that the signaling speed may have to be reduced to that of a single printer channel. The tape boards at the central office begin to fill up with delayed traffic, and one who is familiar with the propagation details comes to see sunspots in the form of perforated paper tape containing messages that are waiting for transmittal.

3.2.5. Other Factors Affecting High-frequency Circuits. If the ground conductivity is high, some useful distances for communication can be obtained by high-frequency ground-wave propagation. From ground propagation curves it is evident that as the frequency becomes higher, the ground-wave attenuation increases very rapidly. Over sea water, the best conductivity that is available in nature, substantial distances can be covered with frequencies of 5 megacycles or sometimes more. This fact has often been utilized for interisland communication and for short-distance shore-to-ship communication, particularly in harbors and estuaries. In such applications, vertical polarization gives best results, and the station sites should be near the shore to avoid excessive attenuation over land.

In airways and aircraft communication using the high frequencies, it is essential to use horizontal polarization and transmission via the ionosphere even for short-distance working. Ground-wave coverage over land is so limited that an aircraft is quickly outside the communication distance. Also, regardless of polarization, the signal strength on the horizon at the high frequencies and typical ground conductivities is vanishingly small by the direct wave. Experience has long proved that best communication with aircraft is via the ionosphere as soon as the craft passes out of the range of the direct space wave. To obtain ionosphere reflections at nearly vertical incidence the frequency used must be below the vertical-incidence maximum usable frequency for the location of the transmitting station.

As a consequence of the randomness of ionospheric waves in azimuth and vertical angles of arrival, as well as the large variations in intensity and the changes in polarization in transit, accurate direction finding at high frequencies has been difficult. Most successful high-frequency direction finding has been with Adcock receiving antennas responsive only to the vertically polarized component of the arriving signal. An extensive metallic ground system around the antennas eliminates wave

tilt in the vicinity so that the electric-flux lines of the wavefronts are vertical. The vertical elements of the Adcock array respond to this electric field with a minimum of response to other components of the wave, as the polarization changes from moment to moment. A carefully calibrated system of this type can accurately indicate the direction of arrival of a wave (in azimuth), though this direction may not always be the true bearing of the transmitting station.

The antenna designer must recognize that high-frequency propagation is more complicated than can be predicted from the best available information. Fortunately, the accumulated information permits the prediction of single-hop circuits with sufficient accuracy for engineering use. It requires the most expert use of the available data to predetermine the variations of vertical propagation angles on multihop circuits through seasonal and sunspot cycles. There is very little information to guide the antenna engineer in the range of variation of azimuthal angles on long circuits, though it is known from observations with modern direction finders that the signals may arrive from angles considerably off the great-circle bearing from the transmitting station (see ref. 12, page 218). Antenna systems should be designed to utilize the optimum vertical angles and suppress others that contribute to multipath delay and distortion. On the other hand, excessive horizontal directivity is often detrimental to circuit performance when the horizontal angle of arrival swings as far as the first null in the receiving-antenna pattern. For this reason, the requisite vertical directivity may have to be associated with a rather broad horizontal pattern.

In using space diversity reception, the pattern for one receiving antenna can be turned slightly with respect to the other, giving the effect of broader horizontal pattern for both. Still more horizontal equalization of this kind can be employed in a third antenna when three-set diversity is employed.

It is essential in the design of communication circuits to direct the beams of the transmitting and receiving antennas at the angle that is most favorable for the particular circuit and operating frequency. In many, if not most, cases the best angle will be the same, within reasonable limits, at both ends of the circuit. On one-hop circuits this seems to be true always, and any departure from this principle seems to increase with the number of hops. To make the best use of this effect, it is desirable to employ complementary antennas for transmitting and receiving—antennas having the same vertical-plane patterns. Figure 3.10*A*, *B*, and *C* gives three examples of uncomplementary antennas; Fig. 3.10*D* and *E* two which are complementary. Example *B* will be recognized as one typical of the high-frequency-broadcasting situation; *C* is an

example of a case often found where a receiving antenna is too low to receive medium-angle signals and gives relatively poor results; and in *A* the receiving antenna is too high and presents low response to the angle of signal arrival. The same result would be obtained if the transmitting and receiving antenna patterns were interchanged. The best operational results can be expected from *D* and *E*, assuming that the

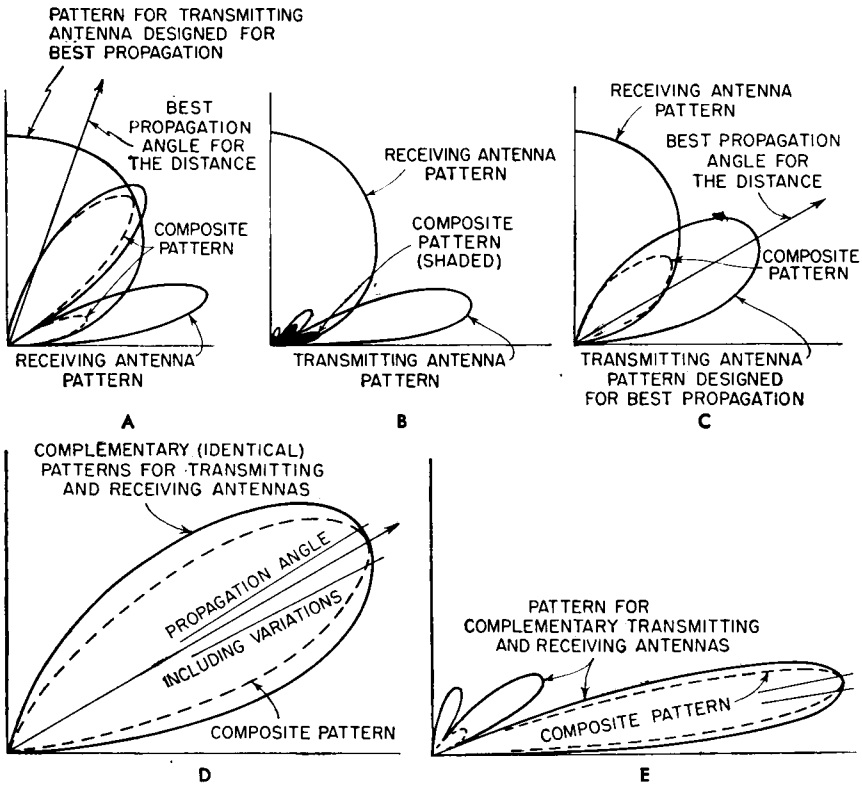

FIG. 3.10. Comparison of uncomplementary and complementary antennas.

angles of maximum transmission and reception are properly chosen propagationwise.

In this discussion we have presented high-frequency wave trajectories on a straight geometric-ray basis, for any number of hops. Owing to ionosphere turbulence, wave trapping, refractions and reflections, and scattering in space and at reflection points on the earth, the actual trajectory of a wave is extremely complex and changes from moment to moment. However, there is a sufficient amount of successful engineering experience now to justify the ray theory for engineering applications.

From extensive measurements that have been made of multipath delays and angles of signal arrival it is indicated that the geometric-ray theory is perhaps a statistical average condition.

It is the utilization of this principle that has led to the use of the principle of complementary antennas for transmitting and receiving. When complementary antennas are used for a communication circuit, the composite radiation pattern for the circuit is the square of the pattern for one of the antennas and the angle of this composite pattern is chosen for the lowest practical order of hop for the distance, using the geometric-ray theory and the known ionosphere heights. When noncomplementary antennas are used, the angle of transmission is chosen to be that of maximum response for the composite pattern for the path obtained by multiplying the transmitting-antenna pattern by the receiving-antenna pattern. This is essential in services, such as broadcasting, where there is no control over the characteristics of the receiving antenna.

REFERENCES FOR HIGH-FREQUENCY PROPAGATION

1. Ionospheric Radio Propagation, *Natl. Bur. Standards (U.S.) Circ.* 462. An essential reference for high-frequency propagation engineering. Obtainable from Superintendent of Documents, Government Printing Office, Washington, D.C.
2. Ionospheric Data. Issued monthly by the Central Radio Propagation Laboratory, National Bureau of Standards, Washington, D.C. Identified as CRPL-F series.
3. Basic Radio Propagation Predictions—Three Months in Advance. CRPL-D series. Issued monthly by the Central Radio Propagation Laboratory, National Bureau of Standards, Washington, D.C., on a subscription basis.
4. Instructions for the Use of Basic Radio Propagation Predictions, *Natl. Bur. Standards (U.S.) Circ.* 465.
5. Radio Progress during 1946—Ionosphere, *Proc. IRE*, **35**:416–417, April, 1947.
6. Radio Progress during 1947—Ionosphere, *Proc. IRE*, **36**:311–313, March, 1948.
7. Radio Progress during 1948—Ionosphere, *Proc. IRE*, **37**:530–553, April, 1949.

NOTE: Subsequent annual reviews similar to the foregoing are excellent guides to current progress and all important publications relating to this subject.

8. Dellinger, J. H., and N. Smith, Developments in Radio Sky-wave Propagation Research and Applications during the War, *Proc. IRE*, **36**:258–266, February, 1948.
9. Hallborg, H. E., Terrestrial Magnetism and Its Relation to World-wide Short-wave Communications, *Proc. IRE*, **24**:455, March, 1936. Auroral-zone effects.
10. Arzinger, A., H. E. Hallborg, and J. H. Nelson, Sunspots and Radio Weather, *RCA Rev.*, **9**:229, June, 1948.

11. Hallborg, H. E., and S. Goldman, Radiation Angle Variations from Ionosphere Measurements, *RCA Rev.*, **8**:342, June, 1947.
12. Feldman, C. B., Deviations of Short Radiowaves from the London–New York Great-circle Path, *Proc. IRE*, **27**:635, October, 1939.

3.3. Factors Affecting Signal Intelligibility

Signal intelilgibility means the reception of communication signals in a form sufficiently unmutilated to provide complete reproduction, at the receiver, of the original intelligence. The amount of mutilation that can be tolerated depends upon the type of emission employed. For example, manual telegraphy can tolerate signal distortion and noise and spurious-signal interference to a greater extent than can automatic teleprinter operation. The amount of mutilation and interference that will provide solid communication is largely dependent upon the ability of each operator. The same is true of telephone working, where experienced operators can understand signals that would appear quite garbled to a casual listener.

Different standards of engineering are required for different classes of services. A teleprinter system must be designed to higher standards of performance than a manual telegraph circuit, and high-speed facsimile or multiplexed teleprinter circuits in turn require superior over-all performance to a single-channel printer circuit. A radiotelephone system intended for public correspondence requires better system performance than does a telephone circuit used only by professional operators as in air-line communication.

In this discussion there are so many factors involved that any remarks must of necessity be quite general. Many of the main factors that control signal intelligibility vary over wide limits for intervals that may be from a fraction of a second to a season or a year. However, these considerations form an important background for the design of antennas.

At the high frequencies, propagation is extremely complex. On any given space circuit, there is always a best working frequency, a best set of transmitting- and receiving-antenna characteristics, and a certain minimum transmitting power that will give the desired signal intelligibility in the presence of propagation variations and other signal and noise interference. One cannot engineer a circuit for such optimum performance because the optimum requirements may be different the following hour and for a high percentage of total working time. One cannot change working frequency, operating power, and antenna characteristics from minute to minute to follow these variations, even if one knows exactly what to anticipate. Accordingly, a circuit is engineered for compromise conditions. The choice of compromise is the essence of

high-frequency communication engineering, and even experienced engineers will not evaluate circumstances equally and select the same compromises. In fact, much of the existing discordance of opinions on system details rests on the fact that there hardly is one optimum compromise, but rather a compromise of compromises.

3.3.1. Antenna Patterns. There are two main divisions of the signal variability to be considered—that due to the signal in space, and that contributed by the characteristics of the transmitting and receiving antennas. Customarily, both are considered as one. Actually, the antennas themselves may introduce a great deal of signal variation that may not be due to the space circuit at all. Consider, for example, a wave of constant field strength that is changing its azimuthal angle of arrival only by several degrees. If the receiving-antenna pattern is too sharp to have uniform response over the angle of azimuthal deviation, the receiving antenna introduces signal variation. If the receiving antenna has a deep null in its pattern 15 degrees off great-circle azimuth and the arriving wave swings as much as 15 degrees, the receiving antenna registers a deep fade which may not have been present in the arriving wave.

If azimuthal variation is a factor on a given circuit, it can be seen that the ideal receiving-antenna azimuthal pattern is one which is uniform over the range of angles of signal arrival and has zero response at all other angles. While it is theoretically possible to accomplish this, it is structurally and economically impractical to do so in present-day operations. In this case it may be the choice of the designing engineer to use a broader pattern, with lower gain and more wide-angle signal and noise pickup, to reduce signal variation caused by his receiving antenna. Another design engineer may find that the opposite choice best fits the circumstances, although usually the best solution is that which ensures the strongest and most constant signal.

The same effect occurs in the vertical plane. There may be several wave groups arriving simultaneously at different vertical angles, although one group will dominate the others in intensity from moment to moment. This gives, in effect, something like a single wave that is constantly changing its vertical angle of arrival. If now the field strength arriving is constant, but changing in angle, the vertical polar pattern of the receiving antenna, if nonuniform in response over the range of arrival angles, introduces signal variations as the signal comes in on different portions of its pattern. If the range passes a null in the pattern, it would look at the receiver as though the signal had faded to a very low value.

These effects due to the antenna response pattern occur in many cases, and the signal itself also varies typically over a considerable range of values. When the horizontal and vertical angles of arrival correspond

to directions of minimum antenna response simultaneously with a minimum arriving signal strength, the signal at the receiver may go far under noise level and produce an interval of unintelligibility. Because of all these causes, the signal at the receiver goes through a wide range of values, sometimes exceeding 80 and 100 decibels, from second to second.

There is another very important aspect of the pattern of the receiving antenna. The fact that more than one wave group often arrives in the vertical plane and that the delay of the signal along each of the paths identified by its different arrival angle is different causes signal distortion even when signals may be strong. The delay is characteristically greater as the arrival angle becomes higher, since each wave traverses a longer path. Wave interference between the different wave groups at the receiving antenna introduces fading and elongation of signals due to the delays. If it were possible to select for reception only one of these wave groups and reject all the others, its field strength might be less variable and the delay differences would be eliminated. As a consequence, the signal intelligibility would be improved.

On some space circuits, there is sufficient angle between the multipath wave arrivals so that the vertical pattern of the receiving antenna can select one, by suitable angular response, and reduce or suppress the others. The shorter the circuit, the more likely is it that substantial angular difference in wave arrival will exist, including the effect of angular changes due to changes of layer height, to permit the selective reception of one dominant wave group by using the appropriate receiving-antenna pattern. However, on longer circuits, two or three orders of hops may arrive at so nearly the same angle that angular selection is impractical. In such a case there is no possibility of improving the intelligibility of the signal by this method, and lower signaling speeds and greater percentage of lost circuit time have to be accepted. If multipath delays cannot be eliminated, there is very little advantage to increasing transmitter power to improve signal intelligibility.

In the same respect as explained for receiving, the transmitting-antenna radiation pattern has a bearing on the situation. If one could radiate all the power at the one optimum vertical angle that gives the best transmission path, there would be relatively little radiated at the angles that give rise to multipath transmission. As stated previously, the angle of departure for a given wave path is roughly the same as that of its arrival a large portion of the time. Then if one is trying to eliminate a certain wave group at the receiver to improve signal intelligibility, it will usually help to transmit less power at the undesired angle. When the transmitting and receiving antennas are complementary, with maximum

responses at the most favorable wave angles and relatively low responses at all the other angles, it is possible to improve operating margins by using greater transmitter power and increased operating speeds in telegraph services. In telephony, the improved intelligibility gives greater speed in completing calls satisfactorily and permits more calls to be placed.

It must be evident that antenna gain, of itself, is a secondary consideration in antenna design. The primary objective in design is to produce the most favorable radiation pattern in both vertical and horizontal planes from the standpoint of minimizing multipath propagation. Excessive directivity may be as detrimental as inadequate directivity. Using random patterns or patterns not expressly designed for the desired path can give results that are definitely bad. In these days of good ionospheric data, there is no longer an excuse to employ the hit-and-miss practices of the past. Years ago, one used high antenna gains to give high effective transmitting power and high-gain receiving antennas to receive as much power as possible—supposedly. Yet there were times when better communication resulted from the use of simple dipoles than from the superarrays. Modern propagation engineering makes this anomaly very clear and points the way to better performance. In years to come, greater and greater attention to these matters will be required as larger traffic volume has to be handled on fewer and fewer frequencies. The compromises employed today for economic expediency may well be intolerable in the future, when each circuit and frequency will be carefully engineered for peak performance, with tailored radiation patterns for that circuit only. A larger portion of the total investment will be in antennas.

3.3.2. Noise. Signal intelligibility is always compromised by the presence of noise. Interference can also be regarded as noise having different statistical properties from receiver noise, or to the broad group of radiations classed generally as static, whether natural or man-made.

Every type of communication system has a certain signal-to-noise ratio below which the intelligibility of the signal is insufficient for communication. If the incoming signal-to-external-noise ratio is below this minimum value, obviously the only thing that can be done to obtain serviceable operation at the optimum working frequency is to increase effective radiated power over the path of propagation. Under some circumstances, advantage may be taken of the directivity of the receiving antenna, making it responsive to the signal and blind to the sources of noise. This works only when signal and noise directions are actually different and when suitable directivity can be obtained. We assume that, beyond the antenna, the receiver bandwidth is no more than necessary

to accept the spectrum of the incoming signal, so that no unnecessary extraband noise is admitted. The received signal-to-external-noise ratio is very often improved by directive antennas, but there are times when this is not at all true. In high-noise regions when signal-to-external-noise ratios are typically low, it is difficult to do anything in the way of antenna engineering that will improve the ratio. Almost any antenna appears to give the same performance. Any reduction of response to the noise makes the system equally unresponsive to signal on the same frequency, with no change in signal-to-noise ratio. Any measures that increase the received power merely reduce the gain required in the receiver, without any net improvement in circuit performance.

In very low noise regions there is a different set of prevailing conditions. Not limited by external noise, very weak signals may be utilized by employing adequate receiver gain. Receiver noise may then be the controlling factor. In this case, signal-to-noise ratio can always be improved by any means that will increase the signal power delivered to the receiver. Directivity will always be beneficial (assuming no angular deviations), and there is reason to be careful with antenna-feeder impedance matching at the working frequency so that system loss will be minimized. These practices are relatively useless in regions of high ambient noise.

In speaking about these extremes it is necessary to remember that the majority of practical cases occur somewhere in between; also, that at any one location it is possible for both extremes to be encountered occasionally. The practices adopted are then based on the percentage of time they occur. Tropical or arctic techniques may prevail according to which is most typical of the location.

3.3.3. Transmitter Power. Assuming optimum radiation engineering for a circuit (frequency, antennas, noise, etc.), a certain amount of effective radiated power is necessary to maintain operating margins over a satisfactory proportion of time. Except for multipath propagation, the principal circuit requirement is that the received signal-to-noise ratio be above a certain minimum. When all other means to this end fail, more transmitter power can be used. Considering the range of variation in signal-to-noise ratio characteristic of high-frequency operation, especially on long circuits, operating economics become an evaluation of the cost of transmitter operation versus the increased percentage of time the minimum operable signal-to-noise ratio is received.

Sometimes enormous power increases would be necessary to make an appreciable improvement in the operating circuit. In such cases it may be far more effective to apply every possible means for decreasing fading range than to increase power. Diversity reception is always a

help in such cases, because it reduces the fading range and makes use of the strongest of two or three arriving signals. Too often, however, excessive power is employed to override other engineering deficiencies, incidentally causing unnecessary interference with other services.

3.3.4. Diversity Reception. Systematic measurements have been made from time to time under many different operating conditions to determine the quantitative value of diversity reception. It has been known for many years, from the works of Beverage and Peterson, that two-set and three-set diversity reception gives greatly improved circuit performance in the presence of the various factors encountered in long-distance high-frequency communication. Measurements made in 1949 using new techniques have shown for the first time that the "gain" in circuit performance due to diversity reception varies with the degree of reliability of the circuit.

For example, on teleprinter operation, the improvement may be of the order of 12 decibels for two-set diversity as compared with non-diversity reception when errors are running at 20 per 1,000 characters. On the other hand, when errors are running at 1 per 1,000 characters with nondiversity, the improvement due to two-set diversity may approach 30 decibels. This means that the transmitter power would have to be increased by 30 decibels to reduce errors by the amount due to the use of two-set diversity. The use of three-set diversity would give even greater improvement, this again being a function of the error count. However, the improvement of three-set over two-set diversity is very much less than that of two-set diversity over nondiversity. It must be mentioned that these figures pertain only to telegraph operation. Comparative measurements on single-sideband and double-sideband telephony are not available yet.

Figure 3.11 shows a set of communication conditions which are arbitrary but which represent in general what occurs on every path. This example may apply to radio communication in general, but for the present it will refer to high-frequency communication. The signal-to-noise ratio (S/N) in decibels is plotted against time for a period of time T_0. This epoch may be a minute, an hour, a day, a season, or a sunspot cycle, according to the case.

The short-period signal-to-noise variations lie between curves AA' for a power P_1 transmitted, and over a longer period the envelope for the instantaneous variations goes through a wide range of variations. These variations may be due to any or all of the causes of signal variation by propagation, by the antennas, and to all the changes in received noise. Let it be assumed that a simple amplitude-modulated telephone service is desired, the lower limit of signal-to-noise ratio for satisfactory com-

munication being 15 decibels. That portion of the time when the signal is below this level may be regarded as lost time.

In the epoch T_1 the range of variation of signal-to-noise is almost all above the working limit, and those values of A' which are below the 15-decibel value are probably of very short duration (sometimes of seconds only) and represent a very small percentage of the time. This epoch represents the conditions for a good circuit.

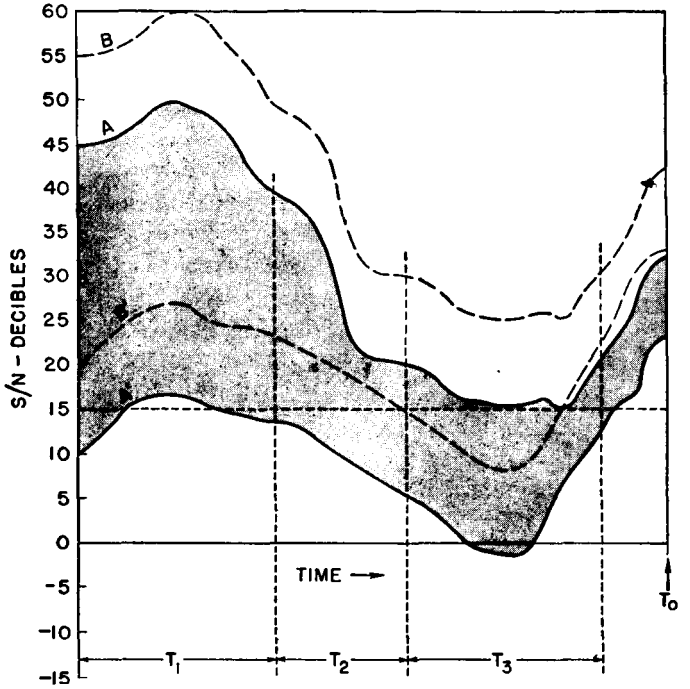

FIG. 3.11. Illustration of communication reliability.

In the epoch T_2 the circuit begins to be marginal because a substantial percentage of the time the signal is below working limits. This condition may be acceptable for an intermittent service by taking advantage of those times when communication can be supported. However, for a commercial service this period of time would be a difficult one.

Finally, the epoch T_3 represents completely unworkable conditions because S/N is greater than the required 15 decibels only a very small percentage of the time.

The curves BB' represent the same conditions but with a 10-decibel improvement in signal-to-noise ratio. This improvement may of course be obtained by increasing transmitter power 10 times or by somehow reducing noise pickup by 10 decibels. During the times when com-

munication is marginal or impractical, it can be seen that a power increase of less than 10 decibels makes only a trivial improvement in circuit performance. Even though any increase in transmitter power will increase S/N, it is in fact necessary to employ substantial power increases to make a worth-while improvement in circuit performance.

If we assume that the circuit is properly engineered with regard to antennas, working frequencies, etc., and the final problem is that of the transmitter power to be used, the power required will be determined entirely by the desired circuit reliability in terms of the percentage of the time the circuit is workable in relation to the times when the service is needed. If a "solid" circuit is required, the power to be used must be sufficient at all times to deliver a signal that will override ambient noise by the amount dictated for the type of emission employed. Amplitude-modulation telephony will require the 15-decibel value that has been used in the above discussion. Frequency-shift teleprinter service may be workable when S/N is as low as 2 or 3, and manual Morse operation with skilled operators may be sufficiently workable at -10 decibels. In any event, the amount of power used at the transmitter may be below the minimum mentioned for solid service only by forfeiting reliability. In choosing a lower power for economic reasons (and this is typical in general in practical communication economics) advantage can often be taken of regular periods of good propagation and low noise for traffic clearance, assuming of course, a tolerable time distribution of these factors.

In practice, this general situation prevails, except that the range of values of S/N may be much greater and perhaps even less than those shown in Fig. 3.11. The range of values used in this example are representative of a fairly good circuit if the epoch T_0 is sufficiently long to embrace the full range of variation encountered on a given circuit.

The range of instantaneous variation between AA' (or BB'), if due mainly to variations in received signal (if noise is relatively constant), can often be reduced by better accommodation of antenna radiation characteristics to the propagation conditions. When this can be done, it is actually as good as an increase in transmitter power because the lower limit of the signal envelope A' will be higher, and at the same time the upper limit of variation A is reduced. If it were possible to eliminate instantaneous wide-range variations entirely, S/N would then lie midway between A and A'. This desirable condition is not likely to be achievable, but before increasing transmitter power it may be worth while to see what can be done to decrease the range of variation between A and A'. Any method that will reduce multipath propagation will usually decrease the range of signal variation from moment to moment. This will also increase signal intelligibility. However, if variation in noise level is the

dominant cause of the variation in S/N, and if directive discrimination against noise is impractical, the only course left to improve the circuit is by a sufficient increase in transmitter power. This latter condition is that prevailing generally in high-frequency broadcasting service, where there is no opportunity to modify the conditions surrounding the receivers.

When the conditions represented in Fig. 3.11 typify short-time variations (seconds or perhaps minutes), it is evident that diversity reception could be employed to equalize them, provided that the same variations occurred at random on a second or third receiving channel.* In such circumstances there is the probability that one diversity channel would provide a satisfactory signal-to-noise ratio at the instant that another experiences a fade-out. The combined output of the diversity receiver would therefore be relatively uniform, and the percentage of total time that the overall signal-to-noise ratio is below threshold value is reduced. The reduction of the time-loss factor due to diversity reception is a system gain equivalent to the power gain that would have to be used at the transmitter to realize the same time loss with a nondiversity system. This gain has been expressed as†

$$\text{Gain} = \frac{20}{m}\left(1 - \frac{1}{n}\right)\log_{10}\frac{1}{k} \qquad \text{decibels}$$

where m is an empirical factor of a nominal value of 2 but which may vary from 1 to 2.5 in practice, n is the number of diversity sets or channels used, and k is the permissible time-loss factor for the system.

3.4. High-frequency Transmitting-station Sites

The choice of a site for a high-frequency transmitting station for efficient radiation is determined almost wholly from considerations of the geometry of the wave-propagation circuits. Any site that has a horizon subtending vertically less than 2 degrees from level in any of the directions of transmission can be considered immediately a satisfactory site from the radiation standpoint.

As a simple rule, one can say that a satisfactory horizon clearance exists when it subtends a vertical angle from the site that does not exceed one-half of the desired beam angle in the vertical plane in that direction. If the vertical beam angle for a given circuit is 10 degrees for the lowest-order hop, then the horizon in that direction can be as much as 5 degrees in elevation as seen from the site or, more exactly, from the antenna location.

* This occurs when the receiving antennas are spaced some 1,000 feet or more. When three antennas are used, the three are best located to form a triangle.

† Jolonek, J., E. Fitch, and J. H. H. Chalk, "Diversity Reception—Statistical Evaluation of Possible Gain, *Wireless Engr.*, **24**:54, February, 1947.

In hilly or mountainous country the choice of a site for long-distance transmission (requiring very low beam angles) can be a difficult problem. In such cases, the best procedure is to set up a transit in the middle of the proposed site and plot the vertical horizon angle for all relevant azimuths in the manner shown in Fig. 3.12. Then on this same profile the beam centers, determined previously from geometrical studies of the desired

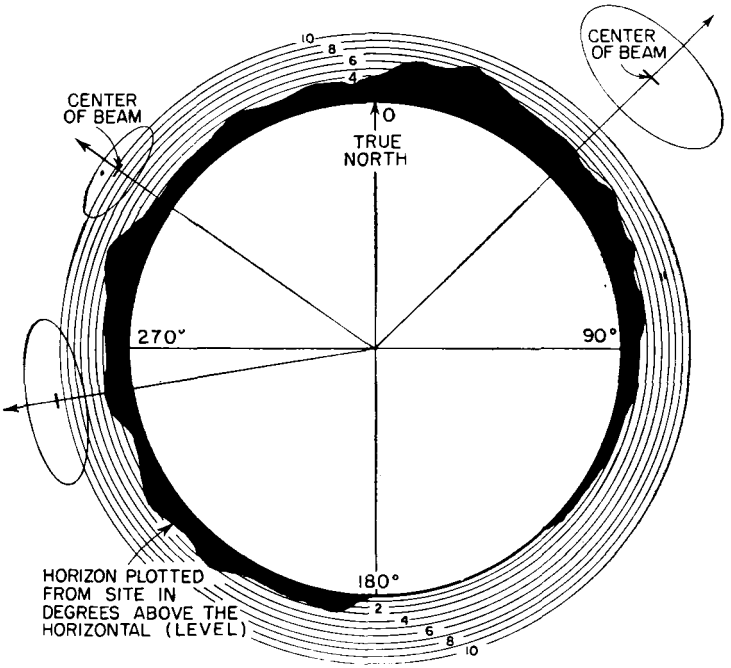

FIG. 3.12. Horizon profile in degrees as seen from a site and three beams from directive antennas having good horizon clearance.

propagation paths depending upon distance, layer heights, and number of hops, can be superimposed.

When the only possible site presents horizon obstructions in the preferred wave path, it may be necessary to design the antennas to use a higher order of hop and to direct the beam at a correspondingly higher angle to obtain the 2-to-1 horizon clearance. If, for example, the computed vertical beam angle for a one-hop circuit was 6 degrees at an azimuth of 332 degrees and the horizon in this direction consisted of a range of mountains with a height of 8 degrees, the performance of the circuit would be greatly compromised by the obstruction of the mountains. In such a case it might be better to work this circuit with two hops. Then a vertical beam angle of 20 degrees can be used instead, with adequate horizon clearance for the wave path. Or if the circuit

required 6 degrees for a two-hop circuit 5,400 kilometers long, with the same obstruction cited, one could change to a three-hop circuit, which for the same layer heights would permit the use of a beam at 14 degrees. This lacks the full 2-to-1 horizon clearance desired, but it may be an acceptable compromise and perhaps preferable to using four hops. This latter example is one of the problems that frequently confronts the engineer where a decision cannot be made in advance.

Short-range high-frequency circuits using one-hop high-angle radiation give a great latitude of choice of sites. For F-layer transmission to distances of 500 miles and less, the beam angles are always greater than 30 degrees. Satisfactory sites for such transmission can often be in

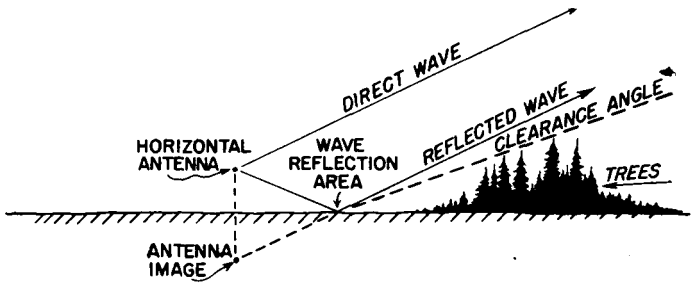

FIG. 3.13. Showing necessary cleared area for good wave reflection for a desired radiation angle.

rather deep valleys without any compromise whatever on the circuit performance.

The presence of forests on or near the site requires some consideration. When it is remembered that the theoretical radiation pattern is calculated on the basis of perfect reflectivity from the ground, as from a mirror surface, it can be foreseen that there are some precautions necessary to obtain performance substantially in agreement with that anticipated. Therefore, attention is directed to choosing conditions as nearly perfect as possible, so far as the wave-reflecting surfaces around an antenna are concerned, by the complete absence or elimination of trees and buildings on the land out to the necessary distance from the antenna.

The point of wave reflection for the desired angle of radiation should be well clear, as shown by Fig. 3.13. Horizontal dipole antennas intended for radiation angles higher than 45 degrees should be located at the middle of a cleared area at least one wavelength square. If the site borders the sea or a lake and the surface of the water can be used as the wave-reflecting surface, this is an excellent choice. One therefore seeks to have the wave-reflecting surface as flat as possible and of the highest possible electrical conductivity and at the same time clear of trees, shrubbery, buildings, and other impediments.

Sites for high-frequency transmitting and receiving stations are not dependent upon soil characteristics to the extent that medium- and low-frequency stations using ground-wave propagation are. Nevertheless, the soil conductivity and inductivity have an important effect on the wave-reflection coefficient in the vicinity of an antenna, which influences the antenna efficiency and the pattern shape. Where a choice of soil exists among several possible sites, good engineering will give consideration to the soils having the highest reflectivity for the frequencies employed, other factors being equal.

It is not always possible to have a site that is on level ground, and here arise many problems of detail that cannot be formulated with precision. In undulating terrain many compromises are necessary. Rhombic antennas may occupy a considerable area encompassing variations of slope of the land. The best way to analyze such a situation is to construct an accurate profile of the terrain through a contemplated location out to a considerable distance in the desired direction of transmission, using the same vertical and horizontal scales. The antenna is shown on this profile to scale. Then from pure geometry one considers the locations of possible wave-reflection points and tries to visualize where spurious reflections may compromise the radiation pattern of the system or where the terrain can be used to advantage to produce reinforced radiation at the desired vertical angle. For instance, if a rhombic antenna can be located on a very long uniform slope of, say, 4 degrees in the direction in which it is desired to transmit (or receive), and it is desired to produce maximum radiation at an angle of 9 degrees from the horizon, then the rhombic-antenna dimensions can be chosen to produce a normal vertical angle of 13 degrees, provided that there is nothing ahead of the antenna to cause spurious reflections or impede this beam. The 4-degree forward slope of the land then brings the beam at the desired 9 degrees with respect to the horizontal. The variations of terrain within the area of a rhombic antenna determine whether different mast heights must be used to maintain the antenna in one plane or whether these variations are negligible.

Another type of problem related to sites is the layout of antennas to minimize interactions between them. A site of limited area may have to accommodate several antennas. Quantitative information of this sort is unavailable; yet situations of this kind are common enough in practice, and tolerable results have been obtained. One should distribute directive antennas in such a manner as to avoid the presence of one antenna in the beam of another by the largest practicable margins. Antennas should be located mutually so that each is in a position of least field strengths from the others. It must be recalled that the radiation pat-

terns for antennas that are usually discussed are the patterns for great distances. Near extended systems, the field distributions are not the same, and one must then consider the effects of proximity to the nearest portions of other antennas. With dipoles and dipole arrays, minimum fields exist in line with the dipoles. In-line assemblies of dipole antennas may use common supports to good advantage. Where dipoles of various azimuthal orientations are to be used, it is well to locate them successively at the minimum angles from a common line, thus tending to form a polygon layout without inverted angles. When this is done, adjacent antennas have minimum coupling angles; and as the coupling angles get more unfavorable, there is a substantial distance between antennas. Such a layout of antennas makes good use of supporting masts and may eventually form a closed circle of antennas with the station house at the center.

Special problems of land utilization arise where several rhombic antennas are to be used and one wishes to know how close adjacent antennas can be without detrimental effects. The only practical advice that can be given with certainty is never to use more than one common mast for two adjacent rhombic antennas and then to have their orientations such that the nearest sides are as far from parallel as possible. The patterns for such antennas are derived from the assumption of an antenna that is completely isolated. The very large electrical dimensions of typical rhombic antennas imply that the radiation pattern is not formed for a very large distance from the system, and therefore the fields of the individual sides must be very strong for a considerable distance from each. Therefore, another antenna nearby will have some energy induced into it, which will cause its reradiation in some undesired manner. In spite of the temptation to place rhombic antennas near each other and to use common masts, good engineering design will provide the maximum available spacing. A rhombic antenna functions as a balanced system, and anything that disturbs its symmetry of fields from the four sides will disturb its performance. Furthermore, a rhombic antenna has almost no selectivity to discriminate against parasitic currents.

3.5. High-frequency Receiving-station Sites

The remarks about the choice of a transmitting-station site apply in exactly the same way to a receiving-station site, with two notable exceptions:

1. The dominant angles of arrival of the incoming waves at the site are determined mainly by the characteristics of the transmitting antenna. Whenever possible, best results are obtained with complementary transmitting and receiving antennas. If a horizon obstruction exists at the

optimum angle of wave arrival, a compromise noncomplementary antenna may be necessary. Whenever possible, the transmitting antenna had best be changed to be complementary with the receiving antenna when an obstruction is unavoidable at the receiving location on a fixed circuit. Figure 3.10 gives some examples of complementary and uncomplementary antenna patterns.

2. The receiving site must be as free as possible from electrical noise. The site should be an adequate distance from a city or other populated place that is a source of noise. Factories and other establishments are to be similarly avoided. Motor highways are also a source of noise (from ignition systems), and a substantial distance from highways that have passing motor vehicles should be allowed. The amount of man-made noise that can be tolerated at a particular receiving-station site depends upon the prevailing natural atmospheric noise levels. At a well-selected site, reception should always be limited only by natural atmospheric noise, which is the limitation imposed by nature. Any man-made noise at the site should always be substantially less than the atmospheric noise received during the low-noise periods.

There is one form of atmospheric noise that can be reduced by suitable antenna design, and that is the kind known as "precipitation static." This occurs when there is wind-blown dust, sand, snow, or fog; electrical noise from these sources is chiefly due to their charged particles hitting and imparting their charges to the metallic portions of the receiving antenna and feeder. It has been found that this kind of interference can be very substantially reduced by using thickly insulated wires for the antenna and feeder and by not having any exposed metallic surfaces. In low-noise regions, precipitation static may be the cause of limiting noise, so that the application of this technique may be very helpful in reducing the noise level.

The suitability of a receiving site will often depend upon the direction of arrival of noise. If, for instance, the dominant noise interference is always from a direction substantially different from that of desired signals, antenna directivity can be employed to favor the signal and discriminate against the noise. Another aspect of this is where man-made noise may be at low angles and the incoming signal at a high angle, in which case the proper antenna pattern will give best response to the signal and have relatively low response to the low-angle noise.

The suitability of a receiving-station site for optimum performance can be seen, from the foregoing, to depend to some extent on the characteristics of the antennas that will be employed for the particular services to be operated and on how antenna directivity can be advantageously employed to obtain the best operating signal-to-noise ratios. The most

severe site-selection problem occurs when reception is required from all directions.

There are instances where a receiving station has to be located in a city or other region of severe man-made noise. It may be necessary to attempt to suppress noise from troublesome dominant sources in the neighborhood of the receiving station to obtain tolerable system performance. The measures that can be applied successfully depend upon

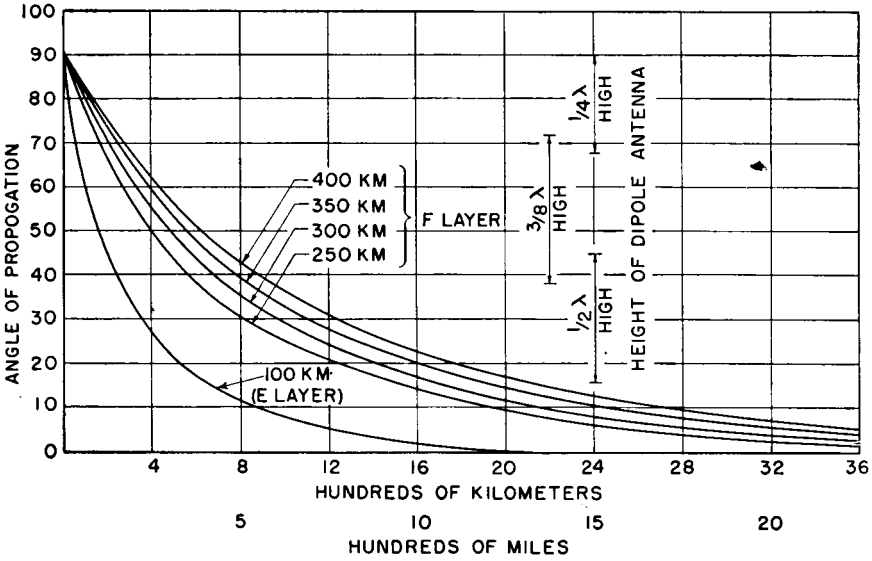

FIG. 3.14. Vertical radiation angles for one-hop circuits.

the nature of the device and the kind of noise it emits, assuming that the source can be located.

3.6. Design of a Horizontal Half-wave-dipole Antenna System

Any antenna must be designed to fit the propagation conditions and the geometry of the particular path required for communication. The radiation pattern for a half-wave dipole is therefore chosen for the best frequency, orientation, and vertical angles of radiation. These factors determine the height, length, and orientation of the antenna. Weather conditions encountered in the locality determine the structural specifications for the antenna.

The required vertical angles of fire as functions of layer height and hop length are shown in Fig. 3.14.

When the radiation pattern has been selected, there follow the steps involved in the circuital design of the system—the potentials and currents to be expected for the power to be transmitted, the insulation and conduc-

tor sizes, the configuration of the feeders and the method of coupling antenna to feeder, the bandwidth requirements for the kind of transmission to be used, and all matters of impedances at certain points in the antenna and feeder system.

Finally, with these all predetermined, there follows the mechanical design of the antenna, feeder, and supports, together with their layout on the available land. The methods of bringing the feeder to the transmitter, of making bends and angles in the line without introducing impedance changes or unbalances, and of switching feeders must be studied in detail. Then there are the problems of stresses, temperature changes, and ice loadings and the other structural details which suit the system to its climatic environment.

When all this is done, the mechanical simplicity of the system completely belies the amount of expert study that preceded its construction.

3.6.1. Radiation Pattern for Horizontal Half-wave Dipole. The radiation pattern in the vertical plane perpendicular to a horizontal dipole over perfectly conducting ground is given by the equation

$$F(\alpha) = \sin (h \sin \alpha)$$

where α is the angle to the horizon and h is the height above ground in electrical degrees.

The values of α at which nulls and maximums occur can be found by equating this to 0 and 1.0, respectively. For heights greater than 180 degrees there will be multiple nulls and maximums, the number increasing with the height. Vertical patterns from this equation are given in Fig. 3.15, and a chart giving the angles of nulls and maximums is given in Fig. 3.16.

In most cases these patterns are used for typical imperfectly conducting grounds such as are encountered in practice. However, to compute the precise pattern that will result from the antenna over ground of the type present at a specified location, its conductivity σ and inductivity ϵ and the frequency f of operation must be determined and used in the following equation:

$$F(\alpha) = 1 + \bar{K} e^{-j2h \sin \alpha}$$

Here, $\bar{K}$ is the complex surface-reflection coefficient for horizontal polarization as found from the following equation:

$$\bar{K} = \frac{\sqrt{\sin \alpha - \left(\epsilon - j\frac{2\sigma}{f} - 1 + \sin^2 \alpha\right)}}{\sqrt{\sin \alpha + \left(\epsilon - j\frac{2\sigma}{f} - 1 + \sin^2 \alpha\right)}}$$

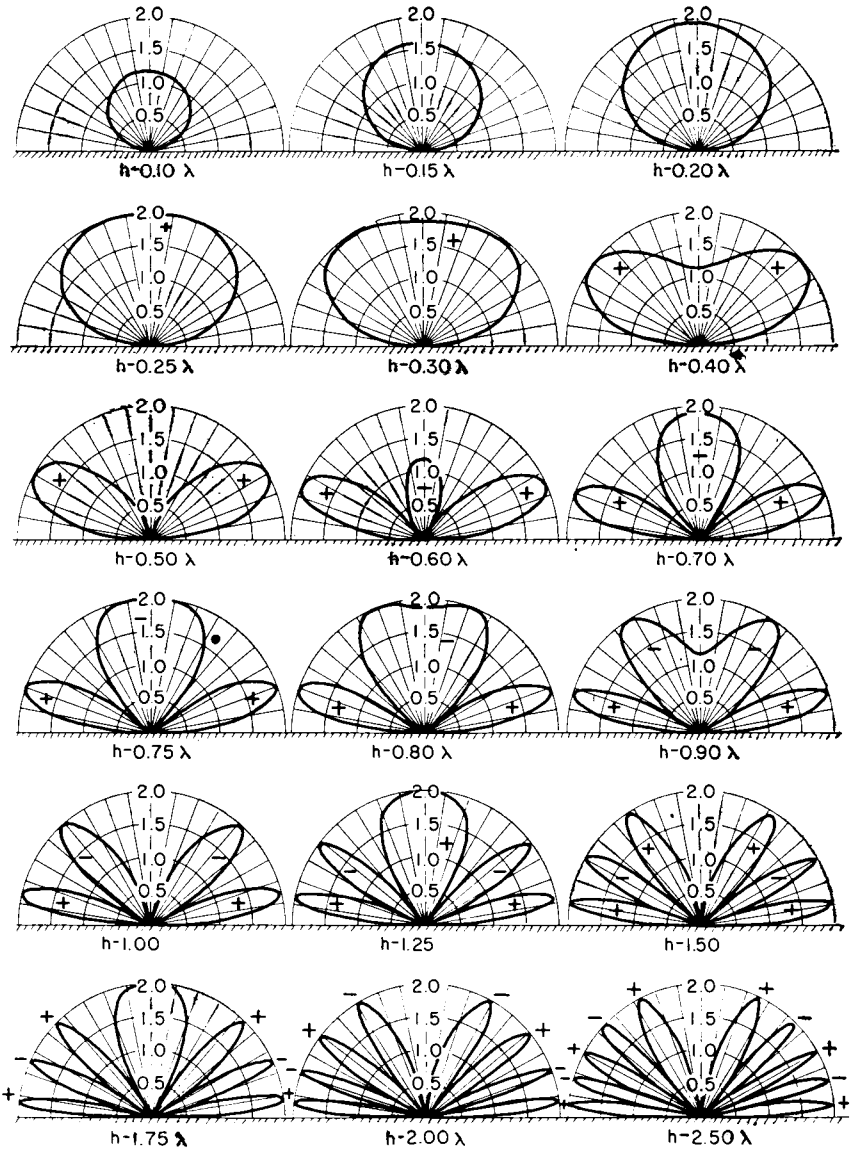

FIG. 3.15. Vertical polar radiation diagrams in the plane normal to a horizontal dipole antenna. (*From RAF Signal Manual.*)

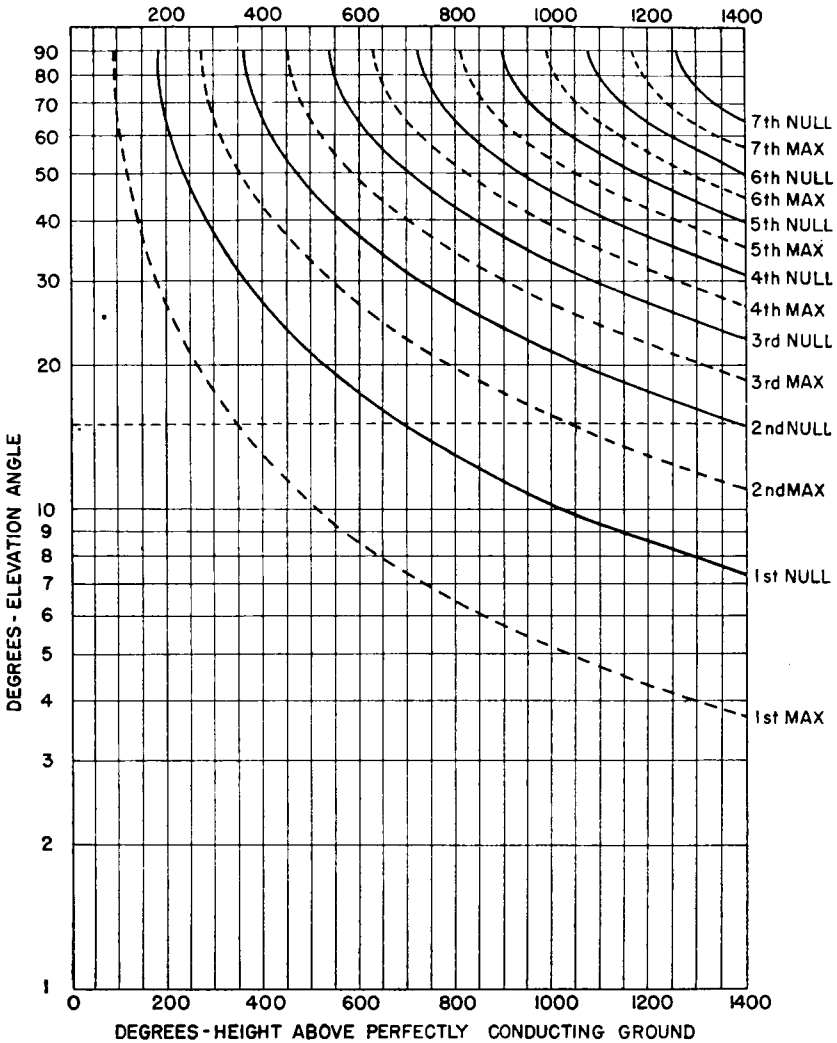

FIG. 3.16. Maximum and null angles in height factor for horizontal dipole antennas.

The phase angle at reflection from the ground is always 180 degrees with a horizontal dipole. The magnitude of $\bar{K}$ varies with α for fixed ground constants. In this equation, ϵ is the ordinary dielectric constant of the soil, σ is the conductivity in *electrostatic* units, which is 9×10^{20} times the conductivity in the more frequently used electromagnetic units, and f is the frequency in cycles.

The effect of ground loss on the maximum field strength, in comparison

with perfectly conducting ground giving zero ground loss, is shown in Fig. 3.17. These data are approximate but show the importance of ground loss for small heights.

This equation influences the pattern primarily with respect to the decrease in the amplitude of the maximums and the slight filling of the nulls due to incomplete cancellation of direct and reflected fields, as

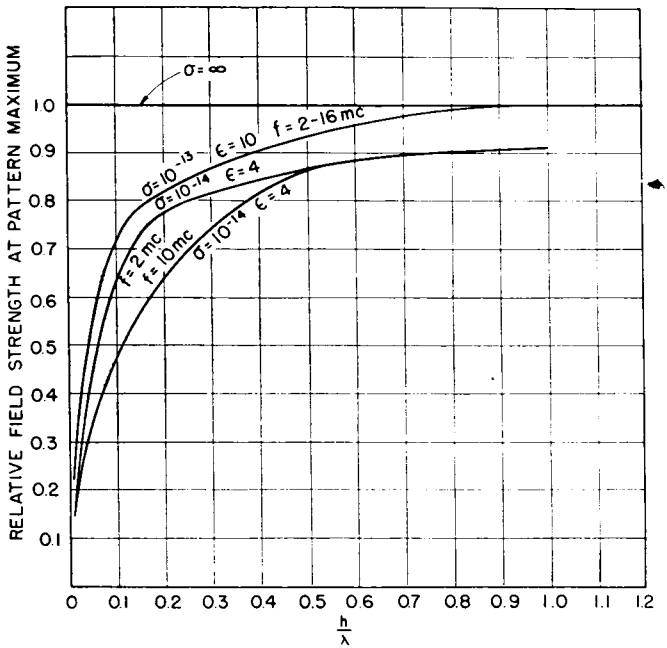

FIG. 3.17. Effect of ground conductivity on maximum field strength from a horizontal dipole antenna.

compared with perfectly reflecting ground. The angles of maximums and minimums are only slightly affected and for most practical uses may be considered to be the same.

If the field about a dipole in free space were uniform (spherical pattern), the vertical pattern for the horizontal dipole above ground would be the same in all directions with respect to the antenna. But the half-wave dipole itself is directional, its pattern in free space when center-fed conforming to the equation

$$f(\theta) = \frac{\cos (90 \cos \theta)}{\sin \theta}$$

where θ is the angle from the antenna axis. The value of this function is 0 at 0 and 180 degrees (in the directions of the axis) and is maximum

at 90 degrees (normal to the axis). Therefore, the antenna should be oriented so as to be perpendicular to the direction in which maximum radiation is desired in point-to-point applications or at the best compromise orientation in broadcasting applications.

The use of simple horizontal dipole antennas for long-distance service requiring multihop ionosphere transmission has serious disadvantages because its broad vertical pattern, or in some cases a multilobe pattern, contributes to multipath interference and delays. To obtain acceptable performance in this regard, antenna arrays are necessary to obtain an optimum vertical radiation pattern for minimizing multipath phenomena.

3.6.2. Circuital Design of a Horizontal Half-wave-dipole Transmitting Antenna. The desired information for the electrical design of this type of antenna is the following:

Length of the antenna conductor and its cross-sectional size
Feed-point impedance (depending upon series or shunt feed)
Potential at the ends (for insulator-selection purposes)
Maximum potential gradient for the power to be used
Antenna current at the middle of the dipole
Method of feeding
Efficiency of antenna and feeder system

It is assumed that the height of the dipole has been determined previously from considerations of its radiation-pattern requirements. The height influences the antenna feed-point impedance as shown in Fig. 3.18.

The tolerance on the antenna length is quite liberal if it is to be series-fed at the center, though the radiation resistance will change with length. The length can be of the order of one-half wavelength, and one can omit considerations of end effect of the wire and the insulator hardware. The reason for this is that a 5 per cent variation in length makes very little difference in the radiation pattern. The changes in the feed-point impedance are quite immaterial when impedance-matching techniques are applied to terminate the feeder at some point near the antenna, which is usually required.

With shunt feed, as in Fig. 3.19 (if one wishes to use a chart such as that given in the upper portion of Fig. 3.18 for impedance matching) the length of the antenna should be more precise and should be one-half wavelength long, less about 5 per cent for end effects. The end effects and the capacitances of strain insulators have the effect of increasing the length of the antenna.

In a typical application one uses a conductor about one-half wavelength long and attaches it to the suspension rigging with the type of insulator suited to the electrical and mechanical duty.

For low-power applications the conductor size will be determined only by the mechanical considerations. However, for medium-power inputs some thought must be devoted to the potential gradients, especially at high altitudes. The larger the conductor diameter, the lower the potential gradients for the same power input and the less possibility of pluming.

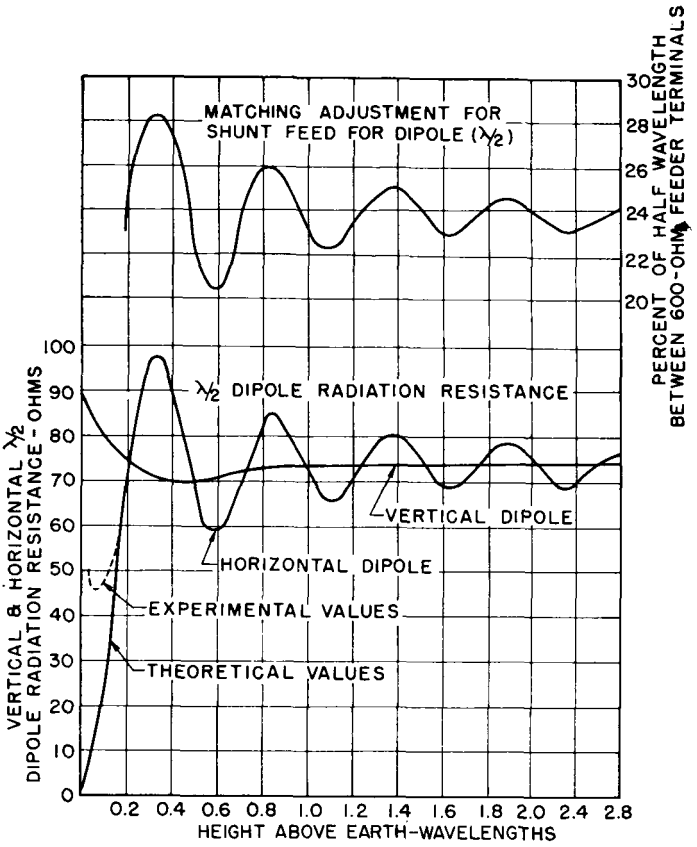

FIG. 3.18. Radiation resistance of horizontal and vertical half-wave dipole antennas. (*After Carter.*)

The calculation of the potential gradients at the high-potential points near the ends of the antenna is dependent upon the power input (on modulation peaks for amplitude-modulated services), the height of the antenna above ground, and the wire diameter. The height affects the radiation resistance as shown in Fig. 3.18, and therefore the antenna current and the antenna potential.

A typical example of the procedure by which these important potential details may be calculated is the following.

Example of Computation of Antenna Operating Potential. A 5,000-watt amplitude-modulated transmitter for an aviation communication application on 5,800 kilocycles requires a horizontal half-wave dipole antenna located three-eighths wavelength above ground. The altitude is 4,000 feet. What antenna dimensions must be used, and what potentials will be encountered?

One-half wavelength at 5,800 kilocycles is 86 feet. With end effect and insulator capacitance considered, we can reduce this about 5 per cent to 81 or 82 feet. The only important reason for doing so is to

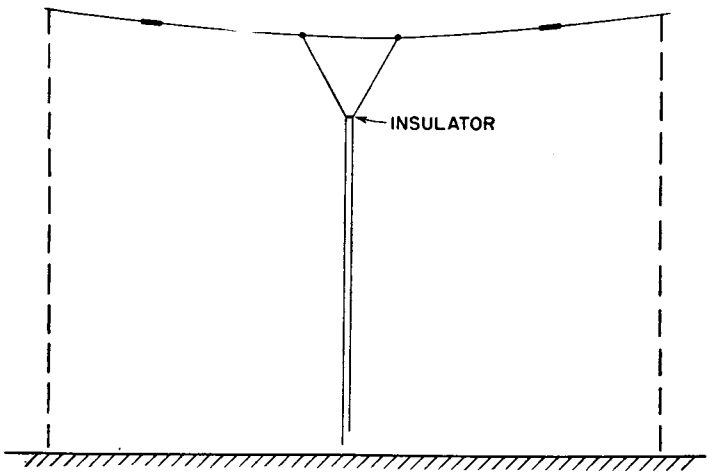

FIG. 3.19. Horizontal dipole antenna with shunt feed.

decrease tower spacing, which is usually desirable for minimizing mechanical loads and the land area required. The end effects make the system appear electrically as a full half-wavelength, and the current and potential distributions can be considered on that basis.

From Fig. 3.18, we read a radiation resistance of 95 ohms at the center of the antenna wire, for a height of three-eighths wavelength (64 feet). For 5,000 watts input on carrier, the antenna current will be

$$I_a = \left(\frac{W}{R}\right)^{1/2} = \left(\frac{5{,}000}{95}\right)^{1/2} = 7.25 \text{ amperes}$$

The current is distributed sinusoidally from the virtual end, that is, from a point which is extended about 5 per cent of length beyond the physical ends of the wire. Maximum current occurs at the center of the antenna.

As measured from the end, the potential distribution is very nearly cosinusoidal, except near the center, where it departs considerably from this form. This departure lies in a region about 10 degrees each side of

center. Beyond these points, the cosinusoidal distribution can be assumed. Therefore, we know the shape of the distribution but not its numerical magnitude. A simple method is now needed to establish this magnitude within limits that are acceptable for engineering purposes. If we can determine the standing-wave ratio Q for the antenna, the voltage *to ground* at the end of the dipole V_m will be $QV_a/2$, where V_a is the balanced voltage applied at the central feed point. $V_a = I_a Z_a$, the antenna current at the feed point times the feed-point impedance.

The Q of a half-wave dipole can be determined approximately from transmission-line theory by considering an open-ended line of characteristic impedance Z_0 having a length of 90 degrees. This is the same as studying relations of voltages and currents in the first one-half wavelength (180 degrees) of an infinite line with attenuation, because when the line is open-circuited at 90 degrees, the reflected wave will be the same as that between 90 and 180 degrees on the infinite line.* By combining the direct wave and the reflected wave from the open circuit, the potential and current distributions can be obtained, and the standing-wave ratio. It will be assumed now that the half-wave dipole has a length such that, with its end effects, $Z_a = R_a + j0$. If the system losses are due entirely to radiation, $R_a = R_r$, the radiation resistance, which can be read from Fig. 3.18 as a function of the height of the horizontal dipole from ground.

Applying this method, we first obtain a factor m which is the ratio of the attenuated voltage 180 degrees from the generator on the infinite line to the generator voltage. This is found to be

$$m = \frac{Z_0 - R_r}{Z_0 + R_r}$$

and

$$Q = \frac{1 + m}{1 - m}$$

Reference to Fig. 3.20 will clarify the derivation of these equations. The dipole antenna, as a balanced transmission line, has a characteristic impedance

$$Z_0 = 276 \log_{10} \frac{l}{\rho}$$

where l is the total length of the dipole in the same linear units as used for its radius ρ.

For low-power and receiving applications the conductor size for the dipole is chosen for its mechanical requirements only. In this example,

*See also Sec. 2.3.

it is desirable to see that the maximum antenna potential is below the critical corona potential for the altitude and temperature of the site, to ensure safe operation. To do this, we first choose a preferred arbitrary wire size and compute the potential that would exist at rated power input. Then the maximum safe operating potential is computed. The ratio of the latter to the former is the safety factor and is greater than 1.0.

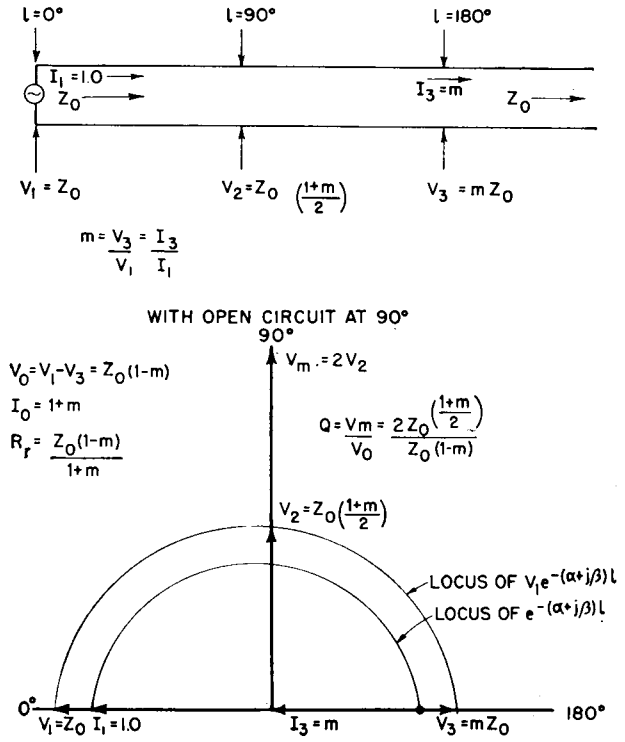

FIG. 3.20. Geometry for computing the approximate Q of the dipole.

Assume that we select a wire for the antenna with a radius of 0.102 inch. Then

$$m \doteq \frac{1{,}100 - 95}{1{,}100 + 95} = 0.84$$

$$Q \doteq \frac{1 + 0.84}{1 - 0.84} = 11.4$$

The *balanced* antenna driving voltage

$$V_a = I_a R_a = 7.25 \times 95 = 690 \text{ volts root-mean-square unmodulated}$$

The potential from one end of the dipole *to ground* is then

$$V_{end} = \frac{QV_a}{2} = \frac{11.4 \times 690}{2} = 3{,}950 \text{ volts}$$

To allow for 100 per cent positive modulation, this value must be doubled, to 7,900 volts root-mean-square. This is the working potential for the strain insulators that will support the dipole.

3.6.3. Feeder Characteristics and Feeder Arrangements. Figure 3.21 shows a typical arrangement for a center-fed horizontal dipole having

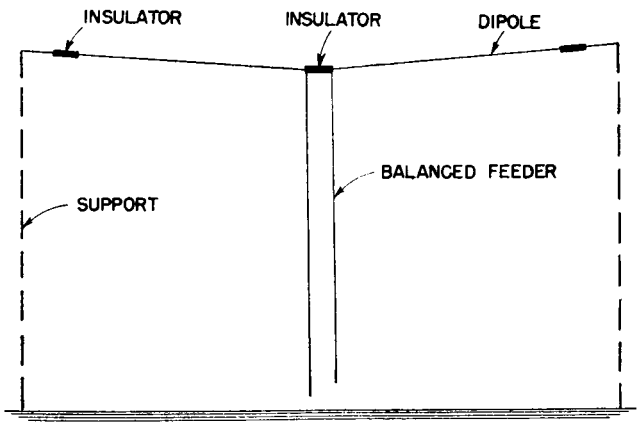

FIG. 3.21. Horizontal dipole antenna center-fed by a balanced feeder.

a length of the order of one-half wavelength, where the design is for one frequency only. However, it will be shown in Sec. 3.10 that such an antenna can be used for a considerable frequency range if adequate measures with respect to impedance matching are taken. In such cases the computation of antenna voltages would proceed from different considerations, which are more involved than the foregoing example.

In general, a half-wave dipole antenna need not be cut to one precise length but may be of the order of one-half wavelength. Small deviations in length will not modify the radiation pattern appreciably, and because in most practical applications the antenna impedance may be considerably different from that of the balanced two-wire feeder that will ordinarily be employed, we can ignore its actual value and prepare for making a proper impedance match in the feeder, as near to the antenna as practicable, by means of a stub section, a coupled section, or a lumped reactance of the proper value at the proper place on the feeder. Standing waves will exist on the feeder on the antenna side of the matching device, and substantially traveling waves only will exist between this device and the transmitter.

A satisfactory impedance match can often be made by shunt-feeding

the antenna, using the Y match which is so well known (see Fig. 3.19). This method is an approximate match in impedance only but can be sufficiently exact to have a low standing-wave ratio on the feeder. The theoretical adjustment for a single half-wave horizontal dipole in terms of its height above ground is shown in Fig. 3.18 (upper curve). Actual conditions cause the exact adjustment to depart slightly from these values in each case, for optimum impedance match.

The calculation of the impedance at the center of a horizontal half-wave dipole cannot usually be accomplished with an accuracy of better than 10 per cent, because of the empirical factors of end loading, conductor diameter, and the complex dielectric constant of the earth underneath. Theoretical computations can be made from the usual idealized assumptions for an infinitely thin wire, together with the mutual impedance with its image in the case of a perfectly conducting ground. Mutual impedances can be read from Fig. 3.61. Idealized values are the starting point for practical adjustment.

In the foregoing remarks it has been assumed that, for transmitting, a two-wire balanced feeder would be used. The common characteristic impedance value of 600 ohms for such a feeder is a matter of convenience only. Values of characteristic impedance as low as 450 ohms may be used with two-wire feeders, and lower values still by using four-wire feeders.* The choice is usually determined by mechanical and cost considerations.

Precautions must be taken to prevent coupling between the antenna and the feeder. This requires exact symmetry of arrangement of the two. The feeder must be perpendicular to the antenna for a distance of several wavelengths, and the feeder connections at the antenna must be symmetrical. When there is radiation coupling between antenna and feeder, currents of the same phase are induced into both sides of the feeder circuit. These induced currents add vectorially at all points along the feeder with the normal feeder currents, causing an unbalance which manifests itself as unequal standing waves on the two sides of the feeder and a displacement of the minimums in the standing-wave patterns on the two sides. The induced currents exist as parallel currents in the two sides of the feeder to ground. This effect makes impedance matching difficult and also causes radiation from the feeder. Parallel currents can be eliminated by using parallel-wave drains, described in Chap. 4. It is better to avoid the condition by proper initial design.

3.6.4. Power Losses in the Antenna System. A horizontal half-wave dipole depends, for its radiation pattern, upon reflection of waves from the surface of the ground in the vicinity of the antenna (image radiation).

* For receiving antennas, various kinds of twisted or flat pairs of much lower impedance can be used for feeders.

The higher the antenna, the greater is the area directly concerned. In applications for short-distance operation, the angles of radiation are high, and the ground area involved in efficient wave reflection is rather small and almost directly beneath the antenna. For high dipoles used for low-angle radiation or reception, the ground should have maximum reflectivity out to a distance somewhat greater than that for the ray which will be reflected into space at the desired angle of radiation. This was illustrated in Fig. 3.13.

For the same reasons, the topography and characteristics of the terrain are important to achieving optimum results on point-to-point circuits. The area of dominant reflection should be as flat and of as high conductivity as possible. The locations of reflecting areas near the antenna can be determined by simple geometrical considerations.

Power losses at reflection from the ground are the most important encountered in ordinary high-frequency applications, even when the site is clear, flat, and of good conductivity. The effect of such losses is evident in Fig. 3.17.

In relation to the foregoing power losses, the loss in insulators and metal of the antenna can be quite negligible. Nevertheless, attention to design of insulation, especially for high-power use, is necessary to prevent mechanical failure due to heating, even though the amount of power lost is immaterial. In intermittent operation this is much less a matter of concern than in continuous service such as broadcasting or frequency-shift telegraph transmission. Insulation specifications should anticipate the most extreme weather conditions likely to be encountered and the possibility of constant reduction of surface resistivity with the accumulation of soot, water, ice, perhaps salt spray, and the deterioration of the glaze.

The gradual accumulation of corrosion on the surface of the wires can eventually increase the resistance of the antenna enough to become a cause of undesirable power loss. Corrosion, especially in salt-spray regions, can be retarded by painting the antenna and feeder conductors with glyptol when they are new and clean. There will be a small power loss in the glyptol but it will be less than with later heavy corrosion.

For a free-space half-wave dipole made of wire and having no end loading except its own natural end effect, the reactance at its center is zero when its physical length is 172 degrees instead of the theoretical 180 degrees. The attachment of insulators produces end loading in an amount that is empirical, so that further shortening is necessary to eliminate all reactance from its center impedance. When this dipole is near the ground, mutual impedance with its image again induces reactance into the center impedance, the amount depending upon its

height above ground and the electrical constants of the ground. Some arbitrary length adjustment is then required to reduce the reactance component of center impedance to zero. The impedance is then restored to a pure resistance.

This resistance R_a can be matched with a balanced feeder of characteristic impedance Z_0 by using a quarter-wave section of line of characteristic impedance Z_{00}, which is the geometric mean of R_a and Z_0.

The reason for eliminating the reactance by adjustment of antenna length is because it may have an appreciable value in relation to the antenna resistance and thus interfere with a correct match using the quarter-wave matching section. When the reactance is small with respect to the resistance, the resulting mismatch can usually be tolerated in practice, as in the case of the Y method of shunt feed. It is assumed that there is no coupling whatever by radiation between the antenna and the feeder.

3.6.5. Horizontal-dipole Antennas for Receiving. For receiving applications, certain points of design covered in the foregoing discussion will not apply. There will of course be no problems of potential gradients and high-voltage insulation. Conductor sizes and insulation will be determined almost solely by bandwidth and mechanical considerations.

In some locations precipitation static is serious at times. Sandstorms, dry snow, and wind-blown fog are well-known causes of precipitation static interference. A substantial reduction in such noise can be realized by embedding all metallic parts of the antenna and feeder system in a low-loss dielectric so that the charged particles hitting the antenna cannot discharge directly to the metal. The antenna and feeder wires can be rubber- or plastic-covered and the metal of insulators and fittings completely incased in paraffin, gutta-percha, polystyrene, or other conveniently cast material. With such precautions to prevent exposure of the metal of the antenna and feeder to the flying charged particles, several decibels reduction in noise level can be realized during conditions of precipitation static.

It must also be recalled that, in the receiving case, energy is flowing from the antenna to the receiver. This requires that the feeder be correctly terminated in an impedance match at the receiver end so that as much as possible of the received energy will be delivered to the receiver input.

Several receivers can be operated from a single antenna and feeder system if precautions are taken for proper impedance match of the feeder over the full range of frequencies to be received. Decoupling resistors can be used in the inputs to the several receivers provided that the power losses they introduce do not require extreme receiver gain and give rise

to intolerable receiver-tube noise. In many regions of the world, atmospheric noise levels are at all times high enough so that one can never use all the intrinsic gain in a modern communication receiver. In such regions, decoupling resistors in the receiver inputs have no detrimental

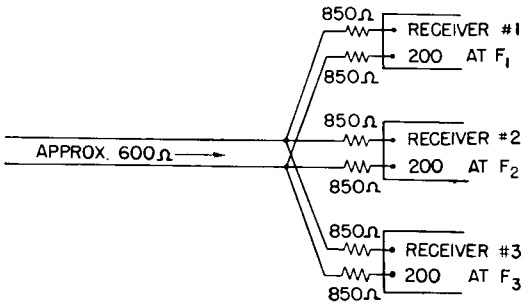

FIG. 3.22. Example of feeder impedance matching using three receivers.

effects on the realizable signal-to-noise ratios. Figure 3.22 shows a method of using three receivers with balanced 200-ohm inputs on a 600-ohm feeder termination.

3.7. Effect of Off-center Feed on Radiation Pattern of Dipole

The radiation pattern for a half-wave dipole is always spoken of as symmetrical about the normal to the antenna axis. This is true only for strictly symmetrical feed at the center. One that is end-fed has its maximum field strength pushed about 20 degrees away from the normal in the direction away from the end that is fed.

When two collinear dipoles are end-fed from a common balanced feeder, the tilt effects of the two patterns are equal and opposite so that they quite thoroughly neutralize each other and produce a combined pattern that is again normal to the axis of the dipoles.

When several collinear cophased dipoles are end-fed one from the other in series, the attenuation of the feed current tilts the resultant pattern away from the normal, toward the free end. Unsymmetrical feed always produces an unsymmetrical pattern. Figure 3.23, abstracted from ref. 1020, illustrates this effect. It is desirable in all cases to employ symmetrical systems of radiators with symmetrical feed in broadside arrays, to obtain symmetrical radiation patterns.

3.8. Bandwidth of a Horizontal Half-wave Dipole

A dipole antenna, like any resonant circuit, has a certain natural selectivity. The selectivity is increased by any influences that reduce its radiation resistance, such as proximity to ground or other reflecting

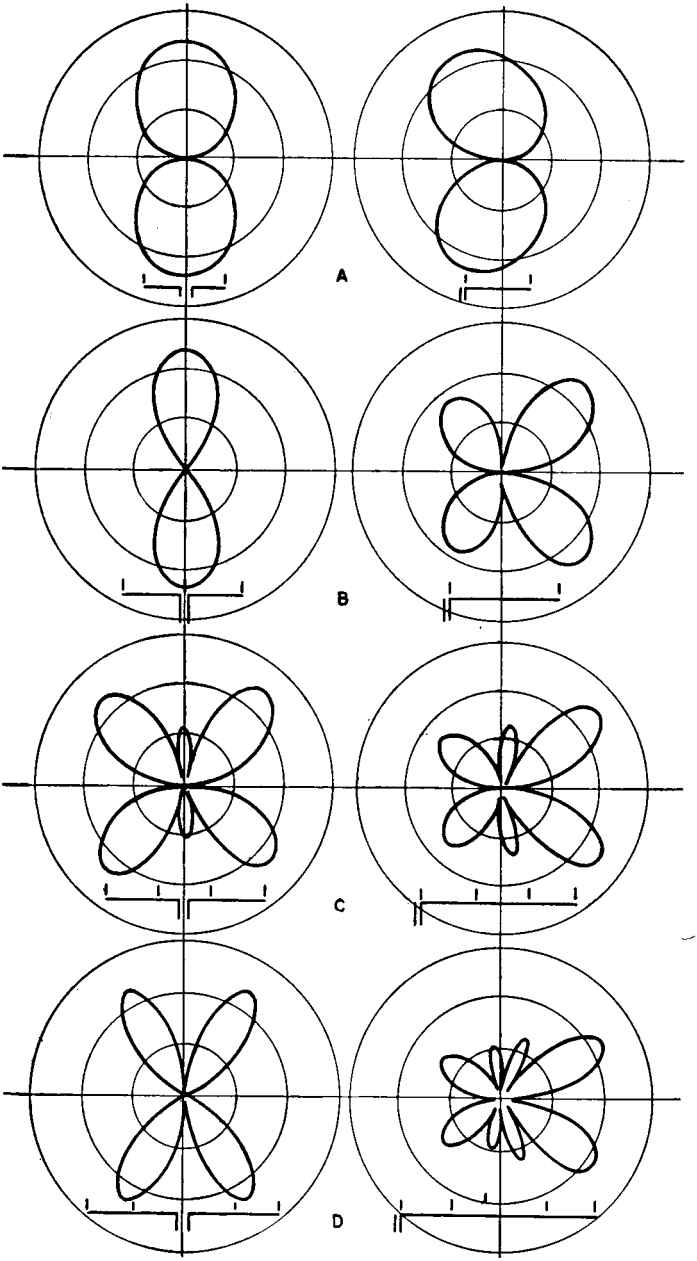

FIG. 3.23. Comparative effects of center feed and end feed. (*After Cleckner.*)

object. The selectivity is decreased by increasing the cross-section area of the dipole.

The bandwidth is defined as that band of frequencies enclosing the frequency f_0 (for which the system has matched impedances), where the feeder standing-wave ratio Q does not exceed some prescribed value, such as 1.41, which is the limit for 3-decibel response for the maximum side frequencies. The actual tolerance in standing-wave ratio throughout the bandwidth required for the emission employed governs the quality of the emission. The standards of performance desired must be taken into account in designing the antenna to accommodate the necessary bandwidth of emission.

The fundamental bandwidth of a straight cylindrical dipole antenna in free space at first resonance is given in Table 3.1. First resonance is defined as the lowest frequency at which the impedance at the feed gap in the center of the dipole is a pure resistance. Owing to end effects, the length of the dipole at first resonance is somewhat less than one-half wavelength, and in the table the exact electrical lengths in degrees are given for various values of the parameter l/d, the ratio of the end-to-end length of the dipole to its diameter. The bandwidths were computed for the condition

$$BW = \frac{2(f_0 - f_1)}{f_0}$$

where f_0 is the resonant frequency where the dipole reactance is zero and f_1 the frequency below f_0 at which the reactance of the dipole equals its resistance, taking into account that both resistance and reactance are changing with frequency. This gives the point at which the response to the lower side frequency is down 3 decibels. The 1-decibel response values shown in Table 3.1 were interpolated.

TABLE 3.1. FREE-SPACE DIPOLE CHARACTERISTICS

Dipole l/d	200	400	1,000	2,000	10,000
Electrical length for $X = 0$, degrees	168.3	170.0	171.8	172.8	176.5
Bandwidth, 3-decibel response	0.112	0.100	0.088	0.076	0.052
Bandwidth, 1-decibel response	0.056	0.050	0.042	0.038	0.026

The rate of change of reactance with frequency for a center-fed horizontal half-wave dipole is much greater than the rate of change of resistance with frequency. For this reason, any means that will reduce the reactance variation rate will increase the intrinsic bandwidth of the dipole. Large-diameter conductors or a cage of small conductors will give increased bandwidths.

Another method of broad-banding a dipole is to use the biconical cage (Fig. 3.27) or its two-dimensional analog, triangular sheets, or simulative wire arrangements.

A cylindrical cage of wires is less effective than a continuous cylinder of the same diameter, as shown by Fig. 3.24, though for large diameters the cage is much the most practical to construct. Using Table 3.1 or Fig. 3.24 in conjunction with Figs. 2.15 and 2.16 (the resistances and reactances read from the latter must be doubled when applied to balanced

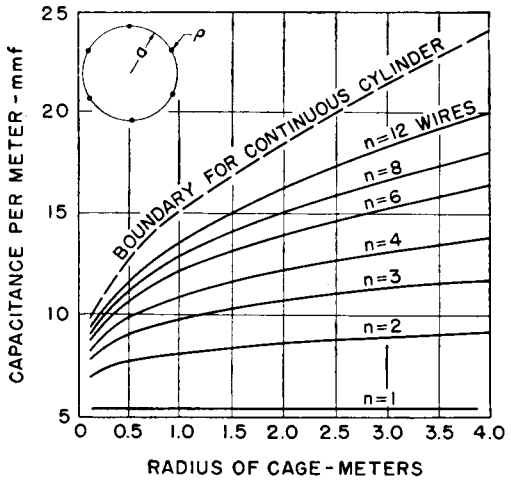

FIG. 3.24. Relation between cylindrical cage and continuous cylinder. (*After Wells.*)

dipoles), one can predict the dimensions to be used for a given bandwidth specification.

The use of a short-circuited stub of the order of one-quarter wavelength long connected across the terminals of a center-fed dipole will also increase its bandwidth. This stub should have a characteristic impedance substantially equal to the characteristic impedance of the half-wave dipole. This combination constitutes an open-circuited quarter-wave line (the dipole) in parallel with the short-circuited quarter-wave stub. Since both parts have the property of virtually opposite changes of reactance with frequency, the stub compensates the dipole in such a way as to maintain a more uniform terminal impedance for the feeder line over a range of frequencies enclosing the frequency for which the system has optimum impedance match.

To center-feed a cage dipole, the inner ends of the side cages can be brought to a point by a conical taper. The length of the taper is important in its effect upon the impedance at the feed point. An optimum

compromise is to make the length of the taper about 75 per cent of the diameter.

Many dipole arrays use half-wave dipoles end-fed from a balanced feeder. If the dipole impedance is to be resistive, the dipole must be shortened as its diameter is increased, owing to end effect. Figure 3.25 shows the proper length of a dipole which is a continuous cylinder, as a function of its diameter in electrical degrees for the case where the resistance is maximum and reactance is zero at one end. The ratio of electrical length to electrical diameter for maximum end resistance is given in Fig. 3.26.

It is misleading to place any general values on the bandwidth of any antenna and feeder system. Bandwidth must be carefully computed or, preferably, measured (using scale models if necessary) for each particular application. The empirical conditions can then be accounted for more precisely. Hence, we only call attention to the means that can be employed to broad-band antennas for applications where bandwidth is a special consideration in the system design.

The power-handling capacity of an antenna is increased by the same methods that increase bandwidth, and the two characteristics are interrelated. The bandwidth is increased as the potential gradients at the surface of the conductors decrease and as the peripheral charge density is decreased. Since the power-handling capacity of an antenna is limited primarily by pluming potentials, the reduction in potential gradients permits greater power input.

In dipole arrays the total power input to the system is divided among several dipoles in some manner so that the power input to any one dipole is correspondingly lower. In high-frequency broadcasting it is sometimes desired to use a single dipole antenna or a pair of collinear dipoles for large power input. In such cases a cage dipole of large diameter or a biconical cage is a suitable antenna design, as shown in Fig. 3.27. In both cylindrical cage and biconical cage antennas it is desirable to use a ring connection to all of the wires at the end. Both types have relatively large bandwidth and power-handling capacity.

For the same reasons, a folded dipole usually has greater natural bandwidth than a single-wire dipole. The folded dipole is an elementary cage antenna of two or three wires.

3.9. Folded Dipoles

The folded dipole is a radiator with a controllable resistive impedance at the feed point. It can therefore be designed to match a particular balanced feeder impedance. To control the feed-point impedance by controlling the current division in the wires of the folded dipole, the number, spacings, and radii of the conductors can be varied if necessary.

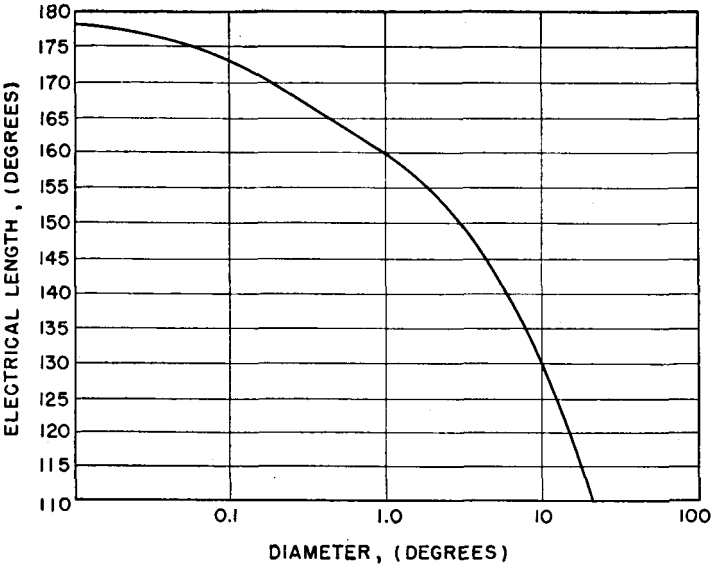

FIG. 3.25. Electrical length of end-fed dipole for maximum resistance and zero reactance. (*After Brown.*)

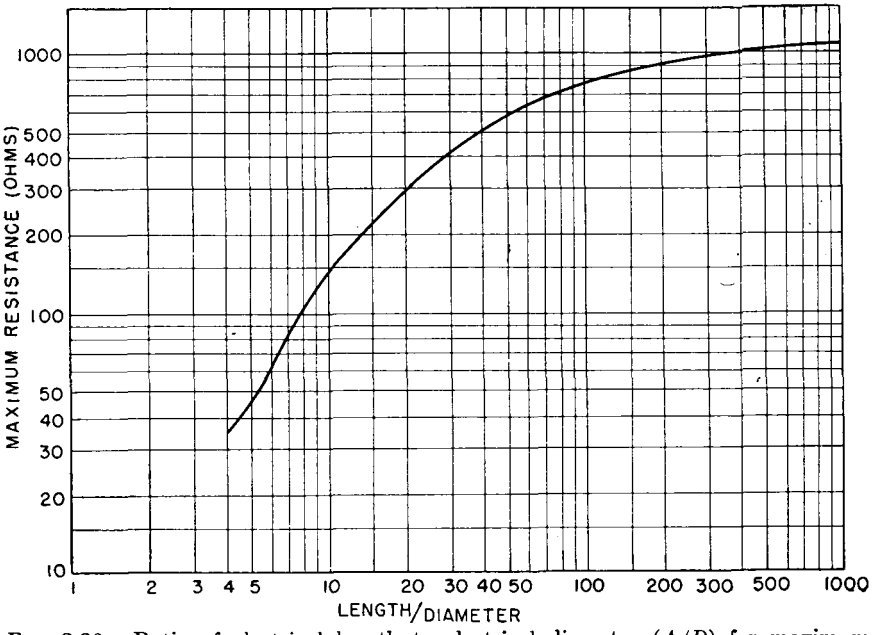

FIG. 3.26. Ratio of electrical length to electrical diameter (A/D) for maximum resistance of end-fed dipole. (*After Brown.*)

The simplest folded dipole is one with two wires of equal radii, straight and parallel, and connected together at their outer ends. The total antenna current is equally divided between the two wires, and by feeding into the middle of one of them, the input resistance is four times that of a single-wire dipole at the same height and with the same cross-sectional configuration. In the case of three equal-radius wires placed at the

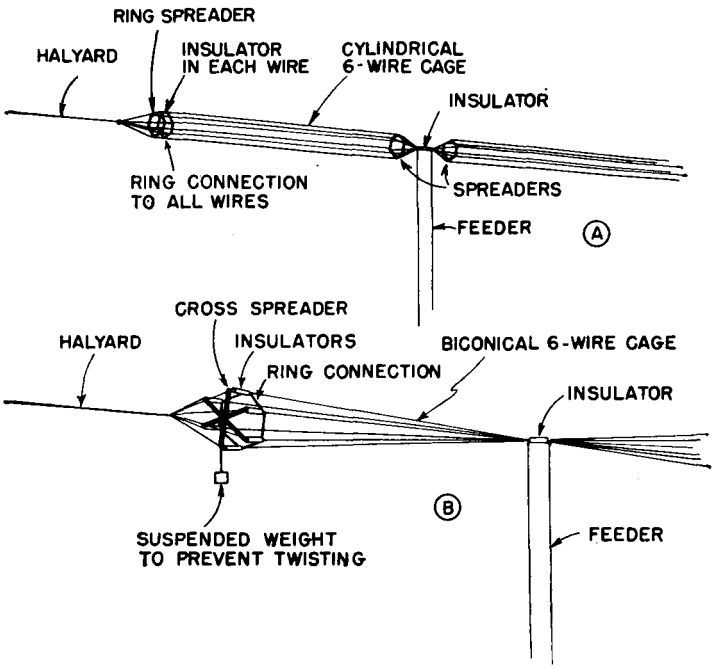

FIG. 3.27. Constructions for cylindrical and biconical cage antennas.

corners of an equilateral triangle to assure equal current division among three wires, the feed-point resistance is nine times that of a simple dipole of the same geometry and height. The radiation patterns are the same as for a simple dipole.

It is easily demonstrated by logarithmic-potential theory (for example, see Chap. 6) that, for a folded dipole of the type of Fig. 3.28*A* having two parallel conductors of radius ρ_1 and ρ_2 and a center-to-center spacing a (all in the same units of measurement), the ratio of the currents I_1 and I_2 in these two conductors is

$$\frac{I_1}{I_2} = \frac{\log_{10} \dfrac{a}{\rho_2}}{\log_{10} \dfrac{a}{\rho_1}}$$

The total antenna current is divided between the two conductors in this ratio.

A three-wire folded dipole of the type of Fig. 3.28*B* provides an endless number of possible combinations of conductor radii and mutual spacings.

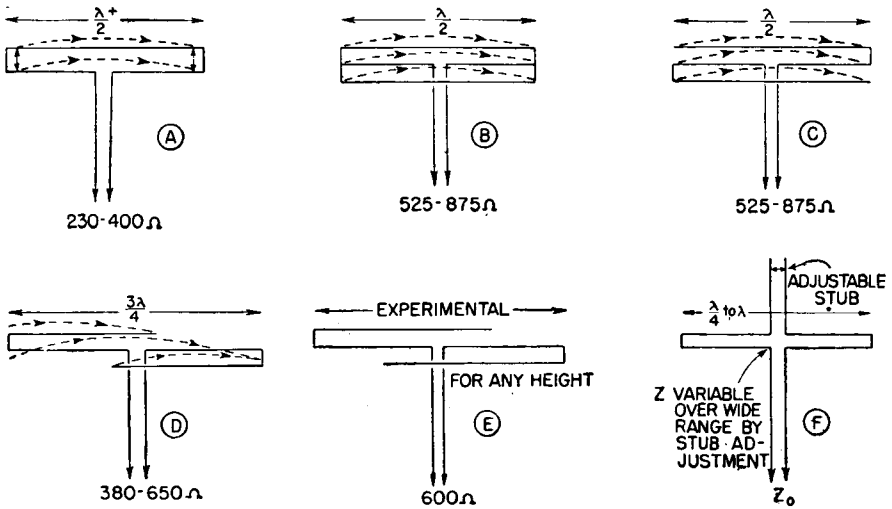

FIG. 3.28. Folded-dipole radiators (resistance limits shown are those due to height of antenna above ground). (*From RAF Shortwave Communication Handbook.*)

If conductors 1, 2, and 3 have radii ρ_1, ρ_2, and ρ_3, respectively, and mutual center-to-center spacings of a between 1 and 2, b between 2 and 3, and c between 3 and 1, the current ratios between I_1, I_2, and I_3 are given in the following equations :

$$\frac{I_2}{I_1} = \frac{\log_{10}\frac{c}{\rho_1}\log_{10}\frac{b}{c} - \log_{10}\frac{a}{\rho_1}\log_{10}\frac{\rho_3}{c}}{\log_{10}\frac{\rho_2}{a}\log_{10}\frac{\rho_3}{c} - \log_{10}\frac{b}{a}\log_{10}\frac{b}{c}}$$

$$\frac{I_3}{I_1} = \frac{\log_{10}\frac{a}{\rho_1}\log\frac{b}{a} - \log_{10}\frac{c}{\rho_1}\log_{10}\frac{\rho_2}{a}}{\log_{10}\frac{\rho_3}{c}\log_{10}\frac{\rho_2}{a} - \log_{10}\frac{b}{c}\log_{10}\frac{b}{a}}$$

The total antenna current for the folded dipole comprises the sum of the component currents I_1, I_2, and I_3.

If I_0 is the total antenna current and I_f is the relative portion of this current in the fed wire of the folded dipole, then the feed-point impedance Z_f is related to the center-point impedance Z_a of the *same* dipole as a simple (nonfolded) system in the following way:

$$Z_f = Z_a \frac{I_0^2}{I_f^2}$$

When half of a folded dipole is used as a vertical antenna operating against ground, the system is called a "folded unipole" or sometimes a "folded monopole." The same principles of current distribution among the conductors will apply as for the folded dipole. The impedances of the unipole will be exactly one-half of those of the equivalent dipole when the ground plane is perfectly conducting. A folded unipole is a form of multiple tuning, and the principle has been discussed in Chaps. 1 and 2.

In high-frequency applications it is practical to use equal-radius wires for the construction of folded dipoles. The types of folded dipoles suitable for high-frequency applications include those shown in Fig. 3.28.

The fact that a folded dipole has generally a larger cross section than a simple dipole gives it a greater intrinsic bandwidth; but this effect is derived wholly from its equivalence to a cage antenna. The bandwidth of a folded dipole depends upon exactly the same geometrical factors as a simple dipole. The direct match between the folded dipole and its feeder adds a further increment to the bandwidth of the system because there is then no excess energy storage to produce selectivity in the impedance-matching circuits.

Figure 3.28*A* shows the elementary two-wire folded dipole. Experience has shown that its adjustment to match precisely a balanced feeder is facilitated by making the outside length slightly greater than one-half wavelength and then placing short circuits between the two wires a small distance in from their ends to obtain the correct center-point resistance. This adjustment should be made for the height at which the dipole will operate, because the impedance will be dependent upon height above the ground.

Figure 3.28 shows five other possible versions of folded dipoles, adaptable to various feeder impedances.

All of the folded dipoles shown, constructed to the indicated dimensions, have a single-lobe pattern with its maximum normal to the antenna axis. Those with lengths greater than one-half wavelength will have sharper lobes.

The three-wire forms are best made in the form of a triangular cage, as shown in Fig. 3.29. A simpler construction but having unequal division of current among the three wires is to place all wires in one plane.

The form shown in Fig. 3.28*F* has an input resistance which is adjustable by varying the length of the stub in the second leg of the antenna by the movable short circuit (see ref. 42, page 365). A construction to utilize this principle is given in Fig. 3.30. The directivity of this type of folded dipole is also adjustable by means of the stub line.

Folded dipoles may be used as elements in directive arrays when

greater bandwidths and great for power-handling capacities per dipole are required than are feasible with single-wire dipoles. For very high power arrays, where potential limitations become a governing design factor, folded dipole elements provide a means for using matched feeders throughout the system, thus avoiding the excessive potentials common to standing-wave feed systems.

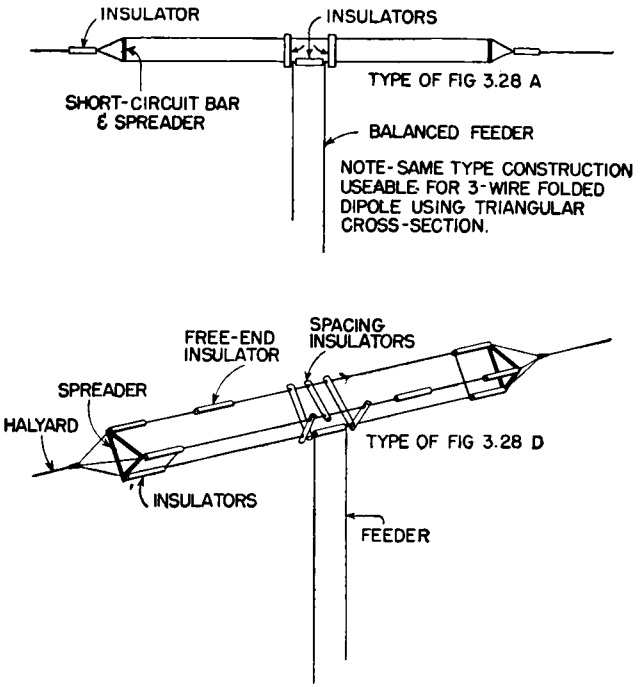

FIG. 3.29. Construction of folded dipoles.

3.10. Universal Antennas

There are circumstances where only one antenna must serve for a number of high frequencies. On shipboard and on buildings, for example, not only must one antenna suffice, but there may be physical limitations in the form and arrangement of the antenna. Obviously in such cases severe compromises in performance must be accepted. One antenna used for a number of different operating frequencies means first of all that the radiation pattern for each frequency will be different—often vastly different. At some frequencies the radiation patterns may be very unfavorable for communication in the desired direction. Some users make up for this radiation deficiency by employing relatively high power. As spectrum space becomes more valuable, this inefficient

expedient will become less tolerable, because it causes more interference than a properly engineered system.

A single antenna used for a number of frequencies also has the characteristic of widely different input impedances so that there cannot be a universal impedance match. This necessitates the switching of individual impedance-matching networks for each frequency or the readjustment of the coupling circuits for each frequency.

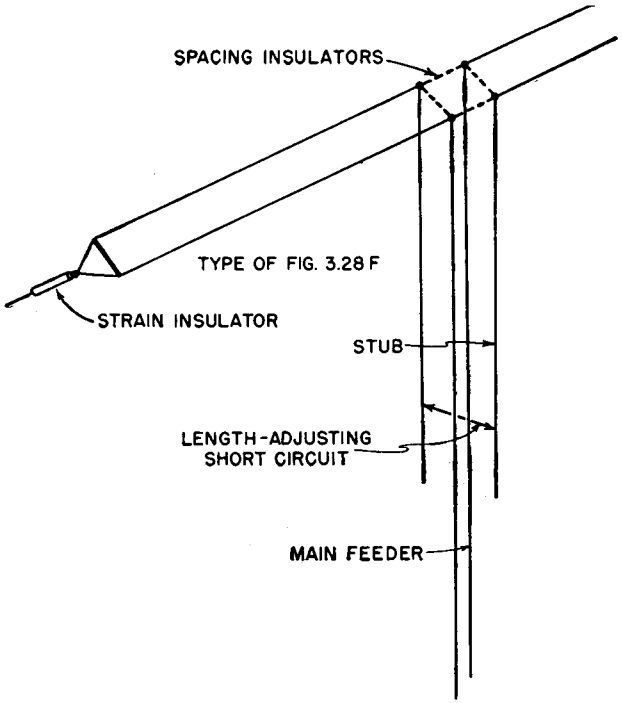

FIG. 3.30. Adjustable two-wire folded dipole.

When service to a fixed point or along a fixed direction is wanted, the double dipole is useful because at least the maximum field strength is always radiated in the same direction as the frequency is changed over a range of more than 2 to 1. However, the vertical beam angle will change with frequency if the physical height remains fixed.

Figure 3.31 represents a very useful form of simple antenna which can be used over a range of frequencies of $2\frac{1}{2}$ to 1. A different matching stub or other impedance-matching device can be used for each operating frequency within this range, if necessary. The merit of the system is that the radiation pattern maintains a constant direction normal to the antenna over the entire range, though the beamwidth of the pattern

changes. Where one antenna must be used for day and night frequencies over a given fixed path, this antenna is useful.

It is dimensioned to have a length each side of center of about 225 degrees at the highest desired working frequency which gives the current distribution and pattern shown in Fig. 3.31*C*. At a slightly lower frequency the length each side of center will be one-half wavelength, and the system, as shown in Fig. 3.31*B*, is two collinear cophased dipoles.

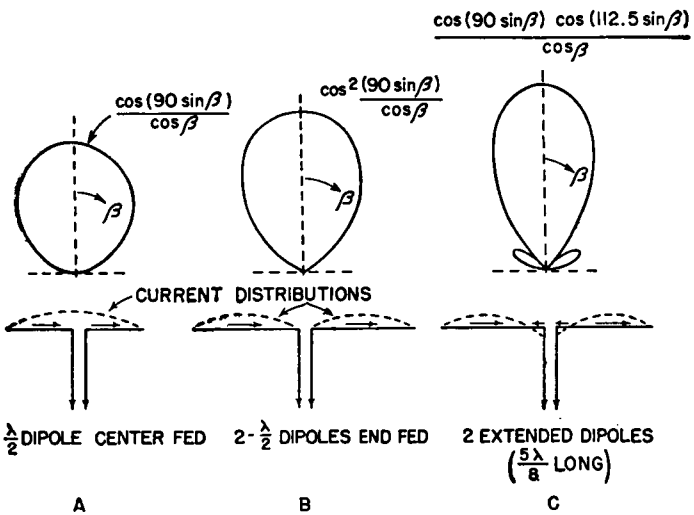

FIG. 3.31. Double dipoles and approximate patterns.

At a frequency one-half this last value, the system becomes a single center-fed half-wave dipole as shown in Fig. 3.31*A*. At a still lower frequency, the antenna would be electrically shorter than one-half wavelength, and its pattern would become a tangent circle.

Antennas of the traveling-wave type, such as rhombics and inverted V's, can be adjusted to have a relatively uniform input impedance over a wide range of frequencies, but the radiation pattern varies with frequency. In applying these antennas, care must be taken to determine that the variation in the pattern varies with frequency in an acceptable manner, to provide the desired service without excessive compromise and without demanding the use of excessive power.

3.11. Simple Directive High-frequency Antennas

In point-to-point communication over fixed circuits it is usually desirable to employ varying amounts of directivity for transmitting or receiving. The reasons for using directivity are:

Transmitting. Power gain in the preferred direction in order to

1. Economize on transmitter power
2. Increase the signal-to-noise ratio at the receiver
3. Increase the margins of reliable operation
4. Reduce interference in other directions
5. Reduce signal distortion due to multipath transmission

Receiving.

1. To obtain better signal-to-noise and signal-to-interference ratios when the disturbances come from other directions than the desired signals
2. To discriminate against multipath signals arriving at different vertical angles
3. To give a larger signal input voltage at the receiver

Additional directivity over that which is typical of a single horizontal dipole can be obtained with director and reflector elements associated with the dipole and fed directly or parasitically.

Broadside dipole arrays have a valuable property—their horizontal and vertical patterns can be separately controlled. The vertical directivity is controlled by the height and the number of radiators in the vertical stack, their spacings, and their current distributions. The horizontal directivity is controlled by the number of radiators in the horizontal line, their spacings, and their current distributions. End-fire and long-wire radiators and arrays lack the feature of independent control of vertical and horizontal patterns.

3.11.1. Dipole with Passive Screen Reflector. One of the simplest directive antennas is a single half-wave dipole associated with a reflecting screen of untuned wires, simulating a continuous metallic sheet, to give essentially unidirectional transmission or reception. Passive screens of practical dimensions give good gains in the forward direction and considerable suppression of backward radiation, as can be seen from Fig. 3.32. The arrangement of Fig. 3.33 is often of great utility. Assuming the screen to be infinite, its principal vertical-plane pattern is

$$f(\alpha) \doteq \sin (h \sin \alpha) \sin (d \cos \alpha)$$

In the horizontal plane, a half-wave dipole with reflector has the pattern

$$f(\beta) = \frac{\cos (90 \sin \beta) \sin (d \cos \beta)}{\cos \beta}$$

All dimensions are in electrical degrees.

A value of d between 40 and 80 degrees is desirable for good reflector action with limited screens and without excessive screen loss.

3.11.2. Horizontal Dipole with Parasitic Elements. This type of array is composed of two parallel horizontal dipoles, one of which is fed and the other is self-resonant and excited by the field of the radiator. Maximum

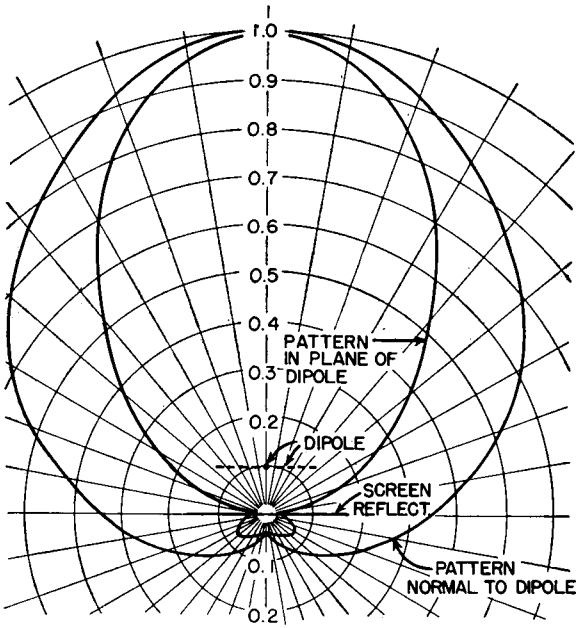

FIG. 3.32. Relative field strength from a half-wavelength dipole parallel to and one-quarter wavelength in front of a sheet reflector 0.85λ square. (*Data by Carter.*)

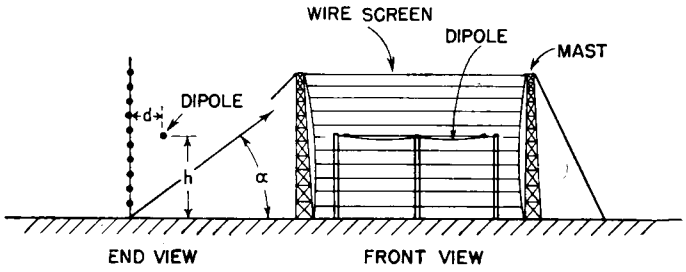

FIG. 3.33. Horizontal dipole with passive screen reflector for unidirectional radiation.

radiation takes place in the direction of the director. When the spacing d is 36 electrical degrees and the height above ground h is about 0.65 wavelength (height at which the mutual impedance with the images is resistive only), the currents in both elements are very nearly equal and the vertical pattern is

$$f(\alpha) \doteq \sin\left(\frac{d}{2}\cos\alpha\right)\sin\left(h\sin\alpha\right)$$

With changes in height it is possible to make small adjustments to maintain a maximum field strength on the beam. A gain of 4 to 6 decibels is available in the arrangement shown in Fig. 3.34.

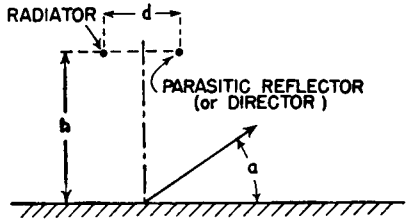

FIG. 3.34. Geometry of horizontal dipole with parasitic reflector.

Using rigid members and operating at a sufficiently high frequency, this array can be mounted on one support, which can be rotated to any azimuth.

The pattern can be inverted and the director changed to a reflector by tuning the parasitic element off self-resonance on the side that will give it a positive reactance. This can be done by inserting inductance at the center or by adjusting the length of the parasitic element. Figure 3.35 shows the relations between two radi-

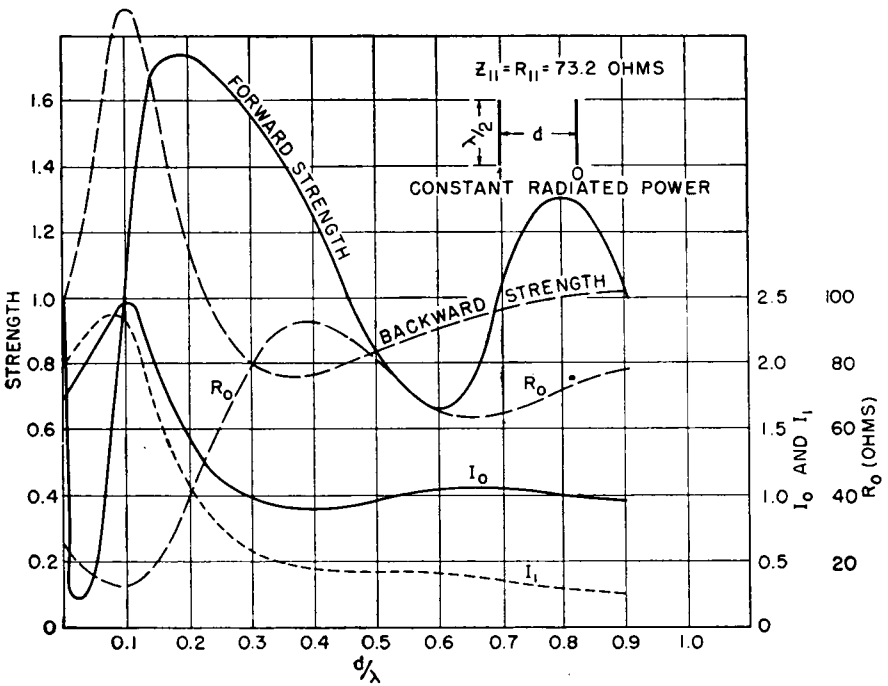

FIG. 3.35. Effect of parasitic dipole. (*After Brown.*)

ation-coupled dipoles in free space when their lengths are such as to have zero self-reactance.

3.11.3. Horizontal Director-Reflector Array. Additional gain can be obtained with two parasitic elements, one a director and the other a

reflector, on opposite sides of the active element. The plan and side views and one set of essential electrical dimensions are shown in Fig. 3.36, together with the horizontal pattern. The vertical pattern for the array

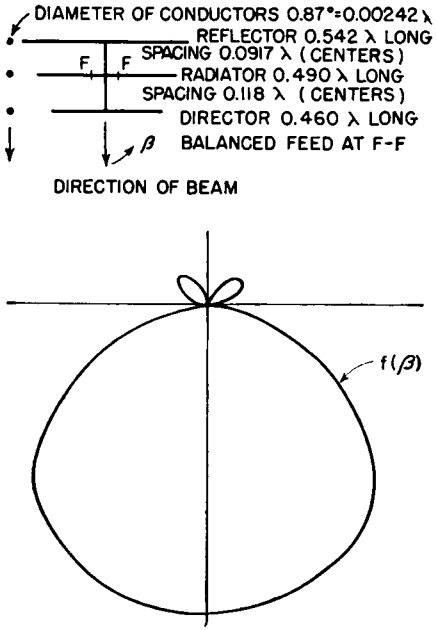

FIG. 3.36. Director-reflector array. (*Data by Brown.*)

over ground at a height h would be derivable from the measured horizontal pattern by the relation

$$f(\alpha) = \frac{f(\beta) \cos \alpha \sin (h \sin \alpha)}{\cos (90 \sin \alpha)}$$

The empirical characteristics of this type of antenna make it necessary to follow closely the principle of similitude in attempting to reproduce a prescribed design. The cross-sectional scale must also be retained faithfully.

This type of antenna can also be used as a single-mast rotary beam for the higher frequencies.

3.12. Vertical Directivity of Stacked Horizontal Dipoles

It was seen from Fig. 3.15 that increasing the height of a single horizontal dipole above the earth lowers the angle of the first lobe, but only at the expense of forming other higher-angle lobes after the height surpasses one-half wavelength. In practical communication it is necessary

for long-distance transmission and reception to focus the energy at low angles and also to suppress partially, if not completely, all higher lobes to reduce fading and multipath signals of long delay. This can be done to a certain extent by increasing the number of cophased dipoles as the height of the lowest dipole is increased. The directivity of two cophased dipoles spaced something of the order of one-half wavelength is such as to reduce the magnitude of the higher lobes that form as the height of the system is increased. Eventually, the second vertical lobe angle is low enough so that two dipoles do not appreciably reduce it, but the third and fourth lobes are effectively reduced. It is then necessary to increase the number of stacked dipoles to achieve the desired reduction of the second lobe. By the time the lowest lobe has been deflected to 5-degree horizon clearance, the lowest dipole is two wavelengths above ground, and if four cophased dipoles spaced one-half wavelength above each other are used, the second lobe has been reduced to 65 per cent of the first in field strength at 15 degrees and the third, fourth, and fifth to 17, 24.5, and 25.5 per cent at 25, 40, 54 degrees elevation, respectively. In order to reduce the second lobe still further, a vertical stack of six or more dipoles would have to be used.

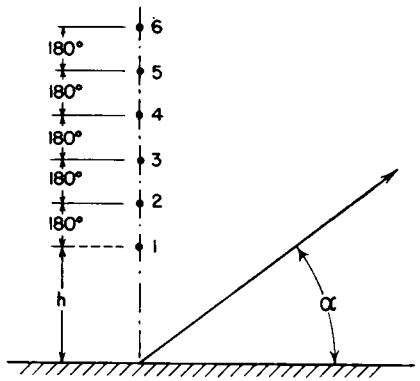

FIG. 3.37. Vertical stack of equal-current cophased dipoles.

This process can lead to very high and expensive structures. Yet such is the problem of obtaining a high concentration of energy at very low angles.

In the following equation, h is the electrical height of the lowest dipole above perfect ground. The other dipoles are assumed to be spaced at half-wavelength intervals with equal currents. The principal vertical pattern, using the method of adding the patterns for individual pairs formed by each dipole and its image (see Appendix V-A), using the geometry of Fig. 3.37, is

$$f(\alpha) = \Big(\sin (h \sin \alpha) + \sin [(h + 180) \sin \alpha] + \sin [(h + 360) \sin \alpha] + \cdots \sin \{[h + (n - 1)\ 180] \sin \alpha\}\Big) N$$

where N is a normalizing factor and n the total number of dipoles in the stack. Each dipole in the stack introduces a term in this equation. When h is a multiple of 180 degrees, quick computation can be made with the aid of Appendix V-A.

The principal vertical pattern can also be written in another form when

the number of dipoles is an integral power of 2. For an array of four stacked dipoles, but otherwise the same geometry as Fig. 3.37, the pattern can be written

$$f(\alpha) = \cos (90 \sin \alpha) \cos (180 \sin \alpha) \sin [(h + 270) \sin \alpha][f_1(\alpha)]$$

The first cosine factor is the pattern for the uppermost pair of dipoles. The second factor is the free-space pattern for two cophased pairs of dipoles. The third factor is the effect of the height of the array above perfectly conducting ground to the *middle of the dipole system* (not to the lowest dipole as in the preceding example). The fourth factor is the

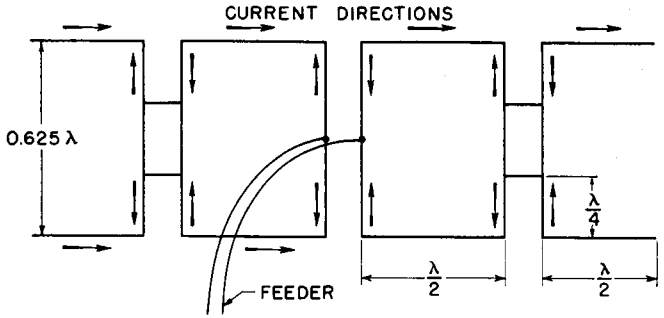

FIG. 3.38. Array with two parallel rows of dipoles arranged vertically but spaced 0.625 wavelength, cophased.

dipole orientation factor, which is unity when the dipole is horizontal and when it is vertical is the familiar dipole-pattern factor

$$\cos (90 \sin \alpha)/\cos \alpha = f_1(\alpha)$$

In a two-stack array, advantage can be taken of the additional gain that results from a spacing of 0.625 wavelength, the optimum spacing from a gain standpoint. This requires a symmetrical feed arrangement similar to that shown in Fig. 3.38. For an array of this type, the vertical pattern through the main beam, assuming perfectly conducting ground, is

$$f(\alpha) = \cos (112.5 \sin \alpha) \sin [(h + 112.5) \sin \alpha]$$

Vertical stacks of dipoles are most conveniently fed in cascade from the bottom upward. It is preferable to use half-wave spacing between dipoles so that the dipoles can be equally excited by the standing waves on the vertical feeder.

It must be remembered that ordinary cascade feeding includes the attenuation that occurs from bottom to top, which means that there is a consequent tapering of the dipole currents upward along the stack. Mutual impedances tend to equalize this somewhat. The reduction of current in successive dipoles causes the pattern to be tilted upward more

than that for equal currents. This effect increases with an increase in the number of stacks.

This upward tilting of the pattern can be corrected by feeding the stack from its center and propagating the currents equally upward and downward from the feed point. Since the expense of high structures is incurred to obtain low angles of radiation, attention to this effect is important in obtaining maximum effectiveness from this height.

A curtain of parasitic (or energized) reflectors or a passive screen reflector of untuned wires influences the vertical pattern because of the additional interference of the fields due to the depth of the array. This effect is used to obtain further suppression of high-angle lobes as well as to suppress backward radiation. A passive reflector of adequate area is a very effective device for suppressing backward radiation. When the reflector wires, parallel to the active radiators, are spaced one-tenth wavelength or less, very little energy is radiated backward and most of what does leak backward is due to diffraction around its edges. The backward-diffraction field is reduced as the directivity of the active curtain is increased. With a highly directive active curtain, the area of the passive reflector can be made equal to the area of the active curtain with relatively small diffraction leakage.

When a stack of four horizontal dipoles spaced 180 degrees is placed in front of a passive reflector, the vertical pattern in the principal vertical plane normal to the forward curtain becomes, assuming perfect earth and perfect infinite reflector,

$$f(\alpha) = \cos (90 \sin \alpha) \cos (180 \sin \alpha) \sin (h \sin \alpha) \sin (d \cos \alpha)$$

The first two factors account for the active curtain, the third for the height of the middle of the curtain, and the last the passive reflector spaced d degrees from the curtain. The application of this equation to a system of two lines of horizontal dipoles spaced 180 degrees with a mid-height of 450 degrees and spaced 36 degrees from a passive reflector, with equal cophased currents in the active dipoles, is shown in Fig. 3.39, step by step. The curtain factor, the height factor, and the reflector factor are all shown, as well as their evolution to the final pattern, shown shaded.

When an identical curtain of parasitically excited dipoles is used for the reflector, the pattern is indeterminate because of complicated mutual effects similar to those shown in Fig. 3.35. The maximum forward field strength is not coincident with minimum backward field. The system is quantitatively so complex that any analysis must be regarded as empirical, although most large dipole arrays used to date have been of this type. It is therefore useless to formulate the pattern shape in the

backward direction, but in the first quadrant of the forward direction one may use the approximate relation, for four stacked cophased dipoles,

$$f(\alpha) \doteq \cos (90 \sin \alpha) \cos (180 \sin \alpha) \sin(h \sin \alpha) \cos (45 \cos \alpha - 45)$$

In this equation the commonly used spacing of one-quarter wavelength between radiator curtain and reflector curtain was assumed in the values used in the last factor.

A simple form of cubical array can be illustrated by the following case: It is desired to obtain a radiation pattern, substantially unidirectional,

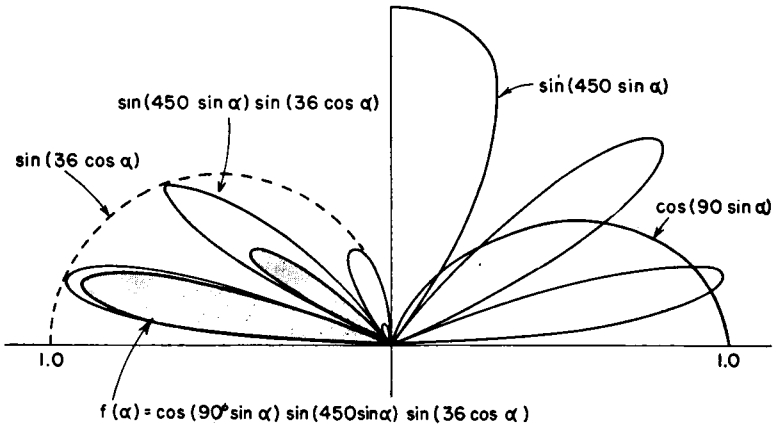

FIG. 3.39. Array pattern derived by multiplication by successive factors.

giving a moderately low angle of radiation in the forward direction in the vertical plane and maximum suppression of other radiation lobes in forward and backward directions consistent with a minimum number of radiators and economical design. Such a need often arises in directive broadcasting on the tropical broadcast frequencies where arrays of large electrical size are uneconomical or impractical.

If we examine the chart of pair patterns, we shall find that a pair with 225 degrees spacing and a phase difference of 45 degrees has a pattern with a submaximum along the line of the radiators in one direction and zero in the other. Two other large lobes occur almost normal to the array axis. This pair has the pattern

$$\cos (112.5 \cos \alpha + 22.5)$$

which has zeros at 37 and 180 degrees.

If now we place the axis of this pair parallel to ground at a height of one-half wavelength, the height factor will have the equation

$$\sin (90 \sin \alpha)$$

which has nulls at 0, 90, and 180 degrees. The zero at 90 degrees will split the major lobe from the radiator pair. What remains is still very large at about 120 degrees (60 degrees above the horizon in the backward direction), and further suppression is desired.

The pattern chart is examined again, and it is noted that a cophased pair spaced 0.75 wavelength has a zero at 42 degrees each side of the line

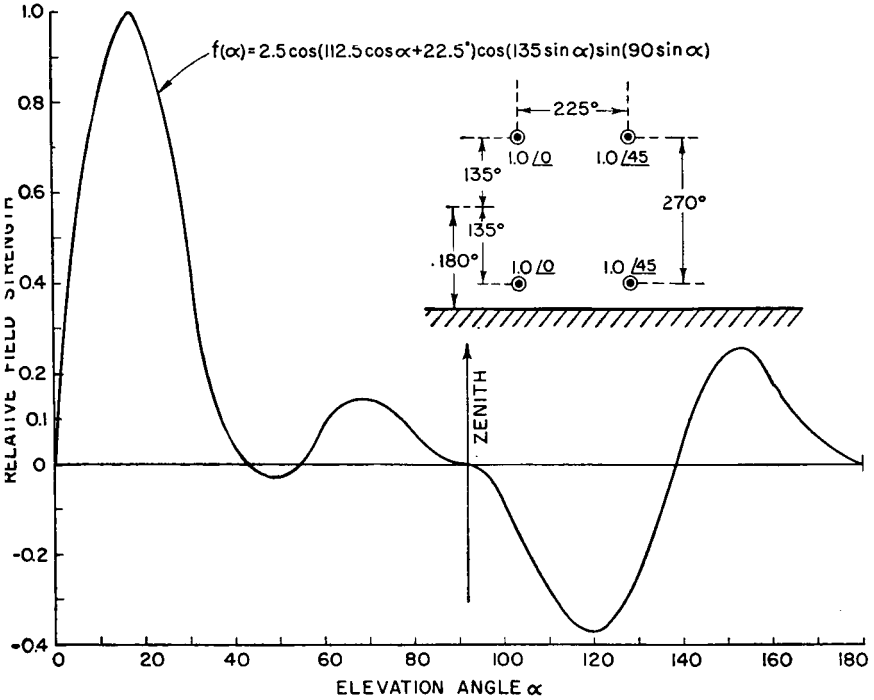

FIG. 3.40. Vertical-plane pattern for the array shown.

normal to the pair. This suggests that each of the original radiators may be replaced by such a cophased pair of radiators centered on the location of the original dipoles, with their axes vertical. Thus the array as seen from the side consists of four dipoles at the corners of a rectangle, with a height of 0.75 wavelength (270 degrees) and a width of 0.625 wavelength (225 degrees) and with an average height of 0.5 wavelength from ground (180 degrees). This brings the two lower radiators 45 degrees above ground, the upper ones 315 degrees. In the vertical plane, with this configuration, the last pair has the pattern

$$\cos (135 \sin \alpha)$$

In the vertical plane this entire array of four dipoles will have the

pattern

$$f(\alpha) = N \cos (112.5 \cos \alpha + 22.5) \sin (90 \sin \alpha) \cos (135 \sin \alpha)$$

When this is computed and plotted we obtain Fig. 3.40. In this figure, the pattern has been "normalized" to restore its maximum value to unity. There are now zeros at 0, 42, 54, 90, 138, and 180 degrees. The maximum field strength occurs at 16 degrees, at which angle the unnormalized maximum value of the above equation is about 0.4. To bring this to 1.0, a normalizing factor of $N = 2.5$ is applied to the equation, which merely enlarges the pattern. A normalizing factor larger than 1.0 means that the radiation resistance of the system has been reduced below normal value, and to obtain normal fields, relatively large currents will be necessary in the radiators. Large currents will result in high system potentials. Both these facts caution the engineer to be considerate of system losses, or low radiation efficiency may result. This condition is characteristic of all radiating systems that give theoretically large gains in relatively small space. This will be confirmed if one makes the computations for the radiator impedances, taking into account all the mutual impedances between radiators and images. A normalizing factor of 2.5 is not excessively large, indicating that with provisions for minimizing conductor and insulation losses, and also ground losses, good working efficiency may be realized. The proximity of the lower radiators to ground suggests the need for improving the effective conductivity of the ground, which can be done by using a surface ground screen of wires spaced 0.05 or 0.1 wavelength and parallel to the dipoles.

If the radiators of this array consist only of single horizontal half-wave dipoles, the horizontal pattern will have the formula

$$f(\beta) = \frac{\cos (112.5 \cos \beta + 22.5) \cos (90 \sin \beta)}{\cos \beta}$$

If additional horizontal directivity is wanted, each radiator may consist of two or more collinear half-wave dipoles.

3.13. Horizontal Directivity of Lines of Cophased Dipoles

The radiation pattern in any plane passing through a half-wave dipole has the equation

$$f_1(\beta) = \frac{\cos (90 \sin \beta)}{\cos \beta}$$

where β is measured from the normal to the dipole. A horizontal line of collinear cophased dipoles has a pattern that can be computed on the basis of isotropic radiators located at the center of each, with a magnitude

proportional to the dipole current, and multiplied finally by the dipole factor $f_1(\beta)$. Thus, for n collinear dipoles with half-wave spacing center to center, the field-strength pattern for equal dipole currents can be computed from the following equations: For n even:

$$f(\beta) = f_1(\beta)\{\cos (90 \sin \beta) + \cos (270 \sin \beta) + \cdots \cos [(n-1)\ 90 \sin \beta]\}$$

For n odd:

$$f(\beta) = f_1(\beta)\{1 + \cos (180 \sin \beta) + \cos (360 \sin \beta) + \cdots \cos [(n-1)\ 90 \sin \beta]\}$$

A set of such patterns is shown in Fig. 3.41. Appendix V-B can be used in the synthesis of such patterns. The space-time reference point for these equations is the geometrical center of the system.

Another form in which these patterns can be expressed is

$$f(\beta) = \frac{\cos (90 \sin \beta) \cos (180n \sin \beta)}{\cos \beta \cos (180 \sin \beta)}$$

These collinear half-wave dipole patterns are for free-space conditions. When they lie parallel to ground, the pattern becomes what is commonly called the horizontal pattern, though actually it is a horizontal plan view of the pattern. When an identical line of radiators is located at the same height above ground, spaced one-quarter wavelength from it, and the system excited so that their currents are equal but differ in phase by 90 degrees, the horizontal pattern is the free-space pattern for one line of radiators multiplied by the couplet factor

$$f_2(\beta) = \cos (45 \cos \beta - 45)$$

Patterns of this type are shown in Fig. 3.42.

When the system of collinear half-wave dipoles is parallel to a perfectly reflecting plane, the pattern $f_0(\beta)$ in the plane through the radiators and their images will be the same as for the original line of dipoles, multiplied by the reflector factor $f_3(\beta) = \sin (d \cos \beta)$. Then

$$f_0(\beta) = f(\beta) f_3(\beta)$$

When the electrical distance d from the reflector is less than 30 or 40 degrees, $f_3(\beta) = \cos \beta$ very nearly. Of course β must lie in the plane through the dipoles and their images.

Figures 3.43, 3.44, and 3.45 show the patterns for two, four, and six collinear half-wave dipoles with equal currents when placed in front of a perfectly reflecting surface.

Arrays of parallel vertical half-wave dipoles spaced one-half wave-

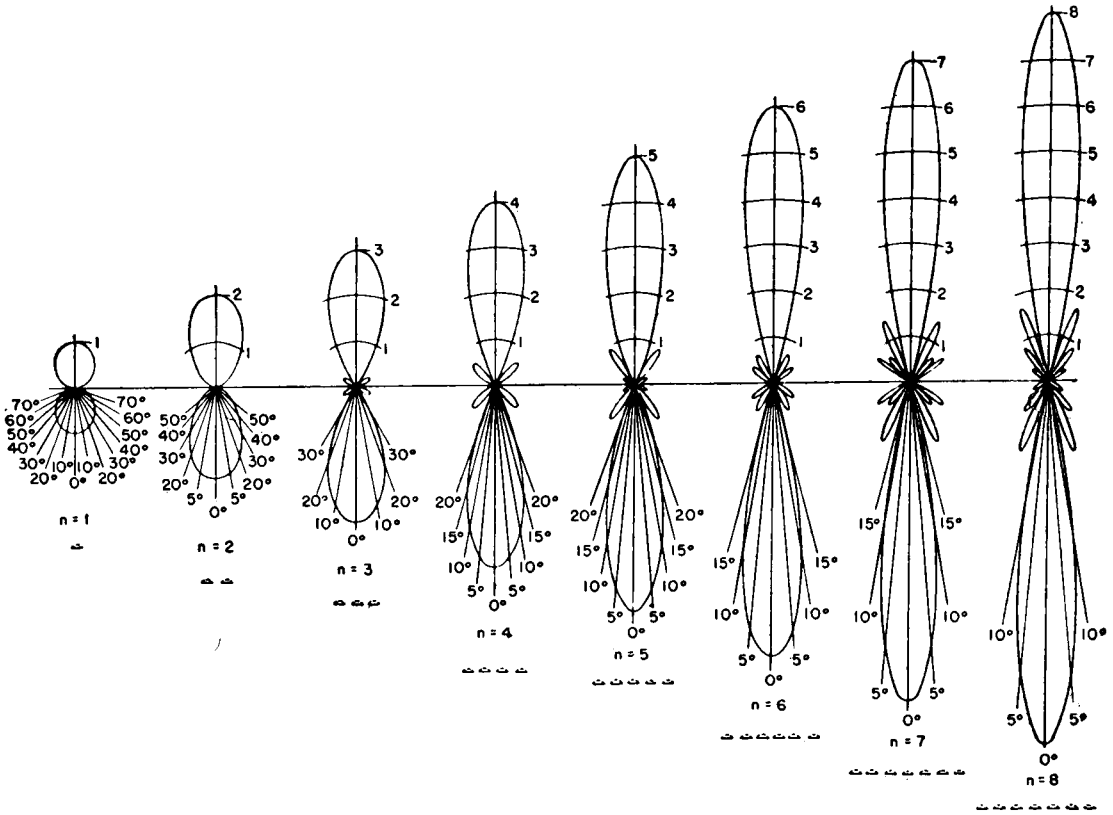

FIG. 3.41. Patterns for collinear cophased equicurrent dipoles. (*From RAF Signal Manual.*)

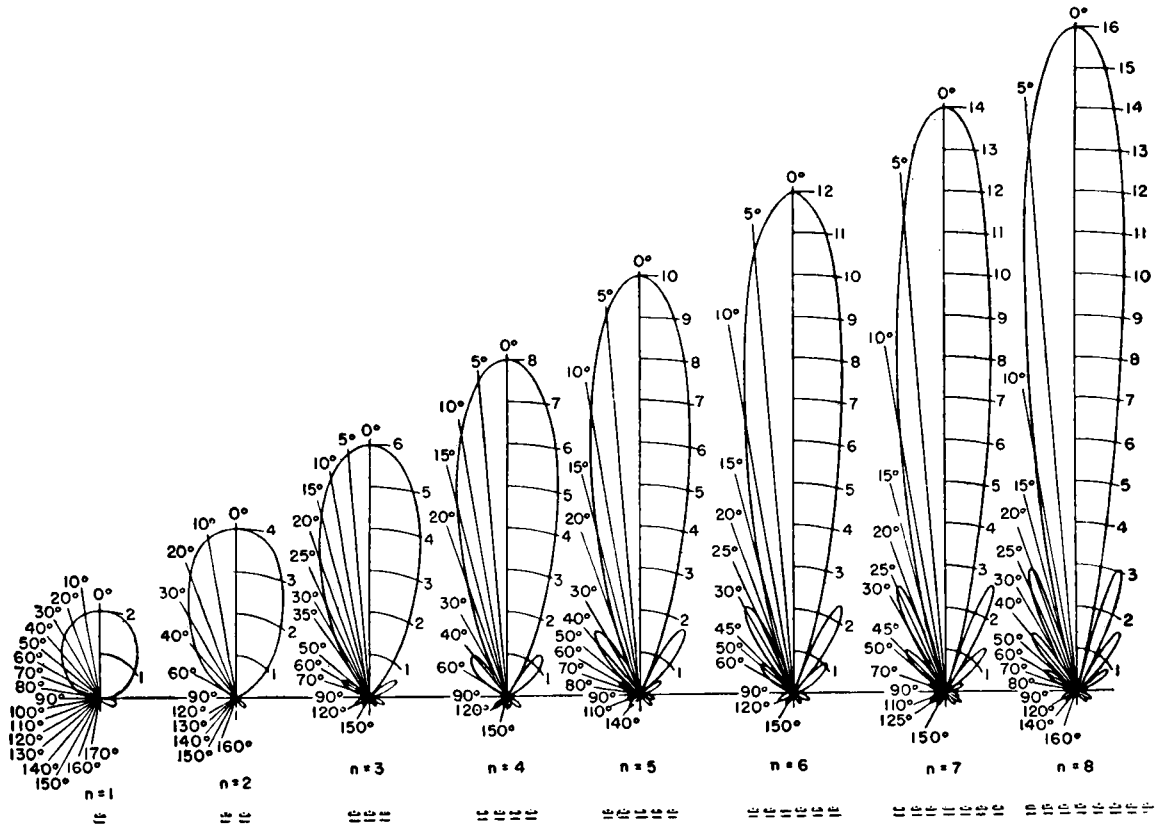

FIG. 3.42. Patterns for collinear cophased equicurrent dipoles with identical parallel row having a quarter-wavelength quarter-phase relation. (*From RAF Signal Manual.*)

length have patterns in the horizontal plane specified by

$$f_0(\beta) = \frac{f(\beta)f_3(\beta)}{f_1(\beta)}$$

Patterns for straight rows of vertical dipoles each having unit current, cophased, are shown in Fig. 3.46.

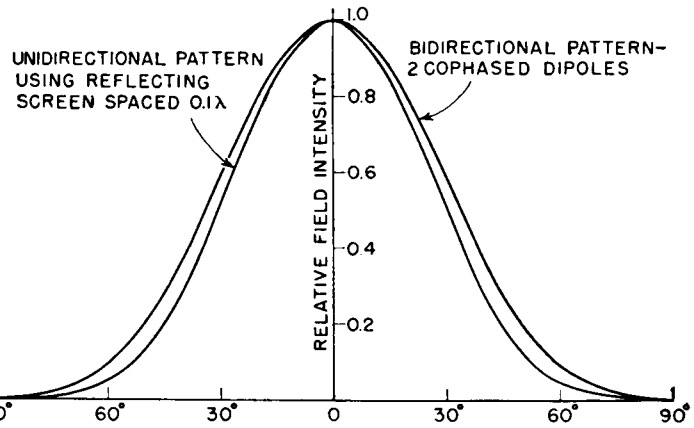

FIG. 3.43. Radiation pattern for two cophased dipoles with and without reflector screen.

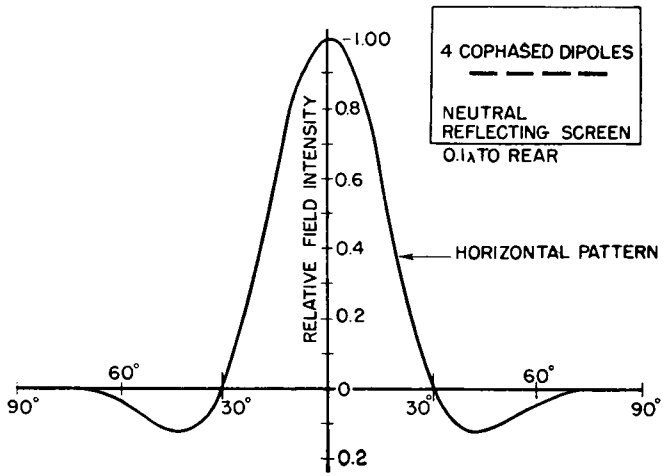

FIG. 3.44. Radiation pattern for four cophased dipoles with reflecting screen.

3.14. Beam Slewing for Broadside Arrays

Beam slewing is a practice often used where one array can serve for two azimuths having a small angular difference. The main beam can be set

off of the normal a few degrees by giving a small phase difference to the currents in the two halves of the array. The method for doing this is indicated in Fig. 3.49*A*, where a phase lag is introduced into the right-hand half by having an extra length of matched feeder on that side.

The horizontal pattern for a slewed unidirectional beam from a horizontal array of four half-wave spaced elements follows the relation

$$f_s(\beta) = \cos (90 \sin \beta) \cos \left(180 \sin \beta + \frac{\phi}{2}\right)$$

The appearance of the constant phase-difference angle ϕ in the last

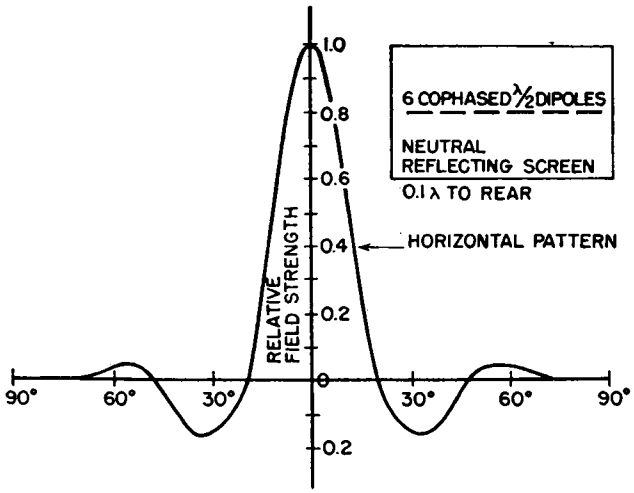

FIG. 3.45. Radiation pattern for six cophased dipoles with reflecting screen.

cosine factor of this equation accounts for the tilting, or slewing. It can be seen from this factor that its maximum will always be to one side or the other of the normal to the array when ϕ is other than zero. It is also evident that a null is going to appear on the off side of a slewed beam, which, when ϕ becomes sufficiently large, causes a split in the pattern. It is this split that sets a practical limit to effective slewing, both from loss of gain on the main beam and the growth of the secondary beam to objectionaable size.

The most effective form of beam slewing is to introduce an equal phase difference in the current of each dipole in succession. The more uniformly the phase difference is distributed across the array, the greater is the slewing angle before the beam splits.

Fig. 3.47 exemplifies two values of beam slewing for an array of four dipoles in line.

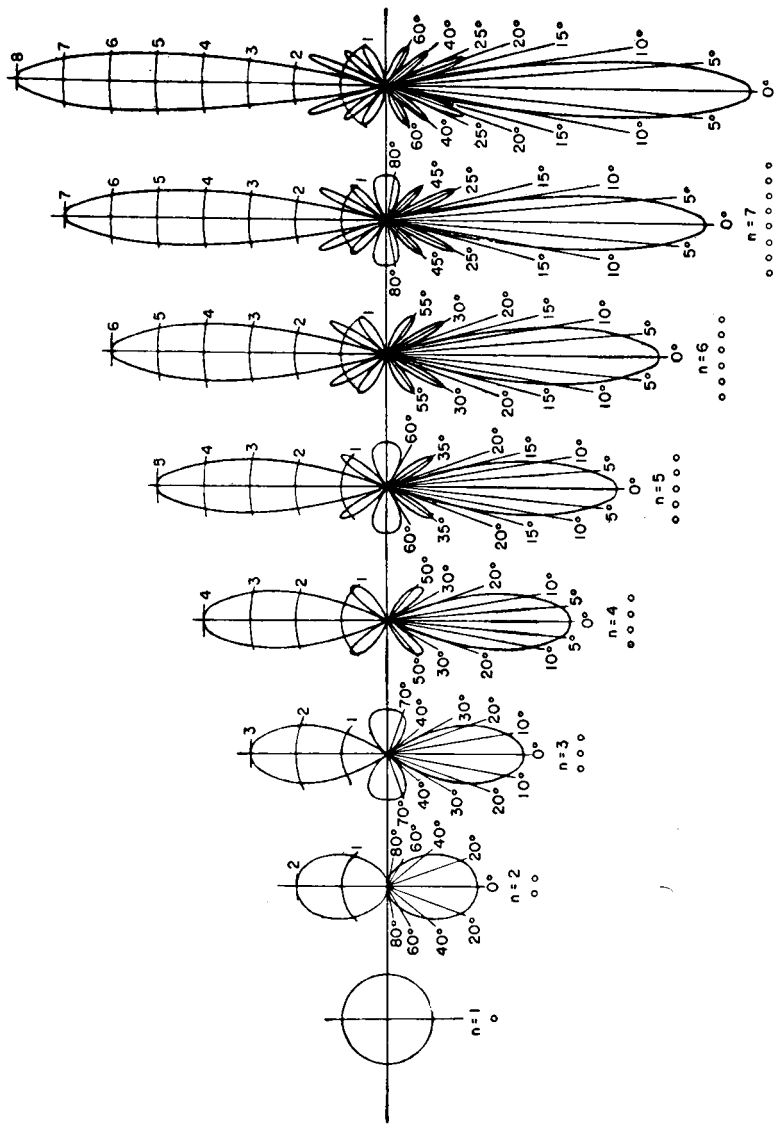

FIG. 3.46. Radiation patterns for horizontal row of vertical dipoles with unit current, cophased. (*From RAF Signal Manual.*)

3.15. Radiation Patterns for Dipole Arrays

The pattern for a dipole array in the main vertical and horizontal directions of interest can be computed separately by the methods outlined in the preceding pages. These patterns are all in terms of relative field strength. If it is desired to compute the radiation patterns in terms of relative power, the field-strength values are to be squared everywhere.

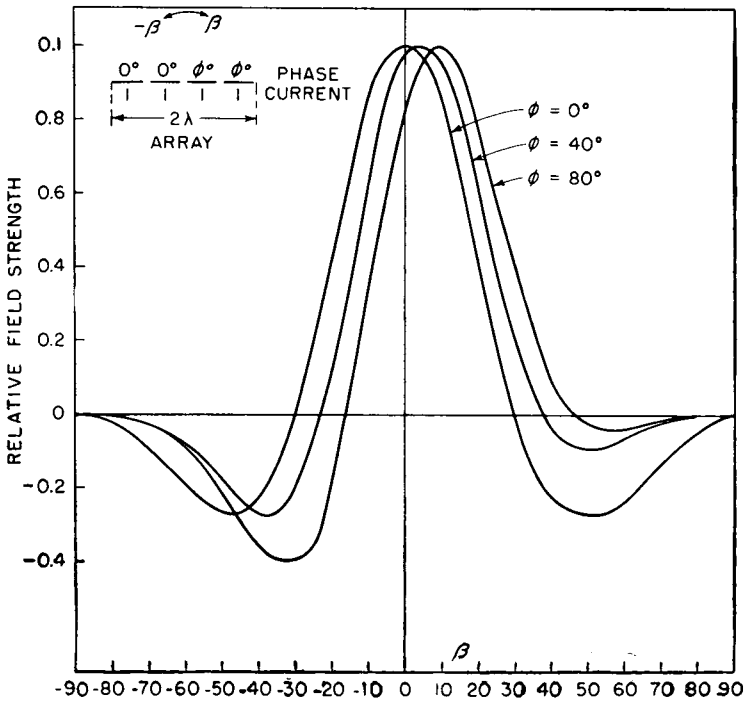

FIG. 3.47. Slewed beam patterns for a row of four horizontal dipoles.

The particular patterns desired for a high-frequency service, such as broadcasting, are chosen after a study of the geography of the service areas to be reached and an analysis of the propagation conditions to be encountered. In broadcasting service it frequently happens that a rather broad pattern in azimuth is required to cover an extended area of population; yet a high concentration of energy is necessary in the vertical plane. Most of the power gain of such a system will come from its vertical directivity.

Directivity is desired in two major planes, called generally the "horizontal" (plan view) and the "vertical" (side view). At times the patterns at other angles may be necessary. Any desired directivity is

obtained by separately utilizing the interference obtained by ground and from reflector-image radiations for the vertical patterns and the interference between the linear current distributions together with any reflector action for the horizontal pattern. The independent control of the pattern in the two major planes is a valuable property of dipole arrays and often dictates their adoption for certain applications. Such antennas are classed generally as broadside antennas, since the main beam is virtually normal to the plane of the dipole curtain.

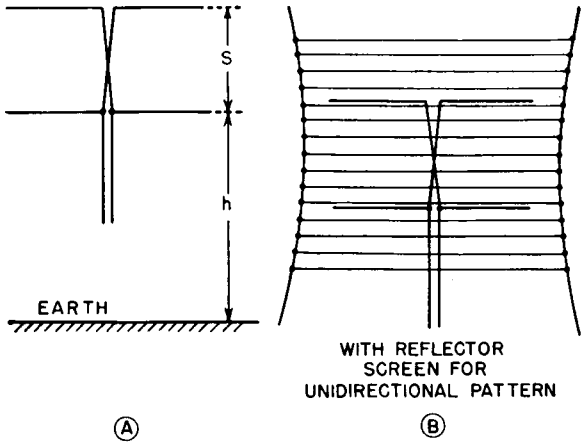

FIG. 3.48. Lazy-H antennas.

One of the simplest arrays with radiation control in the two major planes is the Lazy H, shown in Fig. 3.48*A*. In Fig. 3.48*B* it is shown with a passive reflector of wires for a unidirectional pattern. It consists of four horizontal half-wave dipoles, 2 by 2, voltage-fed from a central feeder.

Using larger numbers of elements, the size of a dipole array can become very large, especially when very low angle radiation and a very sharp beam in the horizontal plane are required. Figure 3.49*A* shows the dipole arrangement for a 4 by 4 curtain with separate feed for each half and provisions for slewing the horizontal beam by changing the relative phases in the two halves. Figure 3.49*B* shows a 6 by 4 curtain with center feed.

The patterns for all extensive dipole arrays using equal currents in the individual dipoles are characterized by secondary lobes of moderate size. This is illustrated in Figs. 3.50, 3.51, and 3.52, except that in these figures the complete pattern for the forward half is displayed in terms of relative power distribution, instead of the usual field-strength distribution.

3.16. Suppressing Secondary Lobes

In the formulas for radiation patterns use can be made of the fact that a null in any one factor of the equation produces a null in the final pattern at the same angle. By placing the nulls in one factor at the angles of secondary lobes in the other factors, these secondary lobes can be split and reduced in amplitude almost as desired. This principle was used in Chap. 2 and will be illustrated here by an example.

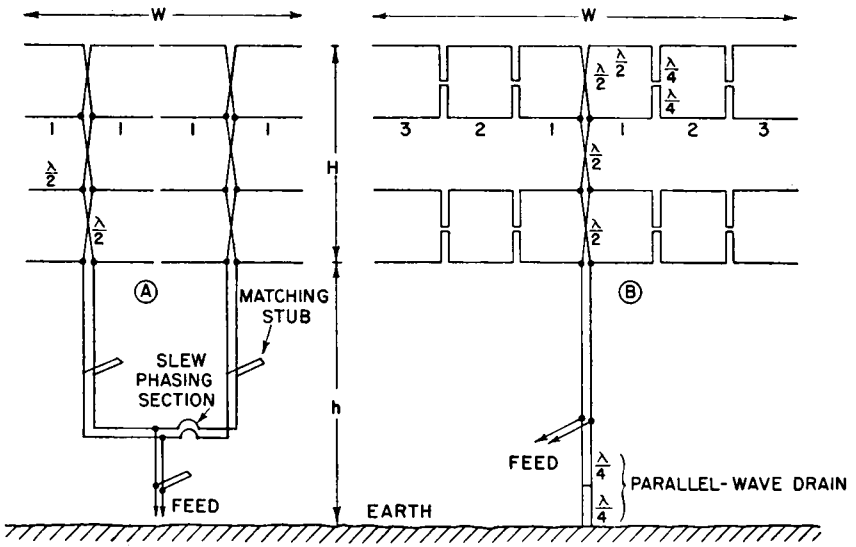

FIG. 3.49. Arrays of horizontal half-wave dipoles and typical feeder connections.

Let it be desired to produce a vertical pattern on the main beam from an array of horizontal dipoles that will have a maximum between 6 and 8 degrees with minimum amplitudes for the secondary lobes.

A single horizontal dipole and its image form an antiphased pair whose pattern has nulls located as shown in Fig. 3.16. For the maximum to be between 6 and 8 degrees the first null must be at about 15 degrees. From Fig. 3.16 we find that the height of the dipole must be 1.94 wavelengths above ground (700 degrees). In addition to the null at 15 degrees there will be other nulls at 31 and 50 degrees.

A cophased pair of dipoles, centered at 700 degrees, can now be substituted for the single dipole. For this pair the spacing can be made such as to bring another null midway between 15 and 31 degrees, where a large secondary lobe should exist. A cophased pair with a null at, say, 22.5 degrees has to have a spacing of 480 degrees. The pair pattern with this spacing has only this one null. So far it is known that the combination pattern has nulls at 15, 22½, 31, and 50 degrees.

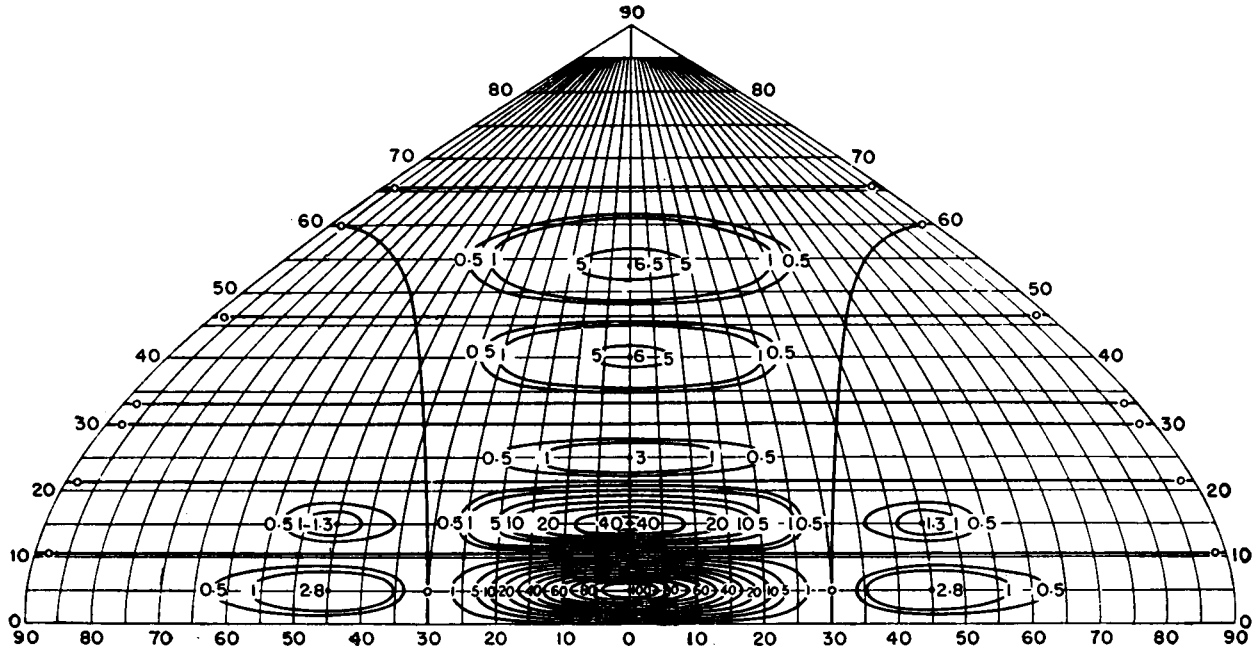

FIG. 3.50. Power-distribution diagram—aerial type same as Fig. 3.49*A* when h equals two wavelengths. (*After Hayes and McLarty.*)

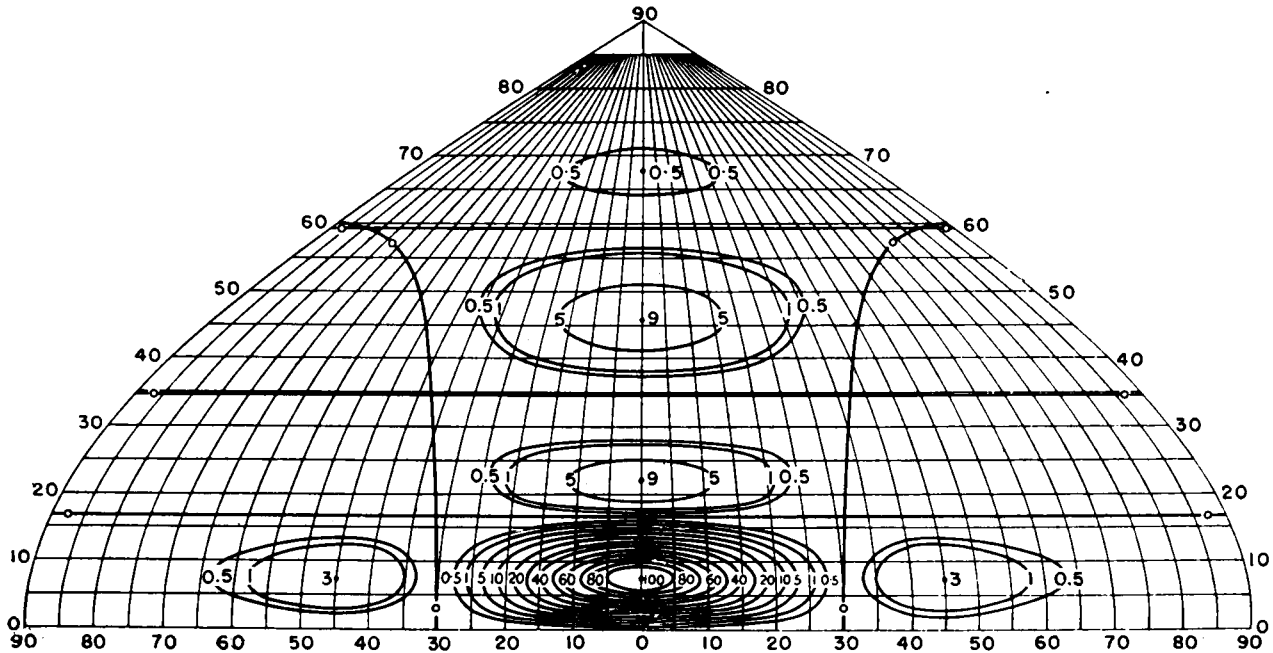

FIG. 3.51. Power-distribution diagram—aerial type same as Fig. 3.49*A* when h equals one wavelength. (*After Hayes and McLarty.*)

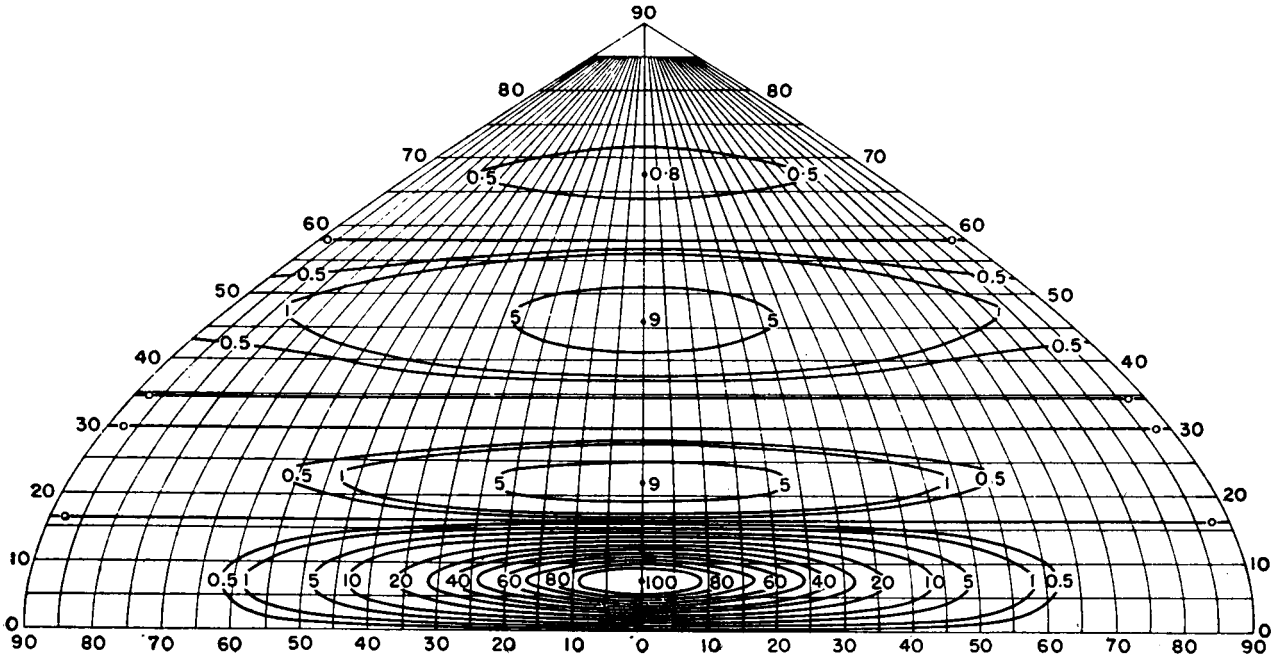

FIG. 3.52. Power-distribution diagram—aerial type same as one-half of Fig. 3.49*A* when h equals one wavelength. (*After Hayes and McLarty.*)

It is now noted that there is a large angle between 31 and 50 degrees in which a large lobe can exist. The next step is to substitute for each of the former two dipoles a pair of cophased dipoles centered at 700 degrees plus and minus 240 degrees. The patterns for these two pairs are identical, and a spacing is chosen that will bring a null at about 40 degrees. The null-angle chart shows that this would result from a pair spacing of 280 degrees.

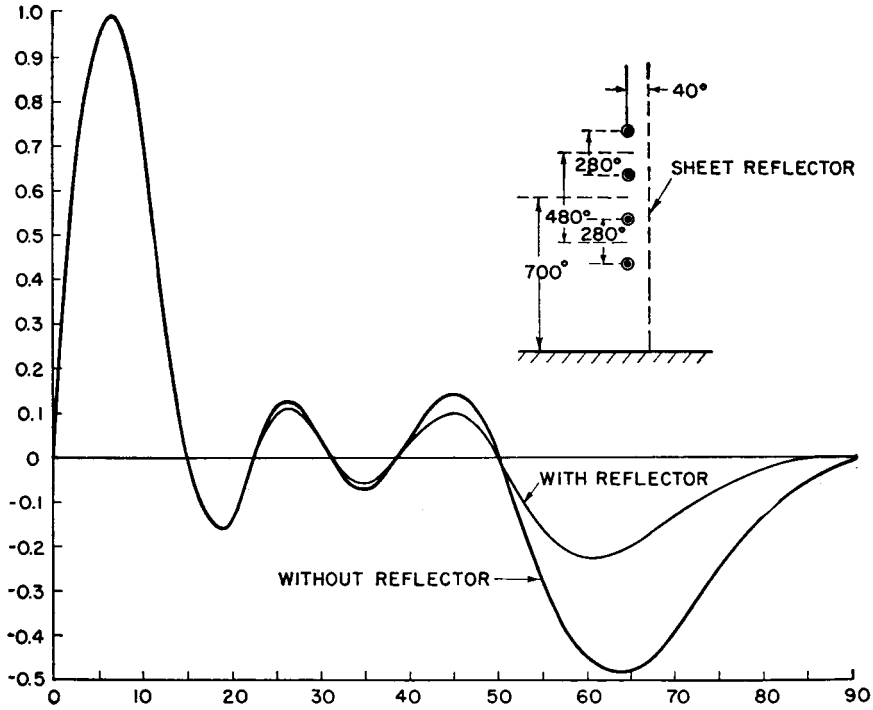

FIG. 3.53. Vertical pattern obtained by splitting secondary lobes.

The array now consists of four dipoles, with equal cophased currents, arranged vertically at heights of 320, 600, 800, and 1,080 degrees. The vertical pattern for this array has nulls at 15, 22½, 31, 40, and 50 degrees. The geometry now permits a computation of the full pattern for examination. The result is shown in Fig. 3.53, with and without a screen reflector. As a first approximation the secondary lobes are suppressed 16 decibels or more at all angles that would cause multipath delays. If the suppression of the uppermost lobe had to be increased, a further extension of the method to put a null at about 60 degrees would provide a possible solution.

Obviously, this characteristic of the pattern equations in factor form adapts itself more readily to the solutions of problems of this kind than

would the form having a series of terms added together. The latter form, however, lends itself more conveniently to binomial, Fourier, and Tchebysheff polynomial distributions, where the current amplitudes across the curtain are graded in some systematic manner to produce a prescribed pattern shape.

3.16.1. Binomial Current Grading. It has been shown that a system of identical radiators with equal currents with specified unequal spacings can be made to produce a main lobe, together with almost any desired degree of suppression of side lobes, by judicious placing of the nulls in the pattern factors. Theoretically this method could be carried so far as to result in almost complete suppression of all side lobes in either the electric or the magnetic plane of a radiator system. The practicality of the principle is limited by the relative difficulty of feeding such an array and by the size and cost of the structures for high-frequency broadcasting or communication.

In order to retain the simplicity of half-wavelength elements with half-wavelength spacings between centers, a method of side-lobe suppression can be used where the current amplitudes are adjusted systematically along a line or a stack of dipoles. The simplest of these current-grading methods is that of symmetrical binomial current amplitudes. Figure 3.54 shows how these amplitudes are derived, using half-wavelength spacings, for a row of parallel dipoles.

With a fundamental pair of identical parallel radiators with cophased and equal current amplitudes, and spaced one-half wavelength,

$$f_1(\beta) = \cos (90 \sin \beta)$$

By overlapping two such pairs by one-half wavelength, there is the equivalent of three radiators in line with currents of 1 to 2 to 1 having the pattern

$$f_2(\beta) = \cos^2 (90 \sin \beta)$$

By continuing this procedure for n successive steps there results a row of $n + 1$ radiators with symmetrical current tapering from the center outward in each direction, the amplitudes being proportional to the values shown in Fig. 3.54. The array pattern will be

$$f_n(\beta) = \cos^n (90 \sin \beta)$$

Any basic pair pattern may be used, and the principle is not limited to half-wavelength spacings as used in this equation.

If the fundamental pair pattern is free of lobes, the patterns corresponding to successive powers of this pattern function must also be free of lobes and the beam increases in sharpness as the length of the array

increases. The same effect takes place in a string of collinear dipoles, with center-to-center spacing of one-half wavelength, but the pattern has the additional directivity of the basic dipole pattern. In this case

$$f(\beta) = \frac{\cos^{n+1}(90 \sin \beta)}{\cos \beta}$$

The principal disadvantage of binomial distributions in practice is that the arrays become relatively large for a given beam width. This

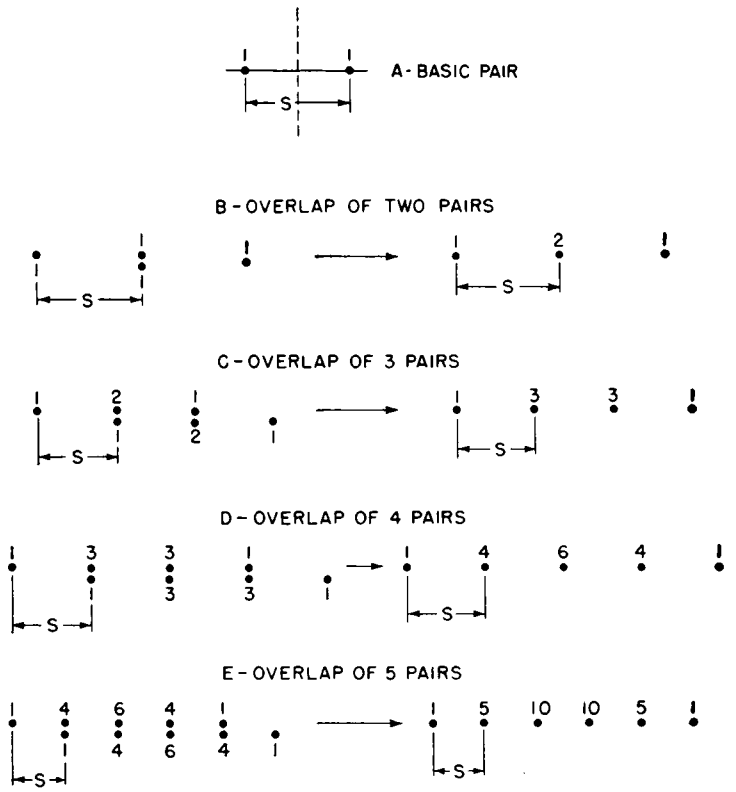

FIG. 3.54. Binomial current distributions for broadside arrays.

is because of the very low current in the outer radiators, which have the greatest electrical spacing and normally contribute most to beam sharpness when uniform currents are employed. The reduction of currents in the outer radiators decreases their effectiveness from a gain standpoint so that a binomial array is much larger than a uniform array for the same sharpness of main beam. The latter, however, is attended with side lobes, as was seen from the study of such systems.

An example of the application of the binomial current grading to a vertical pattern is the following: An antenna consisting of two stacked dipoles spaced 230 degrees, with a mid-height of 450 degrees and located 36 degrees from a passive reflector, has a secondary lobe at 32 degrees having a magnitude 40 per cent of that of the main lobe. How can this lobe be reduced substantially?

This vertical pattern has the equation through the main lobe

$$f(\alpha) = \cos (115 \sin \alpha) \sin (450 \sin \alpha) \sin (36 \cos \alpha)$$

where the first cosine factor is that of the pair of stacked dipoles, the second sine factor that for the height of the mid-point of the array, and the third that for the screen reflector. All factors are functions of α; hence any reduction in the value of any of these factors at any particular angle results in a proportional reduction in the value of the entire function.

What would happen if the first factor, for the pair, were squared? A quick test can be applied for $\alpha = 32$ degrees by comparing

$$\cos (115 \sin 32) = 0.485$$
$$\cos^2 (115 \sin 32) = 0.235$$

According to this, squaring the pair factor reduces the lobe at 32 degrees to 48.5 per cent of its present value, or to a value of 19.4 per cent that of the main lobe, or better than 14 decibels below the field strength of the main lobe. This improvement may be very desirable.

The next step is to determine the antenna configuration and current distribution that will give such a pattern. It is obtained by overlapping two identical pairs, giving a total of three dipoles in the stack, with their center located at the same point as the center of the original pair, and having a 1-to-2-to-1 distribution of current amplitudes, all cophased, and spaced 230 degrees between successive dipoles. The comparative vertical patterns for this array are shown in Fig. 3.55.

It is instructive to interject at this point the application of binomial current grading to a type of array not heretofore discussed. It is a horizontal array of parallel dipoles arranged to give a desirable vertical pattern for low-angle concentration by spreading the array horizontally rather than vertically. At frequencies between 4 and 8 megacycles, vertical stacking of dipoles for a given low-angle beam quickly runs to great heights and becomes relatively expensive. The example to be discussed is an economical alternative, using more land but less height for a certain type of pattern suitable for long-distance transmission or reception.

Consider the pattern for a pair of parallel radiators spaced 0.75 wave-

length (270 degrees) and having a 45-degree phase difference. The equation for this pair is

$$f(\alpha) = \cos (135 \cos \alpha + 22.5)$$

This pattern can be read from the chart, Appendix IV-A, and the precise location of the nulls can be found from Appendix IV-B. It can be seen

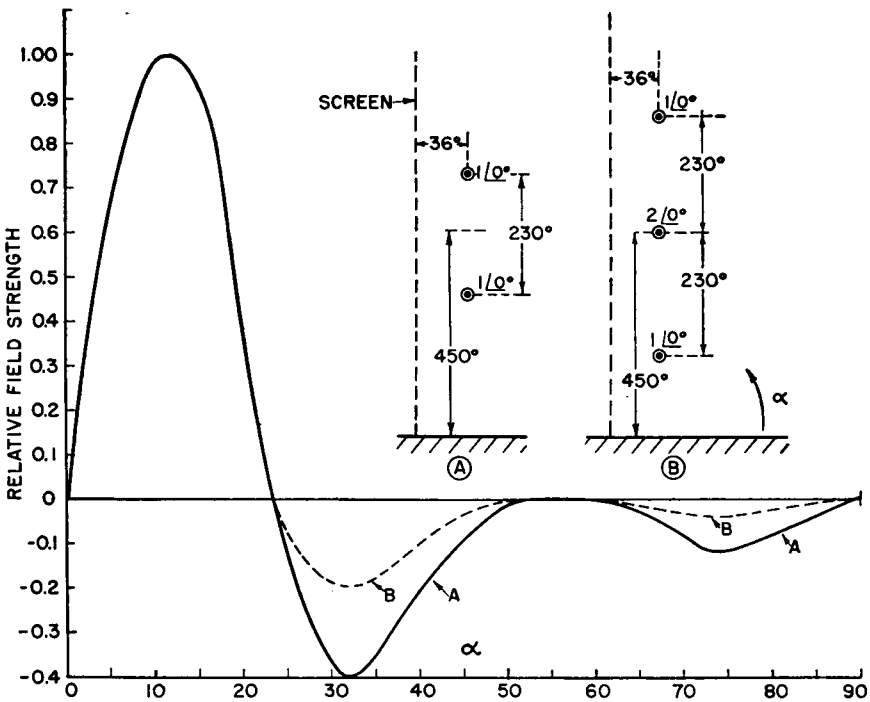

FIG. 3.55. Binomial distribution applied to secondary-lobe reduction in a vertical pattern.

at once that this pattern, when squared, becomes unidirectional in the plane of the array with a narrow beam of large amplitude at high angle in the opposite quadrant. It is now possible to introduce a height factor of such a value as to split this large, parasitic, high-angle lobe. As an exploratory step, let it be assumed that the height of the dipole plane (parallel to the ground) is one wavelength. The height factor therefore has nulls at 0, 30, 90, 150, and 180 degrees. The pair factor, raised to any power, has nulls at 59 and 146 degrees (counting the full semicircle from horizon to horizon in the vertical plane).

Therefore, let the equation take the parameters mentioned so that it becomes

$$f(\alpha) = \cos^2 (135 \cos \alpha + 22.5) \sin (360 \sin \alpha)$$

The pattern for this equation in rectangular coordinates is shown in Fig. 3.56.

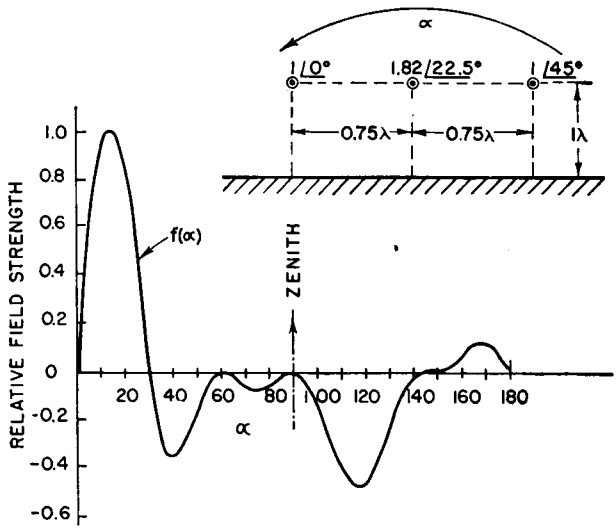

FIG. 3.56. Horizontal binomial current distribution for control of vertical pattern.

This type of antenna is an end-fire array of three elements obtained by squaring the pair factor. The synthesis of the radiators and current distribution for obtaining this pattern results in the following:

Number of horizontal radiators 3
Spacing between radiators 270 degrees
Current distribution, progressing in the direction of the main lobe:
1.0 at angle 0 degrees
1.82 at 22½ degrees
1.0 at 45 degrees

The horizontal pattern for such an array includes the pair factor squared and the directivity factor for the number of dipoles used in line. The height factor is of course not involved in the horizontal pattern. An interesting fact to mention in connection with end-fire arrays generally is that their vertical and horizontal patterns are interdependent, and not separately controllable as with broadside dipole arrays.

3.16.2. Suppressing Secondary Lobes by Splitting. It is possible to suppress side lobes in a broadside pattern from a linear arrangement of horizontal dipoles by using successive pair combinations that split the side lobes resulting from the geometry of the original pair. In this method, the currents in all the dipoles are equal and cophased. The side-lobe suppression is obtained entirely by the geometrical spacings of the dipoles.

Let it be desired to produce a broadside beam that has its first nulls at plus and minus 15 degrees from the main beam, with all side lobes less than 0.1 in strength compared with the main beam.

The equation for a pair of horizontal dipoles that produces first nulls at plus and minus 15 degrees is

$$f_1(\beta) = \frac{\cos (90 \sin \beta)}{\cos \beta} \cos \left(\frac{S_1}{2} \sin \beta \right) = 0$$

Spacing S_1 is found to be 700 degrees. This spacing also gives a second pair of nulls at plus and minus 51 degrees.

It is evident that a large secondary lobe exists between 15 and 51 degrees, and because this is a rather large angular interval, and because we desire a considerable degree of suppression, we can now replace each of these dipoles with a pair of dipoles spaced a distance S_2 between centers such that we bring a null at 27 degrees. The equation for the linear combination is now

$$f_2(\beta) = f_1(\beta) \cos \left(\frac{S_2}{2} \sin \beta \right) = 0$$

From the last factor, S_2 is computed to be 400 degrees. This pair has but one null. Our nulls are now at 15, 27, 51, and 90 degrees, the null at 90 degrees resulting from the dipole factor. It can be assumed that side lobes will exist about halfway between these nulls.

The angular space between 27 and 51 degrees is a large one, and a large side lobe must exist between these nulls. Thus we can pair the radiators again and get

$$f_3(\beta) = f_2(\beta) \cos \left(\frac{S_3}{2} \sin \beta \right) = 0$$

A value for S_3 is now computed that will bring a null at the middle of this side lobe, at about 39 degrees. The center spacing of a pair of dipoles that will achieve this is when S_3 is 290 degrees.

At this stage there are nulls in the patterns at 15, 27, 39, 51, and 90 degrees, and maximums exist at 0, 21, 33, and 45 degrees; and, due to the diminishing value of the dipole factor at the large azimuth angles, we estimate the last lobe at perhaps 65 degrees.

We can now make a quick calculation of the values of the pattern at these angles corresponding to side-lobe maximums to see how we are progressing. We find the following values from the equation above:

0	1.00
21	−0.101
33	0.047
45	−0.048
65	0.345

The desired degree of suppression is obtained in all side lobes except the last. This one can be split up by pairing the radiators in another

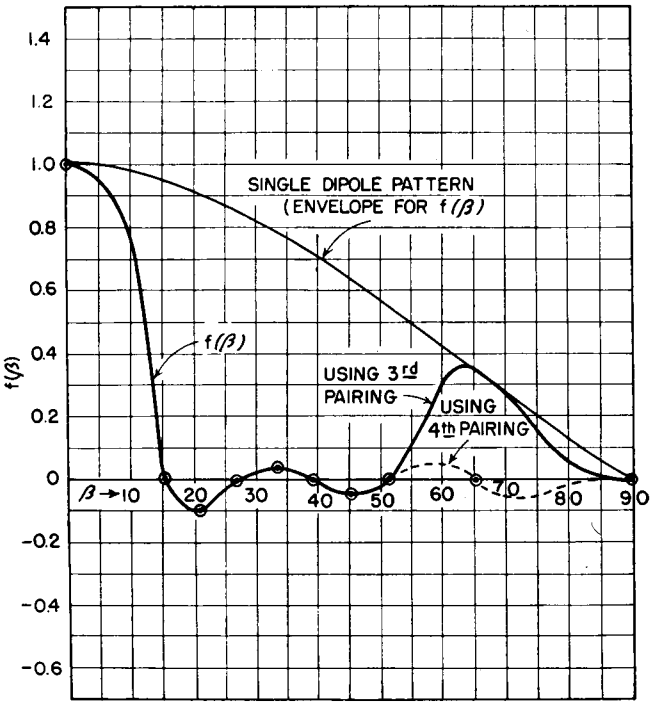

FIG. 3.57

step, obtaining the pattern equation

$$f_4(\beta) = f_3(\beta) \cos\left(\frac{S_4}{2} \sin \beta\right) = 0$$

The value of S_4 that will bring a null at 65 degrees is 210 degrees. Without further computation we can plot the known points and, with accept-

able accuracy for exploratory purposes, sketch in the pattern between these points, as is done in Fig. 3.57. From this we are certain that the specification has been met in principle.

It now remains to synthesize the final arrangement of the dipoles in this linear array. This process is indicated in Fig. 3.58. The resulting arrangement is complicated because we find that the radiators in the

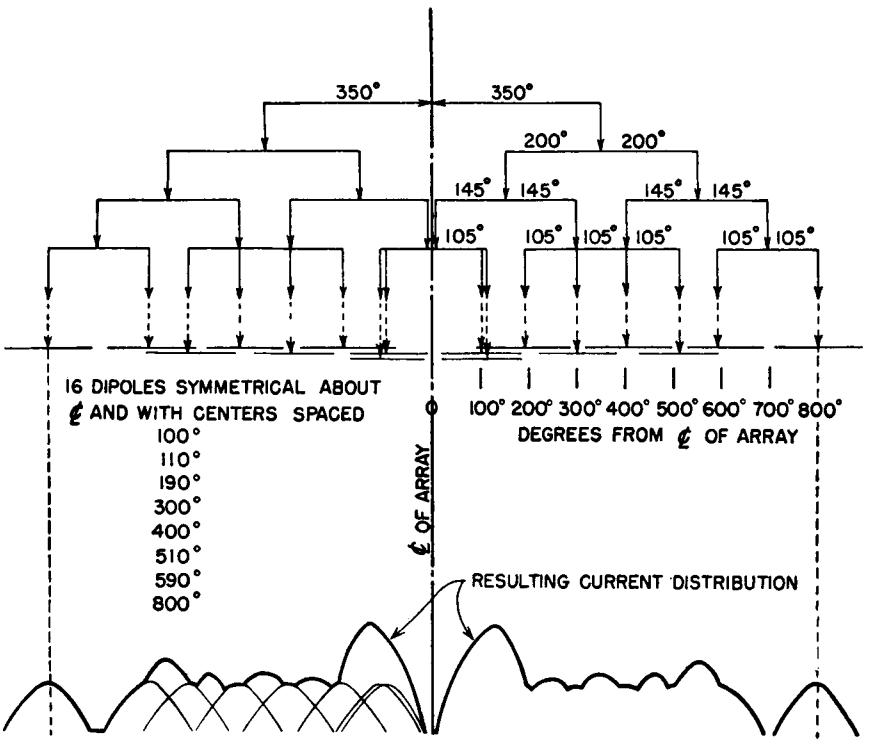

FIG. 3.58. Synthesis of current distribution that gives the horizontal pattern of Fig. 3.57.

successive pairing operations overlap to a considerable extent. Nevertheless, the realization of such a current distribution by this arrangement of dipoles will actually produce the desired pattern. This particular example was chosen at random to describe the application of a useful principle, but the attainment of such an array is not necessarily practical.

Greater practicality of application can be assured in this method if the pair spacings are confined to integral multiples of half wavelengths. Then all the overlapping dipoles will be exactly superimposed in the synthesizing process. It is worth while to test this principle with another example.

Let it be desired to produce a broadside pattern that has its zero at about 10 degrees, and let all secondary lobes be suppressed as much as possible by using the half-wave spacing technique. Following the same procedure as in the preceding example, it is found that the first pair, with a spacing of 1,080 degrees (six half wavelengths) will give nulls at 9.5, 29, and 57.5 degrees. The next pair with five half wavelengths spacing will give nulls at 11.5 and 37 degrees. The third step with four half wavelengths spacing gives nulls at 14.5 and 49 degrees. The fifth step places

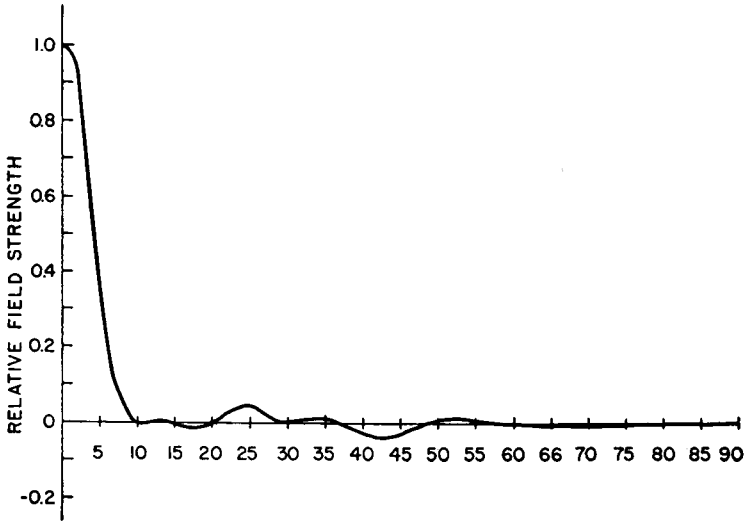

FIG. 3.59. Array horizontal pattern.

another null at 20 degrees, and in the sixth step, when the pair spacing is one-half wavelength, there is another null at 30 degrees. The major side lobes are split by a total of 10 zeros between 9.5 and 90 degrees.

The resulting pattern will have the equation

$$f(\beta) = \cos(540 \sin \beta) \cos(450 \sin \beta) \cos(360 \sin \beta) \cos(270 \sin \beta) \cos(180 \sin \beta) \cos(90 \sin \beta) \text{ (dipole factor)}$$

The computation of this pattern is easy with the aid of Appendix V-B, where each pair pattern has already been tabulated. It is necessary only to multiply across the six columns of cophased pairs together with the column for the dipole directivity pattern. The result is shown in Fig. 3.59. The pattern has a half-power beam width of 13 degrees, and none of the side lobes exceed 4.5 per cent of the field strength of the main beam. There are two lobes of this intensity, at 25 and 42.5 degrees. All the others are 1 per cent or less over the entire range. If a passive reflecting screen were to be used, these would be reduced somewhat more.

The synthesis of the array to give this pattern with half-wave-spaced horizontal dipoles is given in Fig. 3.60. From this we find that the array would require a horizontal width of 22 half-wave dipoles. The loop currents end to end are found to be the following: 1,1,1,2,2,3,4,4,4,5,5,5,5, 4,4,4,3,2,2,1,1,1.

A linear array of this distribution is physically practical to construct and to feed.

The same technique may be applied in the vertical-plane pattern.

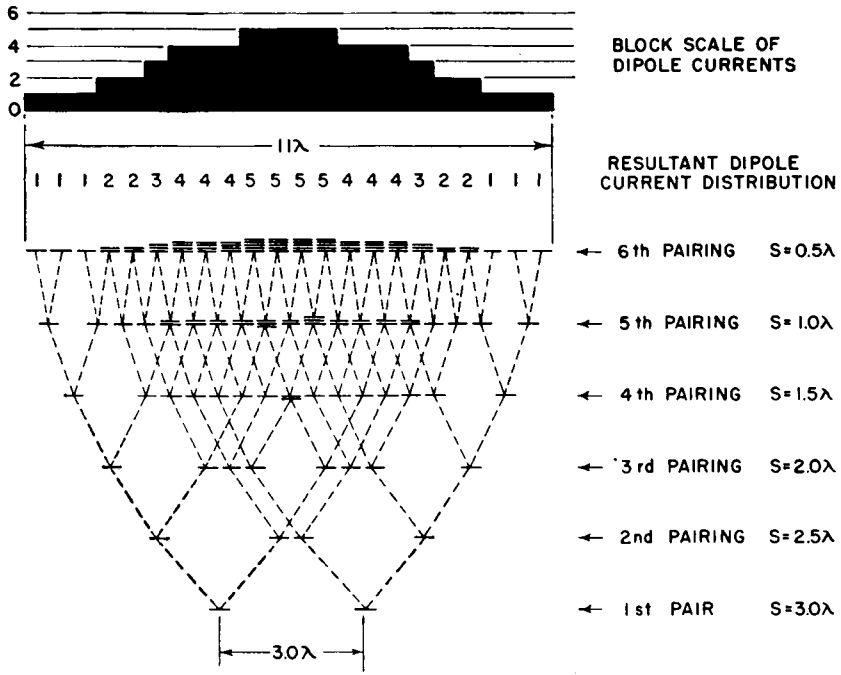

FIG. 3.60. Synthesis of current distribution that gives the pattern of Fig. 3.59.

3.17. Power Distribution among the Half-wave Dipoles of an Array

Certain unique currents must be established in the various dipoles of an array to obtain a specified radiation pattern. The mutual impedances of such a system cause the resistive components of impedance of the various radiators to differ. When fed to provide the specified currents in radiators of different resistances, the power inputs will not be equal. In many systems, this requires that the feeder system divide the power in the specified manner among the different radiators, using appropriate power-dividing circuits and impedance-matching networks, while maintaining control of phase differences within the feeders so as to come

out with the correct phases as well as amplitudes of the various radiator currents. All the techniques of transmission-line transforming and coupling sections are employed in one way or another for this purpose. Chapter 4 outlines some of the common methods that have proved practical. The application of these techniques must be made without introducing couplings between feeders and radiators, and with a high degree of balance when balanced feeders are used.

High-frequency dipole arrays in use at the present time are almost universally of the elementary half-wave-dipole half-wave-spacing type that are intrinsically simple to feed by employing standing waves on the feeders for either current or voltage feed. It is possible that future engineering may tend to more complicated systems, the feeding of which may approach the complexity of the arrays used for directive medium-frequency broadcast transmission.

The simplest type of array of parallel half-wave dipoles is that using half-wavelength spacing and half-wavelength feeders that are unmatched. The currents in the several dipoles of the array are assumed to be equal since presumably they are all fed with equal driving potentials. This implies the further assumption that all the radiators have equal impedances. A simple computation of the driving-point impedance of each radiator in such an array, using mutual impedances between all radiators and their images, reveals that when the desired currents exist in the system the individual impedances are not equal, owing to the effects of radiation couplings with all the other radiators and images in the system. Those on the perimeter of the curtain have the greatest differences from anything that can be called a common value. Proximity to ground and to reflectors has a major influence on the operating impedance of each dipole.

When the radiators are spaced at arbitrary distances, and when specific current amplitudes are required in the various radiators to obtain a specified radiation pattern, the system has then to be fed so that each radiator is correctly excited. This requires a knowledge of the self-impedance and all the mutual impedances in order to determine the driving-point impedance of each radiator. The feeder system must then provide for the correct power, potential, and current phase at each radiator, which are determined by its impedance and its position in the array.

The computation of mutual impedances may be very laborious since the only available precomputed figures are for parallel half-wave dipoles, with their ends opposite each other, and for collinear dipoles (see Figs. 3.61 and 3.62). The echelon dispositions are too numerous to compute for all cases and only a small number of data are published.[1002,1019,1066] Therefore one must compute the impedances according to the circum-

stances of each problem. Unfortunately it is necessary to take into account the most remote dipoles of the system, so that the labor cannot be avoided.

In order to design properly a radiating system with a specified current distribution, the *exact* impedance of each radiator must be *known* and the feeder system designed to provide exactly the required excitation

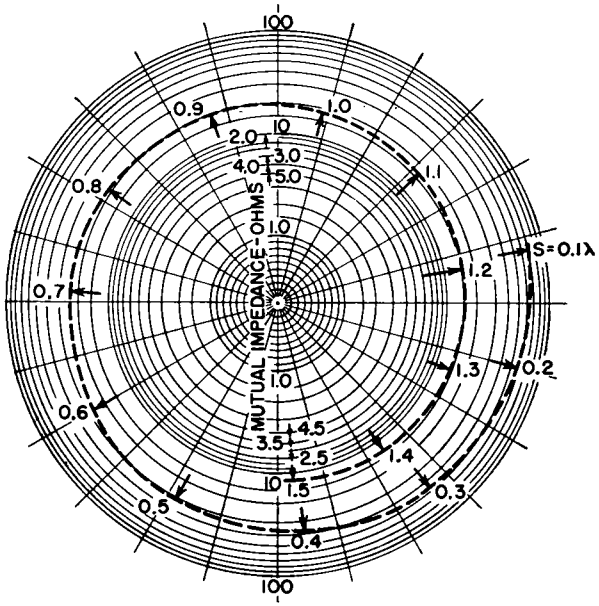

FIG. 3.61. Mutual impedance between two parallel nonstaggered half-wave dipoles with spacing S. (*After Carter.*)

before the system is constructed. Unless the complete project is done in this manner, its objective may not be realizable because it is always impractical, and usually impossible, to cut and try here and there to correct for errors in the system design. There are too many interdependent variables involved to permit adjustment by manipulation, even if the critical locations were accessible after the array is in place.

The system must therefore be built precisely to the final dimensions, and it must work the first time. This requirement is the same as for the medium-frequency broadcast directive systems discussed in Sec. 2.7.3; but there the feed terminals of the various radiators were physically accessible, and it was therefore possible to trim the adjustments slightly to obtain the final degree of correct operation. This is usually impossible in high-frequency antennas.

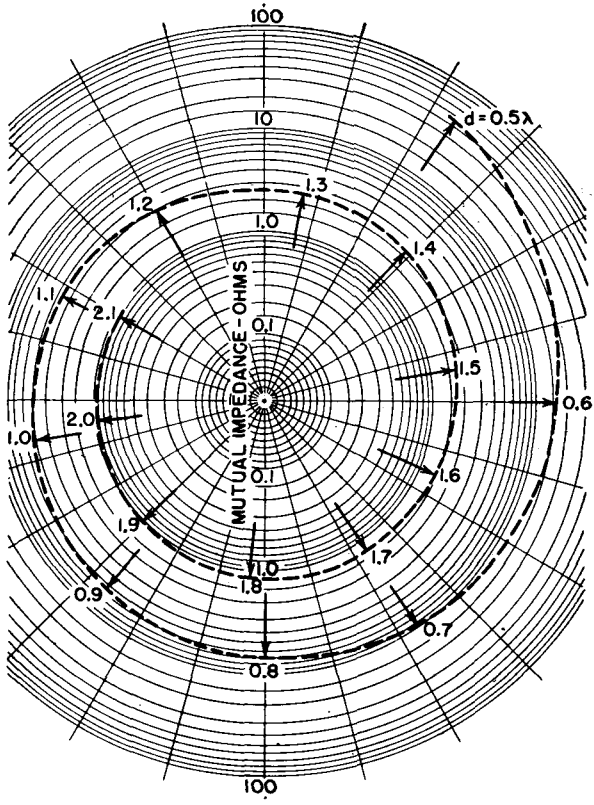

FIG. 3.62. Mutual impedance between two collinear thin half-wave dipoles. (d is the distance between dipole centers.) (*After Carter.*)

3.18. Feeding Power to Dipole Arrays Using Half-wave Spacings

The attainment of a desired radiation pattern depends upon the realization of certain specified spatial current distributions. The radiators are located in a prescribed geometrical arrangement and have current amplitudes and phases that are derived from the design of the radiation pattern. The circuital design of a radiating system starts with a study of ways and means to obtain the prescribed currents in the various radiators of the entire system and to bring the correct impedance at the main feed point to terminate the power transmission line. The other aspects of the circuital design for a system include a determination of the potentials and currents which will exist when the system is energized at specified power input, and the specifications for the conductors and the insulators are based on these.

Feed-system techniques are as varied as the types of systems that

may be used. Considerable inventive ingenuity may be required to design a feed system for one of the more complicated arrays. The simplest feed method occurs in systems where several identical half-wave radiators with equal cophased currents are used in a symmetrical array with half-wave spacing. The properties of a half-wave section of feeder have special utility in such applications, tending to equalize small irregularities in impedances and currents among the various elements. Large beam arrays of the type shown in Fig. 3.100 are constructed for operation on a specified frequency by cutting the radiators to a length slightly less than one-half the free-space wavelength to account for end effects and end capacitance due to insulators and attachments, the feeders being cut to one-half wavelength. If the dipoles are to be end-fed from standing waves on the feeder, the dipoles are located at potential-maximum points on the feeder. Balance of the feeder is maintained by attaching dipoles on opposite sides, which makes a pair of dipoles thus fed have equal cophased currents. The next pair of dipoles is located one-half wavelength along the feeder, where equal potentials, of opposite phase, are located. To cophase this second pair of dipoles with the first, the feeder is transposed 180 degrees. In this way a vertical stack of dipole pairs can be fed. If the number of pairs of such dipoles is very large, the attenuation in the feeder, due to its distributed loading, begins to be a factor to consider, as it will cause the outermost dipoles to have lower current amplitudes than those nearest the source. This effect is usually negligible until the number of pairs of radiators exceeds four. Beyond this number, it is desirable to bring the main power feeder up to the middle of the dipole feeder and branch symmetrically from this point.

In order to transpose a balanced feeder of the two-wire type, it is necessary to use insulators to maintain constant spacing through the transposition. The presence of these insulators can reduce the velocity of propagation in the feeder and change its electrical length. If the velocity reduction is more than 2 or 3 per cent, it may be necessary to reduce the spacing of the dipole pairs along the feeder by an equivalent amount or there will be a cumulative phase discrepancy in the currents in the successive dipole pairs.

The feeding of collinear dipoles from one end, as in Fig. 3.38, requires the employment of means to connect them in series through quarter-wavelength balanced feeder stubs to cophase and equalize currents in the dipoles not directly attached to the main feeder. Figure 3.49*B* is a schematic example of a 6 by 4 array with one central feeder, using series excitation in the three dipoles each side of the center.

Nearly uniform currents can be obtained throughout an array of the larger sizes by the method of Fig. 3.49*A*, where each vertical feeder has

but one pair of dipoles attached at each level. The main power feeder is branched into the desired number of vertical feeders, taking the necessary precautions to excite the resulting sections of the array uniformly in current and phase. However, if there is a phase difference between the two sections of an array of the type of Fig. 3.49*A*, the main beam is deflected away from the broadside position, one way or the other, depending upon the polarity of the phase difference. Use is made of this fact to slew a beam a few degrees.

The feed-point impedance of a pair of end-fed radiators will depend upon the characteristic impedance of the conductors comprising the dipoles, upon their electrical exact length, and upon the radiation couplings to all other dipoles, ground images, and reflector images. The impedance of a pair will change with any change in its position in the system with respect to other dipoles. The dominant element of mutual impedance from other dipoles will of course be from the nearest parallel pair(s) or from the ground images for very low antennas. The nearest collinear pair has a mutual impedance that is relatively small compared with that from the parallel pair. Other echelon pairs will have intermediate effects.

Mutual impedances decrease as distance between dipoles increases. In arrays requiring systematic current distributions it is necessary to compute as accurately as possible, in advance, the impedance at every feed point and to provide the proper excitation at each such point to realize the desired performance.

A broadside array of the horizontal half-wave-dipole type with half-wave spacings is often built to use a second identical curtain of dipoles in a close-spaced parallel plane to obtain reinforcement of fields on one side and partial suppression on the other. One curtain is energized by feeder and the other energized parasitically from the field of the first. A short circuit is placed at the proper point in the main feeder for the reflector curtain to obtain optimum unidirectivity. The radiator and reflector curtains can be interchanged by switching to reverse the direction of the main beam. Unidirectivity can also be obtained, and much more effectively, by using an untuned, passive reflector.

3.19. Input Impedance to Any Radiator in an Array of Dipoles

To excite a radiating system properly, each radiator must have a current of the proper phase and amplitude. Except in the simplest cases, this requires a knowledge of the input impedance of each radiator, due to its self-impedance Z_{kk} and the mutual impedance with all other radiators and images of the system. In practice, certain mutual effects can be neglected when it is known that they are of trivial magnitude

compared with certain dominant ones. A complete solution, however, must account for the total of all these effects, especially if the currents are to be unequal.

When the elements of an array are half-wave dipoles, prepared data given in Figs. 3.61 and 3.62 may be used for the mutual impedances for parallel and collinear dipoles. Echelon and angular configurations must be computed from basic formulas.[1002] Most data of this sort are referred to a current antinode for a half-wave element having sinusoidal current distribution. When half-wave elements are end-fed, the antinode values of impedance must be transformed through one-quarter wavelength of the characteristic impedance of the element used. Such transformations lead to approximations that are of tolerable engineering accuracy.

Mutual impedance is defined as the negative ratio of the induced electromotive force at a current antinode in radiator 2 due to the antinode current in radiator 1.[1019] By reciprocity, the effects both ways are equal. Thus

$$Z_{12} = Z_{21} = -\frac{V_{21}}{I_1}$$

When the values of self- and mutual impedances are known, the system can be computed according to network theory, using the complex form for both currents and impedances. It is emphasized that a vector mutual impedance can lie in any one of four quadrants, and due care must be observed in the computation to account for the most general conditions. When all the currents are equal and cophased, the computations are relatively simple. When the various radiator currents are unequal in amplitude and phase, computations are more complicated.

The equations used to compute the input impedances are as follows: (All V's, I's, and Z's must be in complex (vector) form, indicating magnitude and phase.)

$$\begin{aligned}
V_1 &= I_1Z_{11} + I_2Z_{21} + I_3Z_{31} + \cdots I_nZ_{n1} \\
V_2 &= I_1Z_{12} + I_2Z_{22} + I_3Z_{32} + \cdots I_nZ_{n2} \\
&\cdots\cdots\cdots\cdots\cdots\cdots\cdots\cdots \\
V_n &= I_1Z_{1n} + I_2Z_{2n} + I_3Z_{3n} + \cdots I_nZ_{nn}
\end{aligned}$$

for n radiators numbered in order from 1 to n, having self-impedances Z_{11}, Z_{22}, Z_{33}, etc., and mutual impedances between elements as indicated by the subscripts. Images in the earth and in reflector screens are treated as discreet radiators, taking into account the proper relative directions of currents in corresponding images.

The symmetry characteristic of high-frequency arrays reduces the labor of computation because the computation does not have to be carried

out for every radiator in the system. Unsymmetrical arrays require the full treatment.

An element of the system that is parasitically excited from the radiation field of some other element has its potential equated to zero.

The impedance of any radiator k, when properly functioning in the system to give the required radiation pattern, is then the ratio $Z_k = V_k/I_k$, where in general all values are complex. With a knowledge of the feedpoint impedance in each radiator of a system, the feeder requirements can be developed for impedance, amplitude, and phase matching of all the currents back to the main power feeder.

Figure 3.18 gives the impedance at the center of a half-wave horizontal dipole, taking into account the mutual impedance with its image, assuming perfectly conducting earth.

If a horizontal dipole is located a distance h degrees above a perfectly conducting earth and a distance d degrees in front of a vertical infinite reflecting plane, there will be inverted images of the dipole a distance h below the surface of the earth and another a distance d behind the reflecting screen. In addition, there will be a third image having the same polarity as the radiator, and located below earth level at the corner of the rectangle $2h \times 2d$ formed by the radiator and its two primary images. The impedance of the radiator in this arrangement is

$$Z_1 = Z_{11} - Z_{12} - Z_{13} + Z_{14}$$

where Z_{12} is the mutual impedance with the earth primary image, Z_{13} is the mutual impedance with the screen primary image, and Z_{14} is the mutual impedance with the earth secondary image.

In all cases where there are two or more primary images there may be one or more secondary images. A radiator located in a corner between intersecting 90-degree planes has two primary images and one secondary image. When the radiator is located between two planes intersecting at 60 degrees, there are two primary images and three secondary images, the polarity of successive images being reversed. For intersecting planes at random angles that are not equal fractions of a circle, there may be an infinity of secondary images. Such cases seldom arise in practice except with the corner-reflector type of system or when a radiator is located between parallel and near-parallel conducting planes. One can study the complex images in such cases with mirrors placed at proper angles, as in a kaleidoscope, using a dot to represent the end of the radiator.

Two identical parallel radiators having equal cophased currents have equal input impedances computed from

$$Z_1 = Z_2 = Z_{11} + Z_m$$

In the case of equal antiphased currents,

$$Z_1 = Z_2 = Z_{11} - Z_m$$

This condition explains why a radiator parallel to and with very small spacing from a conducting plane has its input impedance greatly reduced by the effect of the relatively large value of Z_m. Thus, for a given power input, the current must be large, and the potentials on the radiator are relatively large as a consequence. Both these factors contribute to increased losses beyond a certain proximity where losses neutralize theoretical gain. This is an example of a general practical fact that high gain in limited space is always attended with limitations due to losses, since all such systems have low input resistance and low radiation resistance. Bandwidth is also reduced in such systems.

Curves of mutual impedance between parallel and collinear half-wave dipoles are given in Figs. 3.61 and 3.62. For formulas for the mutual impedance between dipoles in echelon and at an angle to each other in a common plane, consult Carter (ref. 1019), Brown (ref. 4, Chap. 2, page 192), Kraus (ref. 1002), and Terman (ref. 1005).

It is seen from Fig. 3.61 that the magnitude of mutual impedance between parallel half-wave dipoles does not fall to one-tenth of the self-impedance of such a dipole until their spacing is greater than two wavelengths. This indicates that mutual impedance should be included in computations for parallel dipoles at least two wavelengths away, and preferably to about twice this distance. For collinear dipoles, Fig. 3.62 shows that the mutual impedance diminishes rapidly as the distance between adjacent ends is increased, so that practical computations for radiator impedances can neglect collinear mutuals when their ends are spaced one wavelength or more. Using these two limits as a guide, we may conclude that practical computations of sufficient engineering accuracy can be obtained by neglecting mutual impedances less than 5 per cent of the self-impedance in cases where there are uniform currents. Since current amplitude is a coefficient for mutual-impedance terms, a system having currents of widely differing amplitudes cannot be simplified in this manner.

The input impedance of a half-wave dipole with a parasitic identical dipole in its field is computed from

$$\begin{aligned} Z_1 &= Z_{11} + kZ_{12} \\ 0 &= Z_{12} + kZ_{22} \end{aligned}$$

in which k is the complex ratio of I_2/I_1. In such a case, with but one parasitic element, the system is determinate and can be computed from known self- and mutual impedances. With more than one parasitic

element, the system is indeterminate because there is insufficient information for a complete solution (see Figs. 3.63*A* and 3.63*B*). Systems using two or more parasitic elements are empirical and must be designed experimentally, though some success by computation can be obtained in simple systems by the method of successive approximations.

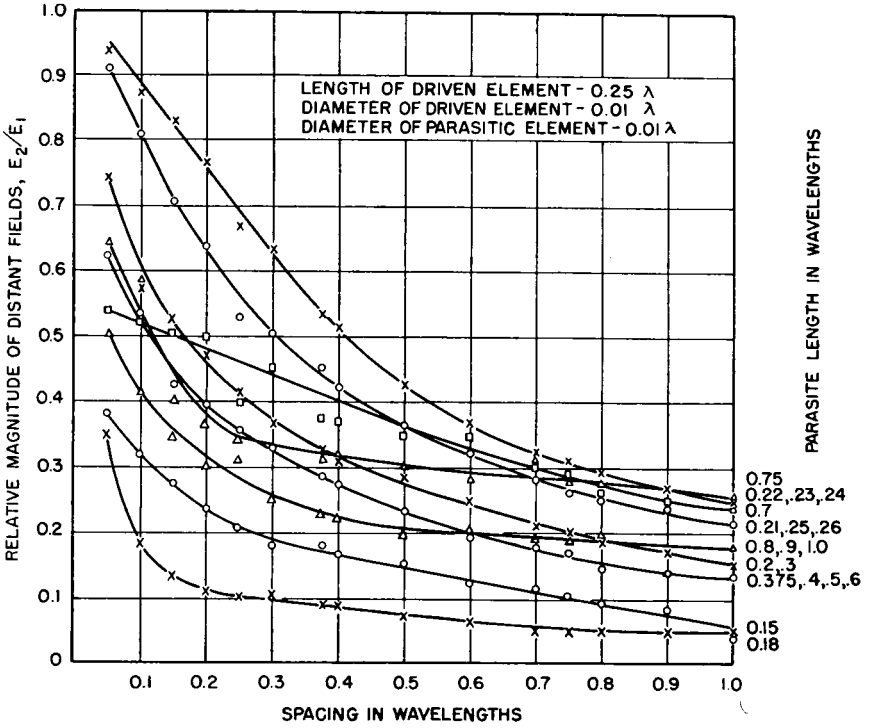

FIG. 3.63*A*. Relative magnitudes of distant fields E_2/E_1 for driven quarter-wave unipole and parasitic unipoles of different lengths and spacings. (*After Abbott and Fisher.*)

The block of simultaneous equations (page 296) applies to any system of radiators having any arbitrary current distributions and any geometrical relationships. The reference points at which the impedances are computed may also be arbitrary. However, the values of self- and mutual impedances will be different in every such case and must usually be computed individually according to the conditions of the case. Equations for most conditions of practical interest have been developed and published for sinusoidal current distributions which are approximated by standing-wave systems. Mutual impedances between radiators carrying traveling waves have to be computed from basic electromagnetic theory.[1021]

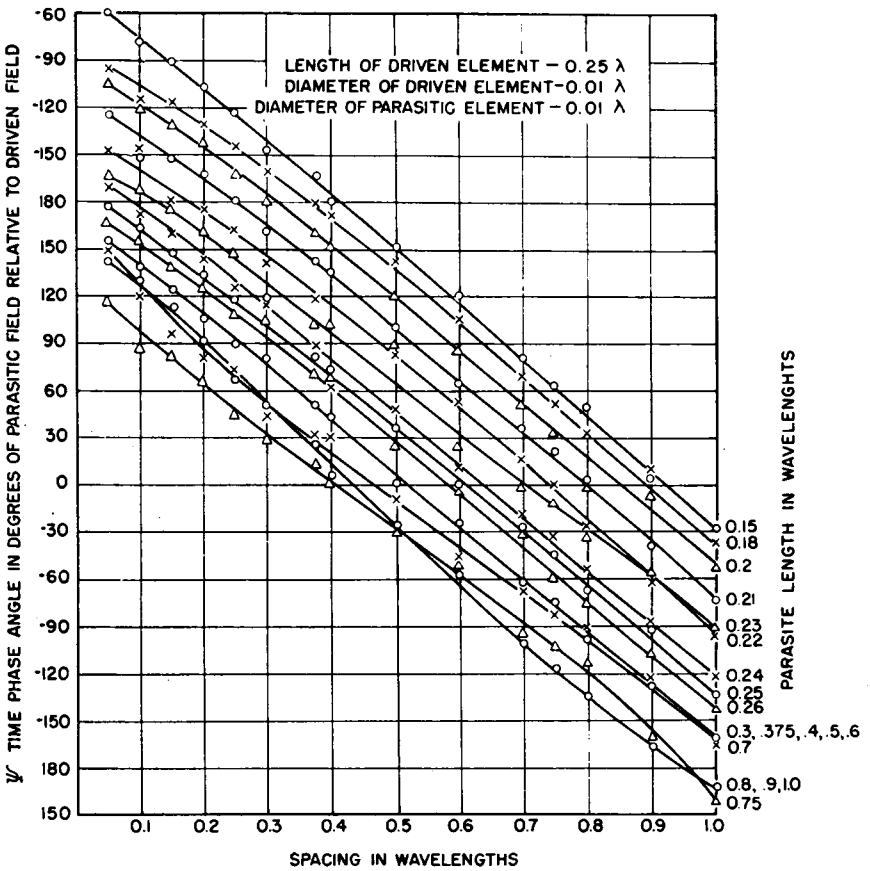

FIG. 3.63*B*. Time-phase angle, in degrees, for driven quarter-wave unipole and parasitic unipoles of different lengths and spacings. (*After Abbott and Fisher.*)

3.20. Fourier Current Distributions[1067,1087]

By the Fourier analysis of a specified radiation pattern, it is possible to find a combination of pairs of radiators with current distributions in accordance with the Fourier coefficients which will produce that pattern, as discussed in Sec. 2.18. When applied to broadside arrays of dipoles with half-wavelength spacings the analysis is made very simply by the well-known methods of alternating-current harmonic analysis, except that in this case the harmonic term is the spherical harmonic, which is the pattern for a symmetrical pair of radiators. Therefore

$$f(\beta) = \text{even function} = A_1 \cos (90 \sin \beta) + A_2 \cos (270 \sin \beta) + A_3 \cos (450 \sin \beta) + \cdots + A_n[(2n-1)90 \sin \beta]$$

$$A_n = \int_0^{90} f(\beta) \cos [(2n-1)90 \sin\beta]\, d\beta$$

Figure 3.64 shows the manner in which the Fourier coefficients are applied to the cophased currents in a symmetrical series of radiator pairs.

The special advantage of Fourier distributions is that a distribution can be found which will produce a pattern of any specified symmetrical shape, the number of pairs used determining the degree of realization

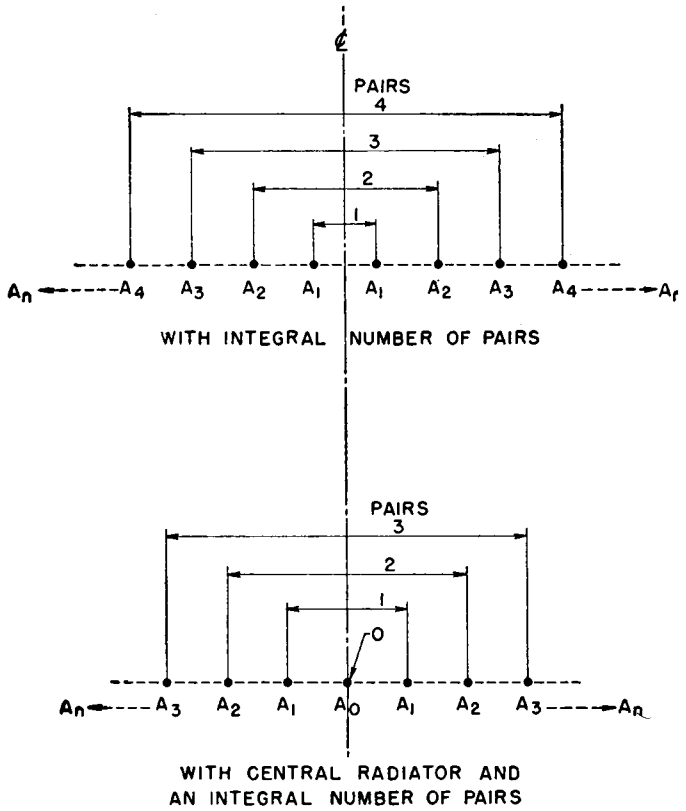

FIG. 3.64. Fourier current distributions for broadside patterns.

of the specified pattern. The above equations apply only to the case where $f(\beta)$ is an even function, though the method may be applied to odd functions or to asymmetric functions that are combinations of both types. One specified characteristic of the desired pattern may be the suppression of secondary lobes over certain ranges of angles and a specified shape of pattern within those angles where radiation is wanted.

3.21. Long-wire Antennas

The simplest high-gain antennas (structurally) are those using electrically long wires in various configurations. The length of the wires may

be from one to eight wavelengths or more, and several of these wires may be used, according to the particular performance desired. Long wires may be excited so as to support standing waves or traveling waves. Practical circumstances of construction and feed, however, are of a compromising nature so that a standing-wave system always contains a substantial component of traveling wave, and vice versa.

It is one of the paradoxes of engineering in this field that the simplest antennas are the most difficult to analyze. Long-wire antennas, which permit the simplest structures for a given performance, involve an enormous amount of computation to determine their performance. Furthermore, an accurate analysis is virtually impossible because of the several empirical factors present.

In view of the importance of long-wire-antenna technology and the difficulties of precise analysis, it is necessary to examine in some detail the principles of long-wire systems of both standing-wave and traveling-wave types.

3.21.1. Long Wires with Standing Waves. If it were possible to excite a long, straight wire so as to have several successive nodes and antinodes of current along its length in the form of a pure standing wave, such a wire, in free space, would have a radiation pattern of the form shown in Fig. 3.65. Such patterns, in general, have the following properties:

Each lobe is actually a cone of radiation, the largest being that between the axis of the wire and the first node in the pattern. The pattern is symmetrical about the normal plane passing through the middle of the wire. Each side of this plane there is a lobe, or cone of radiation, for each full wavelength of wire.

If the amplitude of current at each antinode is identical throughout the wire, and if the wire is an integral number of half wavelengths, then the envelope for the field-strength pattern for the system is a line (or cylinder) parallel to the wire itself and tangent to the main lobe. This is illustrated by the right-hand pattern of Fig. 3.66, which represents the pattern of an eight-wavelength wire with sinusoidal standing-wave current distribution.

If the wire is of arbitrary length, then the various minor lobes are irregular and do not extend as far as the tangent to the main lobe. The left-hand portion of Fig. 3.66 shows the radiation pattern for a $7\frac{3}{4}$-wavelength antenna to illustrate this effect.

When the wire is end-fed, as is often the case in practice, the radiation losses for a long wire cause a substantial traveling wave to exist, which causes the amplitude of successive current maximums to taper off toward the free end. This causes the pattern for a system to become intermedi-

ate between that of a pure standing-wave system and a pure traveling-wave system. This effect is shown in Fig. 3.23.

The shape of the field-strength pattern for a pure standing-wave sys-

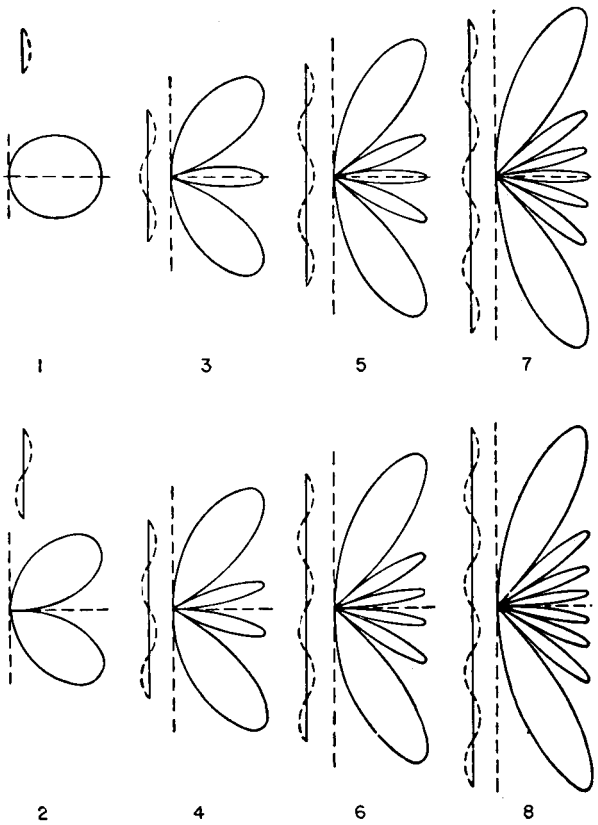

FIG. 3.65. Idealized polar patterns for straight wires with an integral number of half waves of pure standing-wave current distribution.

tem an integral number of half wavelengths long is specified by the relation:

$$f(\theta) = \frac{\sin\left(\frac{m\pi}{2}\cos\theta\right)}{\cos\theta}$$

in which m is the number of half wavelengths in the length of the straight wire bearing a pure standing wave. When m is an even number, the sine is used; the cosine is used when m is odd.

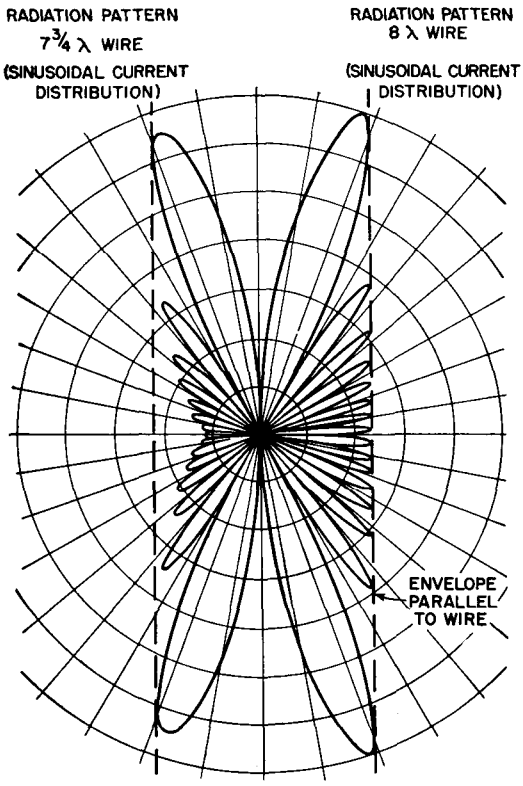

FIG. 3.66. Comparison of pure standing-wave radiation patterns for current distributions of 7¾ wavelengths and 8 wavelengths. (*After Carter.*)

3.21.2. Long Wires with Traveling Waves. If it were possible to excite a long, straight wire in free space so that there would exist on it a pure traveling wave of constant amplitude and uniform phase difference for all elements of length, the radiation pattern would possess the following general characteristics:

The largest radiation lobe would lie between the wire (in the direction of the traveling wave) and its first null. All successive lobes decrease rapidly and regularly in amplitude following the law $\sin \theta_m/(1 - \cos \theta_m)$, where the θ_m are the angles at which the successive maximums occur in the pattern. There is a lobe for each half wavelength of length. Half of these lobes are tilted in the direction of wave travel in the wire, and the other half, which are of relatively smaller amplitude, are tilted away from the direction of wave travel in the wire. The pattern of lobe amplitudes is therefore not symmetrical about the plane normal to the wire and passing through its mid-point, but the angles of nulls are sym-

metrical to this plane when the wire is an integral number of half wavelengths long.

As the length of the wire increases, the direction of the main lobe is pressed closer to the direction of the wire. It cannot ever approach the direction of the wire and in practice is never used closer than 15 or 17 degrees from the direction of the wire.

The complete pattern for a pure traveling-wave current distribution in a straight wire in free space can be quickly constructed with the aid

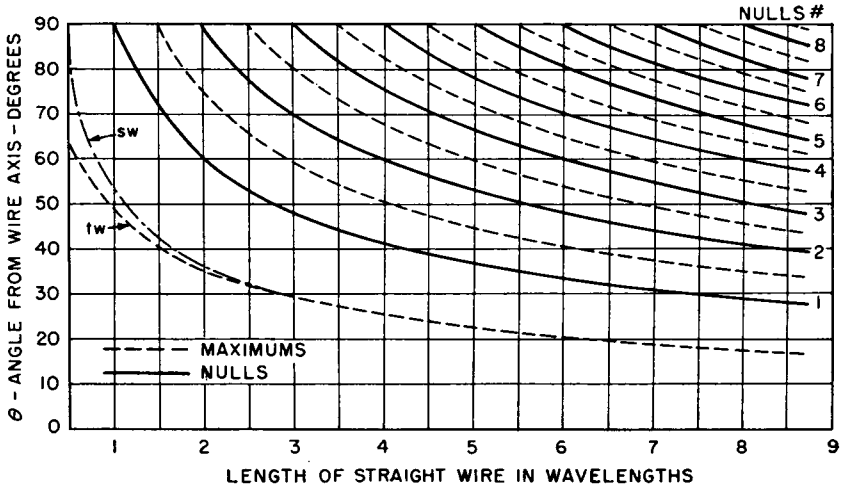

FIG. 3.67*A*. Angles of maximums and nulls in long wires carrying pure standing waves (SW) and pure traveling waves (TW) for the forward half of pattern. (The differences appear only in the direction of the first maximum.)

of Figs. 3.67*A* and 3.67*B*. Figure 3.67*A* provides the angles of the maximums and nulls; Fig. 3.67*B* provides values for the successive maximums. When these points are plotted in rectangular coordinates, the function can be sketched with a fair degree of accuracy through these points. The accuracy is increased if cognizance is taken of the fact that the direction of the field is reversed in successive lobes, using positive and negative values alternately to represent their amplitudes.

The shape of the field-strength pattern for a straight wire in free space carrying an unattenuated traveling wave of current may be found from the equation

$$f(\theta) = \frac{\sin\theta \sin\left(\frac{G}{2}\operatorname{vers}\theta\right)}{\operatorname{vers}\theta}$$

where versine $\theta \equiv 1 - \cos\theta$ and G is the electrical length. Some pat-

terns from this equation for lengths from $\lambda/2$ to 4λ are exhibited in Fig. 3.68.

With the exception of the angle of the maximum in the dominant lobe for a wire less than three wavelengths long, the angles of nulls for both

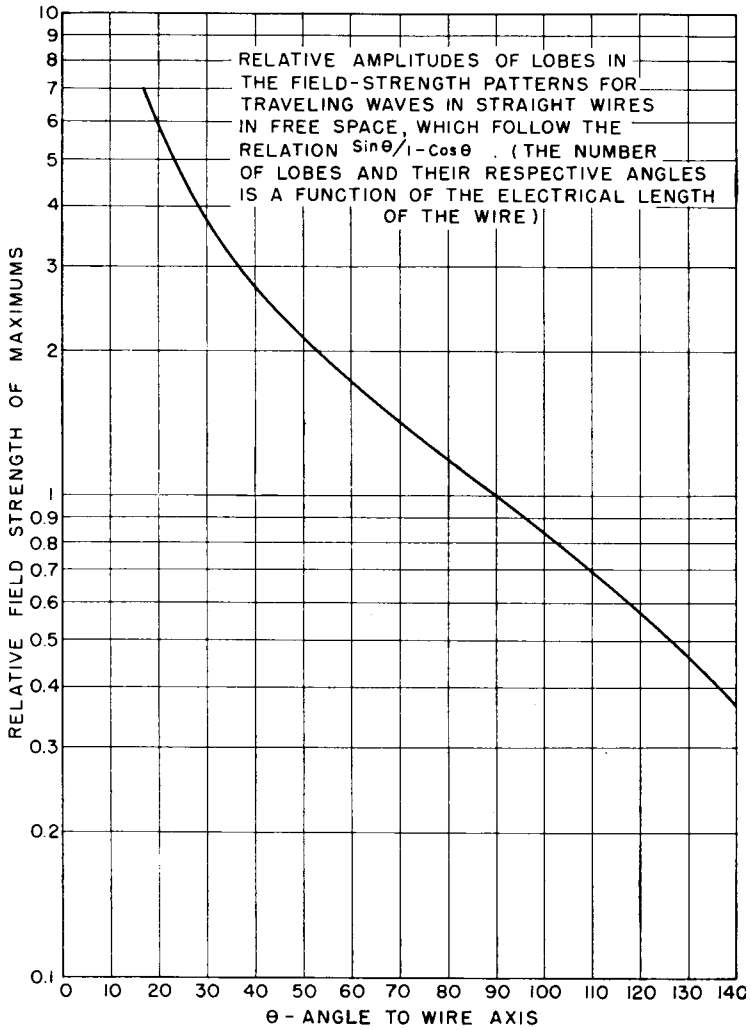

FIG. 3.67*B*

standing-wave and traveling-wave distributions are the same. The difference between the patterns for the two different types of waves rests wholly in the amplitudes of the successive lobes. It is seen from Figs. 3.68 and 3.69 that the pattern for the traveling-wave tends to be uni-

directional, since the envelope for the successive lobes is cardioidal. This fact gives special value to the use of traveling waves for excitation of long wires where a unidirectional characteristic is desired. Otherwise, the number of lobes and nulls being the same for both fundamental forms of excitation of long wires, there is the common characteristic of a radia-

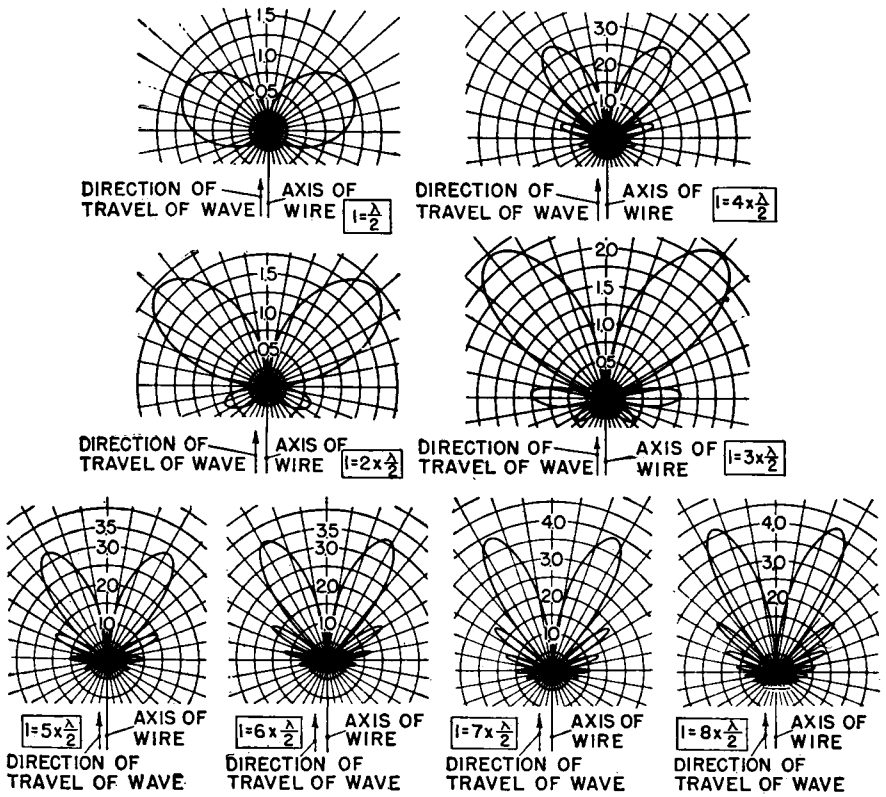

FIG. 3.68. Field patterns due to a straight wire carrying traveling waves. (*From RAF Signal Manual.*)

tion lobe for each half wavelength of wire. The multiplicity of lobes inevitably present when the wire is sufficiently long to give extreme directivity in the main lobe is one of the principal disadvantages of long-wire antennas. When long wires are used as elements of radiating systems, as in rhombic and V harmonic-wire antennas, there are many parasitic lobes extending in many directions. These parasitic lobes limit the directivity of an array made up of long wires. However, the economy and structural simplicity of long-wire antennas have given them

great popularity, in spite of their faults with regard to parasitic lobes. These faults must be kept in mind in applying them practically.

Figure 3.66 also suggests that, in a practical system having some traveling wave and some standing wave, the angles of the nulls would remain constant but that the nulls would degenerate to minimums and the maximums would tend to asymmetry as the ratio of traveling wave to standing wave increased. Also, the angle of the first maximum would be tilted more and more toward the wire as the amount of traveling wave present increased. Indeed, this was already evident in Fig. 3.23.

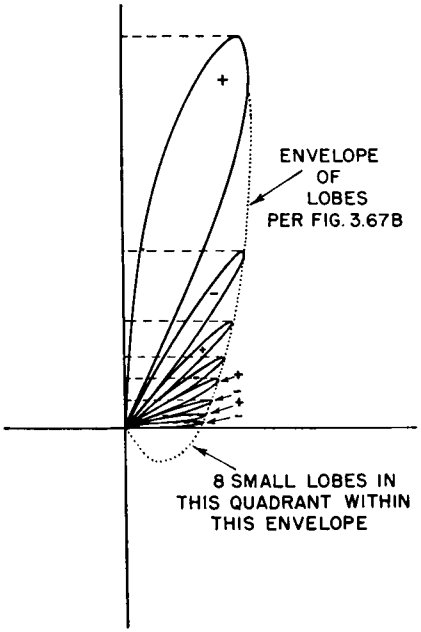

FIG. 3.69. Field pattern for a straight antenna eight wavelengths long with pure traveling wave.

3.21.3. Long Wires as Directive Antennas for High Frequencies. The intrinsic directivity of a single long-wire radiator makes it useful for some elementary applications. The presence of ground beneath the antenna modifies its pattern, of course, the extent of modification depending on the height above ground and its orientation with respect to ground. In such applications, the main lobe resulting from direct and image radiations is focused in the direction of optimum propagation to the desired distant receiving point, and the other lobes fall where they will. Interference between direct and image radiations causes some of the parasitic lobes to be reduced or canceled and others to be reinforced. The orientation of the wire with respect to the propagation path and ground determines the polarization of the wave transmitted (or received) on the main lobe of the pattern.

Figure 3.70 shows how a tilted long wire with standing waves can be constructed for vertical polarization of the main lobe. In this arrangement, the plane through the antenna and its image is oriented directly toward the distant communication point. The angle θ_0 between the wire and ground is usually of the order of the angle between the wire and its first maximum for the electrical length of the wire employed. In some cases the angle of tilt may be as large as the angle of the first null. The

choice is determined by the desired elevation of the beam. The symmetry of lobes in the radiation pattern from a standing-wave antenna gives a bidirectional radiating system. The system is excited unbalanced against ground, and for this reason a radial ground system of wires slightly above, on, or beneath the ground is necessary to avoid terminal ground losses.

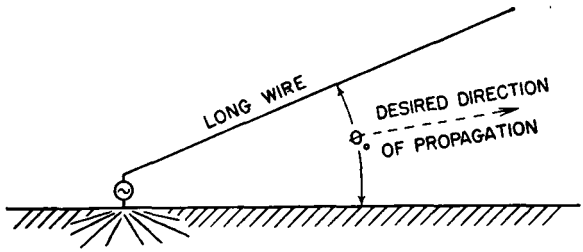

FIG. 3.70. Tilted long wire for directive transmission using standing waves.

An equivalent form of antenna using a traveling-wave current distribution is shown in Fig. 3.71. This is in all respects the same as Fig. 3.70 except that the end of the wire is terminated so as to suppress reflections from the outer end and thus to suppress standing waves. A free end that is one-quarter wavelength long gives an impedance at its inner end that is very low with respect to the characteristic impedance of the system at some chosen frequency of operation. This permits the inser-

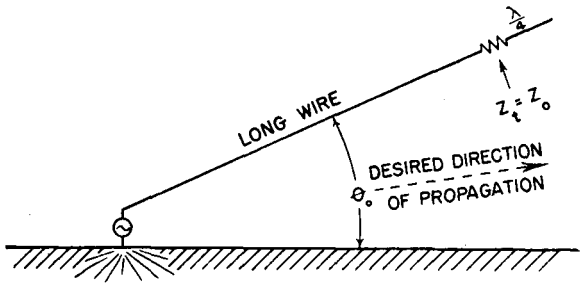

FIG. 3.71. Tilted long wire for directive transmission using traveling waves.

tion of an impedance Z_t which is given a value equal to the characteristic impedance of the system. This termination must dissipate all the power that would otherwise be reflected if the system were not so terminated. The radiation pattern for this system is essentially unidirectional.

The presence of the terminating impedance naturally decreases the selectivity of the system, because the impedance of the open-ended quarter-wave projection will remain low with respect to the impedance Z_t over a band of frequencies on each side of that at which it is resonant.

By making the characteristic impedance of the quarter-wave projection lower than that for the remainder of the system, the bandwidth of the system as a whole can be increased further when necessary.

If still wider bandwidth termination is wanted, two or three mutually perpendicular projections can be used at the end which are resonant to different frequencies within 3 or 5 per cent of the mean frequency. Resonating in turn over the band, the projections serve to maintain a low impedance at the outer end of the impedance Z_t and so maintain a more constant termination impedance over a band of frequencies.

As in all traveling-wave systems, it is advantageous, for improved transmitting radiation efficiency, to use a low characteristic impedance so that the antenna current will be a maximum for a given power input.

Experiment has shown that the correct termination of a long wire in this manner requires a complex impedance and not solely a resistance. The terminal impedance for suppressing standing waves is not a constant value but varies with the length of the wire. The terminal impedance is of the type $R + jX$. The inductive reactance can be obtained from the extension wire by making it longer than one-quarter wavelength. This means that the correct resistance, determined by experiment, must also be located in the correct place along the wire, and that the correct location is more than one-quarter wavelength from the end of the wire. The resistance has an order of magnitude of 400 to 600 ohms in many cases, and 500 ohms is suggested as a starting value for the trials when the antenna consists of a single wire. The reactance values required usually lie between $j150$ and $j250$ ohms, so that, with a thin wire, the extension would be somewhere around 105 degrees long.

Correct termination is best indicated by measuring the current distribution in the wire with inserted ammeters or a sliding ammeter inductively coupled to the wire. The distribution is complicated until the final correct termination is obtained; hence observations of current distribution should be made at several points along the entire length of the antenna.

Horizontal polarization is generally preferred in high-frequency transmission. The same techniques described in the two preceding cases can be applied to systems that transmit or receive horizontally polarized waves. The same long wires are then placed parallel to the ground, but at an angle to the desired direction of propagation equal to that shown in Fig. 3.67*A* for the angle θ_m between the wire and the first lobe maximum. The same lobe on the other side of the wire will also be present when a single wire is used this way, and this is a major disadvantage. If a standing-wave excitation is used, there will also be two main backward lobes. This explains why antennas of this form are very seldom used.

However, it is possible to use two parallel horizontal wires carrying traveling waves to cancel one major lobe and reinforce the other. The radiation pattern then contains one main beam and the usual multiplicity of minor lobes. The plan view of an antenna of this type is shown in Fig. 3.72. The two wires are excited in phase opposition, so that they are balanced to ground. The same end details are used as in Fig. 3.71,

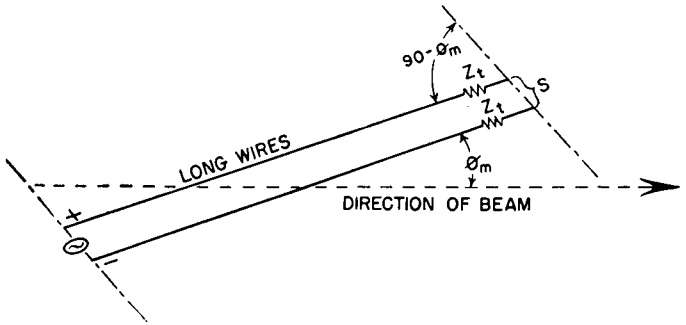

FIG. 3.72. Elementary two-wire traveling-wave antenna.

to suppress standing waves. The ends of the wires are staggered so as to form an angle $90 - \theta_m$ with the direction of the two parallel wires, in order to eliminate the other major lobe. The distance between wires as measured between the staggered ends is made equal to

$$S = \frac{1}{2 \cos (90 - 2\theta_m)}$$

For example, if the lengths of the wires inside of the terminating resistors Z_t were 5 wavelengths, the angle θ_m would be 22.5 degrees. The stagger in the ends of the two wires would be 67.5 degrees with respect to the wire direction, and the spacing would be 0.707 wavelength.

3.22. V Antennas

The V antenna uses two long wires in a balanced arrangement parallel to ground, with a mutual orientation which causes the main lobe from the two sides to add along the axis of the V at some desired elevation angle. The tilt of the horizontally polarized beam depends upon the length of a side, the angle formed by the sides, and also upon the height above ground.

V antennas have the following characteristics:

1. The structural design is simple and economical.
2. The electrical circuitry is simple, when they are fed from the apex.
3. High gain is secured at relatively low cost.
4. They use low supporting structures but require large areas.

5. The horizontal beam width and the elevation of the point of the main beam are not separately controllable but are mutually dependent on the geometry of the array.

Figure 3.73 shows a plan view of the electrical parts of a simple horizontal V made up of two wires, end-fed from a balanced feeder. In this

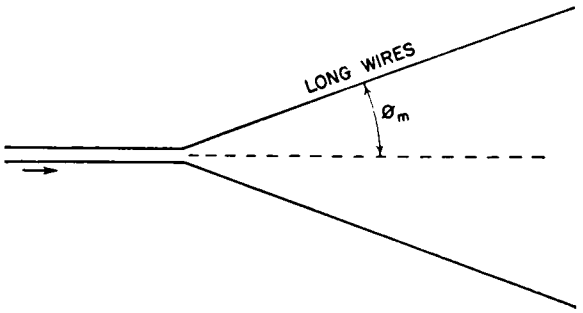

FIG. 3.73. Standing-wave V antenna.

form, there would be standing-wave excitation due to reflections from the open outer ends of the radiating wires. This system would therefore be bidirectional. The apex angle has a value somewhat less than twice the angle between the wire and the maximum of the first cone of radiation (θ_m) for the electrical length of the wire, as determined from Fig. 3.67. To obtain a unidirectional V antenna, the principle shown in Fig. 3.71

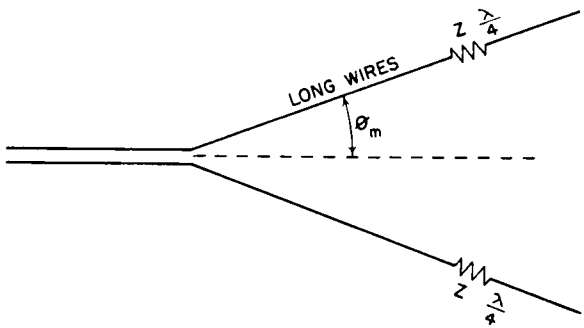

FIG. 3.74. Traveling-wave V antenna.

can be applied to each side, as shown in Fig. 3.74, so that traveling waves result.

It must be recognized that the geometry of long wires that causes the first radiation cones to add along the axis of the V is not that which fully cancels these same cones on the outer sides of the wires. There is characteristically a residual outer lobe of considerable amplitude at an angle of $2\theta_m$ each side of the axis. It is possible to reduce these unwanted lobes

by employing the principle indicated in Fig. 3.72, where a second parallel wire placed on each side, properly spaced, staggered, and excited, will do the necessary canceling at the angle $2\theta_m$ from the axis. For a traveling-wave system, this resulting configuration is shown in Fig. 3.75.

Traveling waves can be obtained by other methods of terminating the wires so that the excess energy arriving at the ends is dissipated. One

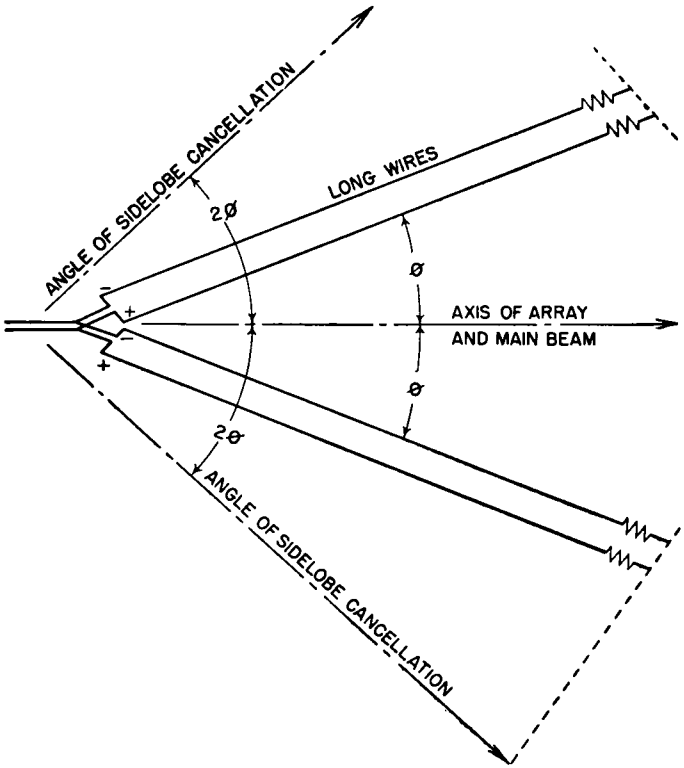

FIG. 3.75. Double traveling-wave V antenna.

such method is to continue each wire outward for a considerable distance very near to ground, after tilting them downward toward the ground from the antenna proper. This is a compromise measure, so devised as to permit very little radiation from the extension wire and at the same time to increase its attenuation rapidly by proximity to ground. The extension wires may be several wavelengths long but are necessarily of such a length that there is some 20 decibels of attenuation. The outer ends may be grounded (providing static drain) or left open-circuited. The extension wires may also be of iron to increase attenuation. In some past applications, the entire antenna has been tilted, using one high

support at the apex of the V and sloping both sides toward ground to the point where the extension wires can continue onward just above the ground. The simplicity of such a structure is very attractive from a cost standpoint, but its use must depend upon the radiation pattern in relation to propagation requirements.

Figure 3.76*A* is an isometric sketch of the arrangement of the RCA Model D antenna of the unidirectional V type excited by standing waves.

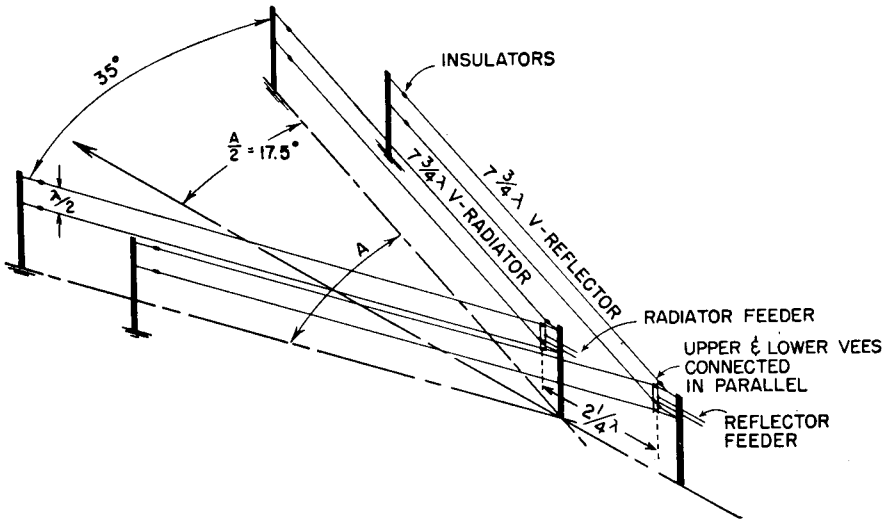

FIG. 3.76*A*. Scheme of the RCA Model D antenna.

One V acts as the reflector for the other to obtain unidirectivity horizontally polarized along the axis in the direction of the open end of the V. In this design, two wires are employed in each side of each V one above the other, cophased and spaced one-half wavelength. The length of each wire is an odd number of quarter wavelengths, which provides appreciable reduction of the amplitudes of some of the minor lobes, as shown in Fig. 3.66. The reflector is excited in quadrature-phase relation with respect to the inner V.

A unidirectional V antenna can be made by combining the fields from two standing-wave systems in close proximity, one obtained from a cosine distribution and the other from a sine distribution in quarter-phase relationship. This is an embodiment of the familiar Argand principle expressed by

$$\underset{\text{(standing wave)}}{\cos\theta} + \underset{\text{(standing wave)}}{j\sin\theta} = \underset{\text{(traveling wave)}}{e^{j\theta}}$$

The geometrical parameters are shown in Fig. 3.76*B*, together with the

elementary circuitry. The lower V, consisting of two wires longer than the driven V and using an adjustable stub section at its apex, is parasitically excited by the field of the driven V. The correct phasing to achieve the quadrature relation between the driven V and the parasitic

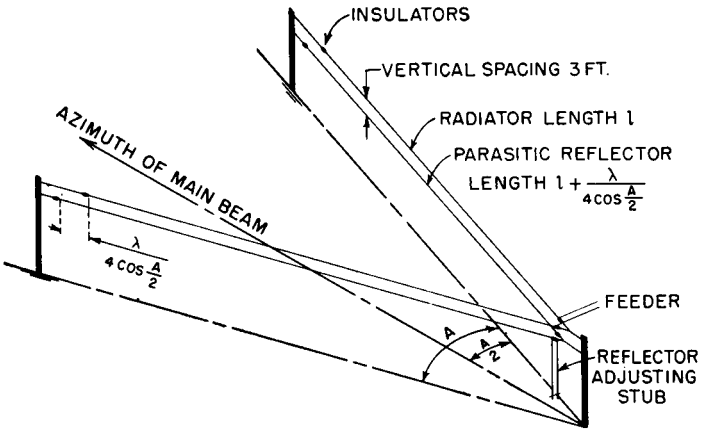

FIG. 3.76*B*. Scheme of the RCA Model G antenna.

V is obtained by adjusting the stub section at the apex. This system is known as the RCA Model G antenna.

3.23. Horizontal Rhombic Antenna

The commonest practical form of high-frequency antenna using the traveling-wave principle is the horizontal rhombic antenna, constructed as shown in Fig. 3.77. It is widely used in high-frequency applications for both transmitting and receiving. It has some marked advantages and disadvantages.

The advantages include simple construction, low-cost supporting structures, low cost of material, relatively high gain for the cost, broad frequency response from the impedance standpoint, minimum antenna potentials and currents for the power transmitted, inconspicuousness, easy maintenance and repair, almost no field adjusting required after installation, and the ease with which the height can be changed to obtain the optimum vertical angle as layer heights change through the sunspot cycle.

The disadvantages include large amount of land required; loss of power in the terminating load; a multiplicity of lobes of radiation in almost all directions, in addition to some rather large secondary lobes under the best conditions of design; compromises necessary from a propagation standpoint as the radiation pattern changes with frequency; limitation of gain and signal-to-noise ratio due to the multiplicity of radiation lobes;

difficulty of predetermining its complete performance due to the complications of computation and to the effects of attenuation and partial standing waves always present in practice; and inability to control the horizontal and vertical patterns separately.

For optimum performance, a rhombic antenna should be designed for use at one frequency or a very small band of frequencies, the pattern

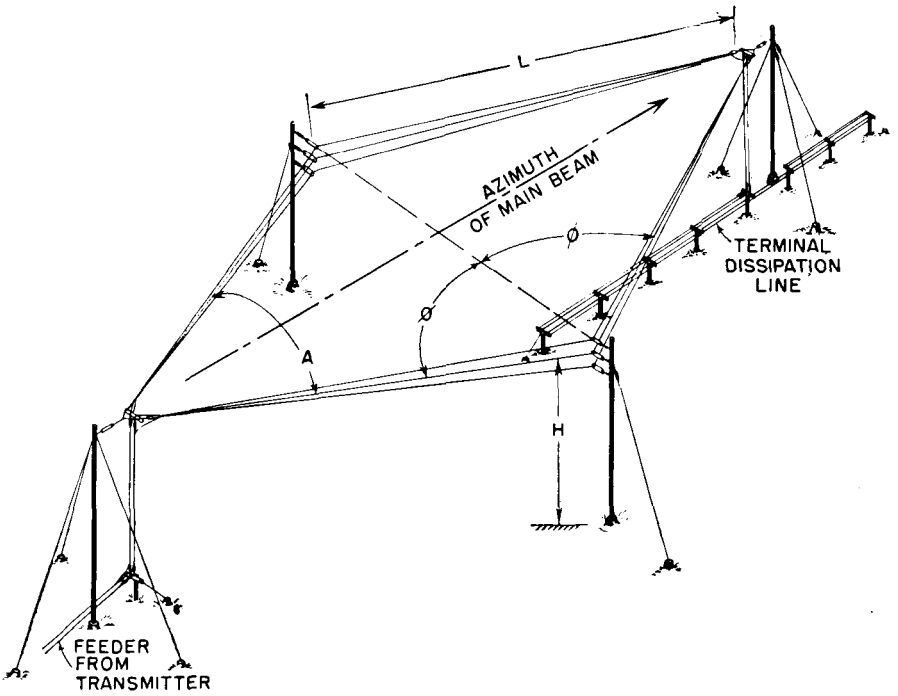

FIG. 3.77. Horizontal rhombic antenna (common three-wire form).

for which is best suited to the propagation conditions of the space circuit. Usually about all that a designer attempts to compute about this system is the characteristic of the main lobe. The enormous labor of computation has obscured its complete radiation characteristics.

There has been widespread confusion between the radiation performance of the horizontal rhombic and its circuitry. The input impedance may be uniform over a frequency range of 8 to 1 but its radiation characteristics are seldom satisfactory over more than 2 to 1 range.

The patterns (ref. 14, page 364) shown in Figs. 3.78 and 3.79 give an idea of the complete radiation patterns for typical rhombic antennas having parameters near the optimum for a frequency within a band of 2.25 to 1. The conditions are for a fixed structure as the frequency

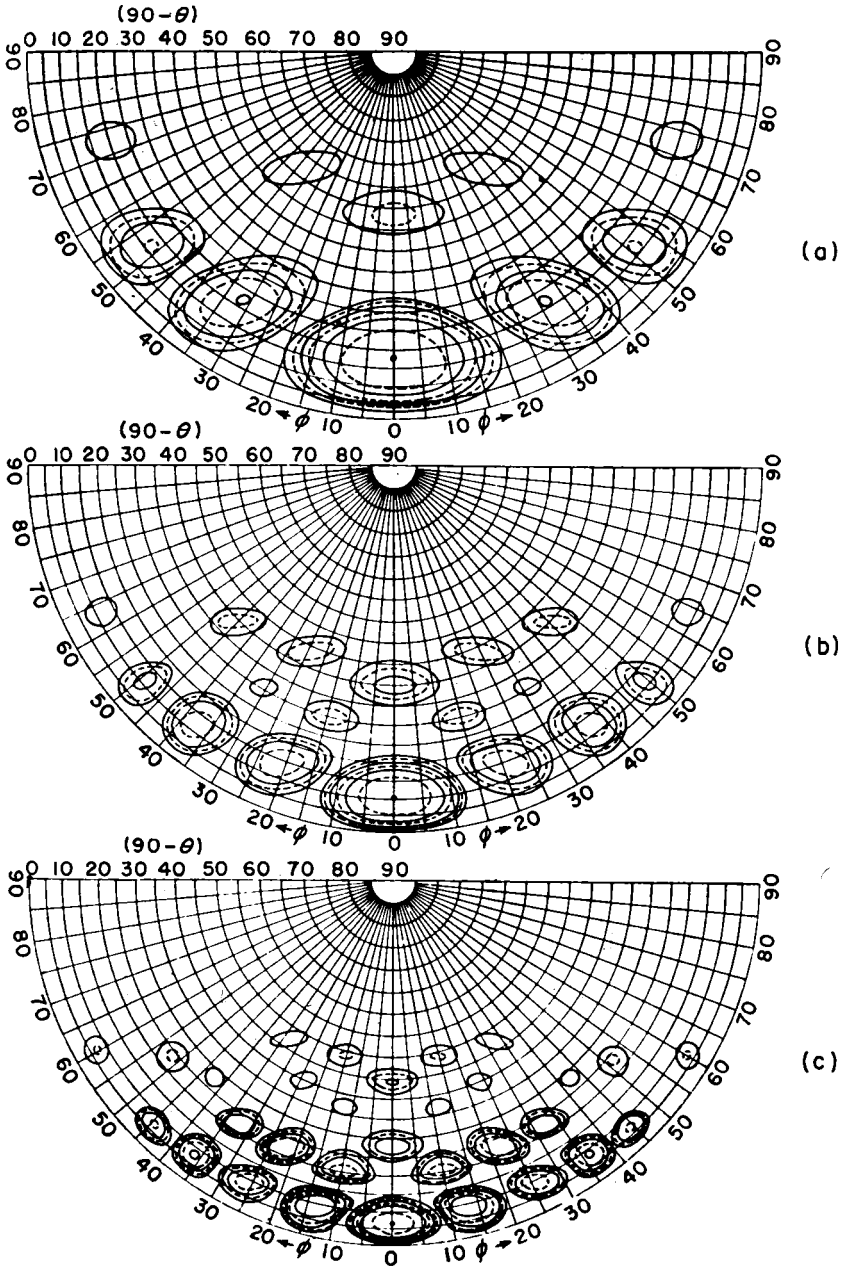

FIG. 3.78. Directive patterns for a rhombic antenna with an apex angle $A = 22$ degrees: (*a*) $l = 3.33\lambda$, $h = 0.8\lambda$; (*b*) $l = 5.0\lambda$, $h = 1.2\lambda$; (*c*) $l = 7.5\lambda$, $h = 1.8\lambda$. (*After Christiansen.*)

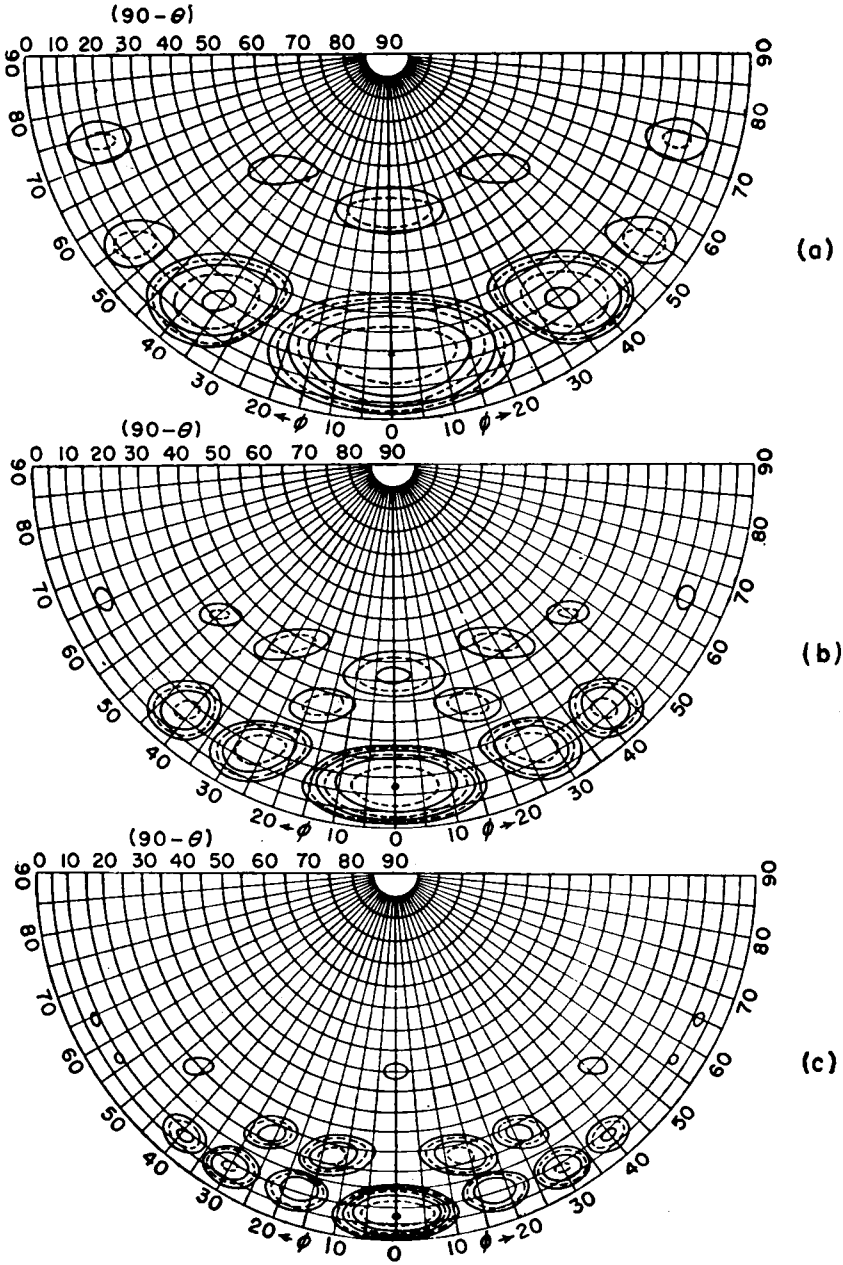

FIG. 3.79. Directive patterns for rhombic antenna same as Fig. 3.78 except that apex angle $A = 18$ degrees. (*After Christiansen.*)

is changed over this range. The outer periphery of each chart is the horizon of a flat earth, and the center is the zenith. The contours are in 3-decibel steps, the smallest shown being only 18 decibels below the amplitude of the main beam. There are many others below this value in the forward half of the hemisphere and also in the rear half, which is not shown. Imperfect construction undoubtedly accentuates these spurious lobes beyond the relatively ideal theoretical conditions represented in these figures. Christiansen has described methods by which

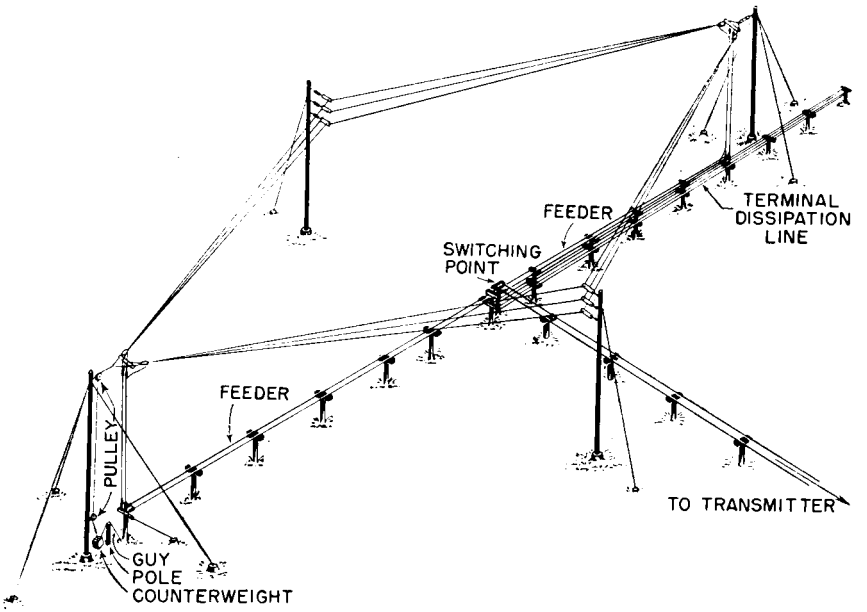

FIG. 3.80. Horizontal rhombic antenna with feeders arranged for reversing pattern.

these patterns can be improved, using tiered, broadsided and overlaid rhombic elements.

3.23.1. Radiation Characteristics. The horizontal rhombic antenna is pictured in Fig. 3.77 (unidirectional) and Fig. 3.80 (reversible). This construction, using two or three wires per side, is the preferred form for both transmitting and receiving. The original single-wire type is suitable only for receiving. The multiwire type has a flatter impedance-frequency response curve and lower characteristic impedance, which is of great importance for transmitting, and smaller pickup of precipitation static when used for receiving. The latter can be improved further by using insulated wires to prevent charged particles from coming in direct contact with the metal of the antenna and feeder system.

Each leg of a rhombic antenna has a radiation pattern which is the

result of an attenuated traveling wave, as indicated in Fig. 3.68. The length per leg l is usually great enough to cause its pattern to have many secondary radiation lobes (one for each half wavelength of length, if the main lobe is included). The over-all pattern is that due to interference between the radiations from the four legs and their images. The height above ground h, the ground constants, the length of the legs, and their included angles are the parameters that control the pattern for each frequency. These parameters are optimum for only one frequency.

With fixed physical dimensions, the elevation of the peak of the main lobe, which is directed along the major axis of the array, is lowered as the operating frequency is raised. If the frequency is increased too much, the main beam will split. At the same time, the horizontal width of the main beam decreases, and there is an increase in the number of secondary lobes of appreciable amplitude appearing near the main lobe. In extreme cases, the main beam is broken into several beams of almost equal amplitude and spread over a considerable range of horizontal and vertical angles, as is seen in Fig. 3.78*c*.

Radiation along the major axis of the array is horizontally polarized. Radiations off of this axis contain both horizontally and vertically polarized components, the proportion of the latter increasing with angle from the axis.

There is one other parameter that can be varied in addition to those named. That is the plane of the rhombus, which can be tilted out of the horizontal plane about the minor axis. The principal effect of tilting is to increase the vertical beam width of the main lobe. The value of this characteristic depends upon propagation conditions, and under some propagation circumstances it can be a disadvantage.

The rhombic antenna is best suited for long-distance circuits where low-angle transmission or reception is wanted. When the beam angle is higher than 30 or 35 degrees, the gain is low and the desired performance can usually be obtained more economically with dipoles.

Figure 3.81 shows the optimum parameters for horizontal rhombic antennas for one frequency only. These data were compiled from stereographic charts which will be described later. The parameters were computed for the conditions that maximize the main beam and minimize the first side lobes to obtain best gain, using idealized factors for the system, including perfectly conducting ground.

The data represent about as much information as can be dependably presented in one figure for the guidance of the designer of a rhombic antenna. The main beam is less sensitive to the influence of variations in the geometric parameters and in the several empirical factors than are the other lobes.

It is always desirable to know the complete radiation pattern for an antenna for every application. While it is very seldom that this pattern is exactly what it is supposed to be, one may at least have an idea of the true state of affairs. This is difficult with rhombic antennas because one must submit to a great amount of labor to compute a single array at a

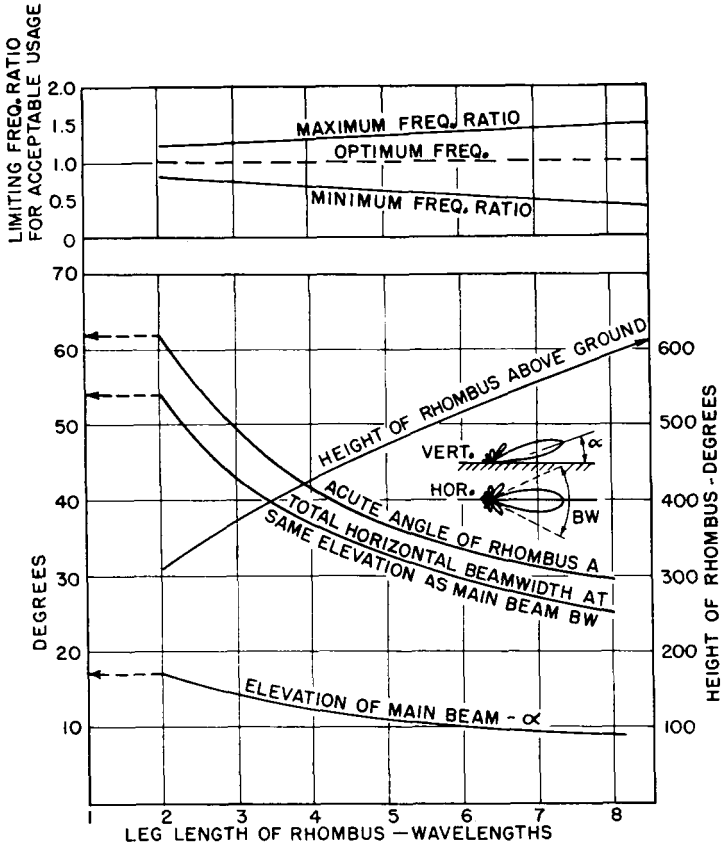

FIG. 3.81. Optimum parameters for the horizontal rhombic antenna, for maximum gain and minimum side-lobe amplitudes.

single frequency. As a consequence, rhombic-antenna performances are customarily taken for granted far more frequently than they are known. This naturally has led to many errors of judgment in rhombic-antenna applications.

If one wishes to compute rigorously the radiation pattern from a rhombic antenna, taking into account the attenuation of the traveling waves of current in the system and the complex reflectivity of the soil, the formulas of Cafferata (ref. 11, page 364) are perhaps the most com-

plete. Harper provides formulas (ref. 25, page 364) which allow for the earth reflectivity but not for the attenuation of the currents in the wires. The method of Foster (ref. 18, page 364) permits location of the main and all the minor lobes of a rhombic-antenna pattern relatively quickly by a graphical method which is very useful in forming an idea of the over-all pattern without excessive labor. The original sources should be consulted for details of formulation and method.

3.23.2. Stereographic Charts for Rhombic Antennas. The rhombic antenna, in common with all long-wire antennas, has an intrinsically

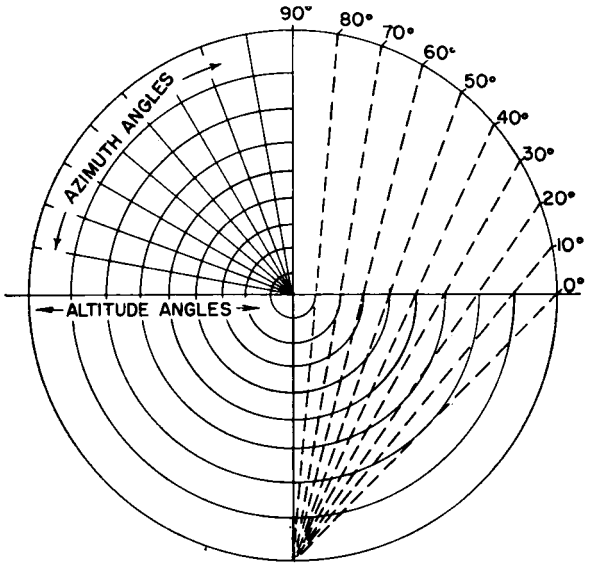

FIG. 3.82. Hemispherical coordinates derived by stereographic projection.

complicated radiation pattern that is difficult to visualize without very extensive and laborious computation for each working frequency. To obtain a main beam of desired orientation and desired width and height, and to minimize undesired lobes in many other orientations, it is necessary to have a method for observing quickly the effects of varying any single parameter in relation to all the others. This is obviously impossible by any system of numerical computation but is practical, and in fact easy, by the graphical method described by Foster (ref. 18, page 364). This is such an important aid to the designer of a rhombic antenna that we shall give a brief review of the method here merely to reveal its possibilities and encourage its use. The original source should be consulted for full details and the development of its principles.

The method makes use of the principle of stereographic projection to obtain a plan view of a hemispheric pattern on a plane. Figure 3.82

demonstrates the definition of stereographic projection and illustrates how the azimuth and altitude angles of a hemisphere are represented in two dimensions, in 10-degree intervals.

Each lobe of radiation from each leg of a rhombic consists of a cone of revolution around the wire. The stereographic projection of the maximum value of one of these cones is a portion of a circle. There will be

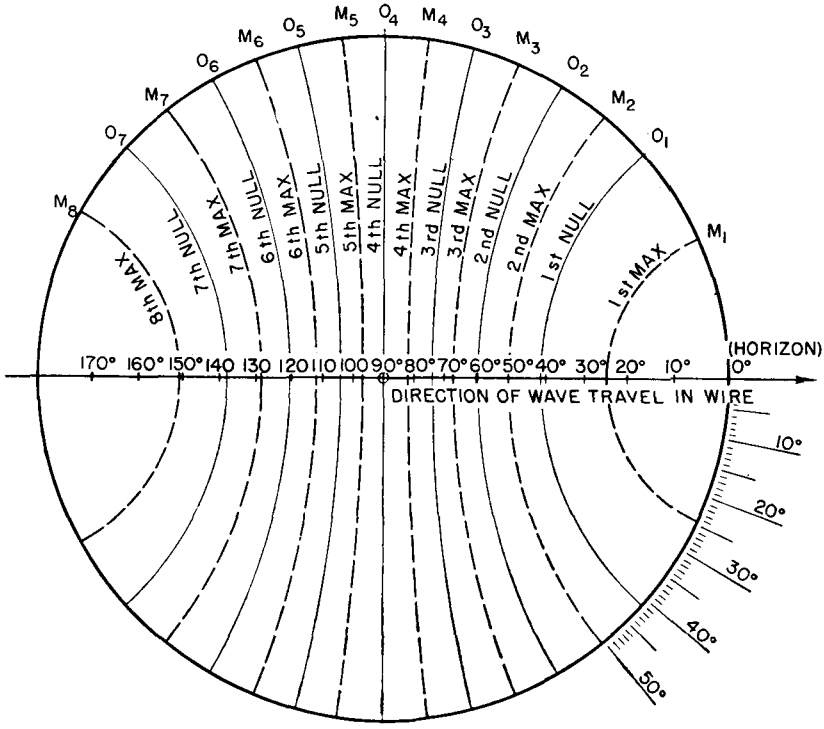

FIG. 3.83. Stereographic map of the radiation pattern for a four-wavelength straight wire in free space with a traveling wave. The maximums for the successive cones of radiation are in broken lines, and the intervening zeros are in solid lines. The altitude angles for the enclosing hemisphere are marked along the axis.

one such cone of radiation for each half wavelength of the length of each leg.

Between successive lobes of radiation are cones which show the locus of intervening nulls. The stereographic projection of a four-wavelength leg of a rhombus is shown in Fig. 3.83. The cones of maximums (shown as broken lines) and the cones of nulls (shown as solid lines) appear in sequence with half of the maximums in the forward half of the hemisphere and the other half in the rear quadrant, reckoned with respect to the direction of current flow in the wires. In other words, in the forward

half of the hemisphere there is one maximum per wavelength of each leg. The same is true of the rear half, when each leg is an integral number of wavelengths long.

This chart locates the stereographic coordinates of the cones of maximums and nulls but does not show the magnitudes of the successive maximums.

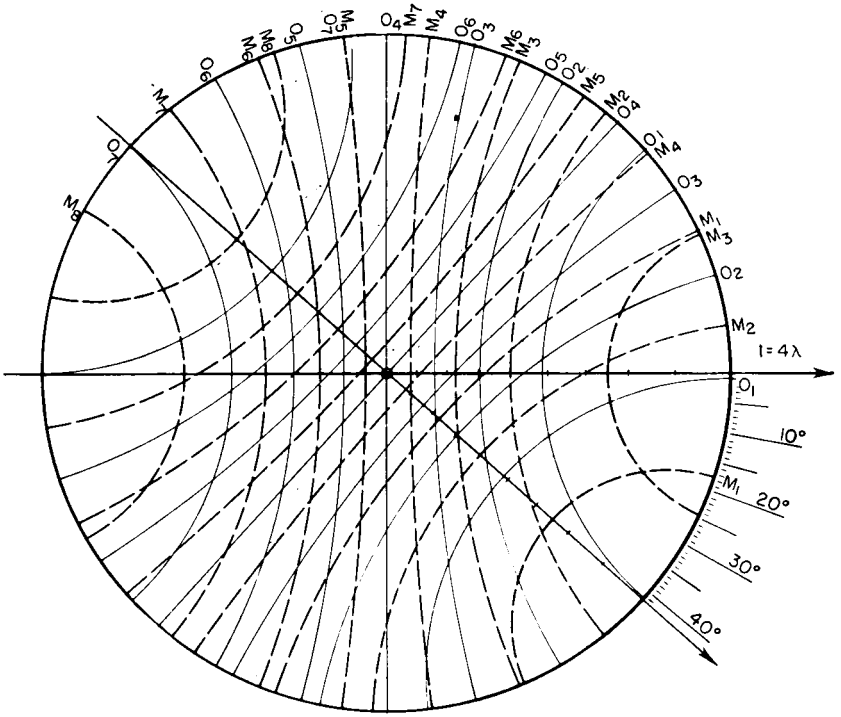

FIG. 3.84. Stereographic map of the pattern for a free-space rhombus four wavelengths per side, with an acute angle of 42 degrees. There are lobes of radiation where maximums of different orders intersect, and the main beam is formed at the intersection of the two first maximums.

Two such charts can be overlaid and set at an angle equal to that of the acute angle of the rhombus to show the pattern for the entire rhombus *in free space*. Figure 3.84 shows such a combination when the acute angle is 42 degrees with a leg length of four wavelengths.

This figure reveals all the null regions in the three-dimensional pattern because each null line for each leg produces a null in the final pattern. Any radiation that occurs must be a lobe of radiation peeking out through each area enclosed by the solid null lines. Strongest radiation occurs where the first maximums (M_1) for the two sides cross. This becomes

the main beam and occurs along the major axis of the rhombus, which is the angle that bisects the acute angle of the antenna.

Figure 3.67*B* shows that, for a traveling wave on a straight wire, the field strength of each successive lobe diminishes in magnitude. Therefore successive maximums for each side of the rhombus diminish in magnitude, so that the lobe formed where two second maximums (M_2) cross will be less than for the main beam, and likewise where the first maximum for one leg intersects the second maximum for the other leg the resulting lobe will also be smaller. The relative magnitudes of these other lobes where successive maximums intersect, with respect to the main beam, are given in Table 3.2.

TABLE 3.2. FREE-SPACE RHOMBUS
(Relative magnitudes of secondary lobes, in decibels, below the magnitude of the main beam)

Order of maximum for other side	Order of maximum for one side				
	1	2	3	4	5
1	0				
2	5.28	11.7			
3	7.52	28.2	50.6		
4	9.00	42.8	65.3	79.7	
5	10.1	53.8	76.2	91	120
6	11.0	62.4			

When the rhombus is placed with its plane parallel to ground, its height produces another interference pattern with the image in the same manner as a horizontal dipole. Figure 3.16 shows where the nulls and maximums occur as a function of the height above ground. In stereographic projection, each such maximum and each such null will appear as a circle concentric with other altitude circles as discussed in connection with Fig. 3.83.

As an example consider the rhombus of Fig. 3.84 and place it 1.18 wavelengths above ground. Figure 3.16 shows that this will put maximums of relative magnitude 1.0 in the height factor at vertical angles of 12.5 and 39.5 degrees and nulls at angles of 25 and 57 degrees. When these values are applied to Fig. 3.84, we obtain Fig. 3.85. This latter figure is marked to show the locations of the maximums of the main beam and several minor lobes. The azimuth of each lobe from the rhombic axis can be measured with a protractor, and the elevation angles are represented stereographically.

The design represented in Fig. 3.85 is an optimum for a horizontal

rhombic antenna having four wavelengths per leg. The term "optimum" is based on the following considerations: The crossing of first maximums for the legs coincides with a maximum in the height factor. The crossing of the first maximum for one leg with the second maximum for the other leg coincides with a null in the height factor, so that these lobes are split

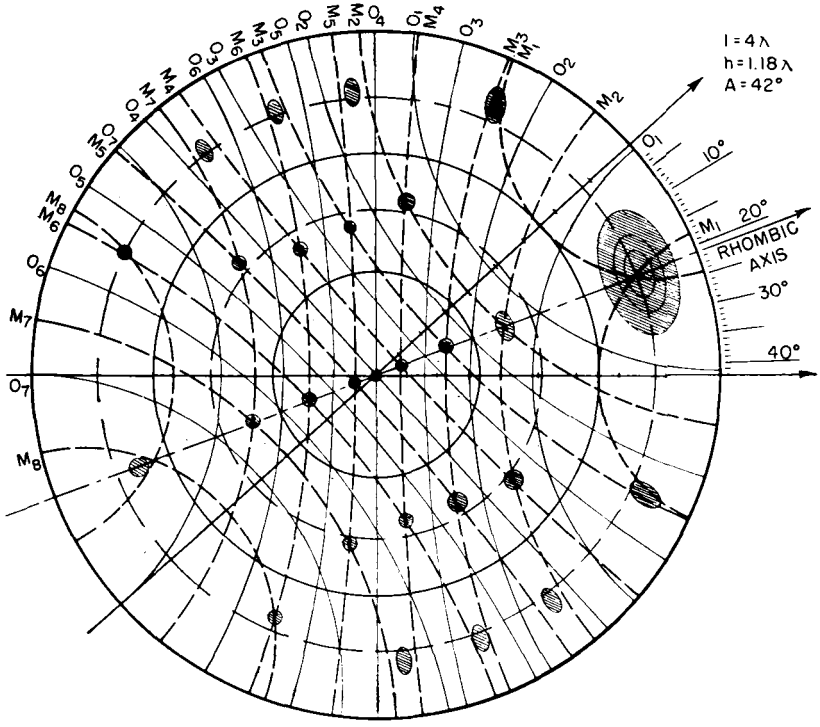

FIG. 3.85. Stereographic map of the radiation pattern for a horizontal rhombic antenna four wavelengths per side, with an acute angle of 42 degrees and a height above ground of 1.18 wavelengths. The successive maximums and zeros in the height factor are shown by the broken-line and solid-line circles, respectively. The main beam and the various secondary lobes are indicated. This pattern is an example of the optimum design.

and reduced to small residual pairs of lobes. The first maximum for one leg intersects with the third maximum for the other leg at zero degrees elevation, where it is canceled by a zero in the height factor. Smaller residual lobes at higher angles do exist, however.

It will be seen that at the lowest angles the higher-order lobes do not meet so that their magnitudes are greatly reduced compared with those which would result from a different apex angle which would permit them to intersect. The intersections of maximums at higher angles cannot be

suppressed, but they are intrinsically of small magnitudes. The intersection of second maximums along the array axis is at a relatively high angle (47 degrees) and is reduced from normal magnitude by the diminishing value of the height factor at this angle. Therefore the pattern for this

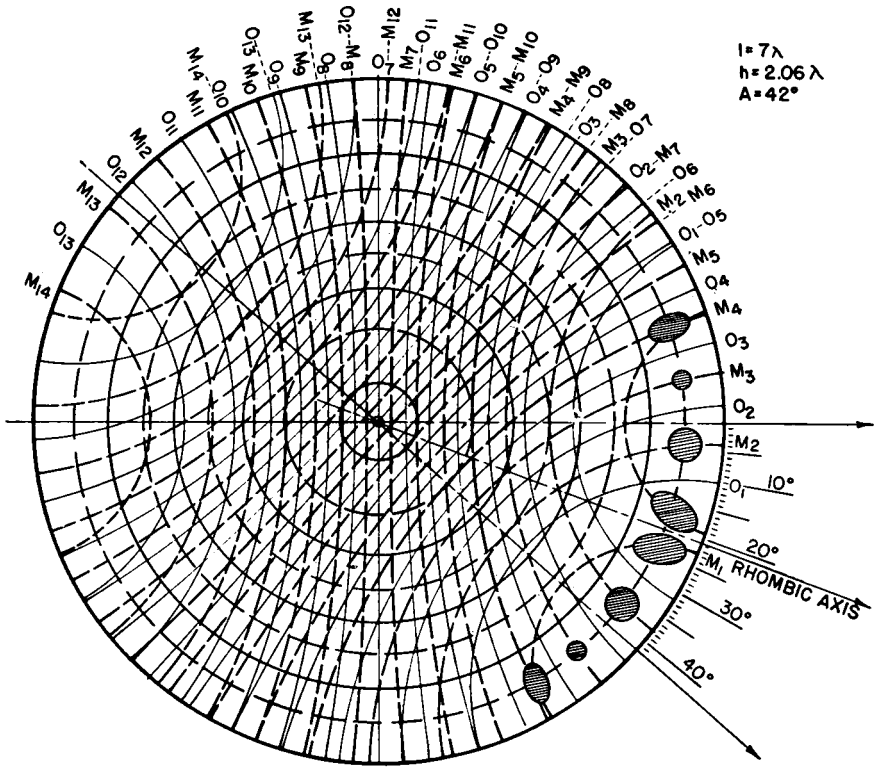

FIG. 3.86. Stereographic map of the radiation pattern for a horizontal rhombic antenna seven wavelengths per side, with an acute angle of 42 degrees and a height of 2.06 wavelengths, obtained when the antenna of Fig. 3.85 is operated at 75 per cent higher frequency. The main beam is split, and the dominant secondary lobes are very large.

system is an optimum because all spurious lobes are minimized and the main beam is maximized.

Let it be assumed that this optimum-design antenna for the frequency corresponding to these electrical parameters is to be constructed; but now it is desired to investigate the performance of this same antenna at another frequency for which the horizontal rhombic antenna has a leg length of 7 wavelengths. The physical dimensions therefore remain fixed, while the frequency is increased in a ratio of 7 to 4. The electrical height at this frequency will be 2.06 wavelengths.

The result is shown in Fig. 3.86, from which it is obvious that a very unsatisfactory pattern is obtained. The main beam is split, and some of the spurious lobes will have magnitudes as great as, perhaps even greater than, the main lobe. Also, the main beam is excessively sharp horizontally; yet in spite of this sharpness the gain must necessarily be very low. The energy of the system is leaking out through other lobes

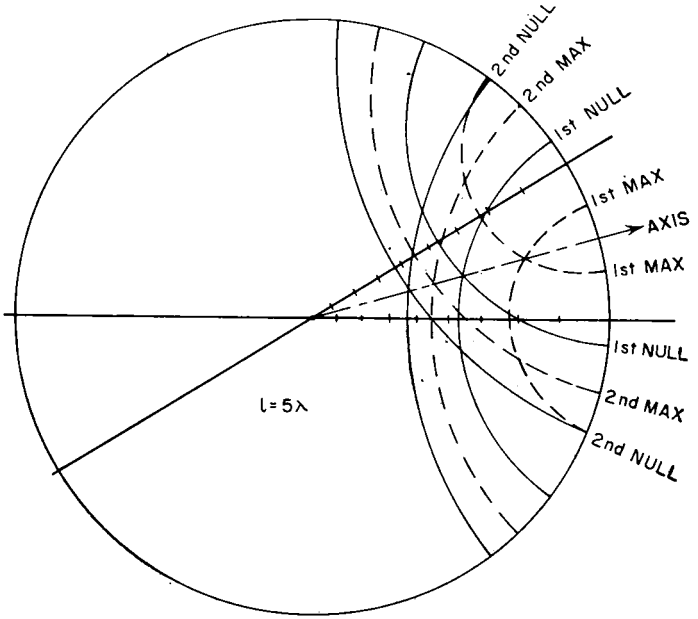

FIG. 3.87. Stereographic construction simplified for the determination of radiation lobes of first and second orders for a rhombic antenna with five wavelengths per side.

in other directions rather than being concentrated in the main beam. It might be difficult to discover this situation by arithmetrical computations, but it is quickly observed by the use of stereographic charts.

The data for Fig. 3.81 were derived on the basis of conditions corresponding to Fig. 3.85.

Abbreviated charts of this type can be prepared very quickly if information is wanted only for the first two or three maximums, instead of for the entire pattern. With the aid of Fig. 3.67*A*, a pair of stereographic charts can be drawn on tracing paper in a few minutes. These may then be used directly to ascertain the antenna parameters for optimizing the main beam or manipulating the spurious lobes of major importance, as shown in Fig. 3.87.

The same design charts can be used for horizontal-V and inverted-V

antennas. A single chart can be used to determine the patterns for other forms of long-wire antennas parallel to ground.

Table 3.2 shows that the magnitudes of secondary lobes formed by intersections with the first maximum for one side diminish slowly. Such lobes usually occur at the lower altitude angles in the forward half of the hemisphere and are bunched around the main beam. When these large secondary lobes occur at angles higher than that of the main beam, the height can be adjusted to diminish or split them. Unfortunately these large lobes often occur at the sides at altitude angles the same as or lower than the main beam so that the adjustment of the height factor has no selective controlling influence.

The application of the stereographic charts for the rhombic antennas enables one to select easily an optimum design for one electrical size of antenna. One can see how the main beam may be broadened, narrowed, raised, or lowered and how the height may be used to control the vertical-plane pattern along the major axis, and in fact in many other directions. When the geometry and height are thus determined for one frequency, the same geometry may be used with corresponding changes in electrical length (using other charts) for other frequencies and the performance studied. If the pattern is found to be undesirable at some frequency, trial and error is used until acceptable compromises are found for a series of working frequencies. Such graphical computations show the conditions to be expected as different charts are used for different leg lengths corresponding to different working frequencies.

One of the dangers associated with blind formulas and design charts for rhombic antennas is that they usually give insufficient information for an optimum selection of parameters and do not indicate reasonable working frequency limits. Figure 3.81 was computed using stereographic charts where the most important secondary lobes were considered. The optimum design minimizes the first side lobes for maximum gain and gives the cleanest horizontal and vertical patterns.

In regular engineering practice a series of charts are drawn on tracing cloth, following Foster's method. These may be, for example, for two, three, four, five, six, and seven wavelengths per leg. Those who have a great deal of rhombic-antenna designing to do may want charts for intermediate lengths. Charts carefully constructed in a circle of 10 centimeters radius are of a very convenient size. Positive transparency films can then be made from the originals by photographic contact printing with cut film sheets or by various copy processes that make direct positives on clear plastic sheets. A pair of positive transparencies for each leg length are then set together at the angle chosen for best performance. A pair may be set together at a chosen angle with transparent adhesive

tape and the combination reproduced by black-line, blueprint, or photographic contact printing to give a work sheet for a thorough analysis of the pattern, as well as for record purposes.

It must be mentioned that all the foregoing is based on idealized conditions—that is, no attenuation of the traveling waves in the antenna, no standing waves whatever due to reflections from the far end or from the side corners, no effects from supports—and it assumes perfectly conducting ground. Because there is radiation from the system, there will be attenuation of the traveling waves. Attenuation causes the nulls to become minimums and the relative values of the maximums to be modified somewhat. However, attenuation does not alter the angles of the maximums and the minimums in the pattern. Then, it is practically impossible to eliminate some small amount of standing wave from the system, either at the termination or at the side corners. The presence of standing waves causes the magnitudes of the smaller lobes, especially those in the rear half of the hemisphere, to be increased. An appreciable amount of reflection may give some of the backward lobes, usually negligible, a considerable magnitude. The effect of imperfect ground fills out the nulls in the height factor and diminishes the maximums. However, all these effects are regarded qualitatively among other unavoidable imponderables and tolerances.

It is especially important to emphasize at this point that the remarks made here concerning "optimum" rhombic-antenna designs mean optimum only in the sense of the best intrinsic radiation performance as an abstract matter. It would obviously not be an optimum antenna from an application standpoint if the antenna pattern was not optimum for fitting the propagation conditions. To make this perfectly clear, consider the following situation:

You have made an analysis of the requirements for a given radio path from the ionospheric data and find that the optimum working frequency (or the nearest available assigned frequency) will permit communication over a sufficient number of hours per day if the angle of fire is 4 degrees; and it is further found that, for the same path, angles of fire higher than 12 degrees will penetrate the ionosphere and be lost during a substantial percentage of the time. The antenna that must be used for this path therefore is one with the main beam aimed 4 degrees above the horizon.

Upon examination of Fig. 3.81, it is noticed that the optimum parameters given do not fit the applicational requirements because the beam angles are much higher than can be used, and the resulting beam angles for the optimum parameters are very near to those which penetrate on the path under consideration. It is evident from this example, which typifies the kind of problems encountered in antenna applications, that

what is optimum from a purely antenna viewpoint is not necessarily optimum from the communication-engineering viewpoint. To adapt an antenna to this particular requirement, it will be necessary to abandon Fig. 3.81 as a source of design data and to seek another design that gives the proper angle of fire to fit the propagation requirements. The rhombic-antenna design ultimately selected to do this will not then be an "optimum" in the sense represented by Fig. 3.85, but it will be an optimum design for the actual radio circuit. If an "optimum" rhombic were to be applied to this case, the antenna would perform well as an antenna but the radio circuit would be unsatisfactory for a large percentage of the time.

It must be explained further that Fig. 3.81 does in fact have great practical utility because the angles of fire for the optimum rhombic-antenna designs will be optimum for a large percentage of actual radio circuits.

When angles of fire lower than those shown in Fig. 3.81 are required, the main beam can be lowered by increasing the acute angle of the rhombus by a small amount; but this angle should never exceed a value somewhat smaller than twice the angle of the cone of first maximum with respect to the wire for one of the legs. In other words, the acute rhombus angle should never quite equal twice the angles given in Table 3.5 in connection with the inverted-V antenna. Otherwise the main beam will split.

If the main beam angle is lowered by changing the acute angle, it is also necessary to increase the height of the rhombus to bring the first maximum in the height factor at the best angle of fire computed for the radio path. When this is done, the antenna pattern is matched to the radio path and will produce the best results operationally.

This discussion brings out what has been said before about antenna "gain" being a purely incidental factor in antenna applications for practical communication, and not a primary objective in antenna design. Unless the gain is effective in the required direction to fit the radio path, it is virtually meaningless.

The design for the antenna is one problem, and the design of the radio circuit is quite another. The design of the radio circuit includes the propagation analysis and also the characteristics of the receiving antenna. There is a large accumulation of data and experience which shows that the transmitting and receiving antennas should be complementary and possess identical patterns.

The dominant angle of arrival of signals has been proved to be essentially the same as the optimum angle of fire for the path when the transmitting antenna is matched to the radio path. If the receiving antenna

also has maximum response to this dominant angle, the results are maximized by two effects—first, the two antennas do not work against each other from the standpoint of angular response; and second, the signal stability is maximum because normal variations in layer height, which cause variations in the optimum fire angle, occur symmetrically with respect to the average angle obtained from the monthly averages given in the ionospheric propagation data. A variation of 2 degrees, for instance, in fire angle gives relatively small variations when this occurs around the peaks of the main lobes, whereas the same angular variation taking place along the underside of the main lobes of both transmitting and receiving antennas, where the response is changing very rapidly with angle, can introduce many decibels of fading unnecessarily.

These remarks relating to the matching of the antenna patterns to the radio path are quite general and do not apply only to the application of rhombic antennas. They are included in this section for this important reason—rhombic antennas are very likely to be used for a wide range of working frequencies, while the antenna itself is correct for only a very narrow band of frequencies around the desired optimum. One may design for one optimum condition and then proceed to let other working frequencies fall where they may, even though they are very far from optimum. The scarcity of available frequencies and the need to make the best possible use of assigned frequencies will certainly require the communication engineer to place optimum performance ahead of capital economy if the latter depreciates performance on other working frequencies for which the system is not optimum. When this occurs, as it often does, there is a tendency to use greater transmitter power to make up for antenna deficiencies. This, of course, causes unnecessary interference and offers little improvement in circuit operation. In the long run there may be economy in using a separate specially designed antenna for each frequency on each path. The rhombic antenna is very economical *when, and only when*, its characteristics at different specific working frequencies are well matched to the propagation medium.

Rhombic receiving antennas designed for low-angle reception inevitably have a narrow main horizontal lobe. Care must be taken not to employ designs having patterns that are too sharp to accommodate the normal range of signal variations in both vertical and horizontal planes.

One advantage mentioned for the rhombic antenna is the ease with which the antenna can be changed in height from season to season or year to year as propagation conditions change through the annual and the sunspot cycle. In planning a system, consideration may well be given in this respect to the height of the supports so that the antenna can be raised and lowered to use the optimum height from one extreme to the other.

3.23.3. Rhombic Antenna Circuitry. From a circuital standpoint the rhombic antenna, when terminated at the far end in its characteristic impedance Z_0, has an input impedance which is predominantly resistive and equal approximately to Z_0. For the three-wire type, this value is of the order of 600 ohms, which matches well with ordinary two-wire balanced feeders. After construction the input impedance should be measured and the feeder impedance matched to the measured value. In practice, true traveling waves never exist on the system. There are always some reflections from the side corners, though it is possible to adjust the termination so that the reflections are minimized on either the forward half or the rear half of the antenna. If a system is constructed carefully so as not to have sharp corners where the feeder and the terminating line attach to the antenna, and if large metallic fittings near the supports are avoided, a satisfactorily uniform input impedance of high power factor is realized, over a large range of frequencies.

When used for receiving, the terminal resistance for a unidirectional system is usually installed directly at the far end in the form of a noninductive resistor. This resistor should have a high impulse rating to maintain stable resistance and to withstand induction from lightning. Some designs include discharge circuits to ground at the termination by dividing the terminal resistance into two sections and connecting the center to one side of a small spark gap, the other side of which is connected to ground with a wire (if wood poles are used), broken by a series of gaps, or by using a steel support as the ground connection.

For medium- and high-power transmitting purposes, the terminal resistance is almost always a balanced lossy line of high dissipation capacity. These are discussed in the following chapter.

Static-charge drains are a necessity in most regions, where the antenna may become highly charged from rain, dry snow or flying sand, and electric storms. Draining is most easily accomplished at the end of a dissipation line but can also be done in the feeder, using resistors or drain inductors having impedances high enough at all working frequencies not to introduce reflections. Drain resistors or coils are connected from each side of the system to ground.

The directivity of a rhombic antenna can be reversed by interchanging the feeder and the terminal resistance. Figure 3.80 shows an arrangement for this purpose, with switches located on the ground near the center of the system where feeders run to each end of the antenna. The main feeder and the dissipation line are also centered at this point and connected into the switching circuits.

For simultaneous reception of unidirectional signals from both directions, lines can be brought from each end to separate receivers. Each line

must be correctly terminated, either by the receiver or by a resistive network, so that there is no reflection from the receiver inputs. To use this system successfully, there must be virtually zero radiation from the receivers, or they may mutually interfere.

In large receiving stations using many antennas and receivers, concentric lines have been used to simplify antenna-receiver switching. The use of concentric lines only to reduce feeder pickup is seldom justified because the spurious directive responses of a rhombic antenna are greater than the direct pickup on ordinary open-wire lines. When concentric lines are used, the balanced antenna impedance is matched to the unbalanced line impedance with a wide-band transformer.

If a balanced four-wire cross-connected open-wire line is used, the two balanced impedances can be matched by using a tapered intermediate matching line designed for the lowest working frequency. Either exponential or linear taper may be used if properly designed.

Here, again, there is no justification for using a four-wire line because of its low pickup quality when it is used with a rhombic antenna having comparatively greater omnidirectional pickup.

3.23.4. Rhombic Antenna Arrays. Some of the basic deficiencies of the rhombic are correctable by more complicated arrays of rhombic elements. For example, a two-layer system on the same supports, one above the other, can do a great deal to suppress the higher angle minor lobes, as shown in Fig. 3.88. Such a pattern has relatively desirable vertical-plane characteristics for the angular discrimination against multipath propagation on some circuits. The horizontal pattern may be undesirable at the higher frequencies, not so much because of the spread of its several forward radiation lobes, but because a signal swinging in azimuth may swing into and past the quasi nulls between the lobes.

When azimuthal swing of signals is a disturbing factor, two such arrays can be used in diversity, by turning the axis of the second array off the great-circle bearing by an angle equal to that between the first null and the peak of the main beam. When two such antennas are spaced as in typical space-diversity operation and oriented in this manner, the maximums of one rhombic pattern will fill the minimums of the other. To obtain this benefit, each rhombic must be associated with its own receiver and their outputs combined in diversity. This form of utilization is obviously a special application to avoid the effects of arriving signals that deviate from the great-circle bearing by an amount which exceeds half the beam width of the main lobe.

Figure 3.89 shows the construction for a two-layer rhombic system having two wires per side in each layer. Figures 3.90 and 3.91 show what is possible by using arrays of these two-layer rhombic systems.

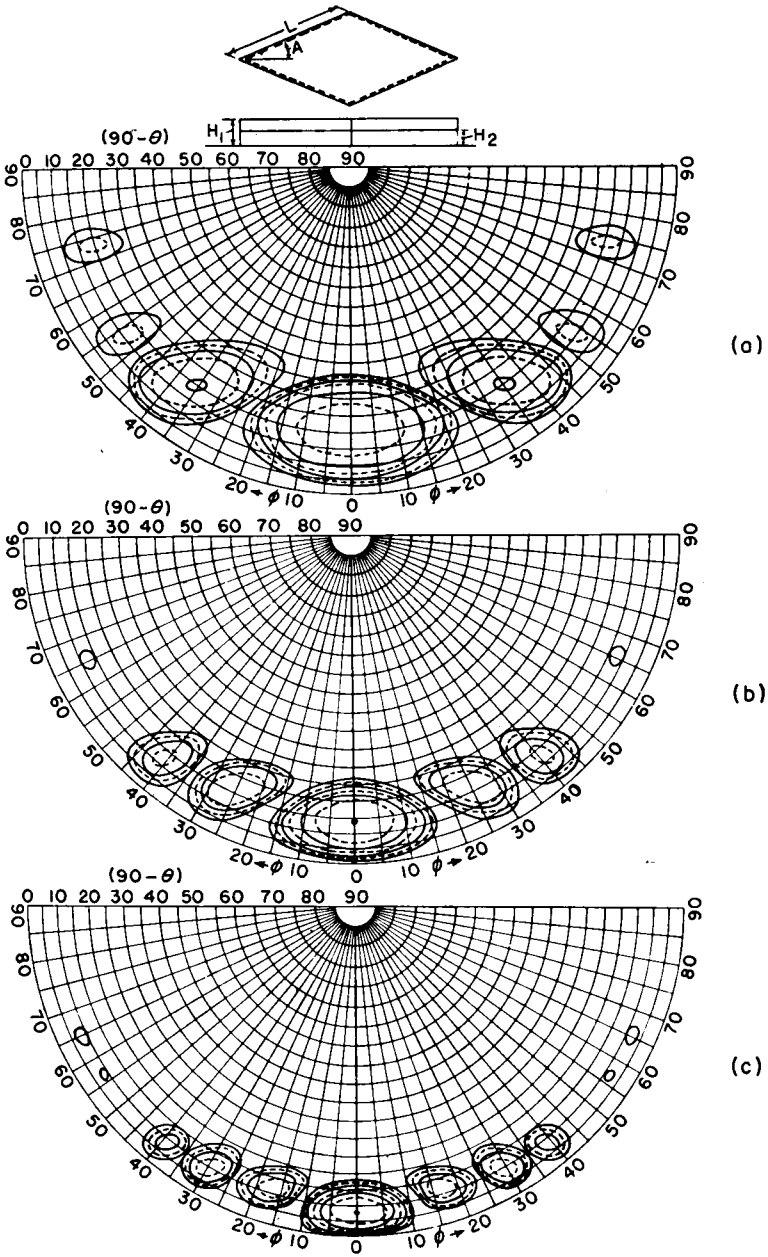

FIG. 3.88. Two-layer rhombic antenna patterns of following geometry (*After Christiansen.*):

	ϕ, degrees	l/λ	h_1/λ	h_2/λ
a	72	3.33	0.8	0.47
b	72	5.00	1.2	0.7
c	72	7.5	1.8	1.05

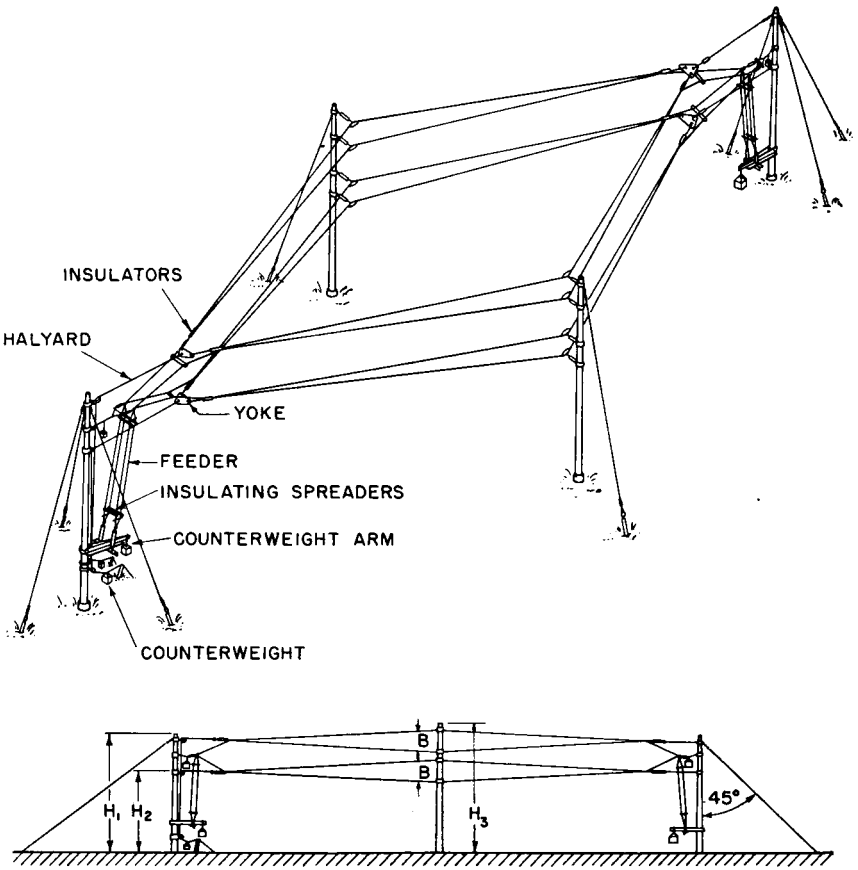

FIG. 3.89. Construction for two-layer rhombic antenna.

TABLE 3.3. COMPARATIVE RHOMBIC-ANTENNA DATA

Type	Fig. 3.79 Single-layer (three-wire)			Fig. 3.88 Two-layer tiered (two-wire)		
Frequency, megacycles	8	12	18	8	12	18
I_{in}	8.9	6.2	4.3	6.7	5.15	3.7
I_{out}	5.7	3.46	2.44	3.74	2.25	1.53
I_{out}/I_{in}	0.64	0.557	0.566	0.557	0.436	0.413
I_{avg}/I_{in}	0.85	0.80	0.77	0.75	0.72	0.65
W_t*	0.41	0.31	0.32	0.31	0.19	0.17
Gain over $\lambda/2$ dipole, decibels	9	11.5	13	9.7	14	14.7
Gain at	18 degrees	10 degrees	7 degrees	18 degrees	14 degrees	8 degress
l/λ	3.33	5.0	7.5	3.33	5.0	7.5
h_1/λ	0.80	1.2	1.8	0.80	1.2	1.8
h_2/λ	.....	.....	.....	0.47	0.70	1.05

* Power lost in terminal resistance for unity power input to antenna system.

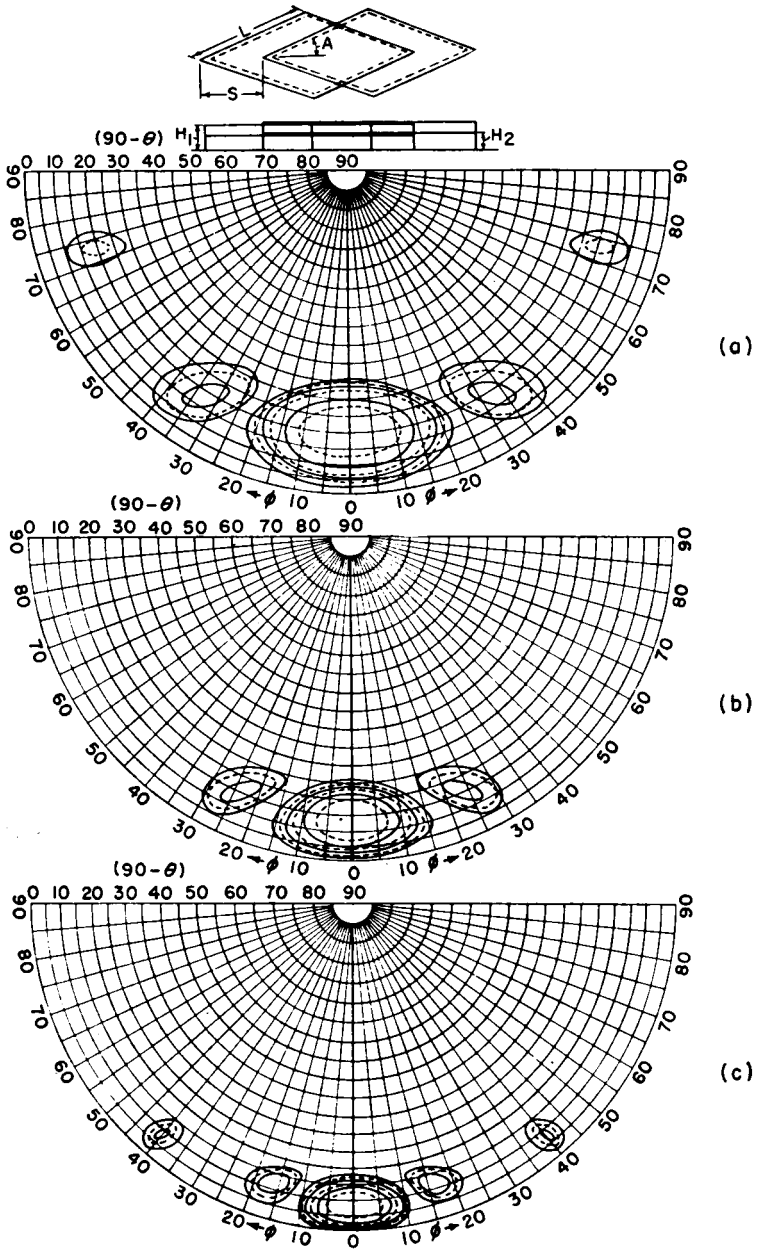

FIG. 3.90. Directive patterns for two two-layer rhombic antennas of the type of Fig. 3.88, with apex spacing as follows: (*a*) apex spacing 1.33; (*b*) apex spacing 2.0; (*c*) apex spacing 3.0. (*After Christiansen.*)

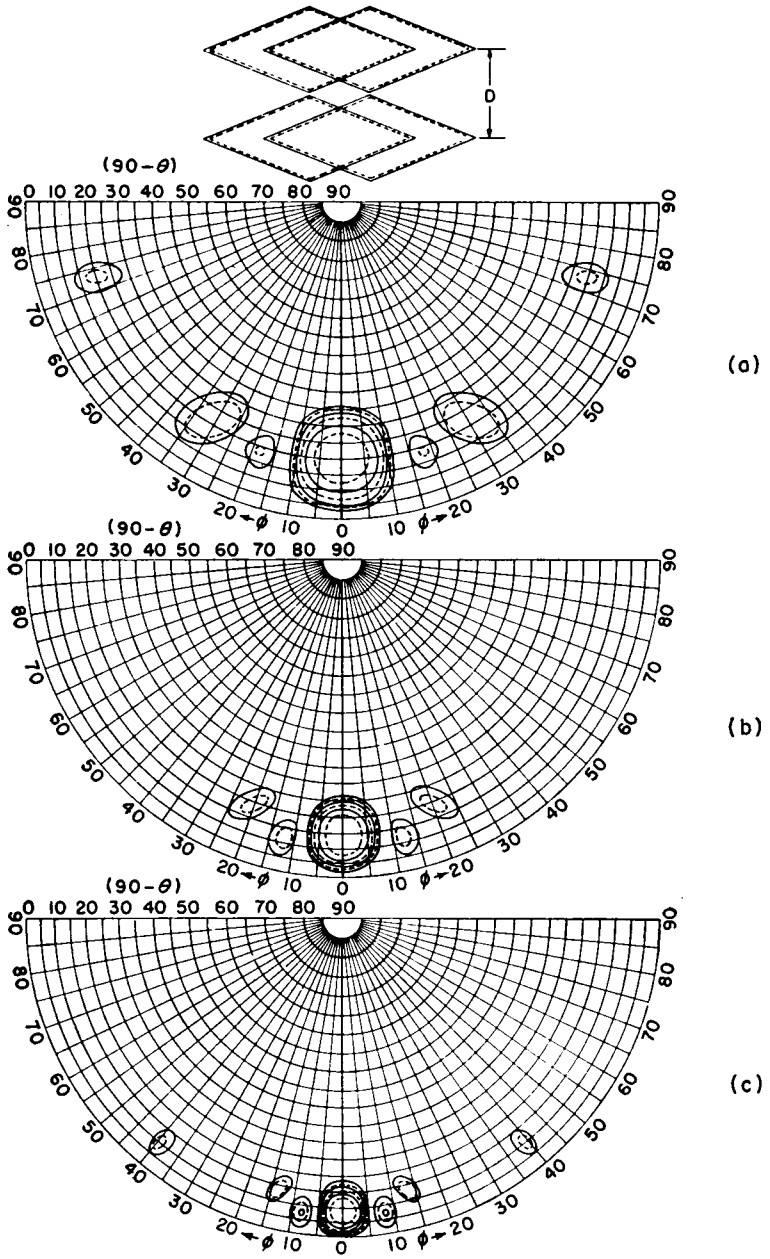

FIG. 3.91. Radiation patterns for two arrays of the type of Fig. 3.90 in broadside but with major axis spacings as follows: (*a*) 2.33λ; (*b*) 3.50λ; (*c*) 5.25λ. (*After Christiansen.*)

These figures, together with Figs. 3.78 and 3.88, represent optimum-design parameters for a frequency range of 2.25 to 1, based on idealized conditions.

Comparison measurements on rhombic antennas of the types having the patterns of Figs. 3.78 and 3.88 are listed in Table 3.3, as published by Christiansen.

3.24. Fishbone Receiving Antenna

The principles of the Beverage wave antenna were first applied to high-frequency reception in the form of the fishbone antenna. Two forms of this antenna have been evolved in the United States and England, both intended for the reception of horizontally polarized waves.

The RCA fishbone antenna is diagrammed in Fig. 3.92 and pictured in Fig. 3.121. To the central feeder are attached horizontal dipoles with a length of the order of one-half wavelength at the center frequency of the response band, on both sides of the central feeder, in series with high-reactance capacitors. The dipoles, with the series capacitors, smoothly load the feeder. The velocity of propagation along the system is adjusted, by means of the capacitors, to be about 90 per cent of free-space velocity. This loading reduces the characteristic impedance somewhat, and the usual design value is about 400 ohms. The maximum directivity is along the line of the feeder. The antenna is made unidirectional by terminating the end toward the transmitting station in a resistance which matches the characteristic impedance. The receiver is fed from the far end over a balanced transmission line of the same impedance.

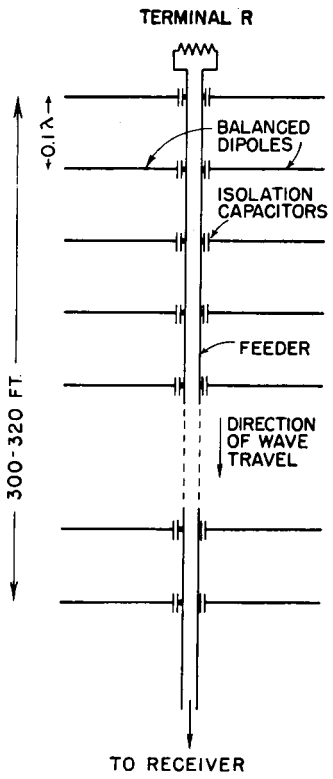

FIG. 3.92. RCA fishbone-antenna circuitry.

Fishbone antennas may be used in various arrays, according to the directivity patterns desired. The one commonly used consists of two fishbones in broadside using common intermediate supporting structures. Typical patterns for single- and two-bay fishbones are shown in Figs. 3.93 and 3.94. The two-bay design unites the transmission lines symmetrically and the main line to the receiver is then of one-half of the antenna characteristic impedance. For this purpose it has been the practice to employ the four-wire cross-connected balanced type of line, a picture of which is shown in Fig. 4.95.

Constructional dimensions for fishbone antennas for various ranges of frequencies in the high-frequency band are given in Table 3.4.

The measured performance of fishbone antennas compares closely with that of a rhombic antenna having the same main beam orientations even

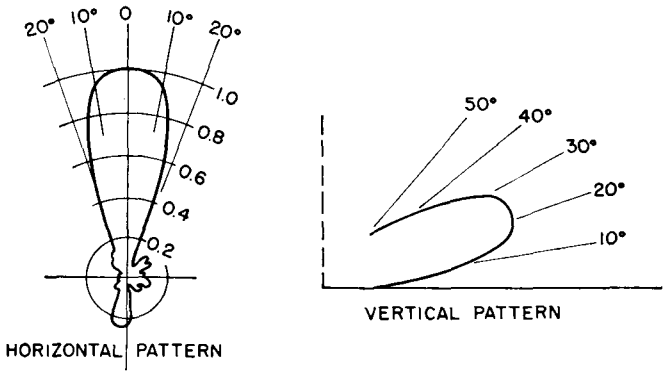

FIG. 3.93. Horizontal and vertical patterns for RCA fishbone unit. (*After Beverage and Peterson.*)

though the former occupies a much smaller land area. The fishbone pattern is relatively free of secondary lobes and the corresponding parasitic directional responses.

TABLE 3.4. RCA FISHBONE-ANTENNA DIMENSIONS

Length dipoles, feet	Optimum frequency, megacycles	Useful range, megacycles	Width (two bays), feet	Length total, feet	Pole height, feet	Useful angle (azimuth), degrees
34	18	13–22	120	312	60	10
48	14	10–19	148	312	90	10
66	9	3–13	200	312	120	10

The number of dipoles used is sufficient to produce the effect of smooth continuous loading of the central feeder. This requires seven or more per wavelength, the wavelength in this case being that in the feeder at the wave velocity employed.

Another version of the fishbone antenna is diagrammed in Fig. 3.95. The dipoles in this system are one-half wavelength long at some chosen frequency and omit the series capacitors. They are spaced at one-quarter-wavelength intervals along the feeder. In all other respects the performance and structural characteristics resemble those of the RCA fishbone.

The fishbone antenna is one of the preferred forms for wide-band response in the high-frequency fixed services. Its higher cost in many cases is offset by the smaller land area required as compared with an equivalent horizontal rhombic antenna.

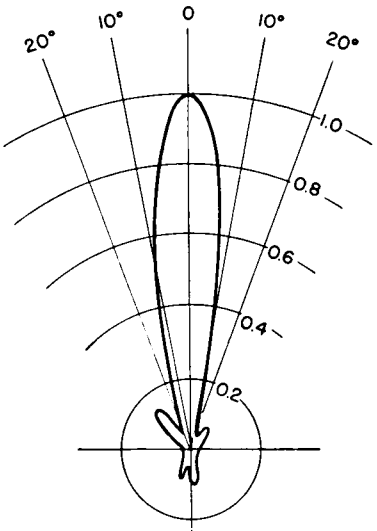

FIG. 3.94. Horizontal pattern for two-bay RCA fishbone array.

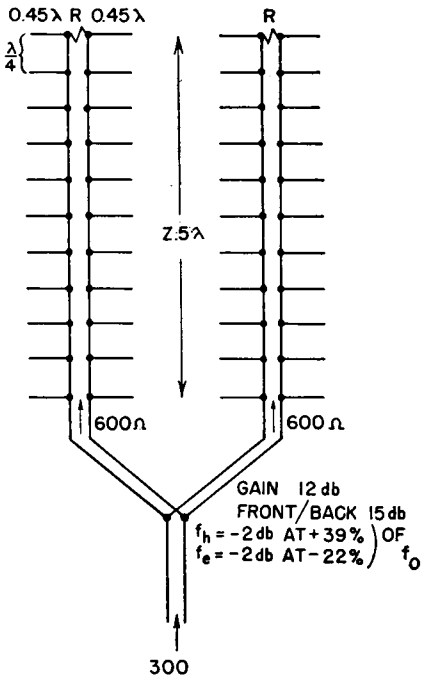

FIG. 3.95. English type HAD fishbone antenna (two-bay).

3.25. Traveling-wave Antenna for Vertically Polarized Transmission

Figure 3.96 shows the construction of an inverted-V antenna. This is essentially one-half of a rhombic antenna split along its major axis and then turned so that its plane is vertical. In this form, the main lobe of radiation is vertically polarized. The system is structurally simple and uses only one supporting pole.

The angle of the wires with respect to ground is a function of the length of the legs. The optimum slope angle is tabulated in Table 3.5. These angles are not the same as one-half of the acute angle of the equivalent horizontal rhombic antenna because, in the latter, the acute angle is adjusted to bring the intersection of the two cones of first maximums a few degrees above the plane of the rhombus, while in this case the angle is that which will maximize the pattern in the plane of the antenna. With

this exception, we can say that the vertical pattern for the inverted-V antenna is the same as that of a free-space rhombus in the plane of the rhombus. In the same sense the horizontal-plane pattern for the inverted-V antenna is the same as that in the major axial plane normal to a free-space rhombus.

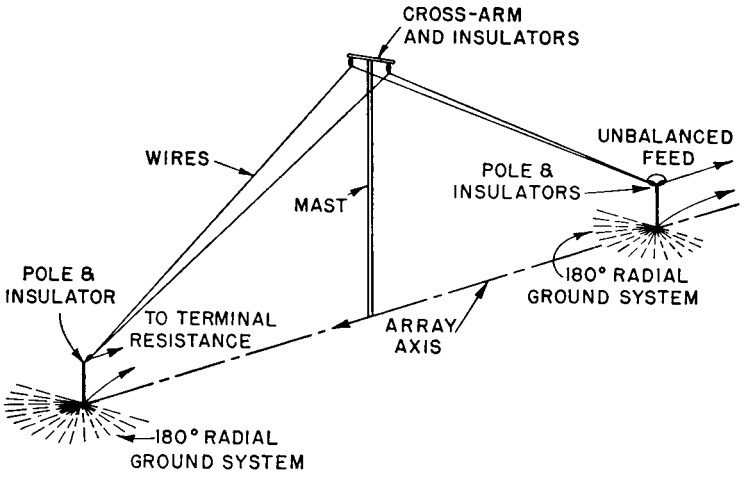

FIG. 3.96. Inverted-V traveling-wave antenna.

Circuitally, the inverted-V antenna is unbalanced, the ground forming one side of its input and output circuits. It is desirable to use a system of ground wires at the input end and also at the far end where the antenna is connected to a dissipation line for transmitting or to a resistor for receiving. Its characteristic impedance is one-half that of the equivalent balanced rhombic antenna.

TABLE 3.5. OPTIMUM SLOPE ANGLES FOR INVERTED-V ANTENNAS

Leg Length, Wavelengths	*Slope Angle, Degrees*
2	36
3	29
4	24.5
5	22
6	20.5
7	19.5

To feed the inverted V, it is usually preferred to use a balanced feeder, similar to those which would be employed for other balanced antennas, and to make a balanced to unbalanced transformation with the proper impedance ratio to excite the antenna.

At the terminal end, the dissipation line can be of the unbalanced type, using the ground itself as the dissipator. If the attenuation per unit

length is small, owing to high ground conductivity or low operating frequency, the required length of the line may be inconveniently large. In such a case, dissipative conductors will increase the attenuation rate by adding conductor loss to the ground loss.

3.26. Construction of High-frequency Antennas

Figures 3.97 to 3.123 are included to provide detailed information on various aspects of mechanical construction of high-frequency antennas. The figures show both low-power and high-power techniques that have

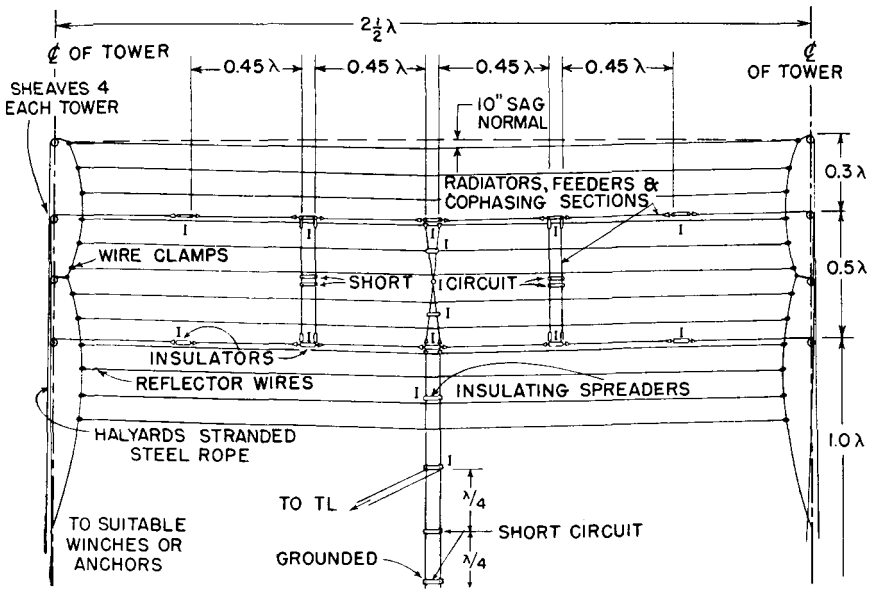

FIG. 3.97. Assembly of a horizontal dipole array using two levels of four dipoles, cophased, with passive screen reflector.

been employed successfully in systems originated by many different engineers, together with various forms of supports. These are but a few of the myriads of details that have been evolved throughout the world during the years of antenna development.

Only an experienced engineer can appreciate the mechanical problems associated with antenna rigging. An antenna is constantly in movement and vibration as winds flow past it from different angles, as tensions of members change with changes of temperature, and as loadings change with winds, contractions, and ice formation on the system. These movements and vibrations cause a great deal of wear and fatigue in the wires and hardware. This necessitates careful consideration in design to

provide an economical structure capable of fulfilling its mechanical duty reliably and for long periods. For this purpose the engineer must consult suppliers' catalogues of wire ropes, cables, wire, electrical-rigging hardware, insulators, etc. These catalogues contain information and data on the physical properties and weights of the parts and materials used in antenna construction.

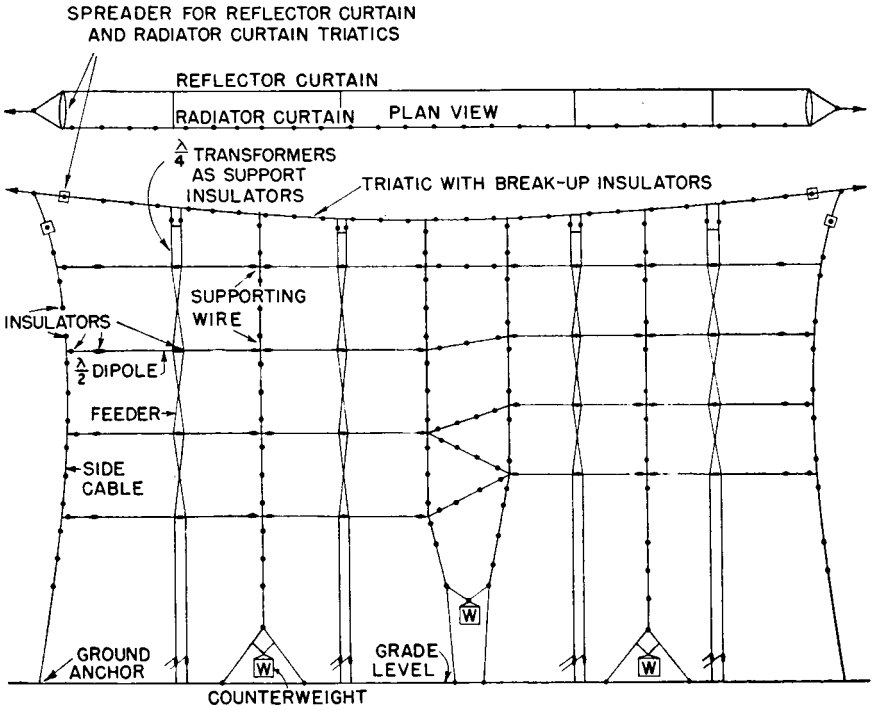

FIG. 3.98. Rigging for two 4 by 4 dipole arrays for two different frequencies, using two supporting masts.

The simplest antennas are rigged between the masts with the active conductors supporting their own weight and that of associated feeders as in Fig. 3.97. The more extensive arrays employ triatics, from which the actual antenna assembly is suspended. Most of the mechanical stress is placed on the triatics, thus reducing the mechanical stresses on the active electrical elements and permitting more accurate dimensioning of radiators and feeders. This eliminates sags and provides better mechanical stability, which in turn gives better electrical stability. Radiator and reflector curtains are usually hung from parallel triatics, using spreaders to maintain the correct spacings between curtains.

Conservative design calls for a minimum factor of safety of 2 on the

principal tensioned members, such as the suspension triatics and halyards, under conditions of maximum wind and ice loadings. The automatic maintenance of predetermined safe tensions in such members is afforded by the use of counterweighted structures.

The computation of simple catenary suspensions with uniformly distributed loadings is the same as that for transmission-line construction,

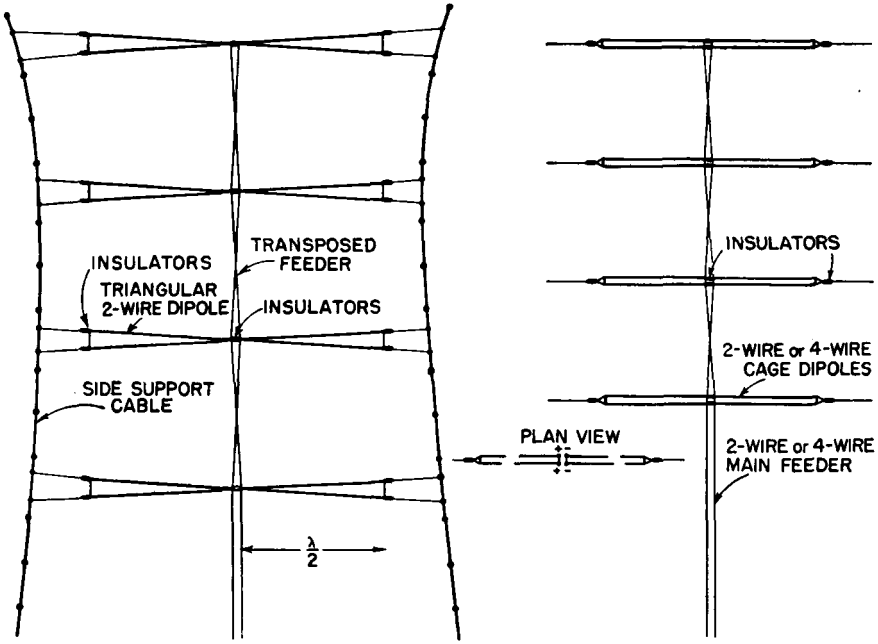

FIG. 3.99. Method of rigging triangular and cage dipoles for curtain arrays requiring large bandwidth.

and formulas are given in Chap. 4. The localized equivalent weight of feeders and other loadings on a simple catenary (such as a single horizontal dipole antenna with a two-wire feeder connected at the middle of its span) modifies the problem to that of the catenary with a central loading equal to the downward pull of the feeder due to its own weight, the static pull of the ground anchor, and the wind and ice loadings.

An approximate method for computing the catenary tensions for center-loaded triatics when the center loading is large with respect to the weight of the triatic proper is the following: Consider the weight of the triatic material lumped at the center of the span and added to the total suspended weight at the center to obtain the total center loading. Consider that a right triangle is formed by one-half of the span and the sag and the straight line drawn from tip to tip of the masts. Let A be the angle

between this line and that of the stressed triatic in the loaded state when the sag is a chosen or specified value. If W is the equivalent total weight of the load at the center, then the tension of the triatic is

$$T = \frac{W}{2 \sin A}$$

where T and W are in identical units.

When the suspended load is more or less equally distributed along a primary triatic, this distributed loading is added to that of the weight of the triatic proper and the tension is computed as for a catenary triatic of that total weight W.

Assuming the catenary to be firmly attached to the top of the mast, the horizontal pull P on each mast is

$$P = T \cos A$$

and the vertical compression load C on the mast is

$$C = \frac{W}{2}$$

When two triatics are used, one for a radiator curtain and one for a reflector curtain, but joined to a common halyard near the tower, their combined stress appears in the main halyard. If the halyard runs down the axis of the tower, the halyard stress is transferred to a compression load on the tower. If the halyard is anchored to ground at some distance from the tower base away from the antenna side, the compression load due to the antenna is reduced in accordance with the relation

$$C = T \cos B$$

where B is the angle between the halyard and the tower axis.

A counterweight in the main halyard is desirable as a means for maintaining uniform tension with transient wind and ice loadings on the antenna system. In small lightweight antenna systems, built for economy, the tension can be released manually at a winch when occasional heavy wind and ice loading is present. In hurricane areas, where complete ability to withstand the extreme conditions would require extravagant structures, one may decide to use light inexpensive construction and expect occasional damage to the system on the theory that its replacement would be a more tolerable expense.

Except for the very simplest structures, the precise computation of stresses in various parts of the antenna rigging becomes very complicated and often indeterminate. One may then use approximate methods,

according to one's ingenuity, or resort to estimates. The uncertainties are allowed for in the safety factors, or "ignorance factors." When insurance against these uncertainties leads to considerable expense, guiding dynamic-tension measurements can often be made with the aid of

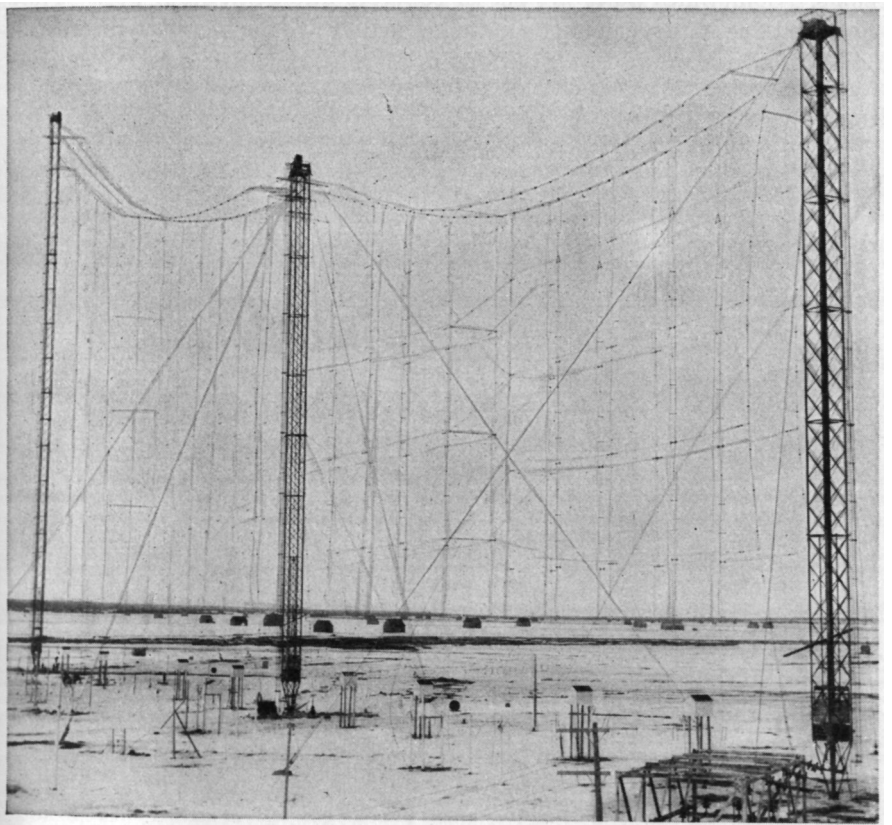

FIG. 3.100. View of the dipole beam-antenna arrays used for the high-frequency broadcasting service to Great Britain and northern Europe from the Sackville, New Brunswick, station of the Canadian Broadcasting Corporation. (*Photograph courtesy of Canadian Broadcasting Corporation.*)

mechanical scale models of the antenna. Such a scale model must accurately simulate distributed weights and all dimensions. Ice loadings can be simulated by judicious distribution of weights on various portions of the model. Wind stresses can be simulated by means of springs or elastic rubber which deforms the assembly by the specified amount corresponding to the wind pressures against the projected areas.

Wood poles, similar to those used for telephone and power-distribution line construction in a large part of the world, are most frequently applied

to the duty of supporting high-frequency antennas when they can be made of sufficient height. Round wood poles can sometimes be obtained in lengths of 70 or 80 feet, and occasionally longer. The length that must be underground depends upon the soil resistance and the guying provisions. Sometimes poles are set in concrete and sometimes not. They have to be set with the aid of a crane since they are too heavy to be erected

FIG. 3.101. Fabricated spreader used to space the radiator and reflector curtains of a large dipole array in the main catenary, shown before being raised into the air. This is part of the array used for 6-megacycle broadcasting. (*Photograph courtesy of Canadian Broadcasting Corporation.*)

with pikes. Figure 3.115 shows an assembled steel mast being erected in this way. Figure 3.120 shows the use of single high poles for rhombic antennas.

Shorter poles may be spliced in different ways to obtain wood supports of moderate heights. Figures 3.112 and 3.113 show the operations for lap-splicing two large poles. Figure 3.114 shows what has come to be called the "A" pole splice, and Fig. 3.111 shows a butt splice. Poles spliced in this way can be seen in Fig. 3.110. A wood mast fabricated from structural timber can be seen in Fig. 3.122.

The advantages of wood in some regions of the world include relatively low cost, easy handling in construction, and the convenience of having

a wide variety of standard items of assembly hardware available. The disadvantage of wood is principally that of rot, which limits the life of the pole. It is good practice to dip the underground wood in creosote, which is an effective preservative. In many applications it is good practice to

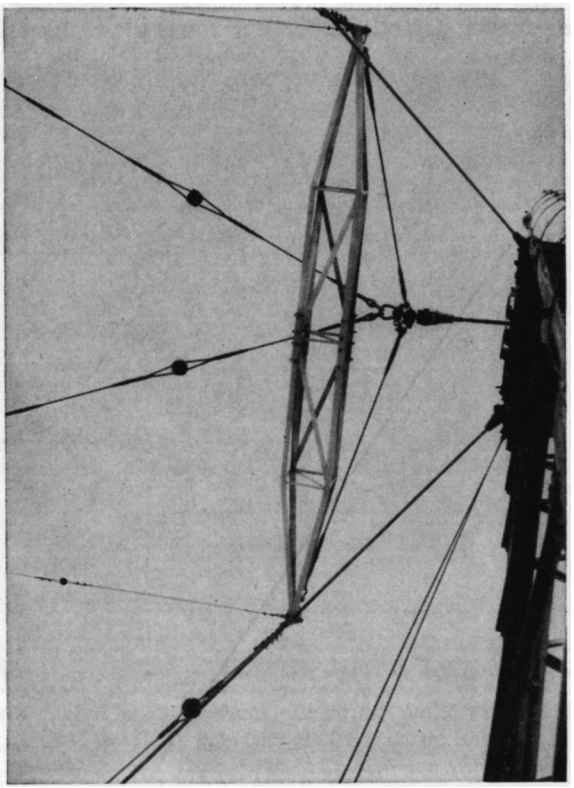

FIG. 3.102. Detail of the top of one tower supporting a high-gain dipole array, showing the cable yoke and the spreader for radiator- and reflector-curtain spacing in the main catenary. The spreader is used to space the side catenary for supporting the ends of the dipoles for the 25-meter array. (*Photograph courtesy of Canadian Broadcasting Corporation.*)

dip the entire pole in creosote, following a process specification familiar to local power and telephone linemen. Wood above ground can be preserved by painting with outdoor-type oil paints.

In places where there is perpetual moisture and fog or in very rainy climates, rot is accelerated because the wood is wet or damp a large part of the time. In other regions where termites and some kinds of wood-eating ants exist, it may not be practical to use wood at all. The greatest risk of rot exists at splices, holes, or the crossarm attachments,

because moisture remains in such cracks, crevices, and unexposed surfaces for long periods.

Steel masts and towers are extensively used for antenna supports where wood is impractical or excessively expensive and for structures higher than can be attained with wood poles. These can be in the form of guyed slender masts or self-supporting towers. Figures 3.100, 3.104,

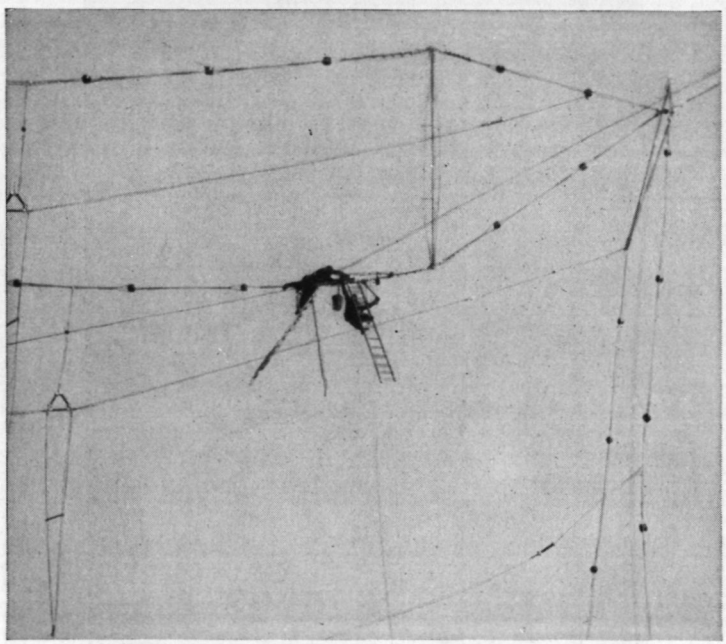

FIG. 3.103. Photograph taken during the construction of a high dipole broadside array, showing riggers working on the main triatics. (*Photograph courtesy of Canadian Broadcasting Corporation.*)

3.106, and 3.115 show guyed masts, while Figs. 3.110 (background) and 3.116 show self-supporting steel towers. Steel structures require painting to preserve them.

Hollow concrete poles, steel-reinforced, are available at reasonable prices in some regions in sizes equivalent to the largest wood poles. They have the advantage of long life in all kinds of weather, but they have the disadvantage that all attachments must be made by means of pole bands, which complicates the original assembly. It is not usually feasible to attach climbing spikes so that it is necessary to employ a boatswain's chair to ascend the pole for construction and maintenance.

Iron-pipe masts can be used for a limited number of very light requirements.

The question of the need for breakup insulators in pole and mast guys is a very frequent one. Actual experience over many years fails to provide a final answer. The purpose of breakup insulators is to avoid any possible self-resonance and reradiation from the guy wires, or stays. Resonance can exist as readily in an insulated guy wire as in a non-

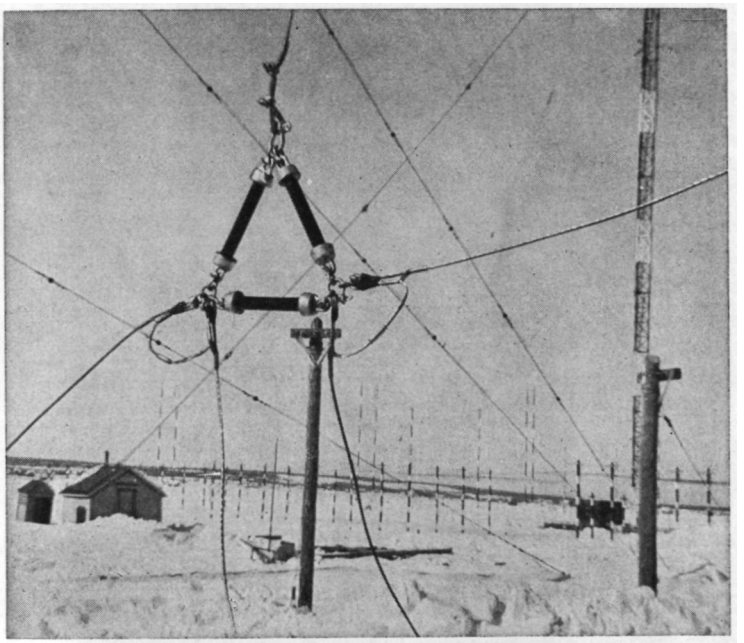

FIG. 3.104. Detail of the assembly of the uppermost dipoles of a high dipole array, showing the upper end of the central feeder and the connections to two dipoles. The cable that supports the feeder and the inner ends of the dipoles from the main triatic is seen in the upper center. (*Photograph courtesy of Canadian Broadcasting Corporation.*)

insulated one, if its natural period is equal to or near the working frequency. The current that will flow in a resonant guy wire is proportional to the induced electromotive force. In any event, one tries to locate guy wires in the weakest possible fields from the radiating system to minimize the induced electromotive force.

If a guy wire is found to be resonant and has a considerable reradiated field, it can be detuned in various ways by altering its distributed electrical constants. Since it is very difficult to predict the resonant frequency of a guy, insulated or uninsulated, the risk of resonance is about the same either way. Therefore it seems that there is slight justification for the

expense of breakup insulators except where the guys are in very strong fields, and this only because of the ease with which a guy can be detuned if necessary by short-circuiting one or more of the insulators or placing inductors across one or more of them.

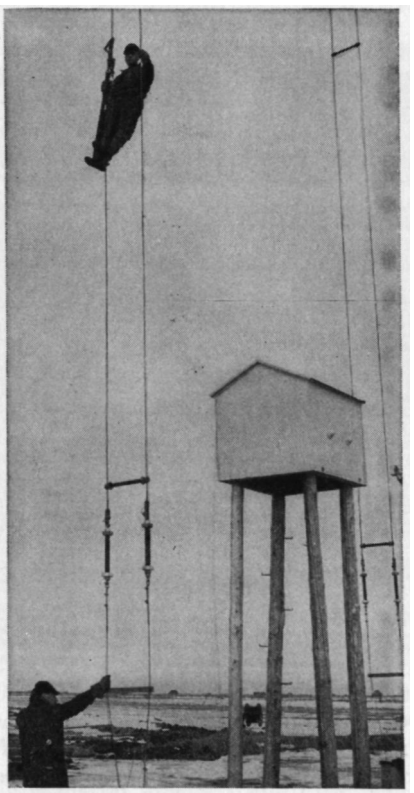

FIG. 3.105. Detail of the lower ends of the vertical feeders for radiator and reflector curtains for a high-frequency dipole beam array, taken during construction. The cabin on posts houses the switching contactors for reversing the direction of the beam by interchanging the feeds to the front and rear (identical) curtains of dipoles. (*Photograph courtesy of Canadian Broadcasting Corporation.*)

It is desirable to explore for parasitic currents in guy wires, using the same technique employed for measuring current in individual wires of a transmission line. Then if a substantial parasitic current is indicated, means can be tried to eliminate it by detuning. This simple precaution is well advised with highly directive systems where spurious reradiation could compromise the radiation pattern of the antenna in the low-field directions.

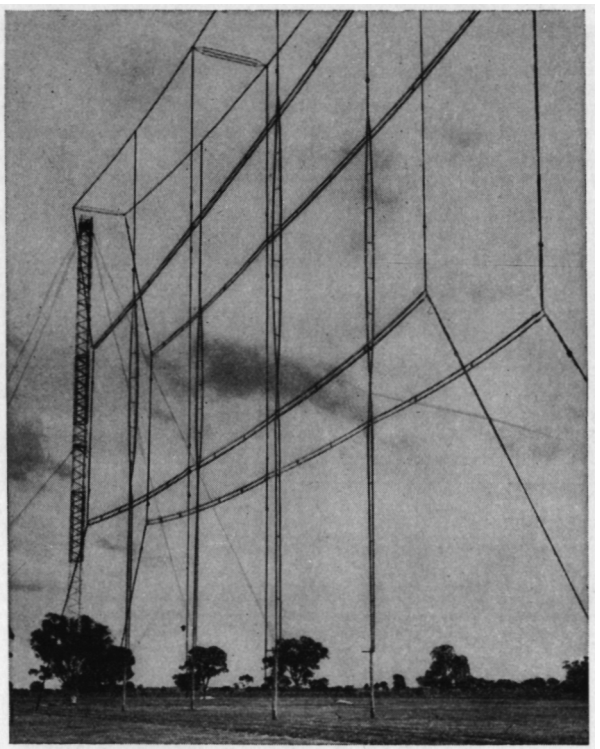

FIG. 3.106. View of a horizontal dipole array using two-wire dipoles. (*Photograph courtesy of Australian Postmaster-General's Office.*)

FIG. 3.107. Inside a rigger's hut during a steel-rope splicing operation. Notice typical rigging equipment in background.

FIG. 3.108. Detail of guy anchor for the pole supports of a high-frequency antenna system.

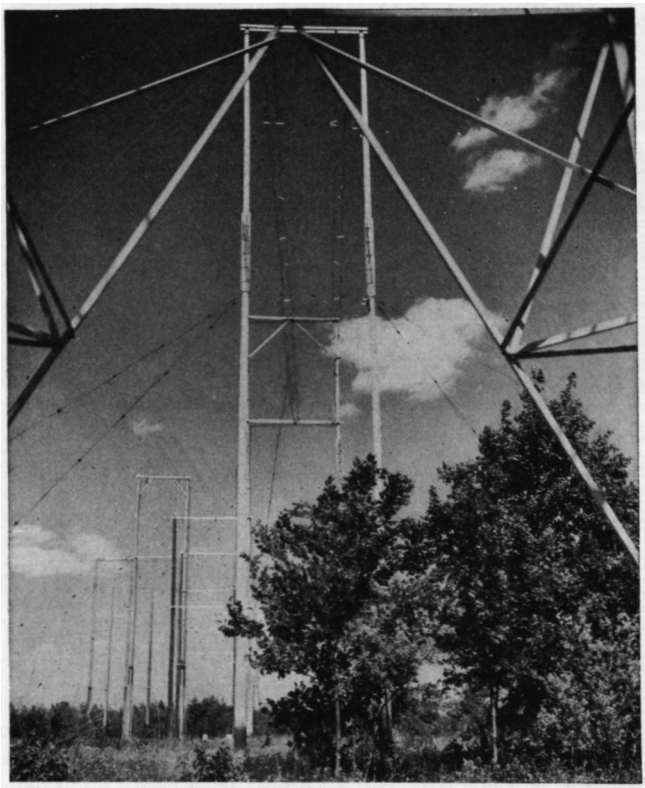

FIG. 3.109. Pole-frame supports for high-frequency-broadcast dipole arrays. (*Photograph courtesy of National Broadcasting Company.*)

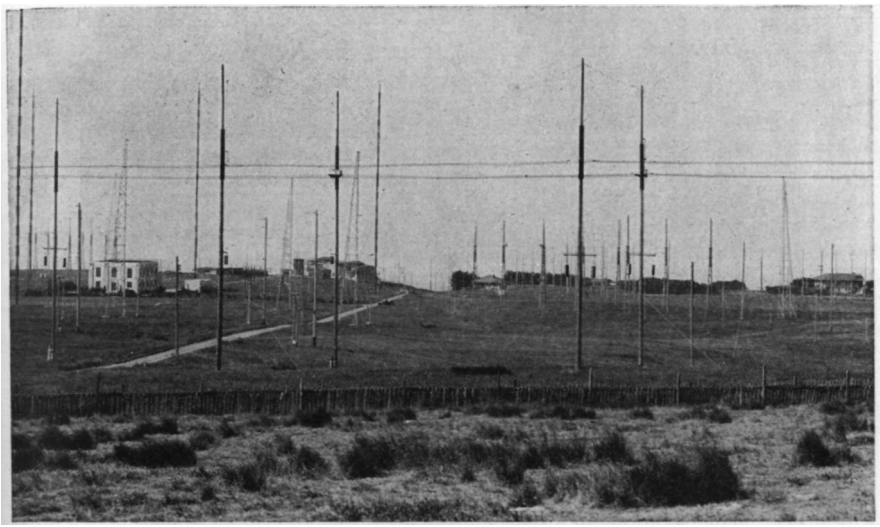

FIG. 3.110. The RCA Communications, Inc., transmitting station at Bolinas, California, showing a forest of poles and towers of different types as used for a large number of high-frequency antennas. Butt-spliced poles and A poles may be seen, together with steel towers. (*Photograph courtesy of RCA Communications, Inc.*)

FIG. 3.111. A butt-spliced pole ready for erection. (*Photograph courtesy of RCA Communications, Inc.*)

FIG. 3.112. The beginning of a pole-splicing operation and the construction of a butt-spliced pole. (*Photograph courtesy of National Broadcasting Company.*)

FIG. 3.113. Preparing the construction of a lap splice for large poles. (*Photograph courtesy of National Broadcasting Company.*)

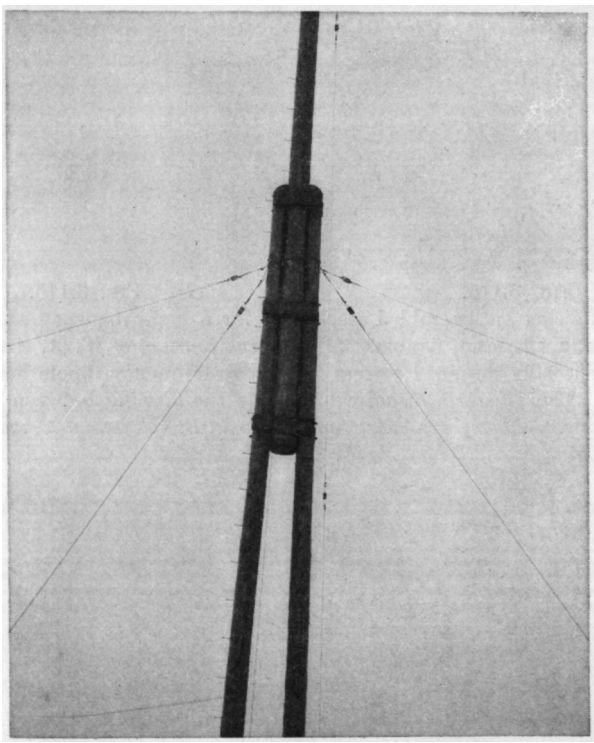

FIG. 3.114. The A pole, a method of splicing wood poles for greater height. (*Photograph courtesy of National Broadcasting Company.*)

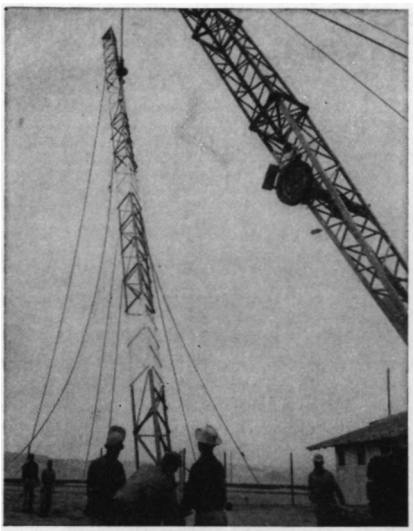

FIG. 3.115.

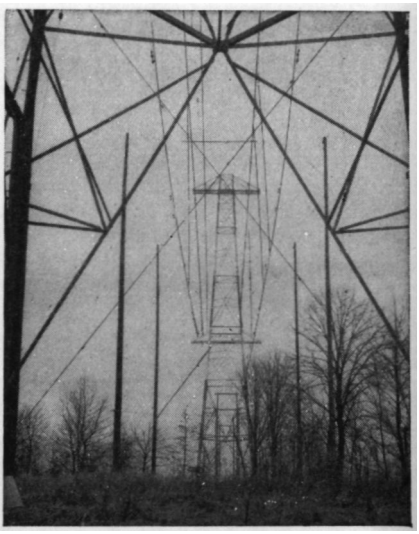

FIG. 3.116.

FIG. 3.115. Raising an assembled steel mast for a high-frequency antenna with a tractor derrick in Dhahran, Arabia. (*Photograph courtesy of W. A. Acton.*)

FIG. 3.116. Specially designed towers for a high-frequency dipole beam array for broadcasting. The crossarm structures provide the spacing between radiator and reflector curtains. (*Photograph courtesy of National Broadcasting Company.*)

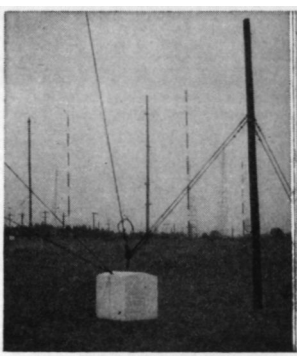

FIG. 3.117.

FIG. 3.118.

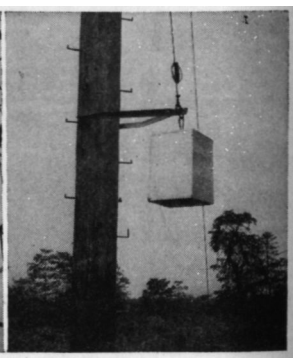

FIG. 3.119.

FIG. 3.117. Counterweight for maintaining constant tension in a large rhombic antenna, with limiting ropes. The wire rope that is most nearly vertical carries the antenna stress.

FIG. 3.118. Counterweight detail for a vertical feeder.

FIG. 3.119. Counterweight lever-arm detail on an antenna pole.

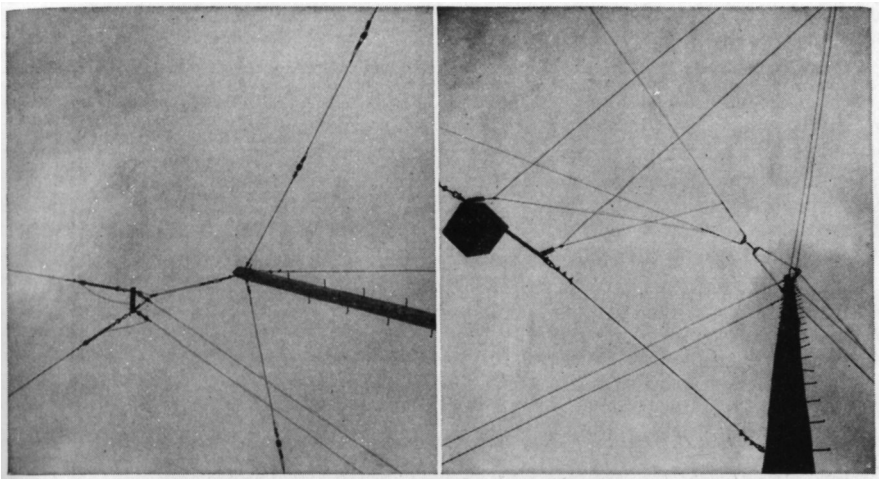

FIG. 3.120. End details for horizontal rhombic antennas built on wood poles. *Left:* View of an antenna with single halyard and sheave, on wood pole. *Right:* Apex of transmitting antenna using yokes for assembly and with a counterweighted vertical feeder. Double halyards and sheaves are used on a crossarm.

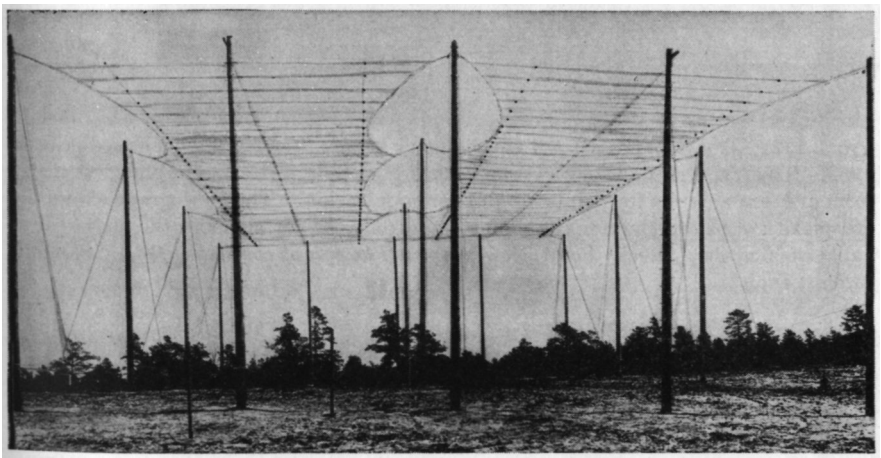

FIG. 3.121. A two-bay fishbone receiving antenna as used at the Riverhead Receiving Station of RCA Communications, Inc.

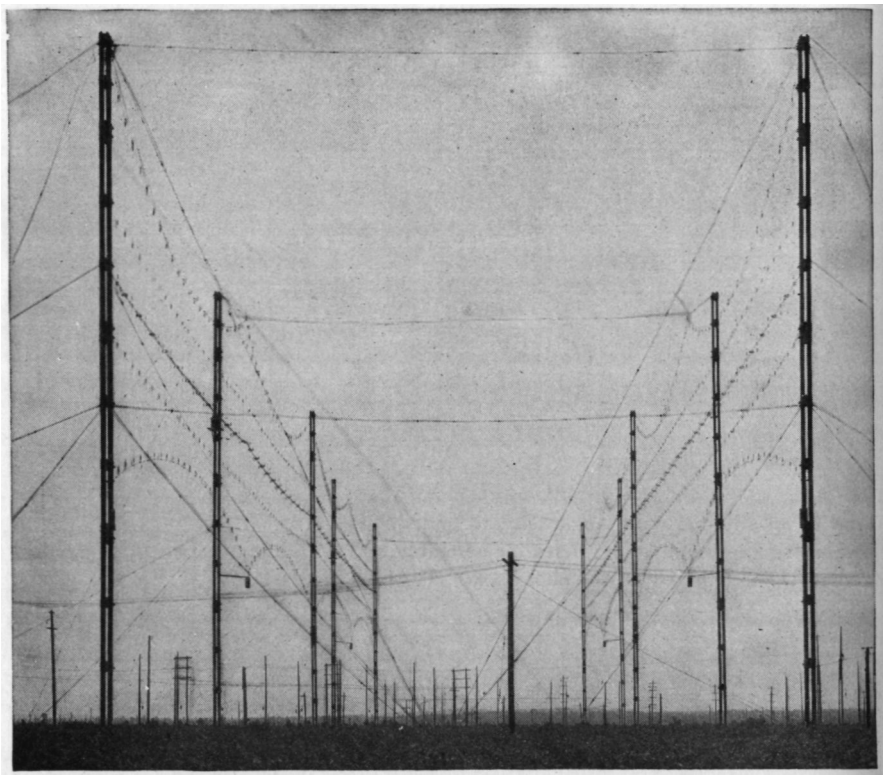

FIG. 3.122. The RCA Model A high-frequency beam-antenna system as used prior to 1935. This type of radiating system for vertical polarization exemplified an early form of beam antenna for point-to-point communication. The photograph shows the complexity of the rigging for the radiator and reflector curtains and the use of fabricated wood masts. Rocky Point, New York. (*Photograph courtesy of RCA Communications, Inc.*)

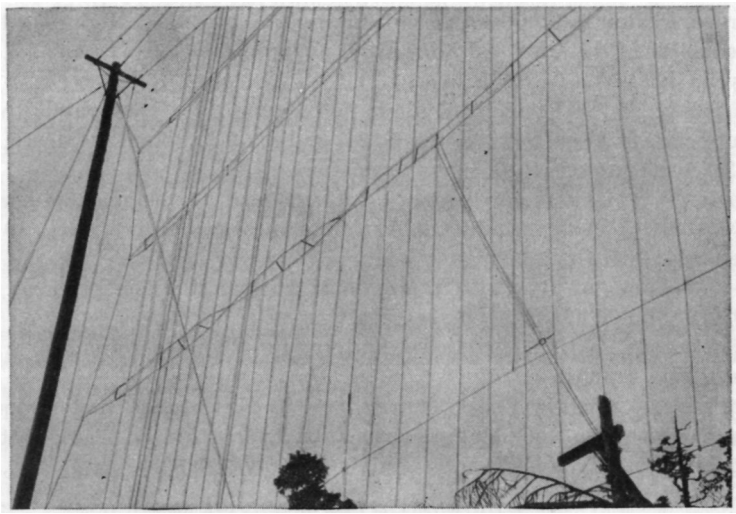

FIG. 3.123. A 24-dipole array for vertically polarized transmission on 45 megacycles. This is an example of the use of high-frequency-antenna techniques in the very-high-frequency region. A screen of parallel wires is used as a neutral reflector. Note use of two-wire balanced feeder, and the use of quarter-wave section at ends of feeders to the radiators as insulators. (*Photograph courtesy of RCA Victor Company, Ltd., Montreal.*)

BIBLIOGRAPHY FOR HIGH-FREQUENCY ANTENNAS

1. Baker, W. G., A Chart for Rhombic Antenna Design, *A.W.A. Tech. Rev.*, **6**:177, 1944.
2. Barfield, R. H., and W. Ross, Short-wave Adcock Direction Finder, *J. IEE*, **81**:683, 1937.
3. Barker, R. H., Rhombic Aerial Design Chart, *Wireless Engr.*, **25**:361, November, 1948.
4. Baumler, M., K. Kruger, H. Plendl, and W. Pfitzer, Radiation Measurements of a Short Wave Directive Antenna at the Nauen High Power Radio Station, *Proc. IRE*, May, 1931, p. 812.
5. Beverage, H. H., and H. O. Peterson, Diversity Receiving System of RCA Communications, Inc., for Radiotelegraphy, *Proc. IRE*, **19**:531, April, 1931.
6. Bown, R., Trans-oceanic Radiotelephone Development; Multiple Unit Steerable Antenna, *Proc. IRE*, **25**:1131, September, 1937.
7. Bown, R., Researches in Radiotelephony; Multiple-unit Steerable Antenna, *J. IEE*, **83**:395, September, 1939.
8. Bruce, E., Developments in Short-wave Directive Antennas, *Proc. IRE*, **19**:1406, August, 1931; *Bell System Tech. J.*, **10**:656, October, 1931.
9. Bruce, E., A. C. Beck, and L. R. Lowry, Horizontal Rhombic Antennas, *Proc. IRE*, **23**:24, January, 1935.

10. Bruce, E., and A. C. Beck, Experiments with Directivity Steering for Fading Reduction, *Proc. IRE*, **23**:357, April, 1935; *Bell System Tech. J.*, **14**:195, April, 1935.
11. Cafferata, H., A Generalized Radiation Formula for Horizontal Rhombic Antennas, *Marconi Rev.*, Issues 80, 81, and 82, **9**(1), January–March, 1946, **9**(2), April–June, 1946, **9**(3), July–September, 1946.
12. Carter, P. S., C. W. Hansell, and N. E. Lindenblad, Development of Directive Transmitting Antennas by RCA Communications, *Proc. IRE*, **19**:1733, October, 1931.
13. Chamberlain, A. B., CBS International Broadcast Facilities, *Proc. IRE*. **30**:118, March, 1942.
14. Christiansen, W. N., Directional Patterns for Rhombic Antennae, *A.W.A. Tech. Rev.*, **7**:33, 1946.
15. Christiansen, W. N., W. W. Jenvey, and R. D. Carman, Radio-frequency Measurements on Rhombic Antennae, *A.W.A. Tech. Rev.*, **7**(2) 131, 1946.
16. Christiansen, W. N., Rhombic Antenna Arrays, *A.W.A. Tech. Rev.*, **7**(4): 361, 1947.
17. Everitt, W. L., and J. F. Byrne, Single Wire Transmission Lines for Short-wave Antennas, *Ohio State Univ. Eng. Expt. Sta. Bull.*, **52**:1, 1930.
18. Foster, Donald, Radiation from Rhombic Antennas, *Proc. IRE*, **25**:1327, October, 1937.
19. Franz, K., Gain and Absorption Area of Large Directional Aerials, *Hochfrequenztech. u. Elektroakustic*, December, 1939, p. 198.
20. Friis, H. T., New Directional Receiving System, *Proc. IRE*, **13**:685, December, 1925.
21. Friis, H. T., and C. R. Feldman, Multiple Unit Steerable Antenna for Shortwave Reception, *Proc. IRE*, **25**:841, July, 1937; *Bell System Tech. J.*, **16**:337, July, 1937.
22. Gill, A. J., Developments in Radio Engineering Carried Out by the Post Office Engineering Department, *J. IEE*, February, 1939, p. 256.
23. Goddess, G., NBC Beam Antennas, *Communications* (*N.Y.*), March, 1939, p. 16.
24. Grosskopf, J., and K. Vogt, Polarisation Measurements in the Field of Horizontal Transmitting Dipole, abstract, *Wireless Engr.*, **21**:437, September, 1944.
25. Harper, A. E., "Rhombic Antenna Design," D. Van Nostrand Company, Inc., New York, 1941.
26. Harrison, C. W., Jr., Characteristics of the Two-antenna Array, *Proc. IRE.*, **31**:75, February, 1943.
27. Harrison, C. W., Jr., Radiation from Vee Antennas, *Proc. IRE*, **31**:362, July, 1943.
28. Harrison, C. W., Jr., Radiation Field of Long Wires, with Application to Vee Antennas, *J. Applied Phys.*, **14**:537, October, 1943.
29. Hayes, L. W., and B. N. McLarty, Empire Service Broadcasting Station at Daventry, *J. IEE*, September, 1939, p. 328.

30. Howe, G. W. O., Polar Diagram of a Simple Broadside Array, *Wireless Engr.*, **19**:193, May, 1942.
31. Kraus, J. D., Multi-wire Dipole Antennas, *Electronics*, January, 1940, p. 26.
32. Lewin, L., Rhombic Transmitting Aerial, *Wireless Engr.*, May, 1941, p. 140.
33. Meissner, A., Directional Radiation with Horizontal Antennas, *Proc. IRE*, **15**:928, November, 1927.
34. Morton, H. B., and J. W. Whitehead, Two Transmitters on One Aerial (3–15 mc/c.), *Elec. Eng.*, **20**(243), May, 1948.
35. Page, H., Measured Performance of Horizontal Dipole Transmitting Arrays, *Electrician*, **133**:408, Nov. 3, 1944; *Elec. Rev.* (*London*), **135**:625, Nov. 3, 1944.
36. Polkinghorn, F. A., Single Sideband MUSA Receiving System for Commercial Operation on Transatlantic Radio-telephone Circuits, *Bell System Tech. J.*, April, 1940, p. 306.
37. Ross, W., Calibration of 4-aerial Adcock Direction Finders, *J. IEE*, August, 1939, p. 192.
38. Royal Air Force Signal Manual, Part II, *Air Pub.* 1093, May, 1937, Chap. 14, Propagation, Chap. 15, Aerials and Aerial Arrays.
39. Smale, J. A., Comparative Merits of Different Types of Directive Aerials for Communications, *J. IEE*, **9**(Part III): 12, March, 1944; *Electrician*, **132**:74, Jan. 28, 1944; *Elec. Rev.* (*London*), **134**:119, Jan. 28, 1944.
40. Smith, N. S., High-frequency Broadcasting in Australia, *Proc. IRE* (*Australia*), October, 1948, p. 4. Multiple-frequency operation of high-frequency antennas. Antenna switching. Use of coupled sections one-half wavelength long. Antenna layouts.
41. Sterba, E. J., Theoretical and Practical Aspects of Directional Transmitting Systems, *Proc. IRE*, **19**:1184, July, 1931.
42. Waidelick, D. L., General Folded Dipole Antenna Design, *Communications* (*N.Y.*), April, 1949, p. 18.
43. Walmsley, T., Beam Arrays and Transmission Lines, *J. IEE*, February, 1931.
44. Walmsley, T., New Type of Directive Aerial, *Wireless Engr.*, **9**:662, November, 1932.
45. Wells, N., Short-wave Dipole Aerials, *Wireless Engr.*, **20**:219, May, 1943.
46. Wells, N., Quadrant Aerial; an Omni-directional Wide-band Horizontal Aerial for Short Waves, *J. IEE*, **91**(3) 182, December, 1944. Brief paper, *Marconi Rev.*, **9**(1), January–March, 1946.

CHAPTER 4

Radio-frequency Transmission Lines

4.1. Propagation of Radio-frequency Currents in Linear Conductors

Radio-frequency energy can be guided by the propagation of transverse electromagnetic waves along systems of parallel conductors called "transmission lines." For brevity they are also called "lines" or "feeders." The input energy is stored in the field of the conductors and is propagated along the system at some finite velocity. For conductors in open air, this velocity is 3×10^8 meters per second. In this discussion it will be understood that the transmission-line phenomena pertain to the quasi-static conditions corresponding to cross-sectional dimensions very small with respect to the wavelength.[60] This means that the time of propagation of the field between conductors is small in relation to a single period. In radio-engineering practice the design of a system is based on the recognition of this condition.

4.1.1. Infinite and Finite Lines. Any line of continuous and uniform parameters exhibits an important circuital property known as the "characteristic impedance." This is usually designated as Z_0. This is the impedance of the line as seen at its input terminals if the line were of infinite length. Such a line would continuously absorb energy from a generator and propagate it outward forever. A line of finite length is simply a portion of an infinite line. The missing remainder, going on to infinity and having the same characteristic impedance Z_0, has been cut away. To simulate this missing portion, any load with an impedance equal to Z_0 can be used to *terminate* or *match* the line and absorb all the energy propagated from the generator. When a line is terminated in an impedance equal to its characteristic impedance, the propagation of currents between the generator and the termination is the same as in an infinite line and energy travels only away from the generator. At radio frequencies the characteristic impedance of low-loss lines is resistive. When open-circuited, close-circuited, or terminated in any arbitrary impedance other

than Z_0, there is reflection of energy from the end back toward the generator. The presence of waves traveling in both directions on the conductors gives rise to various current and potential distributions and causes the input impedance to vary widely in magnitude and phase angle. Because of this, transmission lines have uses as impedance transformers and energy-storage circuits as well as for the guidance of energy from a generator to some load circuit.

4.1.2. Some Important Transmission-line Equations. The following equations, derived from transmission-line theory and proved in the classical literature on this topic, have frequent utility in the design of systems, and are grouped here for reference.

In general

$$Z_0 = \sqrt{\frac{R + j\omega L}{G + j\omega C}} \tag{1}$$

At radio frequencies, when ω becomes very large with respect to other factors

$$Z_0 \rightarrow \sqrt{\frac{L}{C}} = \frac{1}{vC} = vL \tag{2}$$

When the field of the transmission line is entirely within an isotropic dielectric medium having an inductivity, or dielectric constant, ϵ,

$$Z_{0\epsilon} = \frac{Z_{0(\text{air})}}{\sqrt{\epsilon}} \tag{3}$$

The propagation constant γ is in general complex;

$$\gamma = \alpha_0 + j\beta_0 = \sqrt{(R + j\omega L)(G + j\omega C)} \tag{4}$$

At radio frequencies and with lossless lines, γ becomes essentially a phase angle per unit length.

$$\begin{aligned} \gamma = j\beta_0 &= \omega\sqrt{LC} && \text{radians} \\ &= 360f\sqrt{LC} && \text{electrical degrees} \\ \alpha_0 &\doteq \frac{R}{2Z_0} && \text{nepers* per meter} \end{aligned} \tag{5}$$

The velocity of propagation of transverse electromagnetic waves in systems of parallel linear conductors with air dielectric is equal to c, which is the velocity of light in free space (3×10^8 meters per second).

$$c = v = \frac{\omega}{\beta} = \frac{1}{\sqrt{LC}} = \lambda f = \frac{Z_0}{f} = \frac{1}{Z_0 C} \tag{6}$$

* 1 neper = 1 hyperbolic radian = 8.686 decibels, corresponding to a current (or voltage) ratio of $2.7182+ = e$.

For a line in an isotropic dielectric ϵ, the velocity of propagation is

$$v_\epsilon = \frac{c}{\sqrt{\epsilon}} \tag{7}$$

When a radio-frequency line of length βl degrees (or radians) is terminated in a complex impedance Z_t, the input impedance Z_{in} is, in general, complex, in accordance with the equation

$$Z_{in} = Z_0 \frac{Z_t \cos \beta l + jZ_0 \sin \beta l}{Z_0 \cos \beta l + jZ_t \sin \beta l} \tag{8}$$

When $Z_t \neq Z_0$, there is reflection from the termination. The reflection factor is, in general, complex, and is specified as follows:

$$K = |K|e^{j\psi} = \frac{Z_t - Z_0}{Z_t + Z_0} \tag{9}$$

$$|K| = \frac{SWR - 1}{SWR + 1} \equiv \frac{Q - 1}{Q + 1} \tag{10}$$

When $Z_t = 0$ (short circuit),

$$Z_{in} = jZ_0 \tan \beta l \tag{11}$$

When $Z_t = \infty$ (open circuit),

$$Z_{in} = -jZ_0 \cot \beta l \tag{12}$$

For a line of length $\beta l = \pi$ radians $= 180$ degrees (one-half wavelength)

$$Z_{in} = Z_t \qquad \text{and} \qquad V_{in} = V_t\underline{/180}$$

also

$$I_{in} = I_t\underline{/180} \qquad \text{reversed phase} \tag{13}$$

For a line of length $\beta l = \pi/2 = 90$ degrees (one-quarter wavelength)

$$Z_{in} = \frac{Z_0^2}{Z_t} \qquad \text{and} \qquad \frac{V_{in}}{I_{in}} = \frac{Z_0^2 I_t}{V_t} \tag{14}$$

This is an impedance-inverting circuit with a 90-degree change in relative phase between input and output currents and potentials. When $\beta l = 45$ degrees (one-eighth wavelength) and $Z_t = R_t + j0$,

$$Z_{in} = jZ_0 \qquad \text{when} \qquad R_t = 0$$
$$Z_{in} = -jZ_0 \qquad \text{when} \qquad R_t = \infty$$

and in general $|Z_{in}| = |Z_0|$ for all values of R_t, positive and negative, from 0 to ∞. (Only the angle of Z_{in} varies with R_t.)

The standing-wave ratio Q on a transmission line increases with increasing inequality between Z_t and Z_0 both in phase and in magnitude.

$$Q = \frac{\pi f_0}{\alpha_0 v} = \frac{2\pi f Z_0}{RC} = \frac{f_0}{2(f_0 - f)} \tag{15}$$

This equation for Q is useful when transmission lines are used as high-Q resonant circuits.

When a section of transmission line is used as a transformer to match an impedance $Z_t = R_t \pm jX_t$ with another impedance $Z_{in} = R_{in} \pm jX_{in}$, the characteristic impedance Z_{00} of the transforming section is

$$Z_{00} = \sqrt{a + \frac{bd}{C}} \tag{16}$$

and its electrical length must be

$$\beta l = \tan^{-1} \frac{c}{b} Z_{00}$$

in which

$$a = R_t R_{in} - X_t X_{in} \qquad c = R_{in} - R_t$$
$$b = R_t X_{in} + X_t R_{in} \qquad d = X_{in} - X_t$$

In all the preceding equations the following symbols apply:

R = resistance per loop meter, ohms
L = inductance per loop meter, henrys
G = leakage conductance per meter of line, mhos
γ = complex propagation constant per meter of line
C = capacitance per meter of line, farads
α_0 = attenuation constant per meter of line, nepers
β_0 = phase constant per meter of line, radians
$\omega = 2\pi f$
f = frequency, cycles
f_0 = frequency of resonance
c = velocity of propagation of light in free space
$c = 3 \times 10^8$ meters per second
v = velocity of propagation in the line, meters per second
λ = free-space wavelength in meters for a wave of frequency f
Z_{in} = input impedance, ohms (complex)
Z_t = terminal (load) impedance, ohms (complex)
K = reflection coefficient due to terminal mismatch of impedance (complex)
ϵ = specific inductive capacity (dielectric constant) of the medium in which the field of the line is contained

SWR = $Q = V_{max}/V_{min} = I_{max}/I_{min}$—the standing-wave ratio—and is the ratio of energy stored in the line to the energy dissipated per second in the line and in the load termination

βl = the over-all electrical length of a line, radians or degrees

l = the length of a line, meters

$\psi = 4\pi d/\lambda$

d = distance, meters, from the terminal end of a line to the first voltage maximum (or current minimum)

4.1.3. Basic Types of Radio-frequency Transmission Lines. Circuitally there are two basic types of uniform transmission lines for single-phase operation:

1. *Balanced lines*, where there are equal and opposite potentials from both sides of the transmission circuit to ground.

2. *Unbalanced lines*, where one side of the circuit is at high potential and the other side is at ground potential.

Structually there are also two basic forms:

1. *Open-wire lines*, where the conductors are supported in the air above ground.

2. *Enclosed lines*, where one or more conductors forming the transmission circuit are enclosed by a metallic shield that confines the field within the enclosed space. Both balanced and unbalanced lines are included in this class.

Then there are two basic classes of applications for transmission lines:

1. For *guiding* electrical energy from a generator to a load circuit. This is the application implied by the use of the alternative term "feeder." The charges delivered by the generator move along the line to the load in a single traveling wave.

2. For *storing* electrical energy in excess of that dissipated in the load. The charges on the system are moving from the generator to the load, and also in the reverse direction, and form standing waves on the system. In this form lines are used as tuned circuits,[41,42] as reactors, and as impedance transformers.[31] Since a section of transmission line can be used to obtain any desired reactance at any given frequency, a combination of sections can be used to form networks which act as low-pass, high-pass, and bandpass filters of constant-k, m-derived, or lattice types.

4.1.4. Transmission-line Parameters. The fundamental electrical characteristics are derived from the configuration of the electric and magnetic fields surrounding the conductors, which in turn are derived from the parameters of the cross-sectional geometry of the line and the nature of the enclosing dielectric medium. In the quasi-static case, corresponding to typical engineering usage, the transmission lines under consideration

propagate transverse electromagnetic waves (waves in which the electric and magnetic vectors are mutually normal and also normal to the direction of propagation), but the parameters are derivable from electrostatics or magnetostatics. The electrostatic solution, using the theory of logarithmic potentials, is most convenient for the purpose when no ferromagnetic effects are involved. The solution, starting with scalar potentials and charges, yields the unit-length capacitance, characteristic impedance, charge distributions, and velocity of propagation (for example, see Chap. 6). The equipotential surfaces and potential gradients can be calculated from the same information.

An alternative method is that from magnetostatics, using the system of logarithmic vector potentials and currents. The solutions also yield the unit-length inductance, characteristic impedance, current distributions, and the velocity of propagation.

The unit-length resistance and leakance are empirical and depend upon the number of wires and their resistivity, the frequency, the current distribution in the wires, the method and material of insulation, and the conductivity of the soil under the line (when ground-return currents are present). Any concentrated dielectric or ferromagnetic materials in the field of the line can also influence the fundamental parameters to some extent, but ideally they are assumed not to exist. In practice, care is taken to minimize their presence. When the line conductors are of permeable material, the permeability acts with the conductivity as a factor in increasing skin effect and thus increasing the high-frequency resistance.

4.1.5. Characteristic Impedance of a Uniform Low-loss Transmission Line. Any type of feeder with only air dielectric between all the conductors of the system has a characteristic impedance that is determined wholly by the geometry of its cross section, that is, the sizes and shapes of the conductors, their mutual spacings, and their distance from ground or other conducting planes or surfaces. When the entire field of the system is contained within a dielectric material with an inductivity ϵ, Eq. (3) applies. When the conductors have a thin covering of insulating material, the remaining dielectric being air, the presence of the insulation on the wires has the effect of slightly increasing the effective metallic radius of the wires by an amount proportional to the inductivity of the material. For very thin insulating coverings, or for materials of very low inductivity, this effect is usually negligible in practice. In so far as line losses are concerned, any insulation on the wires increases the attenuation. This is because the loss factors for any solid dielectric material are greater than air alone and because the potential gradients are maximum at the surfaces of the conductors. The amount of increase thus caused must usually be

determined empirically and in some cases can be negligible. Beyond a point, loss can affect the value of the characteristic impedance in magnitude and phase angle.

The presence of supporting insulators, or insulators used for maintaining constant spacing, has the effect of increasing the capacitance of the wire system and therefore of reducing its characteristic impedance and the velocity of propagation. In many open-wire lines this effect is virtually negligible (though it should be considered quantitatively in all applications where the electrical length of a line is critical). In enclosed lines with air dielectric, the spacing insulators always have a considerable influence on the characteristic impedance and the propagation velocity and therefore must always be considered.

The manner in which the characteristic impedance is derived from the cross section of a line is developed in Chap. 6, which gives several examples of the computation of characteristic impedance for different types of lines.

In typical practice, round or cylindrical conductors in the form of wires or tubes are used for the conductors. A uniform transmission line means that its cross section is identical at every point throughout its length, and if it be an open-wire line, it is assumed to be straight. In practice, the supporting members, insulators, small variations in cross-section dimensions, corners or bends in the conductors, and the close proximity of other metallic or dielectric objects cause variations in the characteristic impedance. The importance of these irregularities depends upon their magnitude and also upon the frequency of the guided energy. The electrical distance between identical irregularities (such as supporting members) also affects Z_0. If there are at least seven such uniformly spaced irregularities per wavelength, their effect is the same as a uniformly distributed shunt capacitive loading, which reduces the characteristic impedance slightly below its theoretical idealized value and reduces the propagation velocity.

When the frequency is so high that there are fewer than about seven uniformly spaced irregularities per wavelength, there is reflection of energy between these successive points, if the irregularities are sufficiently large, which causes the input impedance to oscillate above or below its characteristic impedance at different frequencies. This is a condition to be avoided because it also increases the attenuation per unit length of line and presents a complex impedance to the generator (regardless of the load termination), which varies with frequency. In this condition the line is said to be "lumpy."

It is possible to reduce the lumpiness of line impedance in the critical region of reflection when open-wire lines are used. For instance, the

presence of insulators, binding wire, metallic insulator caps, and assembly hardware produces the effect of an increase in shunt capacitance over that due to the wires alone in air between supporting poles. The resulting capacitive loading may be of such a magnitude as to constitute a substantial irregularity, especially if the frequency to be transmitted is high.[51] Then, for the short section of line near the pole, Z_0 is reduced. All that is required to maintain constant characteristic impedance is to maintain a constant *ratio* of inductance to capacitance per unit length. A unit of length near a supporting pole has an increased capacitance. Therefore, if the spacing can be increased, or the conductors reduced in diameter, to increase the unit-length inductance by an identical amount, the irregularity due to the support is neutralized and a truly uniform line results.

In practical construction it is usually necessary to change the direction of a feeder. A corner or angular bend introduces an irregularity by changing the series inductance of the line at and near the bend owing to interlinking of fields. For this reason, good construction requires that the bend be gradual and devoid of sharp corners. When such bends are made, it is *necessary* to use exactly the same length of wire on the two sides of a balanced line. It is more important to maintain equal wire lengths on the two sides of a circuit in making a bend than to try to maintain a strictly constant spacing between wires at the bend.

When feeders must pass through switching devices, great ingenuity must be used to avoid discontinuities of magnitudes that are disturbing in their effect on the line impedance. Any dead-end portions of transmission line also produce impedance irregularities that can be very troublesome in switching devices.

In solid-dielectric feeders (both flexible and rigid), there is a close approach to the ideally uniform line. Where connections or junctions are made with other sections of feeder, the connectors may introduce local irregularities. For most standard solid-dielectric feeder material it is possible to obtain constant-impedance connectors that have very little effect on the uniformity of the feeder impedance.

4.1.6. Control of Characteristic Impedance in Design. There are many common applications where the feeder characteristic impedance may be of any convenient though arbitrary value. But in certain types of application one may require a feeder of a specific characteristic impedance.

To obtain a *lower* characteristic impedance the following general conditions apply:

1. The conductor sizes can be increased while maintaining the same center-to-center distances.

2. For given wire sizes, the distances between conductors can be decreased.

3. The number of wires used in each side of the feeder (if balanced) or the high-potential side (if unbalanced) can be increased.

4. Two or more feeders may be used in parallel.

5. Lumped shunt capacitors may be connected across the line at equal distances to produce the effect of smooth loading at the working frequencies, with lower characteristic impedance.

To increase characteristic impedance, opposite methods are used. Instead of increasing the capacitance per unit length as in item 5, inductance may be uniformly distributed in series with the line.

The formulas for the characteristic impedance of several practical forms of transmission lines for radio applications are given in the following section. Formulas for other configurations can be developed by applying the principles of logarithmic potentials from Chap. 6.

4.2. Useful Transmission-line Configurations and Their Formulas

In this section will be found the essential electrical- and mechanical-design information on 19 different types of radio-frequency transmission lines. The formulas for the characteristic impedance and the attenuation of each type of line are left in the form most convenient for arithmetical computation. They have been simplified by omitting small-order effects, which add much to the complexity of usage but which affect the final accuracy of the result by only 1 or 2 per cent. In the form presented, the formulas are sufficiently exact for any ordinary engineering applications. To provide a guide to their application, some representative data are included for each type. All of the formulas are based on quasi-static conditions corresponding to the great majority of engineering applications for frequencies up to about 30 megacycles.

The equations throughout this section will employ the following symbols:

a, b, c, etc. = spatial dimensions in the line cross section
h = height above ground
ρ = wire radius, in the same units as h, a, etc.
Z_0 = characteristic impedance, ohms
k = ratio of return current in the grounded wires to the current in the high-potential wires
$1 - k$ = ratio of ground-return current to the current in the high-potential wires
f = frequency, megacycles
σ = ground conductivity, *electromagnetic* units
α = attenuation, decibels per 1,000 feet

The attenuation of a transmission line without ground-return currents

is composed of a component α_{copper}, due to loss in all the conductors, and α_i, due to loss in the insulation. In a line having all or part of the return current in the ground, there is an additional component α_{earth}, due to loss in the ground. The total attenuation α_{total} is the sum of α_{copper}, α_{earth}, and α_i. In equations for α which include only α_{copper} and α_{earth}, the symbol α_{ce} will be used.

The larger the number of wires used in parallel, the higher the power capacity of the line in general. The charge density per unit surface of the wire and the potential gradients are thus reduced.

In certain configurations, the charges on all the wires at the same potential are not equal, and the formulation must then include the solution for the relative charge distribution. This is set out in a separate formula so that the designer will know its value.

In unbalanced open-wire lines, there is a division of charges between the grounded wires and those induced in the earth under the line. In dynamic operation the line currents and the earth-return currents are in the same proportion as the electrostatic charges. The ratio of the total return current in the grounded wires to the total current in the high-potential wires is an indication of the relative merit of the configuration. For example, when $k = 0.842$, it means that 84.2 per cent of the return current is in the grounded wires and that the remainder, 15.8 per cent, returns in the earth. It is desirable to design for the higher values of k because the smaller the earth-return current, the lower the attenuation and the smaller the radiation from the line.[28] As k approaches unity, there is no more radiation from an unbalanced line than from a balanced line of similar sectional dimensions.

Unbalanced lines are especially convenient for feeding the types of antennas used in the low and medium radio frequencies, which typically have one side of the circuit connected to ground.

An open-wire unbalanced line radiates more than an enclosed line or an open-wire balanced line. The amount of radiation is very small with lines that have large values of k. From a loss standpoint, radiation loss is negligible in proportion to all other losses in the line. A well-designed open-wire unbalanced feeder with a high value of k can always be used without hesitation with nondirective antennas. They have also been used successfully with directive antennas when the ratio of maximum to minimum field strengths is of moderate value.

In the formulas that follow all mechanical dimensions are in the same units, unless subscripted to indicate otherwise. All attenuations are formulated in decibels per 1,000 feet of feeder when working into a perfectly matched termination for a frequency f in megacycles. It is assumed that there are no buried ground wires in the region where the

earth-return currents for the line flow. Buried ground wires parallel to and under the line produce an empirical value for σ that is much greater than for natural earth constants. This reduces attenuation. The attenuation formulas do not include insulation losses. In many cases insulation losses are negligibly low, but in any case they are empirical and not susceptible to formulation.

The losses in a feeder are the sum of the copper loss, earth return loss, insulation loss, and loss due to direct radiation. Radiation loss from a matched feeder is usually so small that it is negligible for carefully designed systems, and it is always very small with respect to all other losses for almost any type of feeder. Insulation loss in a well-designed system is also a minor quantity except in long feeders working in the high-frequency range, where insulation loss on a two-wire balanced line may exceed one-half as much as the copper loss.

The principal losses in an unbalanced open-wire line are copper loss and ground-return loss. Brown[28] has shown that the attenuation factors due to copper and earth-return losses can be formulated as shown here, where m is the number of high-potential wires in parallel and n the number of grounded wires:

$$\alpha_{\text{copper}} = \frac{2.17\sqrt{f}}{\rho_{\text{inches}} Z_0}\left(\frac{1}{m} + \frac{k^2}{n}\right) \quad \text{decibels per 1,000 feet}$$

$$\alpha_{\text{earth}} = \frac{13{,}720}{Z_0 h_{\text{feet}}}(1 - k)^2\sqrt{\frac{10^{-13}}{\sigma}} \quad \text{decibels per 1,000 feet}$$

These equations are restricted to cases of complete symmetry of currents in the feeder cross section and to those configurations which give equal division of current among the high-potential wires and the grounded wires. The constant is derived for hard-drawn copper. Also, all wires must have the same radius. For applications where open-wire unbalanced feeders are used, the total attenuation is simply the sum of the above two equations, plus some small estimated additional allowance for insulation loss.

Balanced feeders, which are used almost exclusively at the high frequencies, also have two major loss components—copper loss and insulation-leakage loss. The latter is proportional to the characteristic impedance of the system but is otherwise empirical. The loss due to heating of the copper is predictable from the equation

$$\alpha_{\text{copper}} = \frac{4.34\sqrt{f}}{\rho_{\text{inches}} Z_0 M} \quad \text{decibels per 1,000 feet}$$

where M is the number of wires in parallel on each side of the circuit provided that the current is equally divided among the M conductors.

McLean and Bolt[31] have made measurements on two-wire and four-wire balanced lines for high-power high-frequency transmission and have found that, for a 550-ohm two-wire line, the insulation and other losses are about 70 per cent of the copper loss, and for a 320-ohm four-wire line the figure is about 22 per cent, at 20 megacycles. These figures provide a

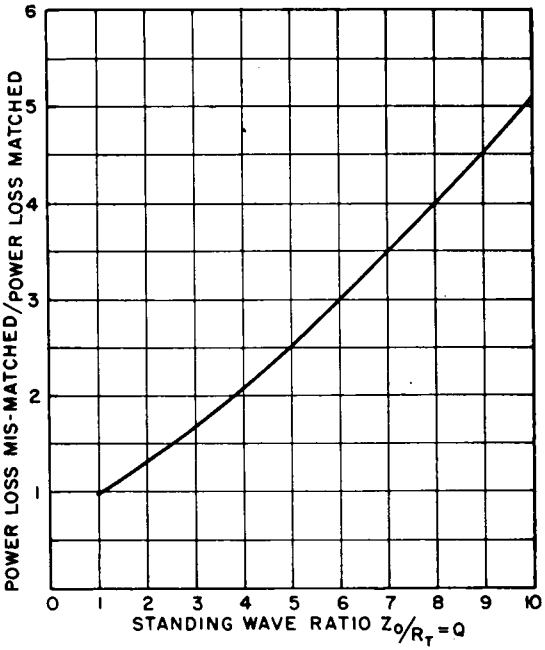

FIG. 4.1. Relative power loss on a transmission line versus standing-wave ratio Q.

basis for estimating the total attenuation of feeders within this impedance range, when the copper conductors are of the order of 0.200 inch diameter. According to Sterba and Feldman[21] the total high-frequency attenuation for a 600-ohm two-wire balanced line using 0.162-inch-diameter hard-drawn copper wires is $\alpha_{total} = 0.152\sqrt{f}$, whereas for copper loss only $\alpha_{copper} = 0.0916\sqrt{f}$. These measurements show insulation and other losses to be 66 per cent of the calculated copper loss.

The increase in attenuation as the standing-wave ratio departs from unity is shown in Fig. 4.1.

A feeder carrying a current I, terminated in its characteristic impedance and having a ground-return current $I_g = I(1 - k)$ amperes, will radiate a small amount of power, the amount being determined from the following equations:[28]

For a feeder one-half wavelength long at a height h above ground, the radiated power P in watts is

$$P = 3{,}500 I_g^2 \left(\frac{h}{\lambda}\right)^2$$

and for a feeder one wavelength long

$$P = 5{,}250 I_g^2 \left(\frac{h}{\lambda}\right)^2$$

One of the causes of radiation from an open-wire line is radiation from the vertical connections at the ends. This can be reduced by decreasing the height of the line; but this in turn increases the ground-return current, which partially offsets the decrease in height. In order to use small heights and retain small relative values of ground-return current, it is necessary to use better shielding of the high-potential wires by using a greater number of grounded wires and perhaps also a smaller line cross section.

The various equations for unbalanced open-wire feeders show that k must be made as near to unity as feasible, which will minimize the ground-return component $1 - k$. The desired properties can, in most cases, be obtained with open-wire lines, thus making it unnecessary to employ concentric lines to avoid radiation troubles.

Whatever radiation occurs from the line will be horizontally polarized at right angles to it and vertically polarized in the direction of the line. The vertically polarized component is the only one likely to cause difficulty, and it can be avoided by running the lines at right angles to the direction of the critical pattern null whenever possible. The precautions taken to avoid end radiation will also aid in suppressing line radiation. Considered application of the various types of lines for which design equations are given, together with the use of still other types that may be developed using more wires, can take care of almost any situation that one is likely to encounter in practice.

By a suitable choice of h and k, radiation can be reduced to any extent desired. The radiation pattern of a terminated feeder follows those of traveling-wave systems, which were discussed in Chap. 3.

4.2.1. Type I. Single-wire Unbalanced Feeder. This design features the utmost structural simplicity, but its use is severely restricted to short runs at low or medium frequencies or to temporary installations. When the line runs over a buried-wire ground system, its attenuation may not be objectionable and when not too high above ground, its radiation is often tolerable. The characteristic impedance, being rather high,

does not lend itself well to matching into low-resistance antennas. Unmatched, it can be used as a direct link between antenna and transmitter, with the tuning elements near the latter. For this type of line

$$Z_0 = 138 \log_{10} \frac{2h}{\rho}$$

$$\alpha_{ce} = \frac{2.17\sqrt{f}}{\rho_{\text{inches}} Z_0} + \frac{13{,}720}{f_{\text{feet}} Z_0} \sqrt{\frac{10^{-13} f}{\sigma}}$$

Typical characteristics are:

ρ, inches	h, inches	Z_0, ohms
0.050	120	509
0.100	120	466

4.2.2. Type II. Two-wire Unbalanced Feeder, with Both Wires in Parallel. This configuration (Fig. 4.2) has lower characteristic impedance than type I, and therefore its attenuation will be higher owing to ground conduction losses. In this case the characteristic impedance is

$$Z_0 = 69 \left(\log_{10} \frac{2h}{\rho} + \log_{10} \frac{2h}{a} \right)$$

and the attenuation is

$$\alpha_{ce} = \frac{1.09\sqrt{f}}{\rho_{\text{inches}} Z_0} + \frac{13{,}720}{h_{\text{feet}} Z_0} \sqrt{\frac{10^{-13} f}{\sigma}}$$

Typical construction values are:

ρ, inches	h, inches	a, inches	Z_0, ohms
0.05	120	10	350
0.10	120	10	329
0.10	120	20	308

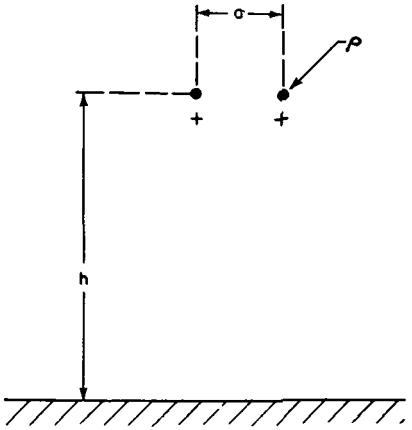

FIG. 4.2.

4.2.3. Type III. Four-wire Unbalanced Feeder, All Wires in Parallel at the Corners of a Square. The application of this type of line (Fig. 4.3) is the same as for types I and II, and it can be used where lower characteristic impedances are desired.

$$Z_0 = 34.5 \log_{10} \frac{16h^4}{\rho a^3 \sqrt{2}}$$

When $h \gg a$,

$$\alpha_{ce} = \frac{0.53\sqrt{f}}{\rho_{\text{inches}} Z_0} + \frac{13{,}720}{h_{\text{feet}} Z_0}\sqrt{\frac{10^{-13} f}{\sigma}}$$

Sample values for a four-wire feeder of this type are:

ρ, inches	h, inches	a, inches	Z_0, ohms
0.100	120	10	254

In types I, II, and III, all of the return current is in the ground. Attenuation tends to be large unless the soil conductivity is reduced by using ground wires parallel to the line and distributed in such a manner as to correspond approximately with the cross-sectional current distribution in the ground.

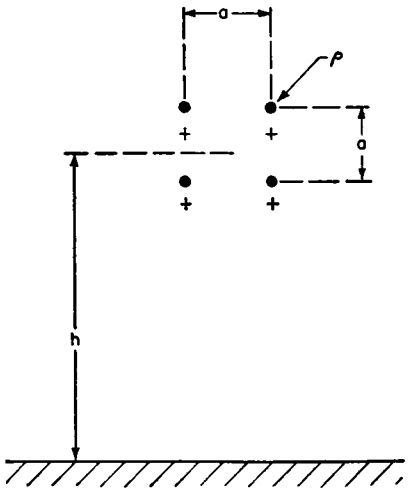

FIG. 4.3.

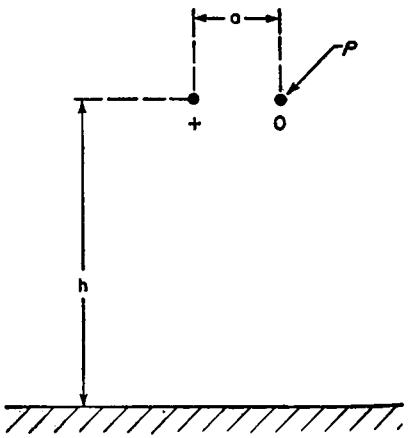

FIG. 4.4.

4.2.4. Type IV. Two-wire Unbalanced Feeder, One Wire Grounded. Applications for this line (Fig. 4.4) are somewhat less restricted than for types I and II, but its use is limited to short runs at low and medium frequencies. The earth-return current is reduced by the presence of the grounded wire. When $h \gg a$,

$$Z_0 = 138\left(\log_{10}\frac{2h}{\rho} + k\log_{10}\frac{2h}{a}\right)$$

$$k = -\frac{\log_{10}\frac{2h}{a}}{\log_{10}\frac{2h}{\rho}}$$

$$\alpha_{ce} = \left(1.09\sqrt{\frac{10^{-13}}{\sigma}} + 0.86\right)\sqrt{f}$$

Typical values include:

ρ, inches	h, inches	a, inches	k	Z_0
0.064	120	10	−0.386	420
0.102	120	20	−0.320	421

4.2.5. Type V. Three-wire Unbalanced Feeder with Outer Wires Grounded. This configuration (Fig. 4.5) is an improvement over that of type IV because a smaller proportion of current returns in the earth. The design is simple and inexpensive to build and can be applied to many low- and medium-frequency situations where short- to medium-distance runs are required.

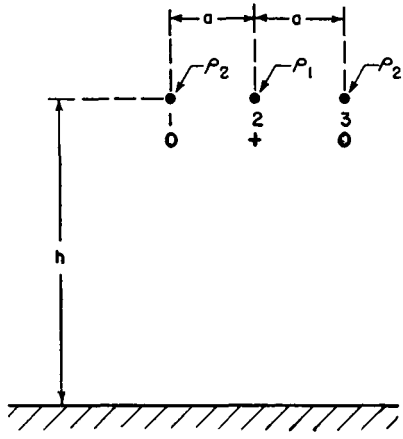

FIG. 4.5.

This is a one-insulator type, where the insulator supports the high-potential wire. No insulators are needed for the grounded wires in low-power applications, but in high-power applications the convergence of the electric-flux lines at the grounded wires can produce large gradients near them, causing dielectric loss in any poor insulating material near the grounded wires. The grounded wires should then be insulated.

Possible constructions for this type of line are shown in Fig. 4.6. Only a very small difference results from having the ground wires slightly below the level of the central wire. When $h \gg a$,

$$Z_0 = 138\left(\log_{10}\frac{2h}{\rho_1} + k\log_{10}\frac{2h}{a}\right)$$

$$k = -\frac{2\log_{10}\dfrac{2h}{a}}{\log_{10}\dfrac{2h^2}{\rho_2 a}}$$

When $\rho_1 = \rho_2$

$$\alpha_{ce} = \frac{2.17\sqrt{f}}{\rho_{\text{inches}} Z_0}\left(1 + \frac{k^2}{2}\right) + \frac{13{,}720}{h_{\text{feet}} Z_0}(1-k)^2\sqrt{\frac{10^{-13}f}{\sigma}}$$

Some typical electrical values are:

ρ, inches	h, inches	a, inches	k	Z_0, ohms
0.064	120	5	−0.678	336
0.064	120	10	−0.592	380
0.064	120	15	−0.537	413

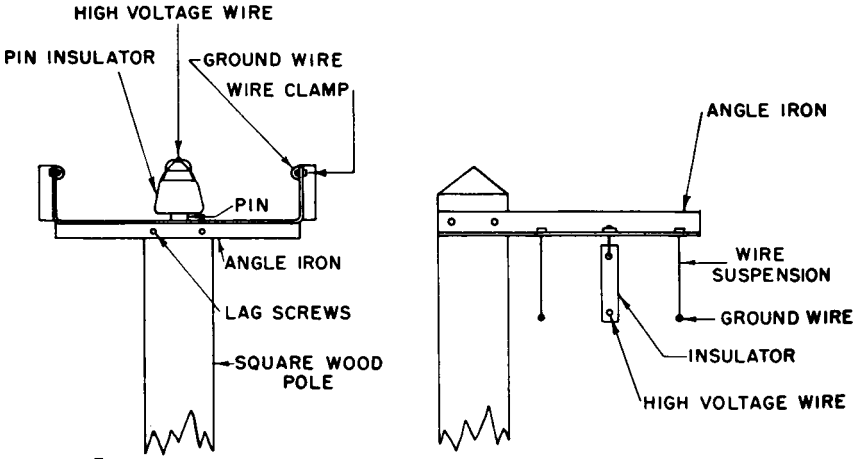

FIG. 4.6. Constructions for type V feeder.

4.2.6. Type VI. Four-wire Unbalanced Feeder with Three Grounded Wires Located at Three Corners of a Square and a High-potential Wire Located at the Center. This is an extension of type V by adding another grounded wire (Fig. 4.7). The same general method of construction can be used except for the additional wire, either above or below the

high-potential wire. The equation is derived on the basis that the height is large enough with respect to other dimensions to give very nearly equal currents in each of the three grounded wires, a condition realized in typical overhead-line constructions. The extra grounded wire increases k and decreases the current returning in the earth. When $h \gg a$,

$$Z_0 = 138\left(\log_{10}\frac{2h}{\rho_1} + k\log_{10}\frac{2h}{a}\right)$$

$$k = -\frac{3\log_{10}\dfrac{2h}{a}}{2\log_{10}\dfrac{2h}{a} + \log_{10}\dfrac{h}{\rho_2}}$$

When $\rho_1 = \rho_2$,

$$\alpha_{ce} = \frac{2.17\sqrt{f}}{\rho_{\text{inches}} Z_0}\left(1 + \frac{k^2}{3}\right) + \frac{13{,}720}{h_{\text{feet}} Z_0}\sqrt{\frac{10^{-13}f}{\sigma}}(1-k)^2$$

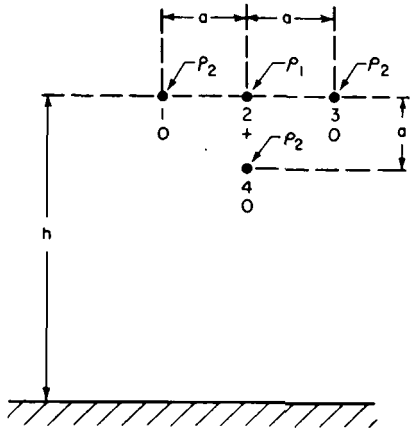

FIG. 4.7.

A sample case, for equal-size wires, is:

ρ, inches	h, inches	a, inches	k	Z_0, ohms
0.064	120	10	0.685	363

Compare this with types IV, VI, and VII. These types, in succession, increase the enclosure of a single high-potential conductor with a circle of ground wires that carry an increasingly large portion of the total return current, and the system gradually approaches equivalence to a coaxial feeder.

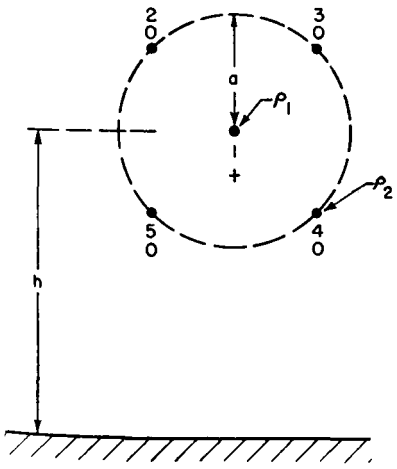

FIG. 4.8.

4.2.7. Type VII. Five-wire Unbalanced Feeder in Quincunx Cross Section, with Four Outer Wires Grounded. This type of feeder (Fig. 4.8) is characterized by a high value of k with consequent reduction in earth-return current and over-all attenuation. The four grounded wires provide a high degree of shield-

ing for the inner wire. The characteristic impedance is too high for some applications because of the single high-potential wire. Construction configurations for this type are discussed in conjunction with type XI.

This quincunx-section feeder has wide application possibilities for low-frequency and medium-frequency power transmission where low attenuation and moderate value of characteristic impedance are desired. When $h \gg a$,

$$Z_0 = 138\left(\log_{10}\frac{2h}{\rho_1} + k\log_{10}\frac{2h}{a}\right)$$

$$k = -\frac{4\log_{10}\dfrac{2h}{a}}{\log_{10}\dfrac{2h}{\rho_2} + \log_{10}\dfrac{2h^2}{a^2} + \log_{10}\dfrac{h}{a}}$$

When $\rho_1 = \rho_2$,

$$\alpha_{ce} = \frac{2.17\sqrt{f}}{\rho_{\text{inches}} Z_0}\left(1 + \frac{k^2}{4}\right) + \frac{13{,}720}{h_{\text{feet}} Z_0}\sqrt{\frac{10^{-13}f}{\sigma}}\,(1-k)^2$$

An example of a set of values is:

ρ, inches	h, inches	a, inches	k	Z_0, ohms
0.064	120	10	−0.775	345

4.2.8. Type VIII. Quasi-coaxial Feeder with Tubular Inner Conductor of Large Diameter and Eight Grounded Wires Enclosing It, the Latter Equally Spaced on a Concentric Circle. For very low impedance lines of very high power transmission capacity, this type of line (Fig. 4.9) has certain mechanical advantages over a full-concentric line. It has the mechanical simplicity and reliability of an open-wire system while giving the electrical characteristics ordinarily desired when a concentric feeder is specified. Its cost of construction is lower than for a full-concentric type, as can be judged immediately by reference to Fig. 4.10. When $h \gg a$,

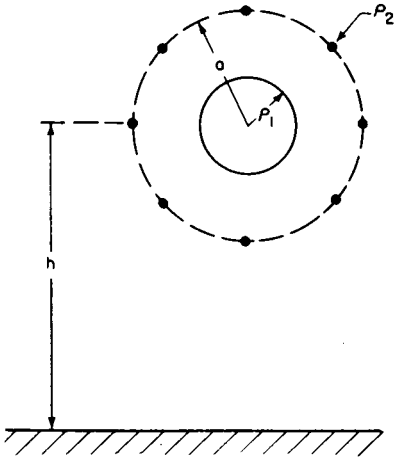

FIG. 4.9.

$$Z_0 = 138\left(\log_{10}\frac{2h}{\rho_1} + k\log_{10}\frac{2h}{a}\right)$$

$$k = -\frac{8 \log_{10} \frac{2h}{a}}{\log_{10} \frac{2h}{\rho_2} + 2 \log_{10} \frac{2h}{0.77a} + 2 \log_{10} \frac{2h}{a\sqrt{2}} + 2 \log_{10} \frac{2h}{1.86a} + \log_{10} \frac{h}{a}}$$

When $h >>> a$, $k \to 1.0$ and $Z_0 \to 138 \log_{10} (a/\rho)$. With ρ_1 and ρ_2 in inches,

$$\alpha_{ce} = \frac{2.17\sqrt{f}}{Z_0}\left(\frac{1}{\rho_1} + \frac{k^2}{8\rho_2}\right) + \frac{13{,}720}{h_{\text{feet}} Z_0}\sqrt{\frac{10^{-13} f}{\sigma}}\,[1 - k]^2$$

An idea of the electrical possibilities is shown by the following values:

h, inches	ρ_1, inches	ρ_2, inches	a, inches	k	Z_0, ohms
100	2.00	0.1625	6.00	−0.950	76

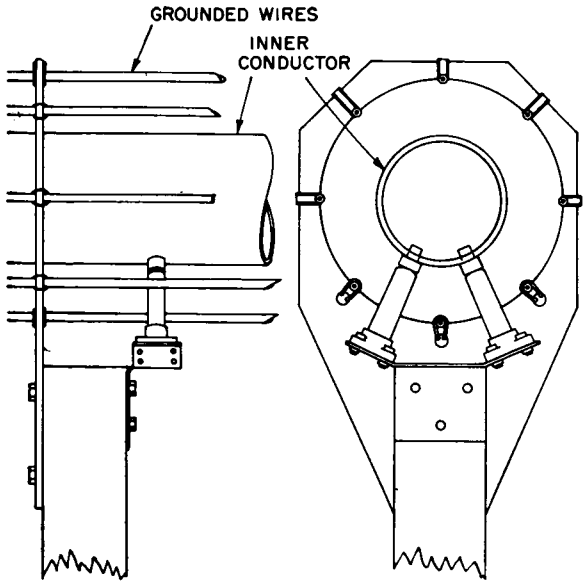

FIG. 4.10. Construction for type VIII feeder.

In regions devoid of ice, the inner conductor may be made of a circle of parallel wires, using a sufficient number closely to approximate, electrically, a continuous tubular conductor. This may allow the cost of the line to be reduced further, both in respect to weight of copper and perhaps also in respect to fewer supports.

4.2.9. Type IX. Four-wire Unbalanced Feeder in a Plane, with Two Outer Wires Grounded. The applications for this design (Fig. 4.11) are similar to those for type IV, and the same type of construction can be used except for the duplication for two inner wires at high potential. The use of two wires provides means for obtaining lower characteristic imped-

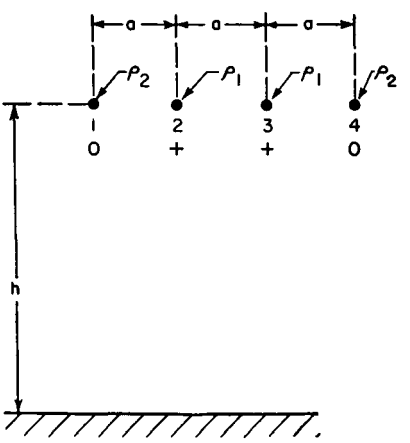

FIG. 4.11.

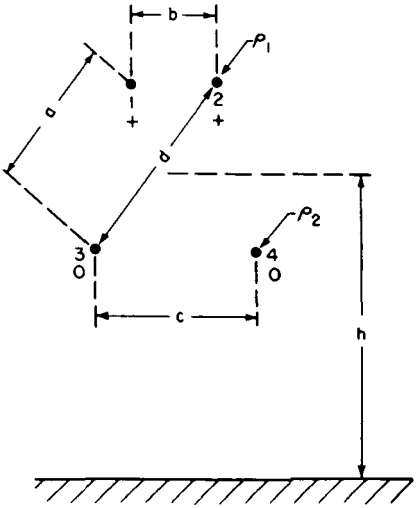

FIG. 4.12.

ances than normally available with the type IV design, when small conductors are used. When $h \gg 3a$,

$$Z_0 = 69\left(\log_{10}\frac{4h^2}{a\rho_1} + k\log_{10}\frac{2h^2}{a^2}\right)$$

$$k = -\frac{\log_{10}\dfrac{2h^2}{a^2}}{\log_{10}\dfrac{4h^2}{3a\rho_2}}$$

When $\rho_1 = \rho_2$ in inches,

$$\alpha_{ce} = \frac{2.17\sqrt{f}}{\rho Z_0}\left(\frac{1}{2} + \frac{k^2}{2}\right) + \frac{13{,}720}{h_{\text{feet}} Z_0}\sqrt{\frac{10^{-13}f}{\sigma}}(1-k)^2$$

A sample set of values for a useful low-power configuration is:

ρ, inches	h, inches	a, inches	k	Z_0, ohms
0.064	120	10	−0.55	248

4.2.10. Type X. Four-wire Unbalanced Feeder with Two Wires in Parallel at High Potential above Two Grounded Wires. This type of feeder (Fig. 4.12) is similar in application to type IX. It is more economical to build if two high-potential wires are attached to a single pin insulator because no crossarm is needed. The grounded wires can be fastened to the pole. A practical construction for this line is shown in

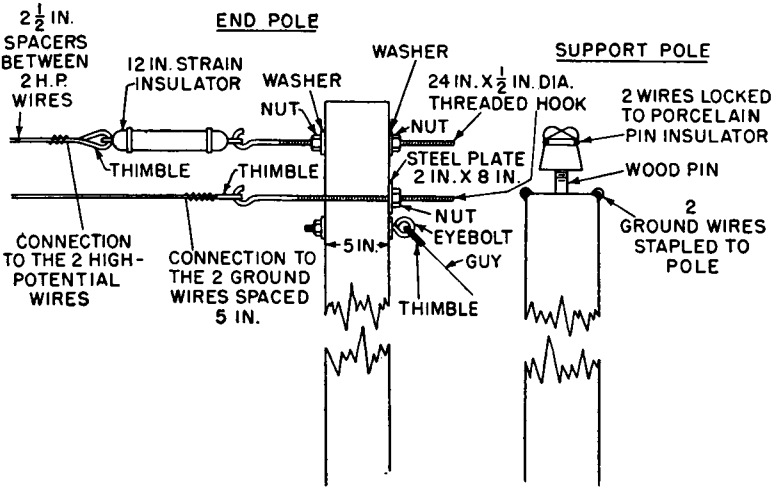

FIG. 4.13. Construction for type X feeder.

Fig. 4.13. This is an excellent type of feeder to use for low-power broadcast stations where extreme economy is essential. If $h \gg a, b, c$,

$$Z_0 = 69\left(\log_{10}\frac{4h^2}{\rho_1 b} + k\log_{10}\frac{4h^2}{ad}\right)$$

$$k = -\frac{\log_{10}\dfrac{4h^2}{ad}}{\log_{10}\dfrac{4h^2}{\rho_2 c}}$$

When $\rho_1 = \rho_2$,

$$\alpha_{ce} = \frac{2.17\sqrt{f}}{\rho_{\text{inches}} Z_0}\left(\frac{1}{2} + \frac{k^2}{2}\right) + \frac{13{,}720}{h_{\text{feet}} Z_0}\sqrt{\frac{10^{-13} f}{\sigma}}\,(1-k)^2$$

The electrical characteristics for two practical configurations are tabulated here:

ρ, inches	h, inches	a, inches	b, inches	c, inches	d, inches	k	Z_0, ohms
0.064	144	4.25	2.50	5.00	5.55	−0.655	235
0.064	144	6.00	2.50	12.0	8.00	−0.643	251

4.2.11. Type XI. Six-wire Unbalanced Line—Two High-potential Wires Enclosed by Four Grounded Wires. This type of feeder (Fig. 4.14) resembles type VII except for its lower characteristic impedance due to the use of a second high-potential wire. Except for this difference, the same method of construction may be used for both types. One insulator per pole is all that is necessary. The grounded wires can be supported in a number of ways, using prefabricated bayonet brackets for attachment to the poles (as in Fig. 4.67) or by pole and crossarm methods similar to those suggested in Fig. 4.6. It is a very popular type, having found wide application in medium-frequency broadcasting and also in low-frequency antenna-feed systems. It was originally introduced by the Radio Corporation of America in 1938 for use with directive broadcast antenna systems, where low feeder radiation was essential, and to avoid the expense and complications of concentric feeders.

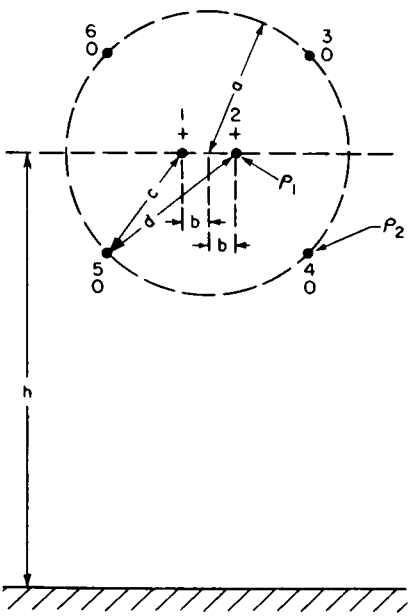

FIG. 4.14.

Figures 4.68 to 4.73 show various constructional details that have been used at different broadcast stations. As constructed using wires of radius 0.064 inch, this line is capable of transmitting a peak power of the order of 600 kilowatts, and with larger conductors this rating can be increased. Its characteristic impedance, of the order of 230 ohms in its usual form, is a very convenient value for broadcasting applications because the coupling networks usually require values of inductance and capacitance readily realizable with available components. When $h \gg a$,

$$Z_0 = 69\left(\log_{10}\frac{2h^2}{\rho_1 b} + k\log_{10}\frac{4h^2}{cd}\right)$$

$$k = -\frac{2\log_{10}\dfrac{4h^2}{cd}}{\log_{10}\dfrac{2h^2}{a\rho_2} + \log_{10}\dfrac{2h^2}{a^2}}$$

When $\rho_1 = \rho_2$,

$$\alpha_{ce} = \frac{2.17\sqrt{f}}{\rho_{\text{inches}} Z_0}\left(\frac{1}{2} + \frac{k^2}{4}\right) + \frac{13{,}720}{h_{\text{feet}} Z_0}\sqrt{\frac{10^{-13} f}{\sigma}}\,(1-k)^2$$

A set of characteristic values is:

ρ, inches	h, inches	a, inches	b, inches	c, inches	d, inches	k	Z_0, ohms
0.064	144	15	2.5	9.7	12.6	−0.792	231

4.2.12. Type XII. Eight-wire Square Line, Unbalanced, with the Four Wires at the Corners Grounded and the Four Wires at the Middle of the Sides at High Voltage. This configuration (Fig. 4.15) is suitable for transmission of high power with low attenuation and where low characteristic impedance is desired. A simplified construction is indicated in Fig. 4.16, where only one post insulator is needed to support the four high-potential wires at each pole on a straight run. This is a relatively low cost assembly. The high-potential wires can be free-running through retaining holes in the metallic star so that transverse stress is minimized in the post insulator. When $h \gg a$,

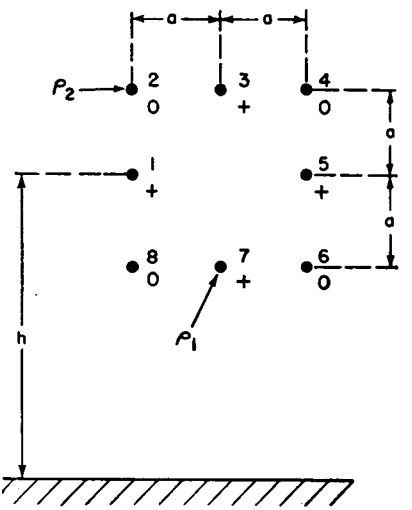

FIG. 4.15.

$$Z_0 = 34.5\left[\log_{10}\frac{2h}{\rho_1} + 2\log_{10}\frac{2h}{a\sqrt{2}} + \log_{10}\frac{h}{a} + k\left(\log_{10}\frac{2h}{a} + \log_{10}\frac{2h}{a\sqrt{5}}\right)\right]$$

$$k = -\frac{2\log_{10}\frac{2h}{a} + 2\log_{10}\frac{2h}{a\sqrt{5}}}{\log_{10}\frac{2h}{\rho_2} + 2\log_{10}\frac{h}{a} + \log_{10}\frac{h}{a\sqrt{2}}}$$

When $\rho_1 = \rho_2$,

$$\alpha_{ce} = \frac{2.17\sqrt{f}}{\rho_{\text{inches}} Z_0}\left(\frac{1}{4} + \frac{k^2}{4}\right) + \frac{13{,}720}{h_{\text{feet}} Z_0}\sqrt{\frac{10^{-13} f}{\sigma}}\,(1-k)^2$$

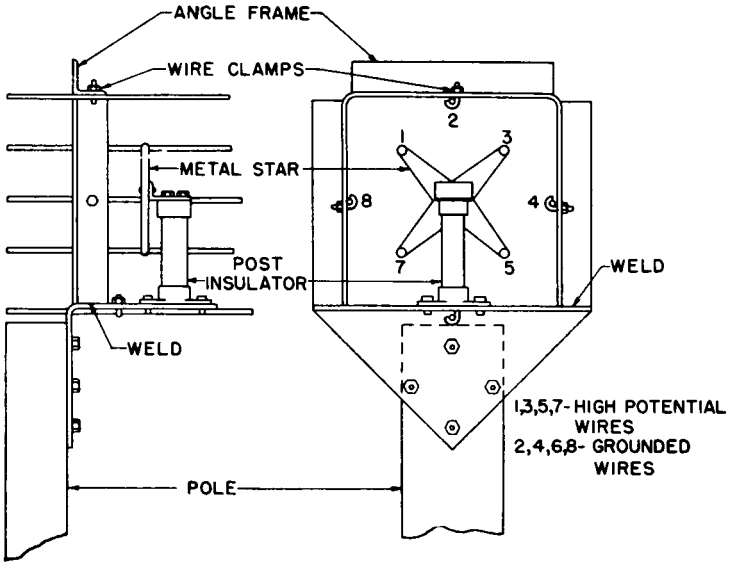

FIG. 4.16. Construction of type XII feeder.

Two sample sets of values for a line of this type for low characteristic impedance are the following:

ρ, inches	h, inches	a, inches	k	Z_0, ohms
0.500	200	8.0	−0.875	70
0.102	120	8.0	−0.773	158

4.2.13. Type XIII. Unbalanced Feeder of the Corner Type. Type XIII (Fig. 4.17), using a 90-degree corner, forms, with its images, one quadrant of the field of a feeder of the cross-connected four-wire balanced type XVIII. When the metallic corner is of sufficiently large width to collect a very high percentage of the electric flux from the high-potential conductor located inside it and on its bisector line, it approaches very closely a sector of the analogous balanced prototype line, but with two adjacent zero-potential surfaces replaced by metallic sheets. There results from this principle the possibility of a line with very high power capacity that may be a good substitute for large concentric feeders.

The metallic corner may be a continuous sheet forming a weather-protective hood for the high-potential conductor, or it may be a multiplicity of parallel wires of small radius. Lines of low characteristic impedance and very low attenuation can be realized with this configuration. The

characteristic impedance can be altered further by setting the high-potential conductor off of the bisector line, in which case the corner becomes a sector of an analogous balanced line that is a quasi-regular polygon. The equations for this latter form can be easily developed as required.

One method of constructing a corner-type line is that shown in Fig. 4.18, where economy is achieved by a simple but substantial structure. Post insulators for the high-potential conductor may not be required at as frequent spacings as for the sheet-metal corner. Longitudinal angle members between support poles, in addition to the one at the ridge, make a solid framework for the entire length of the line and maintain a neat and uniform appearance. When $h >>> s$ and $w \gg s$,

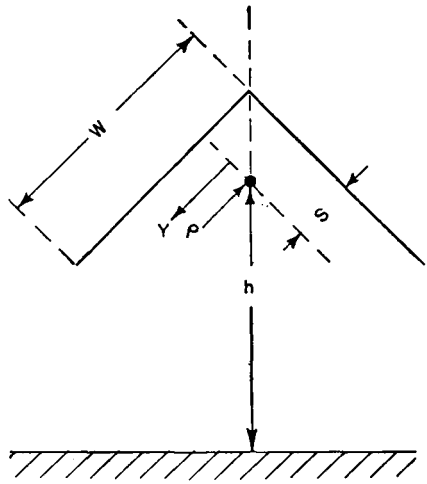

FIG. 4.17.

$$Z_0 = 69 \log_{10} \frac{2s}{\rho \sqrt{2}}$$

When h is small,

$$Z_0 = 69 \log_{10} \frac{2h_0h_2s}{\rho h_1^2 \sqrt{2}}$$

where $h_0 = h$ in the figure, $h_1 = h + s\sqrt{2}$, and $h_2 = h + 2s\sqrt{2}$.

Some electrical characteristics for lines of this type are as follows:

ρ, inches	h, inches	s, inches	By approximate equation, Z_0, ohms	By complete equation, Z_0, ohms
0.500	50	3.00	64	64
1.00	50	4.00	52	51.5

There arises the question of the minimum permissible width w of the corner sheets in order to conform to the principle that the image charges on the sheets be essentially those of infinite sheets. The greatest charge concentration will be on the surfaces nearest the high-potential conductor and will taper off to zero at infinity. In fact, the rate of decrease of the

charge (or the current density) as the distance from this nearest point on the sheet is increased is very rapid in many practical cases. The larger the radius ρ of the high-potential conductor and the smaller the value of s, the greater is the charge concentration on the sheets near the conductor and the more rapid the decay in value with distance.

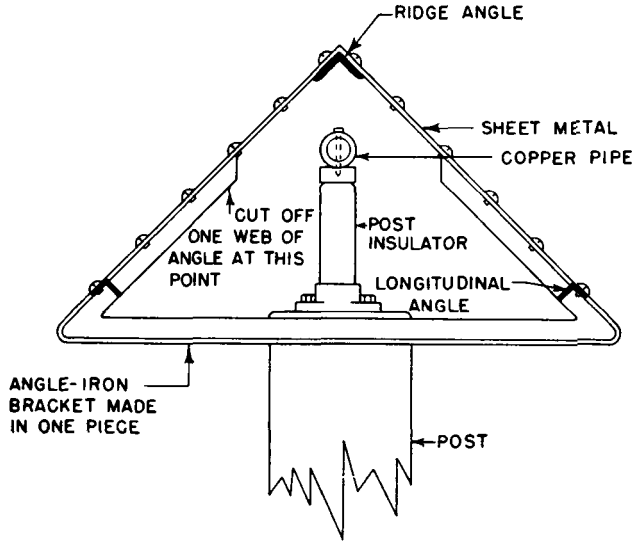

FIG. 4.18. Construction of type XIII feeder.

The following equation* provides the solution of the current density J in the sheet as a function of the distance y from the projection of the axis of the high-potential conductor on the sheet:

$$J = \frac{I}{\pi s} = \frac{\sqrt{1 - \left(\frac{\rho}{s}\right)^2}}{1 - \left(\frac{\rho}{s}\right)^2 + \left(\frac{y}{s}\right)^2} \quad \text{amperes per centimeter}$$

in which I is the current in amperes in the high-potential conductor and ρ and s are the same values used in the equation for the characteristic impedance. A plot of J as a function of y will yield the information that will permit the designer to judge an acceptable minimum current density and thus choose the minimum sheet width w. All the geometrical dimensions are of course in the same units.

4.2.14. Type XIV. Coaxial (Concentric) Feeder. This type of feeder (Fig. 4.19) is well-known in practice and has a long history.[3,21]

* G. H. Brown, C. N. Hoyler, and R. A. Bierwirth, "Radio-frequency Heating," p. 76, Eq. 8.14, D. Van Nostrand Company, Inc., New York, 1947.

Rigid construction feeder line of this type, using straight pipes as inner and outer conductors, with air dielectric except for solid dielectric spacers used to maintain concentricity, is commercially available up to a quite large size for high-power transmission. "Semirigid" line of the same general nature is so called because it is sufficiently small and ductile to be shaped into bends and turns without need for cutting or fittings. There is a third form known as "solid-dielectric concentric" or "coaxial" cable, which, in its commonest form, consists of a flexible inner conductor, embedded in a pliable plastic dielectric material, over which is a flexible sheath forming the outer conductor. There is usually a protective rubber or plastic outer covering over all. Concentric cable of large power capacity has been manufactured with air dielectric and steatite spacers and has a flexibility comparable with ordinary power cables of equivalent diameter. The mechanical details of commercially available coaxial line, cable, and related fittings and hardware are described in various manufacturers' catalogues.

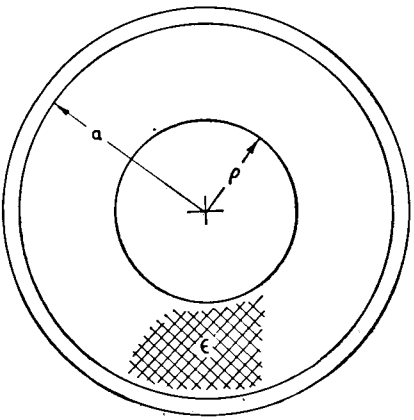

FIG. 4.19.

The coaxial line is theoretically ideal in that all the field is contained within the space bounded by the inside surface of the outer sheath. At radio frequencies, there is no external field, and so there is no energy lost by radiation from the feeder, unless improper termination gives rise to currents on the outside of the sheath. For the same reason, there is no pickup of external fields when used for receiving.

Mechanically this type of feeder involves many problems which compromise its electrical desirability. Within the power capacity of the various designs of cable, with and without solid dielectrics, these problems have been reduced by years of development. Their applications are much more important in the frequencies above those dealt with in this book, but they find considerable use in low-, medium-, and high-frequency practices.[39] Wherever commercial coaxial cable can be used, it provides a very convenient and sometimes economical method for transmitting radio-frequency energy. The rigid form of construction is not so convenient to use, but there are cases where it is a preferred type of feeder. Expansion and contraction introduce problems of considerable complexity, as does internal moisture. A flashover inside such a line can

cause great damage, and its repair entails the labor of disassembly and reassembly. If the line is buried, as is often done to reduce thermal variations or for protection from external damage, an internal failure is very troublesome.

Contraction and expansion have been equalized in many designs, but in applying rigid line one may also take measures to minimize the extremes of temperature to which the line is exposed. In the open, it is desirable to shade the line from direct sunlight (see Fig. 4.74) or to wrap it with heat-insulating material as is done with steam pipes. Burial in the earth below frost line is common practice.

Moisture penetration is prevented by sealing the line as carefully as possible and then pressurizing it with dry compressed air or with dry nitrogen. Reservoirs of hygroscopic material, such as silica gel, are sometimes affixed to the system, and the new gas forced in is also passed through this material for drying. To maintain pressure, great skill and care are needed in the assembly, whether solder or solderless fittings are used. Loss of pressure can subject the line to moisture infiltration. Once moisture gets in, it is not easily removed. Leakage of nitrogen can become a considerable item of expense when the assembly is not completely tight.

Lines are usually pressurized slightly above normal atmospheric pressure for the altitude.

The design of a coaxial feeder for large power transmission becomes a major engineering project.[40] An example of a line for transmitting 2,000 kilowatts peak is shown in Figs. 4.75 and 4.76. The outer conductor has an inner diameter of 10 inches.

Since safety factor is relatively expensive, coaxial lines for high power often have small flashover margins. As a consequence, only small standing-wave ratios can be tolerated. Devices indicating or actuated by standing-wave ratios above predetermined values are sometimes used to interrupt the power source in order to prevent flashover or to minimize the damage in the event of a flashover. These devices are usually in the form of potential probes projecting through the sheath and terminated on an equipotential line in the field of the feeder. Three are used, separated one-eighth wavelength (the wavelength being that in the feeder), and they excite electronic amplifiers. These are connected differentially so that nothing happens as long as the pickups from all probes are identical, but a relay is actuated when the degree of unbalance exceeds a preset limit. Probes have been distributed along a section of line at small electrical intervals and made to actuate a set of milliammeters so that the entire standing wave can be seen in magnitude and position.

As an unbalanced system, a coaxial line is sometimes an inconvenience when it must work from or into balanced generators or loads. Two coaxial lines may be used in a balanced system in many instances. Otherwise it is necessary to use networks or line sections to transform from balance to unbalance, and vice versa. There are several practical methods for this purpose which are discussed in Sec. 4.6. For coaxial feeders,

$$Z_0 = 138 \log_{10} \frac{a}{\rho}$$

For solid dielectric cable,

$$Z_0 = \frac{138}{\sqrt{\epsilon}} \log_{10} \frac{a}{\rho}$$

where ϵ is the dielectric constant of the dielectric.

4.2.15. Type XV. Two-wire Balanced Feeder. This is the commonest type of feeder (Fig. 4.20) for balanced operation and is used for a great variety of applications for high and very high frequencies where open-wire lines are desired. It is simple to construct and is relatively inexpensive. When used for high-power transmission, certain precautions are necessary with regard to potential gradients and details of construction. The conductor size can be increased as much as desired to increase the power-handling capacity, but beyond a point it is more economical to obtain the same effect with two or more conductors in parallel on each side of the circuit, as shown in some succeeding cases. Open-wire lines of this type have generally a characteristic impedance from 500 to 625 ohms in the form most widely used, and 600 ohms is perhaps the value most often chosen. Because of the high characteristic impedance, care is necessary to use insulators of very low capacitance in order to obtain an essentially smooth line. If insulator capacitance causes irregularities in the line constants, their effect can be neutralized by arranging the wires for greater spacing close to the insulators in order to maintain a constant L/C ratio past points of support.

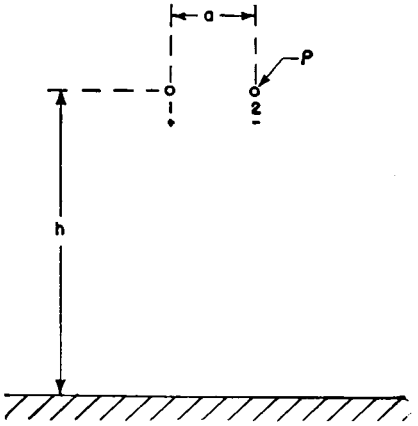

FIG. 4.20.

In all balanced feeder systems, great care must be taken to ensure that the total length of wire is exactly the same for both sides of the circuit

between transmitter and load. When passing through switching devices, transpositions, or bends or turns in the line and entering or leaving the equipment and buildings, the conductor arrangement must always be such as to provide for this essential requirement.[51] When this cannot be done directly, it can be done by means of wire loops inserted in the short side at some convenient point. In making a corner in the line, the arrangement shown in Fig. 4.21 can be used. Another method is to turn the plane of the line 90 degrees before making the turn and bringing it back to horizontal for the next straightaway run (Fig. 4.22). For this type of line,

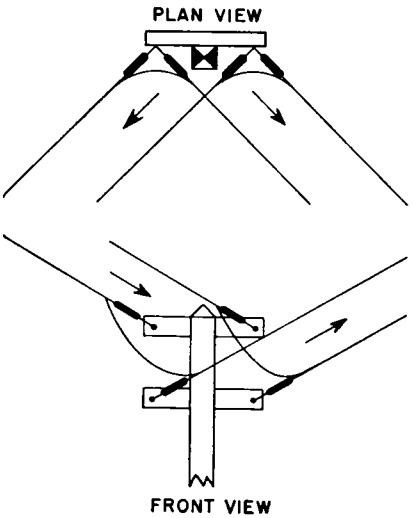

FIG. 4.21. Method of making a corner in a two-wire balanced line to maintain equal wire lengths.

$$Z_0 = 276 \log_{10} \frac{2ha}{\rho \sqrt{4h^2 + a^2}}$$

but when $h \gg a$,

$$Z_0 = 276 \log_{10} \frac{a}{\rho}$$

$$\alpha_{\text{copper}} = \frac{4.34 \sqrt{f}}{\rho_{\text{inches}} Z_0}$$

$$\alpha_{\text{total}} = \frac{7.2 \sqrt{f}}{\rho_{\text{inches}} Z_0}$$

A range of values of characteristic impedance as a function of the ratio of wire spacing to wire radius is shown in Fig. 4.23, which includes the case of small spacings where the proximity effect and the nonuniform peripheral charge distribution on the conductors come into play. In this figure, the spacing is that between the centers of the conductors.

When correctly balanced to ground, the radiation from a feeder of this type with 12-inch spacing is virtually negligible up to 25 megacycles.

Frequently it is necessary to route several such feeders in parallel, as is done with telephone lines. The amount of cross talk that will occur depends upon the spacing between circuits and upon the cross section of any one circuit, the length of the run in parallel, and the selectivity of the load circuit. For a given amount of cross talk between feeders, the circuits can be placed nearer each other if they are arranged to have a common neutral plane (that is, arranged with one circuit above the other) rather than with all the lines in the same plane. The latter, however, is often more convenient, even though it is necessary to use greater

spacing between circuits. To minimize cross talk, various transposition techniques may be applied as in ordinary telephony.

It is difficult to place any specific limitations on tolerable cross coupling between circuits. One might believe that two parallel feeders en route to two different antennas are quite isolated if the power induced into the

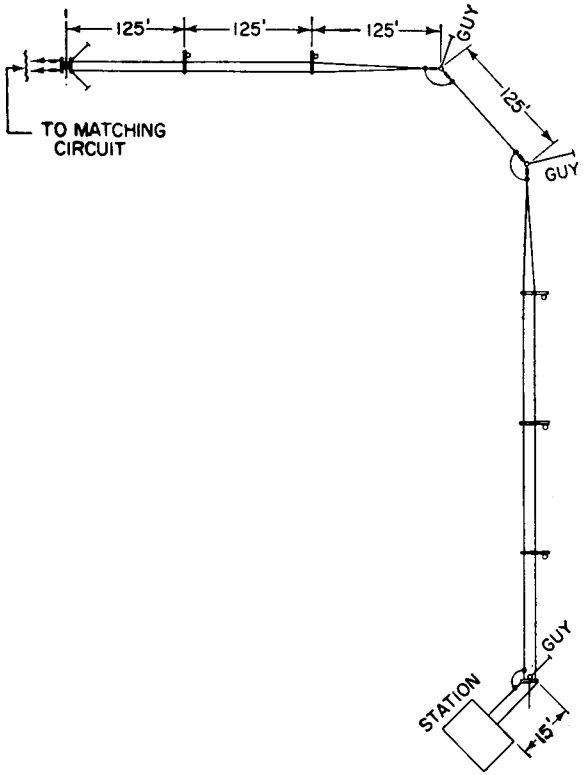

FIG. 4.22. Plan view of a two-wire balanced feeder, including a bend where feeder is turned 90 degrees to maintain equal-length wires.

adjacent circuit is 40 decibels below that in the main circuit. Yet if the antenna to which this cross talk is delivered has no selectivity to discriminate against this signal and radiates it with full antenna gain in some undesired direction, its effect can be undesirable and cause interference out of proportion to the actual power level. This sort of cross talk has not been studied much in the past, but if the most effective use of a crowded frequency spectrum is to be achieved in the future, far greater care will be needed to reduce cross talk between feeder and radiating systems. For the same reasons, directive antennas will require far greater suppression of radiations in undesired directions. Undoubtedly

many existing feeder arrangements, if critically studied, would be found to have intolerable cross-talk ratios because of close proximity.

4.2.16. Type XVI. Four-wire Side-connected Balanced Feeder. This type of balanced feeder (Fig. 4.24) has been extensively applied

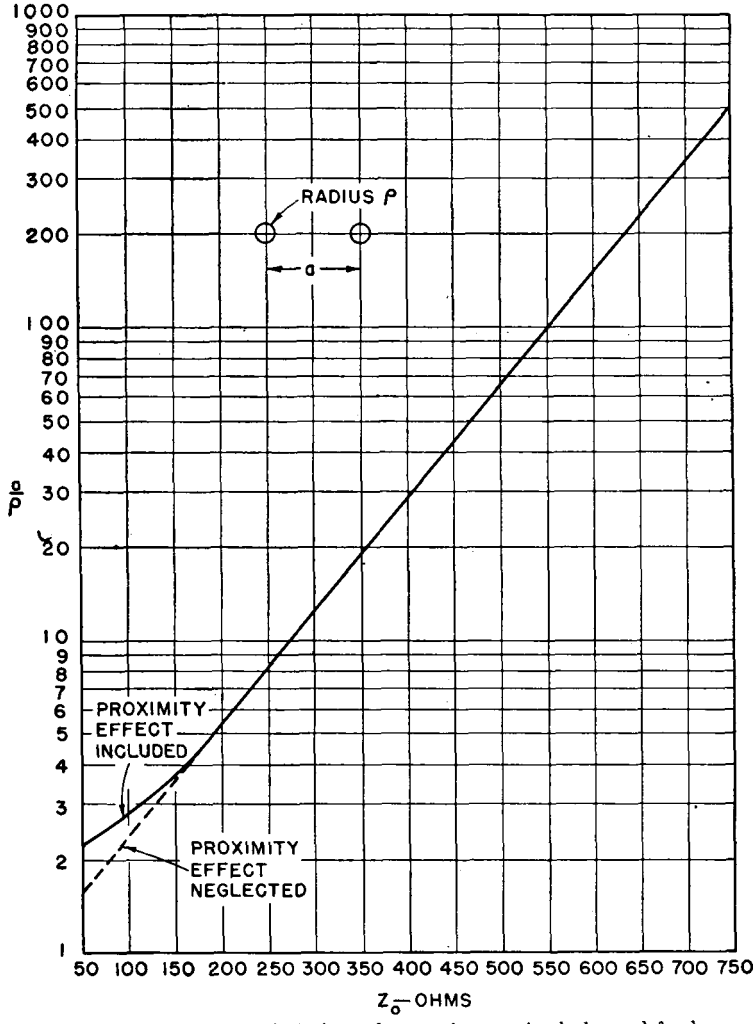

FIG. 4.23. Characteristic impedance of two-wire balanced feeder.

for the transmission of high-power high-frequency energy over the long distances required in large communication stations and in high-frequency broadcast stations where many antennas are located on a single large plot. In some cases the feeder lengths may exceed ½ mile. Its relatively low characteristic impedance makes this type less susceptible to

the irregularities introduced by insulators and switching arrangements. It has a high power-transmission capacity for the amount of copper used, and its attenuation can be less than that of two-wire feeders.[31]

It is interesting to note that when a square-cross-section feeder of this type is used, its characteristic impedance is equal to that of a pair of two-wire feeders in parallel, each having a spacing equal to the diagonal of the four-wire line. Each diagonal pair is in the neutral plane of the other with no intercoupling. Double power rating is therefore obtained on one set of supports and insulators, and the characteristic impedance is one-half that of one pair.

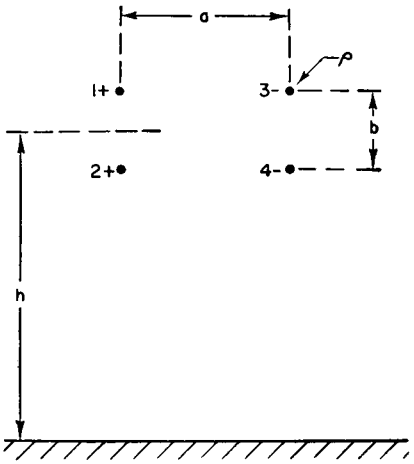

FIG. 4.24.

Figures 4.88 to 4.92 show some of the construction details that have been used, as well as various methods of matching impedances.

The British Broadcasting Corporation has made a systematic study of this type of feeder, and McLean and Bolt[31] report that one composed of wires 0.203 inch in diameter, spaced 10 inches and 6 inches, with a characteristic impedance of 320 ohms, has a safe power-transmission capacity of 130 kilowatts carrier with 100 per cent amplitude modulation at 21.5 megacycles. Its attenuation varies from 0.23 decibels per 1,000 feet at 5 megacycles to about 0.53 decibels per 1,000 feet at 21.5 megacycles. Spans of 150 feet are used with conductor tensions of 150 pounds, with a minimum height of 10 feet at mid-span. Tubular steel frames of the type shown in Fig. 4.89 are now used by the British Broadcasting Corporation instead of wood or steel poles. Metallic spacers suspend the lower wires from the upper ones on each side, and both sides are suspended on porcelain insulators.

Figure 4.88 shows another version of this type of feeder, using a small spacing between the wires in parallel on each side but otherwise following the form of construction commonly used for the two-wire balanced line.

The design formulas for the four-wire side-connected balanced line are

$$Z_0 = 138 \log_{10} \frac{a\sqrt{a^2 + b^2}}{\rho b}$$

When $b = a$,

$$Z_0 = 138 \log_{10} \frac{a\sqrt{2}}{\rho}$$

The attenuation due to copper losses only is

$$\alpha_{\text{copper}} = \frac{2.17\sqrt{f}}{\rho_{\text{inches}} Z_0}$$

and the approximate total attenuation for typical construction is

$$\alpha_{\text{total}} \doteq \frac{3\sqrt{f}}{\rho_{\text{inches}} Z_0}$$

There are tabulated in Table 4.1 the characteristic impedances for a four-wire side-connected line of this type when the diagonal spacing

TABLE 4.1

θ, degrees	a, inches	b, inches	ρ, inches	Z_0, ohms
0	11.65	0	0.102	568
15	11.55	1.55	0.102	405
30	11.25	3.00	0.102	363
45	10.75	4.45	0.102	338
60	10.1	5.8	0.102	316
75	9.25	7.1	0.102	300
90	8.2	8.2	0.102	284

$\sqrt{a^2 + b^2}$ remains constant and the angle θ between the two pairs of 0.203-inch-diameter wires is changed from coincidence (two-wire condition) to 90 degrees (square section).

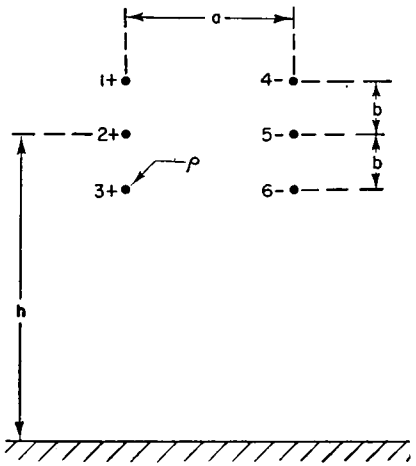

FIG. 4.25.

4.2.17. Type XVII. Six-wire Side-connected Balanced Feeder. This type of line (Fig. 4.25) is one that can be constructed on the same plan as the four-wire side-connected line, but with three wires per side. This decreases the characteristic impedance over that of the four-wire side-connected type for the same sectional dimensions and consequently raises its power-transmission capacity. The spacings between the three wires on one side can be equal or unequal, providing some degree of adjustment of the characteristic impedance for special applications while using the same materials.

The middle wires carry less current than the corner wires so that the

amount of copper used increases somewhat faster than its effectiveness. Nevertheless, the increase in current-transmission capacity and the decrease in the characteristic impedance and the over-all attenuation per unit length are desirable trends as more power has to be transmitted.

Figure 4.35*B* shows how a short section of this construction may be used as a series transforming section in certain impedance-matching operations. For this type of line, when $h \gg a, b$,

$$Z_0 = \frac{276}{2 + A}\left(\log_{10}\frac{a}{\rho} + \log_{10}\frac{\sqrt{a^2 + 4b^2}}{2b} + A\log_{10}\frac{\sqrt{a^2 + b^2}}{b}\right)$$

$$A = \frac{\log_{10}\dfrac{ab\sqrt{a^2 + 4b^2}}{2\rho(a^2 + b^2)}}{\log_{10}\dfrac{ab}{\rho\sqrt{a^2 + b^2}}}$$

$$\alpha_{\text{copper}} = \frac{4.34\sqrt{f}}{\rho_{\text{inches}} Z_0}\left(\frac{1}{2 + A^2}\right)$$

The computed characteristics of a sample line are the following (compare with fifth line of the table for the type XVI line):

ρ, inches	a, inches	b, inches	A	Z_0, ohms
0.1015	10.0	2.91	0.817	271

The current in either middle wire is 81.7 per cent of that in one of the corner wires for this example. This is also a direct measure of the relative effectiveness in copper utilization. The copper loss for this line is 87.5 per cent of that for the four-wire side-connected line of the same cross section, and the insulation loss is 85.5 per cent.

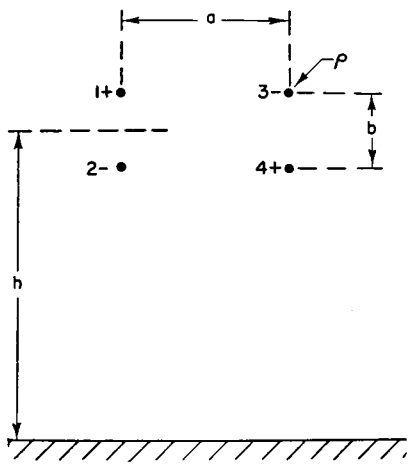

FIG. 4.26.

4.2.18. Type XVIII. Four-wire Cross-connected Balanced Feeder. This type of transmission line (Fig. 4.26) has a smaller external field than the equivalent side-connected line and therefore has lower pickup when used with directive receiving antennas.[47] For the same dimensions it has lower characteristic impedance but higher copper loss. The

insulation loss would be about proportional to the relative characteristic impedances, but since more insulators in parallel are required in its construction, the over-all insulator losses are usually greater. It is therefore not as desirable for transmitting purposes as the four-wire side-connected line using the same amount of copper. Its principal utility is for receiving. A large-scale application of this type of line for receiving is shown in Fig. 4.95, where they connect several fishbone and rhombic receiving beam antennas with the diversity receivers in the station building. When $h \gg a, b,$

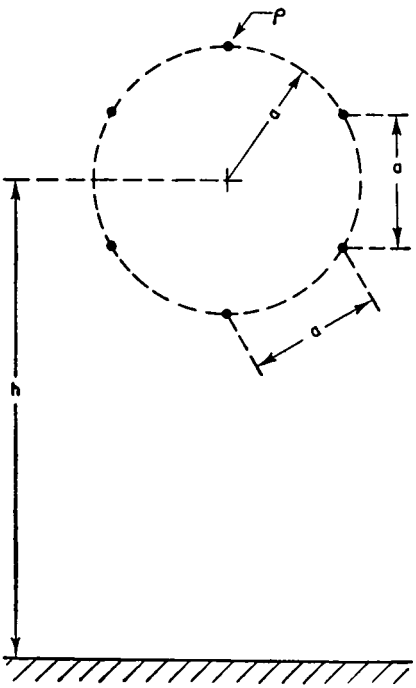

FIG. 4.27.

$$Z_0 = 138 \log_{10} \frac{ab}{\rho \sqrt{a^2 + b^2}}$$

When $a = b,$

$$Z_0 = 138 \log_{10} \frac{a}{\rho \sqrt{2}}$$

$$\alpha_{\text{copper}} = \frac{2.17 \sqrt{f}}{\rho_{\text{inches}} Z_0}$$

Two sets of values for this type of line are given here for reference:

ρ, inches	a, inches	b, inches	Z_0, ohms
0.1015	10.1	5.8	234
0.1015	8.2	8.2	242

4.2.19. Type XIX. Six-wire Hexagonal-section Alternately Connected Balanced Feeder. This type of line (Fig. 4.27) has occasional use, especially when a very low impedance balanced line is required with large power-handling capacity or very low pickup from external fields. The low characteristic impedance reduces insulation loss for a given power-transmission capacity, and the equal current division among the three wires on each side of the circuit ensures maximum copper utilization for the reduction of copper loss.

Figure 4.28 shows a method of construction. Equations for this line are

$$Z_0 = 92 \log_{10} \frac{2a}{3\rho}$$

When $h \gg a$,

$$\alpha_{\text{copper}} = \frac{1.33\sqrt{f}}{\rho_{\text{inches}} Z_0}$$

A set of characteristic values for a line of this design follows:

ρ, inches	a, inches	Z_0, ohms
0.1015	5.8	146

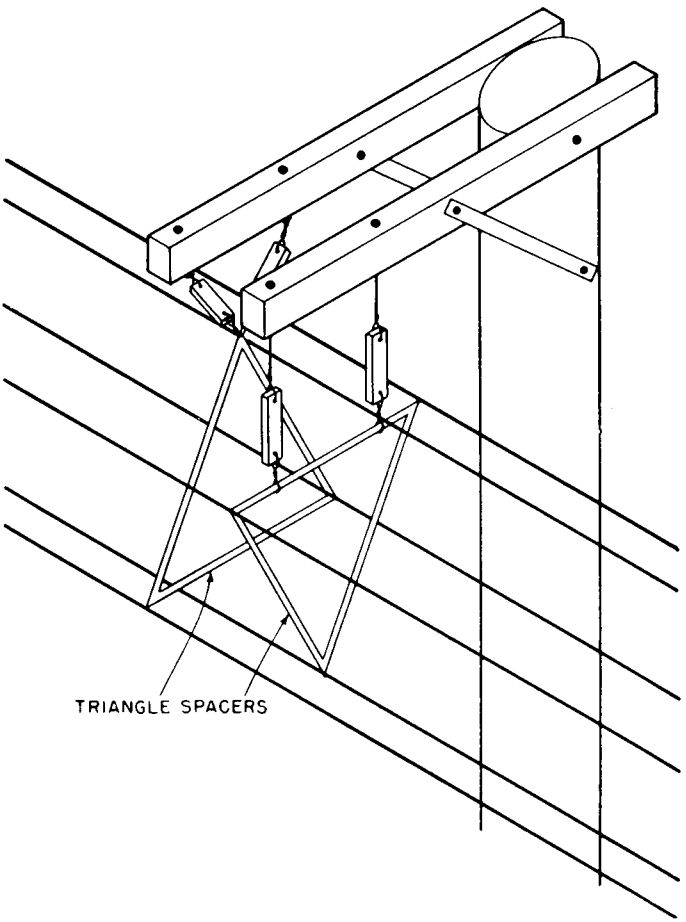

FIG. 4.28. Construction for type XIX feeder.

4.2.20. Summary Remarks regarding Transmission Lines. The 19 different types of transmission lines for which formulas have been given in this section could be expanded to include many other practical and useful types that may have desirable characteristics for certain applications. A sufficient variety of types has been included to offer many ready-made designs as well as to suggest further varieties that may be developed according to need.

The unbalanced types shown represent means for obtaining characteristic impedances from roughly 50 ohms to some 500 ohms with open-wire constructions. They also include alternative configurations having special merits for economy and adaption to low-power transmission and to high-power transmission. The balanced lines discussed have characteristic impedances of the order of 125 to 650 ohms, using a maximum of six wires, and it is evident that lower values can be obtained if needed by employing configurations with a larger number of wires. The 19 configurations therefore cover a wide range of applications, some of which are conventional and common and others more specialized. Engineers should not hesitate to take advantage of special configurations of many sorts that may have particular merits for particular applications.

4.3. Transmission-line Design for Wide-frequency Band

A device such as a transmission line with standing waves, like a lumped reactive element, stores electrical energy. As the amount of energy stored in a system becomes large with respect to the amount of energy transmitted per second, the selectivity of the system is increased. The selectivity of a system limits the bandwidth that can be transmitted without distortion.

There are many common applications where special attention is required to design a system for the band of radio frequencies that must be accommodated. Where the total spectrum of an emission (including upper and lower sidebands) is less than 1 per cent of the carrier frequency, usually no special attention to bandwidth is necessary in ordinary antenna systems and for ordinary services. When the bandwidth surpasses 1 per cent, the designer should always examine the selectivity situation and be prepared to undertake special provisions for circuit design for the bandwidth required.

At all frequencies a transmission line is an aperiodic system when correctly terminated in its characteristic impedance. When the load impedance is frequency-selective, the line may be perfectly terminated at one frequency and improperly terminated at other frequencies.

An antenna system, when properly designed for adequate bandwidth,

will provide a wide-band termination for the line.[51] In this case, the terminated line itself does not add to the selectivity of the system.

The most important first step in system design is to design the antenna for adequate bandwidth whenever possible. When this cannot be fully achieved, it is sometimes possible to employ wide-band coupling circuits between the antenna and the line, which function as impedance equalizers.

A system involving antenna and feeder has its maximum intrinsic bandwidth when their respective impedances are equal and therefore self-matching (see Fig. 4.29). When this is possible, there is no need for

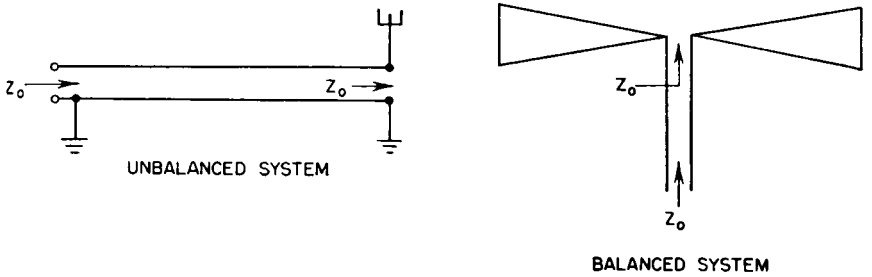

FIG. 4.29. Self-matching antenna and feeder, in which the bandwidth is limited only by the antenna.

reactive coupling elements and the stored energy in the system is minimized. If an antenna has an impedance that is resistive at the operating frequency (or at the middle of the emission band in asymmetric sideband emissions), the feeder should be designed to have a characteristic impedance equal to the input resistance of the antenna.

When the antenna impedance at the feed point is complex, the line impedance can be made equal to the resistive component of the antenna impedance. Then a simple series reactance can be used to neutralize the reactive component and so correctly terminate the line. When the antenna input resistance is lower than realizable characteristic impedances for reasonable transmission lines, the antenna input impedance can be transformed upward by using a single parallel reactance of proper sign to tune the load impedance to parallel resonance. The resistance of the load circuit may then be brought to a value that will match the line.

In certain cases, it may be possible to design the antenna for an impedance that will fit a particular feeder impedance. In other cases, the antenna impedance may not be controllable, and then it is necessary to design the feeder for a particular characteristic impedance to fit the antenna conditions.

In wide-band systems, therefore, the feeder should always be correctly

matched in impedance over the emission band. It is always desirable to use a value of characteristic impedance equal to that of the mid-frequency load resistance after applying the simplest possible power-factor correction. For wide-band receiving systems, there is the additional requirement to provide a wide-band termination for the feeder on the end opposite to the antenna. The receiver input impedance must therefore have a value over the band equal to the characteristic impedance of the feeder.

Bandwidth becomes a problem in high-speed signaling and broadcasting on low and medium frequencies, low-frequency loran, and certain navigational transmissions. Occasionally a bandwidth problem arises in the high-frequency band, such as the transmission and reception of very-high-speed facsimile or multiplexed telephony.

4.4. Transmission-line Impedance-matching Techniques

There are circumstances where a transmission line need not be terminated in its characteristic impedance. In such cases, the feeder, according to its length and characteristic impedance, transforms the load impedance to some different (and usually complex) value at the input terminals of the feeder. This input impedance can then be transformed by a coupling network to a value that will be accommodated by the connected equipment. When mismatched operation *can* be used, it is an extravagance and occasionally an operating inconvenience to use matched-impedance techniques.

Mismatched feeders may be employed when the feeder is electrically very short, say 10 degrees or less. With certain precautions, mismatched feeders may be desirable for feeding two identical loads with identical cophased currents, and where coupling networks would introduce the risk of dissymmetry of coupling-circuit adjustments. There are also occasional cases where half-wave and quarter-wave feeders may be used exactly as in very-high-frequency and ultrahigh-frequency techniques where a whole system may be mismatched except in a common input circuit. The admissibility of such practices depends upon the bandwidth to be transmitted, the magnitudes of mismatch at various points in the system, the magnitudes of potential and current at various points, the losses encountered, and the effect on cost, operating adjustments, and system stability.

Losses in feeders increase with the degree of mismatch, as shown in Fig. 4.1. Since loss is proportional to the feeder length, impedance matching on long feeders is used to obtain optimum efficiency.

For a given design of feeder, the losses also increase with frequency,

and for this reason it is almost universal practice in the high-frequency band to use impedance matching.

There are several methods in use for impedance matching, the choice depending upon the circumstances. The commonest ones are:

1. To design the load and the feeder to have equal impedances so as to be self-matching.
2. To use coupling networks of lumped reactances.
3. To use tapped transmission lines beyond a short circuit.
4. To use a series section of transmission line of proper length and characteristic impedance as an impedance-matching transformer.
5. To use a stub section of line as a reactance in parallel with the feeder at a properly chosen point to make the impedance at this point equal to its characteristic impedance. Either open-circuited or short-circuited stubs may be used.
6. To use a lumped reactance of proper sign and value in place of the stub line and electrically equivalent to it.
7. To use a coupled section of line in parallel with the feeder and of proper length to reflect the correct amount of reactance into the main feeder at the correct point to effect an impedance match.
8. To use a tapered transmission line as an impedance-matching transformer.

The relative desirability of any of these methods depends upon many factors, among which are economics, potentials, currents, frequency, degree of initial mismatch, the amount of electrical and mechanical engineering involved in solving the problem, the available facilities for measurement and construction, the configuration of the feeder cross section and whether balanced or unbalanced, the available space, the ease of adjustment or switching to other working frequencies, the bandwidth to be transmitted (whether transmitting or receiving), the conditions of weather or other exposure to damage, etc. A method preferred for one application may be absurd in another. The choice is therefore made after an appraisal of the prevailing conditions.

4.4.1. Antenna and Feeder Mutually Self-matching. This method (Fig. 4.29) consists in constructing the antenna for its desired radiation properties, then measuring or carefully computing its input resistance, and using a feeder with a characteristic impedance equal to the input resistance of the antenna. The antenna can often be designed to have the proper radiation characteristics and also have an input impedance of a desired predetermined resistive value, to match directly a preferred type of feeder. Examples of this technique are the folded dipoles, folded unipoles, and multiple-tuned antennas. The principle may be applied in a

number of ways in many different kinds of systems. In very-high-frequency and ultrahigh-frequency techniques it is frequent practice to design the antenna input impedance to match that of a preselected type of feeder. Figure 4.30 exhibits two cases where an impedance match can be realized by using only one reactive element.

4.4.2. Coupling Networks of Lumped Reactances. This method of coupling is customary in the range of low and medium frequencies where the use of self-matching line techniques is impractical because of cost. Such networks may be designed for almost any desired impedance match and phase difference. The synthesis of electrical networks[52,53] can be

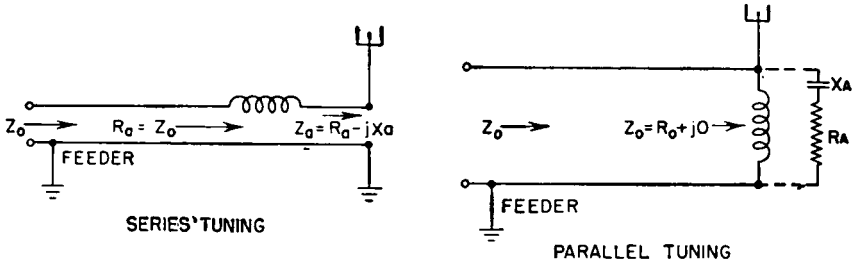

FIG. 4.30. Self-matching of antenna to line, using a single reactive element for power-factor correction.

quickly solved graphically by the methods described in Chap. 5. The elimination of advanced mathematics places this method within reach of any radio technician.

Electrically short antennas are characterized by very low radiation resistance and very high capacitive reactance and by having one input terminal at ground potential. The coupling network must usually have a large impedance transformation ratio, and it therefore introduces considerable selectivity in addition to that associated with the antenna proper. Multiple tuning may be used to present a more favorable value of input resistance at the feed point, as described in Chap. 1. If equal currents can be maintained in each down lead by symmetry of antenna layout, the input resistance will increase approximately as the square of the number of down leads used and the reactance is increased roughly in direct proportion with the increase in the number of down leads. Therefore multiple tuning is a useful device for reducing the impedance transformation ratio of the coupling network, which in turn increases the bandwidth of the antenna proper and of the coupling network.

Figure 4.31 shows an arrangement for coupling a low-frequency antenna to a feeder, where the feeder is electrically short and merely acts as additional shunt capacitance across the antenna terminals. Tuning is performed at the input end of the feeder where it is coupled to the trans-

mitter. With this connection the input impedance will vary as the same antenna is used for different operating frequencies.

Figure 4.32 shows a feeder-terminating and antenna-coupling network where the antenna series inductor does not completely neutralize the

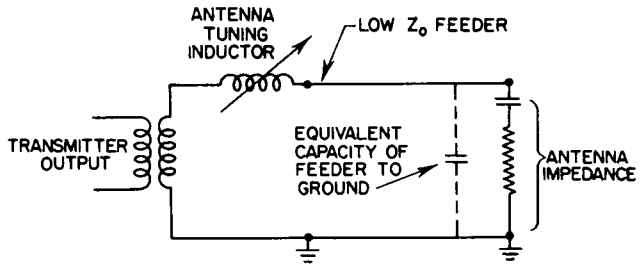

FIG. 4.31. Short feeder used as an extension leadin.

antenna reactance but leaves a value of capacitive reactance which, when tuned to parallel resonance with a parallel inductor, gives a resistive impedance of a value that will match the impedance of an unbalanced feeder of any prechosen value. The advantage of this circuit is its easy

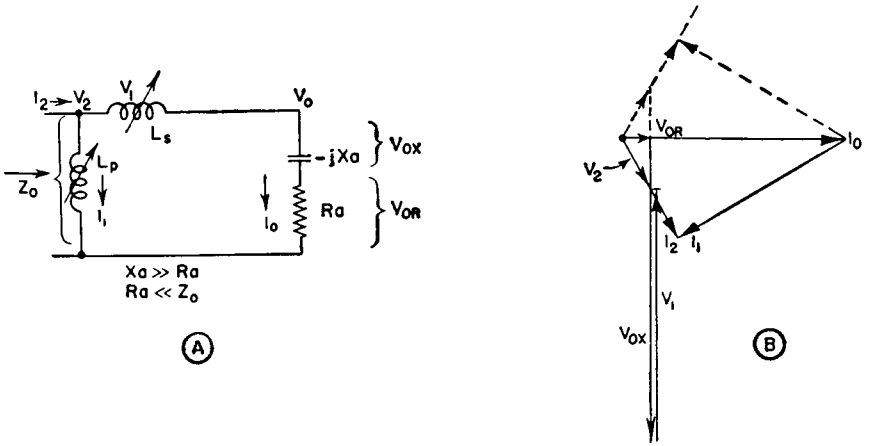

FIG. 4.32. Antenna-coupling circuit.

adjustability to a desired resistance value over a range of operating frequencies with the same antenna. This permits the transmitter to work into a fixed resistive load at all frequencies. Furthermore, the selectivity of the terminal network is nearly the same as that of the antenna itself, assuming the use of high-Q inductors in the circuit. The vector diagram of Fig. 4.32B exhibits these conditions. From this vector diagram one can see immediately how the transformation is made.

The antenna current I_0 flowing through the antenna impedance $R_a - jX_a$ (Fig. 4.32*A*) produces the potential drop $V_{0R} = I_0R_a$, in phase with I_0, and $V_{0X} = I_0X_a$ lagging 90 degrees. Their vector sum is V_0, the potential from the antenna terminal to ground. The antenna current I_0 also flows through the series inductor L_s, producing a potential drop across it which is V_1 and has a direction opposite to that of V_{0X}. Varying the reactance of L_s varies the length of the V_1 vector. When $V_1 < V_{0X}$, their resultant value $V_{0X} - V_1$, added to V_{0R}, gives the vector voltage V_2 in a direction that lags I_0.

Voltage V_2 is across the inductor L_p and sustains the current I_1 through it. The direction of I_1 must lag that of V_2 by 90 degrees, and the reactance of L_p is varied until the vector sum of I_0 and I_1 is in phase with V_2. This makes V_2/I_2 a resistance. By adjusting L_s and L_p the input impedance to the antenna coupling network can always be made to be a resistance that will match a transmission line of characteristic impedance Z_0 provided that $Z_0 > R_a$.

It is interesting to indicate at this point that if $V_1 > V_{0X}$, V_2 then leads I_0. To attain a resistive input impedance to the network, it is then necessary that L_p be changed to a capacitance. The vector conditions for this case are shown in Fig. 4.32*B* by the dotted lines in the upper part of the diagram.

The use of an inductor as shown in Fig. 4.32*A* is preferable to using a capacitor in place of L_p for the following reasons:

The energy storage in the coupling network is less and therefore has less selectivity (desirable in cases where bandwidth is important).

It is sometimes more convenient and economical to use a variable inductor than a variable capacitor (at high power and at low frequencies).

The use of a parallel inductor provides a conductive path to ground which serves as a static drain.

To make this adjustment in practice, one can preset an impedance bridge for balance at a resistance of Z_0 ohms, the feeder characteristic impedance. Then the bridge is connected to the input terminals of the coupling network, and L_p and L_s are manipulated until the bridge is again balanced. The settings of taps and variometers may then be logged and the operation repeated for another frequency. For fixed-frequency operation, permanent connections are made and checked again with the preset impedance bridge. Exact balance is obtained by adjusting the position of the leads themselves by flexing slightly. At exact balance, the movement of the antenna in the wind and the effect of fog and moisture on the system are easily detectable with the bridge. For still more perfect adjustment, the bridge can be connected to the input to the feeder and adjustments made for a specific resistance value at that point. The

coupling adjustments between feeder and power-amplifier anodes can also be made precisely by presetting the bridge to the correct operating value of anode resistance at the sockets and adjusting the power-amplifier circuits until balance is obtained at the anodes.

The use of this coupling circuit permits the power-amplifier output circuits to be designed for working into a fixed value of resistance at all working frequencies. This enables the transmitter designer to use the coupling circuit of Fig. 4.33 between feeder and tank circuit with excellent harmonic-suppression properties, a minimum number of components, and satisfactory tuning flexibility.

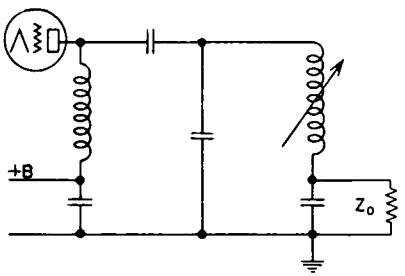

FIG. 4.33. Transmitter output-coupling circuit.

Referring now to the more general ranges of antenna impedances such as those encountered with medium-frequency-broadcast nondirective and directive antennas, one may be required to match almost any antenna impedance whose resistance may be larger or smaller than Z_0 and whose reactance is positive or negative in any degree. If the phase difference between antenna current and feeder current is immaterial, as is usual with nondirective antennas, the impedance match can always be made with two reactive elements in an L network. The low-pass form of L network should always be chosen for its harmonic-reducing property. The L network can transform resistance upward or downward, depending upon whether the shunt element is on the feeder side or the antenna side of the series element. The T and π forms of network provide means for making specified impedance transformations with specified phase differences between load (antenna) current and feeder current, as required in the feeding of directive arrays for medium-frequency broadcasting.

4.4.3. Impedance-matching Series Line Sections. In high-frequency practice, conditions are often favorable for the insertion of a short length of line in series with a main feeder as an impedance-matching device. When this line section has the correct characteristic impedance and length and is located at the correct position in a mismatched feeder, the standing waves can be suppressed for one frequency or a small band of frequencies.

The impedance varies at each point of a feeder with mismatched terminal impedances. At points of current minimums (voltage maximums) the line impedance looking toward the load is resistive and equal to QZ_0. At the current maximums (voltage minimums) the impedance in the direction of the load is resistive and has the value Z_0/Q. Then if

one uses a quarter-wavelength section of transmission line between one of these resistance points and the feeder from the generator, having a characteristic impedance which is the geometric mean between the resistance at that point and Z_0, the standing wave is suppressed on the feeder between the generator and the matching section. This impedance-matching section is located near the load end of the feeder.

In a two-wire balanced feeder, a reduction in Z_0 can be effected by closer spacing, larger conductors, or both. Whereas an increase in Z_0 is

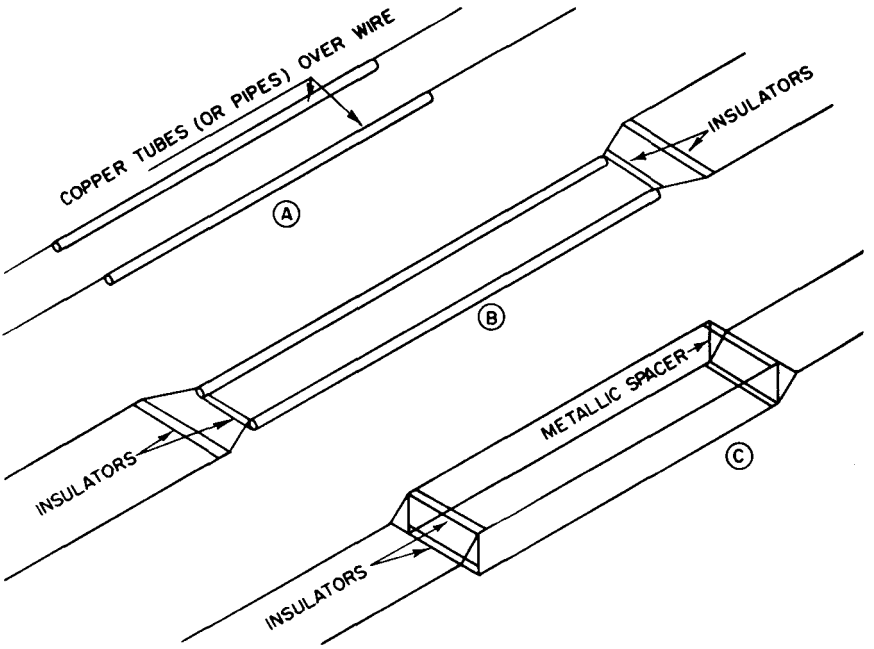

FIG. 4.34. Series impedance-transforming sections (two-wire line).

effected in the opposite manner, a large increase in Z_0 may not be physically realizable. For this reason, the quarter-wave impedance-matching section will usually start at a current maximum so that it can use a characteristic impedance less than that of the main feeder. The matching section may be made with reduced characteristic impedance by using a four-wire cross section, with two spaced wires in parallel on each side, or by using much larger conductors, or by reducing the spacing between wires. For illustrations of these possibilities see Figs. 4.34 and 4.35.

With a four-wire balanced line of type XVI, where there are two wires in parallel on each side of the feeder, the characteristic impedance of a quarter-wave matching section may be made lower or higher than that of the main feeder by contracting or expanding the spacings of the sides

or between the sides, or by changing conductor sizes, or by increasing the number of wires in parallel, or combinations of all these. In such a feeder, this series-section method of impedance matching is convenient and practical.[31,32] Figure 4.35 shows various possibilities. In this figure A and B are sections of reduced characteristic impedance, and C is a section with increased value. Figure 4.89 shows this method in use.

The matching of impedances by this method is not restricted to the use of quarter-wave matching sections. In the generalized case the

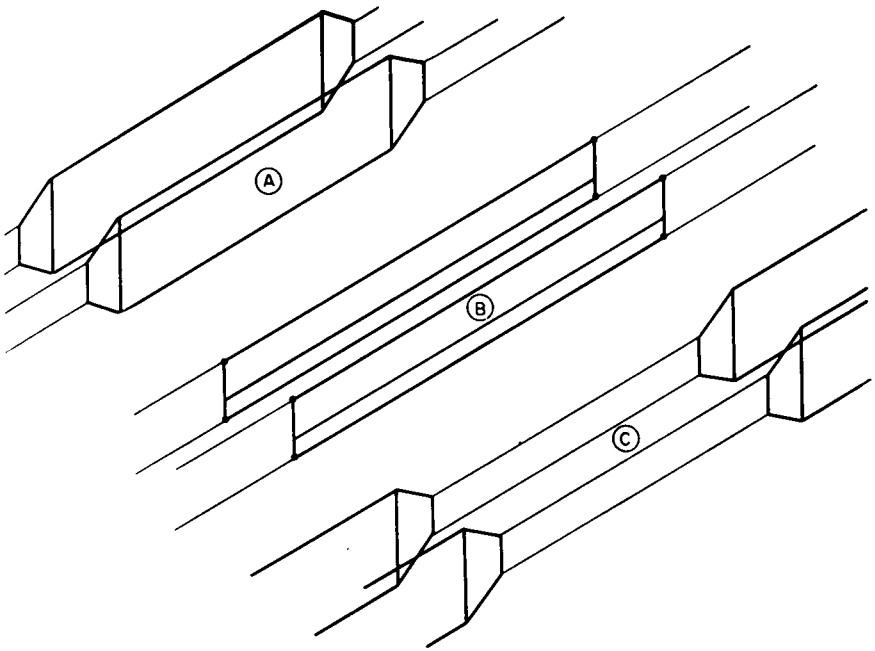

FIG. 4.35. Series impedance-transforming sections (four-wire line).

computations are more involved. For this purpose the circle diagram of a transmission line is useful. Such a diagram is shown in Figure 4.58. These curves are read as follows:

The abscissa of a rectangular system of coordinates is taken as the scale of resistances, and the ordinates, positive and negative, are taken as the scales for positive and negative reactances, using the same scale as for resistance. In order to make the chart as general as possible, a characteristic impedance of 1.0 is used for all computations. This makes all resistances and reactances read directly in proportional parts of the characteristic impedance of *any* transmission line.

The focal point is $1.0 \pm j0$. This is the input impedance of a perfect

line with $Z_0 = 1.0$ and terminated in a resistance $R_t = Z_0$, whatever the distance from the termination.

When the line is terminated in a resistance $R_t > Z_0$, the input impedance Z_{in}, as a function of distance from the termination, will describe a circle enclosing Z_0. This circle will be centered on the resistance axis but will be eccentric with respect to the Z_0 focal point. The distances from the terminal end fall on semicircles centered on the reactance axis where $R_{in} = 0$. The direction of change of Z_{in} with βl in degrees from the termination is clockwise from the resistance axis, starting at the right of Z_0 when $R_t > Z_0$, and sweeps a semicircle in the first 90 degrees and a full circle back to the starting point on the resistance axis in 180 degrees (one-half wavelength from the termination).

To test this method with figures, read from the chart (Fig. 4.58) R_t, βl, R_{in} and X_{in}:

R_t	βl, degrees	R_{in}	X_{in}
2.0	30	1.14	$-j0.74$
3.0	10	2.42	$-j1.10$
3.0	110	0.37	$j0.32$
1.75	90	0.56	0
4.0	160	1.45	$j1.75$

When $R_t < Z_0$, the starting point is on the resistance axis to the left of the focal point and electrical length is read clockwise, starting from this axis as zero and continuing around the complete circle at 180 degrees. The chart is not marked this way, to avoid confusion, but in use one subtracts 90 degrees from the electrical lengths marked on the radial lines in the upper half of the chart and adds 90 degrees in the lower half of the chart.

For example, test the following points on Fig. 4.58:

R_t	βl, degrees	R_{in}	X_{in}
0.45	65	1.3	$j0.9$
0.25	100	2.76	$-j1.77$
0.33	45	0.6	$j0.8$
0.50	125	1.0	$-j0.7$

These relative values of impedance are from the resistive termination or from the current maximum or current minimum nearest to the termination when Z_t is complex, or when $Z_t \neq Z_0$. The ratio $R_t/Z_0 = Q$ is the standing-wave ratio, marked on the confocal circles.

By means of this circle diagram the impedance at any point on a mismatched feeder can be determined if the standing-wave ratio can be measured and the point of minimum or maximum current located.

From the knowledge of the impedance $Z/\underline{\theta}$ at any chosen point on a mismatched line, one can proceed to determine the electrical length βl_{00} and characteristic impedance Z_{00} of a matching line to terminate the main feeder in its characteristic impedance Z_0.

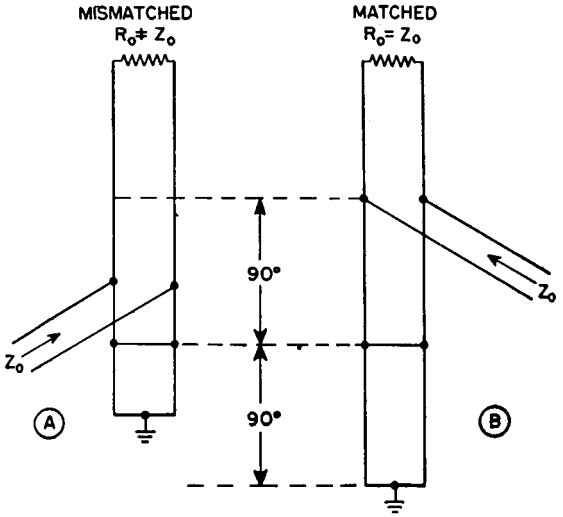

FIG. 4.36. Impedance matching by parallel feed.

4.4.4. Feeder Matching by Means of Tapped Lines. Figure 4.36 shows schematically a simple method of matching a feeder of characteristic impedance Z_0 by tapping it onto another mismatched feeder of the same characteristic impedance some distance above a short-circuiting bar which is located at a maximum current point in the vertical feeder. The distance above the short circuit to obtain a match depends upon the standing-wave ratio in the secondary feeder. For a very high Q the tapping point will be quite near to the short circuit, and as the Q is smaller and smaller, the tapping point increases in distance.

When the secondary feeder has no standing waves, the main feeder is placed one-quarter wavelength above the short circuit, so that the impedance of the lower quarter-wave section is infinite. This is shown in part B of this figure. This quarter-wave section acts as a filter for even harmonics of the working frequency by placing effectively a short circuit across the main feeder at the tapping point for the even harmonics where this section has an equivalent length of an integral number of half wavelengths for the even harmonics. In Fig. 4.36B there is shown an addi-

tional quarter-wavelength section below the short circuit. This is shown to bring out the fact that the one-half wavelength below the tapping point forms a short circuit to ground for any parallel currents that may be flowing in the two wires against ground, while the upper quarter-wavelength section presents a virtually infinite impedance to the desired balanced currents in the feeders.

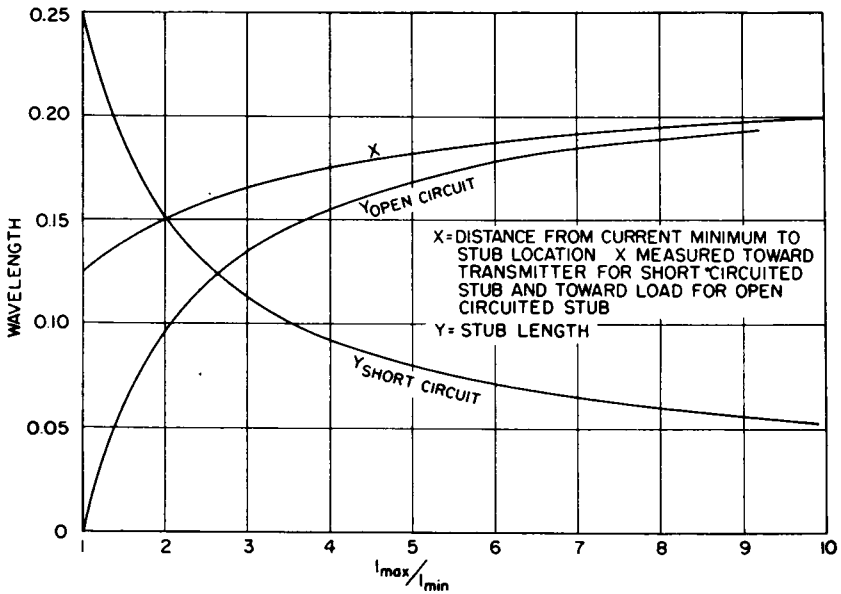

FIG. 4.37. Location and length of impedance-matching stub line when the feeder and stub have the same characteristic impedance.

In tapping into lines in this manner, care must be exercised to avoid mutual couplings between lines. This is best accomplished by bringing the lines together normal to each other.

4.4.5. Parallel Stub Lines for Impedance Matching. In this method, the Q of the line is measured as in previous techniques, and a current minimum is located. The problem is to find a point on the line where the real component G of its admittance $Y = G \pm jB$ is equal to the characteristic admittance Y_0 of the main feeder. At this point, a short stub of line, either open-circuited or short-circuited at its outer end, is bridged across the line. The susceptance of the stub is made equal but of opposite sign to the susceptance of the feeder at the point of attachment.

The circle diagram (Fig. 4.58) may also be read in terms of conductance and susceptance in the same way it was previously used for resistance and reactance, reading conductance in mhos instead of resistance in ohms and susceptance in mhos instead of reactance in ohms.

A stub line that is short-circuited is more easily adjusted than one open-circuited, and is for that reason the commonly preferred type. When its length $\beta l < 90$ degrees, the stub is inductively reactive and therefore has positive susceptance. A point on the feeder can always be

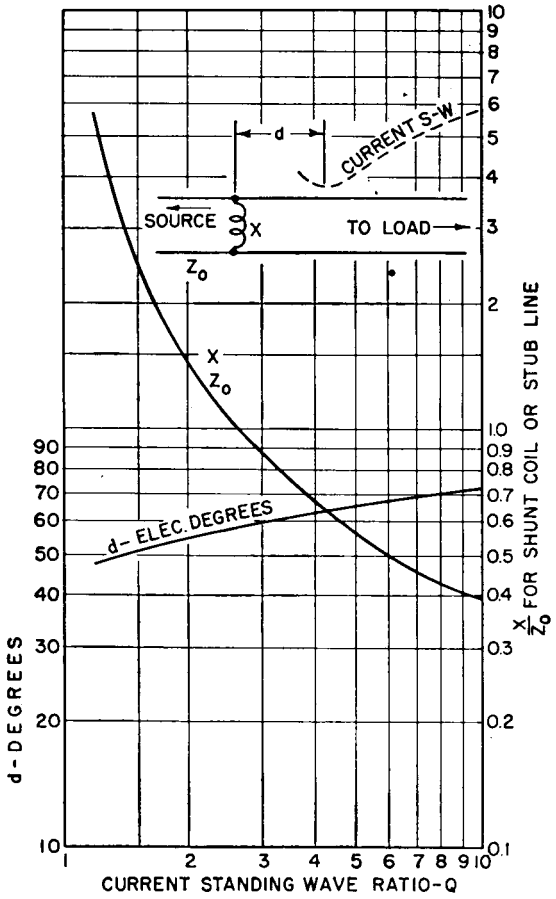

FIG. 4.38. Location and reactance of an impedance-matching shunt coil, derived from Fig. 3.58.

found where the susceptance is negative and therefore requires a stub of positive susceptance to neutralize it.

Such a stub is designed from the equations

$$X_L = Z_0 \tan \beta l \qquad \text{or} \qquad B_L = \frac{1}{Z_0 \tan \beta l}$$

When the stub line has the same characteristic impedance as the feeder, Fig. 4.37 can be used to read directly the location and length of both open-circuited and short-circuited stubs for a correct impedance match.

4.4.6. Impedance Matching with an Inductor or Capacitor. In this case the procedure is identical to that for a stub, except that an inductor or a capacitor of proper value is bridged across the feeder at the proper point to effect the match.

The use of an inductor or a capacitor is much more convenient and economical than a stub line and is therefore frequently preferable to a stub. Figures 4.38 and 4.39 are for use with shunt coils.

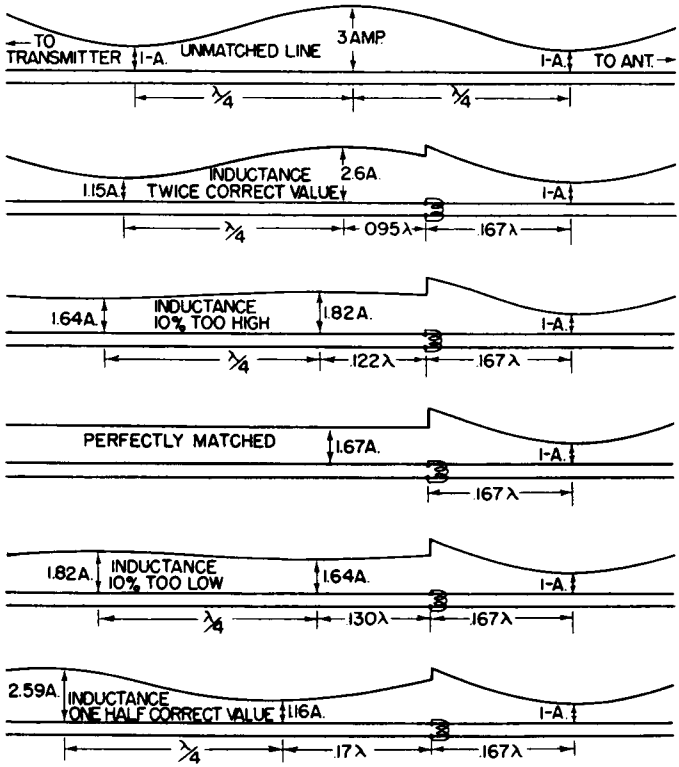

FIG. 4.39. Example of impedance matching by shunt coil. (*After Carter.*)

Figure 4.38 shows the location and relative reactance of a shunt coil that will match a feeder for standing-wave ratios up to 10. These were derived from the circle diagram (Fig. 4.58) in the following way:

The focal point $1 + j0$ is taken as the characteristic *admittance* of the feeder $1/Z_0$. The reactance scales are now read as *susceptance* $Y_i = 1/X$. The standing-wave circles are read directly. If we follow a Q circle from the real axis to the right of the focal point clockwise until it cuts the vertical dashed line through the focal point and read the coordinates of this point, we shall find it is $1 - jY_i$. At this point the admittance of

the feeder consists of a conductance $G_i = 1/Z_0$ and a susceptance $-jY_0$. This is the equivalent of a resistance in parallel with a capacitive reactance. The resistance is $1/G = Z_0$. Therefore, if we add a susceptance jY in parallel at this point, it tunes the susceptance of the line to parallel resonance and makes the total susceptance zero. This leaves only the resistance Z_0, and the line is matched.

In following the Q circles around clockwise to the vertical dashed line through the focal point, an electrical length βl is also read from the chart at this intersection. The distance from a current minimum to the matching point must be the complement of the angle read from the chart. If βl is the value read from the chart, the electrical distance βl_0 to use will be $90 - \beta l$.

Since it is equally important to use the chart (Fig. 4.58) in both impedance and admittance forms, one should become thoroughly familiar with both procedures. To illustrate its use in admittance form, consider the following problem:

Assume that a 500-ohm feeder has been measured and found to have a standing-wave ratio of 3.0 and that the location of a current minimum has been marked for reference. We wish to match this feeder by using a shunt coil, and we must determine where to place this coil and also its reactance. From the chart, we locate the intersection of the circle for $Q = 3.0$ and the vertical dashed line through the focal point $1 + j0$ and read a susceptance of $-j1.15$. This occurs on the curvilinear radial line corresponding to $\beta l = d = 30$ degrees. Since we must take the complement of 30 degrees in this case, the proper distance of the coil from the current minimum will be $d_0 = 90 - 30 = 60$ degrees, or 0.167 wavelength. The relative susceptance of the line is $-j1.15$, and so the relative reactance will be $1/-j1.15 = -j0.87$. These values are now multiplied by the value $Z_0 = 500$ ohms to obtain true working values. At this point, the line appears as a resistance of 500 ohms in parallel with a capacitive reactance of $500 \times 0.87 = 435$ ohms. If an inductance of 435 ohms is bridged across the line at this point, their joint reactances go to infinity, leaving the real value of 500 ohms. The line is then matched.

It is instructive to prove this in the following way:

At a current minimum, the impedance of the line in the direction of the load is identical to a termination in a resistance

$$R_t = 3 \times 500 = 1{,}500 \text{ ohms}$$

The location of the matching coil was found to be 60 degrees toward the generator from the current minimum. These values can be inserted in Eq (8) (page 368), from which it is computed that the impedance of the line looking in the direction of the load is $215 - j248$ ohms.

To transform this impedance to a matching value of 500 ohms resistance, it is found that the inductive reactance required is 435 ohms, connected in parallel with the line.

In this discussion we have used the lower half of the chart, where the susceptance was negative, so that we could perform the match with an inductance. Had we taken the conjugate point in the upper half of the chart, where the susceptance of the line is positive, we should find that the match can be effected in the same way if a capacitor of the correct value is bridged across the line. However, the reversal of the direction in the chart necessitates a reversal in the direction of the matching element from the current minimum, which would be toward the load instead of toward the generator.

Figure 4.38 can also be used to determine the location of an inductive parallel stub line. When a parallel stub is used for matching, its reactance at correct match will be identical to that of a parallel coil. When the characteristic impedance of the stub line is the same as that of the main feeder, its length and location can be read from Fig. 4.37 directly. When the stub has a different characteristic impedance, the required relative reactance is taken from Fig. 4.38, and Eq. (11) is solved for the length βl of the stub, using the value chosen for its characteristic impedance.

Figure 4.39 is a pictorial indication of the effect of varying the value of the reactance of a shunt impedance-matching coil that is correctly located on the feeder to obtain a match.

Figure 4.40 represents another way in which a feeder can be matched by using reactive elements in series with the line, using the correct value at the correct location. Its application is exemplified by the following:

A 600-ohm feeder is found by measurement to have a standing-wave ratio of 1.8, and the location of the current minimum nearest to the load has been marked. Figure 4.58, used in its *impedance* form, is now applied in exactly the same manner as explained for use in its *admittance* form. The Q circle for 1.8 (interpolated) is followed clockwise until it intercepts the vertical dashed line through the focal point, at which point the resistance component of the *series impedance* of the line at that point (37 degrees toward the transmitter from the current minimum) is equal to Z_0. The normalized series component of reactance at that point, read from the chart, is $-j0.60$. If a series inductor of normalized reactance $j0.60$ is placed in series with the line to neutralize the line reactance, the line is matched. In this case the value required is

$$0.60 \times 600 = 360 \text{ ohms}$$

Since the circuit is balanced, coils of one-half this value are placed in each side of the line, as in Fig. 4.40*A*. Following the Q circle counter-

clockwise to obtain the conjugate matching point, and measuring the distance to the matching point in the opposite direction from the current minimum, the same result can be realized with capacitive reactance of the same value, as represented in Fig. 4.40*B*. Figure 4.40*C* represents the use of series stubs to obtain the same effects.

4.4.7. Termination by Means of Coupled Sections. Standing waves on a feeder can be suppressed by means of an open-end quarter-wave

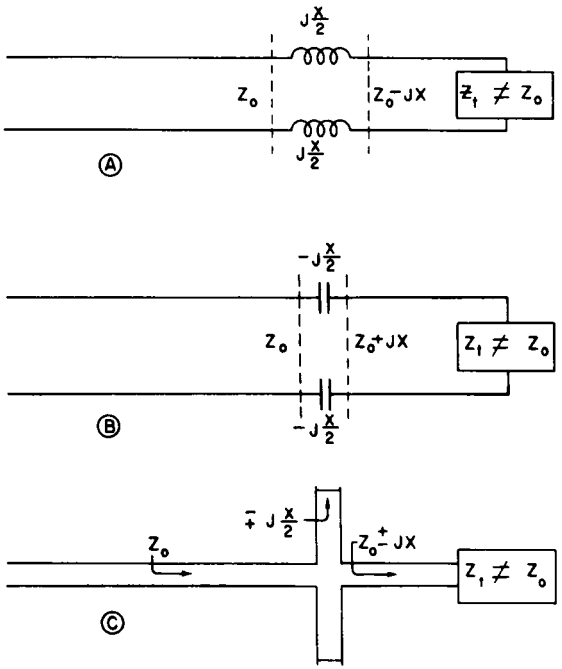

FIG. 4.40. Feeder matching, using series reactances.

section or a half-wave short-circuited section coupled to the feeder,[4,9] provided that the position of the coupled section along the line is correct, as well as the degree of coupling to the feeder. The open end of the quarter-wave coupled section is pointed toward the load end of the feeder, and the standing waves are eliminated on the feeder opposite the closed end of the coupled section. The schematic diagram of this arrangement is given in Fig. 4.41.

Mechanically this method is not very convenient until the frequency is high enough to give a short coupled section that can be easily slid along its support wires to the position that accomplishes the desired result. The method has singular merit due to the fact that the termination of a feeder is selective to the frequency for which it is adjusted, within 1 or 2

per cent, and outside this range the coupled section gives the effect of nonexistence.[54] Therefore, when two or more different frequencies are to be propagated over a common feeder, a separate coupled section can be used to terminate the feeder for each frequency without influencing the other frequencies being transmitted. This provides a means of connecting several generators to a common load over a common feeder and also of using a common feeder to carry power from several generators to several

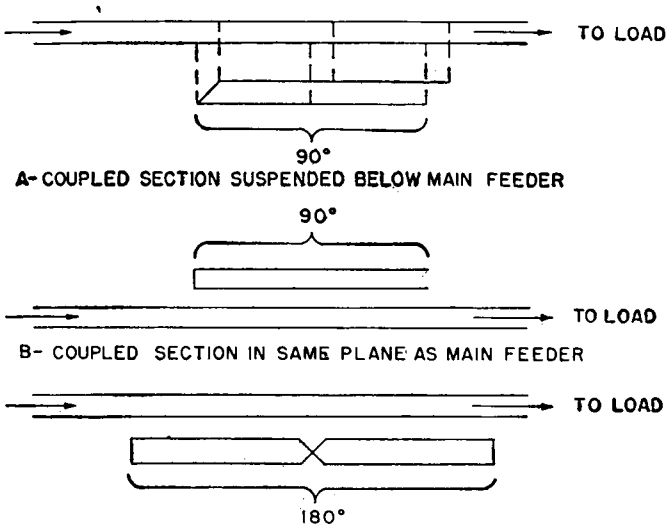

FIG. 4.41. Coupled sections for impedance matching.

loads selectively, using suitable stopper circuits at the branches of the feeder for correct routing of the different frequencies.

4.4.8. Tapered Transmission-line Section as an Impedance-matching Transformer. A transmission line whose characteristic impedance is gradually tapered from one value to another may be used as a coupling transformer between loads and generators of unequal resistive impedances, provided that the change in impedance along the line is sufficiently gradual. The simplest form is a taper that results from converging or diverging straight conductors. The transformation ratio of such an arrangement is somewhat limited, for practical cross-sectional dimensions, as will be evident from the application of the characteristic-impedance formulas. If the tapered-line section has an electrical length of two or more wavelengths, the impedance transformation takes place with negligible reflections over a broad band of frequencies, owing to the smooth and gradual change of characteristic impedance with distance along this line. The shortest length for such a section that will give a

tolerable minimum of reflection at the lowest of a band of working frequencies depends upon the transformation ratio desired, the difficulty increasing as this ratio becomes larger.

The transformation ratio of a tapered line may be increased by changing the number, spacing, configuration, and size of the wires in the cross-section of the line at different points along the system, thus making possible a greater range of characteristic impedances between the ends of this section. The change of characteristic impedance with distance, if made smoothly and over a sufficient length, will provide a substantially reflectionless impedance match between its two limiting resistance values.[25] The practicality of such an application is determined solely by the structural convenience, once the current and potential requirements have been satisfied.

When it is desired to make a tapered-line transformer with a minimum length, the characteristic impedance must be tapered exponentially between its two limiting values.[24,26] In such a case, the design of the transforming section must be carefully computed, because at its minimum length, power-factor correcting networks are necessary for perfect matching. As the length of the exponentially tapered transformer section is increased, the more nearly it approaches a resistance-to-resistance direct match without correcting circuits. When sufficiently long, correcting circuits may be omitted, for most practical applications.[23] One can avoid much complicated design computation by using an exponentially tapered line section with a length of at least one-half wavelength at the lowest frequency to be transmitted and connecting it directly between a resistive load and the main feeder.

The following simple procedure may be used for the design of exponentially tapered lines that are one-half wavelength or more in length at the lowest working frequency:

1. On a sheet of semilogarithmic graph paper, mark the logarithmic scale in terms of characteristic impedances and the uniform scale in terms of length of line in wavelengths or in electrical degrees.

2. When this line is to match two resistive impedances R_1 and R_2, with a line of length x degrees (x at the lowest frequency greater than 180 degrees), mark a point on the chart for R_1 at $x = 0$, and another point for R_2 at $x =$ chosen length of line. Draw a straight line between these points. Read from the logarithmic scale the required characteristic impedance of the tapered line at all intermediate distances along the line.

3. Choose the desired line configurations that provide the range of characteristic impedances required when practical dimensions are used, and apply their formulas at not greater than 20-degree-length intervals from end to end of the tapered section.

Example of Simplified Calculation for a Long Exponentially Tapered Transmission Line. It is desired to match a resistive load of 350 ohms to a feeder of 560 ohms characteristic impedance, over a frequency range of 5 to 12 megacycles. Both ends of the system are balanced to ground. A power of 50,000 watts, amplitude-modulated, is to be transmitted, and

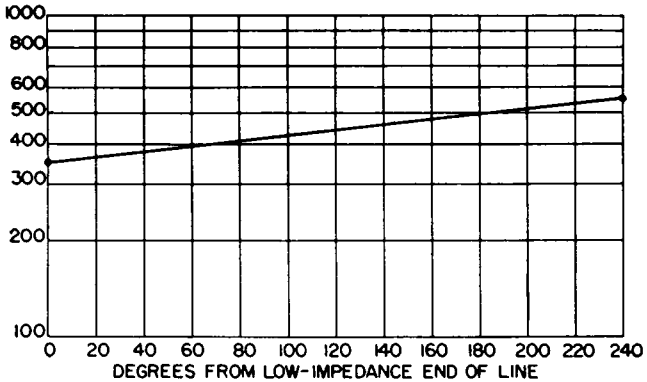

FIG. 4.42. Exponential taper computed graphically.

ample space is available in the open to use a leisurely tapered exponential transformer section. What should be used?

Figure 4.42 shows the first step when the problem is stated on semilogarithmic paper with a length amply chosen to permit the simplified design to be used—in this case, 240 degrees at 5 megacycles. From this figure the values in Table 4.2 are tabulated:

TABLE 4.2

Distance from 350-ohm load, degrees	Characteristic impedance required, ohms	For ρ = 0.102 inch	
		a	b
0	350	6.0	1.0
20	365		
40	380		
60	393	6.0	0.5
80	408		
100	421	5.5	0.25
120	440		
140	460		
160	478	5.5	0
180	496	6.3	0
200	517	7.7	0
220	540	9.2	0
240	560	10.7	0

The higher values of characteristic impedance in Table 4.2 are within the normal range for two-wire balanced lines. Figure 4.23 shows that for the lowest impedance of 350 ohms the ratio of wire spacing to wire radius is 18.5. If the wire to be used were of radius 0.102 inch, the center-to-center spacing would be 1.89 inches. This is obviously a very small spacing mechanically and from a potential standpoint for the power to be transmitted would give excessive potential gradients. We may decide to maintain two-wire design from the 550-ohm end to the point where the

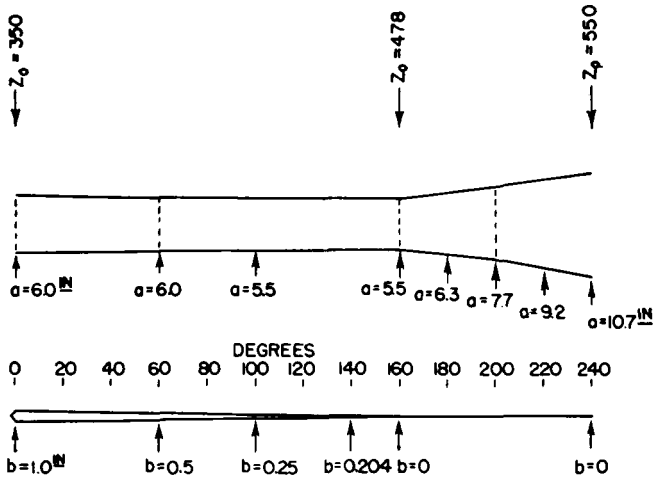

FIG. 4.43. Construction of exponentially tapered matching section from 550 to 350 ohms.

spacing is 5½ inches, at which point a/ρ is 54 for a wire of 0.102 inch radius and $Z_0 = 478$ ohms. It is then decided that from this point to the 350-ohm end a four-wire side-connected design will be used with the same size wire. Applying the equation for Z_0 for the type XVI line and maintaining a substantially constant value of a, the values for a and b (tabulated) were obtained.[23,51] The final electrical design of the tapered line is shown in Fig. 4.43.

It is seen when the arithmetic is developed that the variation of b with distance is very nearly linear with electrical distance from the wide end (low impedance) of the four-wire portion to the place where the two wires in parallel on each side can be soldered together. It is further seen that this particular design is structurally simple to realize with very trivial compromise variations from true exponential continuous taper.

4.5. Network Equivalents of Transmission-line Sections

A matched section of transmission line of electrical length βl produces a phase difference of βl between terminal and input potentials or currents,

and the phase of the terminal current always lags that of the input because of the finite propagation time.

Occasionally it is necessary to use a building-out network to serve as the equivalent of a certain short length of line, having a given phase lag and characteristic impedance.

Figure 4.44*A* shows a T network, and Fig. 4.44*B* shows a π network suitable for producing the equivalent of a section of line less than 180

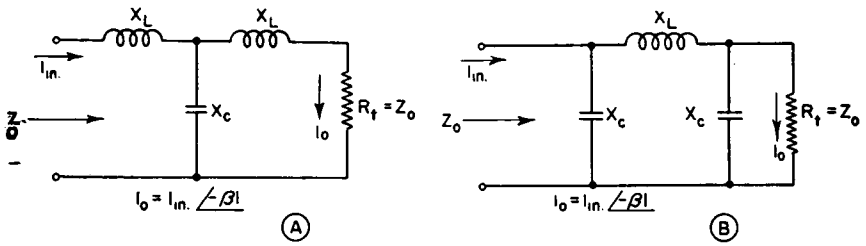

FIG. 4.44. Networks for feeder building-out sections.

degrees long. Practically, it is best to use two cascaded sections when the desired length exceeds 120 degrees, in order to avoid excessive potentials and currents in the elements. Considering Fig. 4.44*A*, the following equations can be used to determine the reactances of the elements:

$$X_L = jZ_0 \tan \frac{\beta l}{2}$$

$$X_c = -j \frac{Z_0}{\sin \beta l}$$

For the π network of Fig. 4.44*B* the following equations apply:

$$X_L = jZ_0 \sin \beta l$$

$$X_c = -j \frac{Z_0}{\tan \frac{\beta l}{2}}$$

If a balanced network is required, the unbalanced solution is used but the series reactances are divided in half and distributed symmetrically in the two sides of the circuit.

Any number of sections can be cascaded to obtain, progressively, any desired electrical length, with any desired phase shift per section that is less than 180 degrees. Good engineering design is that which does not lead to impractical reactance values.

4.6. Balanced to Unbalanced Transformations

The need frequently arises to feed a balanced load from an unbalanced generator, or vice versa. Many practical methods have been developed

for this purpose,[57,58,61] some with coaxial lines and some with open-wire lines. Only a few of the more useful methods are included here.

Using networks of lumped reactances one can always use a single-ended T or a π section to produce a 90-degree advance of phase of current or potential (or both in the case of resistive loads) to go between an unbalanced generator and one end of a balanced load and an equivalent section with equal but opposite-sign corresponding elements to give a phase lag of 90 degrees to go between the same generator and the opposite end of the balanced load. These two networks together provide a balanced

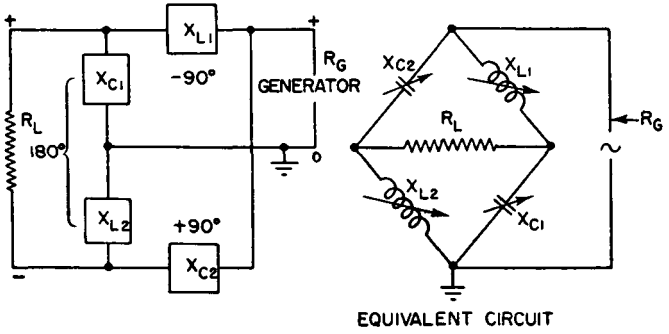

FIG. 4.45. Balance to unbalance transformer network.

potential across the load, and the phase of the source is 90 degrees with respect to the currents or potentials across the load (see Figs. 5.39 to 5.42). The same result can be obtained by using any arbitrary phase shift θ_1 in one side for phase advancing and a phase shift θ_2 of $180 - \theta_1$ in the phase-lagging network. When the impedance transformation ratio is the same in both sides, balanced potentials are produced across the load, while the relative phase of the source is at an angle θ_1. There are very few applications where there is need to control the phase differences between the load and the source, so the 90-90-degree method is the most convenient to use. The most usual application is from a resistive load to a resistive source. In a 90-degree network, all three elements of a T or a π have equal reactances.

The simplest network of this type is one using four equal reactances, two capacitive and two inductive, in a bridge circuit as shown in Fig. 4.45. This is equivalent to the preceding application of plus and minus 90-degree shifts in the two branches, using L networks. Adjustment for perfect balance can be obtained easily. The network is readily adjustable over a band of frequencies by using identical variable capacitors on a common actuating shaft, and the same with the inductors. The inductors are set to some value and the capacitors tuned until they have

the same reactance as that of the inductors. At any given frequency, the transformation ratio of the network can be made anything desired by the choice of the reactances at balance of the bridge. The adjustment for equal capacitive and inductive reactances can be made in two ways: (1) open the balanced resistive load, energize the single-end input at the desired frequency, and tune until the network looks like a short circuit (series resonance) across the source; or (2) short-circuit the balanced resistive load, and tune the network for antiresonance. This network

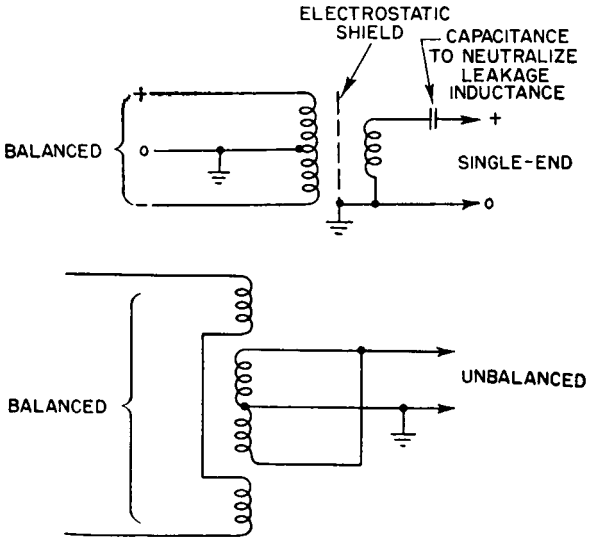

FIG. 4.46. Balance to unbalance transformers.

provides a very simple and versatile balanced-to-unbalanced resistance-to-resistance coupling network that can be used to transform in either direction. The transformation ratio varies with the ratio X/R_G. When $X = \sqrt{R_G R_L}$, $R_L = 4R_G$, when R_G is the unbalanced end.

The foregoing networks are selective in that they accomplish their transformations from balance to unbalance at one frequency only. When it is desired to make this transformation over a wide range of frequencies the inductively coupled electrostatically shielded transformer of Fig. 4.46 can be used, with or without an iron core. One winding is balanced to ground, while the other is grounded at one end. To approach as nearly as feasible an ideal transformer, the coupling coefficient between windings is made very high by interleaving of windings or any other technique common in wide-band transformer design. The leakage reactances on each side of the circuit are thus kept relatively low, and a minimum of power-factor correction can be used in the two circuits. As the leakage

reactances get larger owing to incomplete coupling between the windings, more and more capacitance is required in the two circuits to present resistance-to-resistance matching. The selectivity is thus increased and the bandwidth reduced accordingly. The electrostatic shield eliminates electrostatic couplings, which otherwise would be nonuniformly distributed along the two windings, leading to unbalance to ground of the winding that should be balanced.

The ratio between the coupled balanced and unbalanced resistances is determined by the turns ratio of the transformer and by the coupling factor.

A radio-frequency air-core transformer of this type with a bandwidth of one or two octaves is relatively easy to construct. As the desired band-width is increased to several octaves, the design problem increases rapidly. Toroidal windings on iron-dust cores become useful for wide-band designs. Balanced to unbalanced transformers for use with receiving systems have been successfully developed for a band of 8½ octaves.

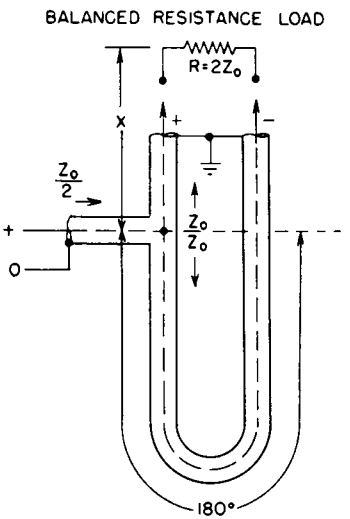

FIG. 4.47. Half-wavelength line transformer from unbalance to balance.

Balance to unbalance networks can be used in one form or another for radio frequencies up to approximately 50 megacycles without serious design problems. The transformers are principally useful for low-energy applications such as receiving circuits but are inconvenient or impractical for most transmitting applications. At the higher frequencies, however, it is often preferred for reasons of cost, simplicity, and convenience to use distributed circuits for balance to unbalance transformations. Where coaxial lines are used, there are certain techniques that have proved very convenient.

Figure 4.47 is one circuit often used to transform reversibly between balanced and unbalanced systems. In one direction of working, a single-end source is branched into two lines of equal characteristic impedance, one branch having an electrical length X between the branch and one side of the circuit, while the other has a length $X + 180$ degrees between the branch and the other side of the balanced circuit. When both branches are terminated in their characteristic impedance, the 180-degree lag in one branch produces the desired inversion of phase to yield balanced potentials across the balanced circuit.

Figure 4.48 is a schematic diagram of the well-known "bazooka," or balun. The outer end is an open double-concentric section 90 electrical degrees long, connected to the sheath of the main feeder one-quarter wavelength from the outer end. The balanced terminals are the innermost conductor and the sheath of the main feeder opposite it. It is not essential that the velocity of propagation in the two parts of the bazooka be identical, and of course the electrical lengths of the system are based on

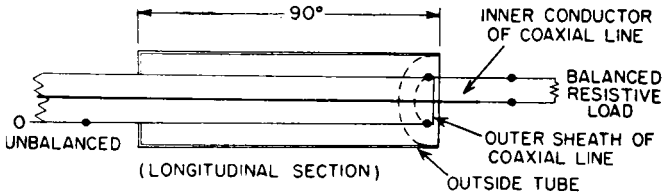

FIG. 4.48. Coaxial "bazooka," or balun.

the velocity in the outer coaxial portion. This is implied in all the foregoing descriptions and in all subsequent ones relating to feeders in which the velocity of propagation is less than that for free-space waves of the same frequency.

Referring now to balance to unbalance transformers in open-wire systems, there are relatively few good choices. Figure 4.49 is one example where the equivalent of a closed quarter-wave stub is placed in series with

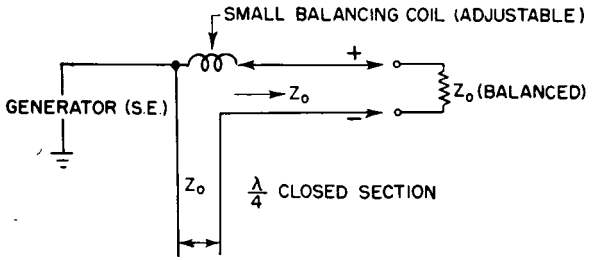

FIG. 4.49. Unbalance to balance transformer for open-wire lines.

one side of the branch to provide a phase lag of 180 degrees across the terminals of this section. Experience has shown that this is sometimes insufficient by itself to make an exact transformation, but by placing a small inductor in series with the straight portion of the balanced side of the branch it can be adjusted to bring an exact balance at the balanced terminals.

Figure 4.50 shows a method that is applicable when substantial standing waves exist on the balanced part of the system. In *A*, when the load resistance on the balanced side is very much greater than the characteristic impedance of this balanced line, the latter should have a

length of 90 degrees, with its lower end grounded. An unbalanced system can now be coupled to this by tapping up from ground on one side of the balanced feeder until the two systems are mutually matched. When the balanced load resistance is much less than the characteristic impedance of the balanced line (*B*), the same scheme can be used, but with a 180-degree line between the load and the ground. To deliver rated power from a balanced system to an unbalanced load of very high resistive impedance, such as an end-fed dipole, a very high voltage is required.

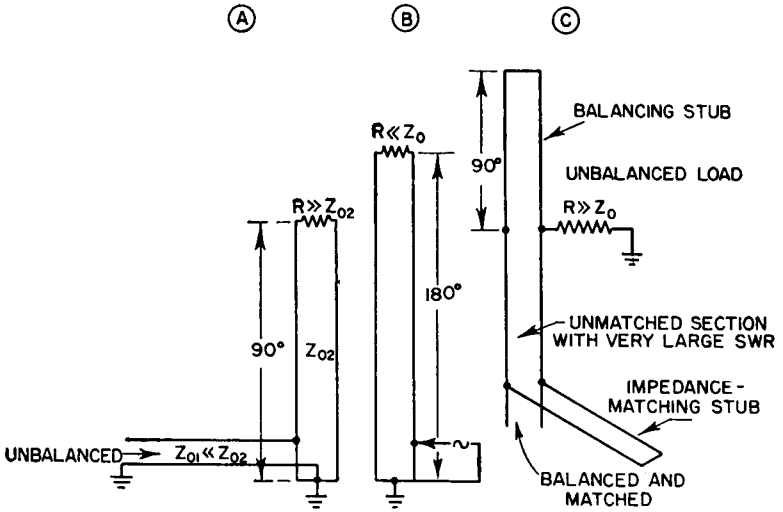

FIG. 4.50. Impedance-matching unbalance to balance circuits.

Very large standing waves on an open-ended feeder will develop a potential many times that in the matched portion of the feeder. When a high-resistance load is connected between one end of this feeder and ground, it introduces an unbalance in the system which usually is intolerable. Balance can be restored to such a system by connecting a balancing quarter-wave stub, short-circuited at its outer end, in parallel with the end of the balanced feeder. This system is shown in Fig. 4.50*C*.

The device shown in Fig. 4.51 has been much used in the ultrahigh-frequency region and can sometimes be used in the range of 4 to 30 megacycles without becoming excessively cumbersome. Its simplicity is its principal merit. The outer conductor has two diametrically opposite longitudinal slots cut for a distance of one-quarter wavelength back from the end which is connected to the balanced load (or generator), and the inner conductor is connected to one half of the outer. The other end is the unbalanced terminal. With uniform characteristic impedance throughout its entire length, the transformation ratio is from Z_0 (unbal-

anced) to $4Z_0$ (balanced). This transformation ratio can be changed by using a different characteristic impedance for that portion of the line which is slotted.

For the lengths that would be used for high-frequency applications, the mechanics are impractical unless rigid tubular line is used. The large-diameter lines that are employed in high-power systems are suited to this purpose. The device is adjustable to different higher frequencies by short-circuiting the slots at various points along their lengths. The slot must withstand a potential twice that existing on the full concentric portion of the line when the impedances are matched.

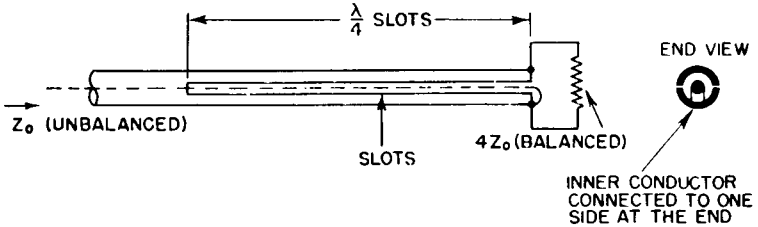

FIG. 4.51. Split-sheath coaxial unbalance to balance transformer.

4.7. High-frequency Transmission-line Switching

One of the engineering problems associated with high-frequency radio-station design is that of switching various antennas to various feeders in order to obtain the best utilization of equipment. In high-frequency operations it is necessary to change the working frequency during a day over a given circuit and also to use the same transmitters at different times on different circuits. To accomplish this, various switching arrangements are employed. The techniques differ with the particular switching requirements, the type of feeder used, and with the power level of transmission.

The one requirement that introduces the greatest complexity to the problem is that of switching without altering the characteristic impedance of the feeder system as it passes through the switches. If the same feeder is to carry power at frequencies that are greatly different from time to time, it is impractical to apply the usual matching techniques that suppress standing waves at particular frequencies. The most practical method results when the switches have the same characteristic impedance as the feeder.

Switching devices of many kinds have been developed for this purpose.[30,31,33,54] There are coaxial and balanced types, for low, medium, and high power. There are manual and automatic types. There are outdoor and indoor types. The switching circuits usually are of two

types—a single transmitter connectible to a multiplicity of antennas, and a multiplicity of transmitters connectible to a multiplicity of antennas. The latter can be one that provides limited flexibility, determined by particular requirements for interconnection, or unlimited flexibility so that any transmitter can be connected with any antenna.

The use of radio-frequency contactors is the simplest method when suitable designs are available and when one or two transmitters only are

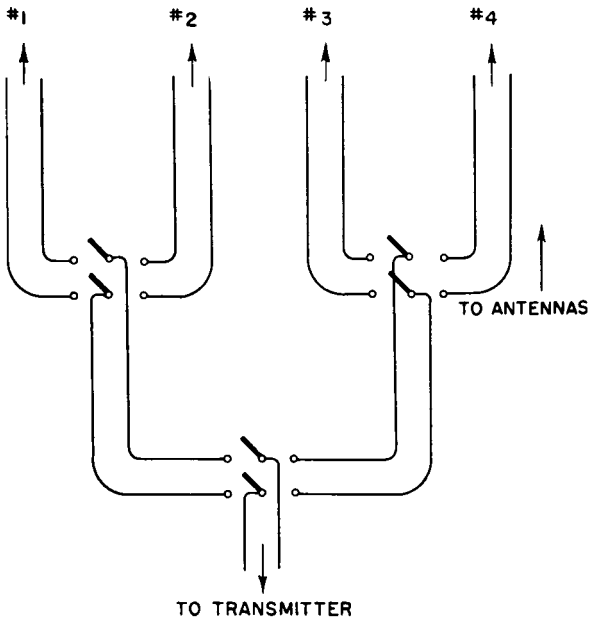

FIG. 4.52. Simple switching of one transmitter to a multiplicity of antennas, using contactors.

involved, with a small number of feeders. Double-pole two-position contactors have been used satisfactorily with two-wire balanced feeders at peak powers of 200 kilowatts, as required for 50-kilowatt amplitude-modulated broadcast transmitters at frequencies used for international short-wave broadcasting. Above this power, specially built switching devices are necessary.

Figure 4.93 shows an installation of contactors for switching one 50-kilowatt transmitter to any one of eight feeders, using a circuit similar to that of Fig. 4.52. The system uses 600-ohm balanced feeders.

Another basic circuit for unlimited flexibility of switching combinations is a form of the crossbar system, as represented schematically in Fig. 4.53. The feeders to the several antennas, with suitable separations to reduce cross talk sufficiently, are distributed in parallel in one plane. The lines

from the several transmitters are similarly distributed in another parallel plane, but with their directions normal to the antenna feeders. To connect any antenna feeder to any transmitter feeder, it is necessary only to provide some form of connection between the appropriate feeders at the places where they cross each other. If the feeder conductors are of fixed lengths, this may leave open-circuited stub sections bridging the connections which constitute a point of reflection. If it is not convenient to open the stub sections near these connections to eliminate this undesirable effect, the stub sections can be constructed to have sufficient length

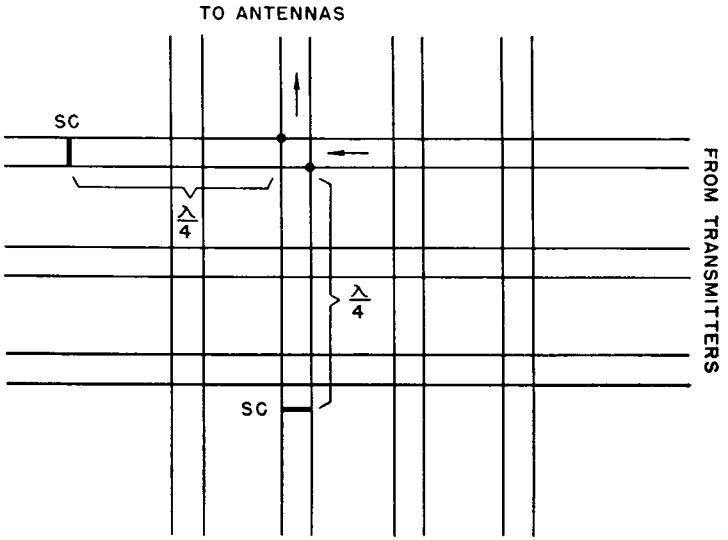

FIG. 4.53. Crossbar switching with dead-end elimination.

to project a quarter wavelength beyond the junction, where they can be short-circuited by contactors or switches. Figure 4.53 shows this principle for one connection between a transmitter and a feeder.

It is possible in the application of the crossbar system to provide an electromechanical device equivalent to two double-pole double-throw switches so that the excess lengths of feeder beyond a junction are open-circuited in the same operation that makes the crossbar connection. A radio-frequency switchboard circuit using this method of eliminating dead ends is shown (for one side of a balanced circuit only) in Fig. 4.54,[30] in which transmitters 1 and 2 are shown connected, respectively, to antenna feeders 3 and 2. The dotted lines between switch sections indicate that they are mechanically interconnected so as to be actuated in one operation. The switches in one transmitter line can be interlocked to prevent more than one antenna feeder being connected at a time, and similarly an

antenna feeder can be interlocked to prevent more than one transmitter being connected to it. The same interlocking provisions can be utilized to actuate indicators showing the status of the connections at a local or a remote location. The realization of a system of this type is simple for low-power applications, and with suitable magnetically operated contacting devices the switching can be wholly electrical. In high-power applica-

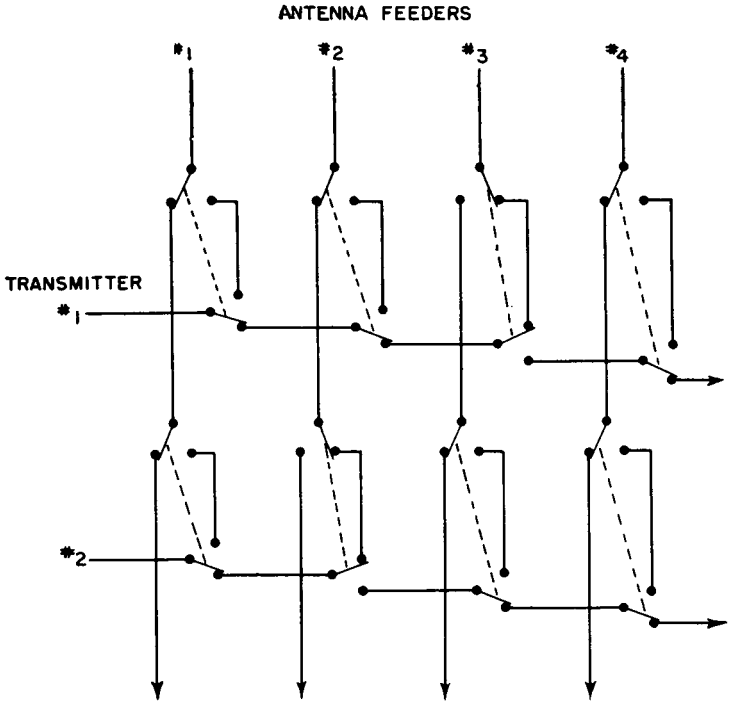

FIG. 4.54. Crossbar switching panel.

tions there are some very involved design problems, for which reason manual operation is usually employed.

There is a class of large multipole multiposition switch that has come to be known as the "boom" switch. Switches of this type require considerable space because sections of two-wire transmission line of the normal proportions are used for the movable sections. They are usually constructed out of doors for high-power applications. Figure 4.55 shows diagrammatically a two-pole multiposition version, suitable for interconnecting one transmitter to a multiplicity of feeders.[33] The transmitter feeder is flexed normal to its plane, and mechanical tie points, usually pairs of insulators, serve as the switch points for each position where the main feeder connects to an antenna feeder. The change of

position is often done manually, but there is a variety of ways by which the operation can be mechanized for remote operation.

Figure 4.56 represents a boom switch, in which are shown three transmitter feed lines leading to a three-level structure (one for each transmitter) in which each transmitter feeder is movable horizontally to a number of pairs of switch points in a horizontal arc. Each pair of switch

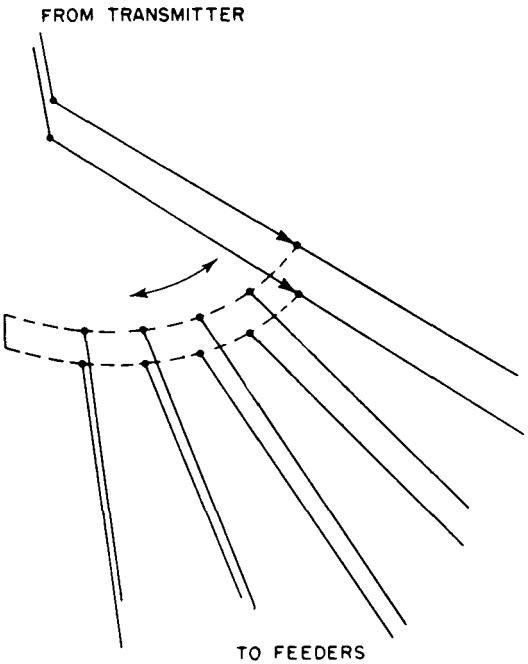

FIG. 4.55. Multiposition switch.

points in each level cooperates with an antenna-feeder movable section that connects it with a transmitter feeder as required. The antenna feeders have flexible sections that can move from level to level in a vertical plane. This circuitry gives direct connections between any transmitter feeder and any antenna feeder without dead ends and without any substantial irregularity in the characteristic impedance of the system as a whole. As shown in Fig. 4.56, the following switching combinations can be noticed:

Transmitter 1 is connected to antenna feeder 2.
Transmitter 2 is connected to antenna feeder 1.
Transmitter 3 is connected to antenna feeder 4.

Since the transmitter feeders are flexed horizontally and the antenna feeders vertically, it is necessary to make a 90-degree transposition in the flexible part of the transmitter feeder. It enters the switch with its plane vertical and turns 90 degrees to cooperate with the insulated switch points, which are horizontally disposed, where the antenna feeders also

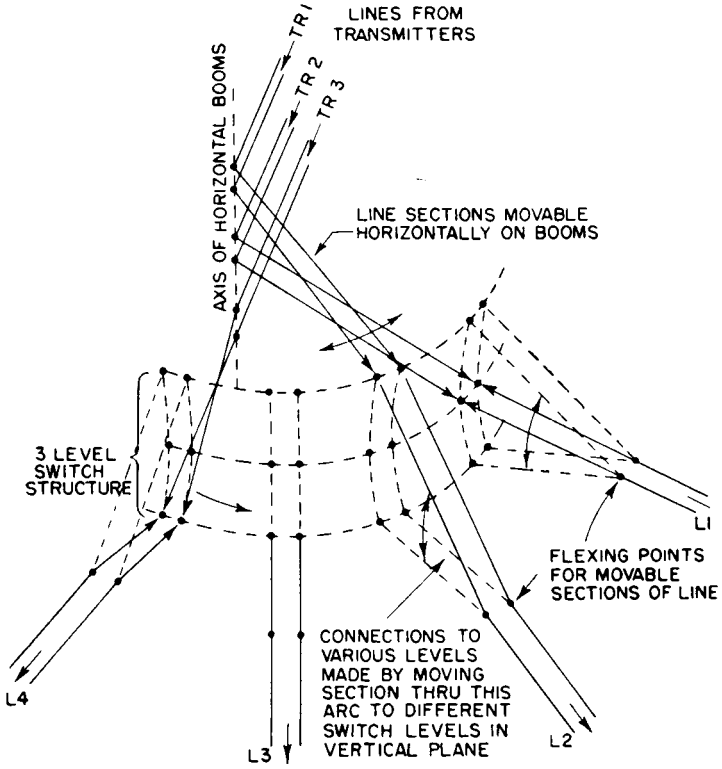

FIG. 4.56. Boom-type switch for three transmitters to four feeders.

connect. The structure supporting the movable transmitter-feeder section of the switch may be supported on a boom structure, the outer end of which may roll on tracks around its full arc.

The design of a structure of this kind is one requiring considerable ingenuity in large-scale electromechanics. It must be operable with ease in high winds and during icing. It must be separately operable by sections while other portions of the switch are energized and in operation, with complete safety to men and equipment. All the principles of the

uniform transmission line must be observed. For these reasons they are quite expensive to design and construct.

Boom and drum switches of the type of Fig. 4.55 can be used in combination to obtain complete flexibility of switching a multiplicity of transmitters to a multiplicity of feeders, as shown in Fig. 4.57.[30] The individual switches may be complete electromechanical assemblies with

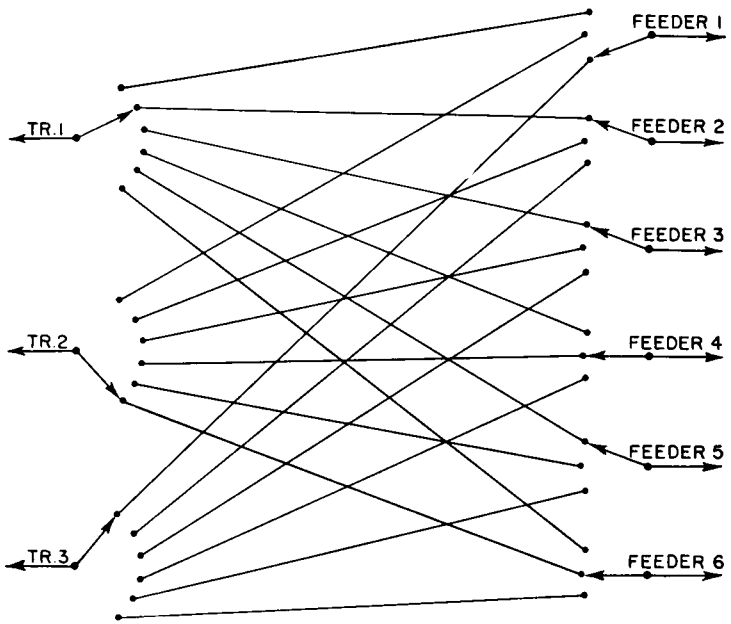

FIG. 4.57. Combination of multiposition switches.

automatic actuating devices for remote control.[31] They may be fully manual also. The movable members for a manual system can be sections of transmission line which are moved to the points desired. Early systems of the Daventry station of the British Broadcasting Corporation used this method.[33]

Other switching needs arise in station design, such as reversing the beam of a dipole array by interchanging radiator and reflector curtains (see Fig. 4.94) or switching the direction of feed and dissipation lines in reversing the directivity of a rhombic antenna. Switching of this sort can be done with a double-pole double-throw switch, though the forms of such switches may be greatly varied by different designers for different particular applications.

4.8. Circle Diagram of a Transmission Line[2,6,7,8,10,17,19,31]

In general, for any short low-loss line,

$$Z_{in} = Z_0 \frac{Z_t \cos \beta l + jZ_0 \sin \beta l}{Z_0 \cos \beta l + jZ_t \sin \beta l} \tag{8}$$

If this equation is computed for a range of values of βl from 0 to 180 degrees when $Z_t \equiv R_t$ varies from 0 (short circuit) to infinity (open circuit), these values can be plotted in rectangular coordinates to give the well-known circle diagram for a transmission line of characteristic impedance Z_0. However, this diagram has a more general application if the values are computed for $Z_0 = 1$, because then it can be used for a line of any characteristic impedance by using its value as a proportionality factor applied to all values read from the circle diagram. A chart of this kind is of great utility in making practical adjustments and measurements of transmission lines.

In plotting such a set of computations in rectangular* coordinates it is found that the locus of $Z_{in} = jX_{in}$ lies on a semicircle centered on the imaginary axis when βl is constant and R_t is varied. Also, it is found that when R_t is constant and βl is varied, the locus of Z_{in} is a circle centered on the real axis. The full range of values for R_t yields a set of confocal circles approaching the focal point $1 - j0$ when $R_t = Z_0$. Since the ratio R_t/Z_0 is the standing-wave ratio Q, an easily measurable quantity, the chart yields all necessary information concerning the impedance at any point in a transmission line having a known standing-wave pattern both in magnitude and in position on the line. It provides the general solution for Eq. (8) for its complete field of values and permits any unknown factor to be read directly when all the other factors are known. Such a chart is shown in Fig. 4.58.

In practice, Z_0 is a resistive quantity that can always be computed with adequate precision for any ordinary engineering uses. The electrical length βl is known from linear measurements, based on the propagation velocity. The position and magnitude of a standing wave can be measured by simple means, in the laboratory and in the field. A current minimum (voltage maximum) point is one where the impedance of the line is *resistive* and equal to QZ_0. A current maximum (voltage minimum) point is one where the line impedance is *resistive* and is equal to Z_0/Q. This information also provides a handy method of determining

* The circle diagram can also be presented in polar form.[10] We use the rectangular form here for convenience in constructing such charts for field use whenever required.

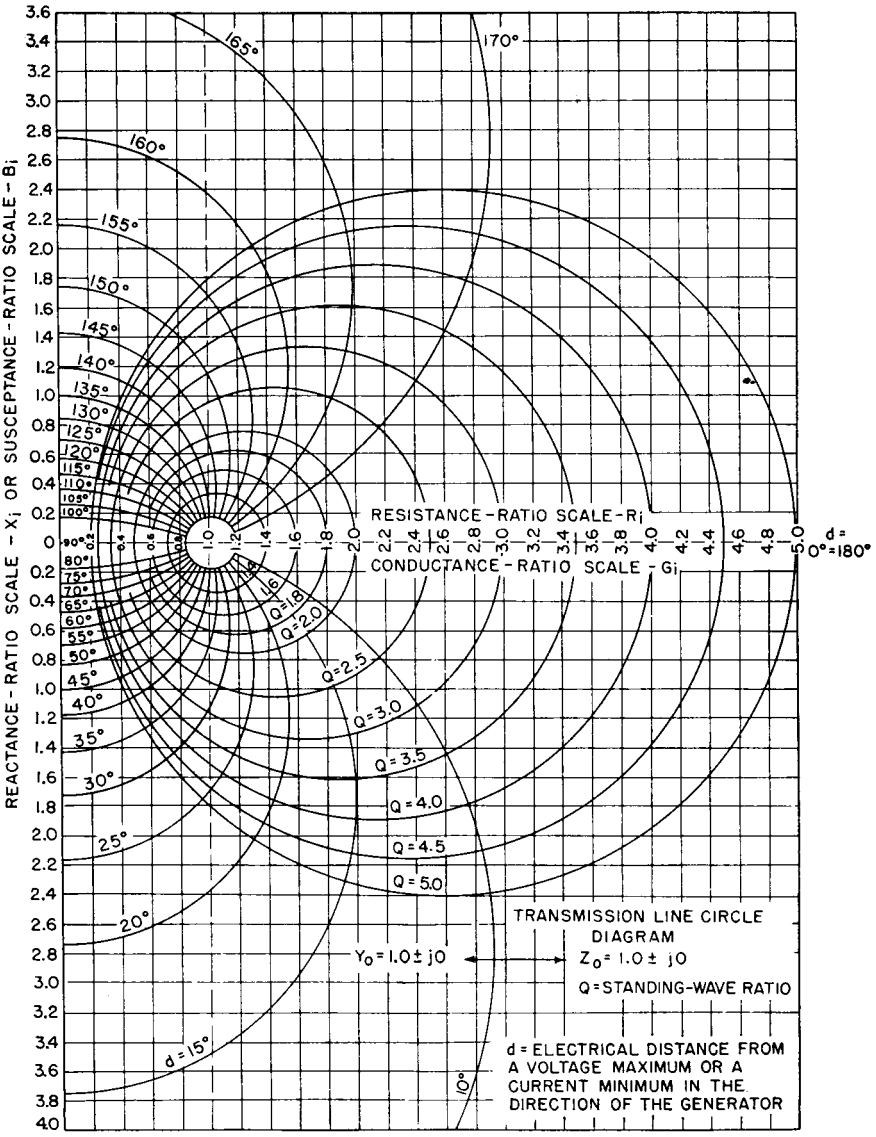

FIG. 4.58. Transmission-line circle diagram in rectangular coordinates.

the value of an unknown complex impedance at the load end of the line.

The same chart may be read and used in terms of admittance, conductance, and susceptance for those applications where the parallel components of impedance are more convenient than the series components. All quantities then are reciprocals except Q and βl.

4.8.1. Details for the Construction of a Circle Diagram for a Transmission Line. For field-engineering purposes it is desirable to have a master chart from which blueprints can be made in any quantity for field use. The following information will enable one to reconstruct a chart like that of Fig. 4.58, the field of which embraces the range of values encountered in all except extreme cases.

1. Use a sheet of graph paper approximately 10 by 15 inches ruled in centimeters with 0.1-centimeter subdivisions or in ½ inches with 10 subdivisions. Locate 0, the origin of coordinates, at the middle of the left-hand long side of the sheet, when the long side is vertical. Then

a. Starting at 0, progressing upward on the left-hand scale, mark each major division in order 0.2, 0.4, 0.6, etc., to the top of the sheet. This will be the ratio scale for positive reactances.

b. Starting at 0, progressing downward along this same scale, mark the major divisions −0.2, −0.4, −0.6, −0.8, etc., to the bottom of the sheet. This will be the ratio scale for negative reactances.

c. Starting at 0, mark the horizontal scale so that successive major divisions are 0.2, 0.4, 0.6, 0.8, 1.0, 1.2, etc., to the right-hand margin. This will be the ratio scale for resistances, or resistance axis.

2. Locate the point where resistance is 1.0 and reactance zero. This will be the focal point for the circle diagram.

3. With centers on the resistance axis, draw the following confocal circles:

Location of center on resistance axis	Circle radius in terms of resistance-scale units	Mark the circle in terms of the following standing-wave ratio Q
1.02	0.18	1.2
1.06	0.34	1.4
1.11	0.49	1.6
1.18	0.62	1.8
1.25	0.75	2.0
1.45	1.05	2.5
1.67	1.33	3.0
1.89	1.61	3.5
2.13	1.88	4.0
2.36	2.14	4.5
2.60	2.40	5.0

4. Draw the following semicircles from centers on the reactance axis, using a radius that causes the semicircle to pass through the focal point $1.0 - j0$.

Location of center on reactance axis	Mark the negative and positive ends of the semicircles	
	Negative end, degrees	Positive end, degrees
−2.74	10	100
−1.74	15	105
−1.20	20	110
−0.84	25	115
−0.58	30	120
−0.36	35	125
−0.17	40	130
0	45	135
0.17	50	140
0.36	55	145
0.58	60	150
0.84	65	155
1.20	70	160
1.74	75	165
2.74	80	170

This gives a set of semicircles which all pass through the focal point and are orthogonal with respect to the Q circles and whose ends are marked in progression clockwise from 10 to 170 degrees in 5-degree steps.

This completes the circle diagram for a transmission line in terms of the ratios of resistance and reactance to that of its characteristic impedance at any distance from a resistive termination in degrees and for any standing-wave ratio from 1.00 to 5.0, the same as shown in Fig. 4.58. If drawn with care and skill, the accuracy of this chart will equal or surpass the usual accuracy of measurements.

4.9. Power-transmission Capacity of Open-wire Transmission Lines

The following discussion will apply to transmission lines that are guiding energy in the form of a *traveling wave*. The line is assumed to be terminated exactly in its characteristic impedance. When standing waves exist, the rating of the system is limited by conditions at some one place along the line where a critical factor, such as potential, determines the limitation. The losses in a line are minimum for the traveling-wave condition and increase with increasing standing-wave ratio as shown in Fig. 4.1. The power-transmission capacity is as much an economic matter as one of physical limitations due to heating or flashover. For

this reason the rating of a system is generally indeterminate within the limits set by flashover, and the latter in turn is so dependent upon the empirical conditions of the construction of the system and its location that flashover potential may also be indeterminate.

At the low radio frequencies, the high-voltage phenomena resemble those associated with commercial power transmission. Corona occurs before pluming or flashover, with consequent increase in system losses due to corona.

As the frequency becomes higher, ionization of the air, which involves a time factor, does not occur as visible corona. The first sign of voltage overstress is manifest by the formation of a standing arc, or plume. The intense heat of a plume can be very destructive, though in some cases it serves to smooth off, by fusion, any small projection in the metallic conductors that produces an excessive gradient. When a system is operated at potentials close to critical pluming or flashover, care must be exercised in all the fine details of splicing wires, removing projecting ends, nicks on the wires, sharp points and corners on the insulator and assembly hardware, binding wires, etc. The potential rating of a system decreases with increased altitude, also. Installations at high altitude require special precautions, and the design of the system is made such that it would be suitable for much higher power if installed at sea level.

It is well known that corona and flashover, especially self-propagating arcs or streamers extending to ground or to other wires of the system, depend upon the energy of the system as well as the voltage. This is familiar qualitatively to radio engineers, who use different space factors for the same potentials in small transmitters, for instance, as compared with high-power transmitters. As soon as an incipient arc starts, current flows into the capacitance of the arc, which lowers its resistance. This changes the electric field configuration in such a way as to reduce the gradients near its base, which in turn moves the regions of critical gradient outward, increasing the capacitance and the entering current at its base, with great heat developing in the plume. This continues until a condition of electric and thermal stability is reached, which determines the size of the plume. The current required to sustain a plume of a given size increases with the frequency because the size of the plume determines its capacitance. In high-power systems, a plume can eventually extend itself to the point where it will bridge the line and cause flashover. Actual flashover is seldom experienced except in rather high power systems, where the size of a plume is not limited by the energy of the system to distances small with respect to the wire spacings.

The potential limit of a feeder system at any given altitude is set by those gradients, distributed or localized, which can cause pluming. The

potential gradients are reduced by the use of relatively large conductors or by the use of two or more conductors in parallel to divide the current. At bends and turns, entrances, and branching points and at insulating points, localized gradients can be very high, therefore creating points of weakness, unless proper precautions are taken in design and construction. Potential-grading rings are sometimes permissible if they do not introduce a disturbance in the line parameters as an irregularity. It is possible to strengthen such points with a coating of insulating material, ceramic, plastic, or varnish, to provide potential grading by the use of intermediate values of dielectric constant between that of unity for the surrounding air and infinity for the metallic conductor. The use of such an insulated control of flux density can in some instances raise the pluming potential of a system at a particular weak point without introducing an intolerable irregularity in the line parameters. It functions in two ways—to prevent ionization near the conductor, where the gradient is maximum, and to limit the amount of current that can flow into an incipient arc. When used, the insulated control is most effective when it is homogeneous. Thickness can be increased to increase its effectiveness.

The maximum potential gradients that can be sustained in air before corona, pluming, or flashover occurs has been the subject of a great deal of research over many years. Thornhill and Beasley[59] have made a synthesis of this available information and have reduced a complex subject to relatively simple form. The values of critical gradients and the equations for maximum working potentials on two elementary types of electrodes have been adapted from their work.

For two clean parallel cylinders in still air at an atmospheric pressure of 28 inches of mercury and a temperature of 45 degrees centigrade, with direct potentials applied between them, the critical potential gradient at which visible corona starts is about 66.7 kilovolts per inch. Under the same conditions concentric cylinders have a critical gradient of about 69.3 kilovolts per inch. However, between the conductor and the zone of visible corona there is formed an ionized conducting layer which has the effect of increasing the radius of the conductor. The actual potential gradient at the surface of the conductor is higher than the critical gradients for visible corona. The amount that it is higher is a function of the geometry of the system. The potential gradient E_0 at the conductor surface that produces visible corona at direct current under these same atmospheric conditions is given by the following relations:

For parallel cylinders,

$$E_0 = 66.7\left(1 + \frac{0.202}{\sqrt{\rho_{\text{inches}}}}\right) \quad \text{kilovolts per inch}$$

For concentric cylinders,

$$E_0 = 69.3\left(1 + \frac{0.208}{\sqrt{\rho_{\text{inches}}}}\right) \quad \text{kilovolts per inch}$$

For very low frequencies, these would represent crest values. As the frequency increases, up to about 2 megacycles, the critical voltage falls to a value of about 80 per cent of direct-current value. For frequencies above 2 megacycles it rises again, eventually approaching the direct-current value, or even more, at around 200 megacycles. As a general principle one may use the 80 per cent value for practical engineering purposes for radio frequencies up to 30 megacycles. Then for ordinary system design the above equations can be rewritten to include this reduction and transformed to root-mean-square values, giving for parallel cylinders in air at 28 inches of mercury and a temperature of 45 degrees centigrade (worst sea-level conditions)

$$E_0 = 37.7\left(1 + \frac{0.202}{\sqrt{\rho_{\text{inches}}}}\right) \quad \text{kilovolts per inch root-mean-square}$$

and for concentric cylinders under the same conditions

$$E_0 = 39.2\left(1 + \frac{0.208}{\sqrt{\rho_{\text{inches}}}}\right) \quad \text{kilovolts per inch root-mean-square}$$

These values will be further reduced by corrosion of conductor surfaces, moisture films, drip water, sharp points, irregularities due to roughness, bends, and other physical conditions. These are all taken into account qualitatively by employing design safety factors. The factor selected will depend upon the consequences of a flashover or the system losses. The safety factor for an open wire line may be less than for a concentric line for these reasons.

The critical gradients will vary with atmospheric pressure and with ambient temperature, which determine the relative molecular density of the air D, which can be found from the relation

$$D = \frac{9.96P}{273 + T}$$

in which P is the barometric pressure in terms of inches of mercury and T is the ambient temperature in degrees centigrade. In the preceding equations for critical gradients, the value used was $D = 0.877$.

Table 4.3 gives values of D as functions of barometer reading P in inches (corrected for temperature) and the temperature, together with

approximate equivalent altitudes based on a corrected sea-level pressure of 30 inches of mercury.

TABLE 4.3. RELATIVE MOLECULAR AIR DENSITY D

P, inches	Altitude, feet	Degrees centigrade					
		0	10	20	30	40	50
16	17,000	0.584	0.563	0.544	0.526	0.509	0.493
18	14,000	0.657	0.634	0.612	0.592	0.573	0.555
20	11,000	0.730	0.703	0.680	0.657	0.636	0.616
22	8,400	0.803	0.775	0.748	0 723	0.700	0.679
24	6,500	0.876	0.845	0.816	0.789	0.765	0.740
26	3,900	0.949	0.916	0.884	0.855	0.828	0.802
28	1,800	1.022	0.987	0.953	0.921	0.892	0.864
30	0	1.095	1.057	1.020	0.988	0.955	0.926
32	−1.250	1.168	1.126	1.088	1.052	1.020	0.988

These relations can be combined in a single equation involving the geometry of the line to give directly the maximum voltage that can be safely applied when the line is terminated in its characteristic impedance. When this is done for a two-wire balanced open-wire line,

$$V_m = \frac{43D}{S}\left(1 + \frac{0.202}{\sqrt{\rho}}\right)\left[\frac{a\left(\frac{a}{2\rho} - 1\right)\cosh^{-1}\frac{a}{2\rho}}{\frac{a}{2\rho}\sqrt{\frac{a^2}{4\rho^2} - 1}}\right]$$

and for an air-dielectric concentric line

$$V_m = \frac{103D}{S}\left(1 + \frac{0.208}{\sqrt{\rho_1}}\right)\rho_1 \log_{10}\frac{\rho_2}{\rho_1}$$

In these equations the symbols have the following meanings:

V_m = maximum root-mean-square applied voltage, *kilovolts*
S = design safety factor, usually between 1 and 3
a = center-to-center wire spacing, inches
ρ = wire radius, inches
ρ_1 = radius, inches, of the center conductor
ρ_2 = radius, inches, of the inside of the outer conductor
D = relative molecular air density

The influence of the spacing of the wires is not immediately obvious from these formulas. Breakdown occurs due to ionization in the gap between the wires, which forms ions and free electrons.

At the low frequencies, there is time for both ions and free electrons to be swept into the wires during an alternation, so that there is no accumulated space charge unless the peak voltage applied exceeds the ionization voltage by a considerable amount. As the frequency is made higher, transit time for the heavy ions becomes too great for the space charge to be cleared during an alternation. Thus the free electrons move into the wires, and a space charge of ions accumulates. This space charge distorts the field and reduces the breakdown voltage. At about 2 megacycles the heavy ions are unable to traverse the gap dimensions, but the electrons, being lighter, are absorbed during the negative alternation. During the positive alternation, they move at high velocity and cause more ionization by impact. Under these circumstances the breakdown potential is at its lowest. This occurs in the high-frequency range, in the vicinity of 2 megacycles.

As the frequency is further increased, the transit time for electrons becomes great with respect to one period. Free electrons are then left in space with the ions, and the space charge is reduced. Finally, at around 25 megacycles, the inability of electrons to be cleared away during the negative alternation leaves the field of the gap in substantial equilibrium, with consequent increase in the breakdown voltage to nearly that for direct current. Experiment shows that, at the worst frequency, the breakdown voltage falls to about 80 per cent of the direct-current value. A design value of 80 per cent of direct-current breakdown voltage is chosen as a safe working limit.

Spurious flashovers may occur at random owing to a number of unusual conditions not necessarily associated with underdesign. Strong ultraviolet bombardment of the air can produce abnormal ionization in still air and cause flashover. Air turbulence tends to minimize this effect on open-wire systems. Ionization due to cosmic rays may be another spurious effect. Insects or birds on the wires may set off a plume or a flashover. High transient potentials may momentarily exceed critical values and strike an arc. Circuits without static drains may accumulate high direct potentials superimposed upon the existing radio-frequency potentials and cause arcing. The same effect can occur when transient potentials are induced into the system by lightning in the vicinity. Drip water on a feeder operated at near-maximum potential can introduce an increase in local gradient and cause flashover. Abnormally high peaks of amplitude modulation are another cause at times. To these must be added momentary mismatches due to arc-overs in the antenna system which cause standing waves.

During on-off keying, and also amplitude modulation, a plume is automatically extinguished with the first interruption of radio-frequency

power. Spurious arcs and flashovers due to most of the above causes may not reoccur. Types of emission that maintain constant radio-frequency power would not extinguish an arc, and unless it is blown out by the wind it is necessary manually to interrupt power to extinguish an arc. For this reason, higher safety factors are usually required for such systems.

The power rating of feeder design also depends upon the total losses resulting from a given feeder design. The power-transmission rating of a feeder thus requires one to weigh the cost of line for a given loss against the annual cost of the power lost in the system. The price of programed radio-frequency power, for instance, reaches some rather high values per kilowatt-hour, and some organizations are accustomed to reckon that a certain reduction in feeder loss would justify an increase in capital outlay for a lower loss system. Long feeders are typical for high-frequency telegraph and broadcasting stations where several antennas are used with several transmitters. Long feeders are also required for many medium-frequency broadcast stations with extensive directive antennas. In such applications, the feeder losses are far from negligible, and considerable engineering may be required to design feeders for higher efficiency.

If we take as an example a two-wire balanced feeder 3,000 feet long, designed for transmitting 100 kilowatts of amplitude-modulated power, its attenuation at 20 megacycles may be about 2 decibels, corresponding to an efficiency of 63 per cent. If a four-wire balanced line is used instead, with about twice as much copper, its efficiency can be increased to something of the order of 73 per cent. A further increase in efficiency can be obtained with more copper and other materials at correspondingly greater cost. This case emphasizes the importance of planning the station and its antenna layout to use feeders of the shortest possible length as the best approach to economy of construction and to over-all efficiency.

Experience has shown that the losses increase in a feeder as the wires become corroded. When feeders are to be located in places subject to salt-spray atmosphere, sulphur smoke or fumes, or other corrosive conditions, the conductors may require protection in the form of electrical enamel, lacquer, or plastic coatings. With such coatings, the initial loss may be higher than for bright, new, bare copper, but it will remain constant over a much longer time than unprotected copper. Thick plastic coatings can provide a substantial increase in maximum operating potential, but at the sacrifice of increased dielectric losses.

4.10. Dissipation Lines[14,21,62]

Resistive loads of high power-dissipation capacity may be of the lumped or the distributed types. A resistive load for a transmitting rhombic

antenna is usually a transmission line built to have high attenuation per unit length, and with a sufficient length to provide the desired over-all attenuation. To terminate a rhombic antenna properly, the dissipation line must have a characteristic impedance equal to that of the rhombic antenna at the point where they are interconnected. The dissipation line may be of uniform or of tapered characteristic impedance. The former has most of its power loss in a relatively short portion of its total length, and the remainder of the line contributes very little in the way of power loss. To equalize the distribution of the power loss over a greater portion of the length of the line, especially when large amounts of power must be dissipated, a tapered line has the desired qualities. If the height of the antenna at the lowest frequency exceeds one-half wavelength, a gradual linear taper of the downcoming line from an impedance which matches the antenna to one of relatively low impedance is easily constructed. An impedance of 600 or 700 ohms at the antenna can be changed to about 400 ohms near ground. If this transformation has to be made in an electrical length less than one wavelength, the tapering would be exponential. Additional tapering can be applied to the pole-line portion of the dissipation system to elongate the effective power-radiating surface.

Where the amount of power to be dissipated is small, tapered lines may be an unnecessary complication in design. Then the line simply acts as a resistance when its attenuative length is great enough to eliminate variations of impedance in the input end of the dissipation line at the lowest working frequency. Various other alternatives are available. The total length of the line can be shortened by substituting a fixed resistor of approximately correct value after the line has dissipated all but the last few watts. If the power delivered at the end of the rhombic antenna is small, a fixed resistor of the correct value of resistance and of very high power factor can be located directly at the rhombic-antenna terminals in place of the terminal-line structure.

A dissipation line with an over-all attenuation of 20 decibels acts virtually as an infinite line so far as its effect on the rhombic antenna is concerned. The total attenuation of 20 decibels to the transmitted and 20 decibels to the reflected wave being 40 decibels (reduction to 1 per cent in voltage), the end of the dissipation line can be open-circuited, short-circuited, or grounded at will without observable influence on the input impedance. A static drain direct to ground is desirable as a protective measure.

Satisfactory termination on the same basis can be had for most cases with a dissipation line having an attenuation of 15 decibels. If a resistor is used to consume the last few watts, attenuative lengths of 12 decibels

are practical. In such a case, the specifications of the resistor are less rigorous with regard to low reactance than when resistors are used for direct termination of the antenna. When resistors are used to save line length, it is desirable to ground the middle for static draining.

The attenuation per unit length is inversely proportional to characteristic impedance when the number and the size of the wires are constant. It is therefore a matter of good design economy to reduce the characteristic impedance of the dissipation line to the lowest value that is mechanically practical without increasing the number of wires.

Experience has established the use of stainless-steel wire as the preferred material for a dissipation line. Its high radio-frequency resistance provides a relatively high attenuation factor. It resists corrosion in the weather, and its electrical characteristics are constant in time. Its cost is reasonable. Since attenuation is desired in the dissipation system, the insulation of the line may be lossy and the line can be attached directly to wood supports provided that the temperature is not sufficient to burn them.

The characteristic impedance of a line using wire of magnetic material is practically the same as one using nonmagnetic materials. The permeability of the material adds only a small and negligible term in the equation for characteristic impedance. Stainless steel is of many different alloys, which vary widely in resistivity and permeability according to their composition. Alloy 430 (18 per cent chromium) has a resistivity forty times that for annealed copper and is magnetic.

The attenuation of balanced lines using steel or iron wires of magnetic permeability μ and resistivity r_1 can be computed from the following equation:

$$\alpha = \frac{4.34 \sqrt{\dfrac{\mu r_1 f_{\text{megacycles}}}{r_0}}}{\rho_{\text{inches}} Z_0}$$

In this equation r_0 is the resistivity of copper, which is 1.724×10^{-6} ohm per cubic centimeter for annealed copper and 1.77×10^{-6} for hard-drawn copper. This attenuation is for conductor loss only. Figure 4.59 shows attenuations for 0.040-inch-radius *steel* wire lines in a two-wire balanced 400-ohm circuit.

Sterba and Feldman[21] have published measurements made on a 600-ohm two-wire balanced line using uncoated iron wires of resistivity 12.3×10^{-6} ohm-centimeter and permeability of 92, with a wire diameter of 0.162 inch. This line follows the relation

$$\alpha_{\text{total}} = 2.32 \sqrt{f_{\text{megacycles}}}$$

A copper line of the same dimensions follows the relation

$$\alpha_{\text{total}} = 0.152 \sqrt{f_{\text{megacycles}}}$$

whereas the copper loss alone for this same line follows

$$\alpha_{\text{copper}} = 0.0916 \sqrt{f_{\text{megacycles}}}$$

The dissipation line is usually located under the rhombic antenna with which it is associated because no additional land is required. The line

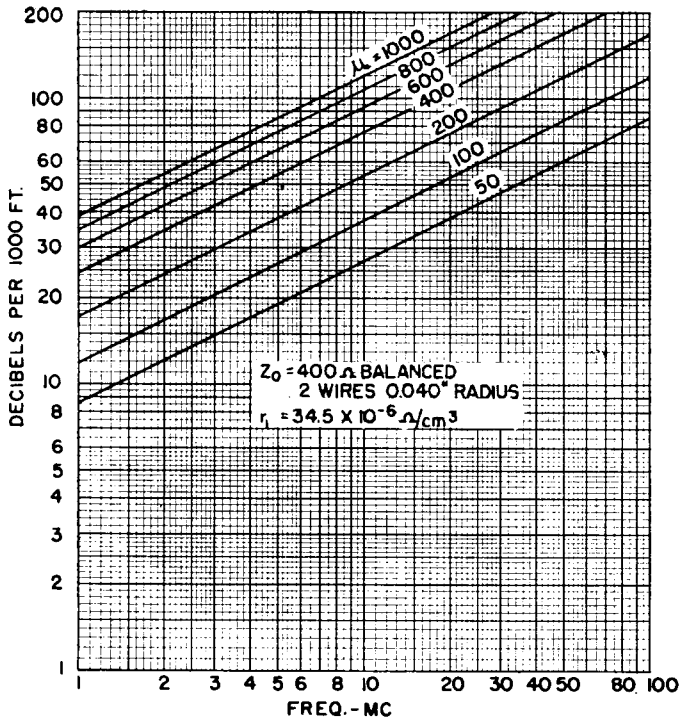

FIG. 4.59. Attenuation of two-wire balanced 400-ohm lines of radius 0.040 inch and a volume resistivity of 34.5×10^{-6} ohm per cubic centimeter as a function of wire permeability.

can be turned back and forth so as to use the smallest number of poles. If the characteristic impedance of the dissipation line is quite low, its spacing is small and one short crossarm can readily support the double line obtained when the line is folded back on itself. Bracket insulators may be attached directly to the poles to eliminate crossarms. When this is done, a sufficient distance between the "go" and "return" lines

can be obtained by putting one of the runs lower down on the opposite side of the pole, as shown in Fig. 4.60.

In certain applications the dissipation line and the feeder can be switched from one end of the rhombic antenna to the other to reverse its directivity. In such cases, the impedance of the ends of the antenna must be equal and brought uniformly to a central switching point for

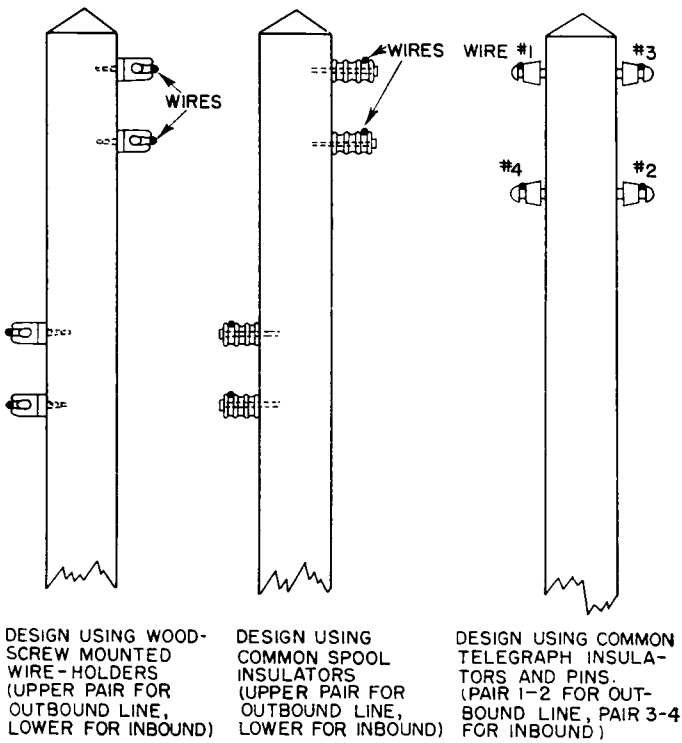

FIG. 4.60. Economical arrangements for dissipation lines.

interchanging the power feeder with the dissipation line. To take advantage of the low characteristic-impedance dissipation line, tapering must then start from the switching position. The same poles can be utilized to carry the transmission line and to support the dissipation line.

Reference to the attenuation formulas for transmission lines types I, II, and III reveals that such lines may also serve as dissipation lines, using the earth as the dissipator. A balanced dissipation line made up of two unbalanced lines of these types is practical and may often be used advantageously, especially for the lower impedances, the higher high frequencies, and the poorer ground conductivities. By studying the possibilities of such applications by setting the relevant values in the

attenuation equations, it will often be found that copper lines using ground dissipation have more unit-length attenuation than lines of dissipative conductors that do not use ground loss. In a limited number of cases the most economical dissipation line may be one using both conductor and ground dissipation. The empirical nature of these possibilities makes the choice dependent upon the particular circumstances surrounding each application.

Lines using ground dissipation require a few simple precautions to ensure stable characteristics as the ground conductivity changes with weather conditions. The input end of the line may require some limited form of ground system which gradually spreads out and disappears in the first decibel or two of line length, after which the effect of varying ground conductivity is relatively unimportant in its effect on the input impedance. The height above ground is an important factor in the design of ground dissipation lines.

An example of the possibilities of using two unbalanced 175-ohm dissipation lines to terminate a 350-ohm balanced system is the following:

The measured values of characteristic impedance and attenuation on a line 300 feet long comprising four parallel copper wires of radius 0.050 inch spaced 20 inches in a horizontal plane 60 inches over ground with a conductivity of about 2×10^{-13} electromagnetic unit were

$$Z_0 = 175 \text{ ohms}$$

Frequency, Megacycles	*Attenuation, Decibels*
10	14
20	16
30	21

4.11. Measurement of Standing Waves on Open-wire Transmission Lines

It is quite sufficient in some cases to determine qualitatively that a feeder is terminated approximately correctly. Some sort of indicator,

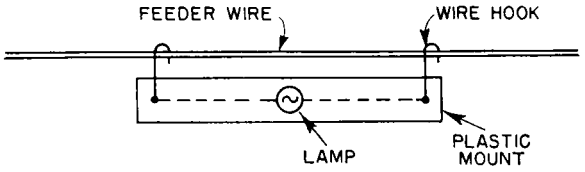

FIG. 4.61. Miniature-lamp indicator.

however simple, is needed. Figure 4.61 exemplifies one of the most elementary forms of indicator, consisting of a small incandescent lamp which is hung on a feeder wire by means of the hooked conductors. The

lamp determines the sensitivity of the device for the amount of power in the system under measurement. Its use is principally that of detecting the existence of standing waves of large magnitude. The device is slid along the wires, and any change in the brilliancy of the lamp in different positions along the wire gives the indication of standing waves. When its brilliancy is apparently uniform in all positions, the standing-wave ratio is fairly small. Expert use of this simple indicator has given indications of Q as low as 1.25. When a substantial standing wave exists, this device is useful in locating the current minimum, and by comparing the locations of the current minimums on both sides of a balanced circuit a very good indication is provided of the degree of balance. If the minimums on the two sides are displaced, this may be due to unequal conductor lengths on the two sides of the circuit, an unbalance in the load itself, or unbalance caused by currents flowing in parallel in both wires against ground.

The same method may be used with a thermocouple milliammeter in place of the lamp, provided that the added capacity on one side of the circuit does not in itself cause unbalance. A dummy device or another similar instrument can be hung on the opposite side to reduce unbalance. The limiting parasitic effect then is if the devices have low enough capacitance not to constitute an irregularity in the line and therefore a source of reflections. The milliammeter will reveal effects not observable with the lamp indicator, but its use requires greater care. This device is only an indicator because it responds not solely to current in the line but also to the potential. It is satisfactory for use for the same rough purposes as the lamp indicator.

The use of these indicators is the same on unbalanced lines, and the measurements may be made on a ground wire or on a high-potential wire.

Neon and argon lamps are very rough indicators of potential distribution, so rough in fact as to have relatively small value for determining the true condition of a line.

Indicating devices of the nature of voltmeters bridging a line must be used with extreme caution. Unless the impedance of the device is very large with respect to the line impedance at the points of maximum potential, the voltmeter device itself causes reflections, the magnitude of which varies with position on the line. The result is that a plot of the measured voltage tends to be abnormal. Voltmeter-type indicating or measuring devices are easier to use on low-impedance lines.

A method of detecting and indicating the magnitude of standing waves in an open-wire feeder is that shown in Fig. 4.62. A short section of line is placed in the field of the feeder to be studied and parallel to it. This secondary line is then terminated in its characteristic impedance at both

ends and an ammeter placed in series with and at the middle of each terminal resistor. If the main feeder is correctly terminated in its characteristic impedance, there will be a wave traveling in one direction only. The coupled line (reflectometer) then has induced in it a wave traveling in the same direction; and since it is also terminated, this energy will be absorbed in its terminal resistance at one end and there will

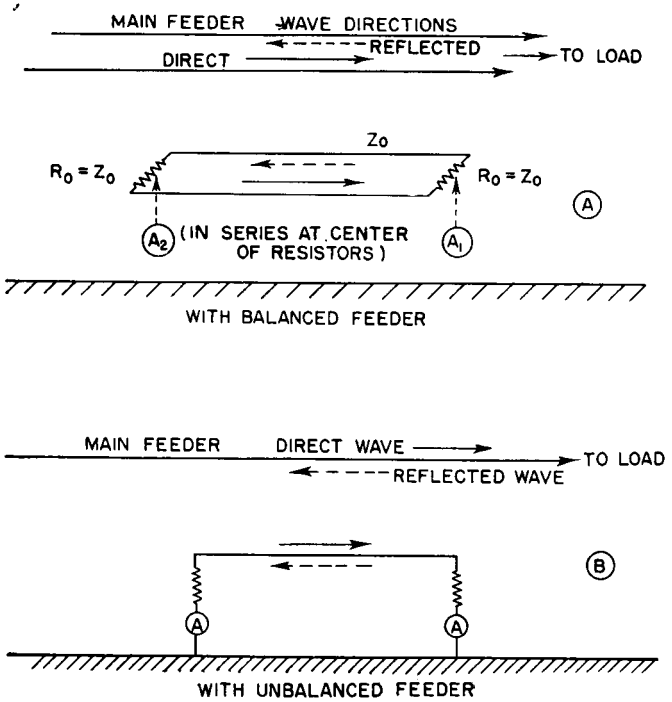

FIG. 4.62. Standing-wave indicators.

not be any reflection. This causes the current at the far end of the secondary line to register on the ammeter there. The near-end ammeter will show zero current.

When there are standing waves on the main feeder, there are traveling waves passing in both directions. The one traveling toward the load will actuate the far-end ammeter in the secondary line as before. The wave traveling from the load toward the generator will act in the same manner to actuate the near-end ammeter in the secondary line. The ratio of the two currents at the terminals of the secondary gives a direct measure of the ratio of the magnitudes of the forward and backward waves in the main feeder, which is a measure of the standing-wave ratio. This method does not provide any information concerning the locations

of the maximums and minimums on the main feeder, but it is very useful as a permanently installed device to indicate the existence and magnitude of standing waves during station operation. The ammeters can be remote-reading and located in a convenient place to be observed. Like all standing-wave detectors, it may also be calibrated to read power directly as a wattmeter.

This principle is applicable to both balanced (Fig. 4.62*A*) and unbalanced feeders (Fig. 4.62*B*). In order not to introduce irregularities upon the main circuit, the coupling of the secondary line should be small and sensitive current-measuring instruments used.

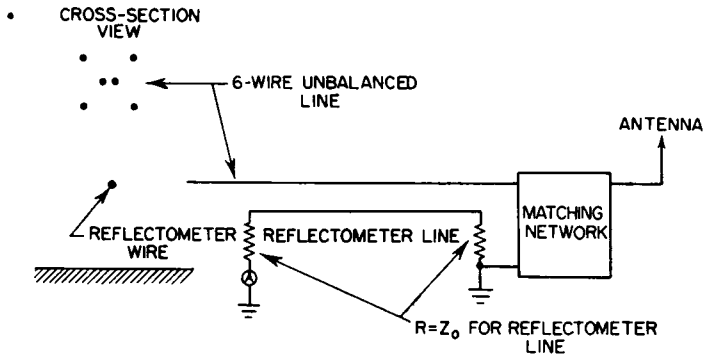

FIG. 4.63. Simplified reflectometer used with unbalanced open-wire line.

When this device is used only for indicating the presence or absence of standing waves in the main feeder, only one ammeter need be used—the one on the generator end of the secondary line. This ammeter will register current only when there is a standing wave. It is possible to precalibrate this one ammeter in terms of standing-wave ratio, using the second ammeter in the load end during the calibration and then removing it.

This standing-wave indicator can be placed anywhere in the system but will usually be wanted near the transmitter, where it can be easily observed by the operating personnel.

This method of measuring or indicating standing waves is especially valuable where a feeder must be matched but where there are no measuring instruments available except a thermogalvanometer or a thermomilliammeter. A coupled line is constructed, its characteristic impedance is calculated, and it is terminated in resistances at each end equal to the characteristic impedance of the reflectometer line. When this is done with *unbalanced* feeders, as in Fig. 4.62*B*, care must be taken to include the resistance of the ground terminal in the matching resistances. Since the load-end termination of the reflectometer is most critical, it can

be connected as shown in Fig. 4.63, where the actual ground resistance is not involved at that end and a known resistance can be used. With the indicating instrument in the transmitter end of the reflectometer line, terminal adjustments may be made. It is possible to determine the correct adjustment of the matching network when the antenna impedance and the line impedance are unknowns. The use of the ammeter in this way is much more convenient than using it as a means for exploring the standing waves on the feeder and adjusting for eventual uniform current distribution. The reflectometer-line method provides an immediate indication of standing waves and the magnitude relative to a previous condition. The adjusting process is continued until the instrument reads zero. This is one of the simplest methods that can be used conveniently for accurate matching.

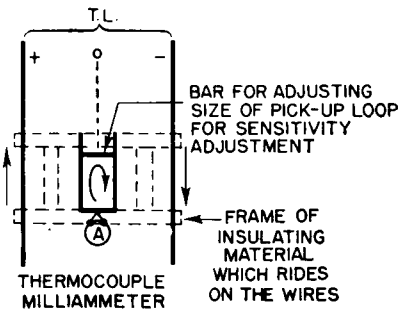

FIG. 4.64. Standing-wave indicator for balanced open-wire lines.

For accurate measurements of standing-wave patterns the measuring device should be so designed as to be responsive solely to the current in the line or to the potential, but not both. Figure 4.64 shows a common form of sliding thermocouple-milliammeter circuit that is responsive wholly to the magnetic field of the line and therefore accurately indicates the current distribution without introducing additional reflections in the balanced line. The sensitivity of the device is adjustable by adjusting the length of the pickup loop by means of the short-circuiting bar. The device must be symmetrically located between the two sides of the circuit and can be in the form of a frame of insulating material that has grooves spaced so that it slides along the wires, always retaining its exact location between the sides of the feeder. There is no response in this type of device to currents that may be flowing in parallel on the two sides of the circuit. In some instances, the milliammeter loop may be tuned with a series condenser in the middle of the short-circuiting bar.

Figure 4.65 is a current-indicating device that is responsive only to the currents on one side of a balanced circuit and is therefore one of the most versatile instruments for open-wire transmission-line measurements. When calibrated against a known current flowing in a straight wire, it can provide absolute measurements of the current in a wire with adequate accuracy for practical field use. It should be constructed on a framework of insulating material which can be set on a wire with constant coupling to the field of the wire and of the sort that has a long handle to facilitate

rapid hanging on a wire and carrying along a line. The current transformer must be symmetrical in the two halves, to eliminate response to the electric field of the wire, and small enough to represent the field of just one wire. With this instrument a complete examination can be made of the magnitude and distribution of currents on each wire of a feeder system.

Currents in a feeder can always be measured directly by inserting matched ammeters in series with the line. When a feeder is exactly matched, ammeters at both ends provide the data necessary to determine the attenuation of the line according to the relation

$$\text{Decibels attenuation} = 20 \log_{10} \frac{I_{in}}{I_{out}}$$

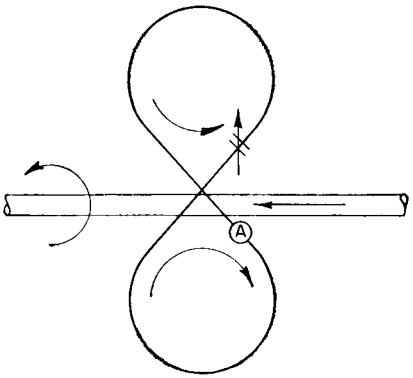

FIG. 4.65. Ammeter connected to respond to current in one wire only by magnetic coupling.

The following sliding-ammeter method is useful for measuring current distributions in antennas and open-wire transmission lines. A suitable radio-frequency ammeter or milliammeter is coupled to the wire with a current transformer consisting of a single-turn loop of rigid wire that is in the form of an equilateral triangle. One side of the triangle is parallel to the wire to be measured and spaced from it a small amount, using an insulated mounting that ensures constant spacing for any position along the wire (see Fig. 4.66).

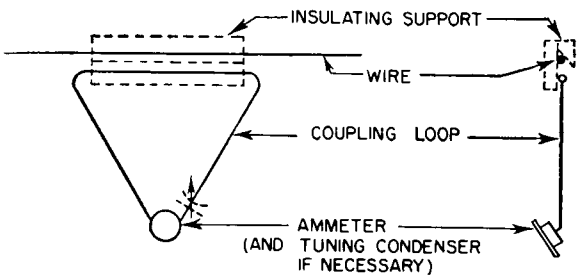

FIG. 4.66. Loop-coupled ammeter for individual open-wire measurements.

The ammeter is connected at the apex of the triangle opposite the side coupled to the wire. This device can then be slid along the wire and the relative current distribution observed for all positions. If the sensitivity is insufficient, the reactance of the loop can be tuned out with a series capacitor. If other parallel wires are nearby, as in a multiwire trans-

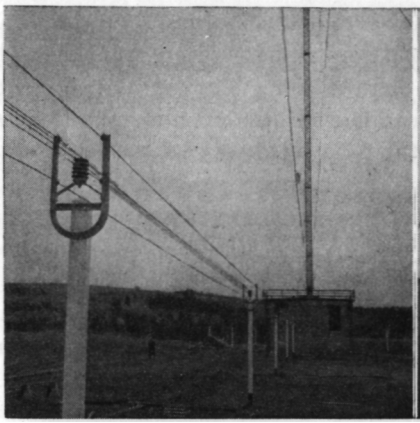

FIG. 4.67.

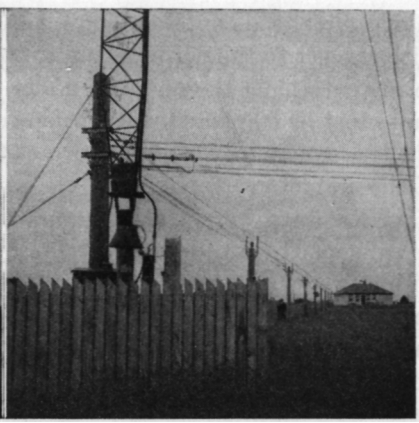

FIG. 4.68.

FIG. 4.67. Details of a bayonet-type assembly for six-wire unbalanced feeder (type XI) mounted on a square wood pole, as used at a 100-kilowatt low-frequency radiotelegraph station. (*Photograph courtesy of RCA Victor Company, Ltd., Montreal.*)

FIG. 4.68. View of a six-wire unbalanced (type XI) feeder from transmitter building to the first radiator of a broadcast directive array. Bayonet-type brackets are used with round wood poles. Base of guyed radiator is fitted with oil-filled safety-core base insulator. Antenna-coupling and power-dividing networks are in a weatherproof metal box mounted on a pole near the antenna. Radio Station CKWS, Kingston, Ontario.

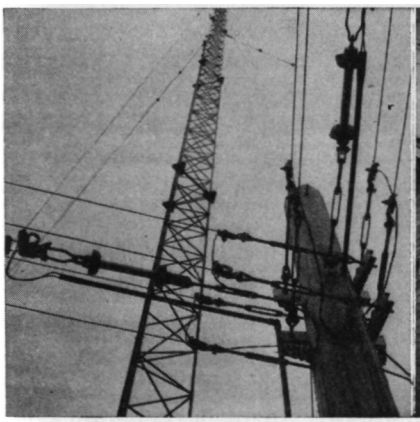

FIG. 4.69.

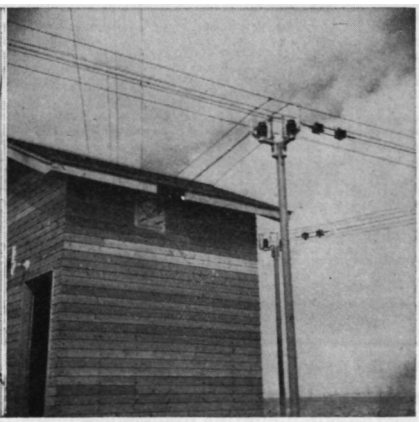

FIG. 4.70.

FIG. 4.69. Details of a corner pole in a six-wire unbalanced (type XI) feeder system for a directive broadcast array. The two lines are connected through a network that divides power between the radiator shown in the photograph and the line to the left that feeds a second radiator. Steel channels are used for crossarms on the wood pile. (*Photograph courtesy of RCA Victor Company, Ltd., Montreal.*)

FIG. 4.70. Details of an application of a six-wire unbalanced (type XI) feeder, showing the use of the side-mounting bracket assembly on a steel pole. Photograph shows a branching of the feeder near one coupling house in a directive broadcast array. (*Photograph courtesy of RCA Victor Company, Ltd., Montreal.*)

mission line, the coupling loop for the current transformer must be small with respect to the wire spacing so that the ammeter responds principally to the current in the one wire under observation. The amount of power that must be transmitted to obtain readable values depends upon the size of the coupling loop, whether or not the loop is tuned, and the sensitivity of the ammeter.

At the very high frequencies, where coaxial feeders are almost universally used, impedances are measured by the standing-wave method with extreme accuracy, using a precision-built slotted section of line with the same characteristic impedance as that of the feeder in use, and probing the field of this slotted line with a voltmeter-type indicator. When the position and ratio of a standing-wave pattern have been measured precisely and the exact characteristic impedance is known, the impedance terminating the line can be quickly read from a circle diagram like that of Fig. 4.58.

4.12. Static Draining of Antenna Feeder Systems

Induction from lightning and the accumulation of charges from wind-blown sand, dust, and dry snow cause very high static potentials to accumulate on an aerial system. These potentials can rise to a value that may cause eventual flashover, with a following power arc in the case of transmitting. In receiving, the system can become excessively noisy owing to precipitation static.

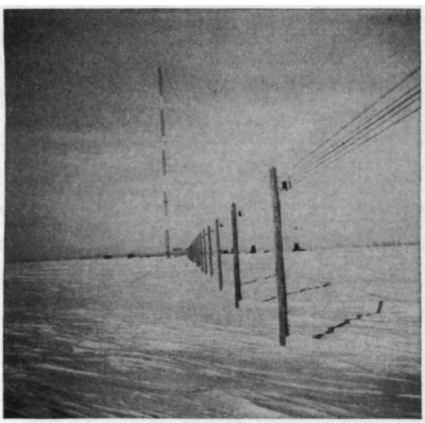

FIG. 4.71. A straight run of six-wire unbalanced (type XI) transmission line using the side-mounting bracket assembly on round wood poles. One radiator of a directive array with its coupling house, is in the distance. (*Photograph courtesy of RCA Victor Company, Ltd., Montreal.*)

It is therefore necessary to provide for static drains in designing a system. A low-resistance, and preferably low-reactance, path from antenna to earth will serve as a drain circuit, but it must be arranged to have a minimum influence on the impedances at the working frequency. Drain choke coils are frequently used in low- and medium-frequency systems for this purpose and occasionally in high-frequency systems. In high-frequency balanced systems, a branch section of line bridging the main feeder, short-circuited one-quarter wavelength from the connection and grounded at or beyond the short circuit, has very desirable draining

characteristics. When a dissipation line is used with a rhombic antenna, the end of the dissipation line can be short-circuited and grounded for draining purposes.

4.13. Mechanical Construction of Open-wire Transmission Lines

An open-wire feeder can be supported in a number of different ways according to the nature of the problem, the conditions met at the site, and

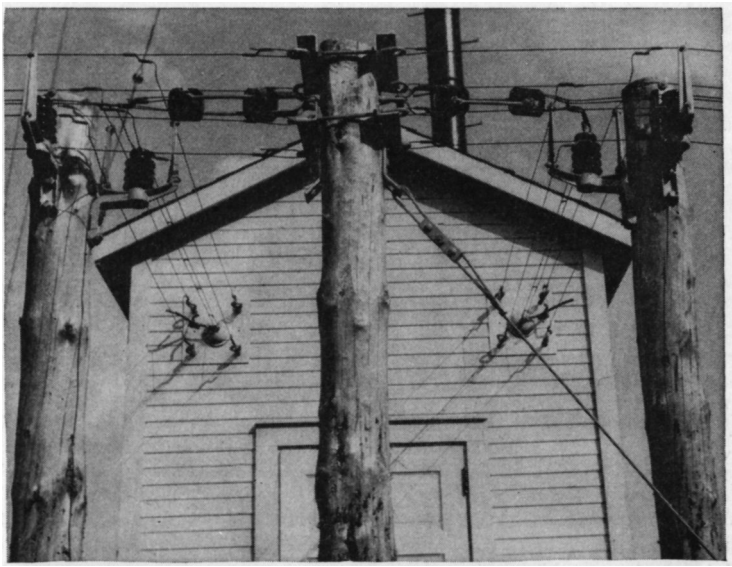

FIG. 4.72. Details for a six-wire unbalanced feeder, showing two right-angle turns to enter the antenna-tuning cabin. Cast aluminum brackets are used for maintaining the line cross section and are designed to attach to the side of a pole. The line is routed into and out of the cabin to divide power for the first radiator of a directive broadcast array and to transmit the remainder on to the other radiators. Radiator tuning and power-dividing and phasing networks are housed in the cabin at this 5-kilowatt broadcast station in Canada. Note building entrance details and typical pole hardware. (*Photograph courtesy of RCA Victor Company, Ltd., Montreal.*)

the kinds of material available. The simplest method is to use single poles of natural round wood or sawed square poles. The size will depend upon the number of wires to be supported and the storm conditions to be endured. The height is determined almost entirely by the clearance desired for men on foot, for horses and cattle, or in some for men on horseback. Some station plots are very large, and the land can be used for agricultural purposes while serving its primary radio-station purpose. When the area is so used, the wires of the transmission lines should be at a safe height.

Crossarms and fabricated steel brackets may be used for the proper

location of the wires, which may be supported on pin or post insulators or suspended on strain insulators. One or more lines may often be supported on the same pole. When several circuits are to be run on the same supports, two or more poles may be set with a cross frame for supporting the wires. There are regions where wood is scarce or where it deteriorates too rapidly; then poles of tubular steel, structural steel, or concrete are more economical in the long run. Poles and frames may require guying

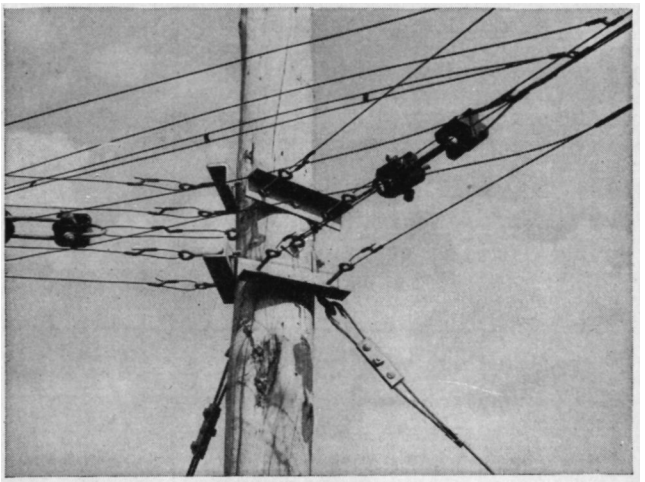

FIG. 4.73. Details of a corner pole for a feeder of the six-wire unbalanced type built on untreated wood pole with steel-angle crossarms. The high-potential pair of wires is insulated by means of double-egg porcelain insulators with steel yokes. Spacers are used between the two inner wires to maintain uniform spacing. (*Photograph courtesy of RCA Victor Company, Ltd., Montreal.*)

to resist displacement due to horizontal loading of the wires. The loadings should be precalculated, taking into account the weight, number and tension of the wires under the most extreme conditions of wind and ice to be encountered at the site, stresses at corners and bends in the line, and the soil resistance (mechanical) for the size and depth at which the poles are set into the soil or rock. The design of the crossarm structures must also be based on these considerations.

The spans between poles may vary between 25 and 150 feet, and the permissible sags may also vary. Allowance must be made for wind and ice loading and displacement for the range of temperatures of the wires through the year. In some cases it may be desirable to use turnbuckles for adjusting line tension from time to time or to eliminate stretching with age or to employ counterweighting to maintain a constant tension automatically.

Certain wire configurations may be susceptible to vibration at certain wind velocities. When this happens, it is desirable to vary the distances of successive spans so that they have different natural periods of vibration. When all the wires of a system are equally stressed, they swing together and maintain mutually normal positions. When small wire spacings are used, wires that are in parallel at the same potential may require the use of metallic spacers and, when of different potentials,

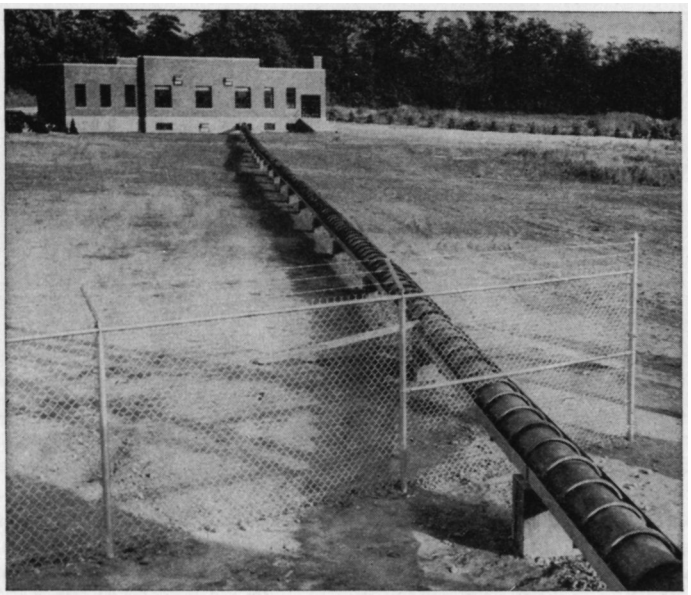

FIG. 4.74. Tile-covered coaxial feeder for 50-kilowatt medium-frequency amplitude-modulation broadcast station WNBC, Port Washington, New York. The station building is in the background. (*Photograph courtesy of National Broadcasting Company.*)

spacers of insulating material. It is more economical to use long spans with rather light wire tensions, and spacers where necessary, than to employ short spans with heavy tensions for the wires.

Pole-line construction is an old art, and there are numerous handbooks available giving detailed information from power-line and telephone practices. There is also a wealth of standardized assembly hardware commercially available, and the designer should have at hand several suppliers' catalogues. Radio insulation is much different from that used for power and telephone transmission, and special catalogues for radio insulators are also available. The engineer thus has a wide choice of the details of construction and assembly.

The various photographs included in this chapter are intended as

examples of what has been done and to serve as suggestions for new installations. They represent a wide variety of individual ideas; yet they are few in comparison with the number of satisfactory methods that one may use. Initial cost will play a prominent role in the detailing of the construction, though the minimum cost will be determined by the amount of power to be transmitted, the frequency, the layout of the station plot in so far as it affects the length of the line, the proximity of the lines to

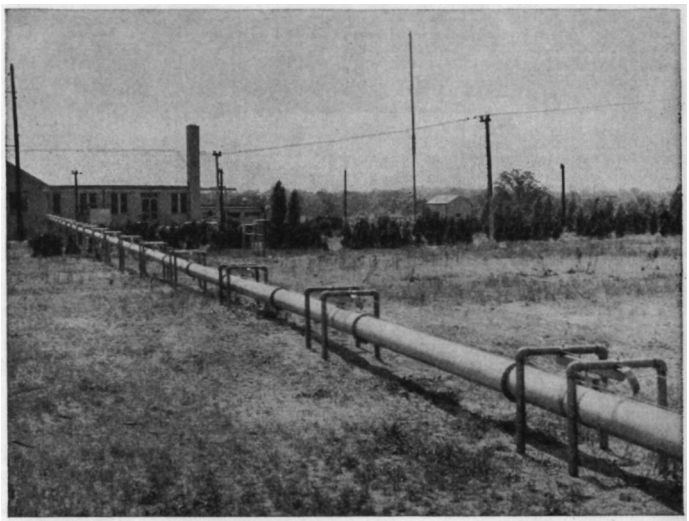

FIG. 4.75. View of a 10-inch coaxial feeder built for Station WJZ in 1937 and designed for 2,000-kilowatt peak power transmission. The feeder is straight and is free to expand and contract with temperature changes. The flanges on the feeder mark the length of each section and the location of the insulator supports for the inner conductor. (*Photograph courtesy of National Broadcasting Company.*)

various antennas, the climatic conditions, and the designer's choice of factors of safety.

4.13.1. Supports. The majority of radio applications in the temperate zones use wood poles for supports because of their availability and relatively low cost, ease of working, and satisfactory durability and strength. Cedar and chestnut poles give long life without protective treatment, and termite damage is relatively infrequent. Other natural round poles may be of many kinds that are locally available. Square-sawed timbers from 5 up to 8 inches square are often used and of course have a neater appearance. The part set in the ground can be dipped in creosote for rot protection and the aerial part of the pole painted. Sometimes the entire pole is creosote-dipped. The pole can be set directly in the ground or in concrete.

A line of poles should be surveyed with a transit and set in a neat line.

Where there are differences in grade level, the pole heights may be varied to keep the line straight in a vertical plane if best appearance is desired. Otherwise the line level can follow the grade with constant wire height above the ground.

A small change in the direction of the line may be made at a suspension-type pole where the suspension insulators hang at an angle, but when the

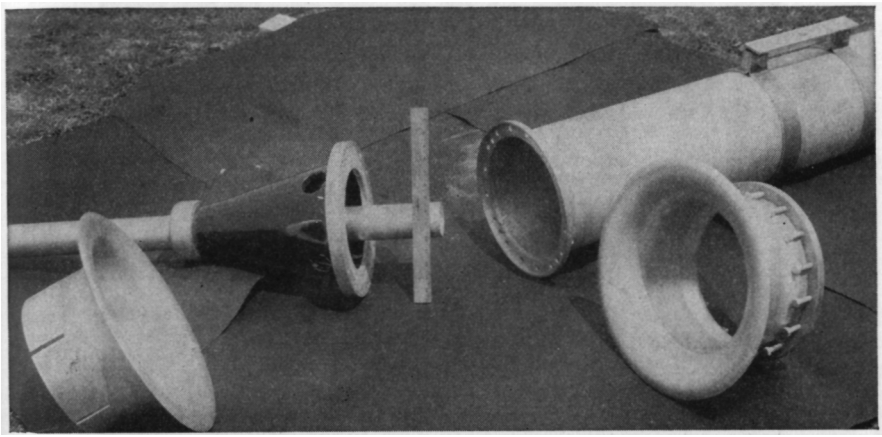

FIG. 4.76. Details of a coaxial feeder, as built for Station WJZ, designed for a transmission capacity of 2,000 kilowatts. The conical porcelain insulator supporting the inner conductor at each 20-foot section joint is assembled to the flange on the outer pipe before the next section is bolted on. A flux-grading flange for the ends of the feeder is shown at right. The line was designed for full rating without pressurizing. (*Photograph courtesy of National Broadcasting Company.*)

direction of the line changes more than 45 degrees, the corner pole should be of the strain type and guyed on the outside to withstand the side stress of the bend. Where a sharp bend is wanted, it is best to make the bend over a distance of two or three spans if there is space enough and there is no interference with other lines or structures. An example is shown in Fig. 4.22.

The recommended depths of setting for poles are shown in Table 4.4.

TABLE 4.4. TYPICAL DEPTHS FOR SETTING RADIO-FREQUENCY TRANSMISSION-LINE POLES

Pole length, feet	Depth of setting in firm ground, feet	Depth of setting in rock, feet
10–18	3½	3
20–22	4	3
25	5	3
30	5½	3
35–50	6	4

Guy anchors in soil should be set at the same depth. In rock, a guy anchor can be set in a drilled hole with molten lead retaining an eyebolt.

4.13.2. Wire Stringing. The tensile strengths of hard-drawn copper and copper-clad steel wires are given in many handbooks and commercial

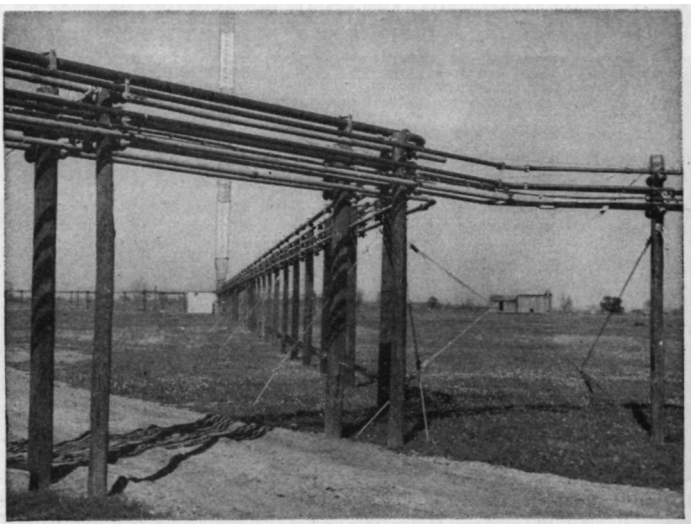

FIG. 4.77. Arrangement of pressurized coaxial feeders from the transmitter building to six radiators of the directive-antenna system for Station KTBS. (*Photograph courtesy of W. M. Witty.*)

catalogues. The relations between span, sag (or dip), wire size, and tension are given in the following equation,

$$S = \frac{WL^2}{8T}$$

in which S is the sag in feet, W the weight of the wire in the span, L the span length in feet, and T the tension in pounds.

The stringing of the wires must take into account the temperature at the time of stringing and also the minimum temperature to which the system will be exposed. In a system that is not counterweighted to retain a constant tension, the contraction of the wire at minimum temperature, together with wind and ice loadings, must not stress the wire beyond the ratio of its ultimate breaking strength and the designer's factor of safety. The weight of ice and the effective weight of the wind loadings are added to W in the above equation, and the maximum expected displacement is computed for this extreme condition. A factor of safety of from 2 to 3 is usually adequate for this purpose. In stringing

the wire in calm weather at some higher temperature, the extreme condition can be approximately simulated by dividing the total calculated weight of ice and wind load into four equal static loads and attaching them to the wire at points of approximately equal distance between the two poles of a span. The sag is adjusted then to be about 10 per cent more than that computed for the extreme condition to allow for the effect of contraction. Sag can be measured with a transit. Another way is to

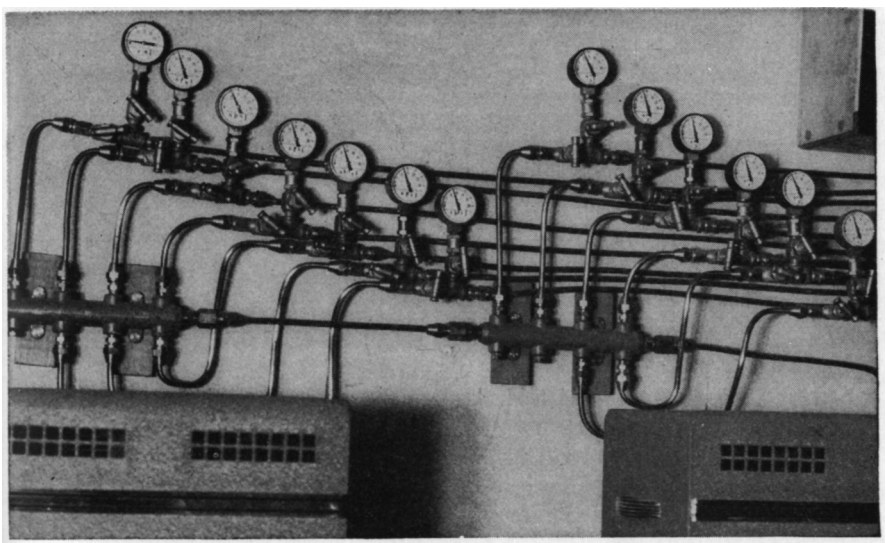

FIG. 4.78. Details showing pressure gages for the dehydrated-air-distribution system for the coaxial feeders of Fig. 4.77 at Station KTBS. (*Photograph courtesy of W. M. Witty.*)

compute the sag as before for the extreme condition and then string the unloaded wire for this same sag. The tension of the wire loaded only by its own weight can then be calculated from the same equation. This tension can then be measured with a dynamometer during stringing or by timing the natural period of vibration of the wire and applying the following equation,

$$T = 1.006 \left(\frac{t}{N}\right)^2$$

in which T is the tension in pounds as derived from the previous equation and t is the time in seconds for N complete fundamental vibrations of the whole span.

This measurement is made as follows: Snap the wire at its mid-point by pulling it to one side and releasing it. At the moment of release a stop

watch is started, and the number of complete swings of the wire are counted (say 10 vibrations), at which moment the watch is stopped. Applying this information to the foregoing equation gives its tension.

Most wires when stressed appreciably will stretch slightly. This stretch is a partial allowance for contraction at lower temperatures.

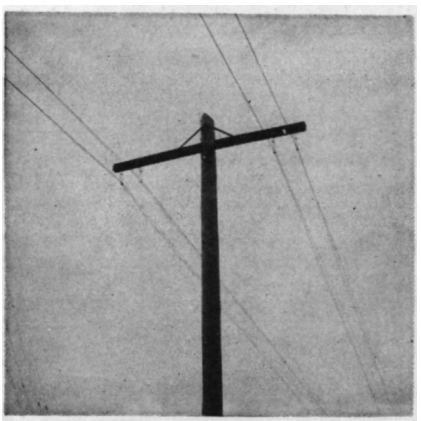

FIG. 4.79.

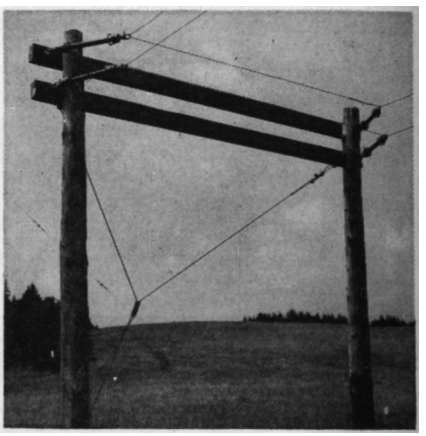

FIG. 4.80.

FIG. 4.79. Two-wire balanced feeders, using the crossarm suspension type of construction.

FIG. 4.80. Double-vertical bend at the mid-point of a two-wire balanced dissipation line where the direction of the line is reversed. (*Photograph courtesy of Royal Canadian Navy.*)

Guy wires can be correctly stressed using the same formulas.

There are three classes of loading used to design pole lines, designated as shown in Table 4.5.

TABLE 4.5. WIRE LOADINGS

Loading	Wind pressure, pounds per square feet, on projected areas	Temperature (minimum), degrees Fahrenheit	Radius of ice, inches
Light	12	30	0
Medium	8	15	¼
Heavy	8	0	½

4.13.3. Vibrational Stress of Wires. In wire systems that are tightly strung there should be a liberal allowance for the additional stress imposed by high-frequency vibration of the wires, over and above the relatively static stresses due to wind and ice loadings. The effect of transverse vibration, regardless of mode, is to increase the lateral displacement and

stretch the wire. The sum of all vibrational and static stresses should, of course, never equal the ultimate tensile strength of the wire, even after allowing for some degree of weakening with time due to fatigue of the metal.

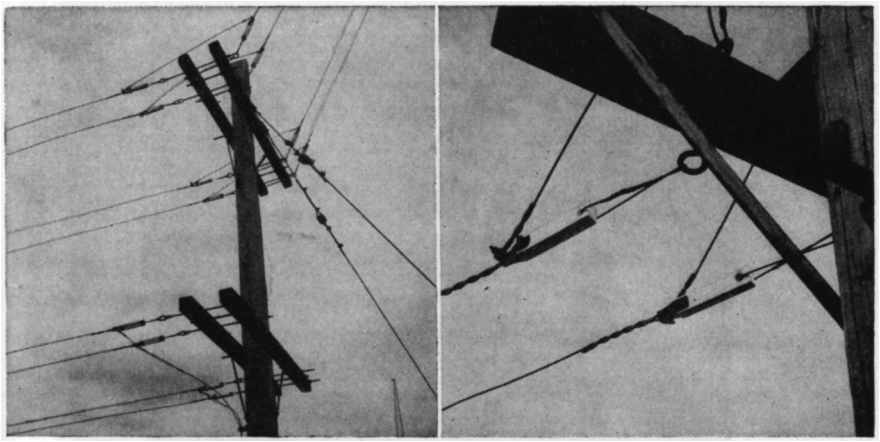

FIG. 4.81. FIG. 4.82.

FIG. 4.81. Details for several two-wire balanced lines for medium-power transmission.

FIG. 4.82. Details showing the use of strain insulators and the use of copper splicing sleeves for terminating wires at the insulators.

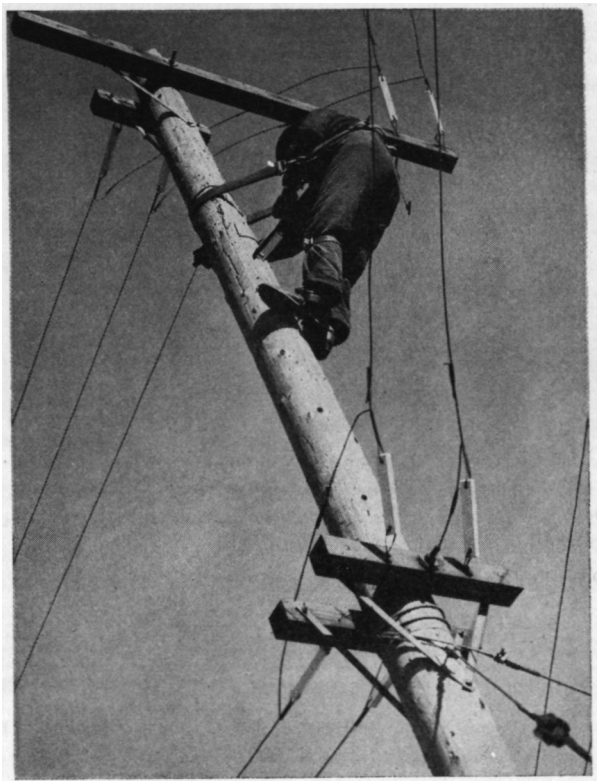

FIG. 4.83. Rigger working on a pole carrying balanced two-wire feeders for high-frequency broadcasting. This typifies many applications of this style of construction and hardware for broadcasting and communication use. This photograph was taken during construction, and the lines are not in final condition. Note the use of copper splicing sleeves at insulators, the attachment of guy wires, and crossarm hardware details. (*Photograph courtesy of National Broadcasting Company.*)

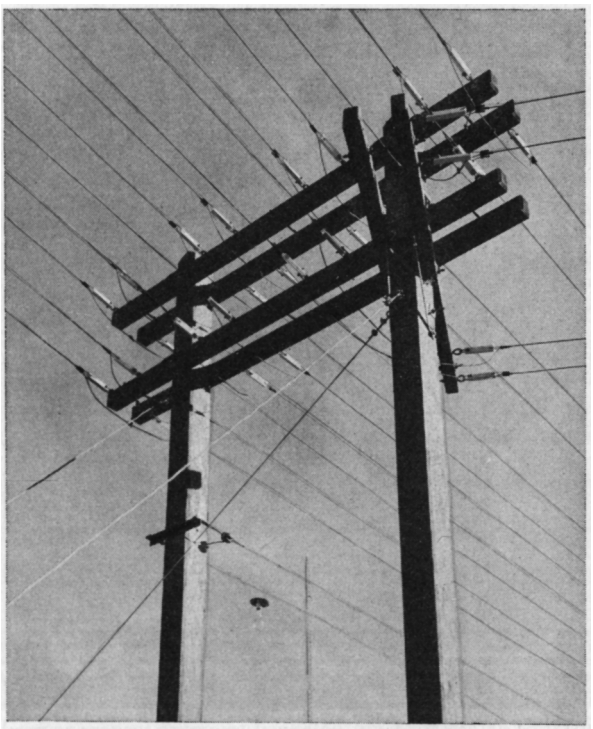

FIG. 4.84. Strain-pole assembly for eight balanced two-wire feeders, with two feeders routed from this support to antennas to the right. These feeders are used to feed any one of eight antennas from a 50-kilowatt high-frequency broadcast transmitter. Steatite block insulators are attached to eyebolts on the crossarms by clevises. The feeder wires are formed in eyes to attach to the insulators and are closed with pressed-metal retainers. (*Photograph courtesy of Radio Nacional, Rio de Janeiro and RCA International Division.*)

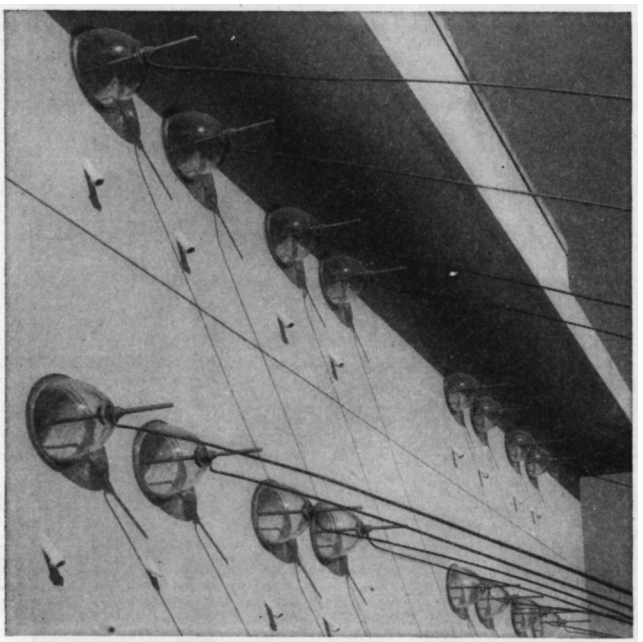

FIG. 4.85. Entrance details for eight balanced two-wire feeders as used by a 50-kilowatt high-frequency broadcast station in Rio de Janeiro. Pyrex bowl insulators (in pairs) serve as entrance insulators. Note the porcelain tubes used as ventilators to remove condensed moisture from the space in the wall between the bowl insulators. (*Photograph courtesy of Radio Nacional, Rio de Janeiro and RCA International Division.*)

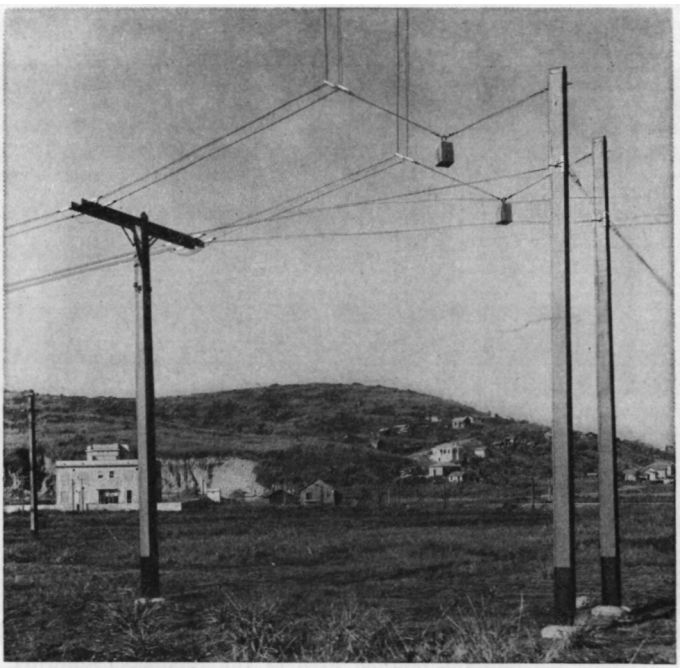

FIG. 4.86. Details showing a terminal pole for two balanced two-wire feeders and the manner of maintaining constant tension on the vertical feeders for a beam antenna. These methods were used for transmitting 50 kilowatts for high-frequency broadcast service. The station building can be seen in left background. (*Photograph courtesy of Radio Nacional, Rio de Janeiro and RCA International Division.*)

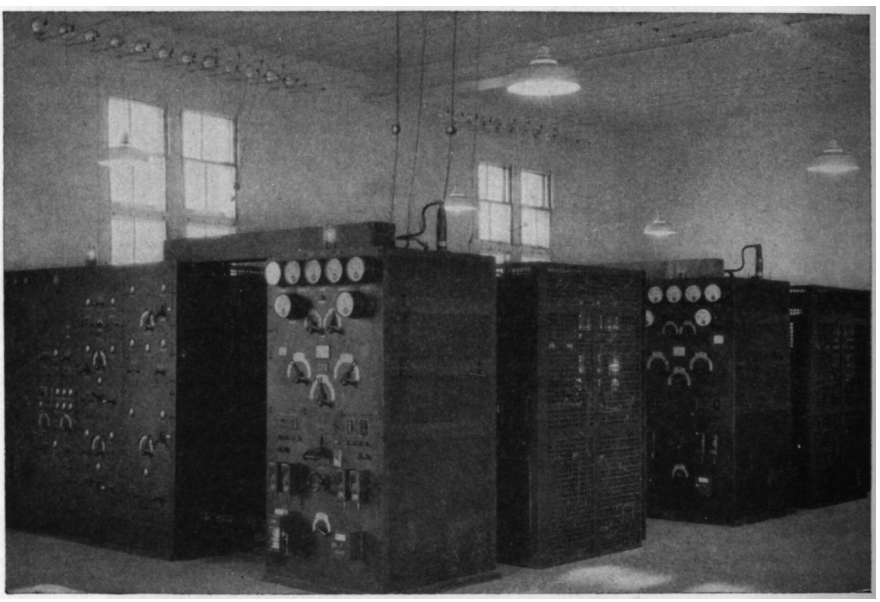

FIG. 4.87. Details showing the method used at the Bolinas, California, high-frequency communication station for distributing balanced two-wire feeders to several 20- to 40-kilowatt radiotelegraph transmitters. (*Photograph courtesy of RCA Communications, Inc.*)

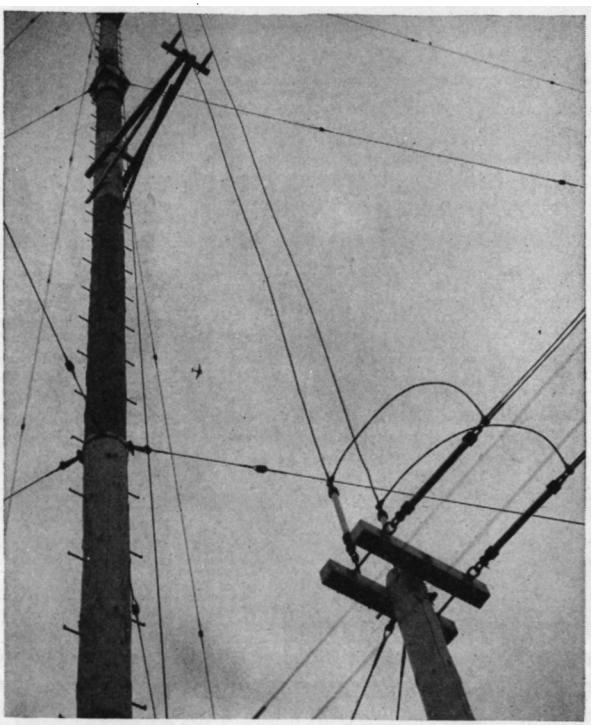

FIG. 4.88. Details showing the guying of a very high wood pole, a strain pole for a four-wire side-connected balanced feeder and the rigging details, a vertical corner, and the use of post insulators on the vertical section of the feeder. This is part of a beam system for 200-kilowatt high-frequency broadcasting at Dixon, California. (*Photograph courtesy of National Broadcasting Company.*)

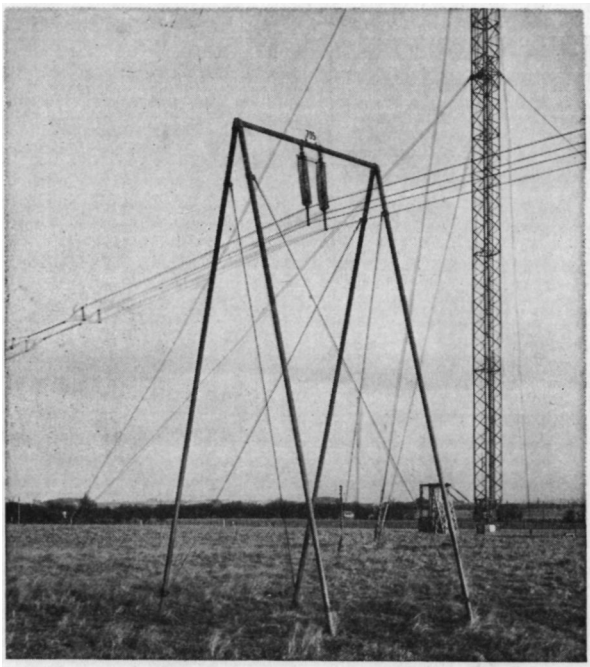

FIG. 4.89. This photograph shows several interesting features. A guyed pipe framework is used instead of a pole to support a four-wire balanced side-connected feeder for high-power short-wave broadcasting in England. Two forms of impedance matching are shown: the pinched section of higher characteristic impedance at the left, and inductors in series (with center grounded to support frame) and surrounding the line insulators as a substitute for an inductive parallel stub line. A guyed steel mast for supporting high-frequency dipole arrays is seen in the background. (*A British Broadcasting Corporation photograph, included here with the permission of the Institution of Electrical Engineers.*)

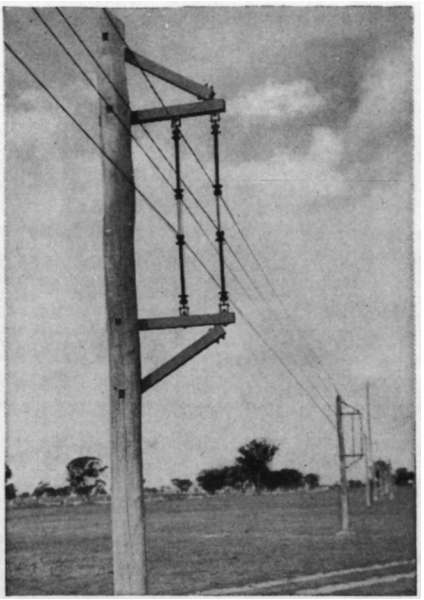

FIG. 4.90. A method of construction for the four-wire side-connected balanced feeder. (*Photograph courtesy of Australian Postmaster-General's Office.*)

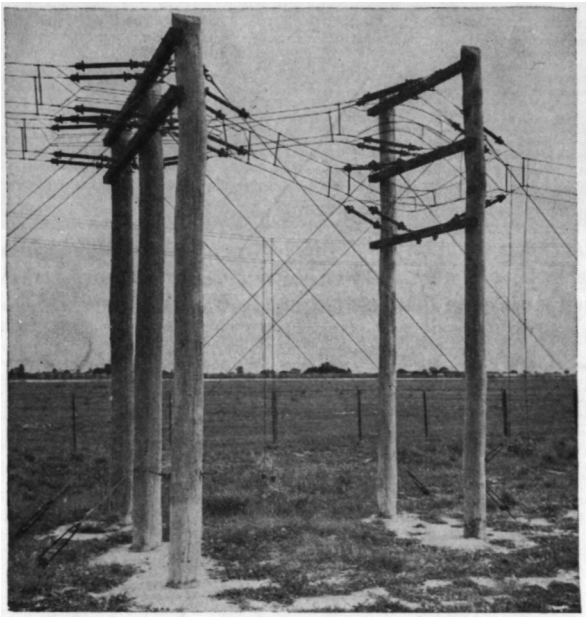

FIG. 4.91. A branching junction in a four-wire side-connected balanced feeder, showing structural detailing where the main line divides to go on to two portions of a dipole array for slewing purposes. The impedance-matching stub is shown at the right, and another is seen in the background associated with another feeder. (*Photograph courtesy of Australian Postmaster-General's Office.*)

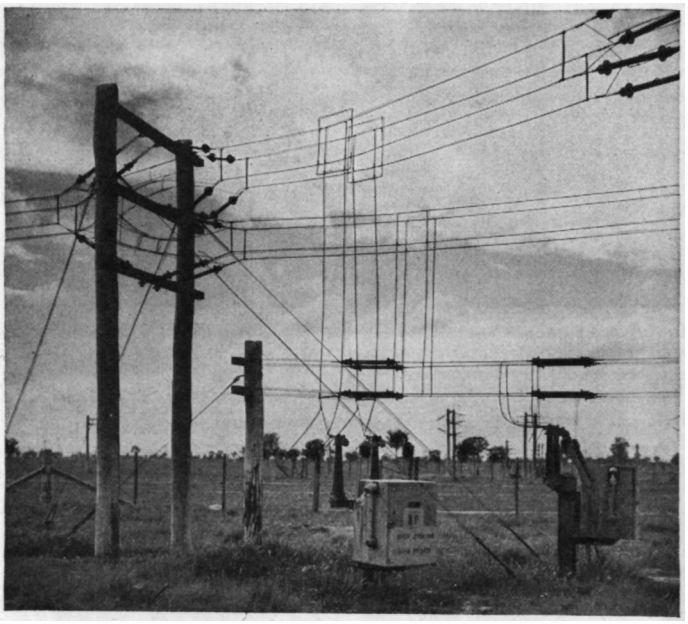

FIG. 4.92. Reversing junction for a dipole-array feed with four-wire side-connected balanced feeders, showing quarter-wave stubs and short-circuiting switches. (*Photograph courtesy of Australian Postmaster-General's Office.*)

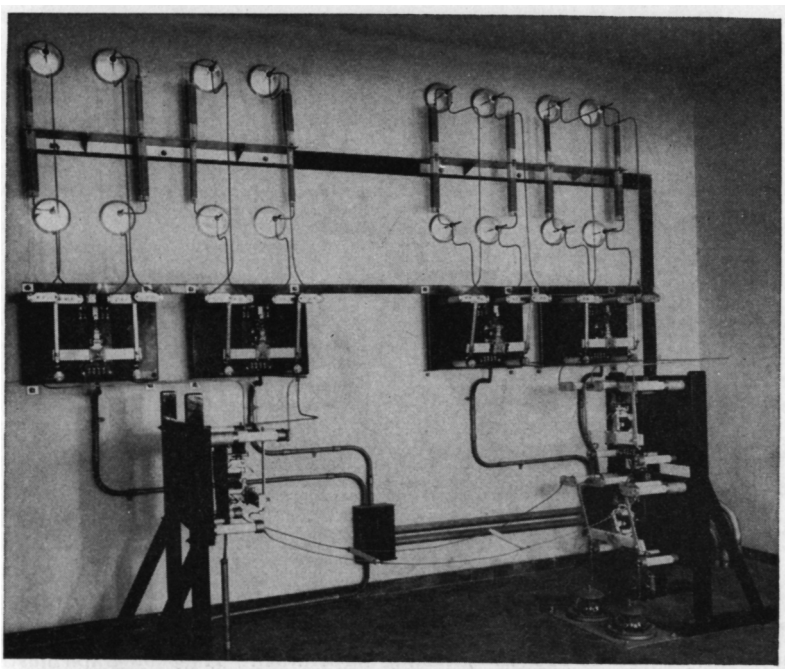

FIG. 4.93. Contactor switching system for a 50-kilowatt high-frequency broadcasting station at Rio de Janeiro, showing the branching circuits from one transmitter to eight two-wire balanced transmission lines feeding separate antennas. The contactors are low-capacitance double-pole double-throw devices designed for radio-frequency service. Balanced static drain coils, center-grounded, are associated with each feeder. (*Photograph courtesy of Radio Nacional, Rio de Janeiro and RCA International Division.*)

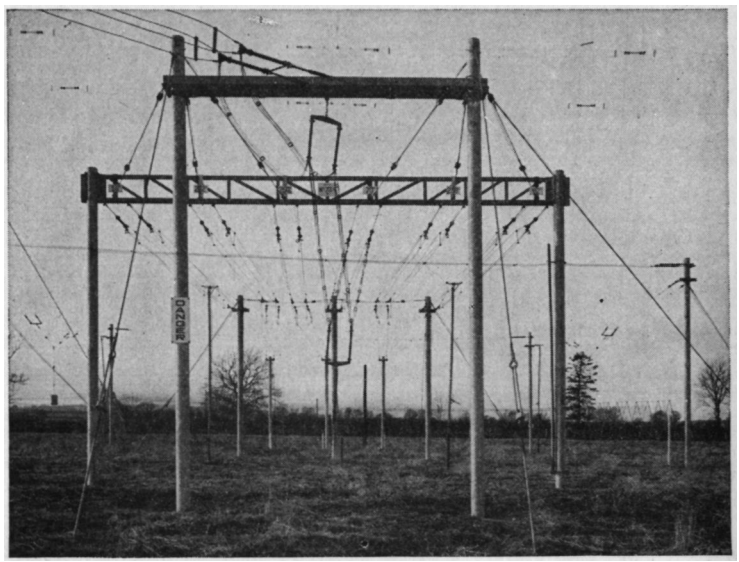

FIG. 4.94. A system of feeder and phasing sections associated with a slewable reversable dipole array with reflector curtain, for 100-kilowatt operation in the high-frequency broadcast service of the British Broadcasting Corporation. The photograph illustrates various assembly and rigging details, steel-post utilization, the use of cages of conductors to maintain uniform characteristic impedances, and the use of four-wire balanced side-connected feeders. A portion of the dipole array is seen in the background. Switching is accomplished manually, moving the flexible cage section to three positions. (*Photograph by British Broadcasting Corporation and reproduced by courtesy of Institution of Electrical Engineers.*)

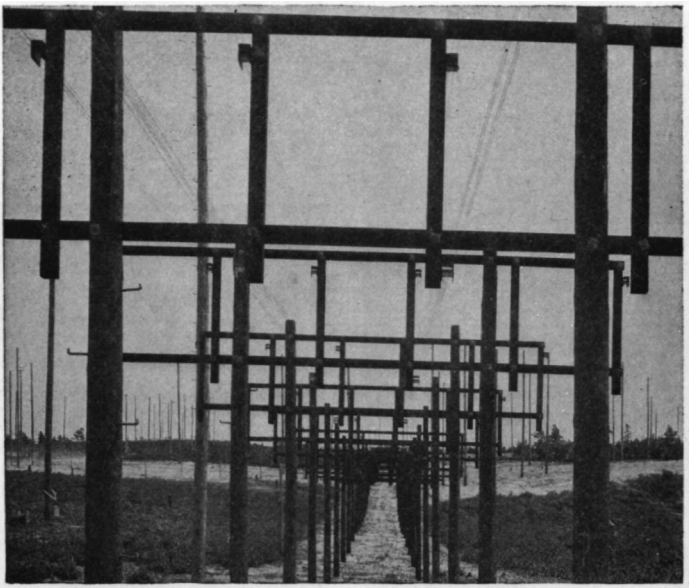

FIG. 4.95. Line construction for supporting several feeders of the four-wire cross-connected balanced type as used at the Riverhead receiving station for connecting diversity high-frequency receiving antennas with the diversity receivers. Note the small cross section of each feeder and the large separation between feeders to obtain very low line pickup and cross talk. RCA fishbone-antenna arrays are in the background. (*Photograph courtesy of RCA Communications, Inc.*)

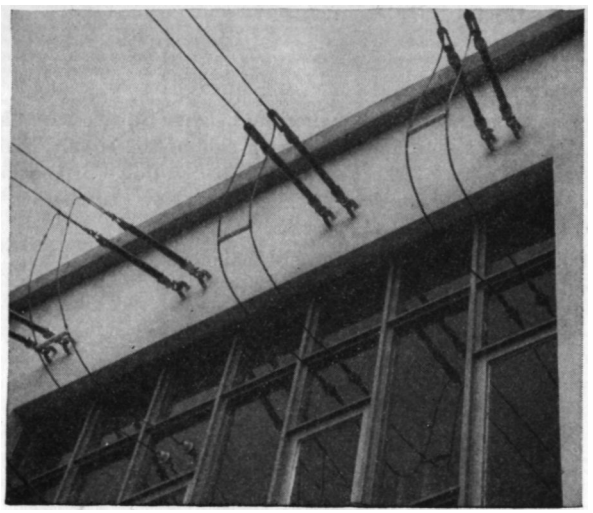

FIG. 4.96. Building entrance detail for several two-wire balanced feeders. (*Photograph courtesy of Canadian Broadcasting Corporation.*)

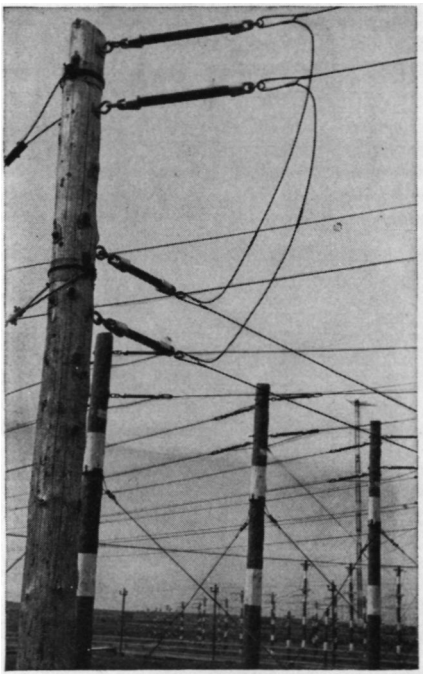

FIG. 4.97.

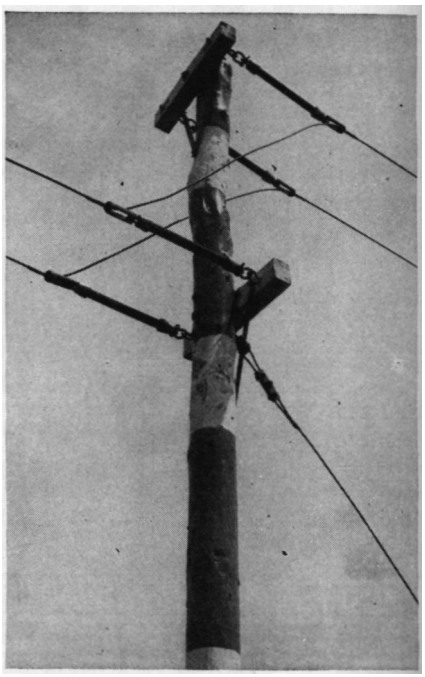

FIG. 4.98.

FIG. 4.97. Turning a corner and changing the height of a two-wire balanced feeder and maintaining constant wire lengths in each side of the circuit. Shown against a background of feeders used at the Canadian Broadcasting Corporation high-power high-frequency broadcasting station at Sackville, New Brunswick. (*Photograph courtesy of Canadian Broadcasting Corporation.*)

FIG. 4.98. Double-strain pole in a two-wire balanced feeder system. (*Photograph courtesy of Canadian Broadcasting Corporation.*)

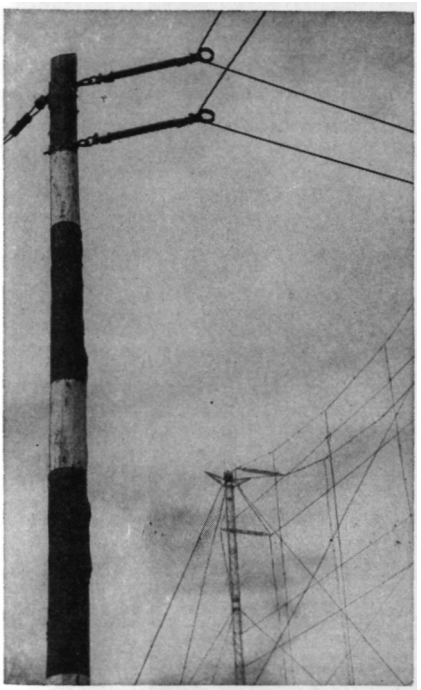

FIG. 4.99. Corner pole in a two-wire balanced feeder system with the feeder plane turned so as to make the turn with the same length of wire in each side of the circuit. (*Photograph courtesy of Canadian Broadcasting Corporation.*)

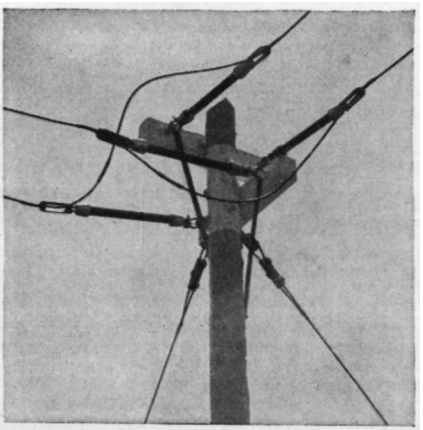

FIG. 4.100. A right-angle bend in a balanced two-wire feeder, made so as to maintain constant length in the wires on each side of the circuit. (*Photograph courtesy of Canadian Broadcasting Corporation.*)

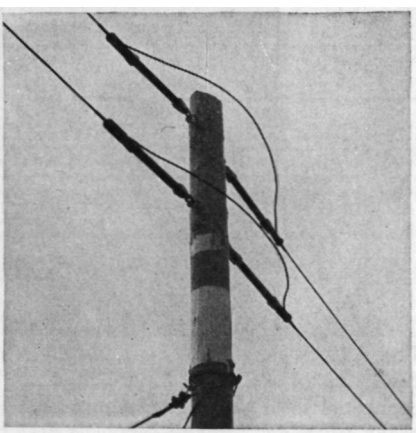

FIG. 4.101. Detail of a double-strain pole in a balanced two-wire feeder. (*Photograph courtesy of Canadian Broadcasting Corporation.*)

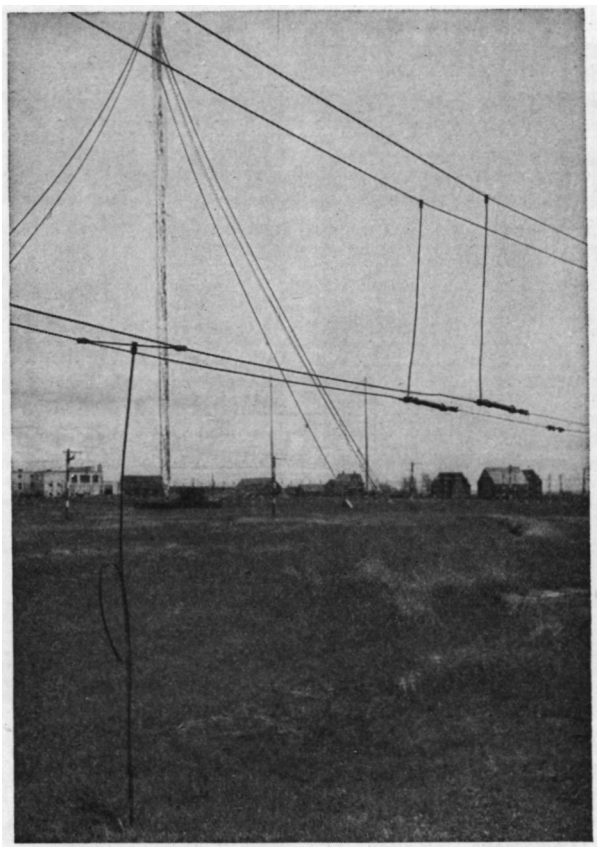

FIG. 4.102. Detail of a parallel-wave drain on a two-wire balanced feeder system, consisting of a quarter-wave balanced stub across the feeder, the end of which is connected to ground with a single conductor one-quarter wavelength long. (*Photograph courtesy of Canadian Broadcasting Corporation.*)

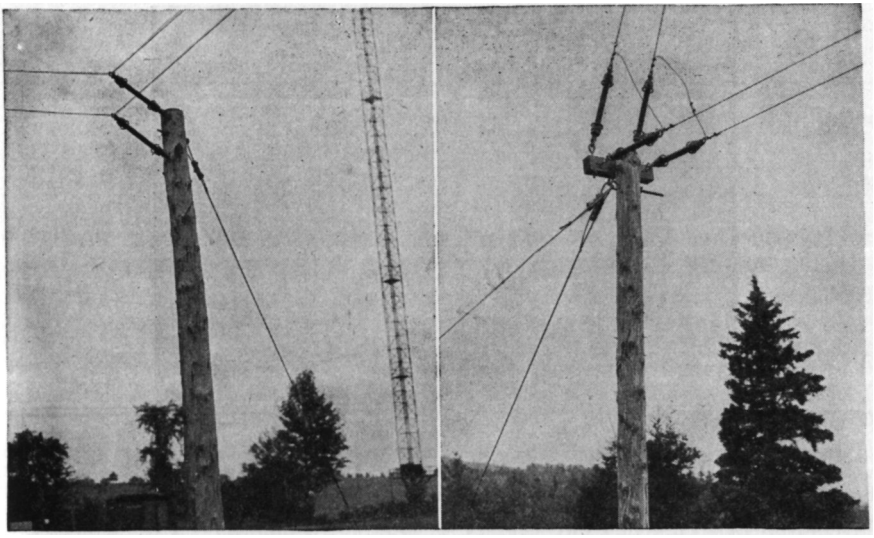

FIG. 4.103. FIG. 4.104.

FIG. 4.103. Corner pole in a two-wire balanced feeder. (*Photograph courtesy of Royal Canadian Navy.*)

FIG. 4.104. End pole in a two-wire balanced feeder, where it rises to the antenna. (*Photograph courtesy of Royal Canadian Navy.*)

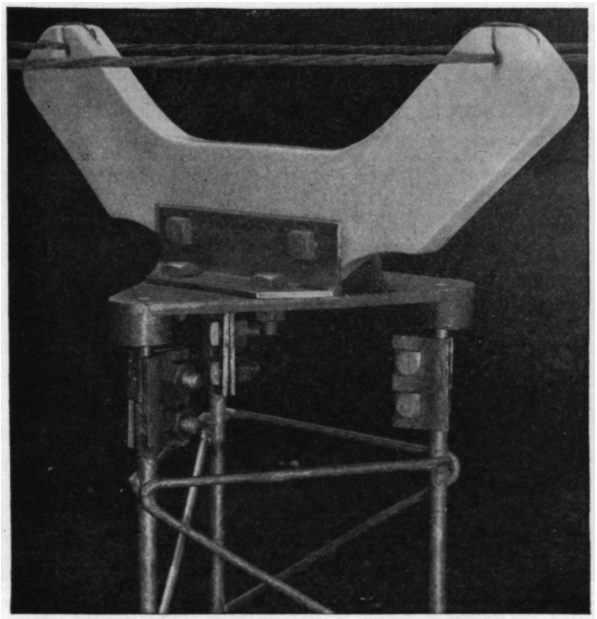

FIG. 4.105. Ceramic insulator crossarm used for two-wire balanced lines. (*Photograph courtesy of Wind Turbine Company.*)

FIG. 4.106. Detail showing the feeders for a receiving installation using four-wire cross-connected open-wire feeders terminating at a building and entering through coaxial feeders. The wide-band high-frequency balance to unbalance transformers are in the weatherproof black boxes on the building. (*Photograph courtesy of Royal Canadian Navy.*)

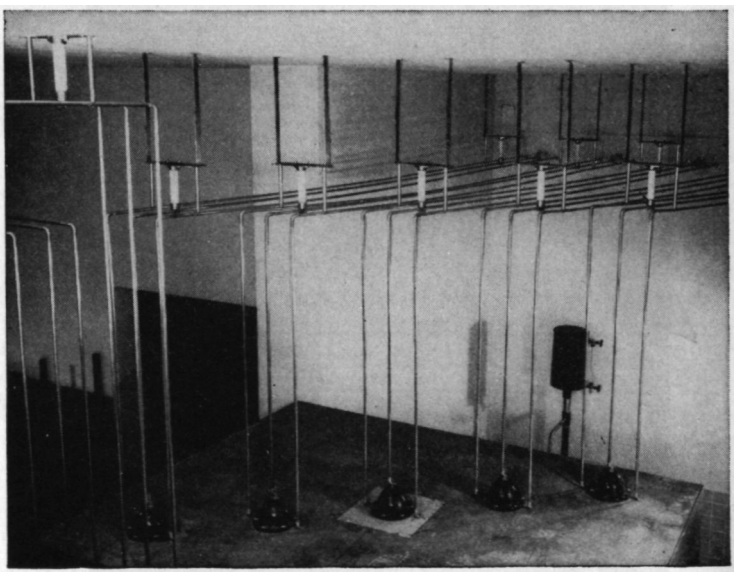

FIG. 4.107. Several feeders of the three-wire type V (two outer wires grounded) with 235-ohm impedance for inside connections to directive-antenna tuning and phasing equipment. (*Photograph courtesy of RCA Victor Company, Ltd., Montreal.*)

BIBLIOGRAPHY

General Theory and Balanced Lines

1. Eaglesfield, C. C., Characteristic Impedance of Transmission Lines, *Wireless Engr.*, **22**:222, May, 1944.
2. Carter, P. S., Charts for Transmission Line Measurements and Computations, *RCA Rev.*, **3**:355, January, 1939.
3. Roosenstein, H. O., Conduction of High-frequency Oscillatory Energy, *Proc. IRE*, **19**:1849, October, 1931.
4. Alford, A., Coupled Networks in Radio-frequency Circuits, *Proc. IRE*, **29**:55, February, 1941.
5. Jamieson, H. W., and J. R. Whinnery, Equivalent Circuits for Discontinuities in Transmission Lines, *Proc. IRE*, **32**:98, February, 1944.
6. Roder, H., Graphical Methods for Problems Involving Radio-frequency Transmission Lines, *Proc. IRE*, **21**:290, February, 1933.
7. Salzberg, B., Graphs for Transmission Lines; Reference Sheet, *Electronics*, **15**:47, January, 1942.
8. Paine, R. C., Graphical Solution of Voltage and Current Distribution and Impedance of Transmission Lines, *Proc. IRE*, **32**:686, November, 1944.
9. Alford, A., High-frequency Transmission-line Networks, *Elec. Commun.*, **17**:301, January, 1939.
10. Smith, P. H., Improved Transmission-line Calculator, *Electronics*, **17**:130, January, 1944.
11. Fuchs, Morton, Intercoupled Transmission Lines, *Elec. Commun.*, **21**:248, 1944.
12. Harris, C. C., Losses in Twisted-pair Transmission Lines at Radio Frequencies, *Proc. IRE*, **24**:425, March, 1936.
13. Bloch, A., Lossless Transmission Lines; Analysis by Means of Two Simple Diagrams, *Wireless Engr.*, **21**:161, April, 1944.
14. Spangenberg, K., Propagation Constant and Characteristic Impedance of High-loss Transmission Lines, *Electronics*, August, 1942, p. 57.
15. Alford, A., and S. Pickles, Radio-frequency High-voltage Phenomena, *Trans. AIEE*, **59**:129, March, 1940.
16. Howe, G. W. O., Reflections from Unmatched Feeder Terminals; Spindle Graphical Method, *Wireless Engr.*, **20**:215, May, 1943.
17. Huxley, L. G. H., and W. Jackson, Solution of Transmission-line Problems by Use of the Circle Diagram of Impedance, *J. IEE*, **91**(part 3): 105, September, 1944.
18. Chestnut, R. W., H. A. Affel, and R. H. Mills, Transmission Lines, *Bell System Tech. J.*, **13**:285, August, 1934.
19. Paine, R. C., Transmission-line Calculator, *Electronics*, March, 1945, p. 140.
20. Pierce, J. E., Transmission-line Equation in Terms of Impedance, *Bell System Tech. J.*, **22**:263, July, 1943.
21. Streba, E. J., and C. B. Feldman, Transmission Lines for Short-wave Radio Systems, *Proc. IRE*, **20**:1163, July, 1932.

22. Colebrook, F. M., Transmission-line Theory in Terms of Propagation Characteristics and Reflection Coefficients, *Wireless Engr.*, **21**:167, April, 1944.

Tapered Transmission Lines

23. Christiansen, W. N., An Exponential Transmission Line Employing Straight Conductors, *Proc. IRE*, **35**:576, June, 1947.
24. Burrows, C. R., Exponential Transmission Line, *Bell System Tech. J.*, **17**:555, October, 1938.
25. Gent, A. W., and P. J. Wallis, Impedance Matching by Tapered Transmission Lines, *J. IEE*, **93**(part 3*a*): 559, 1946.
26. Wheeler, H. A., Transmission Lines with Exponential Taper, *Proc. IRE*, **27**:65, January, 1939.

Open-wire Unbalanced Transmission Lines

27. Duncan, R. D., Characteristic Impedance of Grounded and Ungrounded Open-wire Transmission Lines, *Communications (N.Y.)*, June, 1938, p. 10.
28. Brown, G. H., Characteristics of Overhead Unbalanced Transmission Lines, *Broadcast News (RCA)*, May, 1941.
29. Laport, E. A., Open-wire Radio-frequency Transmission Lines, *Proc. IRE*, **31**:271, June, 1943.

High-frequency Transmission Systems

30. Chamberlain, A. B., CBS International Broadcast Facilities, *Proc. IRE* **30**:118, March, 1942.
31. McLean, F. C., and F. D. Bolt, Design and Use of Radio-frequency Open-wire Transmission Lines and Switchgear for Broadcasting, *Jour. IEE*, **93**(3): 191, May, 1946.
32. Wilkinson, E. J., Testing of High-frequency Aerial Systems and Transmission Lines, *Proc. IRE (Australia)*, February, 1947.
33. Hayes, L. W., and B. N. McLarty, The Empire Broadcasting Station at Daventry, *J. IEE*, **85**:321, 1939.

Concentric (Coaxial) Transmission Lines

34. Andrew, V. J., Applications of Concentric Transmission Lines, *Electronics*, March, 1937, p. 40.
35. Kenney, N. D., Coaxial Cable Design, *Electronics*, May, 1945, p. 124.
36. Whinnery, J. R., H. W. Jamieson, and T. E. Robbins, Coaxial Line Discontinuities, *Proc. IRE*, **32**:695, November, 1944.
37. Hollingsworth, L. M., Concentric-section Resonant Transmission Lines, *Proc. IRE*, **29**:356, June, 1941.
38. Larrick, C. V., and H. H. Race, High-frequency Coaxial Line Calculations, *Elec. Eng.*, **61**:526, July, 1942.
39. Epperson, J. B., Installation of Coaxial Transmission Lines, *Electronics*, July–August, 1939.
40. Duttera, W. S., New Coaxial Transmission Line at WTAM, *Electronics*, March, 1939, p. 30.

41. Hansell, C. W., Resonant Lines for Frequency Control, *Elec. Eng.*, **54**:852, August, 1935.
42. Hansell, C. W., and P. S. Carter, Frequency Control by Low Power-factor Line Circuits, *Proc. IRE*, **24**:597, April, 1936.
43. Dietsch, C. G., Terminating Concentric Lines; Theory and Practice of Coupling Low-impedance Concentric Transmission Lines to Antennas, *Electronics*, December, 1936, p. 16.

Special Subjects and Measurements

44. Frankel, S., Characteristic Impedance of Parallel Wires in Rectangular Troughs, *Proc. IRE*, **30**:182, April, 1942.
45. Brennecke, C. G., Equivalent T and Pi Sections for the Quarter-wavelength Line, *Proc. IRE*, **32**:15, January, 1944.
46. Easton, I. G., Measurements of the Characteristics of Transmission Lines, *Gen. Radio Experimenter*, **18**, November–December, 1943.
47. Harrison, C. W., On the Pickup of Balanced Four-wire Lines, *Proc. IRE*, **30**:517, November, 1942.
48. King, R., Coupled Antennas and Transmission Lines, *Proc. IRE*, **31**:626, November, 1943.
49. Labus, J. W., Measurement of Resistance and Impedance at High Frequencies, *Proc. IRE*, **19**:452, March, 1931.
50. Morton, H. B., and J. W. Whitehead, Two Transmitters on One Aerial, *Electronic Eng.*, **20**:157, May, 1948.
51. Lutkin, F. E., R. H. J. Cary, and G. N. Harding, Wideband Aerials and Transmission Lines for 2 to 85 Mc/s, *J. IEE*, **93**(III*a*): 552, 1946.
52. Laport, E. A., Simplified Network Synthesis, *Broadcast News*, January May, 1939.
53. Brown, G. H., Directive Antennas, *Proc. IRE*, **25**:78, January, 1937.
54. Smith, N. S., High-frequency Broadcasting in Australia, *Proc. IRE* (*Australia*), October, 1948, p. 4.
55. Arnold, J. W., and R. C. Taylor, Linearly Tapered Loaded Transmission Lines, *Proc. IRE*, **20**:1811, November, 1932.
56. Bechberger, P. F., and J. W. Arnold, Sinusoidal Currents in Linearly-tapered Loaded Transmission Lines, *Proc. IRE*, **19**:304, February, 1931.
57. Marchand, N., Transmission-line Conversion Transformers; Methods for Joining a Balanced Two-wire Line to a Coaxial Line, *Electronics*, December, 1944, p. 142.
58. Fubini, E. G., and P. J. Sutro, A Wideband Transformer from an Unbalanced to a Balanced Line, *Proc. IRE*, **35**:1153, October, 1947.
59. Thornhill, W. T., and E. W. Beasley, Influence of Corona Formation upon the Design of High-voltage Apparatus, *Marconi Rev.*, **90**:87, July–September, 1948.
60. Sarbacher R. I., and W. A. Edson, *Hyper and Ultra-high Frequency Engineering*, Chaps. 8 and 9, John Wiley & Sons, Inc., New York, 1943.
61. Terman, F. E., *Radio Engineers' Handbook*, McGraw-Hill Book Company, Inc., New York, 1943.
62. Harper, A. E., *Rhombic Antenna Design*, D. Van Nostrand Company, Inc., New York, 1941.

CHAPTER 5

Graphical Synthesis of Impedance-matching Networks

The design of impedance-matching networks is an important part of antenna engineering. One of the quickest and easiest methods for designing impedance-matching networks is the graphical method described in this chapter. The accuracy of this method is adequate for engineering-design purposes, giving slide-rule accuracy with moderate care in drawing. At radio frequencies this is usually equal to or better than the accuracy of measurements. This type of solution shows at a glance the physical principles of operation that most engineers want to know, as well as the effects of variations in the circuit elements. The method will be demonstrated by a series of typical engineering problems.

There are many ways in which rotating vectors may be employed for circuit analysis, but not all lend themselves to circuit synthesis. The technique best adapted to synthesis is that where only current and potential vectors are used. The results then come out directly in resistance and reactance by using quantitative vector ratios.

The following are general suggestions for obtaining maximum benefit from the graphical method of impedance-matching network synthesis:

1. Reasonable care with drawing will produce 10-inch slide-rule accuracy on 8½- by 11-inch paper. It is a great convenience to use polar coordinate paper for vector calculations, using the printed decimal divisions thereon for scales. Radial vectors and angles are thus directly revealed, while nonradial vectors can be measured with dividers and referred to the basic scale of the paper. This avoids the use of protractor and rule. In using plain paper, the L scale of a slide rule, in combination with dividers, provides a handy decimal-dimension base. Diagrams should be constructed carefully and with a sharp pencil.

2. An impedance is represented by the ratio of a potential vector of assigned value and a current vector of assigned value, related by some phase angle.

3. To avoid confusion, the closed arrowhead A should be used for current, and the open arrowhead V for potential.

4. One scale should be used for all potentials and another scale for all currents, in any single vector diagram. There need be no relation between the scales for potentials and currents, except that the indicated vector ratios be correct for the resistances, reactances, or impedances involved.

5. The current and potential vectors representing the *load impedance* should be drawn as the reference vectors and the network worked backward to the input. This gives vector addition throughout for currents and potentials.

6. The triangle method of addition is ordinarily used instead of the parallelogram, because it makes a simpler, clearer diagram by conservation of lines.

7. Where a network includes two or more stages, each stage is solved separately as an individual problem. The stage that includes the ultimate load is solved first. Then its input impedance is used as the terminal impedance for the next preceding stage, etc. By this method, quite complicated networks can be handled easily.

8. A rotating vector diagram represents steady-state conditions at a single frequency. To analyze the performance of a network at several frequencies, a new vector diagram is required for each frequency.

9. Following generally accepted conventions, advance in time is counterclockwise. A potential across an inductive reactance, leads the current through the element 90 degrees. When the voltage is lagging 90 degrees, it is a capacitive reactance. A current in phase with a potential is a positive resistance, and a current 180 degrees with respect to a potential is a negative resistance.

5.1. Type I Problem*

Problem. Design a network which will match a 500 ohms resistance load to a 100-ohm source with a phase shift of -30 degrees through the network.

Procedure. For vector circuit calculations in general, the first step is to set up the original problem in vector form, using convenient scales for potentials and currents and taking the power derived therefrom into consideration.

Draw a potential vector and a current vector in phase in a reference direction representing, according to some convenient scale, the 500-ohm load (for example, $V_0 = 500$ volts and $I_0 = 1$ ampere). According to

* For an analytical formulation of type I problems, see G. H. Brown, *Proc. IRE*, **25**:130.

this arbitrarily chosen scale for the vectors, the power W_0 represented would be 500 watts. If the impedance-matching network is to have pure reactances, the power input to the network must equal the power represented in the load.

The next step is to draw a potential vector and a current vector, in phase, according to the same scale of vectors, which will have a ratio representing the input resistance, a product which gives a power equal to that in the load, and a direction which gives the specified phase shift.

Since $W_0 = 500$ watts,

$$V_{in} = \sqrt{500 \times 100} = 224 \text{ volts}$$

and

$$I_{in} = \sqrt{500/100} = 2.24 \text{ amperes}$$

Figure 5.1 illustrates these first two steps for the problem outlined. This figure represents the problem written vectorially.

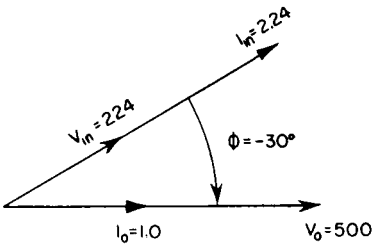

FIG. 5.1

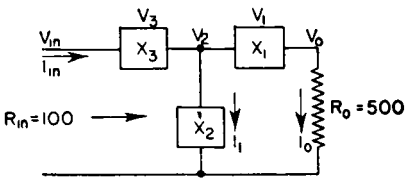

FIG. 5.2

We now have a choice of a T or a π solution. Let us choose a T network first and label all the potentials and currents in the load, network, and input in a manner which will satisfy Kirchhoff's laws (see Fig. 5.2). At this point we know V_0 and I_0, V_{in} and I_{in}, R_0 and R_{in}. We represent the network elements as X's because we do not know what is required yet. We also know, from elementary alternating-current theory, that

$$I_{in} = I_0 + I_1 \qquad \text{vectorially}$$
$$V_2 = V_0 + V_1 \qquad \text{vectorially}$$
$$V_{in} = V_2 + V_3 \qquad \text{vectorially}$$

Similarly, we know that for circuit elements which are purely reactive, V_1 is perpendicular to I_0, V_3 is perpendicular to I_{in}, and V_2 is perpendicular to I_1. These facts give us enough information to complete the vector diagram for the entire network. This vector diagram has all the information necessary to reveal the nature and magnitude of X_1, X_2, and X_3.

There are only three currents in the circuit, and at the outset of the problem we already know two of them. The unknown current I_1 can be drawn immediately by connecting the tips of I_0 and I_{in}. The direction of

I_1 is that which, when added to I_0, gives a vector sum I_{in}. Thus, I_1 is directed toward I_{in}. Its magnitude is determined by its length according to the scale for the current vectors.

The intersection of perpendiculars through V_0 and V_{in} locates V_2, as shown in Fig. 5.3. The directions are found from considering that $V_0 + V_1 = V_2$ vectorially and $V_{in} = V_2 + V_3$ vectorially. From the scales for the diagram

$$V_0 = 500 \text{ volts} \qquad I_0 = 1.0 \text{ ampere}$$
$$V_1 = 418 \text{ volts} \qquad I_1 = 1.5 \text{ amperes}$$
$$V_2 = 670 \text{ volts} \qquad I_{in} = 2.24 \text{ amperes}$$
$$V_3 = 611 \text{ volts}$$
$$V_{in} = 224 \text{ volts}$$

$$X_1 = \frac{V_1}{I_0} = \frac{418}{1.0} = -j418 \text{ ohms}$$

where V_1 lags I_0 by 90 degrees,

$$X_2 = \frac{V_2}{I_1} = \frac{670}{1.5} = -j448 \text{ ohms}$$

where V_2 lags I_1 by 90 degrees, and

$$X_3 = \frac{V_3}{I_{in}} = \frac{611}{2.24} = j273 \text{ ohms}$$

where V_3 leads I_{in} by 90 degrees. The network becomes that shown in Fig. 5.4.

A check on the accuracy of construction is offered by the angle between I_1 and V_2 vectors, which should be 90 degrees.

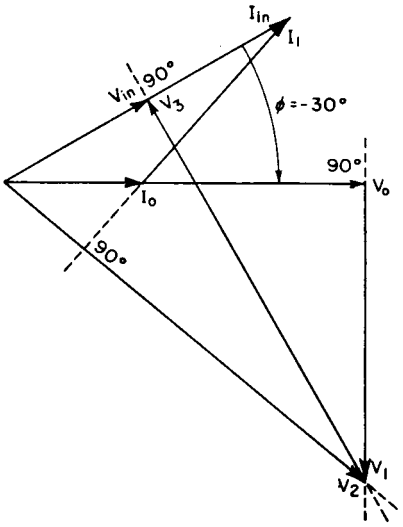

FIG. 5.3

The problem specified a phase difference between V_0 and V_{in}. A different solution results from each different value of phase shift through the network. If phase shift is immaterial, we can find a solution where $X_1 = 0$ and the circuit is simplified to two reactive elements. This is the case where V_3 passes through V_0 and V_1 vanishes; also $V_2 = V_0$. The phase shift ϕ becomes $\cos^{-1}(V_{in}/V_0)$. For values of ϕ greater than the value where $X_1 = 0$, the sign of X_1 changes from $-j$ to $+j$.* When

* When this circuit is used as a tank circuit for a radio-frequency amplifier, its energy-storage ratio Q increases with increasing phase difference between the load current and the input current. This ratio approaches infinity as the phase difference approaches 180 degrees, a physically unrealizable limit. Most practical tank circuits will lie between phase-shift angles of 120 and 165 degrees. (See Fig. 4.33.)

ϕ is positive instead of negative, the signs of all the elements reverse likewise.

Taking now the π-network solution for the same problem, the circuit becomes that shown in Fig. 5.5. In this case, we know V_0, I_0, V_{in}, I_{in}, and ϕ. We also know X_1, X_2, and X_3 to be pure reactances. Therefore

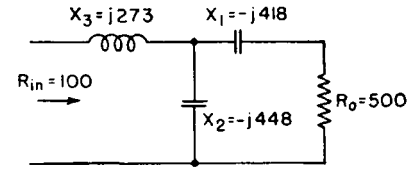

FIG. 5.4

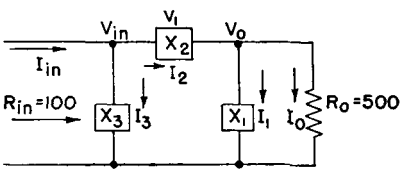

FIG. 5.5

I_1 must be perpendicular to V_0, I_2 must be perpendicular to V_1, and I_3 must be perpendicular to V_{in}. Since we know V_0 and V_{in}, we can draw V_1 immediately, as shown in Fig. 5.6. From the scales of the diagram

$$V_0 = 500 \text{ volts} \qquad I_0 = 1.0 \text{ amperes}$$
$$V_1 = 325 \text{ volts} \qquad I_1 = 2.76 \text{ amperes}$$
$$V_{in} = 224 \text{ volts} \qquad I_2 = 2.95 \text{ amperes}$$
$$I_3 = 1.9 \text{ amperes}$$
$$I_{in} = 2.24 \text{ amperes}$$

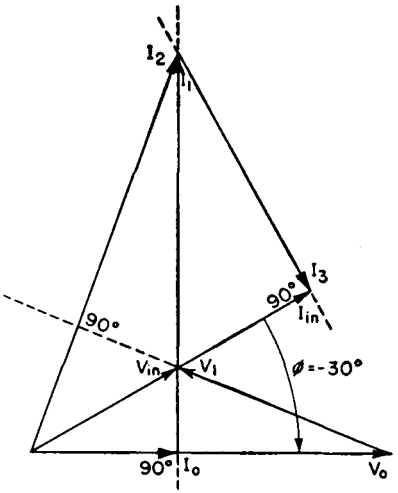

FIG. 5.6

$$X_1 = \frac{V_0}{I_1} = \frac{500}{2.76} = -j181 \text{ ohms}$$

$$X_2 = \frac{V_1}{I_2} = \frac{325}{2.95} = j110 \text{ ohms}$$

$$X_3 = \frac{V_{in}}{I_3} = \frac{224}{1.9} = j118 \text{ ohms}$$

The network becomes that shown in Fig. 5.7.

If the value of ϕ is immaterial, there is a value at which $I_3 = 0$ and $X_3 = \infty$. This particular solution simplifies the circuit to two reactive elements. For values of ϕ greater than this particular value, the sign of X_3 reverses. Study of the vector diagram enables one, by inspection, to foresee the influence of variations in the network for a given impedance transformation and to select a design for maximum circuit economy or energy economy.

To demonstrate the solution for the two-element circuit to obtain this

transformation, we set up input and output vectors but do not specify a phase shift. Instead we allow the input vectors to assume a position which, in the T case, causes V_3 to pass directly through V_0 and, in the π case, causes I_1 to pass through I_{in}. For example in the π case we draw the loci of V_{in} and I_{in} for variable ϕ, as shown in Fig. 5.8. Then we erect I_1 perpendicular to V_0 through I_0. Where this cuts the locus of I_{in} locates the vector I_{in}.

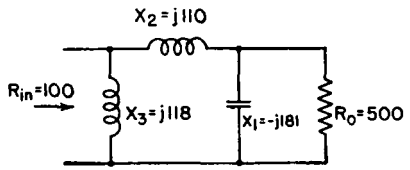

FIG. 5.7

In the case of the T, X_1 becomes 0, and in the case of the π, X_3 becomes ∞. Thus, the T and π solutions merge into a common solution at this

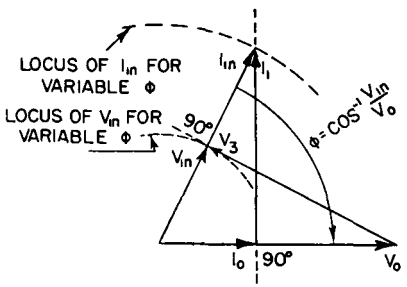

FIG. 5.8

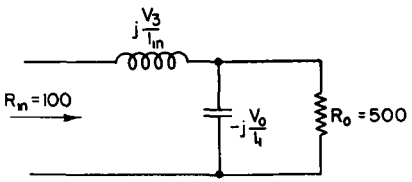

FIG. 5.9

value of ϕ where two reactive elements suffice to solve the problem, as shown in Fig. 5.9.

Where ϕ is larger, for the T case, the diagram becomes that shown in

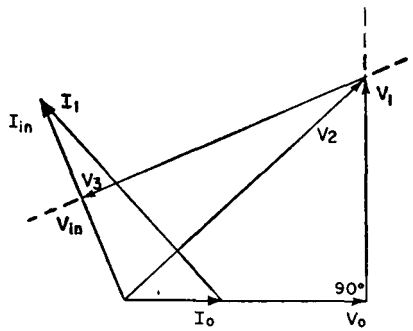

FIG. 5.10

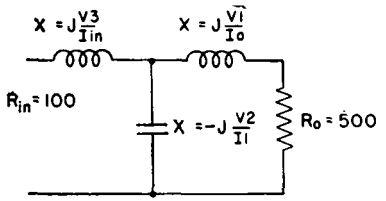

FIG. 5.11

Fig. 5.10. The circuit becomes that shown in Fig. 5.11. Complete curves of reactances for both π and T networks for this transformation as a function of ϕ are reproduced in Figs. 5.12 and 5.13 to show the nature of the variations.

Any impedance-matching problem can be reduced to a type I problem by correcting the power factor of the load or of the generator, when they are other than resistive. This can always be done in either of two ways—by adding series reactance or by adding parallel reactance. The choice

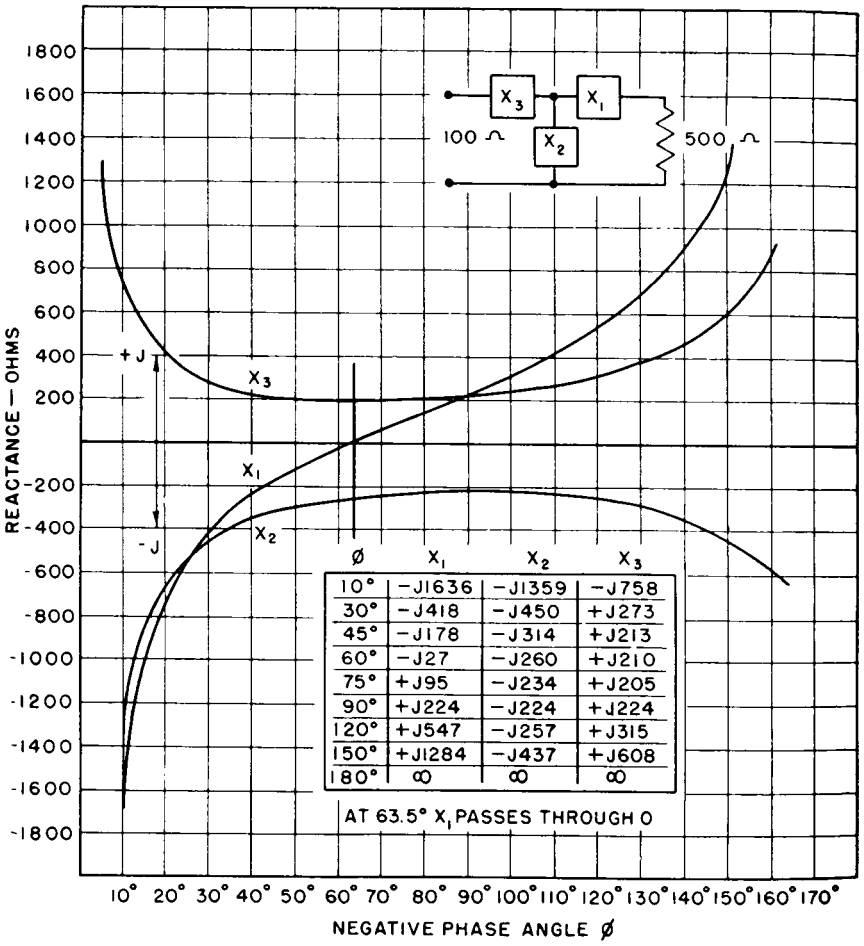

Ø	X_1	X_2	X_3
10°	−J1636	−J1359	−J758
30°	−J418	−J450	+J273
45°	−J178	−J314	+J213
60°	−J27	−J260	+J210
75°	+J95	−J234	+J205
90°	+J224	−J224	+J224
120°	+J547	−J257	+J315
150°	+J1284	−J437	+J608
180°	∞	∞	∞

AT 63.5° X_1 PASSES THROUGH 0

FIG. 5.12

depends upon the relative physical convenience of the ohmic values obtained, whether the desired phase difference is between the currents or the potentials, and the cost or convenience of obtaining the proper reactive components. If a T network is to be used, series power-factor correction of the load impedance or the generator impedance has the advantage that the power-factor-correcting reactors can be combined in value with those found to be necessary from the design synthesis, so that fewer com-

ponents are ultimately required—three instead of four or five. In the same sense, if a π network is chosen, the parallel method of power-factor correction permits the use of three reactive components instead of four or five by combining the power-factor-correcting reactances with those

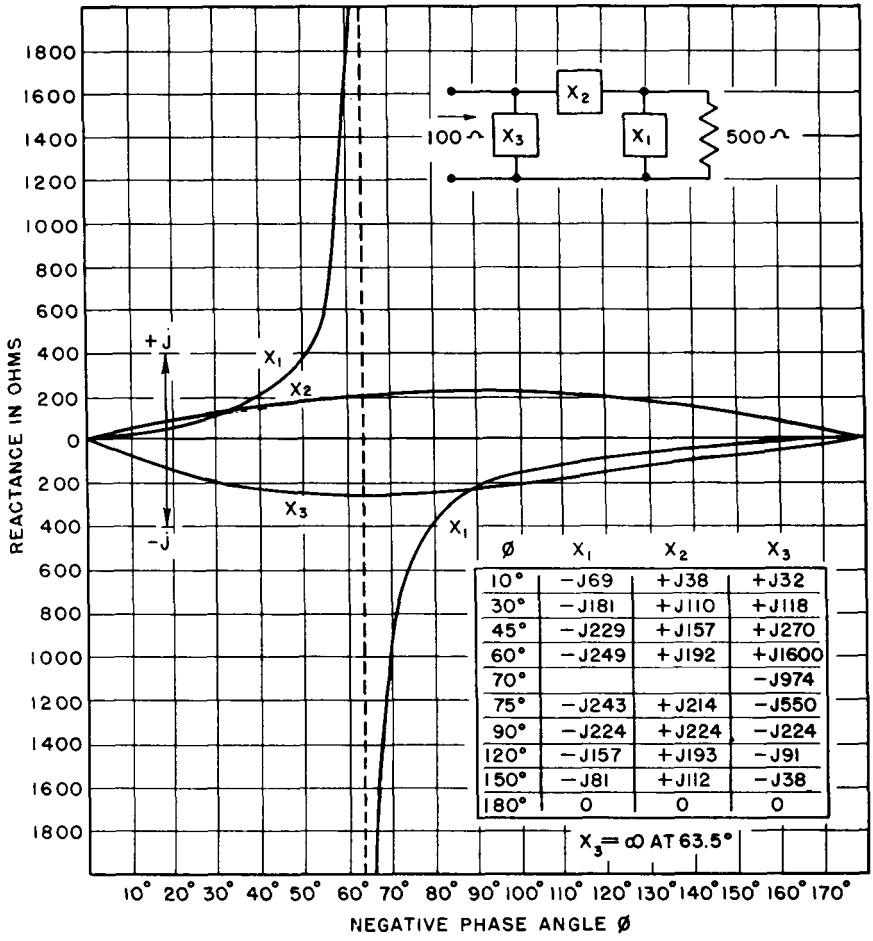

Ø	X_1	X_2	X_3
10°	−J69	+J38	+J32
30°	−J181	+J110	+J118
45°	−J229	+J157	+J270
60°	−J249	+J192	+J1600
70°			−J974
75°	−J243	+J214	−J550
90°	−J224	+J224	−J224
120°	−J157	+J193	−J91
150°	−J81	+J112	−J38
180°	0	0	0

$X_3 = \infty$ AT 63.5°

FIG. 5.13

derived from the network synthesis. This is virtually what is done in the type II problems.

In general, it is always wise to employ network designs requiring the least possible energy storage—that is, the least number of total volt-amperes in all the reactive components. This not only economizes the ratings of the individual components but minimizes the selectivity of the

network. This has special importance whenever the bandwidth to be transmitted exceeds 1 per cent.

The various individual reactances for a network can be made up of lumped capacitance or inductance; or equivalent values of transmission-line sections may be used at frequencies where line sections are preferable.

5.2. Type II Problem

Problem. We desire to couple a load circuit having an impedance of $Z_0 = 75 - j30$ to a circuit which requires a terminating impedance of $Z_{in} = 600 + j150$. The transformation, let us say, must be made with a phase difference between the *load current* and the *input current* of plus 60 degrees. What is the network design required?

Procedure. The problem is set up in vector form first, on the basis that power input equals power output.

Let

$$I_0 = 1.0 \text{ ampere}$$

Then

$$V_{0R} = 75 \text{ volts}$$

and

$$V_{0X} = -j30 \text{ volts}$$

$$V_0 = 81.3 \text{ volts}$$

$$\text{Power in load} = 75 \text{ watts}$$

$$\text{Power input} = 75 \text{ watts}$$

$$V_{in\,R} = \sqrt{75 \times 600} = 222 \text{ volts}$$

$$V_{in\,X} = 0.354 \times j150 = 53 \text{ volts}$$

$$I_{in} = \sqrt{75/600} = 0.354 \text{ ampere}$$

$$V_{in} = 233 \text{ volts}$$

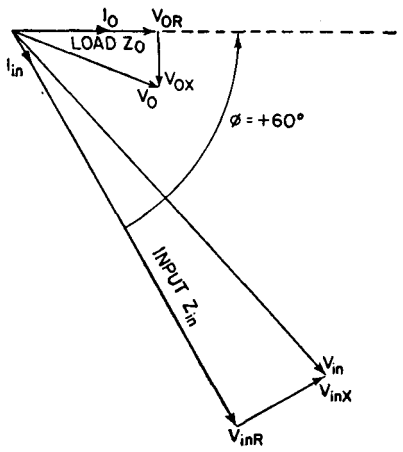

FIG. 5.14

To solve for the network required to make the indicated transformation, complete the vector diagram as shown in Fig. 5.14, and obtain therefrom the nature and magnitude of the required reactances. There is a choice between a π and T network. Let us illustrate by using a T net-

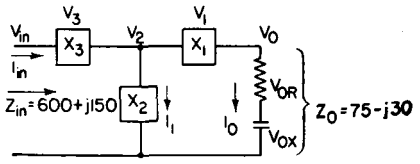

FIG. 5.15

work. Draw the circuit, and label all potentials and currents, as in Fig. 5.15.

$$Z_0 = \frac{V_0}{I_0} = \frac{V_{0R} - jV_{0X}}{I_0}$$

$$Z_{in} = \frac{V_{in}}{I_{in}} = \frac{V_{in\,R} + jV_{in\,X}}{I_{in}}$$

Draw V_1 in a direction perpendicular to I_0, starting at V_0, as shown in Fig. 5.16. Then draw V_3 in a direction perpendicular to I_{in}, through V_{in}. The intersection of these perpendiculars locates the lengths of V_1, V_2, and V_3. Draw V_2 from the origin to the intersection. As a check on accuracy, measure the angle between I_1 and V_2—it should be 90 degrees. As

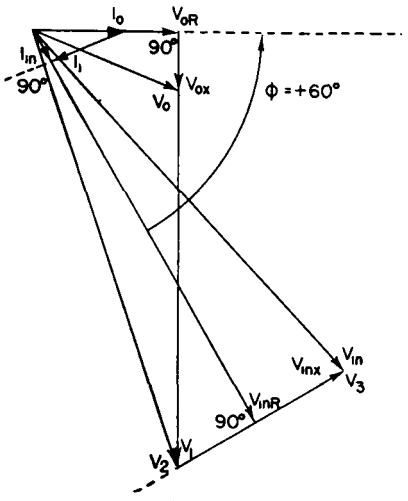

FIG. 5.16

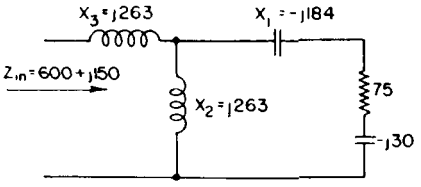

FIG. 5.17

before, I_1 is drawn to connect I_0 and I_{in}. From the scales of Fig. 5.15

$V_0 = 81$ volts $\quad I_0 = 1.0$ ampere
$V_1 = 184$ volts $\quad I_1 = 0.875$ ampere
$V_2 = 230$ volts $\quad I_{in} = 0.354$ ampere
$V_3 = 93$ volts
$V_{in} = 233$ volts

$$X_1 = \frac{V_1}{I_0} = \frac{184}{1.0} = -j184 \text{ ohms}$$

$$X_2 = \frac{V_2}{I_1} = \frac{230}{0.875} = j263 \text{ ohms}$$

$$X_3 = \frac{V_3}{I_{in}} = \frac{93}{0.354} = j263 \text{ ohms}$$

The network becomes that shown in Fig. 5.17.

Solving this same problem on the basis of a π network (Fig. 5.18), we construct Fig. 5.19. Tabulating values from vector scales, we obtain

$$V_0 = 81 \text{ volts} \qquad I_0 = 1.0 \text{ ampere}$$
$$V_1 = 159 \text{ volts} \qquad I_1 = 0.72 \text{ ampere}$$
$$V_{in} = 233 \text{ volts} \qquad I_2 = 1.47 \text{ amperes}$$
$$I_3 = 1.50 \text{ amperes}$$
$$I_{in} = 0.354 \text{ ampere}$$

$$X_1 = \frac{V_0}{I_1} = \frac{81}{0.72} = -j113 \text{ ohms}$$

$$X_2 = \frac{V_1}{I_2} = \frac{159}{1.47} = -j108 \text{ ohms}$$

$$X_3 = \frac{V_{in}}{I_3} = \frac{233}{1.5} = j155 \text{ ohms}$$

The circuit becomes that of Fig. 5.20.

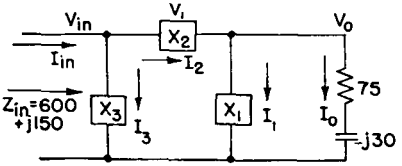

FIG. 5.18

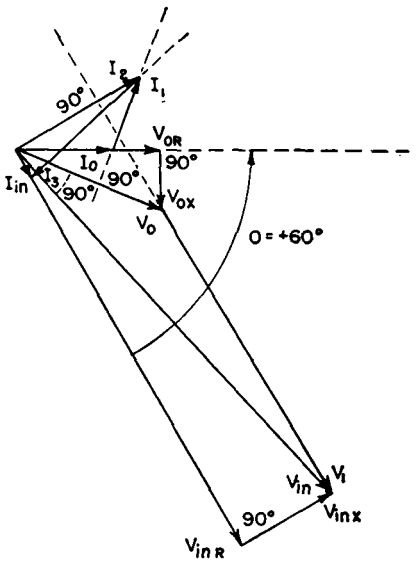

FIG. 5.19

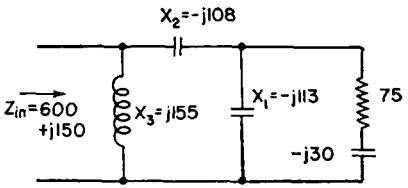

FIG. 5.20

5.2.1. Extreme Case of a Type II Problem

Problem. Calculate the required elements of a network which will make a transformation from 1,500 + $j300$ (load) to 300 − $j400$, so that the potential across the load is in phase with the input potential.

Procedure. Vector statement of this problem is, after resolving the input and load potentials into their resistive and reactive components on the basis of equality of power at input and output, shown in Fig. 5.21 with the scales chosen (for example, 1 inch = 1.0 ampere and 1 inch = 500 volts).

$$V_{in\,R} = \sqrt{1{,}500 \times 300} = 670 \text{ volts}$$

$$I_{in} = \sqrt{\frac{1{,}500}{300}} = 2.24 \text{ amperes}$$

$$V_{in\,X} = 2.24 \times 400 = 893 \text{ volts}$$

$$V_{in} = 670 + j893 = 1{,}118 \text{ volts}$$

This shows V_{in} in phase with V_0 as required, and the relative directions of I_0 and I_{in}. It also is marked to show the potentials and currents prevailing in the load and for the input to the network. From this point, the vector diagram must be completed for either a π or a T network. We shall demonstrate both and compare them.

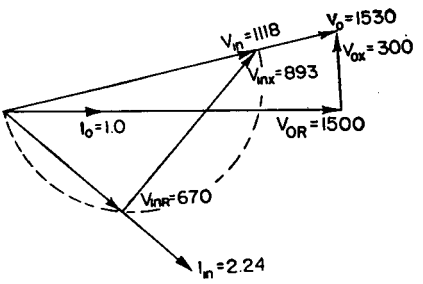

FIG. 5.21

The block diagram of the π network version for this problem is shown in Fig. 5.22. The vector diagram shows that V_0 and V_{in} are in phase. Vectors I_1 and I_3 must both be perpendicular to the direction of V_0 and V_{in}; thus they can never intersect. A solution with a π network is therefore impossible.

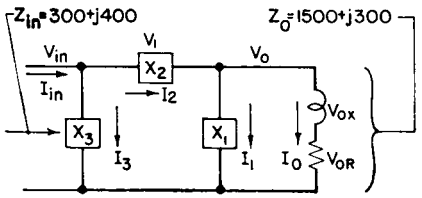

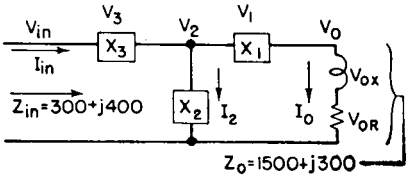

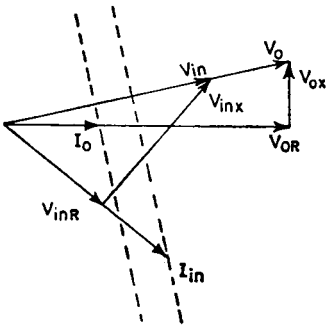

FIG. 5.22

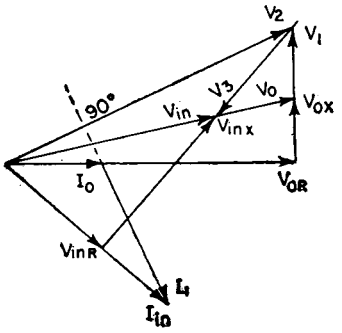

FIG. 5.23

The T network provides a solution for the problem as shown in Fig. 5.23.

$V_0 = 1{,}530$ volts $\quad I_0 = 1.0$ ampere
$V_1 = 364$ volts $\quad I_1 = 1.62$ amperes
$V_2 = 1{,}575$ volts $\quad I_{in} = 2.24$ amperes
$V_3 = 603$ volts
$V_{in} = 1{,}118$ volts

$$X_1 = \frac{V_1}{I_0} = \frac{364}{1.0} = j364 \text{ ohms}$$

$$X_2 = \frac{V_2}{I_1} = \frac{1{,}575}{1.62} = j960 \text{ ohms}$$

$$X_3 = \frac{V_3}{I_{in}} = \frac{603}{2.24} = -j270 \text{ ohms}$$

The network is shown in Fig. 5.24.

NOTE: If the problem had specified that the load and input *currents* be in phase, then a π solution would be possible and the T solution impossible.

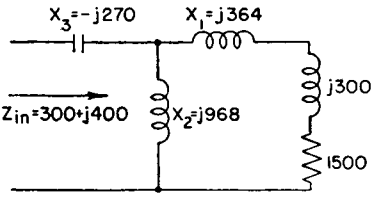

FIG. 5.24

5.3. Type III Problem

Problem. What elements are required for a phase-shifting network which will introduce a phase shift of -120 degrees in a circuit having a characteristic impedance that is 100 ohms resistive?

Procedure. Write the problem vectorially as shown in Fig. 5.25. Because input impedance equals the load impedance, the input is represented by vectors of the same length as for the load, but with the specified phase difference. Then, if we chose a T network (Fig. 5.26), we erect

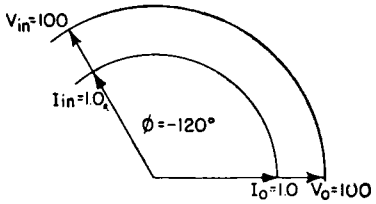

FIG. 5.25

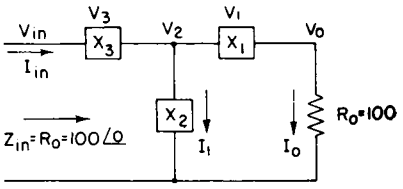

FIG. 5.26

perpendiculars through V_0 and V_{in} and connect I_0 with I_{in} as shown in Fig. 5.27. From this we obtain the solution shown in Fig. 5.28.

Had we chosen the π solution, the vector diagram would have been as shown in Fig. 5.29.

A reversal of the phase angle in any problem reverses the signs of all the elements. For instance, in this problem, if the phase angle had been

+120 degrees, all elements would change from L to C, and vice versa, maintaining the same numerical values.

A phase-shifting network of this type is equivalent to a section of an infinite transmission line having a characteristic impedance R_0 and an electrical length equal to that of the angle of phase shift, which in such cases must be negative. This provides a handy device to study certain properties of lines, such as the 45 degree and the 90 degree sections which

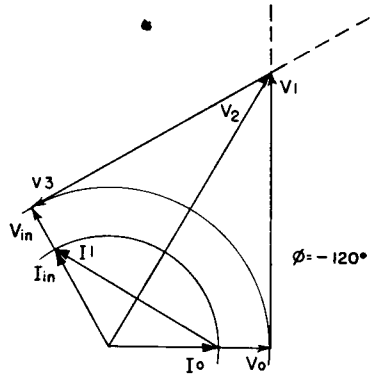

FIG. 5.27

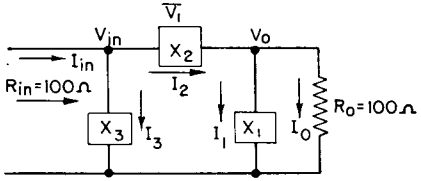

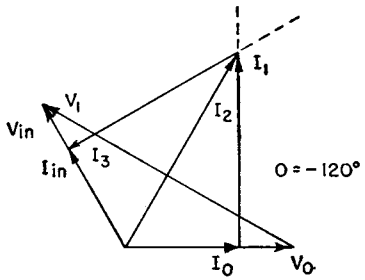

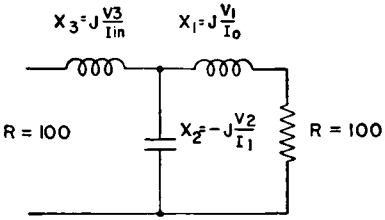

FIG. 5.28

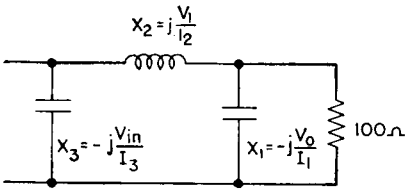

FIG. 5.29

have special properties. For example, how does the input impedance of a 45 degree section of a transmission line change with variation of the terminal resistance from 0 to ∞? Solve for the equivalent single-stage network having a characteristic impedance R_0 when it is terminated in a resistance R_0 by assuming it to be a -45 degree phase-shifting network. (We illustrate with the T network.) The vector diagram is shown in Fig. 5.30. Thus, taking R_0 as unity, we obtain the ratio of all other elements to R_0. We can then assume any value of terminal resistance and calculate the resulting input impedance. We obtain the circuit of Fig. 5.31.

The limiting conditions are quickly examined by assuming open-circuit and short-circuit terminal conditions. For the former, Z_{in} is the sum of $j0.42$ and $-j1.42$, which is $-j1.00$. For the latter, the solution for Z_{in} yields $+j1.00$. So we easily find that Z_{in} remains constant in magnitude for all conditions of resistance termination but varies in character from pure capacitive reactance, through pure resistance to pure inductive reactance as the terminal resistance varies from ∞ to 0.

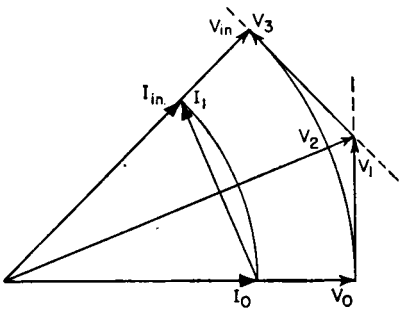

FIG. 5.30

Proceeding in the same manner, the 90-degree network is analyzed.

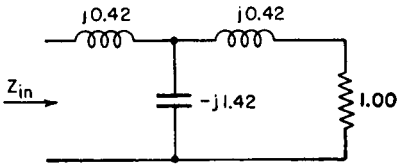

FIG. 5.31

Its special property of impedance inversion is worthy of digression to see why it works as it does. The vector diagram for a -90-degree T network with a characteristic impedance R_0 is given in Fig. 5.32. From this we find the equivalent circuit elements, in terms of R_0, to be those of Fig. 5.33.

All the elements of the network have reactances equal in magnitude to R_0. At this point we can test the circuit for open- and short-circuit terminal conditions and see what happens to Z_{in}. When $R_t = R_0$, $Z_{in} = R_0$. When $R_t = 0$, X_1 and X_2 in parallel give a condition of anti-

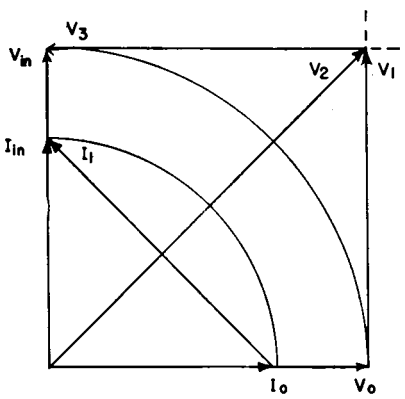

FIG. 5.32

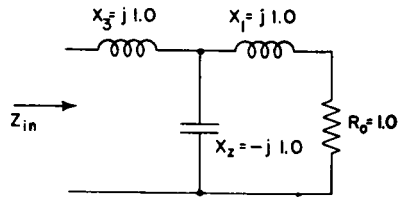

FIG. 5.33

resonance and $Z_{in} = \infty$. When $R_t = \infty$, X_2 and X_3 in series tune to series resonance, making $Z_{in} = 0$. Thus the boundary conditions of impedance inversion in a 90-degree network or transmission-line section are demonstrated.

5.4. Type IV Problem

Problem. Supply two resistance loads with specified potentials in a specified phase relationship from a common generator. Load A is 250 ohms and requires a potential of 800 volts, this potential to lag the generator electromotive force by 90 degrees. Load B is 550 ohms, its

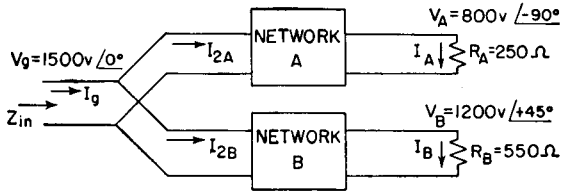

FIG. 5.34

terminal potential must be 1,200 volts, and it must lead the generator electromotive force by 45 degrees. The generator potential is 1,500 volts. What networks are required? What impedance is seen by the generator? The problem is illustrated in Fig. 5.34.

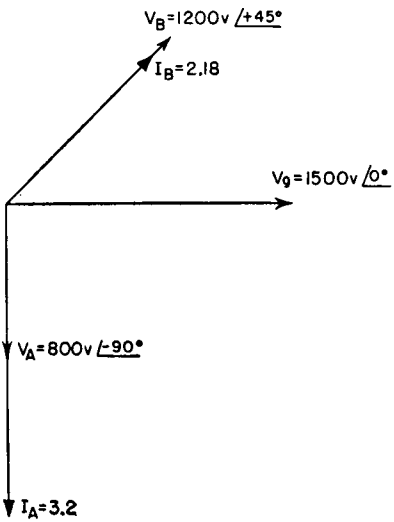

FIG. 5.35

Procedure. Set up the known conditions in the form of a vector diagram of potentials and currents, as in Fig. 5.35. The problem does not specify an input impedance to either network A or network B. If we choose the simplest possible circuit to make the specified potential transformations, we can use a two-element L network for each branch, provided

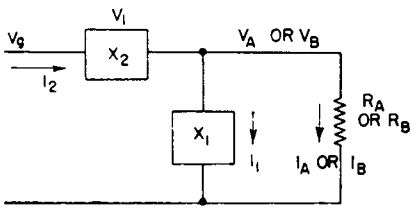

FIG. 5.36

that we are not particular about the power factor of the input impedance. Such a circuit for each branch would be that of Fig. 5.36.

In the vector form of the problem we lack only the potentials for V_1 for each network. We know I_0. We do not know I_1 but know its direction with respect to V_0. We do not know I_2 but know its direction with respect to V_1. We can draw V_1 directly since V_0 and V_g are specified.

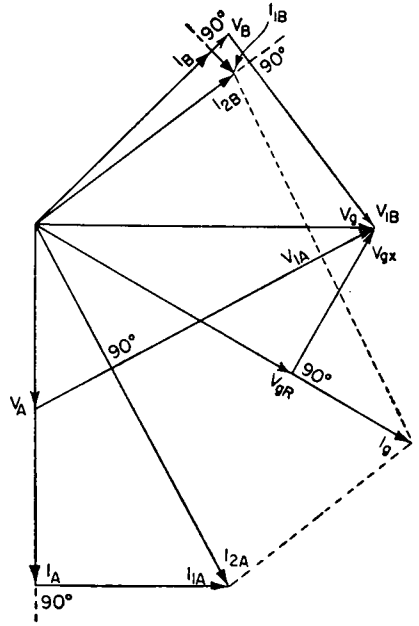

FIG. 5.37

Thus we have enough information to complete the vector diagram of **Fig.** 5.37. This diagram reveals the nature and magnitude of each reactive element, and we obtain

$$\begin{aligned} V_A &= 800 \text{ volts} & I_A &= 3.2 \text{ amperes} \\ V_{1A} &= 1{,}700 \text{ volts} & I_{1A} &= 1.72 \text{ amperes} \\ V_g &= 1{,}500 \text{ volts} & I_{2A} &= 3.6 \text{ amperes} \\ V_{gR} &= 1{,}310 \text{ volts} & I_B &= 2.18 \text{ amperes} \\ V_{gX} &= 700 \text{ volts} & I_{1B} &= 0.28 \text{ ampere} \\ V_B &= 1{,}200 \text{ volts} & I_{2B} &= 2.19 \text{ amperes} \\ V_{1B} &= 1{,}058 \text{ volts} & I_g &= 3.9 \text{ amperes} \end{aligned}$$

$$X_{1A} = \frac{V_A}{I_{1A}} = \frac{800}{1.72} = -j465 \text{ ohms}$$

$$X_{2A} = \frac{V_{1A}}{I_{2A}} = \frac{1{,}700}{3.6} = j472 \text{ ohms}$$

$$X_{1B} = \frac{V_B}{I_{1B}} = \frac{1{,}200}{0.28} = j4{,}290 \text{ ohms}$$

$$X_{2B} = \frac{V_{1B}}{I_{2B}} = \frac{1{,}058}{2.19} = -j483 \text{ ohms}$$

The input impedance to the two networks in parallel is V_g/I_g, where I_g is the vector sum of I_{2A} and I_{2B}. The two series components of the

input impedance are

$$Z_{in} = R_{in} + jX_{in}$$

where

$$R_{in} = \frac{V_{gR}}{I_g} = \frac{1{,}310}{3.9} = 336 \text{ ohms}$$

$$X_{in} = \frac{V_{gX}}{I_g} = \frac{700}{3.9} = j180 \text{ ohms}$$

The entire circuit required to satisfy the problem is shown in Fig. 5.38.

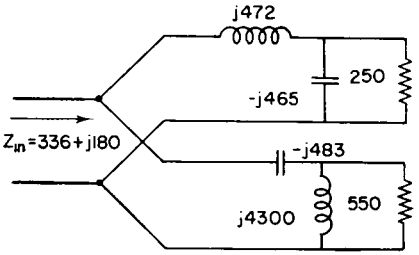

FIG. 5.38

In a similar manner problems having a multiplicity of loads fed in any specified amplitudes and phases of potentials can be solved readily. Some examples of what can be done in this same simple procedure are given herewith.

The following problem represents a special case of potential transformation with two equal loads for *changing from a single-end generator to a balanced (push-pull) load.*

Problem. It is desired to feed two 250-ohm loads in push-pull with 500 volts across each resistance from a single-end generator having a terminal potential of 300 volts. What network is required, and what impedance is presented to the generator?

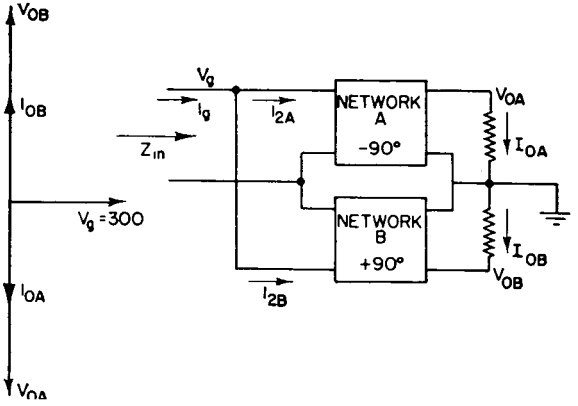

FIG. 5.39

Procedure. Set up vectors representing the desired potentials at 180 degrees for the load, and draw the vector for the generator potential at 90 degrees to each of the load potentials. Thus we have stated the problem vectorially, as shown at the left of Fig. 5.39.

The choice of the direction of V_g at 90 degrees to the load potentials is arbitrary. It could be any angle between the two. The 90-degree choice, however, has symmetry which is usually desirable.

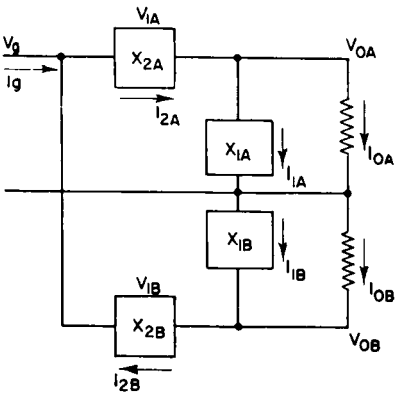

FIG. 5.40

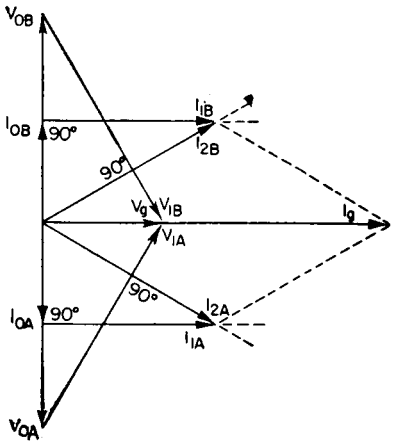

FIG. 5.41

On the basis of L networks, we complete the vector diagram to obtain the desired information, as in the previous problem. The usual elementary considerations provide the basis for this procedure, from which we get Fig. 5.40 and Fig. 5.41. Tabulating vector lengths,

$$
\begin{aligned}
V_{0A} &= 500 \text{ volts} & I_{0A} &= 2.0 \text{ amperes} \\
V_{1A} &= 585 \text{ volts} & I_{1A} &= 3.28 \text{ amperes} \\
V_g &= 300 \text{ volts} & I_{2A} &= 3.84 \text{ amperes} \\
V_{0B} &= 500 \text{ volts} & I_{0B} &= 2.0 \text{ amperes} \\
V_{1B} &= 585 \text{ volts} & I_{1B} &= 3.28 \text{ amperes} \\
& & I_{2B} &= 3.84 \text{ amperes} \\
& & I_g &= 6.65 \text{ amperes}
\end{aligned}
$$

$$Z_{in} = \frac{V_g}{I_g} = \frac{300}{6.65} = 45 \text{ ohms} \qquad \text{(resistive)}$$

$$X_{1A} = \frac{V_{0A}}{I_{1A}} = \frac{500}{3.28} = 152\ (-j) \text{ ohms}$$

$$X_{2A} = \frac{V_{1A}}{I_{2A}} = \frac{585}{3.84} = 152\ (+j) \text{ ohms}$$

X_{1B} = same as X_{1A} except sign = 152 $(+j)$ ohms

X_{2B} = same as X_{1B} except sign = 152 $(-j)$ ohms

These values yield the circuit shown in Fig. 5.42.

5.5. Calculation of Circuit Losses

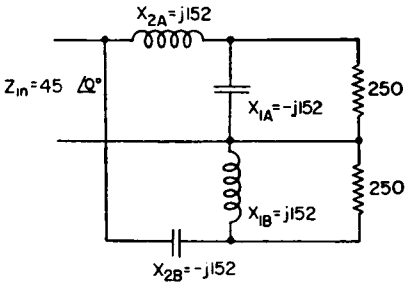

FIG. 5.42

In solving for the reactance required in a network of given performance, the choice of potential and current values at the beginning of the problem is immaterial and determined by convenience only. For definite design applications, however, it may be best to work the problem with potential and current values corresponding to the power expected in reality. The values derived from the completed vector diagram then not only provide the necessary network solution but show the currents and potentials existing at all points in the circuit. On this basis, the power loss and circuit efficiency can be computed with little effort, provided that the dissipation factors (Q's) of the reactive elements are known approximately. The vector diagrams are worked out on the assumption that the reactive elements are lossless. Unless the Q of a reactance is less than 20, this is correct enough for drawing the diagrams. Finally, to determine the losses which were previously neglected, it is necessary only to calculate the energy in each reactance by multiplying the potential across it by the current through it. This reactive energy in volt-amperes, divided by the Q of the reactance, gives the power loss in watts for the element. With synthesis made easy, many networks can be examined with the view of obtaining minimum energy storage and therefore minimum circuit loss.

5.6. Generalized Case of Impedance Transformation

Any four-terminal network whose output power is equal to its input power must be composed of pure reactances. This was the basis of reasoning in all the preceding problem solutions.

It is of some academic value to look at the case where this power equality is not specified. Let us choose a scale of vectors for a given load impedance, and make a specified impedance transformation without equating input and output powers. This is possible since an impedance is merely a *ratio* of a potential to a current. In the preceding problems, we always solved for those particular values which not only gave the correct ratio but also represented the same power. We need discuss the present case only qualitatively to show that, instead of pure reactances, the network elements may be complex and that there are an infinite number of solutions possible.

Let us transform a low value $Z_0 = R_0 - jX_0$ to a large value

$$Z_{in} = r_{in} + jX_{in}$$

with random phase shift (Fig. 5.43). We start from the load as before and set up a vector statement of the problem at that point. We do the same for the input impedance, including phase angle between input and output potentials or currents, as shown in Fig. 5.44. The original problem is written vectorially in solid lines. The unknown current is I_1 (Fig. 5.43), which must connect I_0 with I_{in}. We draw this immediately. But when it comes to determining V_1 and V_3, we find an infinite

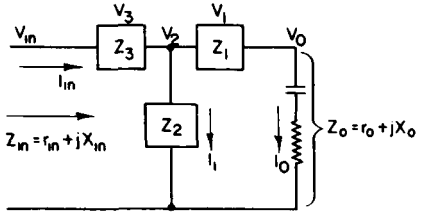

FIG. 5.43

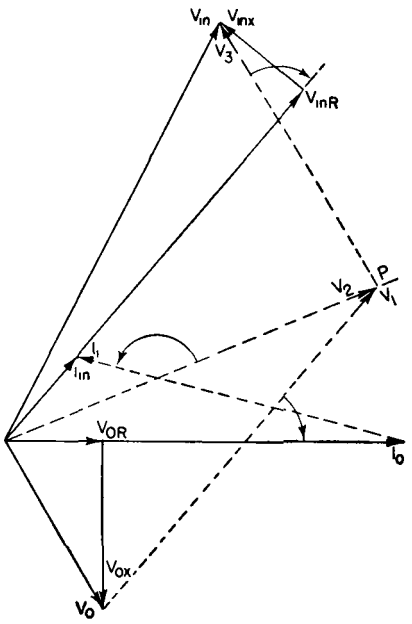

FIG. 5.44

number of choices. Let us select a point P at random, anywhere in the entire plane of the diagram. Completing the diagram through P, we obtain

$$Z_1 = \frac{V_1}{I_0} = R + jX$$

where V_1 leads I_0 less than 90 degrees,

$$Z_2 = \frac{V_2}{I_1} = -R - jX$$

where I_1 leads V_2 more than 90 degrees, and

$$Z_3 = \frac{V_3}{I_2} = R + jX$$

where V_3 leads I_{in} less than 90 degrees.

5.7. Single-phase to Polyphase Transformations

To derive a system of balanced three-phase potentials from a constant-frequency single-phase generator, all that is required is to consider the

original source as one of the phases. The second phase is derived from the original source by connecting it to a 1-to-1 phase-shifting network with a phase shift of -120 degrees and terminated by a resistance R. The third phase is derived in the same manner by bridging the source with a second phase-shifting network with a phase shift of $+120$ degrees, with a 1-to-1 ratio, and terminated in the same value of resistance R. If the

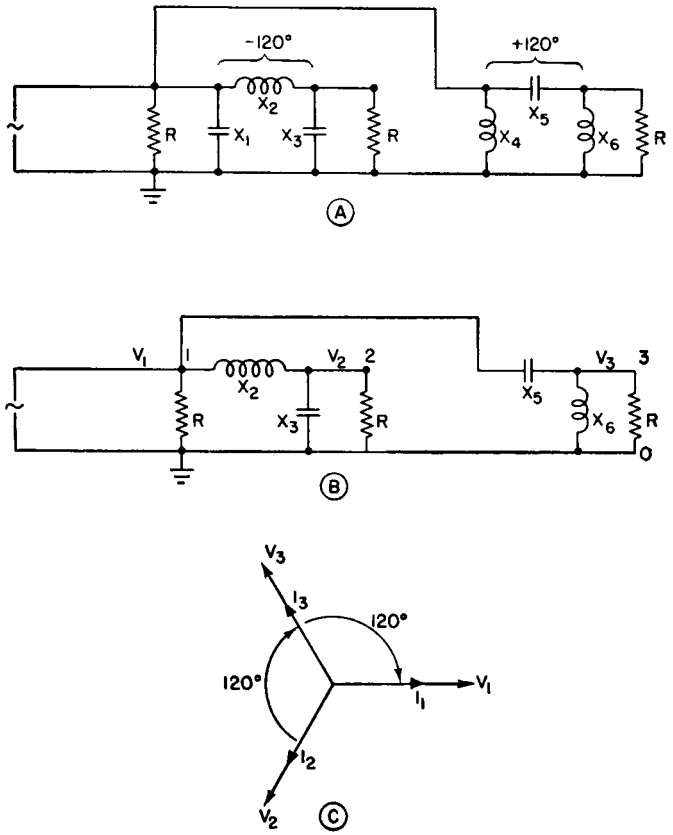

FIG. 5.45

original source has also a resistance R directly across it as the load for the first phase (see Fig. 5.45*A*), the potentials across all three resistors will be equal in magnitude and at successive 120-degree angles. As shown, one side of each resistor is common, so that the balanced three-phase Y arrangement is obtained, as represented in Fig. 5.45*C*.

The circuit of Fig. 5.45*B* is the same as that of Fig. 5.45*A* after taking into account the fact that $X_4 = X_1$. Since both reactances are directly in parallel, they mutually become infinite in impedance owing to anti-

resonance and are eliminated from the real circuit. The other elements are unchanged in value.

If a delta three-phase connection be desired, the resistors R can all be removed and three other resistors with a value R_1 can be substituted but connected, respectively, between points 1 and 2, 2 and 3, and 3 and 1. To maintain correct loadings equivalent to R of the Y arrangement, for which the design was derived, $R_1 = 3R$.

It is evident from the preceding examples that, with networks of this type having fixed values for the reactances, the phase shift will vary with any deviations from the value R which terminates each phase. Therefore, true balanced three-phase potentials are dependent upon the load resistances for each phase remaining constant at the value for which the networks were designed.

It is apparent that other polyphase relations may be derived by the same principle. In fact, any number of vectors at any angle and with any magnitude can be developed from the single-phase source by employing paralleled or cascaded networks of the proper phase shift and transformation ratio, each terminated in some preselected value of resistance, according to the desired power division among the loads.

The design of a feeder system for a multielement directive antenna of the type so frequently required for medium-frequency broadcasting stations is in fact the design of a single-phase to polyphase network, the number of phases being determined by the number of radiators that are to be fed. The relative phases of the currents in the several radiators have to be derived from a common single-phase generator, which is usually the main feeder, or sometimes the transmitter itself.

In general, the impedances of the inputs to the several radiators, when the system is performing correctly so as to obtain the specified radiation pattern, are unequal. Therefore, the power transmitted through each phase to its associated radiator is different from that in the others. The feeder system as a whole is for that reason an unbalanced polyphase circuit, unbalance meaning that the phase relations may be unsymmetrical and the powers in the several phases unequal.

It is evident that the excitation for any one phase can be derived from any other phase instead of connecting every phase directly across the main source. The impedance-matching and the power-dividing networks can be distributed along a series of transmission lines running from radiator to radiator instead of bringing separate transmission lines from each radiator to the transmitter. Both methods are used, the choice being one of cost and convenience. The individual-feeder method may often be preferred when switching is required to change the pattern for a multielement array, as is often done for day and night operation.

CHAPTER 6

Logarithmic-potential Theory

Logarithmic potentials have been mentioned frequently in the previous chapters of this book and have been used to obtain essential design information for antennas and transmission lines. The logarithmic-potential method of calculating various antenna and transmission-line parameters is an invaluable tool for the antenna engineer. With it, he can calculate quickly, and with sufficient accuracy, problems that would otherwise cost him enormous amounts of time and labor.

All students of electrophysics are familiar with logarithmic-potential theory, but as customarily taught it is associated entirely with electrostatic theory. By the straight electrostatic method, the computations for engineering usage are unnecessarily complicated. In engineering one may take advantage of certain well-known dynamic relationships which, at a certain point in the work, lead to valuable direct approaches to the desired answers. In the method to be described,* electrostatic principles are used only for writing the potential equations due to the charges on a system of cylindrical conductors that are parallel to a perfectly conducting plane called the "ground" or "image" plane. After the potential equations have been written and condensed to a compact form, use is made immediately of the dynamic concept of the characteristic impedance of a transmission line expressed in terms of its capacitance per unit length and the velocity of propagation of transverse electromagnetic waves in the system. From then on, in one step one has found the formula for the capacitance per unit length of the system and in the next step the characteristic-impedance formula.

Another dynamic relationship that is employed directly is that which exists between the charge and current. This relationship is as follows: The current I flowing in a wire is related to the charge per unit length Q on the wire by

$$I = vQ$$

Therefore in any system where v is constant, the current is directly proportional to the charge per unit length. This permits one to interpret charge ratios directly as current ratios.

* Due to Brown, ref. 28, p. 488.

The meter-kilogram-second system of units and common logarithms are used, which accounts for the numerical coefficients that appear in all equations. The charge per unit length Q is in coulombs per meter on each conductor, identified by subscript for the conductor of that number and by double subscript for its image charge, which is always of the opposite sign of the charge on the conductor. In order to apply to each logarithmic term the sign of the real or image charge under consideration, reciprocal distances are used for all linear distances from the axes of the conductors. This avoids the problem of signs, because the sign of the logarithm of a reciprocal of a distance will then always be the same as that of the charge from which this distance is measured—otherwise, it would always have the opposite sign. Furthermore, we shall take advantage of the fact that a transmission line of low loss, which includes almost all practical radio-frequency lines, has a characteristic impedance $Z_0 = \sqrt{L/C}$, and since $v = 1/\sqrt{LC}$, $Z_0 = 1/vC$. The velocity of propagation v for air-dielectric systems has the value 3×10^8 meters per second. The capacitance per unit length is defined in the usual way as the charge per unit length divided by the potential difference, Q/V.

The symbols used will have the following meanings:

Q = root-mean-square charge, coulombs per meter
X = constant derived from an indefinite integral
V_1 = root-mean-square potential, volts (with respect to ground), on conductor 1, etc.
k = charge ratio less than unity
K = charge ratio greater than unity
Z_0 = characteristic impedance, ohms
C = capacitance, farads per meter
v = propagation velocity, meters per second
ρ = radius of the conductor in the same units as the other cross-section dimensions
a, b, c, etc. = center-to-center spacings between various conductors
h = height, or in some cases mean height, of the conductor(s) above the image plane
r_1, r_2, r_3, etc. = distances from the conductors, 1, 2, 3, etc., to a point in space
r_{11}, r_{22}, etc. = distances from images of conductors 1, 2, etc., to a point in space

All cross-sectional dimensions must be in the same units (inches or centimeters), and the ground is assumed to be perfectly conducting.

6.1. One Wire above Ground

The simplest case to study is that of a single elevated wire parallel to ground (Fig. 6.1). The potential on the wire, in terms of its charge per meter, is written

$$V_d = \left(138vQ \log_{10} \frac{1}{\rho}\right) + x$$

The induced potential on the wire due to its image is

$$V_i = -\left[\left(138vQ \log_{10} \frac{1}{2h}\right) + x\right]$$

The total potential on the wire is the sum of these direct and induced potentials.

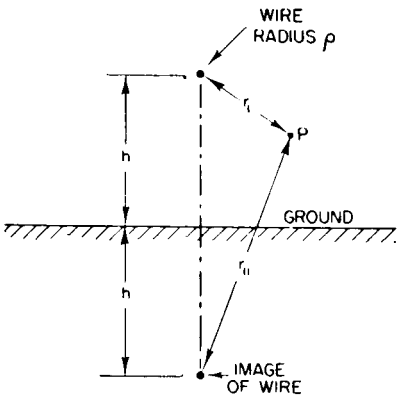

FIG. 6.1

$$V = 138vQ\left[\left(\log_{10} \frac{1}{\rho}\right) + x - \left(\log_{10} \frac{1}{2h}\right) - x\right] = 138vQ \log_{10} \frac{2h}{\rho}$$

In taking the ratio the unknown integration constant x is eliminated. The reciprocal capacitance is

$$\frac{1}{C} = \frac{V}{Q} = 138v \log_{10} \frac{2h}{\rho}$$

The characteristic impedance for this wire is

$$Z_0 = \frac{1}{vC} = 138 \log_{10} \frac{2h}{\rho}$$

In this way the circuital characteristics of the wire system are derived directly from the cross-sectional dimensions of the system, and from now on it can be handled as a typical circuit element. We understand the characteristic impedance to apply to a circuit which is a wire of infinite length in which charges are propagated only in one direction. If reflections exist on the system, the impedance of the wire as a circuit can then be treated by transmission-line theory and derived from its value Z_0.

There are many applications where it is necessary to find the potentials in space in the region of a transmission line, and we may wish to locate the equipotential lines. The electric lines of force are everywhere normal to these equipotential lines. From such calculations the potential gradients can be computed.

For this single-wire line, the potential at a point P in space in the region

of the wire is obtained exactly as before, except that the point at which the potential is calculated, which previously was on the surface of the wire, is now some distance from it. The equations are then written

$$V_{pd} = 138vQ \log_{10} \frac{1}{r_1} + x$$

$$V_{pi} = -\left(138vQ \log_{10} \frac{1}{r_{11}} + x\right)$$

$$V_p = V_{pd} + V_{pi} = 138vQ \log_{10} \frac{r_{11}}{r_1}$$

Then

$$\frac{V_p}{V} = \frac{\log_{10} \frac{r_{11}}{r_1}}{\log_{10} \frac{2h}{\rho}}$$

From this equation the equipotential lines can be completely located and potential gradients found.

In the following developments the same general philosophy applies so that at the outset we can omit the integration constant x in writing the potential equations since it will always fall out when we arrive at the point of taking the ratios in which we are primarily interested and from which all the essential information is derived.

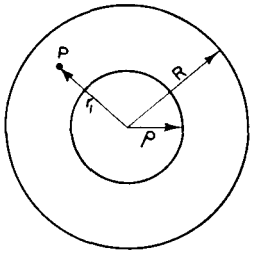

FIG. 6.2

Another application of basic simplicity is the derivation of the characteristic impedance, the capacitance per unit length, and the field distribution for a concentric line (Fig. 6.2).

In this case the potential on the inner conductor due to its own charge is, after omitting the integration constant x,

$$V_\rho = 138vQ \log_{10} \frac{1}{\rho}$$

These charges set up a potential at the inside surface of the outer conductor which is

$$V_R = 138vQ \log_{10} \frac{1}{R}$$

The image charges on the inner surface of the outer conductor set up a field which will reduce the total potential on its surface to zero. This is the same as equating V_R to zero. After this step, we proceed as before

and obtain

$$V_\rho - V_R = 138vQ \log_{10} \frac{R}{\rho}$$

Since

$$V_R = 0$$

$$V_\rho = 138vQ \log_{10} \frac{R}{\rho}$$

$$\frac{1}{C} = \frac{V_\rho}{Q} = 138v \log_{10} \frac{R}{\rho}$$

$$Z_0 = \frac{1}{vC} = 138 \log_{10} \frac{R}{\rho}$$

At a point P in the dielectric space between conductors, the potential will be the same as if the radius of the inner conductor were increased to the value r_1, the distance of the point P from the axis. Therefore we can substitute V_p for V_ρ and write

$$V_p = 138vQ \log_{10} \frac{R}{r_1}$$

Then

$$\frac{V_p}{V_\rho} = \frac{\log_{10} \frac{R}{r_1}}{\log_{10} \frac{R}{\rho}}$$

6.2. Two-wire Balanced Transmission Line

The wire potentials are always with respect to ground, or zero potential. A balanced two-wire line has two parallel wires of radius ρ, spaced a distance a and located at a height h above ground. The potential between wires is twice that of each wire to ground. The calculation of the capacitance, the characteristic impedance, and the field equipotential surfaces proceeds in this case as follows (see Fig. 6.3):

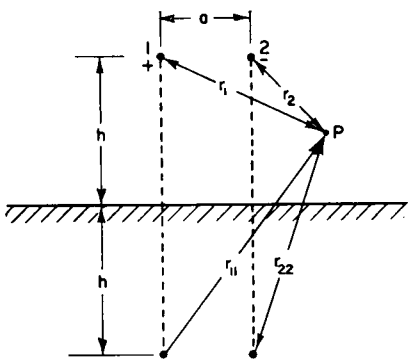

FIG. 6.3

The potential of wire 1 is written

$$V_1 = 138vQ \left(\log_{10} \frac{1}{\rho} - \log_{10} \frac{1}{2h} - \log_{10} \frac{1}{a} + \log_{10} \frac{1}{\sqrt{4h^2 + a^2}} \right)$$

$$= 138vQ \log_{10} \frac{2ha}{\rho \sqrt{4h^2 + a^2}}$$

and for wire 2, $V_2 = -V_1$. Then

$$\frac{1}{C} = \frac{2V_1}{Q} = 276v \log_{10} \frac{2ha}{\rho \sqrt{4h^2 + a^2}}$$

and so

$$Z_0 = \frac{1}{vC} = 276 \log_{10} \frac{2ha}{\rho \sqrt{4h^2 + a^2}}$$

When $h \gg a$,

$$Z_0 \rightarrow 276 \log_{10} \frac{a}{\rho}$$

It is evident from this development that when the height is very large with respect to the wire spacing the effect of the presence of ground becomes negligible and the line may be considered to be in free space.

The electric field around a balanced line parallel to ground can be completely calculated in the following way:

The potential at a point P in space is the sum of the potentials from the two wires and their images. This gives

$$\begin{aligned} V_P &= 138vQ \left(\log_{10} \frac{1}{r_1} - \log_{10} \frac{1}{r_{11}} - \log_{10} \frac{1}{r_2} + \log_{10} \frac{1}{r_{22}} \right) \\ &= 138vQ \log_{10} \frac{r_{11}r_2}{r_1 r_{22}} \end{aligned}$$

In terms of the potential at the surface of wire 1

$$\frac{V_P}{V_1} = \frac{\log_{10} \dfrac{r_{11}r_2}{r_1 r_{22}}}{\log_{10} \dfrac{2ha}{\rho \sqrt{4h^2 + a^2}}}$$

When a two-wire balanced transmission line is far enough removed from ground so as to be considered to be in free space, r_{11} and r_{22} are eliminated and the field can be plotted from the relation

$$\frac{V_P}{V_1} = \frac{\log_{10} \dfrac{r_2}{r_1}}{\log_{10} \dfrac{a}{\rho}}$$

A field map derived from this equation is shown in Fig. 6.4. It is instructive to examine this map to determine what additional information it can yield. The equipotential lines are plotted at intervals corresponding to 10 per cent of the wire potentials, which are actually confocal cylindrical surfaces enclosing the charged wires. As the potential

in space approaches zero, the cylinders become larger, until when the potential is zero their radii are infinite. This makes the zero-potential surface a flat plane midway between the wires. The fields each side of this plane are mirror images of each other and have reversed polarities.

According to the principles of electrostatics, any equipotential surface in space can be replaced by a coincident metallic surface without disturbing the field in any way. If this metallic surface is closed, and its charge is on the outer surface, the external field is undisturbed but the

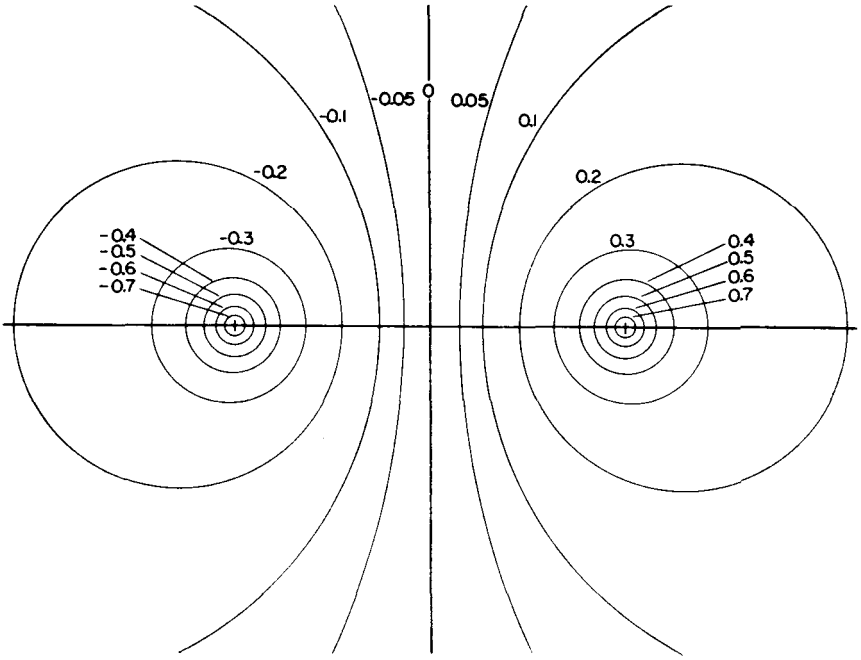

FIG. 6.4

internal field vanishes. In this particular case where the equipotential surfaces are cylinders it would be physically practical to substitute a metallic cylinder for those shown in the map. Remembering that $C = Q/V$ and therefore that $Z_0 = V/vQ$, one can read from the map the relative capacitance C_{00}/C_0 per unit length and the relative characteristic impedance Z_{00}/Z_0 in proportion to the values for which the map was originally plotted, for any combination of two cylindrical conductors lying on the equipotential lines shown. Figure 6.4 was plotted for a 600-ohm balanced transmission line. The contours higher than 0.7 of the wire potential cannot be legibly shown for the scale selected for this figure.

The confocal circles of this figure represent one of the simplest field

configurations. If the zero-potential plane is taken to be ground, the field on one side can be that of a single-wire transmission line with a characteristic impedance of 300 ohms.

Let a transmission line be formed by conductors lying on the equipotential surfaces 0.7 and -0.7 of Fig. 6.4. The original conductors forming the 600-ohm line lie on the surfaces 1.0 and -1.0 (not shown), so that their total potential difference is 2.0. For the 0.7 surfaces, the total potential difference becomes 1.4. Since the propagation velocity and the charge per unit length are constant for this map, the characteristic impedance Z_{00} for the two conductors on the 0.7 surfaces can be found from the relation

$$Z_{00} = 0.7 \times 600 = 420 \text{ ohms}$$
$$C_{00} = \frac{C_0}{0.7} = 1.43C_0$$

The field between these two conductors remains unchanged by this substitution. The field inside each of the two cylindrical conductors vanishes.

Next consider a balanced transmission line composed of two cylindrical conductors of unequal radii, one lying on the 0.5 line of Fig. 6.4 and the other on the -0.3 line. The potential difference is now 0.8. For this arrangement

$$Z_{00} = \frac{600 \times 0.8}{2} = 240 \text{ ohms}$$

Then consider the eccentric transmission line formed by one cylinder lying on the 0.5 line and the other enclosing it with its inner surface on the 0.2 line. Their potential difference is 0.3, and

$$Z_{00} = \frac{600 \times 0.3}{2} = 90 \text{ ohms}$$

The same kind of analysis applied to any equipotential field map will yield similar information, but the equipotential surfaces usually do not have shapes which are easily obtained practically, such as the cylinders which result from this particular map.

6.3. Systems in Which One or More of the Conductors Are Grounded

Unbalanced lines employing both high-potential and grounded wires, all parallel to ground, can be computed by equating the potentials on the grounded wires to zero. In such cases another step of procedure is necessary to solve for the charge ratios among the various wires and the ground

charge, since in practical systems of this type there is always some stray capacitance direct from the high-potential wires to ground, as well as to the grounded wire(s).

To illustrate the procedure, consider a six-wire unbalanced line having the sectional geometry of Fig. 6.5. The two middle wires on each side are in parallel at high potential. The four outer wires located at the corners of a square are grounded. The configuration is located at an average height h which is sufficiently large with respect to a to allow the convenience of employing a constant value of h for all the wires with negligible numerical error.

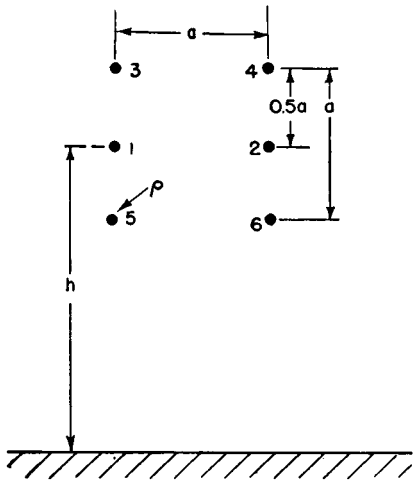

FIG. 6.5

We see that there is symmetry to this problem, which makes evident at once that the charges on the wires on the left will be the same as for those on the right. If h is sufficiently large with respect to a, as assumed and as justified in the majority of practical applications, there will be symmetry of charge distribution across the upper and lower halves of the configuration. In other words, the total ground-wire charge will be equally divided among the four grounded wires. From these considerations the potential equations are written as follows: For the two high-potential wires 1 and 2,

$$V_1 = V_2 = 138v\left[Q_1\left(\log_{10}\frac{2h}{\rho} + \log_{10}\frac{2h}{a}\right) + Q_2\left(2\log_{10}\frac{2h}{0.5a} + 2\log_{10}\frac{2h}{\sqrt{a^2 + 0.25a^2}}\right)\right]$$

$$= 138vQ_1\left(\log_{10}\frac{4h^2}{a\rho} + \frac{2Q_2}{Q_1}\log_{10}\frac{4h^2}{0.5a^2\sqrt{1.25}}\right)$$

For the four grounded wires 3, 4, 5, and 6,

$$V_3 = V_4 = V_5 = V_6 = 138v\left[Q_1\left(\log_{10}\frac{2h}{0.5a} + \log_{10}\frac{2h}{a\sqrt{1.25}}\right) + Q_2\left(\log_{10}\frac{2h}{\rho} + 2\log_{10}\frac{2h}{a} + \log_{10}\frac{2h}{a\sqrt{2}}\right)\right] = 0$$

or

$$V_3 = 138vQ_1\left(\log_{10}\frac{4h^2}{0.5a^2\sqrt{1.25}} + \frac{Q_2}{Q_1}\log_{10}\frac{16h^4}{\rho a^3\sqrt{2}}\right) = 0$$

Solving for the ratio

$$\frac{Q_2}{Q_1} = -\frac{\log_{10}\dfrac{4h^2}{0.5a^2\sqrt{1.25}}}{\log_{10}\dfrac{16h^4}{\rho a^3\sqrt{2}}} = k$$

Making this substitution in the first equation permits the desired information to be derived. Since Q_1 is the charge on *one* high-potential wire and Q_2 the charge on *one* grounded wire, the characteristic impedance becomes (using the manipulations previously employed and remembering that there are two high-potential wires in parallel),

$$Z_0 = 69\left(\log_{10}\frac{4h^2}{a\rho} + 2k\log_{10}\frac{4h^2}{0.5a^2\sqrt{1.25}}\right)$$

It is always of importance to know the ratio of the return current in the grounded wires to the current in the high-potential wires. In this example, where there are four grounded wires each with charge Q_2 and two high-potential wires each with charge Q_1, the total charge ratio on the wires (and therefore the current ratio) will be $4Q_2/2Q_1 = 2k$. Therefore, if I is the total current in the high-potential wires, the total return current in the grounded wires will be $2kI$.

That portion of the total current I which does not return in the grounded wires must return through the ground. Therefore the ground-return current $I_g = I(1 - 2k)$.

6.4. Application to Noncylindrical Conductors

We shall now apply the theory for cylindrical wires to the calculation of empirically shaped conductors. By a series of successive steps, accurate determinations of the capacitance and characteristic impedance can be made for lines made of conductors of any arbitrary shape. In practice one must often use a certain structural member as a transmission line. The calculations are tedious since they sometimes involve sets of several simultaneous equations to solve for the charge ratios. The urgency of the situation would determine the actual need to submit to this procedure. The method is based on the premise that a sufficient number of small wires would eventually assume the complete outline of the empirical surfaces. This process automatically solves the charge-distribution problem over all the surface in terms of those on the discrete wires

assumed in the development. Actually, one need not pursue this development through many steps to have adequate information for extrapolation to the limit and the final result.

An example of this process is the case of two parallel flat strips of half thickness ρ with spacing a, used as a balanced transmission line. The

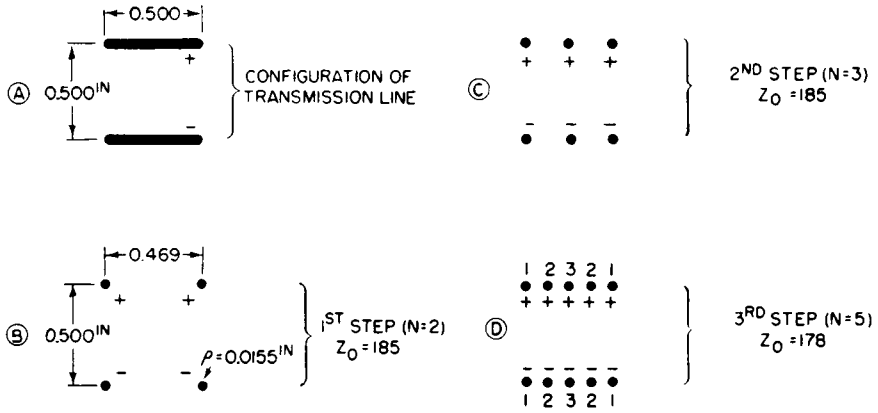

FIG. 6.6

numerical results of each step only are included. The dimensions used are as follows (see Fig. 6.6):

Thickness 0.031 inch (ρ = 0.0155 inch)
Width 0.500 inch
Spacing 0.500 inch between center lines

In step 1, the extremities of each strip are replaced by four wires of diameter equal to the thickness of the strips and having the same outside dimensions. Solving this as a balanced line,

$$Z_0 = 138 \log_{10} \frac{a\sqrt{2}}{\rho} = 227 \text{ ohms}$$

In step 2, another wire is placed midway between each of the above pairs and given the same potentials, and for this step Z_0 = 185 ohms. The charge ratios for step 3 (Fig. 6.6) for the inner wires are found to be $Q_3/Q_1 = 0.418$ and $Q_2/Q_1 = 0.600$. The computed value Z_0 = 178 ohms.

These values can now be plotted in Cartesian coordinates. If we call N the number of wires in one side of the circuit and plot the computed values of Z_0 against $1/N$, as in Fig. 6.7, the ultimate value of a continuous strip of wires conforming to the originally desired flat strips can be found at the intersection of this curve with the value $1/N = 0$. This value is seen to be about 175 ohms.

The process can be applied to complex surfaces such as angles, channels, or other structural forms which are much more complicated than this simple example.

6.5. Application to Antennas

An example of a very-low-frequency antenna closely resembling a transmission-line problem is that of the Rocky Point type of antenna (see Fig. 1.39). The dimensions of the flat-top cross section are shown in Fig. 6.8. The configuration is symmetrical and so can be analyzed with six potential equations for the 12 wires. All wires are at the same potential to ground, and one may wish to know the ratio of currents in the various wires or the capacitance per meter of length for the wire system only.

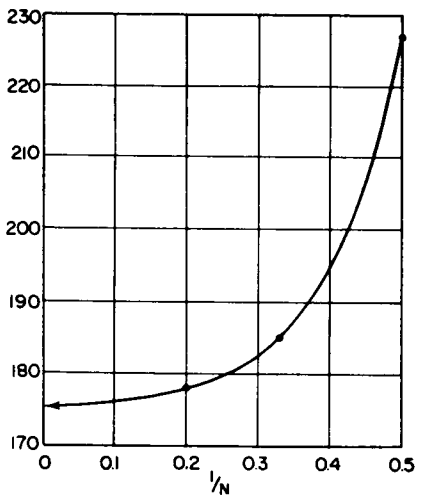

FIG. 6.7

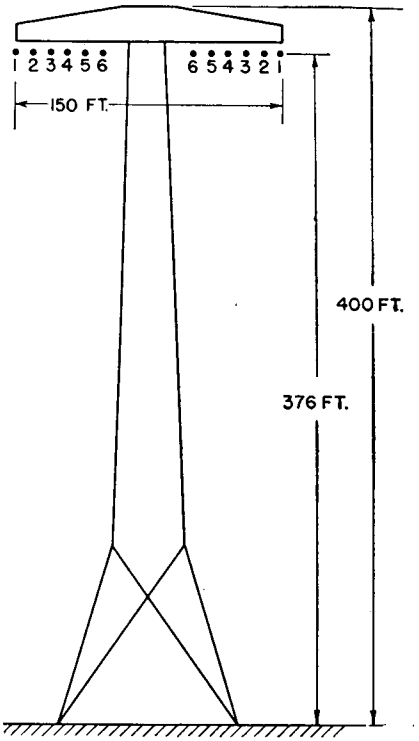

FIG. 6.8

One proceeds with logarithmic potentials by writing the potential of each wire, numbers 1 to 6. The equation for wire 1 is, for example,

$$V_1 = 138v\left(Q_1 \log_{10}\frac{4h^2}{15a\rho} + Q_2 \log_{10}\frac{4h^2}{14a^2} + Q_3 \log_{10}\frac{4h^2}{26a^2} + Q_4 \log_{10}\frac{4h^2}{36a^2} + Q_5 \log_{10}\frac{4h^2}{44a^2} + Q_6 \log_{10}\frac{4h^2}{50a^2}\right)$$

After solving all six such equations simultaneously, the charge (current) ratios are found to be

$$\frac{Q_2}{Q_1} = 0.756 \qquad \frac{Q_3}{Q_1} = 0.654 \qquad \frac{Q_4}{Q_1} = 0.613 \qquad \frac{Q_5}{Q_1} = 0.621 \qquad \frac{Q_6}{Q_1} = 0.720$$

Proceeding through the successive steps to solve for Z_0, it is found to be 201 ohms. The capacitance is 16.6 micromicrofarads per meter.

An obstacle to the application of logarithmic potentials to many of the problems of engineering is the enormous labor of solving large blocks of simultaneous equations. Electronic calculators for several simultaneous equations facilitate such work and thus make it feasible to study a large variety of such problems rapidly. The above charge ratios were solved with the RCA Simultaneous Equation Computor in less than 10 minutes. A great deal of new information can be obtained with such a calculator by eliminating the tedious arithmetical labor required by manual solution, which has always impeded comparative analyses of complicated systems.

6.6. Computation of Potential Gradients

Any solution for the potential at a point in space near the conductors of a transmission line can be applied to the computation of the potential gradient at the surface of a conductor. The potential can be computed for a point very near to the conductor and compared with the potential at the surface. The fall in potential from the conductor surface to the point in space, divided by the distance between them, will yield an average gradient. The exact solution can be obtained by differentiating the potential equation at the surface of any of the conductors, which would give the rate of change of potential versus distance from the conductor. A practical approximation which is simpler will suffice for engineering usage. If the distance between the surface of a conductor and a point in space at which the potential is computed is very small with respect to the radius of the conductor, the potential difference across this space divided by the distance will give a gradient that can be converted to standard units, such as volts per inch or volts per centimeter. For example, if we compute the potential on a wire of a system of radius ρ_1, and then compute the potential at a point distant $\Delta\rho$, where $\Delta\rho$ is very small with respect to ρ_1, the gradient across $\Delta\rho$ will be very nearly the maximum gradient. If the wire radius is 0.100 inch and we take the point in space 0.005 inch from the surface, the potential at the point would be the same as if the wire was increased in radius by 0.005 to become 0.105 inch, with the same charge on the wire.

One is usually interested to know the gradient near the high-potential wires of a feeder when a power W is being transmitted into the feeder that is correctly terminated in its characteristic impedance. Then

$$V = \sqrt{WZ_0}$$

Then, since the potential gradient $\nabla V = f(\rho)$ for a given configuration of wires,

$$\nabla V_1 = f(\rho_1) \qquad \text{and} \qquad \nabla V_p = f(\rho_1 + \Delta\rho)$$

Then the approximate potential gradient ∇V will be

$$-\nabla V = \frac{V_1 - V_p}{\Delta\rho}$$

This is applied to practical design problems as follows: Assume that it is desired to find the approximate potential gradient at the surface of a cylindrical wire of radius 0.100 inch when its potential with respect to ground is 10,000 volts. The wire is far removed from all other wires so that its peripheral-charge distribution is uniform and its electric field strictly radial.

We can employ the device of assuming that this wire is the inner conductor of a coaxial transmission line of very high characteristic impedance —say 400 ohms arbitrarily. For such a value the radius R of the outer conductor must be (from the characteristic-impedance formula for the coaxial line)

$$R = \rho \log_{10}^{-1} \frac{Z_0}{138} = 79.17 \text{ inches}$$

and the ratio $R/\rho = 791.7$.

If now we increase ρ by 0.005 inch, so that we can compute the potential at a point 0.005 inch from the wire, and apply the equation previously derived for the potential at a point in the dielectric space of a coaxial line, we obtain, by using five-place logarithms,

$$\frac{V_P}{V_\rho} = \frac{\log_{10} \dfrac{R}{\rho + 0.005}}{\log_{10} \dfrac{R}{\rho}} = \frac{2.87737}{2.89855} = 0.9927$$

The fall in potential across the first 0.005 inch from the wire is

$$10{,}000(1 - 0.9927) = 73 \text{ volts.}$$

The average gradient across this distance is then $73/0.005 = 14{,}600$ volts per inch.

The same method can be applied to determine the potential gradient at the surface of the high-potential wires of any transmission line for which the characteristic-impedance formula is known. The reason for this is that when the charge per unit length remains constant, the potential of a wire decreases as its periphery increases, or, as a consequence, as its characteristic impedance decreases. Since the accuracy of the results depends upon the accuracy of very small differences, slide-rule accuracy is not sufficient and the computations should be carried out to four or, preferably, five significant decimal places.

APPENDIX I

General Bibliography on Antenna and Radiation Theory

General Textbooks

1001. Stratton, J. A., *Electromagnetic Theory*, McGraw-Hill Book Company, Inc., New York, 1941.
1002. Kraus, J. D., *Antennas*, McGraw-Hill Book Company, Inc., New York, 1950.
1003. Institute of Radio Engineers, *Standards on Antennas, Modulation Systems and Transmitters—Definitions of Terms*, New York, 1948.
1004. Skilling, H. H., *Fundamentals of Electric Waves*, 2d ed., John Wiley & Sons, Inc., New York, 1948.
1005. Terman, F. E., *Radio Engineers' Handbook* (Chapter 11), McGraw-Hill Book Company, Inc., New York, 1944.
1006. American Radio Relay League, *ARRL Antenna Handbook*, West Hartford, Conn.

Radiation and Antenna Theory

1007. Alford, A., Discussion of Methods Employed in Calculation of Electromagnetic Fields of Radiating Conductors, *Elec. Comm.* **15**:70, July, 1936.
1008. Ballantine, S., On the Optimum Transmitting Wave Length for a Vertical Antenna over Perfect Earth, *Proc. IRE*, **12**:833, December, 1924.
1009. Ballantine, S., On the Radiation Resistance of a Simple Vertical Antenna at Wave Lengths below the Fundamental, *Proc. IRE*, **12**:823, December, 1924.
1010. Barrow, W. L., Impedance of a Vertical Half-wave Antenna above an Earth of Finite Conductivity, *Proc. IRE*, **23**:150, February, 1935.
1011. Barzilai, G., Mutual Impedance of Parallel Aerials, *Wireless Engr.*, **25**:343, November, 1948.
1012. Bechmann, R., Calculation of Electric and Magnetic Field Strengths of Any Oscillating Straight Conductors, *Proc. IRE*, **19**:461, March, 1931.
1013. Bechmann, R., Calculation of Radiation Resistance of Antennas and Antenna Combinations, *Proc. IRE*, **19**:471, August, 1931.
1014. Born, H., Energy Distribution in the Near Field of Electromagnetic Radiators, in Particular in Front of Diaphragms and Reflectors (Treated by Acoustical Methods); abstract, *Wireless Engr.*, **21**:188, April, 1944.
1015. Bouwkamp, C. J., Hallén's Theory for a Straight, Perfectly Conducting Wire, Used as a Transmitting or Receiving Aerial, *Physica*, **9**:609, July, 1942.

1016. Brown, G. H., and R. King, High-frequency Models in Antenna Investigations, *Proc. IRE*, **22**:457, April, 1934.
1017. Brown, G. H., Phase and Magnitude of Earth Currents near Radio Transmitting Antennas, *Proc. IRE*, **23**:168, February, 1935.
1018. Brown, G. H., and O. M. Woodward, Experimentally Determined Impedance Characteristics of Cylindrical Antennas, *Proc. IRE*, **33**:257, April, 1945.
1019. Carter, P. S., Circuit Relations in Radiating Systems and Applications to Antenna Problems, *Proc. IRE*, **20**:1004, June, 1932.
1020. Cleckner, D. C., Effect of Feed on Pattern of Wire Antennas, *Electronics*, August, 1947, p. 103.
1021. Colebrook, F. M., Electric and Magnetic Fields for a Linear Radiator Carrying a Progressive Wave, *J. IEE*, **89**:169, February, 1940.
1022. Colebrook, F. M., and A. C. Gordon-Smith, Method of Calibrating Field Strength Measuring Set, *J. IEE*, **90**:15, March, 1941.
1023. Cox, C. R., Mutual Impedance between Vertical Antennas of Unequal Heights, *Proc. IRE*, **35**:1367, November, 1947.
1024. Essen, L., and M. H. Oliver, Aerial Impedance Measurements, *Wireless Engr.*, **22**:587, December, 1945.
1025. Forbes, H. C., Re-radiation from Tuned Antenna Systems, *Proc. IRE*, **13**:363, June, 1925.
1026. Foster, R. M., Directive Diagrams of Antenna Arrays, *Bell System Tech. J.* **5**:292, January, 1926.
1027. Friis, H. T., A Note on a Simple Transmission Formula, *Proc. IRE*, **34**:254, May, 1946. (Effective areas of transmitting and receiving antennas.)
1028. Gray, M. C., Modification of Hallén's Solution of the Antenna Problem, *J. Applied Phys.*, **15**:61, January, 1944.
1029. Green, E., Extended Aerial Systems; Calculating the Polar Diagrams, *Wireless Engr.*, **19**:195, May, 1942.
1030. Grosskopf, J., Radiation Field of a Vertical Transmitting Dipole over Stratified Ground, *Wireless Engr.*, **20**:245, May, 1943.
1031. Hallén, E., Theoretical Investigations into the Transmitting and Receiving Qualities of Antennas, *Nova Acta Upsaliensis*, ser. IV, **11**:No. 4, 1938.
1032. Hansen, W. W., and J. G. Beckerley, Concerning New Methods of Calculating Radiation Resistance, either with or without Ground, *Proc. IRE*, **24**:1594, December, 1936.
1033. Hansen, W. W., and J. R. Woodyard, A New Principle in Directional Antenna Design, *Proc. IRE*, **26**:333, March, 1938.
1034. Harrison, C. W., Jr., and R. King, Receiving Antenna in a Plane-polarized Field of Arbitrary Orientation, *Proc. IRE*, **32**:35, January, 1941.
1035. Harrison, C. W., Jr., Mutual Impedance of Antennas, *J. Applied Phys.*, **14**:306, June, 1943.
1036. Harrison, C. W., Jr., Approximate Representation of the Electromagnetic Field in the Vicinity of a Symmetrical Radiator, *J. Applied Phys.*, **15**:544, July, 1944.

1037. Howe, G. W. O., Equivalent Inductance and Capacity of an Aerial with Inserted Tuning Coil or Condenser, *Exp. Wireless*, **5**:297, June, 1928.
1038. Howe, G. W. O., Applying Transmission Line Theory to Aerials, *Wireless Engr.*, **15**:1, January, 1939.
1039. Howe, G. W. O., Radiation Resistance of a Half-wave Dipole Aerial, *Wireless Engr.*, **22**:153, April, 1945.
1040. Jachnow, W., Mutual Impedance of Inclined Rectilinear Conductors with Progressive Waves, *ENT*, July, 1939, p. 177.
1041. Jachnow, W., Theoretical Investigations of Radiation Diagrams and Radiation Resistance for Progressive Waves of Various Phase Velocities; abstract, *Wireless Engr.*, **20**:87, February, 1943.
1042. Jordan, E. C., Acoustic Models of Radio Antennas, Ohio State Univ. Engineering Series, Vol. 10, No. 3, May, 1941.
1042A. Jordan, E. C., and W. L. Everitt, *Proc. IRE*, **29**:186, April, 1941.
1043. Kelvin, W., Radiation Field of an Unbalanced Dipole, *Proc. IRE*, **34**: 440, July, 1946.
1044. King, D. D., Measured Impedance of Cylindrical Dipoles, *J. Applied Phys.*, **17**:844, October, 1946.
1045. King, L. V., On the Radiation Field of a Perfectly Conducting Base Insulated Cylindrical Antenna over a Perfectly Conducting Plane Earth, and the Calculation of Resistance and Reactance, *Phil. Trans. Roy. Soc. (London)*, **236**:381, Nov. 2, 1937.
1046. King, R., and B. C. Dunn, Currents Excited on a Conducting Plane by a Parallel Dipole, *Proc. IRE*, **36**:221, February, 1948.
1047. King, R., and F. G. Blake, Jr., Self-impedance of a Symmetrical Antenna, *Proc. IRE*, **30**:335, July, 1942.
1048. King, R., and C. W. Harrison, Distribution of Current along a Symmetrical Center-driven Antenna, *Proc. IRE*, **31**:548, October, 1943.
1049. King, R., Coupled Antennas and Transmission Lines, *Proc. IRE*, **31**:626, November, 1943.
1050. King, R., and C. W. Harrison, Jr., Impedance of Short, Long, and Capacitively Loaded Antennas with a Critical Discussion of the Antenna Problem, *J. Applied Phys.*, **15**:170, February, 1944.
1051. King, R., and C. W. Harrison, Jr., Mutual and Self-impedance for Coupled Antennas, *J. Applied Phys.*, **15**:481, June, 1944.
1052. Labus, J., Recherische Ermittlung der Impedanz von Antennan, *Hochfrequenztechnik und Elektroakustic*, January, 1933, p. 17.
1053. Levin, S. A., and C. J. Young, Field Distribution and Radiation Resistance of a Straight Vertical Unloaded Antenna Radiating at One of Its Harmonics, *Proc. IRE*, **14**:675, October, 1926.
1054. McPetrie, J. S., Graphical Method for Determining the Magnitude and Phase of the Electric Field in the Neighborhood on an Antenna Carrying a Known Distribution of Current, *J. IEE*, **69**:290, February, 1931.
1055. McPetrie, J. S., Method for Determining the Effect of the Earth on the Radiation from Aerial Systems, *J. IEE*, **70**:382, March, 1932.

1056. McPetrie, J. S., and J. A. Saxon, Theory and Confirmation of Calibration of Field Strength Sets by Radiation, *J. IEE*, **88**:11, May, 1941.
1057. Moullin, E. B., Radiation Resistance of Aerials Whose Length Is Comparable with the Wavelength, *J. IEE*, **78**:540, May, 1936.
1058. Murray, F. H., Mutual Impedance of Two Skew Antenna Wires, *Proc. IRE*, **21**:154, January, 1933.
1059. Neiman, M. S., Principle of Reciprocity in Antenna Theory, *Proc. IRE*, **31**:666, December, 1943.
1060. Neissen, K. F., Ground Absorption for Horizontal Dipole Aerials, *Ann. der Physik*, July, 1938, p. 444.
1061. Neissen, K. F., Choice between Horizontal and Vertical Dipole Aerials for Minimum Earth Absorption with Given Wavelength and Soil Type, *Ann. der Physik*, November, 1938, p. 403.
1062. Neissen, K. F., Radiation from a Dipole, *Ann. der Physik*, p. 209, February, 1937.
1063. Neissen, K. F., and G. de Vries, Receiving Impedance of a Receiving Antenna, *Physica*, July, 1939, p. 601.
1064. Neissen, K. F., Calculation of Field Strength of a Half-wave Aerial, *Physica*, September, 1940, p. 23.
1065. Pippard, A. B., O. J. Burrel, and F. F. Cromie, The Influence of Re-radiation on Measurements of the Power Gain of an Aerial, *J. IEE*, **93**:IIIa:720, March–May, 1946.
1066. Pistolkors, A. A., Radiation Resistance of Beam Antennas, *Proc. IRE*, **17**:562, March, 1929.
1067. Ramsay, J. F., Fourier Transforms in Antenna Theory, *Marconi Review*, Nos. 83–87, October–December, 1946.
1068. Roubine, E., Les Récentes théories de l'antenne, *L'Onde électrique*, **27**:32, 57, 104, 160, January–April, 1947; Same paper in Spanish, Las nuevas teorías de la antena, *Revista de telecomunicación*, **3**:2, December, 1947.
1069. Schelkunoff, S. A., On Diffraction and Radiation of E-M Waves, *Phys. Rev.*, August, 1939, p. 308.
1070. Schelkunoff, S. A., General Radiation Formula, *Proc. IRE*, **27**:660, October, 1939.
1071. Schelkunoff, S. A., Theory of Antennas of Arbitrary Size and Shape, *Proc. IRE*, **29**:493, September, 1941.
1072. Schelkunoff, S. A., and C. B. Feldman, Radiation from Antennas, *Proc. IRE*, **30**:511, November, 1942.
1073. Schelkunoff, S. A., Mathematical Theory of Linear Arrays, *Bell System Tech. J.*, **22**:80, January, 1943.
1074. Schelkunoff, S. A., Antenna Theory and Experiment, *J. Applied Phys.*, **15**:54, January, 1944.
1075. Smith, P. D. P., The Conical Dipole of Wide Angle, *J. Applied Phys.*, **19**:11, January, 1948.
1076. Southworth, G. C., Certain Factors Affecting the Gain of Directive Antennas, *Proc. IRE*, **18**:1502, September, 1930.

1077. Sommerfeld, A., and F. Renner, Radiation Energy and Earth Absorption for Dipole Antennae, *Wireless Engr.*, **19**:351, 409, 457, August–October, 1942.
1078. Starnecki, B., and E. Fitch, Mutual Impedance of Two Center-driven Parallel Aerials, *Wireless Engr.*, **25**:385, December, 1948.
1079. Stratton, J. A., and L. J. Chu, Diffraction Theory of E-M Waves, *Physic. Rev.*, July, 1939, p. 99.
1080. Tai, C. T., Coupled Antennas, *Proc. IRE*, **36**:487, April, 1948.
1081. Thomson, W. T., Development of the General Antenna Array Equation, *J. Applied Phys.*, **15**:420, May, 1944.
1082. Walmsley, T., Impedance Characteristics of Short-wave Dipoles, *Phil. Mag.*, June, 1938, p. 981.
1083. Wells, E. M., Radiation Resistance of Horizontal and Vertical Aerials Carrying a Progressive Wave, *Marconi Review*, No. 83, October–December, 1946.
1084. Wells, N., Aerial Characteristics, *J. IEE*, 89 III:76, June, 1942.
1085. Zinke, C., Fundamental Consideration of the Current and Potential Distribution on Antennas, *Wireless Engr.*, **18**:377, September, 1941.
1086. *Tables of Sine, Cosine and Exponential Integrals*, Vols. I and II, Work Project Administration for the City of New York, Project 765-97-3-10, National Bureau of Standards, Washington, D. C.,1940.
1087. Wolff, I., Determination of the Radiating System Which Will Produce a Specified Directional Characteristic, *Proc. IRE*, **25**:630, May, 1937.

APPENDIX II

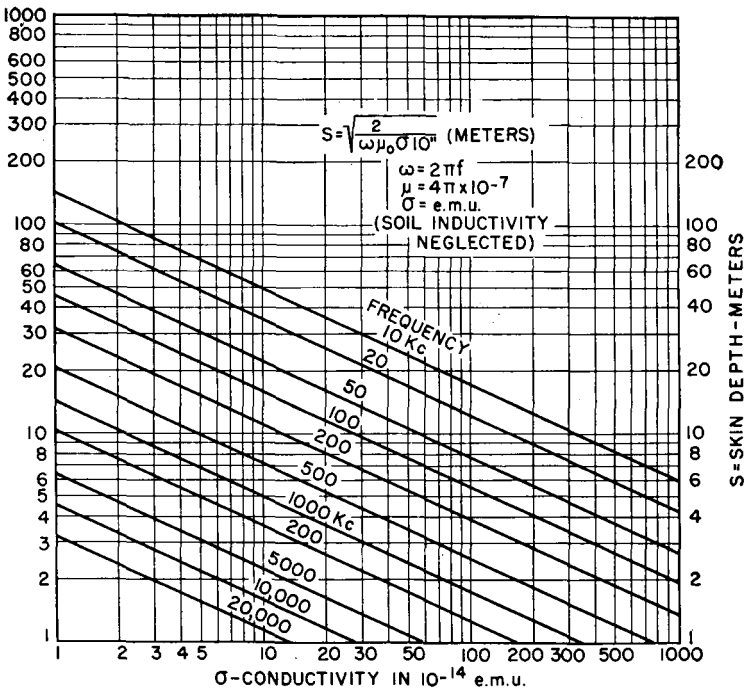

Penetration of earth currents (skin depth) as a function of frequency and ground conductivity, with inductivity of unity.

APPENDIX III-A

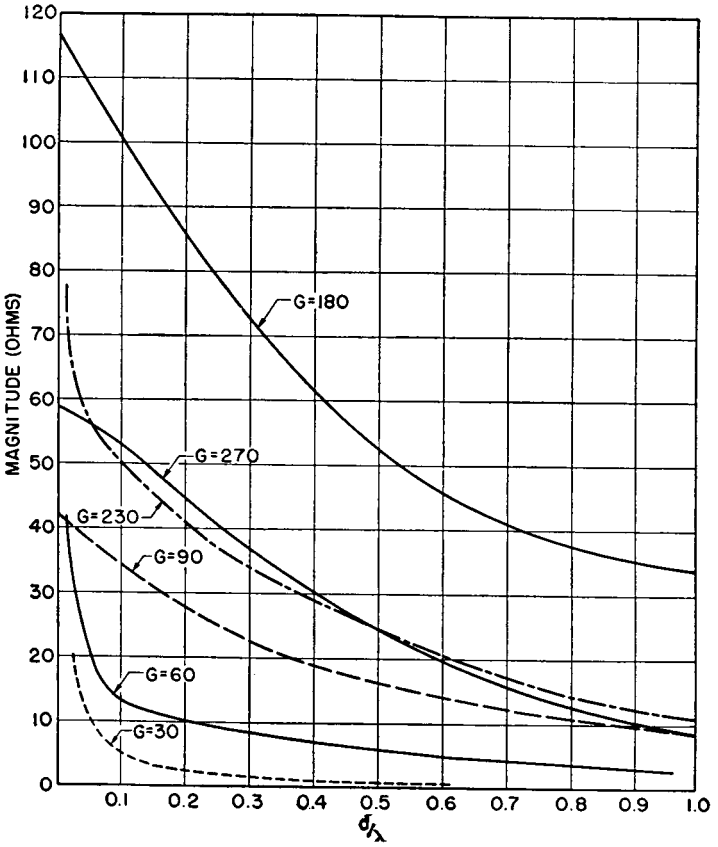

Magnitude of mutual impedance between identical thin vertical cylindrical radiators as a function of height and spacing. Values are those referred to the base of the antenna, except for the 180-degree height which is referred to current antinode. (*After G. H. Brown.*)

APPENDIX III-B

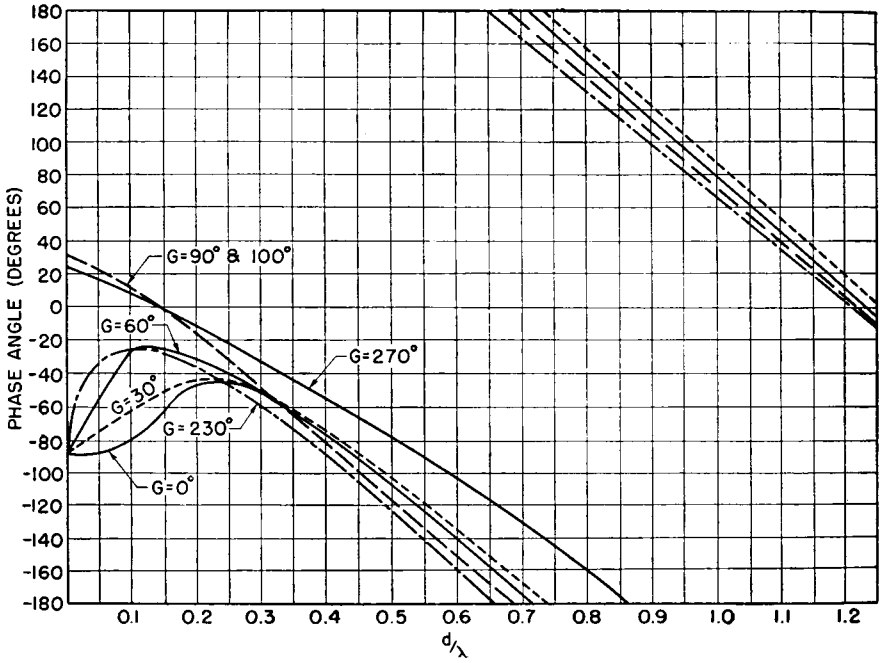

Angle of the mutual impedance vector under conditions identical to those for Appendix III-A. (*After G. H. Brown.*)

APPENDIX III-C

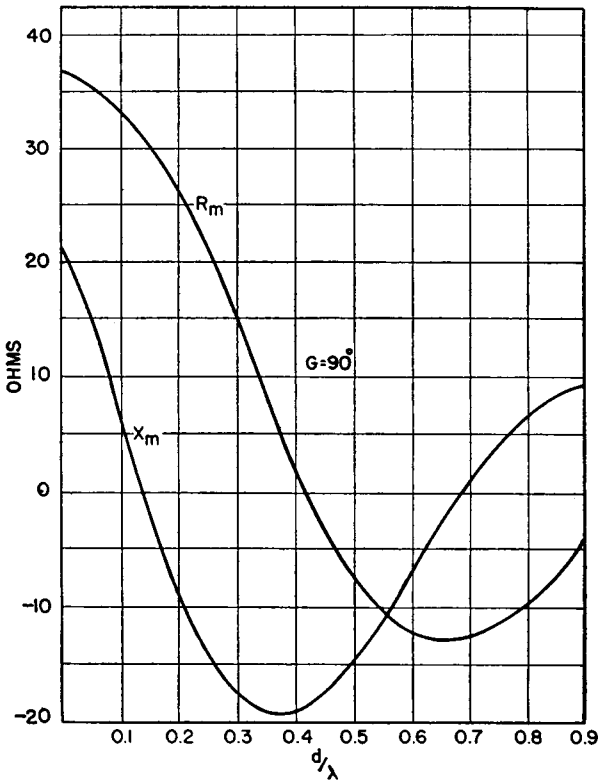

Resistive and reactive components of the mutual impedance for two identical thin vertical cylindrical radiators one-quarter wavelength high. (*After G. H. Brown.*)

APPENDIX III-D

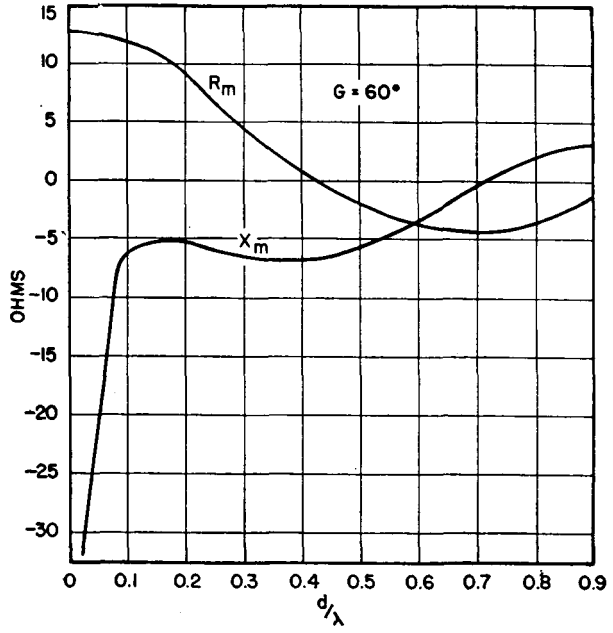

Resistive and reactive components of the mutual impedance for two identical thin vertical cylindrical radiators one-sixth wavelength high. (*After G. H. Brown.*)

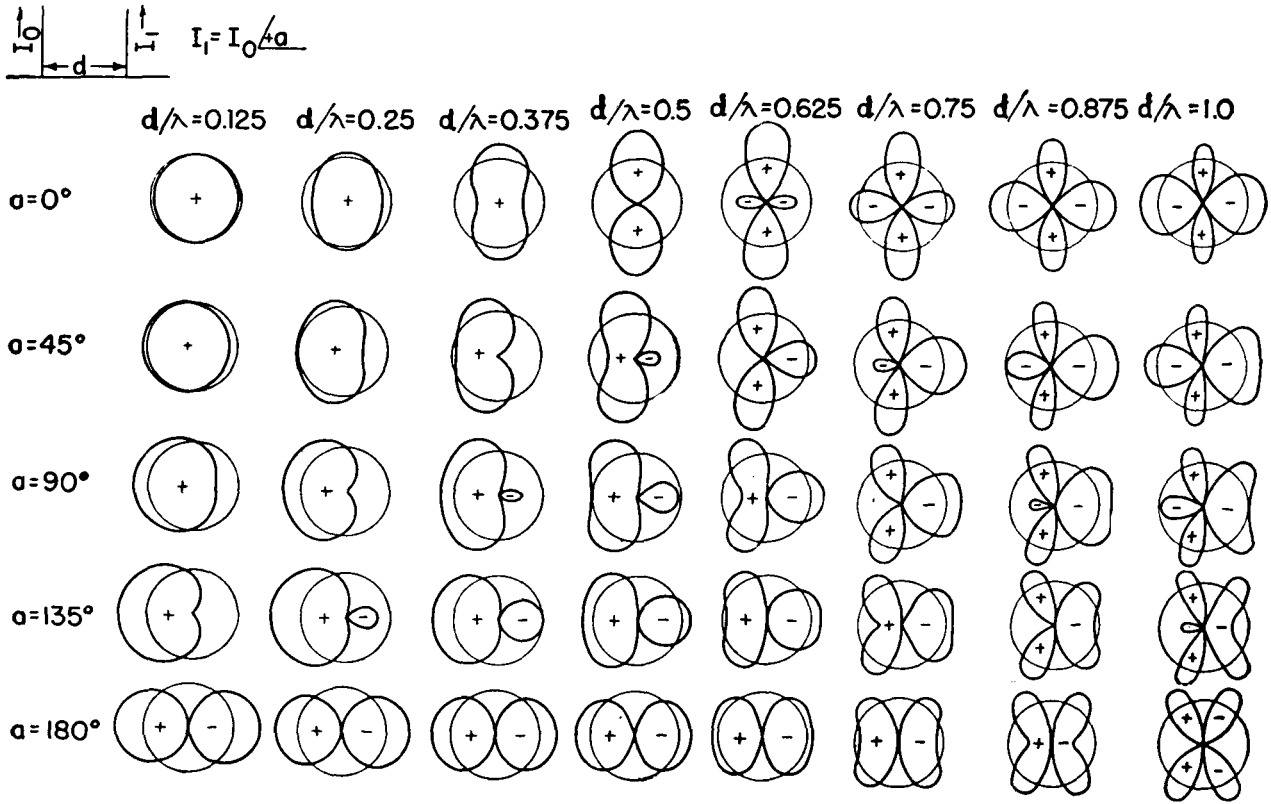

Chart of radiation patterns from two point sources having equal radiation fields, as functions of spacing and time-phase difference. For identical vertical radiators with equal currents, these are horizontal patterns. The radiating sources have their axis along the horizontal axis of each pattern, and the current in the right hand radiator has a leading time-phase with respect to that in the left-hand radiator. Polarity of fields of lobes is indicated. (*After G. H. Brown.*)

APPENDIX IV-B

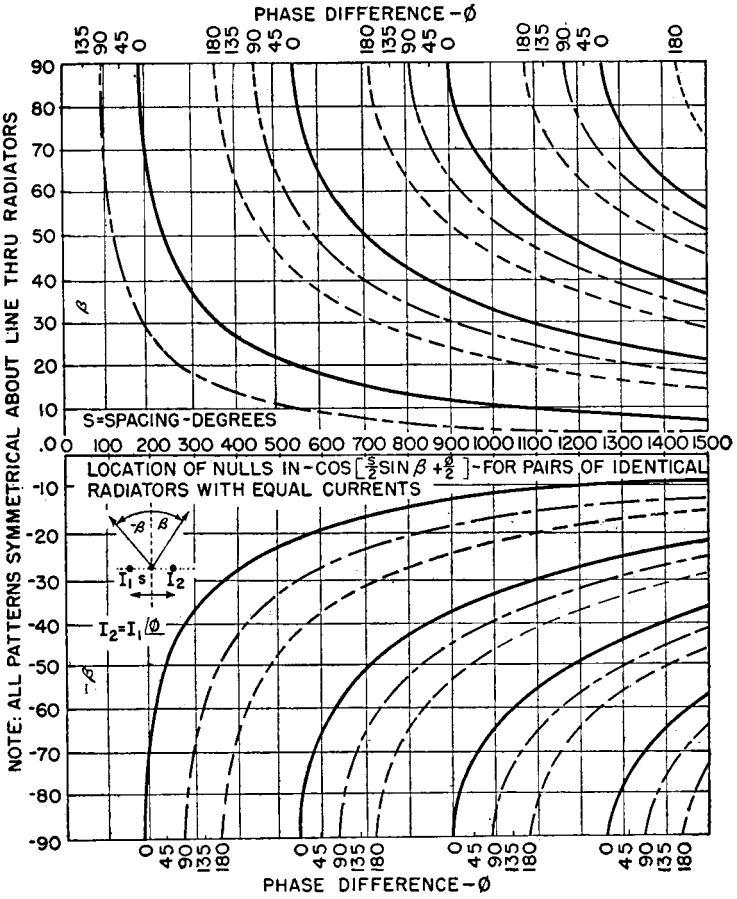

Chart of angles of nulls in the function

$$\cos\left(\frac{S}{2}\sin\beta + \frac{\phi}{2}\right)$$

The angles of nulls in the patterns of Appendix IV-A as measured from the normal to the axis of the radiators are read from this chart.

TABULATION OF THE FUNCTIONS SIN $\left(\frac{S}{2} \text{ SIN } \phi\right)$ AND SIN $\left[\frac{S}{2} \text{ SIN } (90 - \phi)\right]$

$S(\lambda) \rightarrow$		0.5	1.0	1.5	2.0	2.5	3.0	3.5	4.0	4.5	5.0	5.5	6.0	6.5	7.0
S (Degrees) $\rightarrow$		180	360	540	720	900	1080	1260	1440	1620	1800	1980	2160	2340	2520
$90 - \phi$	ϕ														
90	0	0	0	0	0	0	0	0	0	0	0	0	0	0	0
87.5	2.5	0.06	0.14	0.195	0.26	0.320	0.40	0.462	0.47	0.574	0.610	0.682	0.735	0.777	0.819
85	5.	0.135	0.27	0.400	0.52	0.630	0.73	0.820	0.89	0.941	0.980	0.998	0.997	0.982	0.948
82.5	7.5	0.205	0.40	0.570	0.76	0.845	0.95	0.980	1.00	0.961	0.884	0.777	0.629	0.454	0.259
80.	10.	0.270	0.515	0.734	0.82	0.981	1.00	0.938	0.81	0.629	0.330	0.139	−0.139	−0.407	−0.629
77.5	12.5	0.333	0.62	0.857	0.97	0.993	0.93	0.682	0.39	0.087	−0.250	−0.574	−0.819	−0.961	−0.998
75	15.	0.398	0.72	0.938	1.00	0.892	0.64	0.255	−0.11	−0.500	−0.797	−0.970	−0.985	−0.848	−0.537
72.5	17.5	0.455	0.80	0.985	0.97	0.503	0.33	−0.160	−0.53	−0.891	−1.000	−0.891	−0.588	−0.156	0.309
70.	20.	0.515	0.88	0.998	0.84	0.438	0	−0.588	−0.92	−0.995	−0.790	−0.391	0.174	0.642	0.940
67.5	22.5	0.568	0.93	0.970	0.72	0.100	−0.40	−0.885	−1.00	−0.766	−0.230	0.309	0.799	0.997	0.848
65	25.	0.615	0.97	0.915	0.48	−0.174	−0.74	−1.000	−0.83	−0.326	0.310	0.848	0.993	0.707	0.122
62.5	27.5	0.665	0.99	0.828	0.25	−0.465	−0.95	−0.927	−0.45	0.280	0.825	0.990	0.777	0.191	−0.500
60.	30	0.707	1.00	0.705	0	−0.707	−1.00	−0.707	0	0.707	1.000	0.707	0	−0.707	−1.000
57.5	32.5	0.745	1.00	0.563	−0.24	−0.866	−0.94	−0.380	0.42	0.961	0.830	0.174	−0.629	−0.999	−0.695
55.	35.	0.785	0.98	0.425	−0.44	−0.978	−0.78	−0.040	0.79	0.990	0.400	−0.485	−0.988	−0.743	0.500
52.5	37.5	0.817	0.95	0.268	−0.65	−1.000	−0.47	0.325	0.98	0.755	−0.100	−0.883	−0.900	−0.139	0.731
50.	40.	0.850	0.92	0.122	−0.79	−0.944	−0.17	0.707	0.98	0.342	−0.618	−0.993	−0.423	0.530	1.000
47.5	42.5	0.884	0.87	−0.035	−0.89	−0.810	0.11	0.914	0.82	−0.110	−0.895	−0.777	0.156	0.934	0.766
45.	45.	0.894	0.81	−0.191	−0.96	−0.668	0.37	0.997	0.53	−0.500	−0.996	−0.358	0.669	0.970	0.191
42.5	47.5	0.915	0.74	−0.333	−1.00	−0.485	0.61	0.965	0.15	−0.790	−0.835	0.174	0.980		
40.	50.	0.932	0.67	−0.455	−1.00	−0.277	0.81	0.840	−0.21	−0.985	−0.500	0.629	0.956		
37.5	52.5	0.945	0.59	−0.562	−0 96	−0.092	0.93	0.620	−0.51	−0.982	−0.110	0.906	0.680		
35.	55	0.960	0.53	−0.655	−0.90	0.100	0.99	0.420	−0.77	−0.829	0.295	1.000	0.242		
32.5	57.5	0.970	0.46	−0.741	−0.83	0.300	0.99	0.155	−0.91	−0.586	0.630	0.914	−0.250		
30.	60.	0.980	0.40	−0.808	−0.75	0.500	0.95	−0.093	−1.00	−0.309	0.865	0.669	−0.602		
27.5	62.5		0.34	−0.862	−0.67	0.638	0.88	−0.316	−0.99	0	0.980	0.375	−0.820		
25.	65.	0.994	0.29	−0.905	−0.57	0.744	0.78	−0.530	−0.94	0.276	0.993	0.052	−0.985		
22.5	67.5		0.24	−0.937	−0.47	0.825	0.67	−0.683	−0.84	0.500	0.918	−0.242	−0.990		
20.	70.	1.000	0.19	−0.960	−0.38	0.890	0.55	−0.788	−0.69	0.669	0.805	−0.500	−0.914		
17.5	72.5		0.15	−0.975	−0.29	0.930	0.44	−0.870	−0.53	0.793	0.666	−0.682	−0.780		
15.	75.	1.000	0.11	−0.986	−0.22	0.965	0.34	−0.935	−0.39	0.875	0.500	−0.829	−0.629		
12.5	77.5		0.08	−0.993	−0.16	0.985	0.23	−0.968	−0.28	0.936	0.340	−0.914	−0.466		
10.	80.	1.000	0.05	−0.997	−0.10	0.996	0.14	−0.986	−0.17	0.978	0.225	−0.966	−0.292		
7.5	82.5		0.03	−1.000	−0.06	1.000	0.08	−0.992	−0.11	0.990	0.135	−0.988	−0.146		
5.	85.	1.000	0.02	−1.000	−0.03	1.000	0.04	−0.996	−0.07	0.999	0.071	−0.998	−0.070		
0.	90.	1.000	0	−1.000	0	1.000	0	−1.000	0	1.000	0	−1.000	0		

NOTE:
When applied to radiation patterns of straight antennas parallel to perfectly reflecting surfaces (such as "ground" or passive reflectors), S represents the electrical spacing between the antenna and its *image*. Therefore $S/2$ is the electrical height h of the antenna above ground, or the electrical distance d from a reflecting screen.

Tabulation of the functions sin $\left(\frac{S}{2} \sin \phi\right)$ and sin $\left[\frac{S}{2} \sin (90 - \phi)\right]$ for values of S from 180 to 2,520 degrees in 180-degree steps. These are the patterns in the equatorial plane of two identical parallel nonstaggered radiators with equal currents in antiphase relation. By dividing the column headings for S (degrees) by 2, each column can be read as a vertical pattern for a horizontal antenna over perfectly conducting ground.

TABULATION OF THE FUNCTIONS cos $\left(\frac{S}{2} \sin \phi\right)$ AND cos $\left[\frac{S}{2} \sin (90 - \phi)\right]$

$S(\lambda) \rightarrow$		0.5	1.0	1.5	2.0	2.5	3.0	3.5	4.0	4.5	5.0	5.5	6.0	6.5	7.0
S (Degrees) $\rightarrow$		180	360	540	720	900	1080	1260	1440	1620	1800	1980	2160	2340	2520
$90 - \phi$	ϕ														
90.	0	1.00	1.00	1.00	1.00	1.00	1.00	1.00	1.00	1.000	1.000	1.000	1.000	1.000	1.000
87.5	2.5	1.00	0.99	0.97	0.96	0.95	0.93	0.90	0.86	0.819	0.777	0.731	0.678	0.629	0.534
85.	5.	0.99	0.96	0.92	0.85	0.77	0.68	0.56	0.43	0.334	0.165	0.070	−0.073	−0.208	−0.342
82.5	7.5	0.98	0.92	0.88	0.70	0.49	0.33	0.12	−0.07	−0.276	−0.470	−0.629	−0.777	−0.891	−0.966
80.	10.	0.96	0.86	0.69	0.46	0.20	−0.07	−0.34	−0.57	−0.777	−0.914	−0.991	−0.990	−0.914	−0.777
77.5	12.5	0.94	0.79	0.53	0.20	−0.11	−0.40	−0.75	−0.90	−0.996	−0.980	−0.819	−0.574	−0.276	0.070
75.	15.	0.92	0.69	0.35	−0.05	−0.43	−0.76	−0.95	−1.00	−0 866	−0.618	−0.242	0.139	0.545	0.819
72.5	17.5	0.89	0.58	0.17	−0.29	−0.68	−0.94	−0.99	−0.83	−0.454	0	0.454	0.809	0.988	0.951
70.	20.	0.86	0.47	0	−0.55	−0.90	−1.00	−0.81	−0.41	0.122	0.615	0.921	0.985	0.766	0.342
67.5	22.5	0.83	0.37	−0.18	−0.71	−0.99	−0.94	−0.47	0.10	0.642	0.965	0.951	0.602	0.052	−0.530
65.	25.	0.79	0.27	−0.36	−0.85	−0.99	−0.84	−0.07	0.56	0.951	0.965	0.530	−0.122	−0.707	−0.993
62.5	27.5	0.75	0.14	−0.54	−0.94	−0.88	−0.37	0.32	0.89	0.996	0.558	−0.139	−0.629	−0.982	−0.867
60.	30.	0.71	0	−0.70	−1.00	−0.71	0	0.71	1.00	0.707	0	−0.707	−1.000	−0.707	0
57.5	32.5	0.67	−0.11	−0.83	−0.98	−0.45	0.30	0.93	0.90	0.276	−0.558	−0.985	−0.777	−0.035	0.719
55.	35.	0.62	−0.23	−0.91	−0.90	−0.21	0.63	1.00	0.62	−0.242	−0.915	−0.875	−0.156	0.643	0.867
52.5	37.5	0.57	−0.33	−0.96	−0.78	0.06	0.85	0.92	0.15	−0.656	−0.995	−0.450	0.375	0.991	0.682
50.	40.	0.53	−0.44	−0.99	−0.63	0.32	0.97	0.71	−0.31	−0.939	−0.777	0.122	0.906	0.848	−0.018
47.5	42.5	0.48	−0.52	−1.00	−0.45	0.53	1.00	0.40	−0.65	−0.996	−0.340	0.629	0.988	0.358	−0.642
45.	45.	0.44	−0.60	−0.99	−0.27	0.74	0.93	0.09	−0.86	−0.867	0.100	0.934	0.742	0.292	−0.982
42.5	47.5	0.40	−0.68	−0.95	−0.09	0.88	0.79	−0.21	−0.97	−0.550	0.544	0.985	0.230		
40.	50.	0.36	−0.74	−0.90	0.08	0.96	0.60	−0.53	−0.99	−0.174	0.866	0.777	−0.292		
37.5	52.5	0.32	−0.79	−0.83	0.25	0.99	0.38	−0.75	−0.87	0.210	0.995	0.423	−0.676		
35.	55.	0.28	−0.84	−0.76	0.41	0.99	0.14	−0.91	−0.66	0.559	0.955	0	−0.970		
32.5	57.5	0.24	−0.88	−0.67	0.56	0.94	−0.07	−0.98	−0.38	0.783	0.777	−0.407	−0.990		
30.	60.	0.21	−0.91	−0.59	0.67	0.87	−0.29	−1.00	−0.11	0.951	0.500	−0.743	−0.799		
27.5	62.5	0.18	−0.93	−0.51	0.76	0.78	−0.46	−0.96	0.13	1.000	0.190	−0.927	−0.490		
25.	65.	0.15	−0.95	−0.43	0.83	0.68	−0.63	−0.86	0.37	0.965	−0.140	−0.999	−0.174		
22.5	67.5	0.12	−0.97	−0.35	0.88	0.56	−0.75	−0.74	0.57	0.858	−0.410	−0.970	0.110		
20.	70.	0.10	−0.98	−0.28	0.92	0.45	−0.84	−0.62	0.73	0.743	−0.588	−0.866	0.407		
17.5	72.5	0.08	−0.98	−0.22	0.96	0.36	−0.90	−0.49	0.85	0.618	−0.745	−0.731	0.625		
15.	75.	0.06	−0.99	−0.16	0.98	0.28	−0.94	−0.37	0.91	0.485	−0.866	−0.560	0.777		
12.5	77.5	0.04	−0.99	−0.10	0.99	0.20	−0.97	−0.25	0.96	0.338	−0.940	−0.407	0.887		
10.	80.	0.03	−1.00	−0.05	1.00	0.14	−0.99	−0.15	0.98	0.208	−0.975	−0.259	0.956		
7.5	82.5	0.02	−1.00	−0.03	1.00	0.09	−1.00	−0.09	0.99	0.105	−0.990	−0.156	0.985		
5.	85.	0.01	−1.00	−0.01	1.00	0.05	−1.00	−0.04	1.00	0.052	−1.000	−0.070	0.998		
0	90.	0	−1.00	0	1.00	0	−1.00	0	1.00	0	−1.000	0	1.000		

Tabulation of the functions cos $\left(\frac{S}{2} \sin \phi\right)$ and cos $\left[\frac{S}{2} \sin (90 - \phi)\right]$ for values of S from 180 to 2,520 degrees in 180-degree steps. These are the patterns in the equatorial plane of two identical parallel nonstaggered radiators with equal cophased currents.

APPENDIX V-C

ψ Degrees	Function	θ Degrees
0	1.000	90
2.5	0.997	87.5
5.0	0.990	85.0
7.5	0.983	82.5
10.0	0.976	80.0
12.5	0.962	77.5
15.0	0.950	75.0
17.5	0.933	72.5
20.0	0.916	70.0
22.5	0.891	67.5
25.0	0.869	65.0
27.5	0.843	62.5
30.0	0.816	60.0
32.5	0.785	57.5
35.0	0.756	55.0
37.5	0.725	52.5
40.0	0.695	50.0
42.5	0.660	47.5
45.0	0.628	45.0
47.5	0.594	42.5
50.0	0.559	40.0
52.5	0.523	37.5
55.0	0.488	35.0
57.5	0.453	32.5
60.0	0.414	30.0
62.5	0.380	27.5
65.0	0.345	25.0
67.5	0.309	22.5
70.0	0.271	20.0
72.5	0.240	17.5
75.0	0.204	15.0
77.5	0.171	12.5
80.0	0.138	10.0
82.5	0.103	7.5
85.0	0.070	5.0
87.5	0.036	2.5
90.0	0.000	0.0

Tabulation of the functions $\frac{\cos(90 \sin \psi)}{\cos \psi}$ and $\frac{\cos(90 \cos \theta)}{\sin \theta}$, the radiation pattern for a half-wavelength cylindrical dipole in free space, with the angle ψ measured from the normal to the dipole, and the angle θ measured from the dipole axis.

APPENDIX VI

World Noise Zones and Required Minimum Field Strength for Commercial Telephone Communication*

Natural atmospheric noise frequently is the limiting factor in radio communication. Until recent years the existing magnitudes of atmospheric noise were known only in a qualitative way. Recent systematic measurements made throughout the world have given some statistical values for such noise which is of basic engineering importance. More data on this subject are needed, and the available information will increase as the result of work that is now in progress.

Atmospheric noise varies throughout the day and throughout the yearly cycle. It also varies with frequency, being of greatest magnitude statistically at the lowest radio frequencies and decreasing as the frequency increases. An arbitrary system of designation for average noise levels of different values has been devised through international cooperation on the problems of noise cataloguing, and are indicated as various noise grades from 1 to 5. The world's noise zones, under this system of grading, are shown for the four seasons in Appendix VI-A, B, C, and D. In the absence of more specific data on particular locations, these figures may be used as a general guide to probable noise grades in any locality. Because of the fact that reliable radio communication depends upon the signal-to-noise ratio at the receiver, antenna engineers must be as interested in the subject of noise as they are in the power of their transmitters, because a 10-decibel rise in noise level is equivalent to reducing the transmitter power to one-tenth its original value. It is therefore of prime importance to make atmospheric noise measurements at locations where important receiving facilities are to be installed. Such measurements should be made in such a way as to reveal the diurnal and yearly range of noise field strengths in the parts of the radio spectrum that would be used for radio communication. The choice of a site for a receiving station must take noise into account always, although both atmospheric and man-made noise are involved in site selection.

Appendix VI-E to J is included here to show the average values of field strength required for standard double-sideband amplitude-modulated radiotelephony to secure 90 per cent reliability with different frequencies for different noise grades at different hours of the day during different seasons. It is useful to replot these data curves for specific operating frequencies for any particular receiving location to obtain the necessary information in simpler form. It must be emphasized that these data apply only to atmospheric noise. If other sources of electrical noise are present near a receiving location, and such noise equals or exceeds the atmospheric noise, the required minimum received field strengths

* Data for Appendix VI after Central Radio Propagation Laboratory.

for the signal, shown in these figures, must be increased in the same ratio as the extraneous noise exceeds the atmospheric noise. If locally received noise exceeds atmospheric noise at certain times by 10 decibels, the minimum required received field strength of the signal must be 10 decibels higher than shown by these figures. It is for this reason that extraneous noise picked up at a receiving site should preferably always be less than the minimum atmospheric noise in order that radio communication will not be limited more than nature permits.

It is evident from these data curves that atmospheric noise is a severe limitation on the lower radio frequencies, because relatively high field strengths are needed to give the same degree of communication reliability.

APPENDIX VI-A

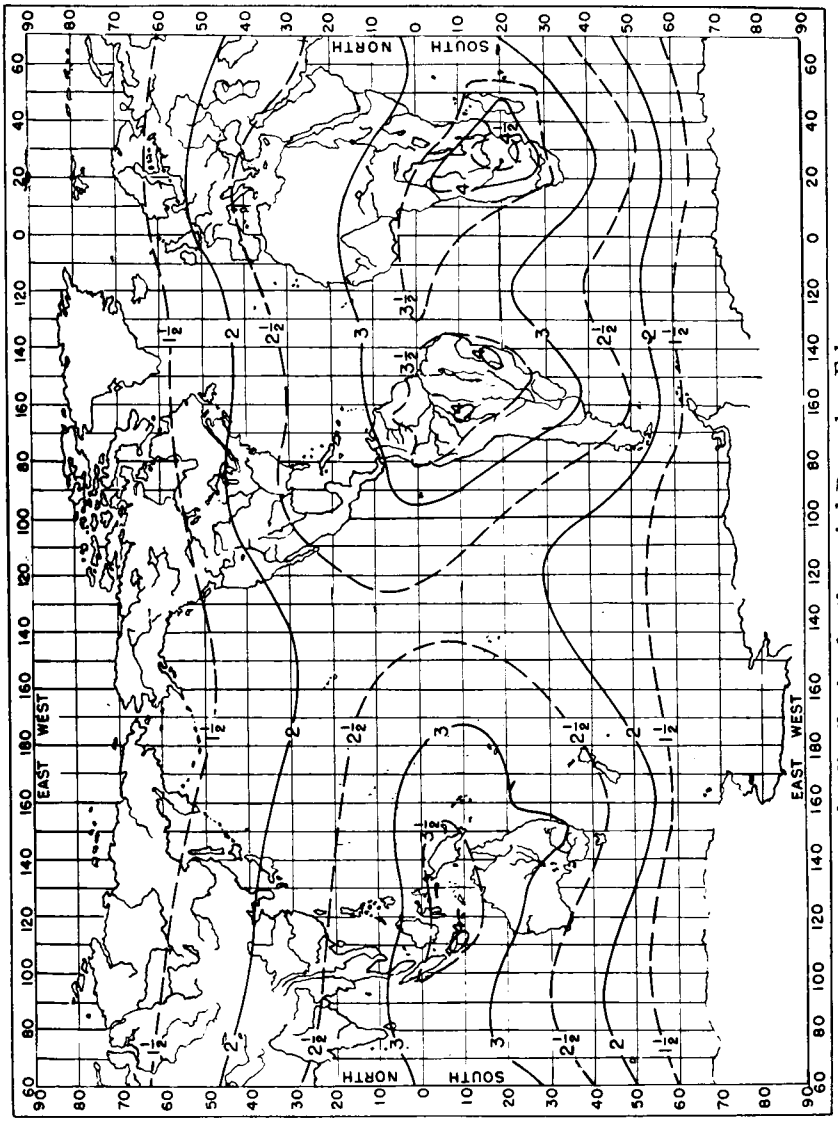

Noise distribution for the period December–February.

APPENDIX VI-B

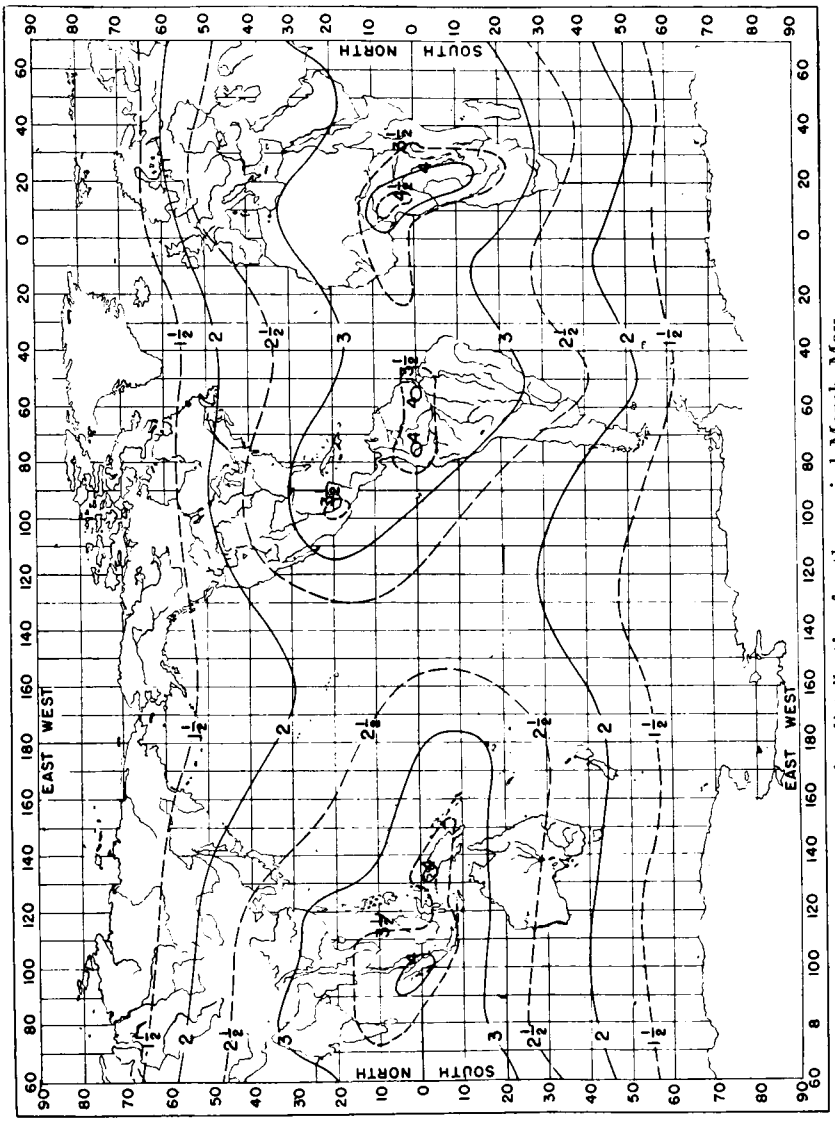

Noise distribution for the period March–May.

APPENDIX VI-C

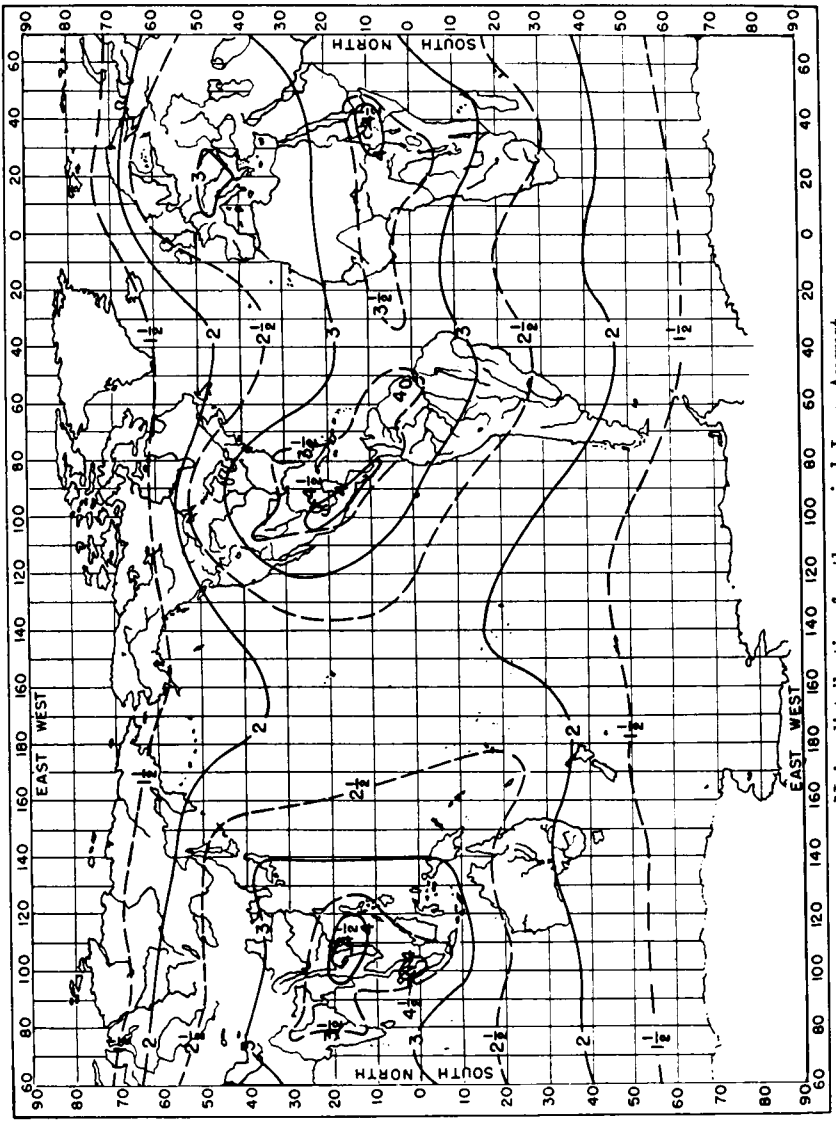

Noise distribution for the period June–August.

APPENDIX VI-D

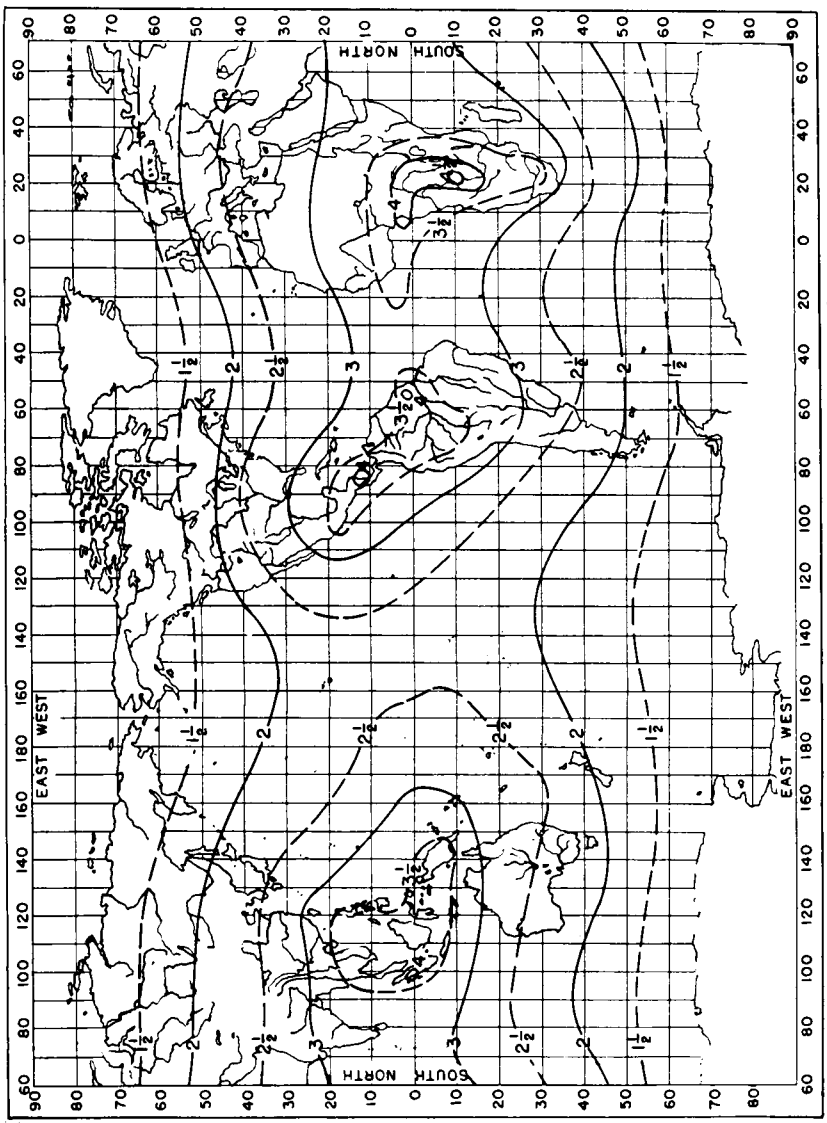

Noise distribution for the period September–November

APPENDIX VI-E,F

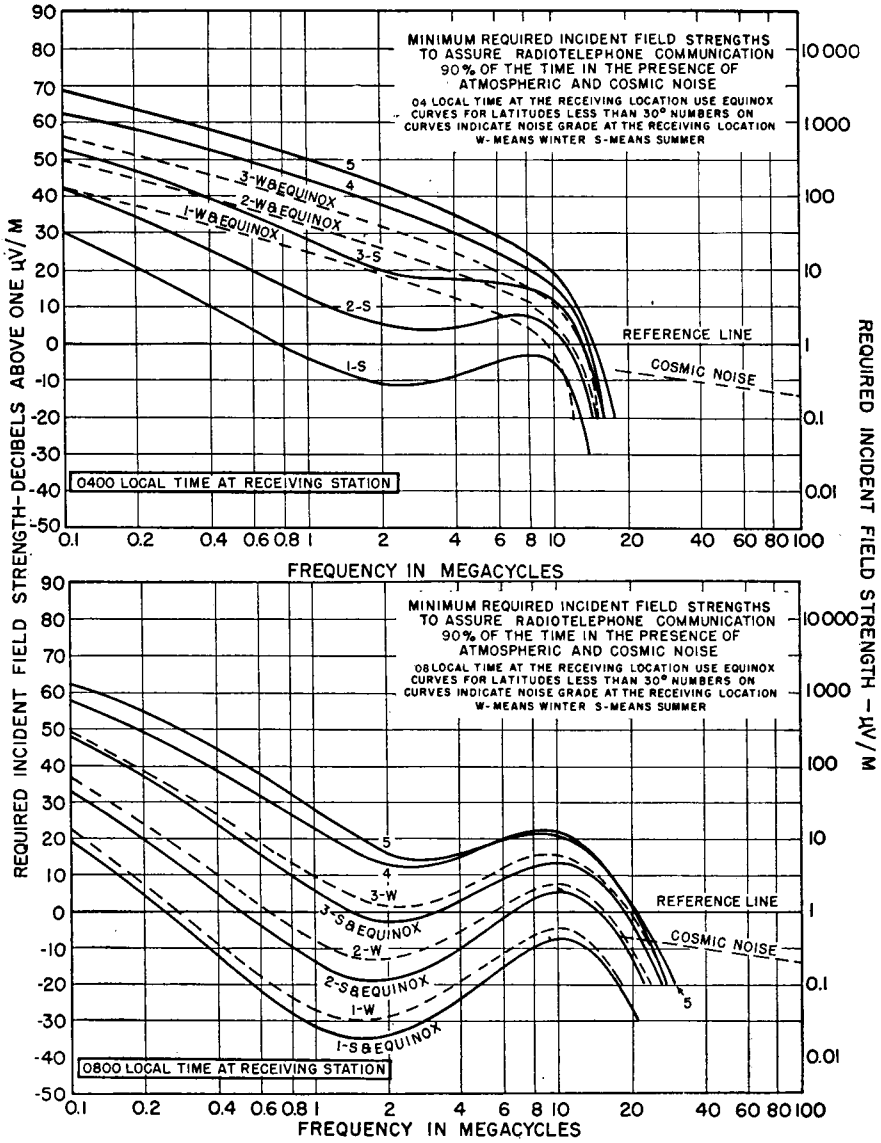

APPENDIX VI-G,H

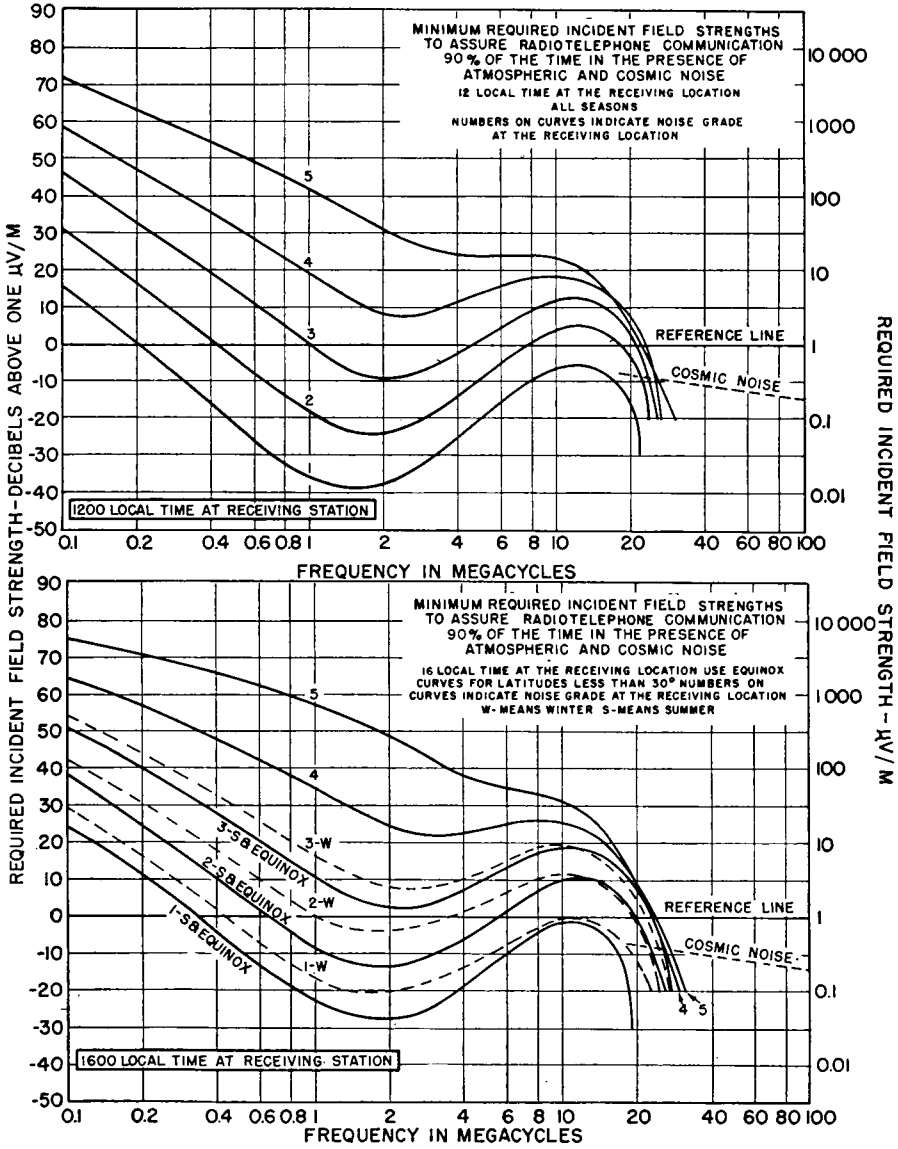

APPENDIX VI-I,J

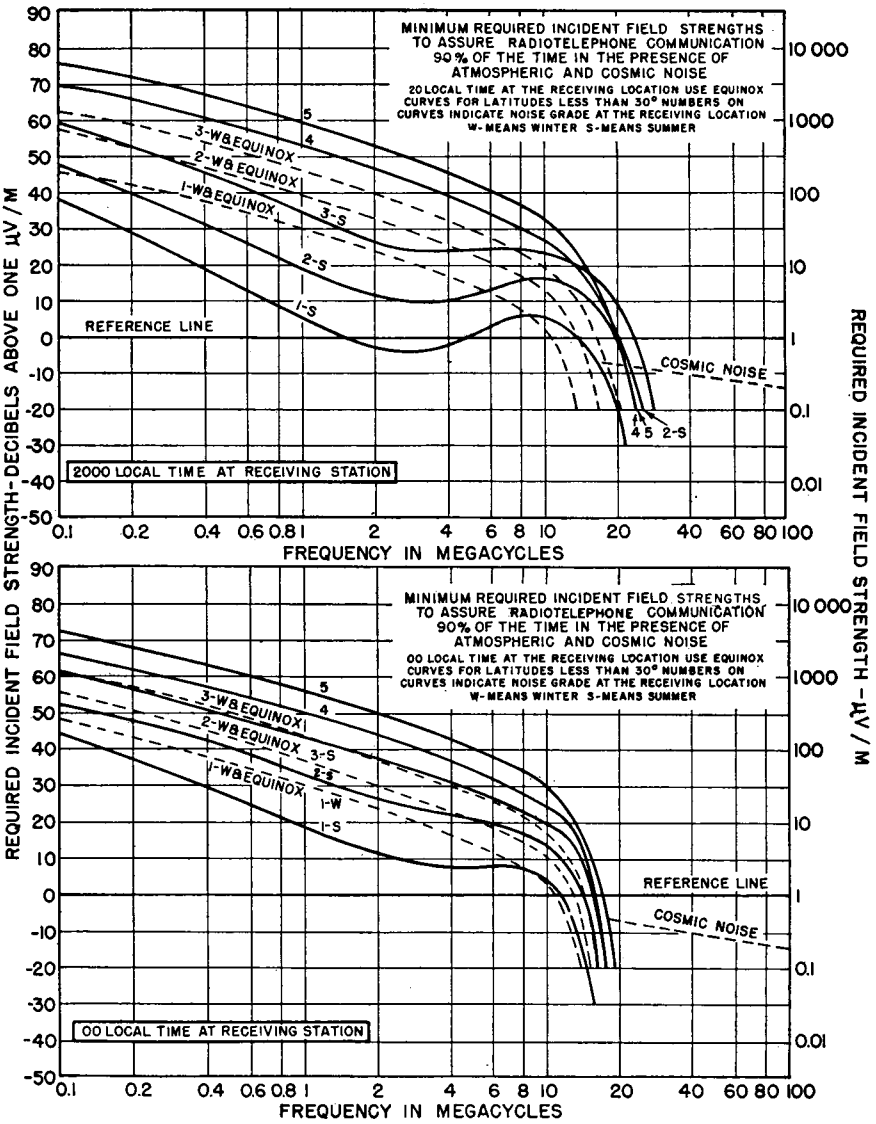

APPENDIX VII

Minimum Operating Signal-to-noise Ratios for Various Classes of Commercial Service in Telecommunication

Type of Radio Service	*Approximate Minimum S/N (Decibels)*
1. Double-sideband radiotelephony (3-kilocycle bandwidth)	15
2. Single-sideband radiotelephony (3-kilocycle bandwidth)	9
3. Broadcasting (5-kilocycle bandwidth)	26
4. Manual Morse radiotelegraphy (for average operators)	0
5. Frequency-shift radiotelegraphy (60-word teleprinter speed)	6
6. Single-sideband two-tone radiotelegraphy, one tone marking and one tone spacing, 60-word speed	8
7. Single-sideband four-tone radiotelegraphy, two tones marking and two tones spacing, 60-word speed	6
8. Radio facsimile with 8-decibel contrast ratio using double-sideband amplitude modulation	18
9. Radio facsimile with 8-decibel contrast ratio using carrier-shift	12

NOTE 1: The signal-to-noise ratios given are those required for reliable commercial operation, assuming the limiting factor is only noise.

NOTE 2: Noise includes all extraneous interference due to atmospheric static, man-made static, or interfering signals from other stations.

NOTE 3: Professional operators engaged in handling telegraph or telephone traffic often are able to copy faithfully when S/N is 10 to 15 decibels below the values stated for 1, 2, and 4. The others, with the exception of 3, are intrinsically machine methods.

NOTE 4: Consult documents of the International Radio Consulting Committee (CCIR) for standards under study on this subject.

APPENDIX VIII

Example of the Use of Directive Antennas for Minimizing Interference between Cochannel Medium-frequency Broadcasting Stations

The map shows the broadcasting stations on 620 kilocycles as they existed in North America in 1949. Under the North American Regional Broadcasting Agreement (NARBA) 620 kilocycles is a regional channel. The directive antenna pattern for each station on this channel is shown. Those in broken lines are used during local daylight hours, while those in solid lines are for night hours. In some cases a station is nondirective during daylight. It is seen that WROL and KCOM, for example, use different directive patterns day and night. Stations like WDNC and WHJB use the same pattern day and night but with different power.

The purpose of directive antennas is to provide a local service and, at the same time, to protect the service areas of stations that were already on the channel before a new station is installed. It will be noted that protections are not mutual in all cases. This is because existing stations are not required to change their antenna systems when a new station enters the channel, but the new station must protect the existing stations to rigidly prescribed limits. Directivity is also used to protect stations on adjacent channels when necessary.

The patterns shown indicate their shape only, and the size of the pattern as drawn does not in any way indicate a station's coverage. Each pattern is marked with the station call letters and its licensed power day and night. The symbol 5.U indicates 5 kilowatts unlimited (day and night); 0.5–1 LS means 1 kilowatt during daytime until local sunset and 0.5 kilowatt after local sunset. The symbol CP means that at the time the map was prepared the station had a construction permit to install the antenna system and the transmitter power using the pattern shown. (*Map supplied through courtesy of Mutual Broadcasting System.*)

Index

T

U

V

W

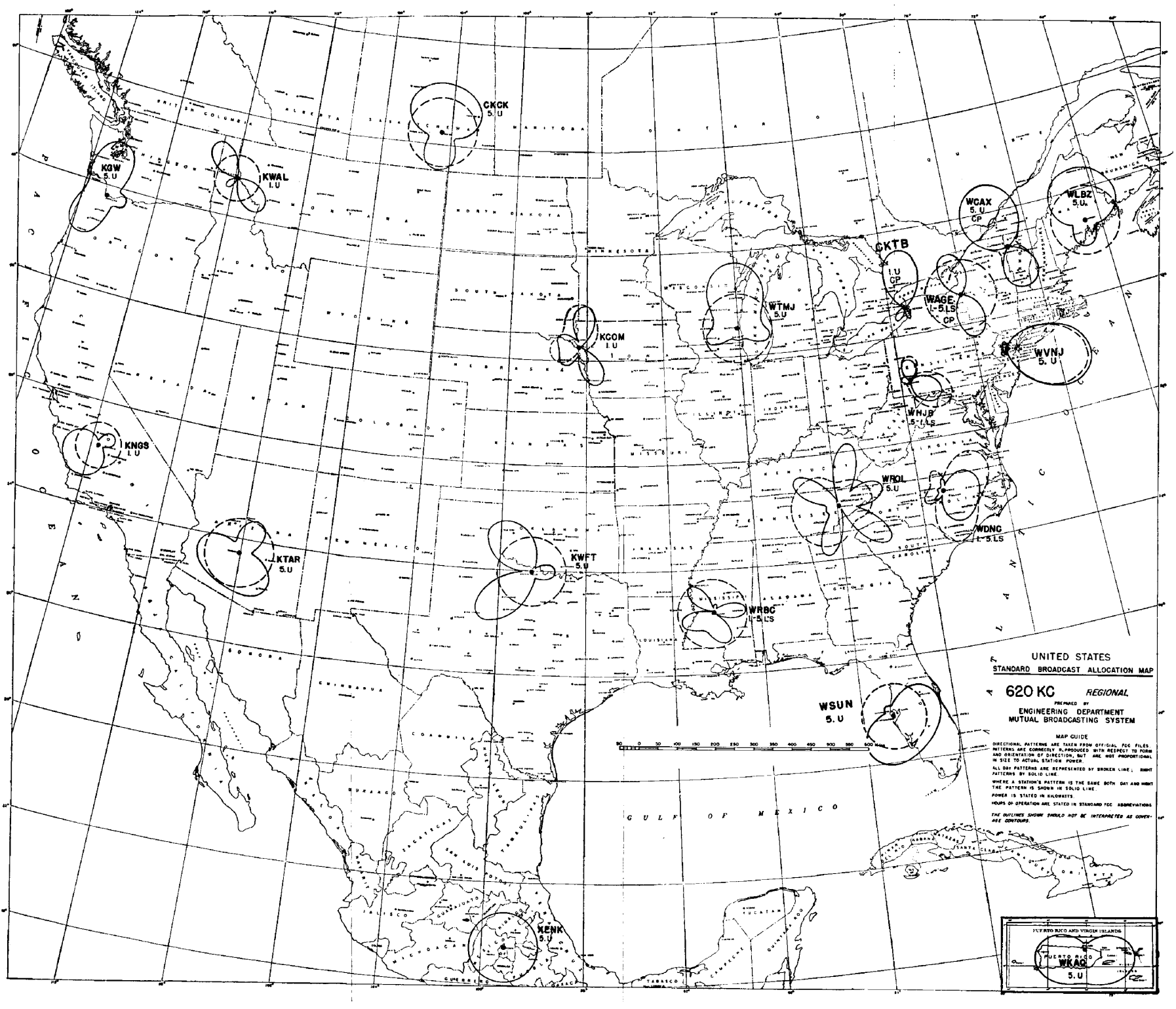
CKCK
5.U
KGW
5.U
KWAL
I.U
KCOM
I.U
WTMJ
5.U
CKTB
I.U
CP
WCAX
5.U
CP
WLBZ
5.U
WAGE
I-5.LS
CP
WVNJ
5.U
WHJB
5-I.LS
KNGS
I.U
KTAR
5.U
KWFT
5.U
WROL
5.U
WDNC
I-5.LS
WRBC
I-5.LS
WSUN
5.U
XENK
5.U
WKAQ
5.U
PUERTO RICO AND VIRGIN ISLANDS
PUERTO RICO
GULF OF MEXICO
ATLANTIC OCEAN
PACIFIC OCEAN
UNITED STATES
STANDARD BROADCAST ALLOCATION MAP
620 KC REGIONAL
PREPARED BY
ENGINEERING DEPARTMENT
MUTUAL BROADCASTING SYSTEM
MAP GUIDE
DIRECTIONAL PATTERNS ARE TAKEN FROM OFFICIAL FCC FILES. PATTERNS ARE CORRECTLY REPRODUCED WITH RESPECT TO FORM AND ORIENTATION OF DIRECTION, BUT ARE NOT PROPORTIONAL IN SIZE TO ACTUAL STATION POWER.
ALL DAY PATTERNS ARE REPRESENTED BY BROKEN LINE; NIGHT PATTERNS BY SOLID LINE.
WHERE A STATION'S PATTERN IS THE SAME BOTH DAY AND NIGHT THE PATTERN IS SHOWN IN SOLID LINE.
POWER IS STATED IN KILOWATTS.
HOURS OF OPERATION ARE STATED IN STANDARD FCC ABBREVIATIONS
THE OUTLINES SHOWN SHOULD NOT BE INTERPRETED AS COVERAGE CONTOURS.